SYNTHESES AND BIOCHEMICAL EVALUATION OF *TROPOLONYLATED* PEPETIDE AND NUCLEIC ACID ANALOGUES

By

BIBHUTI BHUSANA PALAI

CHEM11201604002

National Institute of Science Education and Research (NISER)
Bhubaneswar

A thesis submitted to the

Board of Studies in Chemical Sciences

In partial fulfillment of requirements
for the Degree of

DOCTOR OF PHILOSOPHY

of

HOMI BHABHA NATIONAL INSTITUTE

January, 2022

Homi Bhabha National Institute[1]

Recommendations of the Viva Voce Committee

As members of the Viva Voce Committee, we certify that we have read the dissertation prepared by **BIBHUTI BHUSANA PALAI** entitled "**SYNTHESIS AND BIOCHEMICAL EVALUATION OF *TROPOLONYLATED* PEPETIDE AND NUCLEIC ACID ANALOGUES**" and recommend that it may be accepted as fulfilling the thesis requirement for the award of Degree of Doctor of Philosophy.

Chairman – Prof. A. Srinivasan	17.05.22
Guide / Convener – Dr. Nagendra K. Sharma	17.05.22
Examiner - Prof. Kana M. Sureshan	17.05.2022
Member 1- Dr. Chandra Sekhar Purohit	17.05.22
Member 2- Dr. Jogendra Nath Behera	17.05.22
Member 3- Dr. Tirumala K. Chowdary	17.05.22

Final approval and acceptance of this thesis is contingent upon the candidate's submission of the final copies of the thesis to HBNI.

I/We hereby certify that I/we have read this thesis prepared under my/our direction and recommend that it may be accepted as fulfilling the thesis requirement.

Date: 17.05.22
Place: NISER - Bhubaneswar

Signature
Co-guide (if any)

Signature
Guide Dr. Nagendra K. Sharma

[1] This page is to be included only for final submission after successful completion of viva voce.

STATEMENT BY AUTHOR

This dissertation has been submitted in partial fulfillment of requirements for an advanced degree at Homi Bhabha National Institute (HBNI) and is deposited in the library to be made available to borrowers under rules of the HBNI.

Brief quotations from this dissertation are allowable without special permission, provided that accurate acknowledgement of source is made. Requests for permission for extended quotation from or reproduction of this manuscript in whole or in part may be granted by the Competent Authority of HBNI when in his or her judgment the proposed use of the material is in the interests of scholarship. In all other instances, however, permission must be obtained from the author.

BIBHUTI BHUSANA PALAI

DECLARATION

I, hereby declare that the investigation presented in the thesis has been carried out by me. The work is original and has not been submitted earlier as a whole or in part for a degree / diploma at this or any other Institution / University.

BIBHUTI BHUSANA PALAI

List of Publications arising from thesis

Journal

1. **Palai, B. B**.; Sharma, N. K.* *N*-Arylated peptide: troponyl residue influences the structure and conformation of *N*-troponylated-(di/tri)-peptides. *CrystEngComm*, **2021**, *23*, 131-139.

2. **Palai, B. B**.; Soren, R.; Sharma, N. K.* BODIPY Analogues: Synthesis and Photophysical studies of difluoro Boron complexes from 2-Aminotropone Scaffolds through N,O-Chelation. *Org. Biomol. Chem*., **2019**, *17*, 6497-6505.

Chapters in books and lectures notes: NA

Conferences

1. Oral Presentation: “New DNA Binding Agents: Synthesis of Cyclotropoimine from ketene intermediate via [2+2] cycloaddition” in National Bioorganic Chemistry Conference-2018, NBCC-2018, 22-24th December 2018, NISER-Bhubaneswar.India

2. Oral presentaation: “Synthesis and Structural Studies of N-Troponyl-Amino acids/Peptides”. IC-CBSDD-2019, 8-10th March 2019, Berhampur University, Bhanja Bihar, Odisha. India

3. Poster presentation: “Syntheses and Photophysical studies of functionalized Boron-Aminotropones”. XV J-NOST 2019, 18-21st Oct 2019, University of Delhi. India

4. Participant: International Conference in Chemistry, iconChem2018, 24-26th May, 2018, IISER-Tirupati, India.

5. Participant: ACS on Campus, 23rd July, 2018, NISER-Bhubaneswar, India.

Others (Manuscripts)

1. **Palai, B. B**.; Sharma, N. K.* Synthesis and photophysical studies of Tropolonyl dihydropyrazine molecules as DNA Binding Agents

2. **Palai, B. B**.; Sharma, N. K.* Synthesis and Photophysical Study of BODIPY Analogue from *Troponylalkyl Chain* via *N, O*-Chelation.

3. **Palai, B. B.;** Sharma, N. K.* Synthesis of *Troponyl*- BODIPY DNA and *Troponyl* RNANucleoside analogues

4. N. Dalabehera, N.; Meher, S; **Palai, B. B**.; Sharma, N. K.* Instability of Amide Bond With TFA (20%): Synthesis, Conformational Analysis and Mechanistic Insights of Cleavable Amide Bond Comprising β-Troponylhydrazino Acid. *ACS Omega*, **2020**, *5*, 26141–26152.

BIBHUTI BHUSANA PALAI

Dedicated
To
My Family

ACKNOWLEDGEMENTS

I am extremely grateful to **God** for blessing this life and giving strength.

I sincerely acknowledge the National Institute of Science Education and Research (NISER) and its prosperous research environment. It is my privilege to be part of esteemed institution. I thank the University Grant Commission (UGC) for the Junior/Senior Research Fellowship

I would like to express my heartfelt gratitude to my supervisor, **Dr. Nagendra Kumar Sharma** for accepting me to work under his guidance. I am grateful to him for his care, help, support, and other countless reasons that I cannot enumerate in this journey. His extraordinary vision, excellent knowledge of the subject, and kind heart made me today what I am.

I would like to thank the faculty, School of Chemical Science (SCS), my current and past research lab members, Dr. Chandrasekar Reddy, Dr. Balachandra, Dr. Amarnath, Dr. Smitha, Dr. Supriya Dr. Raghunath. Sagarika, Chinmay, Manish, Subhashree, Ankita , Ramu, Nihar, Saideep, Bhagya and Asmita. I am thankful to our collaborator Dr. Manjusha Dixit and lab members Saket and Vinay from School of Biological Sciences (SBS) for their valuable scientific discussion and support. I also thank my doctoral committee Prof. A. Srinivasan, Dr. Chandrasekhar Purohit, Dr. Jogendra Nath Behera and Dr. Tirumala Kumar Chowdary.

I express my sincere gratitude to my teacher prof. (Dr.) Panchana Goud and Dr. Santosh Kumar Choudhury for their encouragement and moral support during my Ph.D.

A special thank goes to my dear friend Shaikh Samser for his cooperation, moral support, fruitful advice and continuous encouragement during my Ph.D.

I thank my dear friends Dr. Tapan, Pragya, Mona, Smurti, Jiban, Shreeni, Pragati, and my Ph.D batch mates (Jan-2016, Chemistry).

Finally, I convey my heartfelt gratitude to my parents, sisters for their sacrifices for me, constant encouragement, unconditional love, support, and blessings which helped me overcome many difficulties during my Ph.D. and in my life**.**

SYNOPSIS

Introduction

Amino acids/peptides and nucleic acids (DNA/RNA) are bio-macromolecules, which are involved in the various biochemical process. Recently, the synthetic amino acid and nucleic acid analogues are developed to regulate the sequence specific bioactivities, and considered as potential therapeutic drug candidates. The bioactivities of peptides depend upon their secondary structures, which acquired by the side chain residues of amino acids. The various unnatural amino acids are synthesized and incorporated into native peptides to tune the structure and function of peptides, including aromatic amino acid derivatives. Mostly, the aromatic amino acids are derived from benzenoid aromatic moiety. However non-benzenoid aromatic molecule and related derivatives are also occurred in nature, such as Tropolone, Thujaplicinols, Stipitatic acid, and Colchicine. Tropolone is seven-membered conjugated cycloheptene aromatic molecule possessing unique structural and photophysical properties. For examples, Tropolone exhibit intramolecular hydrogen bonding and metal chelation with bivalent transition metals, Be, Cu (II), Zn (II) and Ni (II).

Scope and Organization of the Present Thesis

Tropolone is non-benzenoid natural molecule comprising unique structural and photophysical properties. It is part of various bioactive natural products as *Tropolonoids*. This thesis describes the role of tropolone in amino acid and nucleic acid derivatives which is classified into Five chapters as following: (a) Introduction of modified amino acids and nucleic acid (DNA/RNA) analogues (Chapter 1); (b) Structural and conformational analyses of *N*-tropolonylated *di-/tri*-peptide (Chapter-2); (c) Synthesis and photophysical studies of Troponyl BODIPY analogues (Chapter 3);

(d) Synthesis and photophysical studies of Tropolonyl dihydropyrazine molecules (Chapter 4); (e) Synthesis and Photophysical studies of Troponyl DNA and RNA analogues (Chapter 5).

Chapter-1. Introduction of modified amino acids and nucleic acid analogues
This chapter describes the brief introduction of synthetic amino acid, peptides, fluorescent DNA/RNA analogues and tropolonoid natural products. Many of them are promisable analogues for the development of new nano-materials and therapeutic drugs.

Chapter 2. Structural and conformational analyses of *N*-tropolonylated *di-/tri*-peptide

Synthesis and Conformational Analysis of N-Troponylated *di-/tri*-Peptides (Palai, B. B.; Sharma, N. K.* *CrystEngComm*, **2021**, *23*, 131-139)

The *N*-arylated peptides have reportedly a significant role in the structural organization of peptides,[1] which are mainly derived from benzenoid aromatic moieties. This chapter demonstrates the synthesis of *N*-troponylated amino acid and their peptides from naturally occurring *Tropolone* scaffold by following the synthetic Scheme-1. Their structural conformations are established by NMR (1D/2D), HRMS, CD, and single-crystal X-ray techniques. The comparative CD spectra of control native *di-tri*-peptides and *N*-tropolonylated *di-tri*-peptides are depicted in Figure-1 which strongly support the role of tropolonyl scaffold in the formation of β-turn type of secondary structures in solution phase. The single-crystal analyses of troponlylated *di*-peptides also support the formation of a unique supramolecular self-assembly β-sheet/turn type of structure. Hence, the *N*-tropolonyl unit has a significant role in the tunning of native peptides structure and conformation

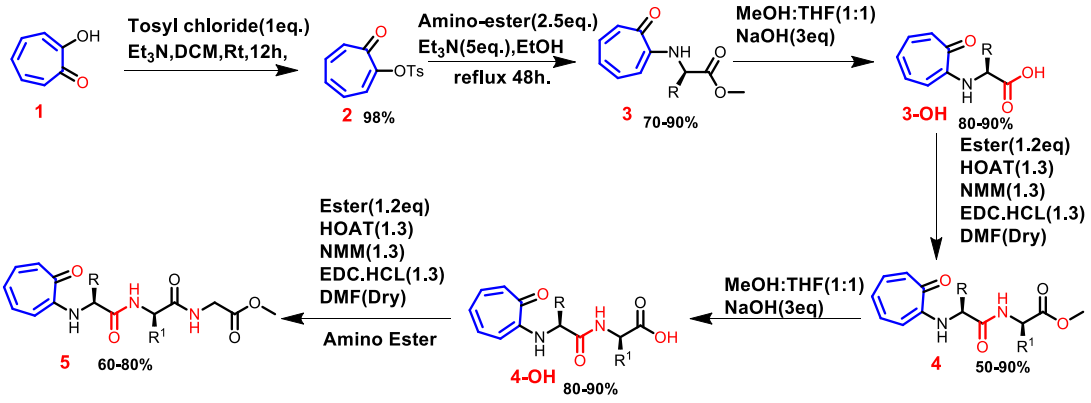

tr-dipeptide(4) (Tr-NH-AA$_1$CO-NH-AA$_2$-OMe)
4a. Tr-NH-Gly-CO-NH-Gly-OMe
4b. Tr-NH-Gly-CO-NH-Ala-OMe
4c. Tr-NH-Val-CO-NH-Gly-OMe
4d. Tr-NH-Val-CO-NH-β-Ala-OMe
4e. Tr-NH-Gly-CO-NH-β-Ala-OMe
4f. Tr-NH-Leu-CO-NH-β-Ala-OMe
4g. Tr-NH-Val-CO-NH-β-Ala-OMe
4h. Tr-NH-Ala-CO-NH-β-Ala-OMe
4i. Tr-NH-Ile-CO-NH-β-Ala-OMe
4j. Tr-NH-Phe-CO-NH-β-Ala-OMe
4k. Tr-NH-Pro-CO-NH-Val-OMe
4l. Tr-NH-b-Ala-CO-NH-Pro-OMe

tr-tripeptide(5) (Tr-NH-AA$_1$CO-NH-AA$_2$-CO-NH-AA$_3$-OMe)
5a. Tr-NH-Gly-CO-NH-β-Ala-CO-NH-Gly-OMe
5b. Tr-NH-Ala-CO-NH-β-Ala-CO-NH-Ala-OMe
5c. Tr-NH-Val-CO-NH-β-Ala-CO-NH-Val-OMe
5d. Tr-NH-Leu-CO-NH-β-Ala-CO-NH-Leu-OMe
5e. Tr-NH-Ile-CO-NH-β-Ala-CO-NH-Ile-OMe

Control-tripeptide(6) (Tr-NH-AA$_1$CO-NH-AA$_2$-CO-NH-AA$_3$-OMe)
6a. Boc-NH-Gly-CO-NH-β-Ala-CO-NH-Gly-OMe
6b. Boc-NH-Ala-CO-NH-β-Ala-CO-NH-Ala-OMe
6c. Boc-NH-Val-CO-NH-β-Ala-CO-NH-Val-OMe
6d. Boc-NH-Leu-CO-NH-β-Ala-CO-NH-Leu-OMe
6e. Boc-NH-Ile-CO-NH-β-Ala-CO-NH-Ile-OMe

Scheme 1. Synthesis of N-Troponylated dipeptides

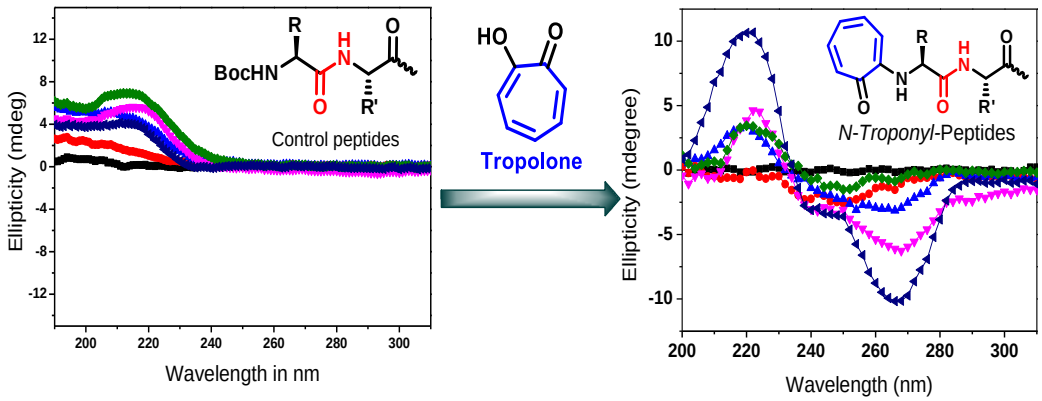

Figure 1. CD Spectra of troponyled peptide and control tripeptides

Chapter 3. Synthesis and photophysical studies of Troponyl BODIPY analogues

BODIPY and related compounds are versatile fluorescent dyes molecules which are being used for labeling of biomolecules for imaging inside the living system in real-time and fluorescent nano-materials for various purposes.[2] This chapter describes the

synthesis of BODIPY analogs from tropolone scaffold which is classified into two as Part A and Part B**.**

Part A: Synthesis and Photophysical Studies of Functionalized *Troponyl*-BODIPY Analogues (Palai, B. B.; Soren, R.; Sharma, N. K.**Org. Biomol. Chem.***,** 2019,**17**, 6497-6505).

Part A (Chapter-2) demonstrates the synthesis of various boron-aminotropones derivatives (*Troponyl*-BODIPY) from *N*-troponly amino acids and *difluoro*-Boronating reagent by following Scheme-2. *Troponyl*-BODIPY compounds contain aminotropone and boron complexes through *N,O*-chelation. Their structures are confirmed by NMR ($^{1}H/^{13}C/^{19}F$, ^{11}B) HRMS, and single-crystal X-ray analyses. These BODIPY analogues exhibit characteristic UV/Fluorescence properties organic polar solvents (MeOH/CH_3CN). Their quantum yields are varied from ~0-15% because of different amino acids acid residues. Theses analogues also exhibit solvent-dependent fluorescence properties. Their electrochemical studies confirm only one irreversible reduction reaction with Epc = −1.3 (V). Their structure has been optimized with DFT and their optimized structures show that the amino acid residues affect fluorescence characters in the respective troponyl-BODIPY analogues. Hence, Chapter-2 (Part A) provides the opportunities to develop the amino acid-functionalized troponyl-BODIPY analogues for labelling peptides and other biomacromolecules.

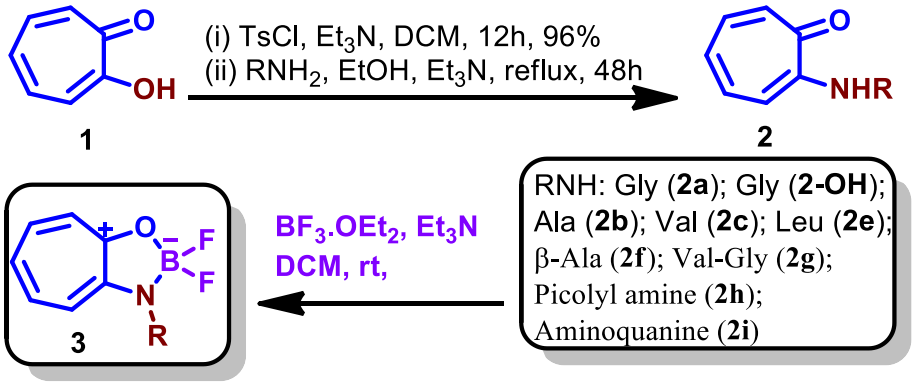

Scheme 2. Synthesis of difluoroboron-aminotropone complex

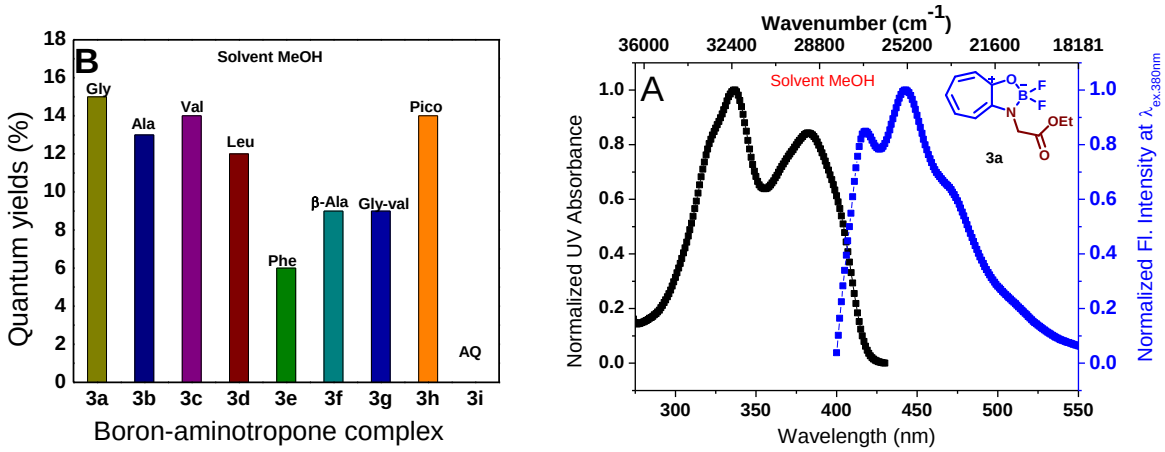

Figure 2. (A) Absorption and Emission spectra of boron-aminotropone complexes (**3a**) in methanol at concentration ($5x10^{-4}$M). (B) Quantum yield bar diagram of boron-aminotropone complexes (**3a-3i**) in methanol.

Part B: Synthesis and Photophysical Studies of Lipophilic *Troponyl*-BODIPY Aanlogues

(Palai, B. B. and Sharma, N. K.* *Manuscript under preparation*)

Part B (Chapter-2) describes the synthesis and photophysical studies of lipphilic BODIPY analogues which are derived from *N*-Tropolonyl of various alkylamines by following the given synthetic Scheme-3. The various *N*-tropolonyl alkylamines have

been prepared from alkylamines and *O*-tosylate tropolone before complexing with difluoroboronating reagents. These complexes have been characterized NMR ($^{1}H/^{13}C/^{19}F$, ^{11}B), HRMS, and single-crystal techniques. Their photophysical studies (UV/Fluorescence) reveal that these analogues are fluorescent with quantum yield 10-15% in organic polar solvents, MeOH/CH_3CN, (Figure 3). Importantly these analogues contain long chain hydrocarbons, lipophilic nature, in the BODIPY analogues which could be useful to find non-polar microenvironment.

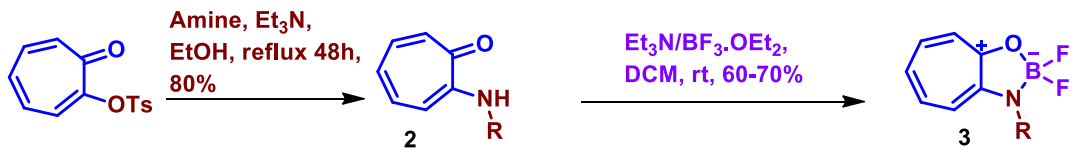

RNH: Sec-*butyl* amine **(2a)**; Cyclohexyl amie **(2b)**; Propagyl amine **(2c)**; n-*butyl* amine **(2d)**; Hexyl amine**(2e)**; Octyl amine **(2f)**; Dodecyl amine **(2g)**; Octadecyl amine **(2h)**

Scheme 3. Synthesis of boron-aminotroponimine complexes.

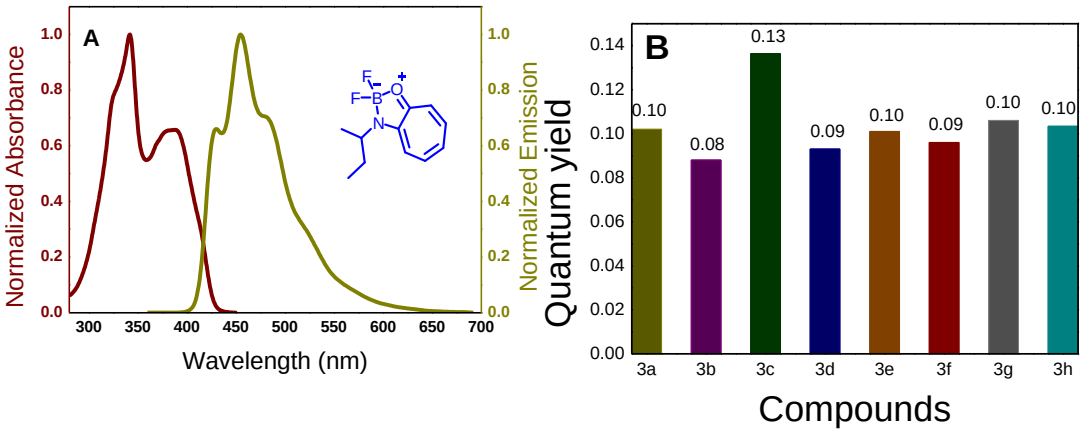

Figure 3. (A) Absorption and Emission spectra of boron-aminotropone complexes (**3a**) in methanol at concentration ($5x10^{-4}$M). (B) Quantum yield bar diagram of boron-aminotropone complexes (**3a-3h**) in methanol.

Chapter 4. Synthesis and photophysical studies of Tropolonyl dihydropyrazine molecules as DNA Binding Agents

(Palai, B. B. and Sharma, N. K.* *Manuscript under preparation*)

Dihydropyrazine molecules are bioactive molecules which are considered as promisable therapeutic drug candidates. Troponyldihydrapyrazine core moeities are also bioactive molecules possessing anticancer properties.[3] This chapter describes the synthesis of various substituted dihydrapyrazine derivatives from *N*,*N*-dialkylated 2-aminotropone ester derivatives and imines under acidic conditions (Scheme 4). The product has been formed by the 2+2 cycloaddition reaction of imine and troponyl ketene and then rearrangment. Interestingly, we new adduct has been isolated as aryl-substituted troponyl dihydropyrazine derivatives from N-troponyl alkyl glycinate and imine derivative under acidic conditions (Figure 3). So far, there is no such report about the formation of dihydropyrazine from imine derivatives. This thesis describes the synthesis, mechanistic studies of product formation, and structural features of newly synthesized dihydropyrazine derivatives. For biological importance, we examine the inhibition of cancerous cell proliferation with representative troponyl dihydropyrazine molecule by MTT-assay. Importantly, amino troponyl ketene has formed from the *N*,*N*-dialkylated 2-aminotropone ester under mild acidic conditions.[4, 5] Interestingly these derivative are fluorescent in nature with the quantum yield ~10-15%. This thesis also describes their bioactivies by MTT assay. Initial their bio-screening results strongly support the binding with DNA and anticancer activities. Hence these derivatives are potential fluorescent therapeutic drug candidates.

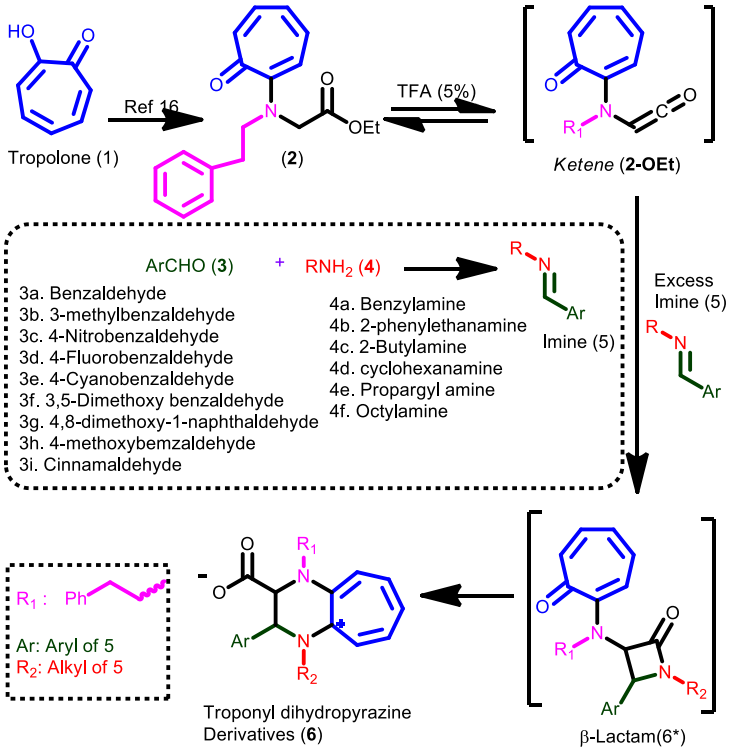

Scheme 3. Synthesis of *Troponyl* dihydropyrazine derivatives

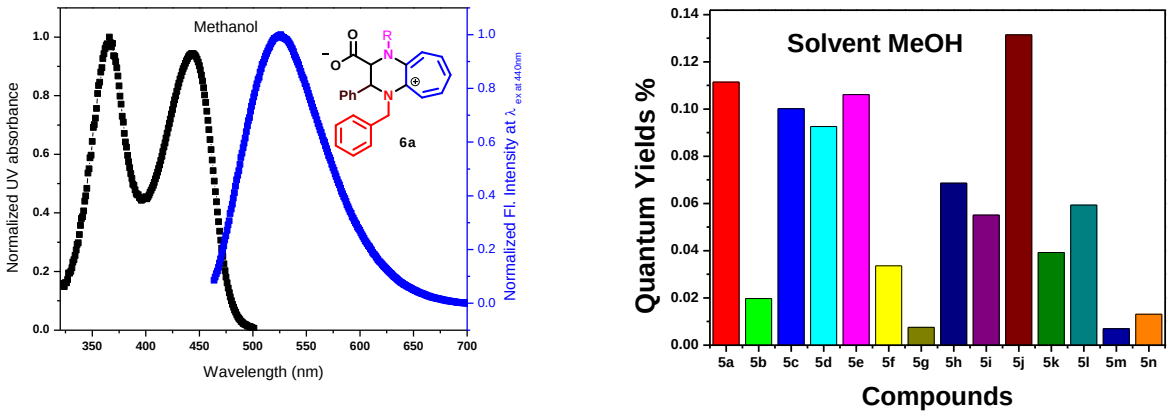

Figure 4. (A) Absorption and Emission spectra of *Troponyl* dihydropyrazine derivatives (**6a**) in methanol at concentration ($5x10^{-5}$M). (B) Quantum yield bar diagram of *Troponyl* dihydropyrazine derivatives (**6a-6n**) in methanol.

Chapter 5. Synthesis of *Troponylated*-Uridinyl Nucleoside Analogues

Previously, troponyl-DNA analogue has shown the remarkable duplex DNA formation and photophysical properties. This chapter describe the synthesis photophysical studies of troponyl BODIPY containing DNA nucleosides and troponyl linked RNA nucleoside analogues, There are two main objectives of this chapters:

Part A: *Troponyl* BODIPY DNA Nucleoside analogues

(Palai, B. B. and Sharma, N. K.* *Manuscript under preparation*)

This chapter describes the synthesis and photophysical studies of *troponyl*-BODIPY containing deoxyuridinyl nucleoside analogue as dU^{trBOD}. Its synthetic route is described in Scheme-4. Then this modified nucleoside analogue is studied by UV and fluorescence spectrophometer. Its UV and fluorescence spectra exhibit that dU^{trBOD} is fluorescent molecules though its quantum yield is weak in aquesous solution ~1.0%. This modified nucleoside has converted into phosphoramidites by following the given synthetic route and attempted to incoprporate into DNA oligos at different position. Triphospahte of dU^{trBOD} is also synthesized by following the previous procedure. Thus this nucleoside analogue could be useful to prepare the fluorescent label DNA oligo enzymatically.

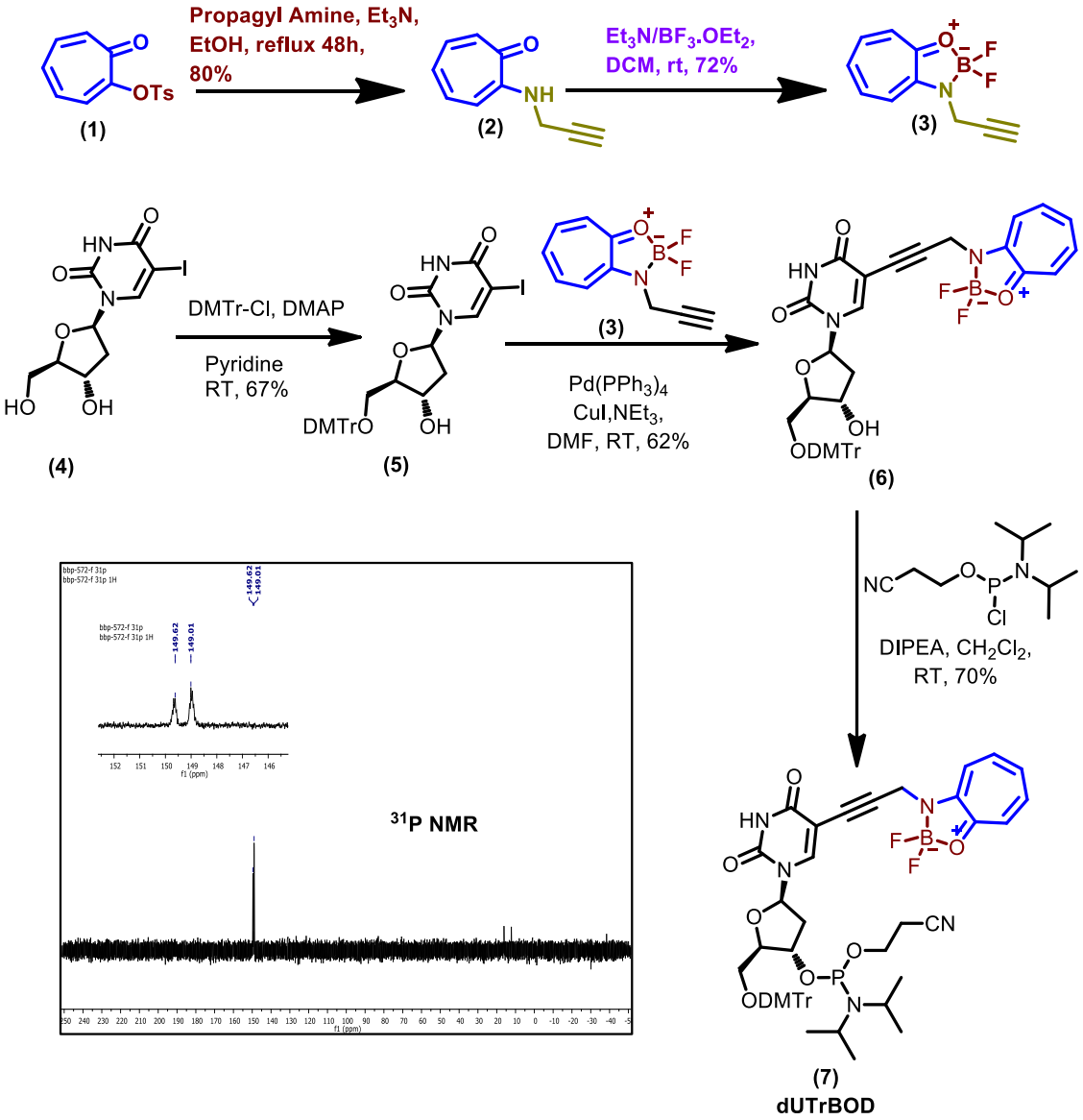

Scheme 4. Synthesis of Trpoponylated BODIPY thymidine phoshporaamdities **dU^{TrBO}**

Part B: *Troponyl* conjugated RNA analoues

(Palai, B. B. and Sharma, N. K.* *Manuscript under preparation*)

Part B of this chapter describes the synthesis of tropolone conjugated uridine nucleoside by following the synthetic route (Scheme 5). Next, this nucleoside has converted into troponyl uridinyl phosphoramidites. This modified phosphoramidite

has incorporated into RNA oligo to examine the effect of troponle in RNA:RNA and RNA:DNA duplex formation. Hence this troponyl RNA analogue could be useful to examine role of tropolone in RNA dependent biological process.

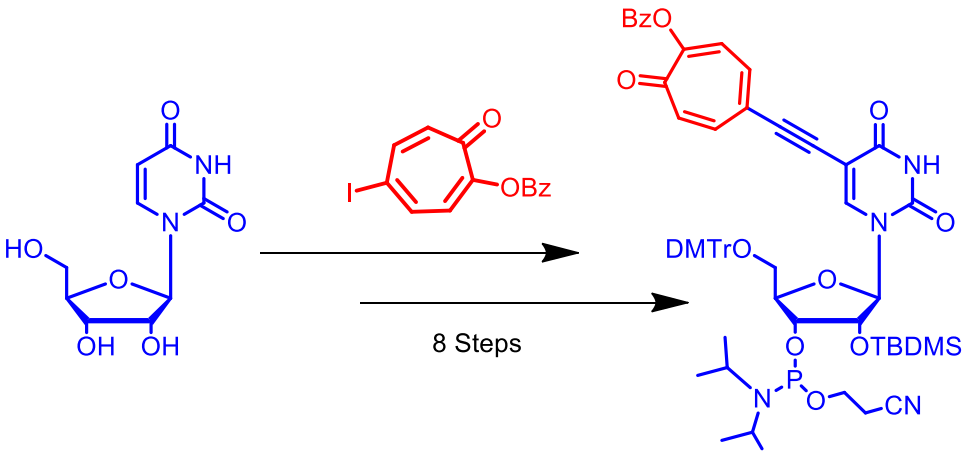

Scheme 5. Synthesis of Trpoponyl conjugated Uridine phoshporaamditie

References

1. B. Paul, G. L. Butterfoss, M. G. Boswell, P. D. Renfrew, F. G. Yeung, N. H. Shah, C. Wolf, R. Bonneau and K. Kirshenbaum, *J. Am. Chem. Soc.*, 2011, **133**, 10910-10919.
2. A. Bessette and G. S. Hanan, *Chem. Soc. Rev.*, 2014, **43**, 3342-3405.
3. R. Bentley, *Nat. Prod. Rep.*, 2008, **25**, 118-138.
4. C. Balachandra and N. K. Sharma, *Org. Lett.*, 2015, **17**, 3948-3951.
5. C. Balachandra and N. K. Sharma, *ACS Omega*, 2018, **3**, 997-1013.

CONTENTS

Page No.

SUMMSRY **1**

List of Figures

Figure 1.1 First synthetic peptides: dipeptide (A); polypeptide (B). 2

Figure 1.2 Advantages of peptidomimetics over peptides 4

Figure 1.3 A) general representation of solution-phase peptide syntheses, B) Coupling reagents and additives C) Mechanism of carbodiimide mediated solution-phase peptide syntheses. 6

Figure 1.4 General representation of solid-phase peptide syntheses 7

Figure 1.5 Examples of different peptide to α-helix mimetics 9

Figure 1.6 Crystal and NMR analyzed α/γ APCH peptides 9

Figure 1.7 α/γ containing APCH peptides structures 10

Figure 1.8 Crystal structure of α-helix A) α-helix with Poly L-Alanine, B) 14-helix Poly *β*-Alanine. 10

Figure 1.9 Secondary structures of natural, synthetic peptides A) *β*-hairpin in solution state B) Antiparallel β-sheet in single-crystal structures 11

Figure 1.10 Synthesis of short α, γ-hybrid tripeptide 12

Figure 1.11 Synthesis of novel tetra and hexa pseudo peptides 12

Figure 1.12 Structure of DNA duplex 13

Figure 1.13 Nucleotide structure of DNA and RNA 14

Figure 1.14 Chemically modified nucleobase analogues 15

Figure 1.15	Incorporation of BodU and modified non-nucleosidic DNA base having Bo into DNA using automated phosphoramidite chemistry	16
Figure 1.16	Synthesis of fluorescently modified DNA oligonucleotides	17
Figure 1.17	Synthesis of diarylethene-modified DNA Olionucleotides	17
Figure 1.18	Synthesis of modified DNA ONs from 8-aryl-dG phosphoramidite derivatives using different protecting Groups	18
Figure 1.18	Synthesis of tetrazole-modified DNA ON by automated phosphoramidite chemistry	19
Figure 1.20	Synthesis of norbornene-modified uridine phosphoramidite into RNA olionucleotides.	19
Figure 1.21	Chemical structue of tropolonoid natural products	20
Figure 1.22	Chemical structure (a) *Traeg* peptide, (b) hydroen bonding in *Traeg* peptide	21
Figure 1.23	Chemical structure **(a)** *Traeg* peptide analogues (b) *N-Troponylated*-β-hydrazino Acid/Peptide	21
Figure 1.24	Synthesis of *Troponyl*-modified DNA ON by automated phosphoramidite chemistry	22
Figure 2.1	(a) *N*-aryl peptide; *N*-troponyl cleavable peptides; and (b) *N*-troponyl noncleavable peptides	40
Figure 2.2	Crystal structure of compound **4a**, **4b**, **4d**, **4e**, **4f** and **4j**	42
Figure 2.3	Structural analysis of N-trponyl-peptide (**4a**): (a) structure and ORTEP diagram; (b) Unit cell packing diagram; (c-e) Supramolecular self-assembly structure	43

Figure 2.4	Structural analysis of *trponyl*-peptide (**4b**): (a) structure and ORTEP diagram; (b) Unit cell packing diagram; (c-g) Supramolecular self-assembly structure	44
Figure 2.5	Structural analysis of *trponyl*-di-peptide (4d): (a) structure and ORTEP diagram; (b) Unit cell packing diagram; (c) Supramolecular self-assembly structure	45
Figure 2.6	Structural analysis of trponyl-peptide (4e): (6a) structure and ORTEP diagram; (6b) Unit cell packing diagram; (6c) Supramolecular self-assembly structure	46
Figure 2.7	Structural analysis of *trponyl-di*-peptide (**4f**): (a) structure and ORTEP diagram; (b) Unit cell packing diagram; (c-h) Supramolecular self-assembly structure	47
Figure 2.8	Structural analysis of trponyl-peptide (4j): (a) structure and ORTEP diagram; (b) Unit cell packing diagram; (c) Supramolecular self-assembly structure	48
Figure 2.9	Ramachandran Plots of Individual *N*-troponyl Peptides (**4a/4b/4d/4e/4f/4j**)	50
Figure 2.10	CD spectra of tr-peptides in solvent MeOH/CH_3CN: (A) CD spectra of peptide (**4a-4l**) in Methanol (MeOH), (B) CD spectra of peptide (**4a-4l**) in Acetonitrile (CH_3CN), (C) non-characteristic CD signals in peptides (**4a**/**4b**/**4c**/**4f**/**4h**/**4j**/**4k**/**4l**) and (D) Characteristic CD signals of peptides (**4d**/**4e**/**4g**/**4i**).	52
Figure 2.11	DMSO-d_6 titration ^{1}H-NMR experiment of peptide of **4c** (A)/ **4e**(B)/**4j** (C) and NOE and possible intramolecular hydrogen bonding in respective tr-peptides (D)	54
Figure 2.12	CD Spectra of *tr-tri*-peptides and control *tri*-peptides in CH_3CN	56
Figure 2.13	DMSO-d_6 titration ^{1}H-NMR experiment of peptide **5c (A)/5d(B) and** NOE and possible intramolecular hydrogen bonding in respective tr-peptides (C)	57

Figure 3A.1	Chemical structures of A) BODIPY complex; B) Boron-aminotroponimine complex; and C) Boron-aminotropone complex	119
Figure 3A.2	11B NMR and 19F NMR of **3a** in $CDCl_3$. HRMS spevtrum of **3a**	121
Figure 3A.3	ORTEP diagrams of boron complex (3a, 3a-OH, 3b, 3c, 3h, and 3i) with 50% probability of ellipsoids	123
Figure 3A.4	Structural description of crystal BF_2-Aminotropone analogue 3a (CCDC 1888899): a. ORTEP diagram with 50% probability of ellipsoids and important bond length; b. Packing diagram; π-π interaction (side view), c. interaction (top view); and d. ORTEP diagram with 50% probability of ellipsoids and important bond length	124
Figure 3A.5	Absorption spectra of boron-aminotropone complexes (**3a-i**) in methanol at $5x10^{-4}$M concentration (A); and Bar diagram of their molar extinction coefficient (B)	126
Figure 3A.6	(A) Absorption and Emission spectra of boron-aminotropone complexes (**3a**) in methanol at concentration ($5x10^{-4}$M). (B) Quantum yield bar diagram of boron-aminotropone complexes (**3a-3i**) in methanol	128
Figure 3A.7	Optimized structure and HOMO- LUMO energy gap (atomic unit in eV) of boron aminotropone (**3a, 3a-OH, 3b, 3h, 3i**) at B3LYP/6-31+G* level of theory in vacuum	131
Figure 3B.1	Chemical structures of A) aminotroponimine ligand. B) boron dipyrromethene core. C) boronaminotroponimine core (this work)	192
Figure 3B.2	ORTEP diagrams of boron complex (3a, 3b, 3c, and 3g) with 50% probability of ellipsoids.	195
Figure 3B.3	(A) Absorption and (B) Emission spectra of boron-aminotropone complexes (**3a-h**) in methanol at $5x10^{-4}$M concentration	198
Figure 3B.4	**3** (A) Absorption and (B) Emission spectra of boron-aminotropone complexes (**3a-h**) in Acetonitrile at $5x10^{-4}$M concentration	198
Figure 3B.5	(A) Absorption and Emission spectra of boron-aminotropone complexes (**3a**) in methanol at concentration ($5x10^{-4}$M). (B) Quantum yield bar diagram	199

of boron-aminotropone complexes (**3a**-**3h**) in methanol

Figure 3B.6 FE-SEM images of **3f** 2μm, 10μm, 20μm 200

Figure 3B.7 FE-SEM images of **3g** 2μm, 10μm, 20μm

Figure 3B.8 FE-SEM images of **3h** 2μm, 10μm, 20μm 200

Figure 3B.9 Confocal images **3f/3g** of 3 μm, 4μm, 10μm 201

Figure 4.1 Chemical structure of troponyl derivatives 250

Figure 4.2 **2** ORTEP diagram of cyclohetapyrazine derivatives: A. Compound 2; B. Compound 6a; C. Compound 6d; D. Compound 6k; and E. C-C bond length comparison of troponyl ring ester and dihydrapyrazine 255

Figure 4.3 Plausible mechanism for synthesis of dihydropyrazine derivatives 257

Figure 4.4 UV-Vis and Fluorescence spectra of ct-DNA under different concentration of *Troponyl dihydraopyrazine* derivatives (**6a/6e/6j/6n)** with EtBr and Hoechst dyes 258

Figure 4.5 UV-Vis and Fluorescence spectra of EtBr under different concentration of with ct-DNA. 259

Figure 4.6 UV-Vis and Fluorescence spectra of ct-DNA under different concentration of *Troponyl dihydraopyrazine* derivatives (**6a/6e/6j/6n)** with EtBr and Hoechst dyes 260

Figure 4.7 CD-spectra *Troponyl dihydraopyrazine* derivatives **6a/6e/6j/6n** under different concentration of DNA at pH 7.0 (Room temperature) 261

Figure 4.8 MTT asaay profile f compound **6a** 262

Figure 5.1 **(a)***Troponylated*-BODIPY deoxyuridine phosphorsmidite, **(b)** *Troponylated*-BODIPY deoxyuridine Triphosphate **(c)** *Troponylated*-uridine Phoshpramidite. 325

LIST OF SCHEMES

Scheme 2.1 Synthesis of N-Troponylated dipeptides 41

Scheme 2.2 Synthesis of *N*-Troponylated tri-peptides and control peptides 55

Scheme 3A.1 Synthesis of difluoroboron-aminotropone complex 120
Scheme 3B.1 Synthesis of boron-aminotroponimine complexes 194

Scheme 4.1 Syntheses of aryl substituted troponyl dihydropyrazine compounds 253

Scheme 5.1 Synthesis of Trpoponylated BODIPY thymidine phoshporamdities **dU^{TrBO}** and Triphosphate **dU^{TrBOD}TP** 326

Scheme 5.2 Synthesis of *Trpoponylated* uridine phosphoramidite 328

List of Tables

Table 2.1 Torsional angles of the amide backbone φ, ψ, Ω and χ 50

Table 3A.1 Photophysical parameters of Boron-aminotropone complexes 129

Table. 3B. 1 Selected bond lengths and bond angles of Boron complexes **3a, 3b,3c and 3g** in solid state 195

Table. 3B. 2 Photophysical parameters of Boron-aminotropone complexes 197

CHAPTER-1

CHAPTER 1. Introduction of Modified Amino acid, Peptide and Nucleic acid Analogues

1.1 Introduction 2

1.2 Conclusion and objective of the present thesis 22

1.3 References 26

CHAPTER-2

CHAPTER 2. Synthesis and Conformational Analysis of *N*-Troponylated *di-/tri*-Peptides

2.1 Introduction 38

2.2 Objective of our work 40

2.3 Result and discussion 40

2.4 Conclusion 58

2.5 Experimental Section 59

2.6 References and Notes 69

2.7 Appendix 74

CHAPTER-3

CHAPTER 3A. Synthesis and Photophysical Studies of Functionalized *Troponyl*-BODIPY Analogues

3A.1 Introduction 116

3A.2 Objective of our work 118

3A.3 Result and discussion 119

3A.4 Conclusion 132

3A.5 Experimental Section 132

3A.6 Reference and Notes 142

3A.7 Appendix 148

CHAPTER 3B. BODIPY Analogues: Synthesis and Photophysical Study of BODIPY Analogue from *Troponylalkyl Chain* via *N, O*-Chelation

3B.1 Introduction 190

3B.2 Objective of our work 192

3B.3 Result and discussion 293

3B.4 Conclusion 202

3B.5 Experimental Section 202

3B.6 Reference and Notes 209

3B.7 Appendix 215

CHAPTER-4

CHAPTER 4. Synthesis and Biochemical Evaluation of *Troponyl* dihydropyrazine Molecules as DNA Binding Agents

4.1 Introduction 249

4.2 Objective of our work 250

4.3 Result and discussion 251

4.4 Conclusion 262

4..5 Experimental Section 263

4.6 Reference and Notes 273

4. 7 Appendix 277

CHAPTER-5

CHAPTER 5. Synthesis of *Troponylated*-Uridinyl Nucleoside Analogues

5.1 Introduction 324

5.2 Objective of our work 325

5.3 Result and discussion 325

5.4 Conclusion 330

5.5 Experimental Section 330

5.6 References and Notes 341

5.7 Appendix 345

6. Thesis Summary 378

List of abbreviations

A	Adenine
Å	Angstrom
Aa/AA	Amino acid
Ac	Acetyl
aq.	Aqueous
Bn	Benzyl
Boc	Tert-butyloxycarbonyl
BODIPY	boron-dipyrromethane
Bnaeg	Benzylaminoethyl glycine
br	Broad
C	Cytosine
CAT	Cyclic-2-aminotropoimine
°C	Degrees Celsius
CCDC	Cambridge Crystallographic Data Centre
CSD	Cambridge Structural Database
CD	Circular Dichroism
COSY	Correlation Spectroscopy
Cys	Cysteine
d	Doublet
DNA	Deoxy ribose nucleic acid

DMF	N,N-dimethylformamide
DCM	Dichloromethane
DMSO	Dimethyl sulfoxide
DIPEA	Diisopropylethylamine
EDC.HCl hydrochloride	N-(3-Dimethylaminopropyl)-N′-ethylcarbodiimide
equiv.	Equivalent
ESI-MS	Electrospray ionization Mass Spectrometry
Et	Ethyl
EtOAc	Ethylacetate
FDA	Food and Drug Administration
G	Guanine
g	Gram(s)
h	Hour(s)
HCL	Hydrochloric acid
Hf	Hafnium
HIV	Human Immunodeficiency Virus
HOMO	Highest Occupied Molecular Orbital
HRMS	High Resolution Mass Spectrometry
Hx	Hexyl
Hxhpn	N- Hexyl Hydrazine Propyl
Hz	Hertz
IR	Infrared (spectroscopy)
J	Coupling constant

K	Kelvin
λ	Wavelength
L	Liter
LiOH	Lithium Hydroxide
LUMO	Lowest unoccupied Molecular Orbital
Lys	Lysine
m	Multiplet or milli
m/z	Mass to charge ratio
μ	Micro
Me	Methyl
MeOH	Methanol
mg	Milli gram
MHz	Megahertz
min	Minute(s)
mol	Mole(s)
mL	Milli litre
μL	Micro litre
mp	Melting point
NMR	Nuclear Magnetic Resonance
NOE	Nuclear Overhauser Efect
NOESY	Nuclear Overhauser Enhancement Spectroscopy
nm	Nanometers
NTP	Nucleoside Tri-phosphate
ORTEP	Oak Ridge Thermal Ellipsoid Plot Program

p	Para
Ph	Phenyl
Phe	Phenyl alanine
pH	Hydrogen ion concentration in aqueous solution
ppm	Parts per million
Prop	Propyl
q	Quartet
rt	Room temperature
s	Singlet
t	Triplet
T	Thymine
TFA	Trifluoroacetic acid
THF	Tetrahydrofuran
Thr	Threonine
TLC	Thin layer chromatography
Trp	Tryptophan
Ts	p-toluenesulfonyl (tosyl)
Trag	*N*-Tropolonylaminoalkylglycinate
Traeg	Troponyl aminoethylglycine
UV	Ultraviolet

CHAPTER-1

Introduction of Modified Amino acid, Peptide and Nucleic acid Analogues

1.1 Introduction

1.2 Conclusion and objective of the present thesis

1.3 References

Chapter 1. Introduction of Modified Amino acids Peptide, and Nucleic acid Analogues

1.1 Introduction

This thesis comprises about the synthesis and structural analysis of two biomacromolecules' building blocks. Herein we provide their literature reports into two sections- (a) Amino acid Peptide Chemistry; (b) Nucleic acid Chemistry.

Section-A

The first part of my thesis is related to aminoacid peptide. Protein and peptides are bio-macromolecules derived from α-amino acids through amide bonds. These molecules form characteristic secondary structures such as β-sheets/turn and α-helixes, which provide unique biological functions.[1-3] The short peptides have been synthesized chemically from natural and synthetic amino acids. For example, Emil Fischer had synthesized the first dipeptide glycylgycine in 1901.[4]. This was considered the beginning of peptide chemistry. In 1953, du Vigneaud had synthesized the first polypeptide, Oxytocin (**Figure 1.1**).[5] The classical synthesis of polypeptides are tedious with overall low yields. In 1963, Bruce Merrifield accelerated and automated the synthesis of polypeptides by using solid support peptide synthesis (SSPS) method.[6]

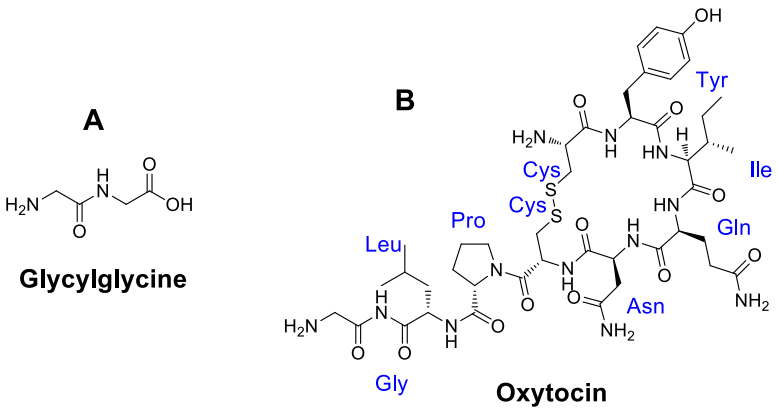

Figure 1.1. First synthetic peptides: dipeptide (A); polypeptide (B).

This method is simple, rapid, and effective for the preparation of peptides, which remarkably sparked the progress of peptides-based molecular biology and pharmacology.

Peptidomimetics

The natural short peptides have some structural and functional limitations to directly employ as a therapeutic candidate, such as poor aqueous solubility, serum stability and target specificity. Thus, the synthesis of structurally modified amino acids and their peptides have started to mimic the structure and function of naturally occurring peptides. These modified peptide are called as peptidomimetics.[7] On the basis of structures and functions, peptidomimetics are generally classified into three categories.[8]:

- Type-I (Structural mimetics)- Generally show an analogy of a local tropology with the amide bond, and responsible for the interaction with enzymes or receptors in the well-defined spatial orientation.
- Type-II (Functional mimetics)- is a small molecule based on the interaction with the receptor or enzyme in distinct three-dimensional orientation.
- Type-III (Functional and structural mimetics) type-III peptidomimetics are generally represented as possessing as a scaffold with a structure different from that of the substate: all actions required or biological interaction. Many of the reported unnatural amino acids substitute the peptide functional groups carry the biological activities.

The examples of peptidomimetics scaffold is given by a thyrotropin-releasing hormone (TRH) mimetics based on the cyclohexane scaffold **1** (**Figure 1.2**).[9] other example of peptidomimetics is the replacement of peptidic fragment in somatostatin receptor binding with cyclopeptide in a D-glucose scaffold **2 .**[10] The third one is RGDFV cyclopeptide which is steroidal scaffold **3** and contains the type-II β-turn structure.[11]

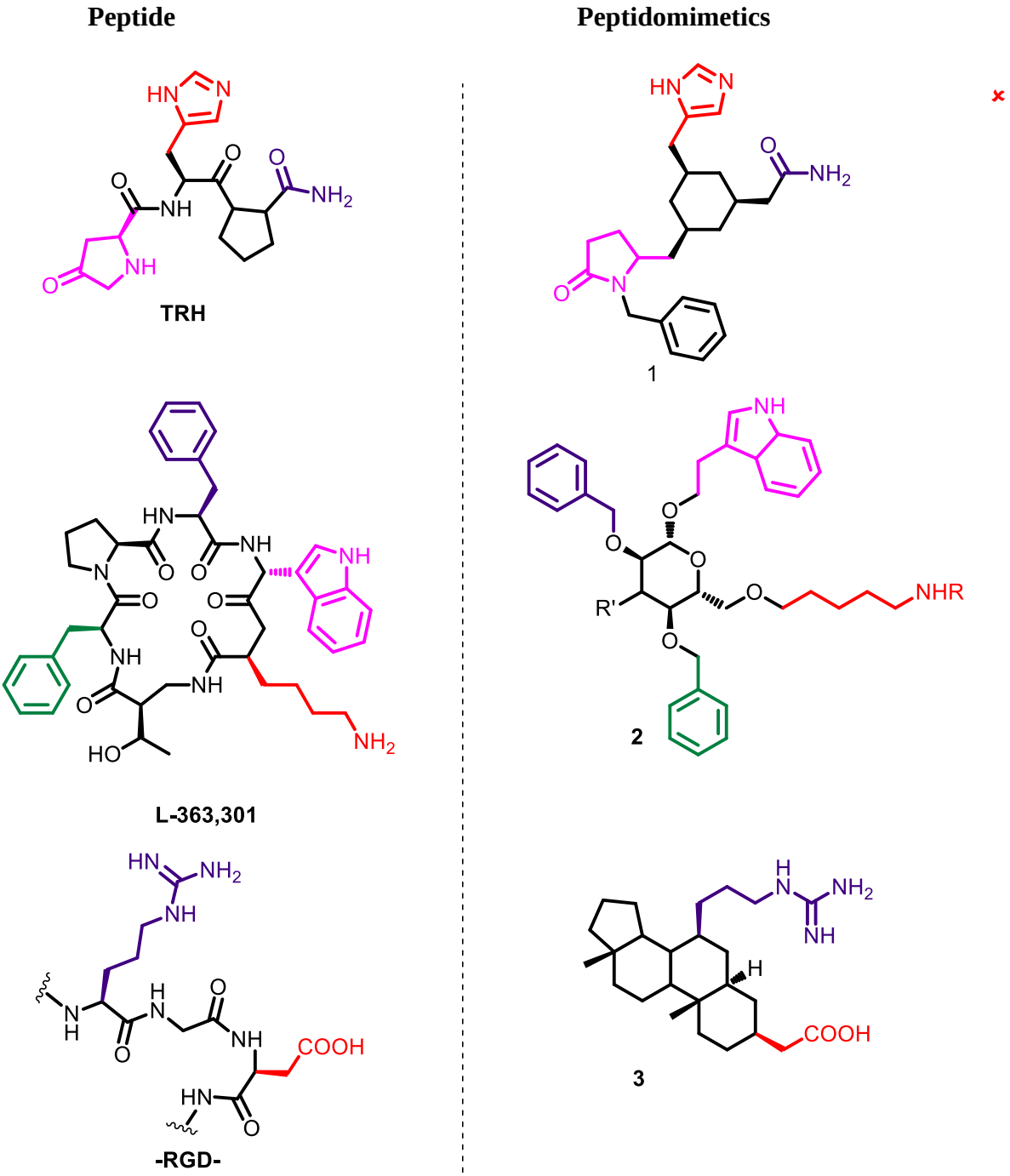

Figure 1.2. Advantages of peptidomimetics over peptides.

Synthetic approach towards peptide in the laboratory

In peptide syntheses, study their secondary structure and biological properties is an important task. Now synthesis of peptides are well-established in both solution and solid phase.[12-17] Generally the solution phase method of polypeptide syntheses gives low yield as compared to the solid phase method. Howover, solution phase peptides syntheses are economical for the large quantity synthese. In the solution phase peptide syntheses, the partial protected amino acids such as PG-NH-AA-COOH and NH_2-AA-COOPG are coupled throuh amide bond by using coupling reagent (DIPCDI, DCC, EDC.HCL, Di-p-TCDI), and carboxylate activators. (HOAT, HOBT, HOTM, Oxyma) under anhydrous conditions (**Figure 1.3**).

A) General representation of solution phase peptide syntheses:

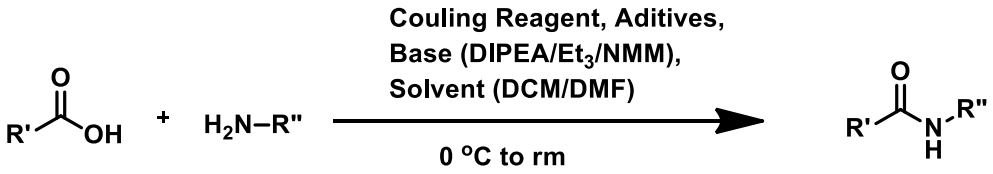

B) Widley using carbodiimide coupling reagents and additives:

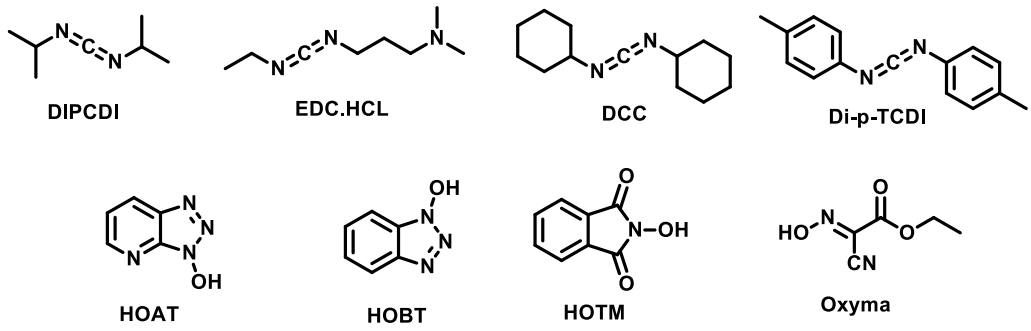

C) Mechanism of carbodiimide mediated solution-phase peptide syntheses:

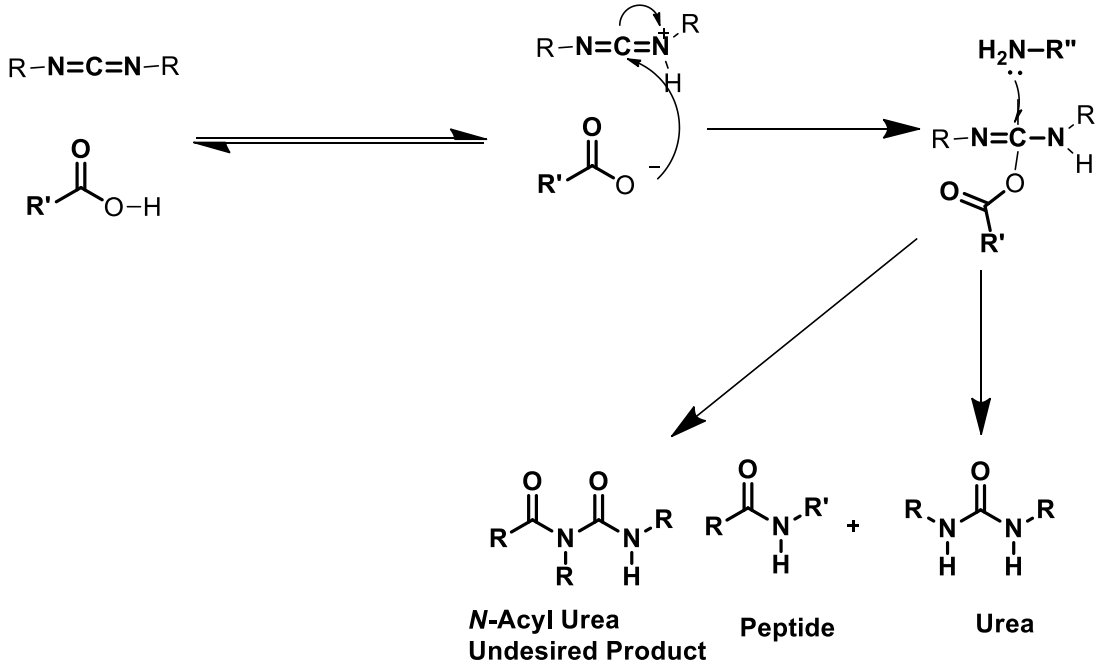

Figure 1.3. A) general representation of solution-phase peptide syntheses, B) Coupling reagents and additives C) Mechanism of carbodiimide mediated solution-phase peptide syntheses.

In the solid-phase peptide synthesis (SPPS), first amino acid residue is tethered to insoluble polymeric resin via a linker. The growing peptide chain is attached to a solid support, and unreacted starting materials and reagents are washed out. After completion of the syntheses' desired peptide sequence, the peptide chain has to be cleaved from the solid support and purified by preparative HPLC. The principle of solid-phase peptide synthesis is represented in **Figure 1.4**.

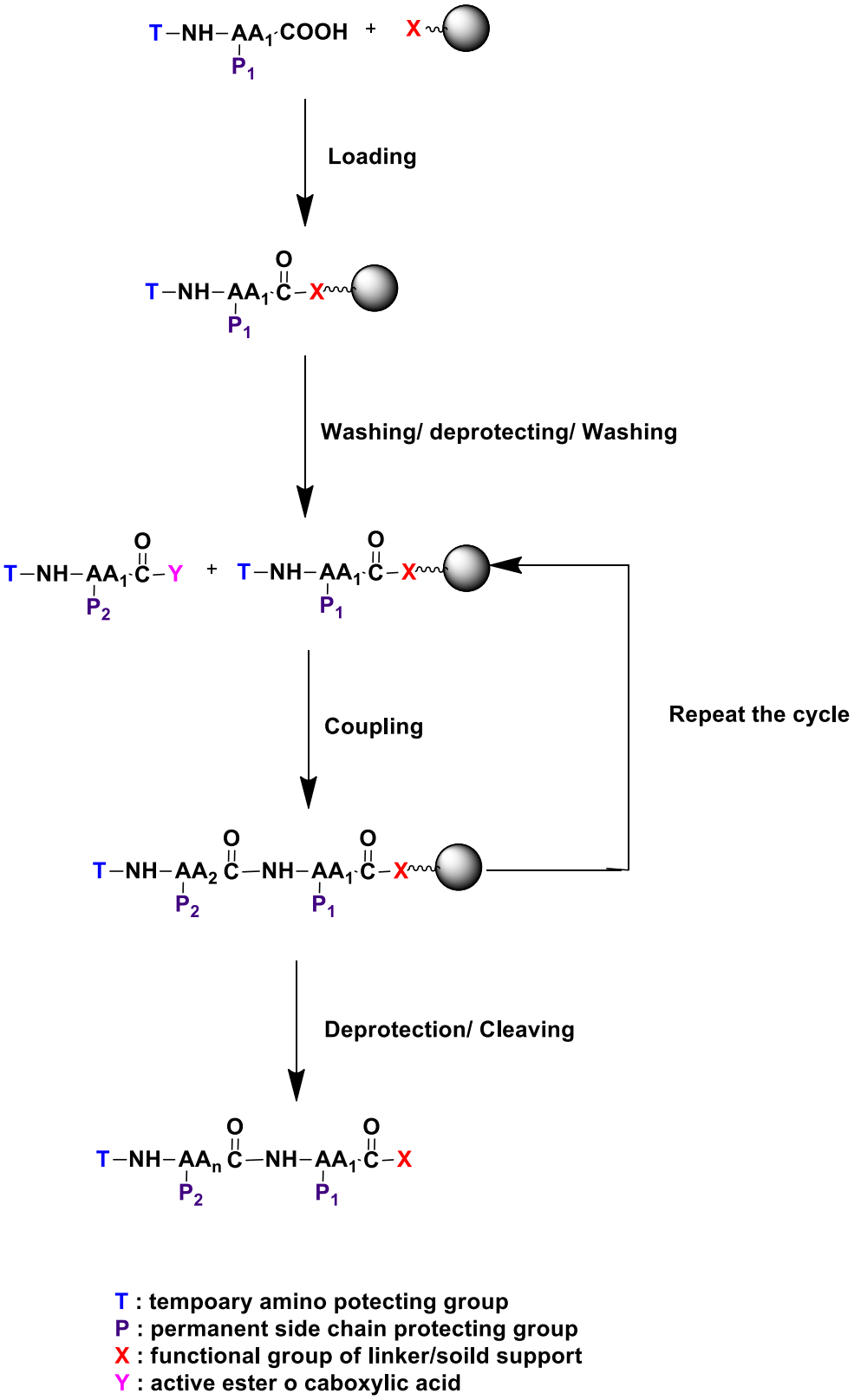

Figure 1.4. General representation of solid-phase peptide syntheses

Synthetic polypeptides and their structural analysis

Proteins and peptides are the ubiquitous structural and functional macromolecules that occur in the living system. Proteins/peptides perform several physiological and biological functions in the live system, such as enzymes, hormones, etc. The natural protein peptides are constructed from 20 proteomic amino acid residues connected through amide bond linkages.[1, 18] Protein-Protein interactions (PPIs) are involved in numerous biological process which plays a vital role in the various pathological conditions. [19] peptide and protein form secondary structures such as beta-sheet, beta-turn, alfa-helix, which play a vital role in their biochemical activities. Peptide and protein secondary structures are well defined through side-chain amino acid residues.[20] the driving force of structural organization of peptide/protein depends upon the amino acid residue and hydrogen bonding interactions between NH and CO functional group of the peptide backbone. Most importantly, the specific amino acid sequence is responsible for three-dimensional structural organizations.[21, 22] synthetic peptides with natural amino acids were extensively studied to understand the structural aspects and function of natural protein/peptides. And learned that the synthetic peptide are the potential to mimic the function of naturally occurring protiens/peptides.

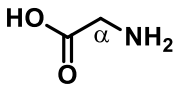

General Structure of α–amino acid

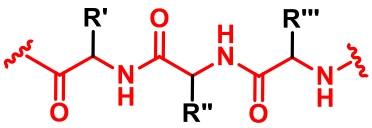

Peptide bacbone

Hamilton has first proposed α-helix mimetics that contain molecular templates as terphenyl and terpyridyl moieties **(Figure 1.5).**[23]-[24] these peptides give the *i*+3 and *i*+7 hydrogen bonded secondary structures. Subsequently, Boger has described 3-alkoxy-4-benzoic acid-based oligoamines that contains aromatic building block.[25]

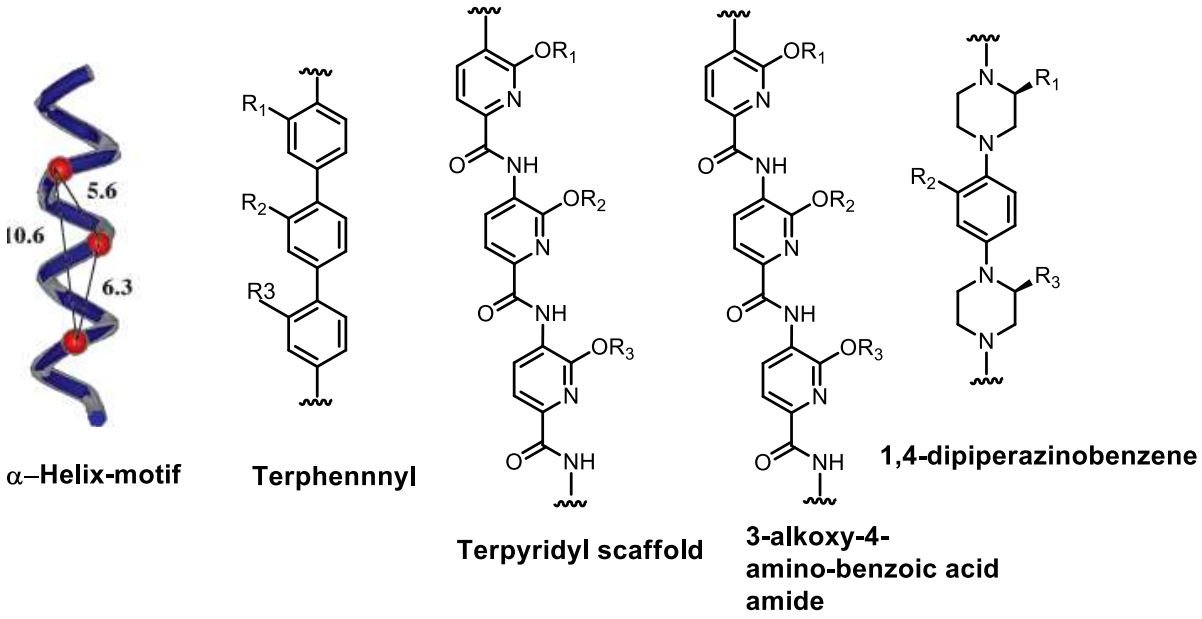

Figure 1.5. Examples of different peptide to α-helix mimetics

Gellman and co-worker proposed a novel γ-amino acid (1*R*,2*R*,3*S*)-2-(1-aminopropyl)-cyclohexanecarboxylic acid (APCH) residue which contains a six-member ring around its C*α*-C*β* bond (**Figure 1.6**). They studied the secondary structure of these peptides through NMR-spectrometry and crystallography. These APCH peptides intensely observed that it was the α/γ peptides which peptide contains 12/10-helical secondary structure.[26]

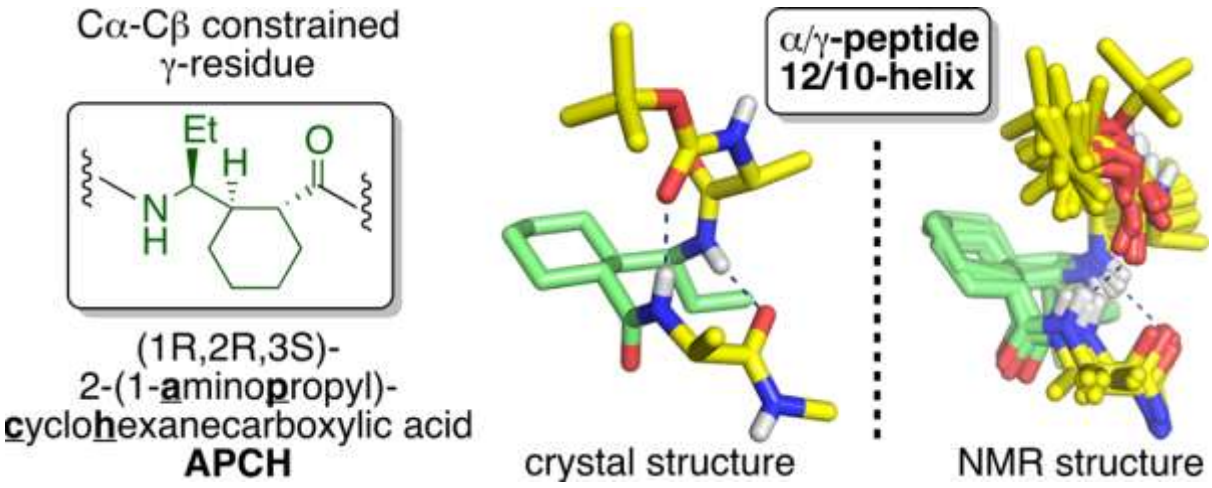

Figure 1.6. Crystal and NMR analyzed α/γ APCH peptides

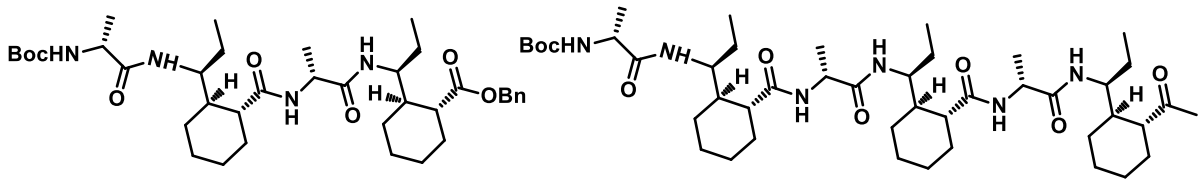

Figure 1.7. α/γ containing APCH peptides stuctures

Degradoe has reported a poly L-Alanine peptide forms α- helical secondary structure in solid-state (F**igure 1.8A)** with 3.6 residues per turn, i+4 to i hydrogen bonding.[27] Seebach has reported β-alanine polypeptides also shows alfa-helical 14-helix proposed (F**igure 1.8B**).[13]

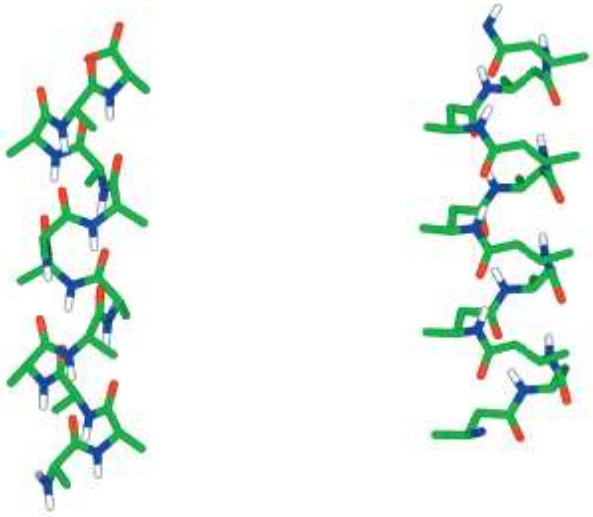

α-helix Poly L-Alanine **14-helix Poly *β*-Alanine**

Figure 1.8. Crystal structure of α-helix A) α-helix with Poly L-Alanine, B) 14-helix Poly *β*-Alanine.

The **β**-sheet/turn is another regular secondary structure of protein and peptides. The **β**-sheet consists of **β**-strands connected through two or three hydrogen bonds and that lead to the more organised tertiary structures *via* side-chain hydrophobic interaction.[28] for example, a

octapeptide (Leu-Phe-Val-DPro-LPro-Leu-Phe-Val) shows a *β*-hairpin type secondary structure in solution (**Figure 1.9**).[29] Another *α,β*-unsaturated-γ^4-alkyl-substituted *E*-vinylogous *γ*-amino acid containing tetrapeptides shows the *β*-sheet type secondary structure.[30] Many more synyhetic peptides are synthesized and explored their structural properties. Over all the synthetic peptides are potential mimics of biomolecules for the development of peptide based therapeutic drugs.[13, 15-17, 31-33]

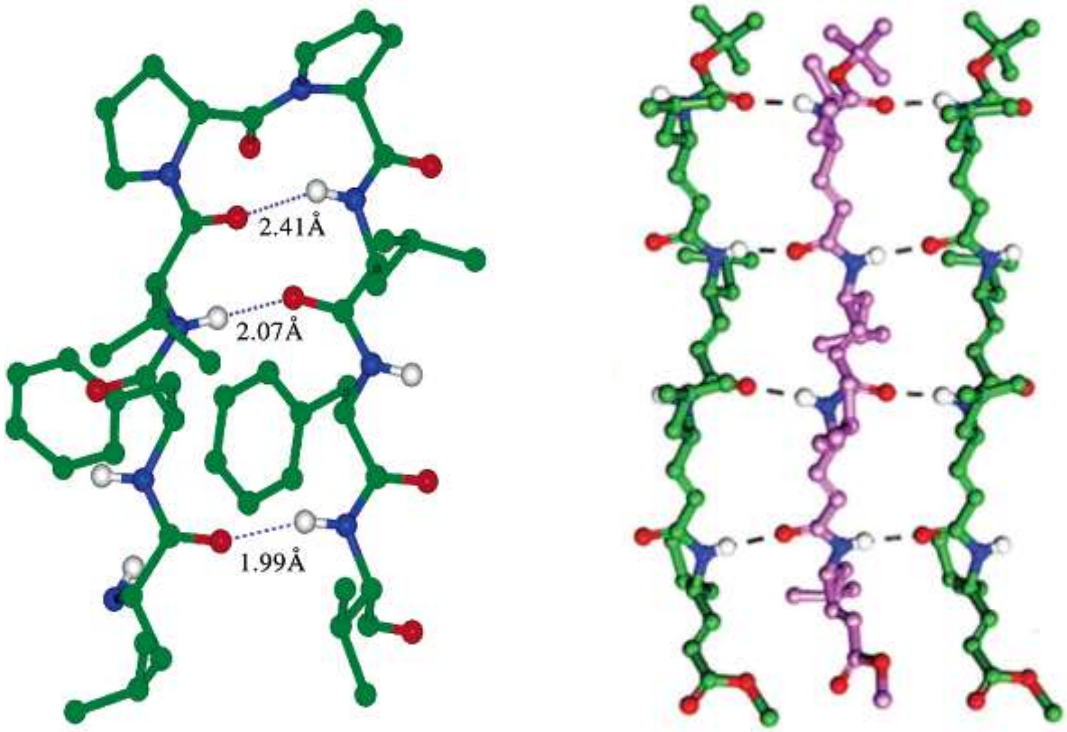

Figure 1.9. Secondary structures of natural, synthetic peptides A) *β*- hairpin in solution state B) Antiparallel β-sheet in single-crystal structures**.**

In addition, peptides are natural ligand of coordinating metals which produce various type of peptide-metal complexes. These complexes exhibit unique metal induced secondary structures.[34 35, 36] Gopi and co-workers have reported the synthesis and conformational studies

of *α, γ*-hybrid tripeptides (**Figure 1.10**).[37] These hybrid tripeptides fold into the helix even in the presence of two typical *β*-sheet favouring amino acid like Val and Leu residues. These hybrid tripeptides contain pyridine moiety at the peptide terminals which coordinates with metal ions (Ag^{+}, and Cu^{+}) and assemble into the polymerized helical structure.

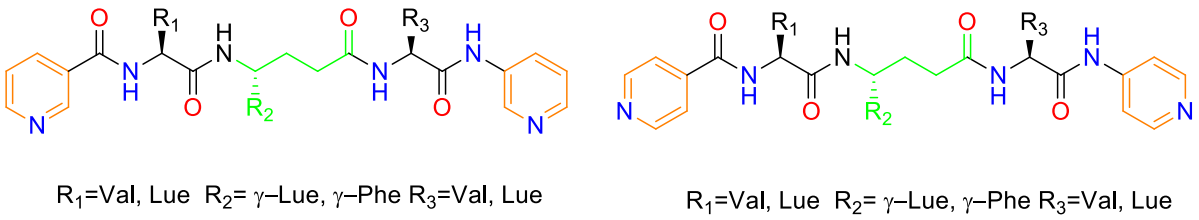

Figure 1.10. Synthesis of short α, γ-hybrid tripeptide

Another class of synthetic peptides are pseudopeptides which contain two native peptides through diamine/dicarboxylate linkers.[38, 39] Recently our groups has reported the synthesis and structural studies of novel pseudo peptide ethylenediprolyl of *tetra* and *hexa* peptides (**Figure 1.11).**[40] These pseduopeptides adopt *β*-turn type structures in organic solvents (ACN/MeOH). The X-ray structure of representative *tetra*-peptide crystal reveals the formation of a unique self-assembly structures as *β*-strand type in the solid-state. These pseduopeptides form cupper complex with Cu (ll) ions through its diamine functionality.

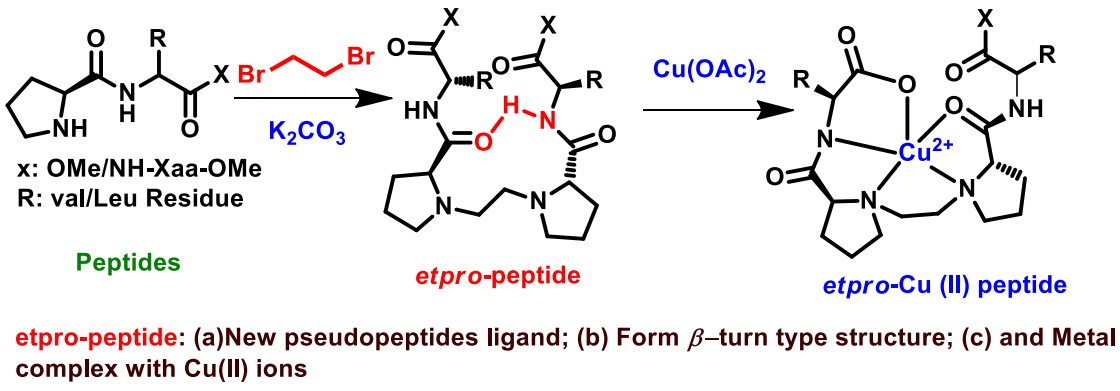

Figure 1.11. Synthesis of novel tetra and hexa pseudo peptides

Section-B

Second part of my thesis is releted to the structrually modified nucleoside analogues. Thus this section describes the summary of various nucleoside analogues. Nucleosides are constituents of nucleic acids, Deoxyribonucleic Acid (DNA)/Ribonucleic Acid (RNA) that store or transfer the genetic informations of living systems.[41, 42] The structure of native DNA is double helix, formed by two single DNA strands through hydrogen bonding between their nucleobases (**Figure 1.12).**[43, 44] There are four Nucleobases in native DNA structure such as adenine (A), cytosine (C), guanine (G) and thymine (T).[45]

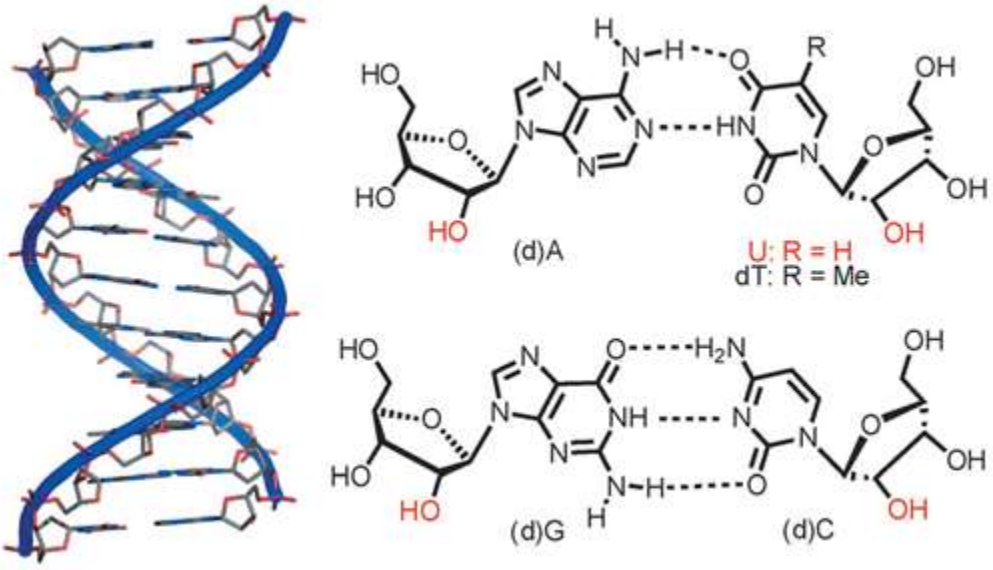

Figure 1.12. Structure of DNA duplex

Nucleoside Analogues

The chemical structure of nucleosides contains five-member sugar ring (ribose/deoxyribose) and nitrogenous nucleobases (pyrimidines/purines). Pyrimidine has six-member aromatic heterocyclic structure. while purine has fused (five-six membered) aromatic heterobicyclic structure. There are two types of pyrimidine nucleobases (thymine and cytosine) and two types

of purine nucleobases (adenine and guanine). In nucleosides, the N1-atom of pyrimidine is attached to the C1 of sugar ring whereas the N9-atom of purine is attached to the C1 of the sugar ring through the glycosidic bond (**Figure 1.13**).

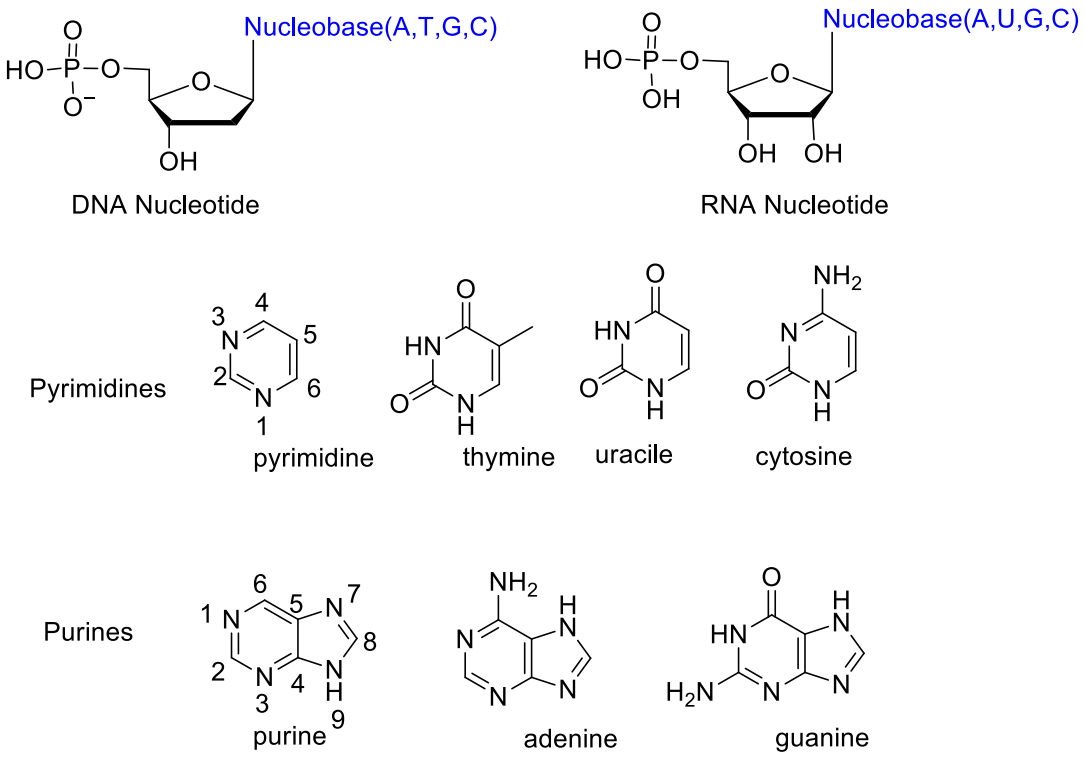

Figure 1.13. Nucleotide structure of DNA and RNA

Modified Nucleosides (DNA/RNA)

In the recent past, various structurally modified nucleosides are synthesized to explore the novel structures and functions of DNA. A group of chromophores and flurophores have been conjuated at the nuclobase of nucleosides to pepare the fluroscent-lebelled nucleic acid analogues [44, 46-49]. The fluroscent lebelled nucleic acids are in demand to study the DAN dependent chemical events in the cellular envionment at the real time.[50] These modified nucleoside analogues are being incorported into DNA/RNA to prepaed the lebelled and rective

nucleic acid analogues.[51] The incorporation of modified nucelosides are generally acomplist by to ways- a) chemically from resective nucleoside phosporamidite and b) enigametically from respective nucleoside triphosphate (NTP).[52] Herein, a few nucleobase modified DNA/RNA analogues are described. Various functional group such as aryl, heteroyl, chromophore or flurophore are attached by cross coupling reaction at nucleosides containing *halo*-functionalized nucleobses (**Figure 1.14**). These functionalized nucleosides are being used by palladium catalysed cross couplig reaction throuh Organostannanes,[53-55] organo boranes,[56-58] alkynes,[59-62] alkenes.[63, 64]

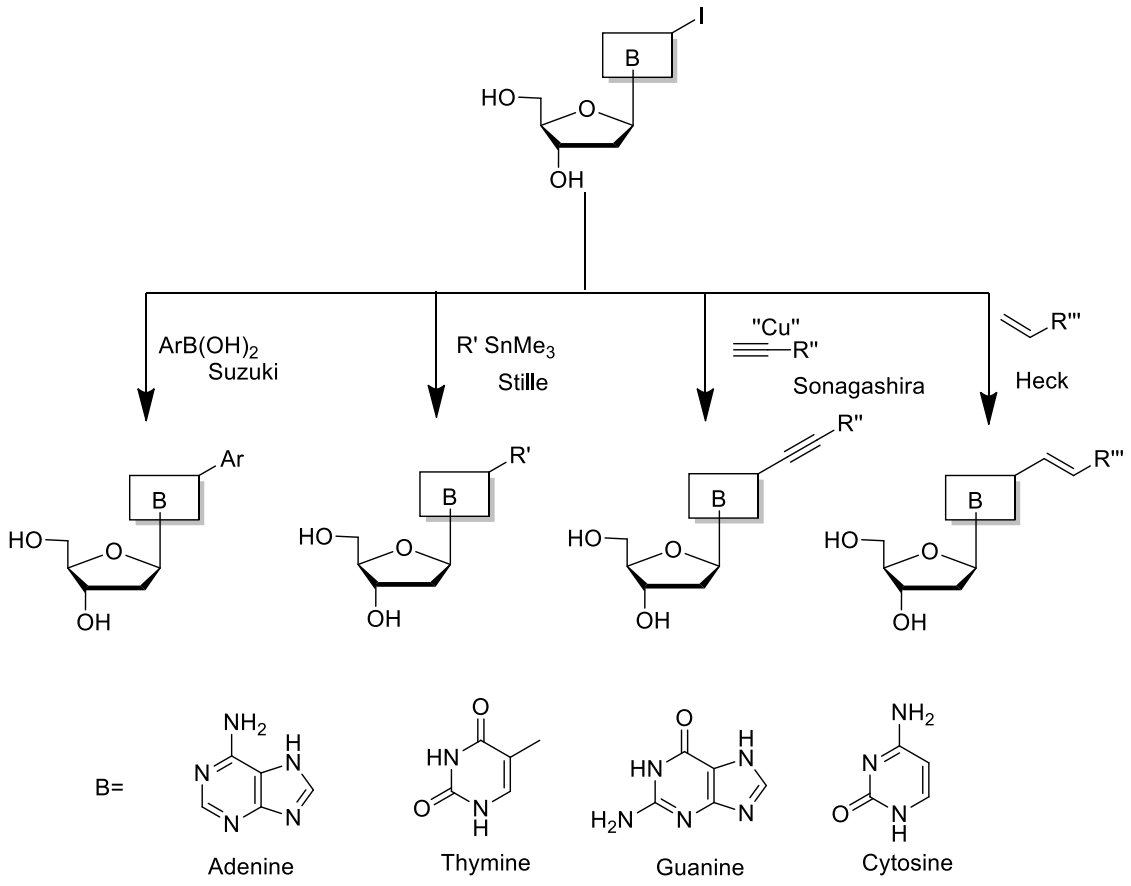

Figure 1.14. Chemically modified nucleobase analogues

Fluroscence nucleosides. Non-fluroscence native DNA and RNA can be converted into the the fluroscence by indroducing the modified fluroscent nucelosides.[51] The conujation of flurophore or chromophore at the nucelobase of nucleosides are the most common methods for the

synthesis of fluroscence nucelosides,[65-68] for example BODIPY and Benzofuran containing deoxyuridine analogues. Wagenknecht and co-workers reported the incorporation of 4,4-difluoro-4-bora-3a,4a-diaza-s-indacene (BODIPY) dye-modified uridine, BodU, and non-nucleosidic DNA base surrogate containing Bo into DNA using standard automated phosphoramidite chemistry **(Figure 1.15).**[69] The BodU modified DNA hybridize with complementry with DNA strands and form duplexes which quench the fluorescence. However the Bo analogue exhibts strong fluroscence after duplex formtion but non preferential base pairing with adenine.

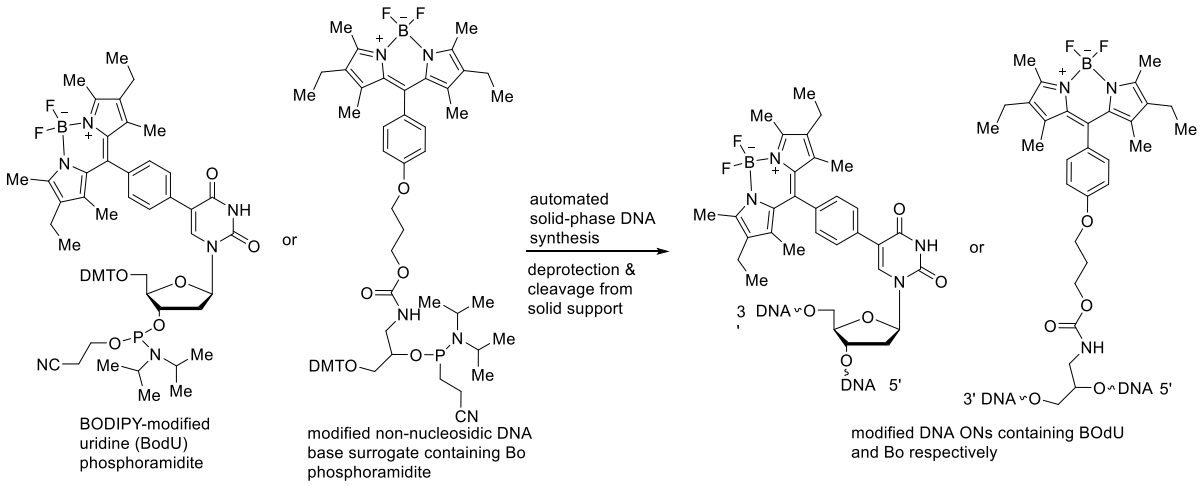

Figure 1.14. Incorporation of BodU and modified non-nucleosidic DNA base having Bo into DNA using automated phosphoramidite chemistry.

Srivatsan and co-workers have reported the benzofuran containing deoxyuridine analogues at C5-position of uridine (**Figure 1.16**).[70] This analogue exhibit microenvinroment-sensetive fluorescence properties. Its phosphoramiditie has been incorporated into DNA oligonucleotides which form a duplex with complementary RNA. This DNA-RNA duplex exhibits strong emissive properties as compare to the modified nucleoside.

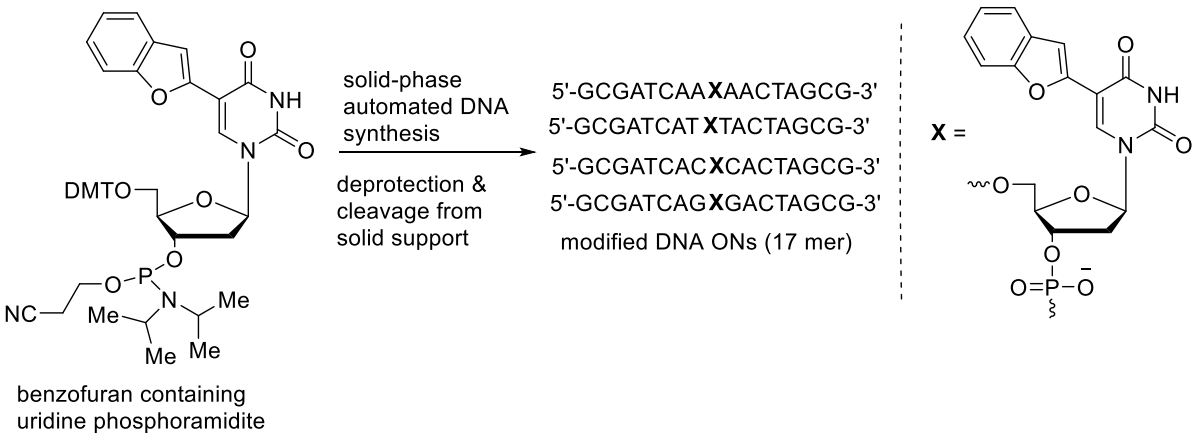

Figure 1.16. Synthesis of fluorescently modified DNA oligonucleotides

Barrois and coorkers have reported this synthesis of *diarylethene*-deoxyuridine nucleoside analogues *via* Sonogashira-type cross-coupling reaction and then phosphoramidite (**Figure 1.17**). Its DNA exhibits photoswitching behaviour at the modified uridine nucleosides. [71]

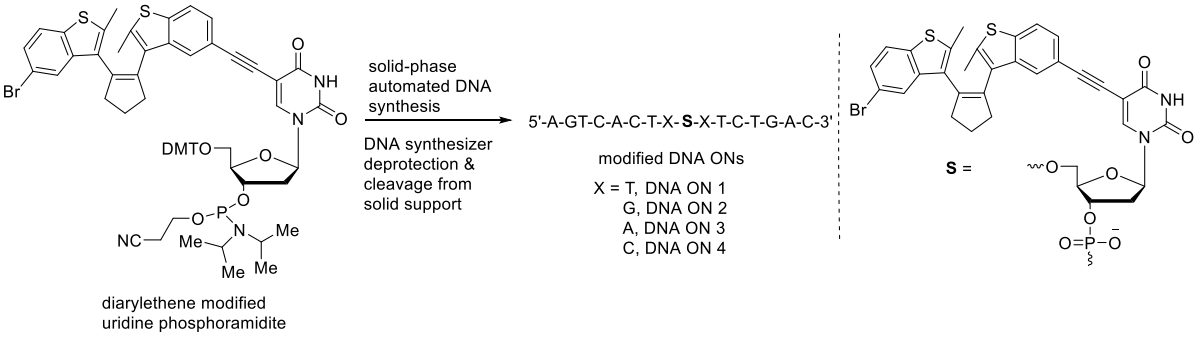

Figure 1.17. Synthesis of diarylethene-modified DNA Olionucleotides

Manderville and co-workers have reoported the synthesis of 5′-O-2,7-dimethylpixyl (DMPx) containing 8-aryl-deoxyguanosine analogues followed by a series of 8-aryl-dG phosphoramidite derivatives containing 8-substituents such as furyl (^{Fur}dG), phenyl (^{Ph}dG), 4-cyanophenyl (^{CNPh}dG), and quinolyl (^{Q}dG). These phosphoramidites have been incorporated into DNA oligonucleotides (**Figure 1.18**).[71] Outcome of this study reveals that 5′-O-DMPx group is superior (4-fold) in yield for the incorporation of ^{Fur}dG into DNA as compared to 5′-

O-DMT. Moreover, these adducts also exhibit strong fluorescent properties, which allow them to use as fluorescent nucleobase probes.

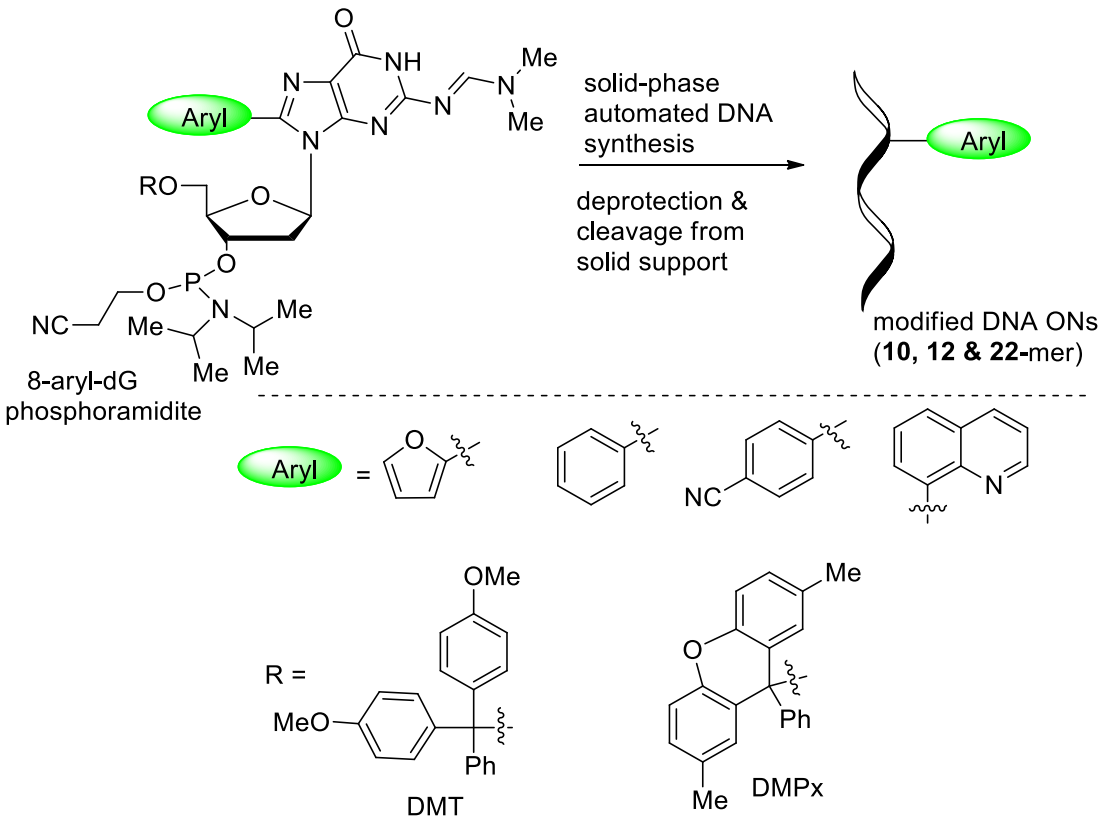

Figure 1.18. Synthesis of modified DNA ONs from 8-aryl-dG phosphoramidite derivatives using different protecting groups.

Wagenknecht and co-workers have reported a synthesis of new modified DNA building block, which contains diaryltetrazole unit, attached to the 5-position of 2'- deoxyuridine through an aminopropynyl linker. These phosphoramidite have been incorporated into DNA oligonucleotides (**Figure 1.19**).[72] The modified DNA hybridize with its complementary DNA strands and form a duplexes. The tetrazole group of DNA oligonucleotide have been utilized for the chemically post-synthetic functionalization with commercially available sulfo-Cy3 dye by using photoclick cycloaddition reaction.

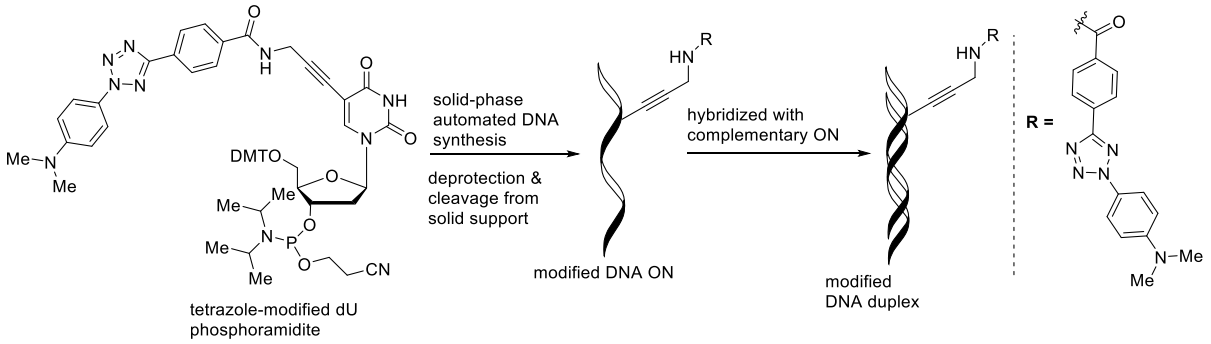

Figure 1.19. Synthesis of tetrazole-modified DNA ON by automated phosphoramidite chemistry

Kath-Schorr and co-workers have reported a novel synthesis of norbornene-modified uridine phosphoramidite. These base modified norbornane phosphoramidite have been incorporated into RNA oligonucleotide at different position of RNA within the required sequences (**Figure 1.20**).[73] further, they have been utilized these modified RNA oligonucleotides for Diels-Alder cycloaddition of norbornene moiety with tetrazines to attach small fluorophore molecules at specific positions within RNA sequences both in vitro and in mammalian cells.

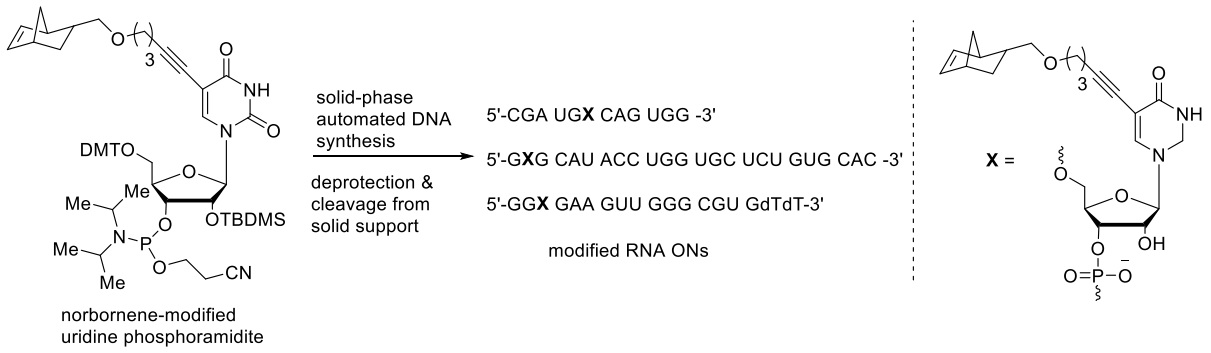

Scheme 1.20. Solid phase incorporation of norbornene-modified uridine phosphoramidite into RNA ONs.

Structure and general properties of Tropolone

Tropolone is non-benzenoid aromatic molecule which presents in nature as bioactive molecules.[74, 75] For examples Cholchicine, Stiptatic acid, α-/β-/γ-Thujaplicine, Pycnidione, Manicol (**Figure 1.21**). Tropolone and its related derivatives are found in nature as tropolonoids. Tropolone and related derivatives possess various biological activities such as antibacterial,[76] antifungal,[77] antitumor,[78] and antiviral,[79] agents. Tropolone, unlike benzene, tropolone is chemically functionalized aromatic compounds with conjugated carbonyl and α-hydroxyl groups in cyclohexatriene ring system which has ability to form stable metal complexes. Tropolone and its derivatives are excellent ligands for transition metals (Cu, Zn, Ni) and form stable tropolone-Metal complexes. The chelating characters of tropolone are further improved by its amino/imino derivatives. Tropocoronand, macrocycle ligands are synthesized and *via* by

hydroen bonding.

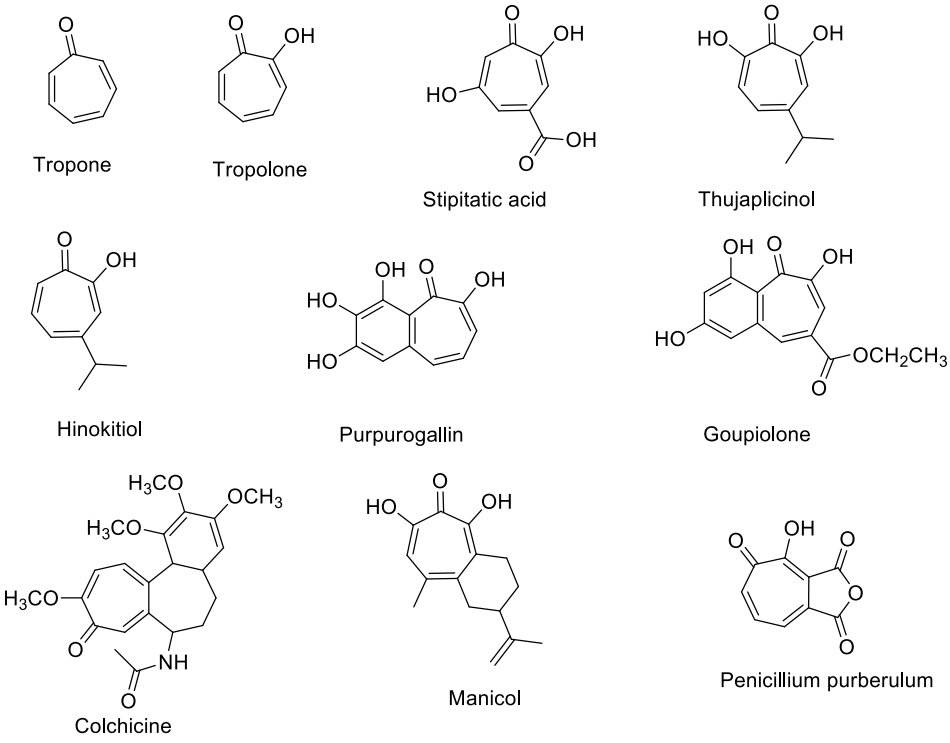

Figure 1.21 Chemical structue of tropolonoid natural products

Our group have explored the troponyl moiety into amino acids/peptides as *Traeg*-amino acid/peptides for tuning their secondary structures, and established the role of troponyl carbonyl group of *Traeg* containing peptides in hydrogen bonding with adjacent amide N-H as C=O-----H-N (**Figure 1.22)**. [80]

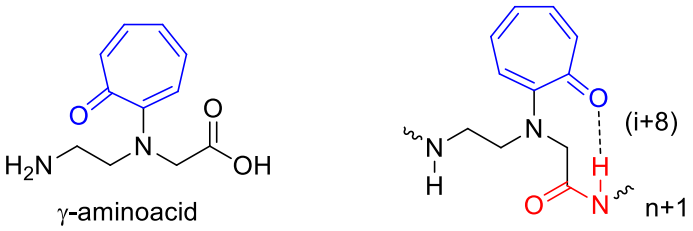

Figure 1.22 Chemical structure (a) *Traeg* peptide, (b) hydroen bonding in *Traeg* peptide

However, the synthesis of *Traeg*-homologous peptides have become difficult due to the instability of amide bond under mild acidic conditions.[81, 82] The role of troponyl residue has serious implications in cleavage of amide bond (**Figure 1.23**). Further direct amidation and reversible amidation are also established with *Trag* amino acids under acidic conditions. Importantly amide bonds of only *di*-alkylated 2-aminotropone derivatives as *Treg/trag* peptides are cleavable under basic conditions. Interestingly, the amide bond of *mono*-alylated 2-aminotropone containing peptide are pretty stable as like regular amide bonds.

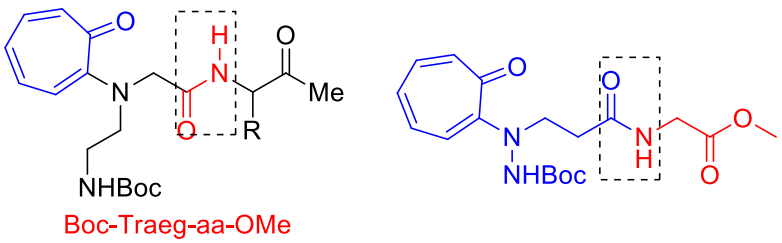

Figure 1.23 Chemical structure **(a)** *Traeg* peptide analogues (b) *N-Troponylated*-β-hydrazino Acid/Peptide

Our group has also reported a new class tropolone conjugated thymidine nucleoside and corresponding DNA oligonucleotides **Figure 1.24.**[83] Tropolone is a seven-membered non-

benzenoid aromatic with a weak chromophoric, pH-dependent fluorescent compound.[84, 85] The UV/fluorescent properties of tropolone conjugated nucleoside/oligonucleotide have been demonostarted. Hoever,the enhancement of fluorescence properties of the oligonucleotides after the formation of DNA duplex structures.

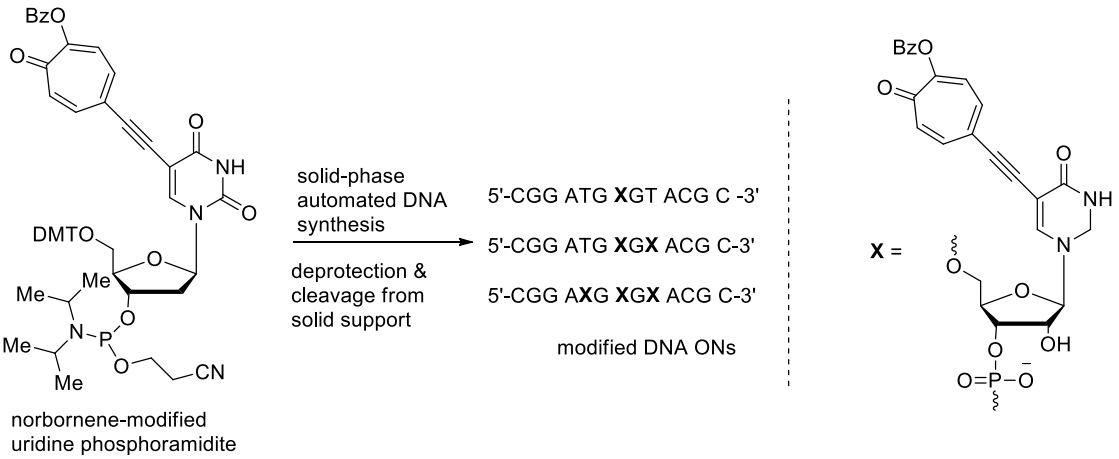

Figure 1.24. Synthesis of *Troponyl*-modified DNA ON by automated phosphoramidite chemistry

1.3 Conclusion and objective of present thesis

Tropolone is non-benzenoid natural molecule comprising unique structural and photophysical properties. It is part of various bioactive natural products as *Tropolonoids*. This thesis describes the role of tropolone in amino acid and nucleic acid derivatives which is classified into Five chapters as following: (a) Introduction of modified amino acids and nucleic acid (DNA/RNA) analogues (Chapter 1); (b) Structural and conformational analyses of *N*-tropolonylated *di-/tri*-peptide (Chapter-2); (c) Synthesis and photophysical studies of Troponyl BODIPY analogues (Chapter 3); (d) Synthesis and photophysical studies of Tropolonyl dihydropyrazine molecules (Chapter 4); (e) Synthesis and Photophysical studies of Troponyl DNA and RNA analogues (Chapter 5).

Chapter-1, This chapter describes the brief introduction of synthetic amino acid, peptides, fluorescent DNA/RNA analogues and tropolonoid natural products. Many of them are promisable analogues for the development of new nano-materials and therapeutic drugs.

Chapter-2, The *N*-arylated peptides have reportedly a significant role in the structural organization of peptides,[86] which are mainly derived from benzenoid aromatic moieties. This chapter demonstrates the synthesis of *N*-troponylated amino acid and their peptides from naturally occurring *Tropolone* scaffold. Their structural conformations are established by NMR (1D/2D), HRMS, CD, and single-crystal X-ray techniques. The comparative CD spectra of control native *di-tri*-peptides and *N*-tropolonylated *di-tri*-peptides. which strongly support the role of tropolonyl scaffold in the formation of *β*-turn type of secondary structures in solution phase. The single-crystal analyses of troponlylated *di*-peptides also support the formation of a unique supramolecular self-assembly β-sheet/turn type of structure. Hence, the *N*-tropolonyl unit has a significant role in the tunning of native peptides structure and conformations.

Chapter-3, BODIPY and related compounds are versatile fluorescent dyes molecules which are being used for labeling of biomolecules for imaging inside the living system in real-time and fluorescent nano-materials for various purposes.[87] This chapter describes the synthesis of BODIPY analogs from tropolone scaffold which is classified into two as Part A and Part B**.**

Part A (Chapter-3) demonstrates the synthesis of various boron-aminotropones derivatives (*Troponyl*-BODIPY) from *N*-troponly amino acids and *difluoro*-Boronating reagent by following Scheme-2. *Troponyl*-BODIPY compounds contain aminotropone and boron complexes through *N,O*-chelation. Their structures are confirmed by NMR ($^{1}H/^{13}C/^{19}F$, ^{11}B) HRMS, and single-crystal X-ray analyses. These BODIPY analogues exhibit characteristic UV/Fluorescence properties organic polar solvents (MeOH/CH_3CN). Their quantum yields are varied from ~0-15% because of different

amino acids acid residues. Theses analogues also exhibit solvent-dependent fluorescence properties. Their electrochemical studies confirm only one irreversible reduction reaction with Epc = −1.3 (V). Their structure has been optimized with DFT and their optimized structures show that the amino acid residues affect fluorescence characters in the respective troponyl-BODIPY analogues. Hence, Chapter-3 (Part A) provides the opportunities to develop the amino acid-functionalized troponyl-BODIPY analogues for labelling peptides and other biomacromolecules.

Part B (Chapter-3) describes the synthesis and photophysical studies of lipophilic BODIPY analogues which are derived from *N*-Tropolonyl of various alkylamines by following the given synthetic Scheme-3. The various *N*-tropolonyl alkylamines have been prepared from alkylamines and *O*-tosylate tropolone before complexing with difluoroboronating reagents. These complexes have been characterized NMR ($^{1}H/^{13}C/^{19}F$, ^{11}B), HRMS, and single-crystal techniques. Their photophysical studies (UV/Fluorescence) reveal that these analogues are fluorescent with quantum yield 10-15% in organic polar solvents, MeOH/CH_3CN. Importantly these analogues contain long chain hydrocarbons, lipophilic nature, in the BODIPY analogues which could be useful to find non-polar microenvironment.

Chapter-4, Dihydropyrazine molecules are bioactive molecules which are considered as promisable therapeutic drug candidates. Troponyldihydrapyrazine core moeities are also bioactive molecules possessing anticancer properties.[88] This chapter describes the synthesis of various substituted dihydrapyrazine derivatives from *N*,*N*-dialkylated 2-aminotropone ester derivatives and imines under acidic conditions. The product has been formed by the 2+2 cycloaddition reaction of imine and troponyl ketene and then rearrangment. Interestingly, we new adduct has been isolated as aryl-substituted troponyl dihydropyrazine derivatives from N-troponyl alkyl glycinate and imine derivative under acidic conditions. So far, there is no such

report about the formation of dihydropyrazine from imine derivatives. This thesis describes the synthesis, mechanistic studies of product formation, and structural features of newly synthesized dihydropyrazine derivatives. For biological importance, we examine the inhibition of cancerous cell proliferation with representative troponyl dihydropyrazine molecule by MTT-assay. Importantly, amino troponyl ketene has formed from the *N*,*N*-dialkylated 2-aminotropone ester under mild acidic conditions.[89, 90] Interestingly these derivative are fluorescent in nature with the quantum yield ~10-15%. This thesis also describes their bioactivies by MTT assay. Initial their bio-screening results strongly support the binding with DNA and anticancer activities. Hence these derivatives are potential fluorescent therapeutic drug candidates.

Chapter-5, Previously, troponyl-DNA analogue has shown the remarkable duplex DNA formation and photophysical properties. This chapter describe the synthesis photophysical studies of troponyl BODIPY containing DNA nucleosides and troponyl linked RNA nucleoside analogues. This chapter describes the synthesis and photophysical studies of *troponyl*-BODIPY containing deoxyuridinyl nucleoside analogue as dU^{trBOD}. This modified nucleoside has converted into phosphoramidites and Triphospahte of dU^{trBOD}. Thus this nucleoside analogue could be useful to prepare the fluorescent label DNA oligo enzymatically.

Further the synthesis of tropolone conjugated uridine nucleoside have synthesized. Next, this nucleoside has converted into troponyl uridinyl phosphoramidites. This modified phosphoramidite has incorporated into RNA oligo to examine the effect of troponle in RNA:RNA and RNA:DNA duplex formation. Hence this troponyl RNA analogue could be useful to examine role of tropolone in RNA dependent biological process.

1.3 References

1. Vella, F., Introduction to protein structure. By C Branden and J Tooze. pp 302. garland publishing, New York. 1991 ISBN 0–8513–0270–3 (pbk). *Biochemical Education* **1992,** *20*, 121-122.

2. Uzman, A., Molecular biology of the cell (4th ed.): Alberts, B., Johnson, A., Lewis, J., Raff, M., Roberts, K., and Walter, P. *Biochemistry and Molecular Biology Education* **2003,** *31*, 212-214.

3. Hecht, S.; Huc, I., *Foldamers: structure, properties and applications*. John Wiley & Sons2007.

4. Fischer, E.; Fourneau, E., Ueber einige Derivate des Glykocolls. *Berichte der deutschen chemischen Gesellschaft* **1901,** *34*, 2868-2877.

5. Babu, V. V. S., One hundred years of peptide chemistry. *Resonance* **2001,** *6*, 68-75.

6. Jensen, K. J.; Shelton, P. T.; Pedersen, S. L., *Peptide synthesis and applications*. Springer2013.

7. Vagner, J.; Qu, H.; Hruby, V. J., Peptidomimetics, a synthetic tool of drug discovery. *Current opinion in chemical biology* **2008,** *12*, 292-6.

8. Ripka, A. S.; Rich, D. H., Peptidomimetic design. *Current Opinion in Chemical Biology* **1998,** *2*, 441-452.

9. Olson, G. L.; Bolin, D. R.; Bonner, M. P.; Bös, M.; Cook, C. M.; Fry, D. C.; Graves, B. J.; Hatada, M.; Hill, D. E.; Kahn, M.; et al., Concepts and progress in the development of peptide mimetics. *Journal of medicinal chemistry* **1993,** *36*, 3039-49.

10. Hirschmann, R.; Nicolaou, K. C.; Pietranico, S.; Leahy, E. M.; Salvino, J.; Arison, B.; Cichy, M. A.; Spoors, P. G.; Shakespeare, W. C., De novo design and synthesis of somatostatin non-peptide peptidomimetics utilizing .beta.-D-glucose as a novel scaffolding. *Journal of the American Chemical Society* **1993,** *115*, 12550-12568.

11. Mega, J. L.; Close, S. L.; Wiviott, S. D.; Shen, L.; Hockett, R. D.; Brandt, J. T.; Walker, J. R.; Antman, E. M.; Macias, W.; Braunwald, E.; Sabatine, M. S., Cytochrome p-450 polymorphisms and response to clopidogrel. *The New England journal of medicine* **2009,** *360*, 354-62.

12. Spiegel, J.; Mas-Moruno, C.; Kessler, H.; Lubell, W. D., Cyclic Aza-peptide Integrin Ligand Synthesis and Biological Activity. *The Journal of Organic Chemistry* **2012,** *77*, 5271-5278.

13. Seebach, D.; Gardiner, J., β-Peptidic Peptidomimetics. *Accounts of Chemical Research* **2008,** *41*, 1366-1375.

14. Seebach, D.; Hook, D. F.; Glättli, A., Helices and other secondary structures of β- and γ-peptides. *Peptide Science* **2006,** *84*, 23-37.

15. Seebach, D.; L. Matthews, J., β-Peptides: a surprise at every turn. *Chemical Communications* **1997**, 2015-2022.

16. Gellman, S. H., Foldamers: A Manifesto. *Accounts of Chemical Research* **1998,** *31*, 173-180.

17. Hill, D. J.; Mio, M. J.; Prince, R. B.; Hughes, T. S.; Moore, J. S., A field guide to foldamers. *Chemical reviews* **2001,** *101*, 3893-4012.

18. Gahan, P. B., Molecular biology of the cell (4th edn) B. Alberts, A. Johnson, J. Lewis, K. Roberts and P. Walter (eds), Garland Science, 1463 pp., ISBN 0-8153-4072-9 (paperback) (2002). *Cell Biochemistry and Function* **2005,** *23*, 150-150.

19. Lenci, E.; Trabocchi, A., Peptidomimetic toolbox for drug discovery. *Chemical Society Reviews* **2020,** *49*, 3262-3277.

20. Bullock, B. N.; Jochim, A. L.; Arora, P. S., Assessing Helical Protein Interfaces for Inhibitor Design. *Journal of the American Chemical Society* **2011,** *133*, 14220-14223.

21. Clark, A., Foldamers: Structure, Properties, and Applications. Edited by Stefan Hecht and Ivan Huc. *ChemMedChem* **2008,** *3*.

22. Lubell, W. D., Peptide Chemistry. *The Journal of Organic Chemistry* **2012,** *77*, 7137-7142.

23. Orner, B. P.; Ernst, J. T.; Hamilton, A. D., Toward Proteomimetics: Terphenyl Derivatives as Structural and Functional Mimics of Extended Regions of an α-Helix. *Journal of the American Chemical Society* **2001,** *123*, 5382-5383.

24. Ernst, J. T.; Becerril, J.; Park, H. S.; Yin, H.; Hamilton, A. D., Design and application of an alpha-helix-mimetic scaffold based on an oligoamide-foldamer strategy: antagonism of the Bak BH3/Bcl-xL complex. *Angewandte Chemie (International ed. in English)* **2003,** *42*, 535-9.

25. Shaginian, A.; Whitby, L. R.; Hong, S.; Hwang, I.; Farooqi, B.; Searcey, M.; Chen, J.; Vogt, P. K.; Boger, D. L., Design, synthesis, and evaluation of an alpha-helix mimetic library targeting protein-protein interactions. *J Am Chem Soc* **2009,** *131*, 5564-72.

26. Serrano-Chacón, I.; Mir, B.; Escaja, N.; González, C., Structure of i-Motif/Duplex Junctions at Neutral pH. *Journal of the American Chemical Society* **2021**.

27. Cheng, R. P.; Gellman, S. H.; DeGrado, W. F., β-Peptides: From Structure to Function. *Chemical reviews* **2001,** *101*, 3219-3232.

28. Harper, J. D.; Lansbury, P. T., Jr., Models of amyloid seeding in Alzheimer's disease and scrapie: mechanistic truths and physiological consequences of the time-dependent solubility of amyloid proteins. *Annual review of biochemistry* **1997,** *66*, 385-407.

29. Rai, R.; Raghothama, S.; Balaram, P., Design of a Peptide Hairpin Containing a Central Three-Residue Loop. *Journal of the American Chemical Society* **2006,** *128*, 2675-2681.

30. Veeresh, K.; Singh, M.; Gopi, H. N., Impact of substituent effects on the design of β-sheet mimetics and β-double helices from (E)-vinylogous γ-amino acid oligomers. *Organic & Biomolecular Chemistry* **2019,** *17*, 9226-9231.

31. Chatterjee, S.; Roy, R. S.; Balaram, P., Expanding the polypeptide backbone: hydrogen-bonded conformations in hybrid polypeptides containing the higher homologues of α-amino acids. *Journal of The Royal Society Interface* **2007,** *4*, 587-606.

32. Prabhakaran, P.; Priya, G.; Sanjayan, G. J., Foldamers: They're Not Just for Biomedical Applications Anymore. *Angewandte Chemie International Edition* **2012,** *51*, 4006-4008.

33. Avan, I.; Hall, C. D.; Katritzky, A. R., Peptidomimetics via modifications of amino acids and peptide bonds. *Chemical Society Reviews* **2014,** *43*, 3575-3594.

34. Soler, M.; Feliu, L.; Planas, M.; Ribas, X.; Costas, M., Peptide-mediated vectorization of metal complexes: conjugation strategies and biomedical applications. *Dalton Transactions* **2016,** *45*, 12970-12982.

35. Ousaka, N.; Takeyama, Y.; Yashima, E., Dinuclear metal complexes composed of peptide chains: Solvent-induced switching and inversion of the metal-centered chirality. *Chemical Science* **2012,** *3*, 466-469.

36. Zou, R.; Wang, Q.; Wu, J.; Wu, J.; Schmuck, C.; Tian, H., Peptide self-assembly triggered by metal ions. *Chemical Society Reviews* **2015,** *44*, 5200-5219.

37. Dey, S.; Misra, R.; Saseendran, A.; Pahan, S.; Gopi, H. N., Metal-Coordinated Supramolecular Polymers from the Minimalistic Hybrid Peptide Foldamers. *Angewandte Chemie* **2021,** *133*, 9951-9956.

38. Faggi, E.; Gavara, R.; Bolte, M.; Fajarí, L.; Juliá, L.; Rodríguez, L.; Alfonso, I., Copper(ii) complexes of macrocyclic and open-chain pseudopeptidic ligands: synthesis, characterization and interaction with dicarboxylates. *Dalton Transactions* **2015,** *44*, 12700-12710.

39. Luis, S. V.; Alfonso, I., Bioinspired Chemistry Based on Minimalistic Pseudopeptides. *Accounts of Chemical Research* **2014,** *47*, 112-124.

40. Gupta, M. K.; Jena, C. K.; Balachandra, C.; Sharma, N. K., Unusual Pseudopeptides: Syntheses and Structural Analyses of Ethylenediprolyl Peptides and Their Metal Complexes with Cu(II) Ion. *The Journal of Organic Chemistry* **2021,** *86*, 16327-16336.

41. Cobb, M., Who discovered messenger RNA? *Current biology : CB* **2015,** *25*, R526-32.

42. Dahm, R., Friedrich Miescher and the discovery of DNA. *Developmental biology* **2005,** *278*, 274-88.

43. Judson, H. F., *The eighth day of creation*. New York1979.

44. Watson, J. D.; Crick, F. H., Molecular structure of nucleic acids: a structure for deoxyribose nucleic acid. *Nature* **1953,** *171*, 737-738.

45. Shivalingam, A.; Brown, T., Synthesis of chemically modified DNA. *Biochemical Society transactions* **2016,** *44*, 709-15.

46. Xu, W.; Chan, K. M.; Kool, E. T., Fluorescent nucleobases as tools for studying DNA and RNA. **2017,** *9*, 1043-1055.

47. Seo, T. S.; Bai, X.; Kim, D. H.; Meng, Q.; Shi, S.; Ruparel, H.; Li, Z.; Turro, N. J.; Ju, J., Four-color DNA sequencing by synthesis on a chip using photocleavable fluorescent nucleotides. *Proceedings of the National Academy of Sciences* **2005,** *102*, 5926-5931.

48. Ju, J.; Kim, D. H.; Bi, L.; Meng, Q.; Bai, X.; Li, Z.; Li, X.; Marma, M. S.; Shi, S.; Wu, J., Four-color DNA sequencing by synthesis using cleavable fluorescent nucleotide reversible terminators. *Proceedings of the National Academy of Sciences* **2006,** *103*, 19635-19640.

49. Carell, T.; Brandmayr, C.; Hienzsch, A.; Müller, M.; Pearson, D.; Reiter, V.; Thoma, I.; Thumbs, P.; Wagner, M., Structure and function of noncanonical nucleobases. *Angewandte Chemie (International ed. in English)* **2012,** *51*, 7110-31.

50. Ivancová, I.; Leone, D. L.; Hocek, M., Reactive modifications of DNA nucleobases for labelling, bioconjugations, and cross-linking. *Curr Opin Chem Biol* **2019,** *52*, 136-144.

51. Xu, W.; Chan, K. M.; Kool, E. T., Fluorescent nucleobases as tools for studying DNA and RNA. *Nature chemistry* **2017,** *9*, 1043-1055.

52. Traube, F. R.; Carell, T., The chemistries and consequences of DNA and RNA methylation and demethylation. *RNA biology* **2017,** *14*, 1099-1107.

53. Manna, S.; Sarkar, D.; Srivatsan, S. G., A Dual-App Nucleoside Probe Provides Structural Insights into the Human Telomeric Overhang in Live Cells. *Journal of the American Chemical Society* **2018,** *140*, 12622-12633.

54. Nuthanakanti, A.; Boerneke, M. A.; Hermann, T.; Srivatsan, S. G., Structure of the Ribosomal RNA Decoding Site Containing a Selenium-Modified Responsive Fluorescent Ribonucleoside Probe. *Angewandte Chemie International Edition* **2017,** *56*, 2640-2644.

55. Pawar, M. G.; Nuthanakanti, A.; Srivatsan, S. G., Heavy Atom Containing Fluorescent Ribonucleoside Analog Probe for the Fluorescence Detection of RNA-Ligand Binding. *Bioconjugate Chemistry* **2013,** *24*, 1367-1377.

56. Hopkins, P. A.; Sinkeldam, R. W.; Tor, Y., Visibly Emissive and Responsive Extended 6-Aza-Uridines. *Organic Letters* **2014,** *16*, 5290-5293.

57. Hervé, G.; Sartori, G.; Enderlin, G.; Mackenzie, G.; Len, C., Palladium-catalyzed Suzuki reaction in aqueous solvents applied to unprotected nucleosides and nucleotides. *RSC Advances* **2014,** *4*, 18558-18594.

58. Flynn, B. L.; Macolino, V.; Crisp, G. T., Synthesis of modified nucleosides. Palladium-catalysed couplings of organostannanes or organoboranes with pyrimidine nucleosides. *Nucleosides & nucleotides* **1991,** *10*, 763-779.

59. Matyašovský, J.; Tack, L.; Palágyi, A.; Kuba, M.; Pohl, R.; Kraus, T.; Güixens-Gallardo, P.; Hocek, M., Nucleotides bearing aminophenyl- or aminonaphthyl-3-

methoxychromone solvatochromic fluorophores for the enzymatic construction of DNA probes for the detection of protein–DNA binding. *Organic & Biomolecular Chemistry* **2021,** *19*, 9966-9974.

60. Güixens-Gallardo, P.; Hocek, M., Acetophenyl-thienyl-aniline-Linked Nucleotide for Construction of Solvatochromic Fluorescence Light-Up DNA Probes Sensing Protein-DNA Interactions. *Chemistry – A European Journal* **2021,** *27*, 7090-7093.

61. Ondruš, M.; Sýkorová, V.; Bednárová, L.; Pohl, R.; Hocek, M., Enzymatic synthesis of hypermodified DNA polymers for sequence-specific display of four different hydrophobic groups. *Nucleic Acids Research* **2020,** *48*, 11982-11993.

62. Panattoni, A.; Pohl, R.; Hocek, M., Flexible Alkyne-Linked Thymidine Phosphoramidites and Triphosphates for Chemical or Polymerase Synthesis and Fast Postsynthetic DNA Functionalization through Copper-Catalyzed Alkyne–Azide 1,3-Dipolar Cycloaddition. *Organic Letters* **2018,** *20*, 3962-3965.

63. Mačková, M.; Pohl, R.; Hocek, M., Polymerase Synthesis of DNAs Bearing Vinyl Groups in the Major Groove and their Cleavage by Restriction Endonucleases. *ChemBioChem* **2014,** *15*, 2306-2312.

64. Slavíčková, M.; Pohl, R.; Hocek, M., Additions of Thiols to 7-Vinyl-7-deazaadenine Nucleosides and Nucleotides. Synthesis of Hydrophobic Derivatives of 2′-Deoxyadenosine, dATP and DNA. *The Journal of Organic Chemistry* **2016,** *81*, 11115-11125.

65. Güixens-Gallardo, P.; Humpolickova, J.; Miclea, S. P.; Pohl, R.; Kraus, T.; Jurkiewicz, P.; Hof, M.; Hocek, M., Thiophene-linked tetramethylbodipy-labeled nucleotide for viscosity-sensitive oligonucleotide probes of hybridization and protein–DNA interactions. *Organic & biomolecular chemistry* **2020,** *18*, 912-919.

66. Güixens-Gallardo, P.; Zawada, Z.; Matyašovský, J.; Dziuba, D.; Pohl, R.; Kraus, T.; Hocek, M., Brightly Fluorescent 2′-Deoxyribonucleoside Triphosphates Bearing Methylated

Bodipy Fluorophore for in Cellulo Incorporation to DNA, Imaging, and Flow Cytometry. *Bioconjugate Chemistry* **2018,** *29*, 3906-3912.

67. Deore, P. S.; Soldatov, D. V.; Manderville, R. A., A 5′-BODIPY End-label for Monitoring DNA Duplex-Quadruplex Exchange. *Scientific Reports* **2018,** *8*, 16874.

68. Kim, K. T.; Kim, B. H., A fluorescent probe for the 3′-overhang of telomeric DNA based on competition between two interstrand G-quadruplexes. *Chemical Communications* **2013,** *49*, 1717-1719.

69. Ehrenschwender, T.; Wagenknecht, H.-A., 4,4-Difluoro-4-bora-3a,4a-diaza-s-indacene as a Bright Fluorescent Label for DNA. *The Journal of Organic Chemistry* **2011,** *76*, 2301-2304.

70. Tanpure, A. A.; Srivatsan, S. G., Synthesis and photophysical characterisation of a fluorescent nucleoside analogue that signals the presence of an abasic site in RNA. *ChemBioChem* **2012,** *13*, 2392.

71. Sproviero, M.; Rankin, K. M.; Witham, A. A.; Manderville, R. A., Utility of 5′-O-2, 7-dimethylpixyl for solid-phase synthesis of oligonucleotides containing acid-sensitive 8-aryl-guanine adducts. *The Journal of organic chemistry* **2014,** *79*, 692-699.

72. Arndt, S.; Wagenknecht, H. A., "Photoclick" postsynthetic modification of DNA. *Angewandte Chemie International Edition* **2014,** *53*, 14580-14582.

73. Pyka, A. M.; Domnick, C.; Braun, F.; Kath-Schorr, S., Diels–Alder cycloadditions on synthetic RNA in mammalian cells. *Bioconjugate Chem.* **2014,** *25*, 1438-1443.

74. Pauson, P. L., Tropones and tropolones. *Chemical reviews* **1955,** *55*, 9-136.

75. Nozoe, T., Seventy Years in Organic Chemistry. *Profiles, Pathways, and Dreams (Autography)* **1991**.

76. Saleh, N.; Zwiefak, A.; Mordarski, M.; Pulverer, G., Antibacterial activity of selected tropones and tropolones. *Zentralblatt für Bakteriologie, Mikrobiologie und Hygiene. Series A: Medical Microbiology, Infectious Diseases, Virology, Parasitology* **1988,** *270*, 160-170.

77. Angawi, R. F.; Swenson, D. C.; Gloer, J. B.; Wicklow, D. T., Malettinin A: a new antifungal tropolone from an unidentified fungal colonist of Hypoxylon stromata (NRRL 29110). *Tetrahedron letters* **2003,** *44*, 7593-7596.

78. Yang, P.-S.; Wang, M.-J.; Jayakumar, T.; Chou, D.-S.; Ko, C.-Y.; Hsu, M.-J.; Hsieh, C.-Y., Antiproliferative activity of hinokitiol, a tropolone derivative, is mediated via the inductions of p-JNK and p-PLCγ1 signaling in PDGF-BB-stimulated vascular smooth muscle cells. *Molecules* **2015,** *20*, 8198-8212.

79. Lomonosova, E.; Daw, J.; Garimallaprabhakaran, A. K.; Agyemang, N. B.; Ashani, Y.; Murelli, R. P.; Tavis, J. E., Efficacy and cytotoxicity in cell culture of novel α-hydroxytropolone inhibitors of hepatitis B virus ribonuclease H. *Antiviral research* **2017,** *144*, 164-172.

80. Balachandra, C.; Sharma, N. K., Synthesis and conformational analysis of new troponyl aromatic amino acid. *Tetrahedron* **2014,** *70*, 7464-7469.

81. Balachandra, C.; Sharma, N. K., Instability of Amide Bond Comprising the 2-Aminotropone Moiety: Cleavable under Mild Acidic Conditions. *Organic Letters* **2015,** *17*, 3948-3951.

82. Dalabehera, N. R.; Meher, S.; Bhusana Palai, B.; Sharma, N. K., Instability of Amide Bond with Trifluoroacetic Acid (20%): Synthesis, Conformational Analysis, and Mechanistic Insights into Cleavable Amide Bond Comprising β-Troponylhydrazino Acid. *ACS Omega* **2020,** *5*, 26141-26152.

83. Bollu, A.; Sharma, N. K., Tropolone-Conjugated DNA: Fluorescence Enhancement in the Duplex. *ChemBioChem* **2019,** *20*, 1467-1475.

84. Doering, W. v. E.; Knox, L. H., Tropolone. *J. Am. Chem. Soc.* **1951,** *73*, 828-838.

85. Breheret, E.; Martin, M., Electronic relaxation of troponoids: tropolone fluorescence. *J. Lumin.* **1978,** *17*, 49-60.

86. Paul, B.; Butterfoss, G. L.; Boswell, M. G.; Renfrew, P. D.; Yeung, F. G.; Shah, N. H.; Wolf, C.; Bonneau, R.; Kirshenbaum, K., Peptoid Atropisomers. *J. Am. Chem. Soc.* **2011,** *133*, 10910-10919.

87. Bessette, A.; Hanan, G. S., Design, synthesis and photophysical studies of dipyrromethene-based materials: insights into their applications in organic photovoltaic devices. *Chem. Soc. Rev.* **2014,** *43*, 3342-3405.

88. Bentley, R., A fresh look at natural tropolonoids. *Nat. Prod. Rep.* **2008,** *25*, 118-138.

89. Balachandra, C.; Sharma, N. K., Instability of Amide Bond Comprising the 2-Aminotropone Moiety: Cleavable under Mild Acidic Conditions. *Org. Lett.* **2015,** *17*, 3948-3951.

90. Balachandra, C.; Sharma, N. K., Direct/Reversible Amidation of Troponyl Alkylglycinates via Cationic Troponyl Lactones and Mechanistic Insights. *ACS Omega* **2018,** *3*, 997-1013.

CHAPTER-2

Title: Synthesis and Conformational Analysis of *N*-Troponylated *di-/tri*-Peptides

2.1 Introduction

2.2 Objective of our work

2.3 Result and discussion

2.4 Conclusion

2.5 Experimental Section

2.6 References and Notes

2.7 Appendix

2.1 Introduction

Protein and peptides form secondary structures such as *β*-sheets/turns and α-helixs, which are vital role in their biochemical activities.[1, 2] The non-covalent interactions as hydrogen bonding and π-π interactions guide the formation of the secondary structure in peptides as foldamers.[3-5] Generally, the amide carbonyl (-C=O)/amine (N-H) of peptides are involved in the hydrogen bonding and form stable secondary structures.[6, 7] The sequence-specific structured peptides interact with a specific protein and nucleic acid to maintain the biochemical process. Nowadays, the protein-peptide interactions and nucleic acid (DNA/RNA)-peptide interactions studies have emerged as powerful tools for the development of peptide-based therapeutic d, for practical applications in biochemical research. Thus several structurally modified amino acids and their peptides are prepared as foldamers and considered to employ in the development of new potent drugs.[8, 9] The aromatic amino acids, mainly phenylalanine-rich di-/tri-peptides, have shown a high tendency, because of π-π interactions, for the formation of various types of self-assembled materials.[10] The aromatic tripeptides containing aromatic amino acids (tyr & Trp) and methionine (or cysteine) are reportedly known to form fibrous aggregate.[11] Bag and co-workers have reported novel scaffolds for *β*-turn peptidomimetics from the triazole amino acid-containing peptides.[12] The gabapentin-based hybrid small peptides reportedly form double turn conformation by C_{12}/C_{10} hydrogen bonding.[13] *N*-terminal aromatic acid-containing peptides have the ability for spontaneous self-assembly because of hydrogen bonding and π-π interactions.[14-17] The attachment of the *alkyl/aryl* group at the *N*-terminal of peptides alters the structure and function of peptides. Recently, *N*-alkylated/arylated peptides or peptoids are explored in the structural and conformational changes of peptides.[18-22] The *N*-alkylated peptoids form a unique oligomeric structure and are being tested as potential antifreeze agents for food production and biomedicine.[23] Importantly, the *N*-arylated peptoids exhibit atropisomerism and unique foldamers properties.[24-26] The synthesis of *N*-arylated peptides is

reported by a metal catalyst and metal-free catalysts.[27-29] So far, *N*-aryl peptides are prepared from benzenoid aromatic compounds. In nature, the non-benzenoid aromatic molecules also occur as bioactive natural products but are poorly explored to link with aminoacid/peptides. Tropolone and related derivatives occur in various natural products such as *Cholchicine, Stiptatic acid, α-/β-/γ-Thujaplicine, Pycnidione, Manicol. Tropolone*.[30-32] Tropolone-related derivatives are natural chromophore, a weak fluorophore, and excellent metal chelating agents, mainly with transition metal ions (Cu, Zn, and Ni).[33-36] Recently, we have introduced the non-benzenoid aromatic molecules, *Tropolone,* into unnatural amino acids/peptides and explored the role of troponyl residue into hydrogen bonding with adjacent amide-NH (Figure. 2-1A).[37-39] Importantly, their amide bond is cleavable under mildly acidic conditions (~5.0% TFA). Recently, *N*-troponylated amino acid esters are employed for the development of small fluorescent molecules as BODIPY analogues (Figure.2-1B).[40, 41] These results encourage attaching troponyl moiety at the *N*-terminal of peptides and exploring the role of troponyl scaffold in structural changes of native short *di*-/*tri*-*pe*ptides.

We assume that the carbonyl group of *N*-troponylated peptides may involve in hydrogen bonding with N-H of peptides in intramolecular and intermolecular fashions and produce supramolecular self-assembly dimer/β-turn types of structures. Recently we have explored the troponyl moiety into amino acids/peptides as *Traeg*-amino acid/peptides for tuning their secondary structures. We have established the role of troponyl carbonyl group of *Traeg* containing peptides in hydrogen bonding with adjacent amide N-H as C=O-----H-N. However, the synthesis of *Traeg*-homologous peptides have become difficult due to the instability of the amide bond under mildly acidic conditions. The role of troponyl residue has serious implications in the cleavage of the amide bond. Further direct amidation and reversible amidation are also established with *Trag* amino acids under acidic conditions. Importantly amide bonds of only *di*-alkylated 2-aminotropone derivatives as *Treg/trag* peptides are

cleavable under basic conditions. Interestingly, the amide bond of *mono*-alkylated 2-aminotropone containing peptide is pretty stable as like regular amide bonds. Thus, we planned to introduce troponyl residue at *N*-terminal *α*-/*β*-amino acid to explore the role of troponyl carbonyl in the peptides' secondary structure formation.

2.2 Objective of our work

In this chapter, we have to explain the syntheses and importance of *N*-arylated peptides as peptoids, the structural and conformation changes of small peptides that lead to the unique foldamers, even *di*-/*tri*-peptides. We have also explored the role of troponyl group in structural and conformational changes by single crystal X-ray analyses NMR and CD studies.

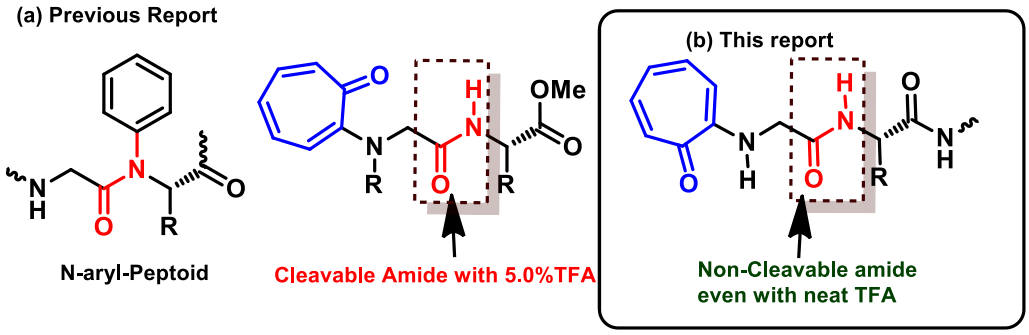

Figure. 2.1. (a) *N*-aryl peptide; *N*-troponyl cleavable peptides; and (b) *N*-troponyl noncleavable peptides

2.3 Results and Discussion

We began the chemical syntheses of rationally designed *N*-troponyl amino acid ester from Tropolone (**1**) and amino acids ester derivatives (Scheme 1). Tropolone was tosylated as *O*-tosylate tropolone derivative (**2**) and then treated with *α*-/*β*-amino acid ester derivatives such as NH_2-Gly-OMe, NH_2-Ala-OMe, NH_2-Val-OMe, NH_2-Leu-OMe, NH_2-Ile-OMe, NH_2-Phe-

OMe, NH-Pro-OMe, and NH_2-*β*-Ala-OMe. These troponylated amino acid derivatives were hydrolyzed into respective carboxylic acid derivatives with NaOH (MeOH: THF) and coupled with *α*-amino acid esters/*β*-amino acid ester (H_2N-AA_2-OMe) *via* amide bond under peptide coupling conditions. Pleasantly, we isolated *N*-troponylated-*di*-peptides esters (**4a**-**4l**) in excellent yield (Scheme 1). We used both *α*-/*β*-amino acid ester derivatives for peptides coupling that produced *N*-troponyl-dipeptides (**4a**-**4l**). These derivatives were characterised by NMR and HRMS. Their characterization data (^{1}H-/^{13}C-NMR/ESI-HRMS) are provided in Appendix (Figure. A1-A24).

Scheme 2.1 Synthesis of N-Troponylated dipeptides

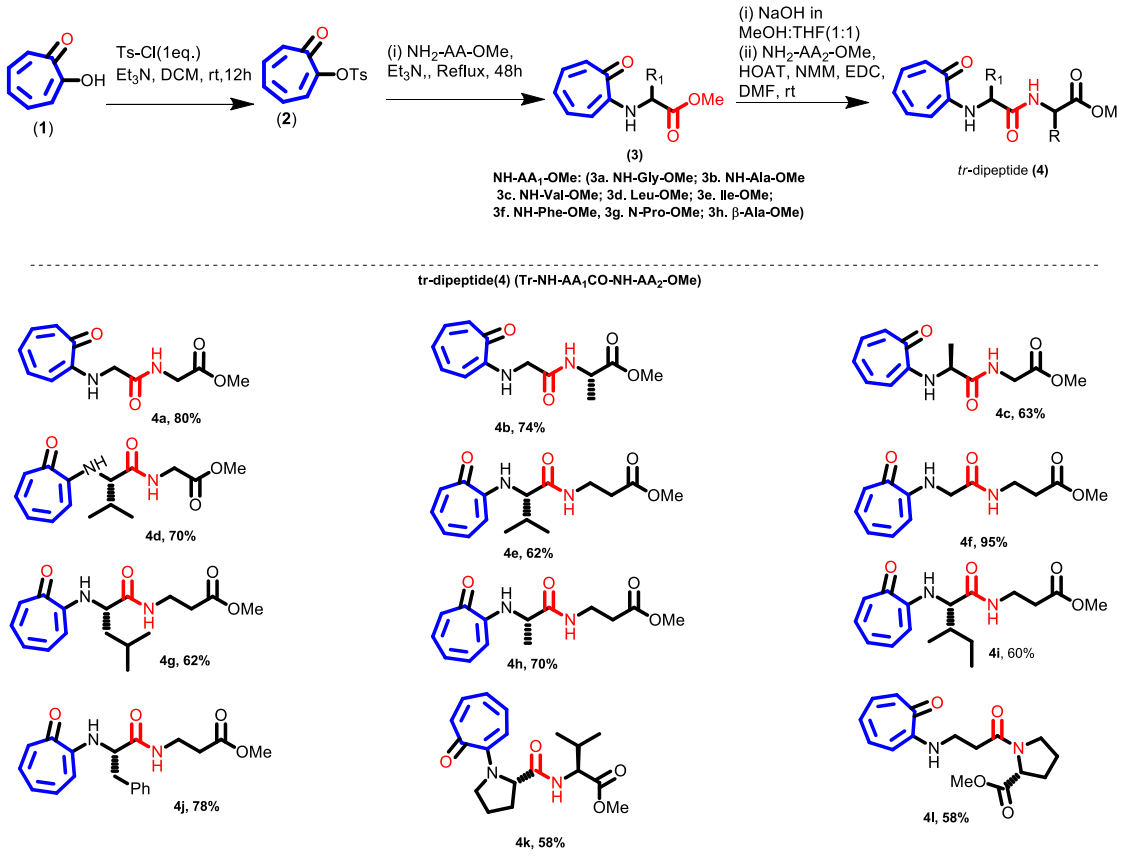

Further, we planned to study the role of troponyl carbonyl in the structural and conformational changes of those peptides in solid-state. We then attempted to crystalize under different solvent systems. Pleasantly we obtained the single crystal of six di-peptide under EtOAc/Hexane (1:1) solvent mixture and confirmed their chemical structure by the X-ray data analyses of respective crystals. Their crystal data are deposited to the Cambridge Crystallographic Data center (CCDC). Their CCDC numbers are CCDC 1889029 for compound (**4a**) CCDC 1889030 for compound (**4b**) CCDC 1889031 for compound (**4d**) CCDC 1889033 for compound (**4e)** CCDC 1889034 for compound (**4f**) CCDC1889032 compound (**4j**). To examine the role of Tropolone-containing peptide conformations in their solid states, we studied the crystal packing arrangement of troponyl peptides (**4a,4b,4d,4e,4f,** and **4j**) by using diamond visualizing software (Diamond version 3.2k). Their X-ray data are summarized in the Supporting Information (Table S1). We also demonstrate their supramolecular self-assembly structure in solid-state from respective single-crystal data.

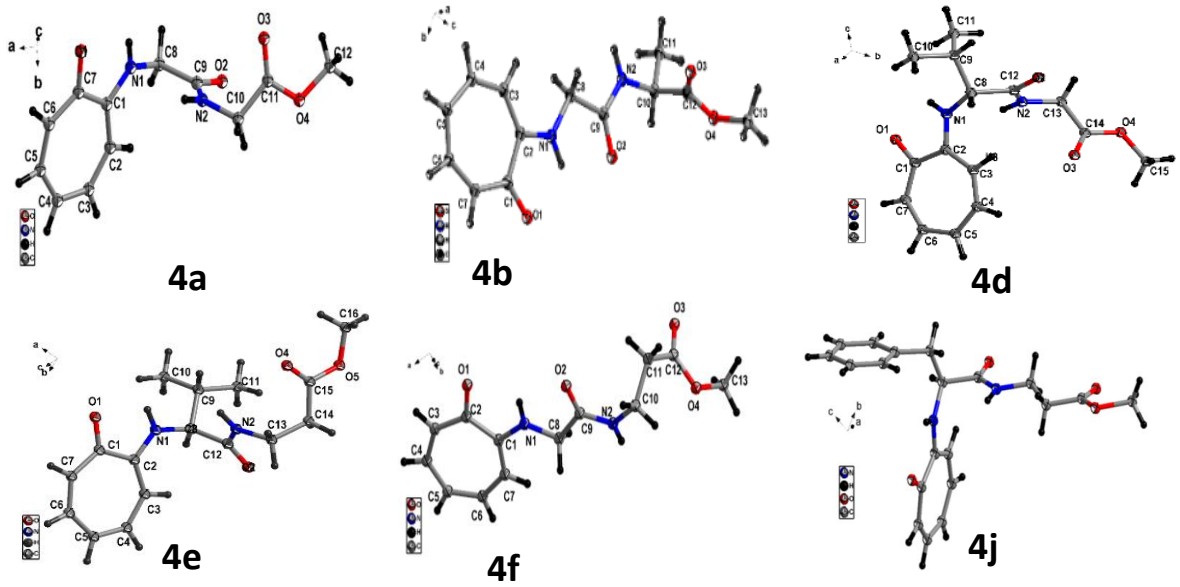

Figure2.2. Crystal structure of compound **4a**, **4b**, **4d**, **4e**, **4f** and **4j**.

*Troponyl-peptide **4a***. We have performed structural analysis of peptide **4a**, which are described in **Figure 2.3**. as the ORTEP diagram, unit cell packing diagram, and self-assembly structure. The *tr-Gly-Gly-OMe* dipeptide (**4a**) forms a unique self-assembled supramolecular structure *via* intermolecular hydrogen bonding, between troponyl carbonyl (tr-C=O) and troponyl amine (tr-N-H)/amide N-H with bond length 2.1Å. These interactions lead to the antiparallel double helical type of structure along axis-a with pitch value 4.8Å. The formation of such kind of supramolecular structure from native dipeptide (NH_2-Gly-Gly-OMe) is not known in the literature. Thus, tropolone residue plays an important role in influencing the structure changes of peptides.

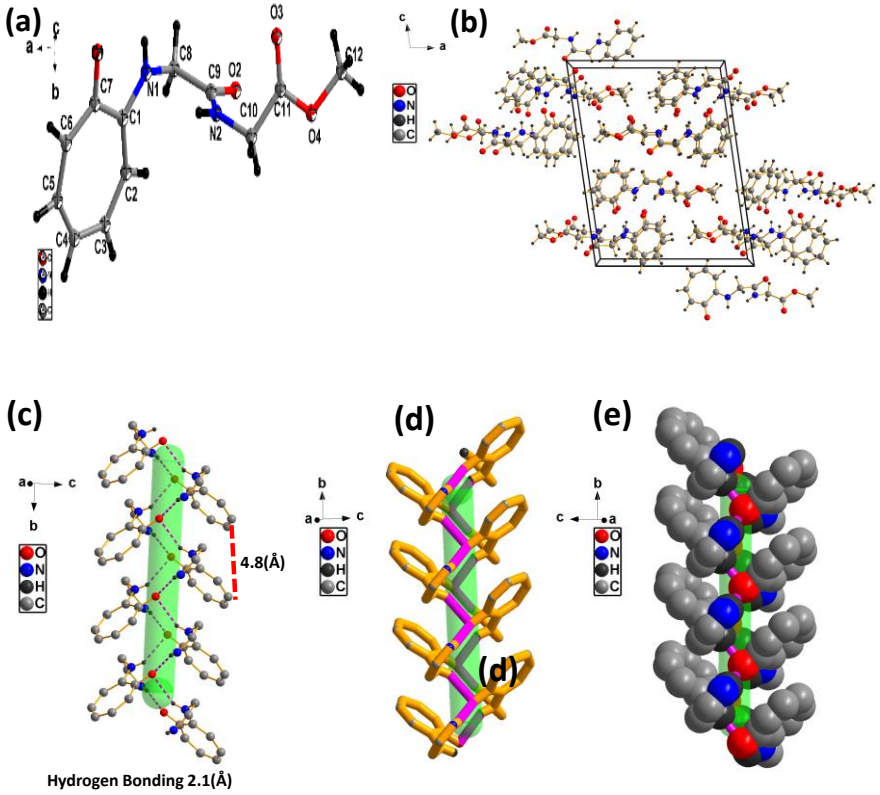

Figure 2.3. Structural analysis of N-trponyl-peptide (**4a**): (a) structure and ORTEP diagram; (b) Unit cell packing diagram; (c-e) Supramolecular self-assembly structure.

We have performed the structural analysis of troponyl peptide **4b** in **Figure 2.4**. Herein we describe the ORTEP diagram (a), unit cell packing diagram (b), and packing diagram (Figure. 4c), and hydrogen bond self-assembled structure (d-g). The *tr-Gly-Ala-OMe* dipeptide (**4b**) forms a unique self-assembled supramolecular structure *via* intermolecular hydrogen bonding such as Ala-residue (N-H) of one molecule is non-covalently interacted with tropolonyl carbonyl (O=C-tr) of another molecule with bond length 2.1Å. As resultants, dipeptide **4b** forms sheet type of structure along axis-a. These β-sheets structures exist at equal distances along axis-b that lead to the ladder-type of supramolecular structure in solid-state of **4b**. A similar self-assembly is not noticed with lone native dipeptide (NH_2-Gly-Ala-OMe).

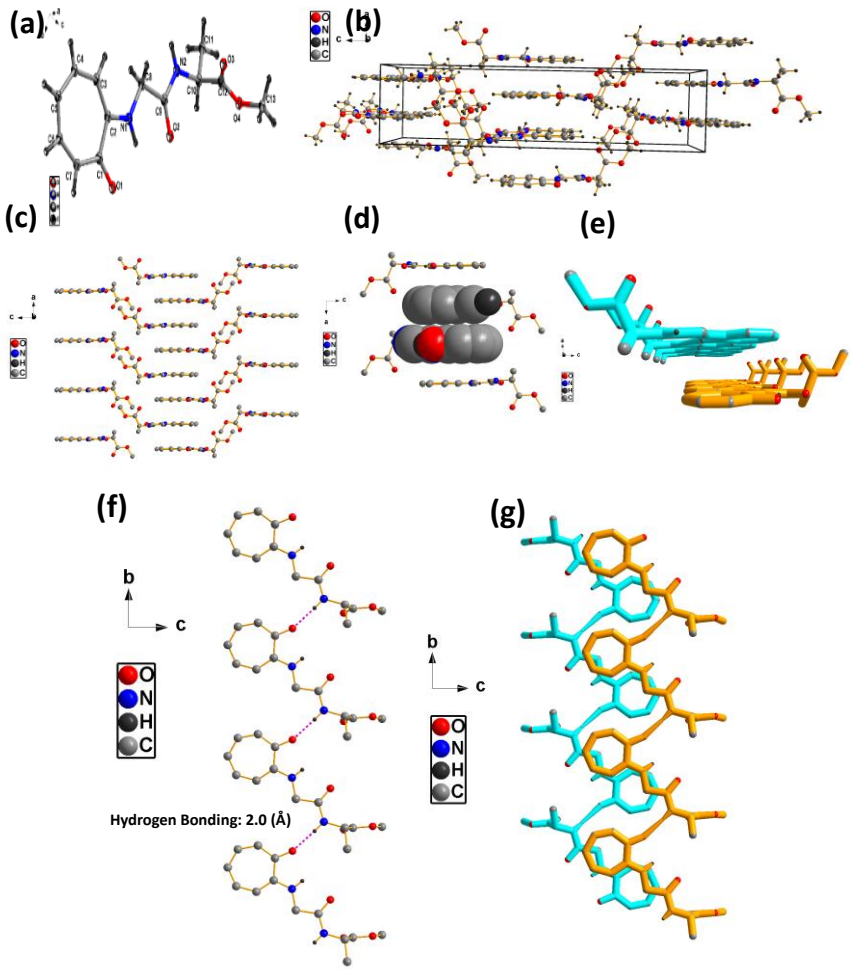

Figure 2.4. Structural analysis of *trponyl*-peptide (**4b**): (a) structure and ORTEP diagram; (b) Unit cell packing diagram; (c-g) Supramolecular self-assembly structure.

We have performed the structural analysis of troponyl peptide **4d** in **Figure 2.5**. which describes the ORTEP diagram (a), unit cell packing diagram (b), and hydrogen bond self-assembled structure (c). The *tr-Val-Gly-OMe* dipeptide (**4d**) forms *β*-strand (antiparallel *β*-sheet) type of self-assembled supramolecular structure by non-covalent interactions, two intermolecular hydrogen bonding with distance 2.1Å. In this assembly, the glycine N-H of one molecule is hydrogen-bonded with tropolonyl carbonyl (O=C) of another molecule that is oriented in antiparallel fashion in a solid crystal.

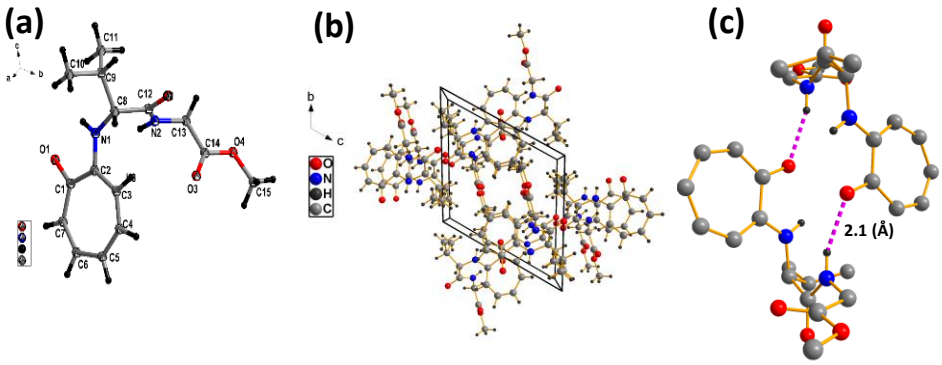

Figure 2.5. Structural analysis of *trponyl*-di-peptide (4d): (a) structure and ORTEP diagram; (b) Unit cell packing diagram; (c) Supramolecular self-assembly structure.

We have performed the structural analysis of troponyl peptide **4e** in **Figure 2.6**. which describes the ORTEP diagram (a), unit cell packing diagram (b), and hydrogen bond self-assembled structure (c). The *tr-Val-β-Ala-OMe* dipeptide (**4e**) also forms a *β*-sheet type of self-assembled supramolecular structure in solid-state via two hydrogen bonding with distance 2.0Å as *β*-Ala's N-H of one molecule is hydrogen-bonded with tropolonyl group O=C of another molecule in the antiparallel manner **Figure 2.6**. Importantly, the π-π interaction between two tropolonyl residues is existed along to give a stable structure.

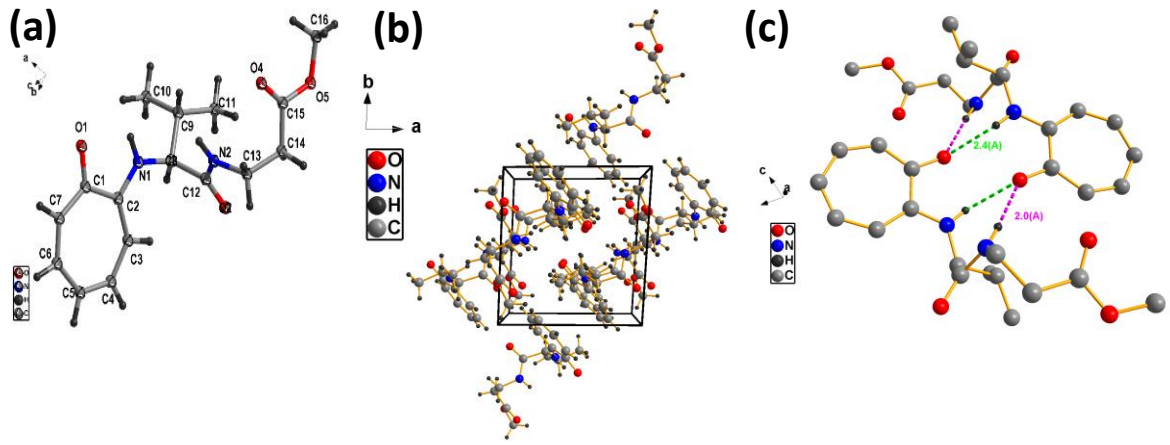

Figure 2.6. Structural analysis of trponyl-peptide (4e): (6a) structure and ORTEP diagram; (6b) Unit cell packing diagram; (6c) Supramolecular self-assembly structure.

We have performed the structural analysis of troponyl peptide **4f** in **Figure 2.7**. which describes the ORTEP diagram (a), unit cell packing diagram (b), and packing diagram (c), and hydrogen bond self-assembled structure (d-h). The tr-Gly-*β*-Ala-OMe dipeptide (**4f**) forms a self-assembled supramolecular complex structure by hydrogen bonding between Tropolonyl carbonyl with *β*-Ala N-H form with a distance of 2.0Å (g). Two molecules are oriented in an antiparallel direction. Importantly, this dipeptide forms a chair-form type of planner *β*-sheet-type structure along with tilted axis-b. This sheet is interconnected via hydrogen bonding between πC-H with ester carbonyl C=O. Such kind of structure is not known with control peptide NH_2-Gly-*β*-Ala-OMe dipeptide. Importantly, this troponyl peptide forms sheets and is separated by weak Van der Waal interactions. Each layer (*β*-sheet) is formed by intermolecular hydrogen bonding.

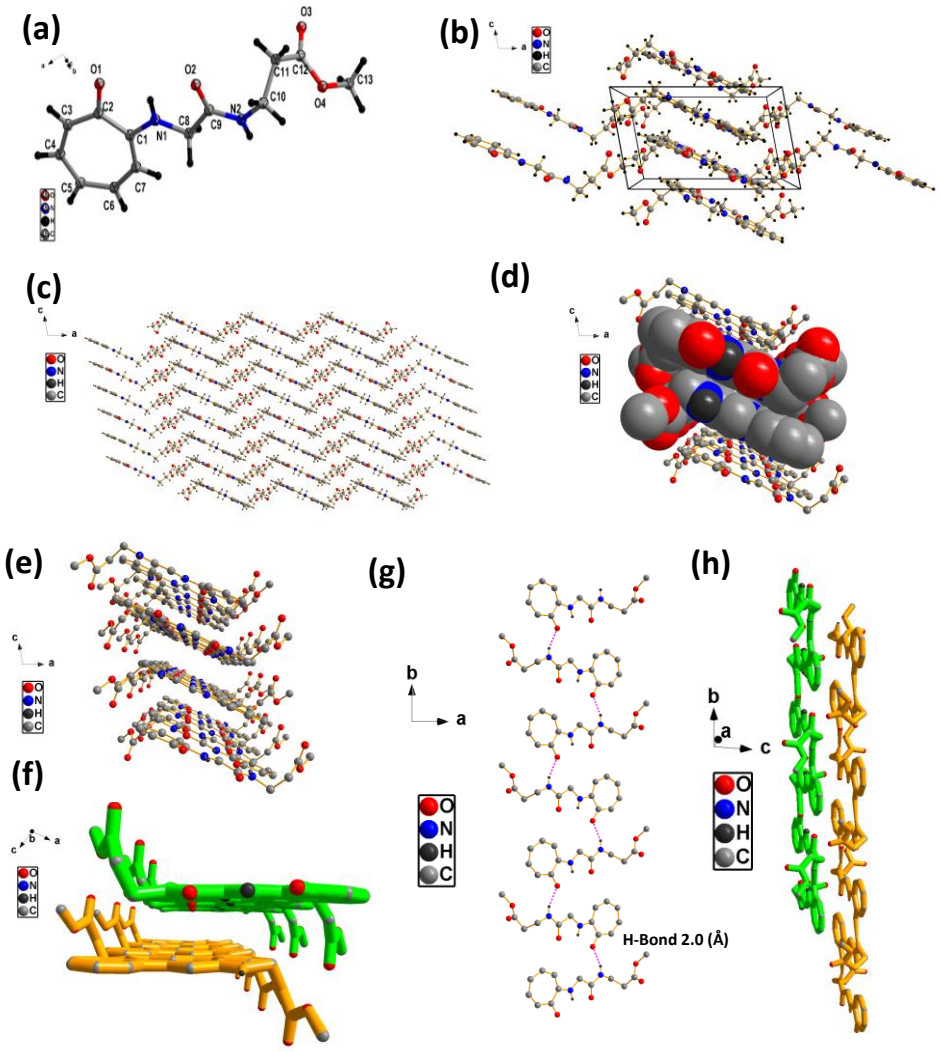

Figure 2.7. Structural analysis of *trponyl-di*-peptide (**4f**): (a) structure and ORTEP diagram; (b) Unit cell packing diagram; (c-h) Supramolecular self-assembly structure.

We have performed the structural analysis of troponyl peptide **4j** in **Figure 2.8**. that describes the ORTEP diagram (a), unit cell packing diagram (b), and hydrogen bond self-assembled structure (c). The tr-Phe-*β*-Ala-OMe (**4j**) dipeptide forms a unique self-assembled supramolecular quadrilateral structure via hydrogen bonding as *β*-Ala-N-H with tropolonyl carbonyl (C=O) with distance 2.0Å (Figure. 7c). This self-assembled structure contains two molecules that are oriented in the opposite direction in a twisted manner. Importantly,

tropolonyl residue is almost perpendicular to the linear backbone Phe-*β*-Ala residue. No such structure is reported with native dipeptide (NH_2-Phe-*β*-Ala-OMe).

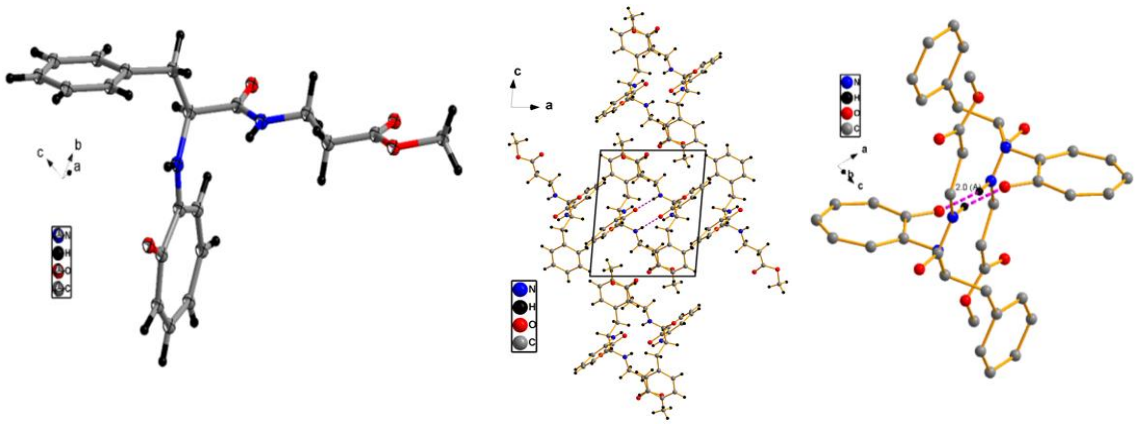

Figure 2.8. Structural analysis of trponyl-peptide (4j): (a) structure and ORTEP diagram; (b) Unit cell packing diagram; (c) Supramolecular self-assembly structure.

The torsional angles of the amide backbone have a critical role in the conformational changes of peptides to form the regular secondary structures such as α-helices and *β*-strands. The torsional angles around N-Cα (ϕ) and Cα-C (Ψ) of amide backbones mostly depend upon the nature of amino acid residues in native peptide. These angles are employed for Ramachandran plot (ϕ vs Ψ) which reveal the role of amino acid residue for the formation of peptides' secondary structures such as right α-helix, *β*-strand, and *β*-turn.[42] In literature, the Ramachandran plot of α-amino acid-containing peptides has the following allowed regions: (i) α-helical region with torsion angle range $-180<\varphi<0^{o}$, $-100<\psi<45^{o}$; (ii) *β*-sheet regions with torsional angle range $-180<\varphi<-45^{o}$, $45<\psi<225$; (iii) β-turn regions with torsional angle range $0<\varphi<180^{o}$, $-90<\psi<90^{o}$.[42, 43] Herein, we also extracted φ/ ψ angles of *N*-troponylated peptides,

tr-peptides **4a**/**4b**/**4d**/ **4e**/**4f**/**4j,** from the respective single-crystal structure (**Table 2.1**) and plotted as φ *vs* ψ plot, Ramachandran Plot **Figure 2.9**. These values and plots are compared with reported data for α-amino acid peptides. The φ/ ψ angles of *tr*-peptide **4a** (tr-Gly-Gly-OMe) are not fallen in the allowed region of Ramachandran plot, so it may not form the regular secondary structure in the peptide. The φ/ ψ angles of *tr*-peptide **4b** (tr-Gly-Ala-OMe) and **4f** (tr-Gly-β-Ala-OMe) are fallen in *β*-sheet forming allowed region. The φ/ ψ angles of *tr*-peptide **4d (**tr-Val-Ala-OMe**)** is fallen in the *β*-turn allowed region. However, the φ/ ψ angles of **tr**-peptide **4e** (*tr*-Val-β-Ala-OMe) and **4j** (*tr*-Phe-*β*-Al-OMe) are fallen α-helix forming allowed region. Another torsional angle around the amide bond (ω) is close 180^{o} in native peptides that support the planarity of the amide bond. The ω angles of *tr*-peptides' crystal are also close to 180^{o} with little deviations (~8^{o}), so amide bonds of tr-peptides are a planner. These results may help in the prediction of secondary structure in long peptides containing troponyl residue at *N*-terminal. In *N*-aryl peptides, another the torsion angle (χ) depends upon the nature of amino acid residue and ortho substituents of the aryl group and guide the orientation of aryl group peptide backbone which generate atropoisomers.[24] Herein, we also extracted such torsional angle C1-C2-N-Cα (χ) in *tr*-peptides (**4a/4b/4d/4e/4f/4j**) from the respective single crystal structure (Table 1, Column 6). The χ-value of are in negative (~ -175^{o}) while that of **4b/4d** are in positive (~ +175^{o}). The troponyl carbonyl group of *tr*-peptides **4a/4e/4f/4j** is oriented in the opposite plane than those of tr-peptides **4b/4d**. The Cα' of **4b/4d** is non-chiral in nature, in contrast to *tr*-peptides **4a/4b/4d/4e/4f/4j**. Thus, the Cα'-substituents play important role in orientation of the *N*-troponyl group in *tr*-peptides.

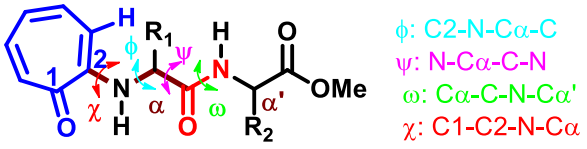

***N*-Troponyl Peptide**

Table 2.1 Torsional angles of the amide backbone φ, ψ, Ω and χ

Entry	Tr-Peptide	ϕ	Ψ	Ω	χ
1	**4a**	-92.6	-1.9	178.7	-172.6
2	**4b**	-177.6	175.8	-179.9	177.6
3	**4d**	76.0	12.0	-178.2	175.1
4	**4e**	-74.2	-54.0	-176.7	-178.4
5	**4f**	-177.1	-178.1	-173.8	-178.4
6	**4j**	-71.0	-47.9	-175.0	-174.6

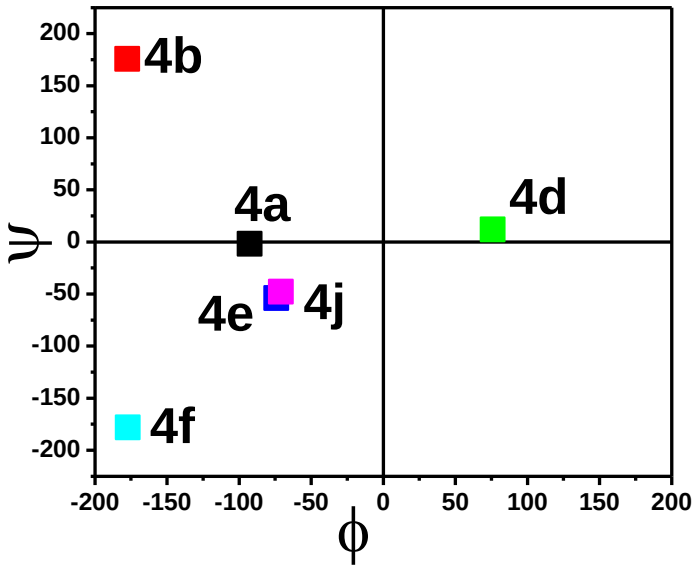

Figure 2.9. Ramachandran Plots of Individual *N*-troponyl Peptides (**4a/4b/4d/4e/4f/4j**).

Secondary structure studies by Circular Dichroism (CD) techniques

Herein, the X-ray studies of *tr*-peptides crystals reveal the ability and importance of troponyl group in the formation of unique self-assembled supramolecular structure in solid-state. We attempted to evaluate the formation of secondary structure in those *tr*-peptides by Circular

Dichroism (CD) technique. In literature, the secondary structure of peptides are well characterized by CD-spectral analyses.[44] We recorded the CD spectra of tr-peptides (**4a-4l**) in two different solvent systems: MeOH (protic polar) and CH_3CN(aprotic polar). Their CD spectra in both MeOH and CH_3CN are provided in **Figure2A.10**. In literature, the typical β-strand structure of native peptides exhibits maxima (~λ 195nm) and minima at ~λ220nm, while their α-helical structure exhibits maxima at ~λ190nm and two minima at ~λ_{208nm} and ~λ_{220}.[45] The CD signals of native peptides structure occur due to electronic transition of n-π* and π-π*. The CD spectra of chromophore rich peptides depend upon the electronic transition of chromophores.[46] Herein, the CD signal of *tr*-peptides also depend upon the electronic transition of troponyl group. The CD spectra of *tr*-peptides **4a**, **4c**, **4f, 4h**, **4j**, **4k**, and **4l** exhibit non-characteristic signal, only a broadminima at (~λ_{26onm}) while CD spectra of **4d/4e/4g/4i** exhibit strong CD signal because of cotton effect on troponyl residue. The CD spectra of *tr*-peptide **4d/4i** exhibit maxima at wavelength 222nm (~λ_{220nm}), and minima at 266nm (~λ_{266nm}). The CD spectra of *tr*-peptide **4e/4g** exhibits a maxima at wavelength 222nm (~λ_{220nm}), and two of minima with different intensities such as weak signal at wavelength 248nm (~λ_{248nm}) and strong signal 266nm (~λ_{266nm}). Thus the *tr*-peptides **4d/4i** form only *β*-strand type of structure in solution (CH_3CN), and *tr*-peptides **4e/4g** possibly form two types of secondary structures (*α*-helix and *β*-sheet and turn) in acetonitrile solution. The CD spectra of *tr*-dipeptides are almost similar in MeOH, protic polar solvent.

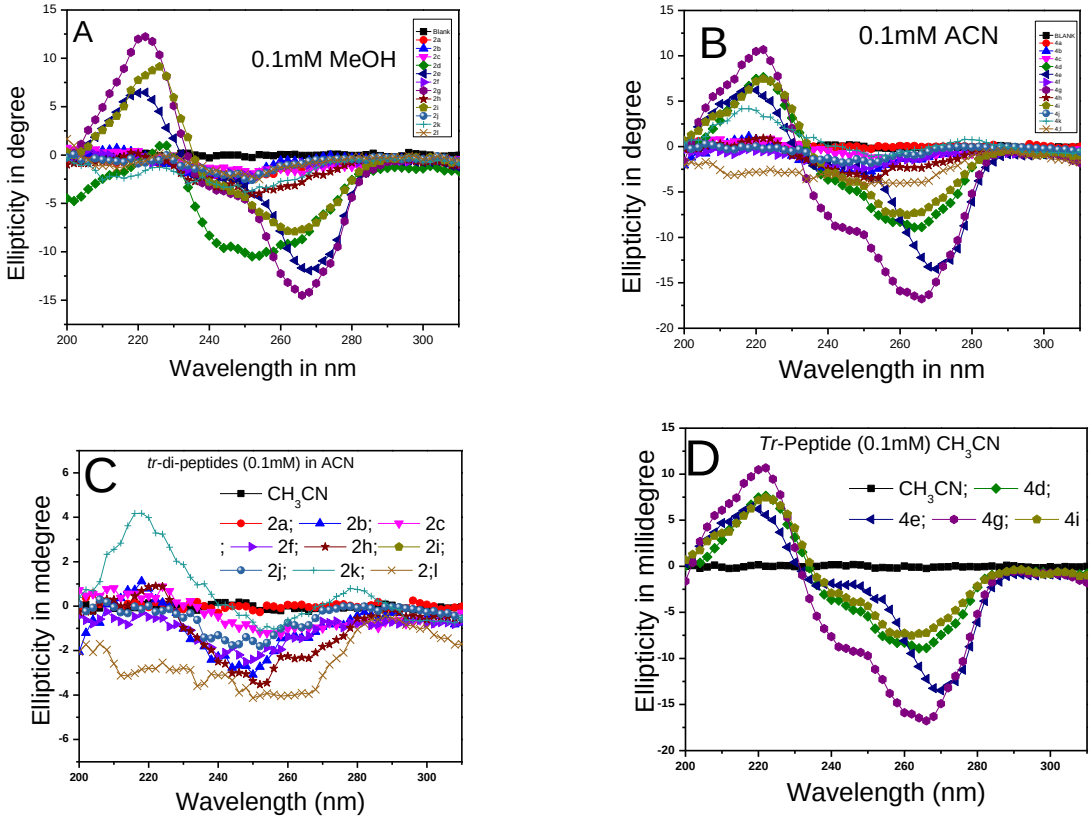

Figure 2.10. CD spectra of tr-peptides in solvent MeOH/CH_3CN: (A) CD spectra of peptide (**4a-4l**) in Methanol (MeOH), (B) CD spectra of peptide (**4a-4l**) in Acetonitrile (CH_3CN), (C) non-characteristic CD signals in peptides (**4a**/**4b**/**4c**/**4f**/**4h**/**4j**/**4k**/**4l**) and (D) Characteristic CD signals of peptides (**4d**/**4e**/**4g**/**4i**).

Confirmational analysis and hydrogen bonding studies by NMR analysis

The formation of *β*-turn/helix type of secondary structure in solution state of *tr*-peptides is mainly due to the intermolecular hydrogen bonding between aminotroponyl-N-H (NH1)/amide-N-H (NH2) with aminotroponyl carbonyl/amide carbonyl oxygen as N-H-----O=C. Generally, DMSO-d_6 titration ^{1}H-NMR experiment reveals the nature of hydrogen bonding as intermolecular or intramolecular.[39] It is well known that *intra*-molecular hydrogen-bonded protons remain unaffected in ^{1}H-NMR spectra with the addition of DMSO-d_6, while

inter-molecular hydrogen-bonded protons exhibit significant downfield shift with the addition of DMSO-d_6. Thus we assigned the chemical shifts of all protons, including N-H's, of representative *di*-/*tri*-peptides (**4a**/**4b**/**4d**/**4e**/**4f**/**4j**) by 2D-NMR analyses. Their spectra are provided in the Supporting Information (Figure. A45-S54). We, then, performed the DMSO-d_6 titration experiment with representative *tr*-peptides such as **4c**/**4j** (exhibit non-characteristic CD- signal) and **4e** (exhibit *β*-strand type of characteristic CD signal)**.** Their NMR spectra are provided in the Supporting Information (Appendix. S59-64). We generated a titration plot, DMSO-d_6 concentration *vs.* chemical shift (ppm) from respective sequential ^{1}H-NMR data. Their NMR-titration plots and outcomes are depicted in **Figure 2.11**. We noticed that the significant increment in the chemical shift of amide-N-H (**4c**/**4e/4j**) after increasing the concentration of DMSO-d_6 in $CDCl_3$. The chemical shift of NH-1 and NH-2 are sequentially increased after the addition of DMSO-d_6 in *tr*-peptide (**4c**) $CDCl_3$ solution, though that increment in NH-1 is higher than NH-2. It suggests that NH-2 has some sort of intramolecular hydrogen bonding with the carbonyl. With help of its NOE data (2D-NMR), we propose the conformation of *tr*-peptide (**4c**) as Figure. 10A, (bottom). The CD signal of *tr*-peptide (**4c**) is also non-characteristic. In case of *tr*-peptide (**4e**), there is no significant changes in the chemical shifts of both NH-1 and NH-2, so both are involved in the *intra*-molecular hydrogen bonding. With help of its NOE data, we propose the conformation of *tr*-peptide (**4e**) in solution ($CDCl_3$) as Figure. 10B (bottom). This proposed conformation resembles like the unique *β*-strand type of structure. Importantly, its CD signals (in both solvents CH_3CN & MeOH) strongly support the formation of *β*-strand type of secondary structure. In case of tr-peptide (**4j**), the chemical shift of N-H1 (in $CDCl_3$) is almost constant with addition of DMSO-d_6, though the chemical shift of N-H2 (in $CDCl_3$) is increased with DMSO-d_6 addition (Figure. 2A.11C). It suggests that only NH-1 is involved in intra-molecular hydrogen bonding. With the help of its NOE

data, we propose the conformation of *tr*-peptide (**4j**) in solution ($CDCl_3$) as Figure. 2A.11C, (bottom). The CD signal of tr-peptide (**4j**) is also non-characteristic.

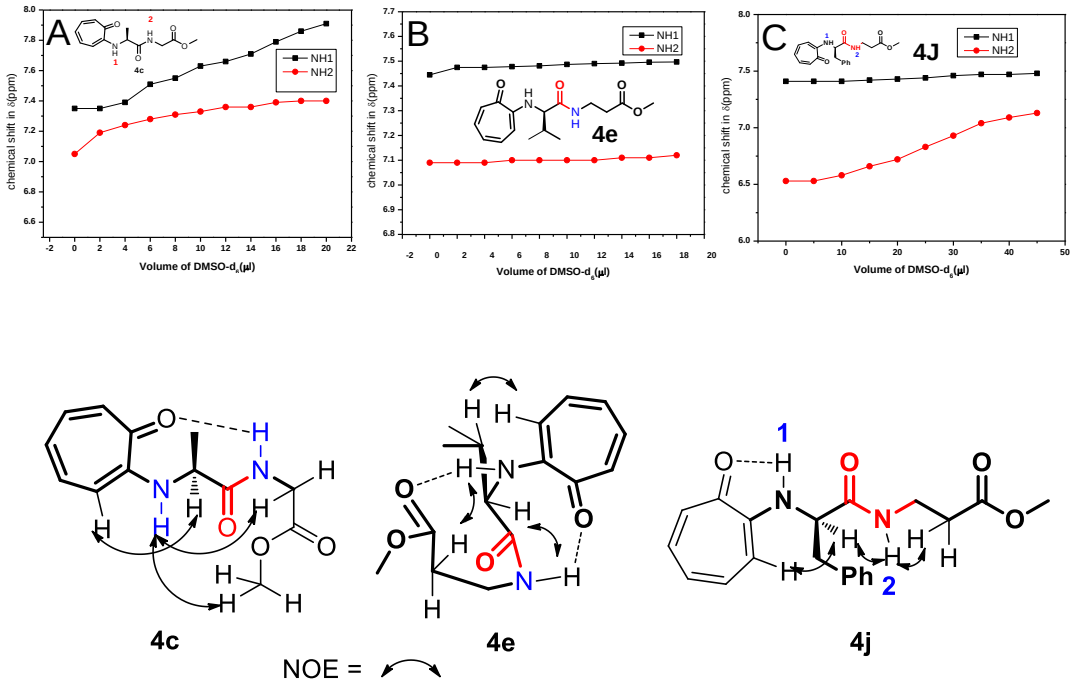

Figure 2.11. DMSO-d_6 titration ^{1}H-NMR experiment of peptide of **4c** (A)/ **4e**(B)/**4j** (C) and NOE and possible intramolecular hydrogen bonding in respective tr-peptides (D)

Our X-ray, NMR titration, and CD studies results reveal that the troponyl substituted *di*-peptides adopt *β*-strand type of secondary structure in a few *tr*-*di*-peptides. We notice that the formation of *β*-sheet structure is more pronounced with troponyltaed hybrid peptides, containing *α*-amino acid and *β*-alanine dipeptides. Thus, for practical utilities, we synthesized hybrid peptides such as *roponyl*-*α*-*β*-*α*-hybrid *tri*-peptides (**5a**-**5e**) by following **Scheme 2**. For control studies, we also synthesized non-troponyl *α*-*β*-*α*-hybrid *tri*-peptides (**6a**-**6e**) by following a similar synthetic procedure (**Scheme 2.2**).

Their characterization data are provided in the appendix (**Figure. A25-A44**). We also synthesized *tr*-peptides (**5a-5e)** from the free amine derivative of control peptides by troponylation reaction with *O-tosylatetropolone.*

Scheme 2.2. Synthesis of *N*-Troponylated tri-peptides and control peptides

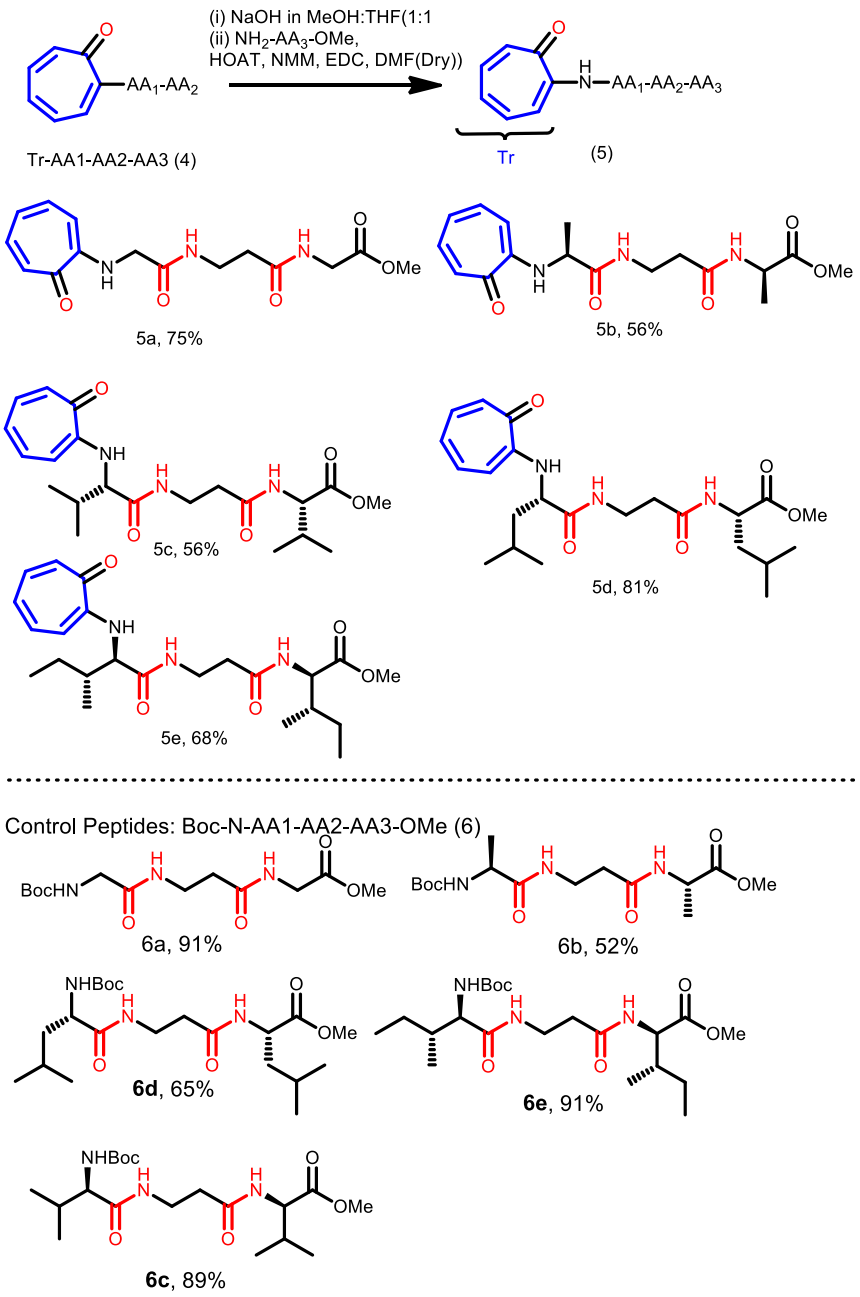

We recorded the CD-spectra of *tr*-tripeptides (**5a-5e**) in two different solvent systems (MeOH & CH_3CN). For comparative studies, we also recorded CD spectra of control peptides (**6a-6e**). These CD spectra in solvent CH_3CN are provided in **Figure. 2A.12** (A & B), while those in MeOH are given in the appendix (Figure S70-71). In solvent MeOH, the CD spectra of tripeptides **5b**, **5c** & **5e** exhibit similar pattern as *tr-di*-peptide (maxima at λ_{220nm} and minima ~λ_{260nm}) which are characteristic of *β*-strand type of secondary structure. The CD spectra of **5e** exhibit similar strong maxima (λ_{220nm}) and minima (λ_{260nm}) and more stable. The CD spectra of tr-peptide (**5d**) exhibits a characteristic signal such as broad minima (-λ_{250nm}) and one maxima (λ220nm). This CD data strongly support the formation of helical types of structure. However, the CD spectra of *tr*-peptide (**5a)** exhibit only minima (λ_{250nm}), non-characteristic in the peptide. In contrast, the CD spectra of control hybrid peptides (**6a-6e**) exhibit only maxima at λ_{220nm} in MeOH, which are non-characteristic signals. The comparative CD studies of troponyl *tri*-peptides (**5a-5e)** are almost similar in another solvent MeOH. Hence troponyl residue influence the formation of *β*-strand/turn types of secondary structure in *tr-tri*-peptides, hybrid peptides.

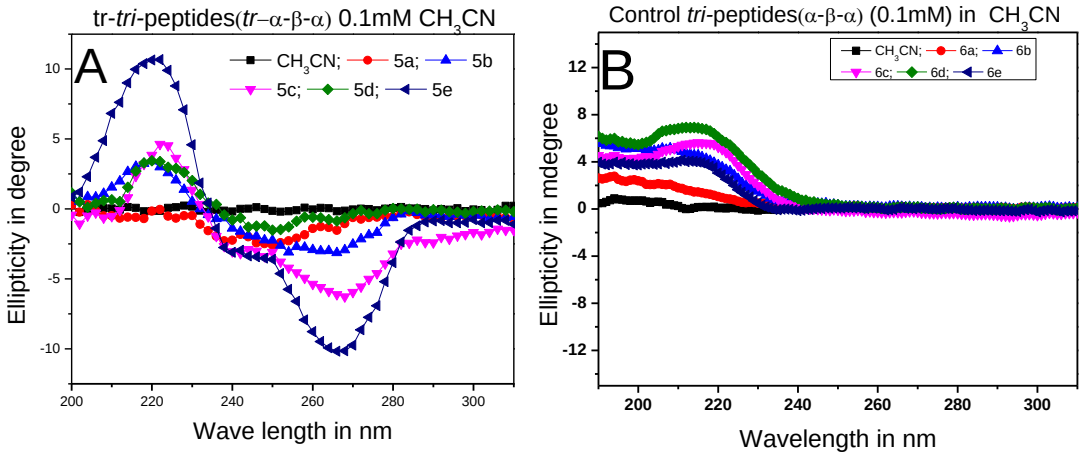

Figure. 2.12. CD Spectra of *tr-tri*-peptides and control *tri*-peptides in CH_3CN.

Nevertheless, we assigned all protons, along with the N-H's, of tr-tri-peptides (**5c/5d**) by 2D-NMR analyses (appendix, Figure S55-S58). We, then, performed DMSO-d6 1H-NMR titration experiments with tr-peptide **5d/5e** and generated a titration plot, DMSO-d6 concentration vs chemical shift (ppm) from respective sequential 1H-NMR data (**Figure 2.13**.). Though, subsequent 1H-NMR data are provided in the appendix (Figure S65-S68). In case of tr-peptide (**5d**), there is no significant changes in the chemical shifts of both NH-2 and NH-3, so both are involved in the *intra*-molecular hydrogen bonding. Though the chemical shift of NH-1 in *tr*-peptide (**5d**) is significantly shifted with the addition of DMSO-d_6. With help of its NOE data, we propose the conformation of *tr*-peptide (**5d**) in solution ($CDCl_3$) as Figure **Figure2.13**, (bottom). This proposed conformation supports the formation of helical structure as like i+8 helix. Importantly, its CD signals (in both solvents CH_3CN & MeOH) also support the formation of a helix type of secondary structure. In the case of *tr*-peptide (**5e**), there is no significant changes in the chemical shifts NH-1/NH-2, so these are involved in the *intra*-molecular hydrogen bonding. Though the chemical shift of NH-3 in tr-peptide (**5e**) are marginally increased with the addition of DMSO-d_6. It means NH-3 is not involved/weakly involved in intramolecular hydrogen bonding. With the help of its NOE data, we propose the conformation of *tr*-peptide (**5e**) in solution ($CDCl_3$) as Figure. 10B, (bottom). This proposed structural conformation supports the formation of β-strand (*β*-turn) types of secondary structure in tr-peptide (**5e**). Importantly, its CD signals (in both solvents CH_3CN & MeOH) also support the formation of β-strand (β-turn) types of secondary structure.

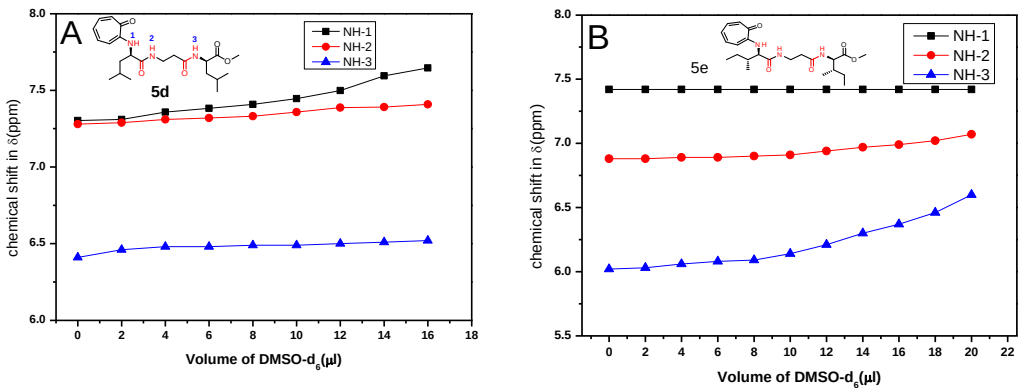

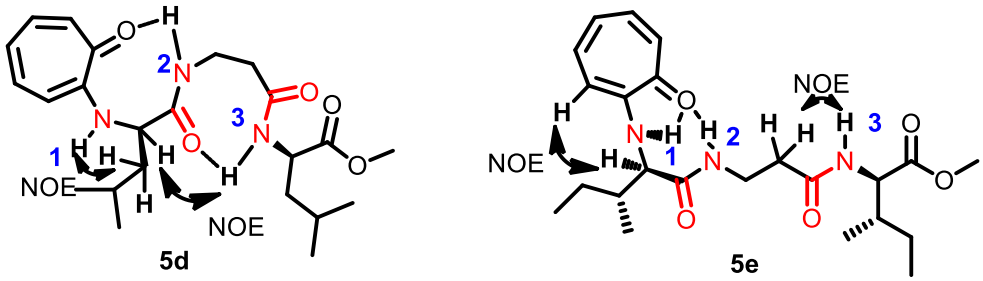

Figure 2.13. DMSO-d_6 titration ^{1}H-NMR experiment of peptide **5c (A)/5d(B) and** NOE and possible intramolecular hydrogen bonding in respective tr-peptides (C).

2.4 Conclusions

The synthesis of *N*-tropolonylated *di-/tri*-peptides are accomplished containing native α-amino acids and *β*-alanine. Herein, the role of tropolone residue is demonstrated the formation of unique secondary structure, even in *di-/tri*-peptides, by NMR, X-Ray, and CD-studies. The X-ray studies of *di*-peptides confirm the establishment of a unique self-assembled supramolecular structure as *β*-sheet and helical type of secondary structures in a respective single crystal solid. The DMSO-d_6 NMR titration studies reveal that aminotroponyl N-H's are involved in the inter/intramolecular hydrogen bonding in the solution state. The CD spectral analysis of tropolonylated *di-/tri* peptides strongly supports the formation of *β*-sheet/turn type of structure in solution (MeOH and CH_3CN) in contrast to native control peptides. Hence, the *N*-tropolonylation of peptides influences the formation of regular secondary structures even in a small peptide which could be useful in the synthesis of novel peptidomimetics for practical applications including therapeutic drug candidates and novel biomaterials.

2.5 Experimental Procedure

Material and Instrumentation: All required chemical materials were obtained from commercial and used without purification. Anhydrous DMF was freshly prepared by distilling over calcium hydride. The reaction was monitored by thin-layer chromatography (TLC), purification by Column chromatography (230-400/100-200 mesh silica). Mass spectra were recorded by Bruker MicrOTOF-Q II Spectrometer. NMR spectra were recorded on Bruker AV-700MHz and Bruker AV-400 (^{1}H:400MHz ,^{13}C:100.6 MHz),^{1}H and ^{13}C-NMR chemical shift were recorded in ppm downfield from tetramethylsilane, splitting patterns are abbreviated as: s, singlet; d, doublet; dd, doublet of doublet; t, triplet; q, quartet; dq, doublet of quartet; m, multiple. CD experiment were performed on JASCO-J 1500 all CD experiment were performed at 20°C.All CD spectra recorded two scans averaged, CD spectra recorded from 310-190 nm.

Syntheses of Troponyl monomer: A solution of 2-tosyloxy tropone (1.00g, 3.61 mmol) in ethanol (50mL), was added in neutralized amino methyl ester (1.2mg,7.23mmol) and refluxed. The reaction was monitored by using thin layer chromatography and found the completion of reactions after 36 hours. After cooling the reaction mixture to room temperature it was concentrated under reduced pressure. The reaction mixture was dissolved in DCM(50mL) and washed with water(50ml) three times and then brine(50mL) solution one time using the separating flask. The organic layer was kept Na_2SO4 for 20 minutes and then concentrated under vacuum. The concentrated crude residue was purified by the column chromatography method. The product was purified by using solvent 30% ethyl acetate in hexane[1]; the N-troponyl aminomethyl ester was dissolved in EtOH and THF (1:1), to this reaction mixure 2 eq. of NaOH was dissolved in little amont of disstiled water was added and allowed to stir under the room temperature. The reaction mixture was monitered by TLC, after 15min. After the completion of reaction, the solvent was removed under the reduced pressure and 1N HCl

was added to the crude product followed by extraction with EtOAC. The organic layers were combined together, dried over Na_2SO_4 and concentrated under low pressure to afford the pure product as yellow gelatinous liquid. This Troponyl momnomer acid was futher used for peptide synthesis[2].

General procedure for peptide synthesis: L-amino methyl ester (1.2 eq) was neutralized with Et_3N and to the reaction mixture of troponyl monomer amino acid (1.0 eq.) in anhydrous DMF (10 ml) with NMM (3.0 eq.), HOAT (1.3 eq.), and EDC-HCL (1.3 eq.) and then allow to stir overnight. After complication of reaction, the reaction mixture was concentrated under reduced pressure. Concentrated reaction mixture was extracted three times with methylene chloride. The organic layer was combined, dried over saturated sodium bicarbonate. The washed organic layer was combined together and concentrated under reduced pressure and purified using silica gel to obtain desired product. The obtained product was characterised by ^{1}H -/^{13}C-NMR and ESI-ToF-HRMS mass techniques. The characterization of all synthesized hybrid peptide data is provided in bellow.

Analytical data

Methyl-(2-((7-oxocyclohepta-1,3,5-trien-1-yl)amino)acetamido)acetate ***(4a)****. (tr-Gly-Gly-OMe)* The dipeptide was synthesized by the following general procedure. The Pure product was obtained as yellowish solid (60 mg, 80% yield,) ^{1}H NMR (400 MHz, $CDCl_3$) δ 7.57 (s, 1H), 7.35 – 7.16 (m, 4H), 6.92 (s, 1H), 6.81 (t, *J* = 9.5 Hz, 1H), 6.54 (d, *J* = 10.2 Hz, 1H), 4.12 (d, *J* = 6.3 Hz, 2H), 4.06 (d, *J* = 5.5 Hz, 2H), 3.71 (s, 3H), 3.49 (s, 1H). ^{13}C NMR (101 MHz, $CDCl_3$) δ 177.34, 169.77, 168.64, 154.90, 137.90, 136.28, 130.75, 124.64, 110.24, 52.42, 47.04, 41.00. HRMS (ESI-TOF) m/z: $[M+Na]^+$ Calcd. For $C_{12}H_{14}N_2O_4$ 273.0846, found 273.0852.

Methyl-(2-((7-oxocyclohepta-1,3,5-trien-1-yl)amino)acetamido)propanoate ***(4b).*** *(tr-Gly-ala-OMe)* The dipeptide was synthesized by the following general procedure .The Pure product was obtained as light-yellow solid (66 mg, 74% yield) ^{1}H NMR (400 MHz, $CDCl_3$) δ 7.68 (t, *J* = 5.7 Hz, 1H), 7.33 – 7.08 (m, 4H), 6.78 (t, *J* = 9.5 Hz, 1H), 6.53 (d, *J* = 10.2 Hz, 1H), 4.63 (p, *J* = 7.3 Hz, 1H), 4.10 (d, *J* = 6.2 Hz, 2H), 3.69 (s, 3H), 1.37 (d, *J* = 7.2 Hz, 3H). ^{13}C NMR (101 MHz, $CDCl_3$) δ 177.23, 172.88, 167.99, 155.04, 137.84, 136.29, 130.50, 124.40, 110.20, 52.48, 48.05, 47.06, 29.69, 17.92. HRMS (ESI-TOF) m/z: $[M+H]^+$ Calcd. For $C_{13}H_{16}N_2O_4$ 265.1183, found 265.1210.

Methyl-(2-((7-oxocyclohepta-1,3,5-trien-1-yl)amino)propanamido)acetate ***(4c).*** *(tr-ala-Gly-OMe)* The dipeptide was synthesized by the following general procedure .The Pure product was obtained as light red Viscous liquid (86 mg, 63% yield) ^{1}H NMR (400 MHz, $CDCl_3$) δ 7.31 (dd, *J* = 6.5, 5.1 Hz, 1H), 7.27 – 7.15 (m, 3H), 7.09 (s, 1H), 6.80 (t, *J* = 9.5 Hz, 1H), 6.53 (d, *J* = 10.2 Hz, 1H), 4.13 – 4.04 (m, 1H), 4.01 (dd, *J* = 5.8, 2.3 Hz, 2H), 3.70 (s, 3H), 1.68 (d, *J* = 7.0 Hz, 3H). ^{13}C NMR (101 MHz, $CDCl_3$) δ 177.20, 172.69, 169.78, 154.24, 137.91, 136.44, 130.68, 124.64, 110.98, 77.36, 77.04, 76.72, 53.99, 52.33, 40.98, 19.14. HRMS (ESI-TOF) m/z: $[M+Na]^+$ Calcd. For $C_{13}H_{16}N_2O_4$ 287.1002, found 287.1026.

Methyl-(3-methyl-2-((7-oxocyclohepta-1,3,5-trien-1-yl)amino)butanamido)acetate ***(4d).*** *(tr-Val-Gly-OMe)* The dipeptide was synthesized by the following general procedure .The Pure product was obtained as yellowish solid (200 mg, 70% yield,) ^{1}H NMR (700 MHz, $CDCl_3$) δ 7.48 – 7.44 (m, 1H), 7.44 – 7.36 (m, 1H), 7.29 – 7.20 (m, 3H), 7.15 – 7.07 (m, 1H), 6.80 (dd, *J* = 20.6, 11.1 Hz, 1H), 6.57 (d, *J* = 10.3 Hz, 1H), 4.59 (s, 1H), 4.09 (dd, *J* = 17.9, 6.0 Hz, 1H), 3.96 (dd, *J* = 17.9, 5.7 Hz, 1H), 3.87 (t, *J* = 5.7 Hz, 1H), 3.69 (s, 3H), 2.53 – 2.48 (m, 1H), 1.12 (dd, *J* = 30.4, 6.9 Hz, 6H). ^{13}C NMR (101 MHz, $CDCl_3$) δ 177.01, 171.43, 169.78, 155.00, 137.95, 136.68, 130.04, 126.74, 124.53, 111.08, 63.79, 52.26, 40.98, 31.26, 19.60, 17.87. HRMS (ESI-TOF) m/z: $[M+H]^+$ Calcd. For $C_{15}H_{20}N_2O_4$ 293.1496, found 293.1515.

Methyl-(3-methyl-2-((7-oxocyclohepta-1,3,5-trien-1-yl)amino)butanamido)propanoate ***(4e).*** *(tr-Val-β-ala-OMe)* The dipeptide was synthesized by the following general procedure .The Pure product was obtained as light red Viscous liquid (551 mg, 62% yield,) ^{1}H NMR (700 MHz, CDCl3) δ 7.44 (d, J = 6.3 Hz, 1H), 7.32 – 7.25 (m, 1H), 7.20 – 7.16 (m, 1H), 7.13-7.10 (m, 2H, 6.75 (q, J = 9.5 Hz, 1H), 6.45 (d, J = 10.3 Hz, 1H), 3.78 (t, J = 6.0 Hz, 1H), 3.54 – 3.45 (m, 5H), 2.53 – 2.47 (m, 2H), 2.47 – 2.38 (m, 1H), 1.11 – 1.05 (m, 6H). ^{13}C NMR (176 MHz, CDCl3) δ 176.89, 172.17, 170.88, 154.95, 137.62, 136.46, 129.69, 123.79, 110.15, 63.97, 51.60, 35.22, 33.85, 31.11, 19.58, 18.24. HRMS (ESI-TOF) m/z: $[M+H]^+$ Calcd. For $C_{16}H_{22}N_2O_4$ 307.1652, found 307.1674.

Methyl-(2-((7-oxocyclohepta-1,3,5-trien-1-yl)amino)acetamido)propanoate ***(4f).*** *(tr-Gly-β-ala-OMe)* The dipeptide was synthesized by the following general procedure .The Pure product was obtained as light-yellow solid (160 mg, 95% yield) ^{1}H NMR (400 MHz, $CDCl_3$) δ 7.35 – 7.27 (m, 2H), 7.14 (d, *J* = 11.6 Hz, 1H), 6.82 (t, *J* = 9.5 Hz, 1H), 6.60 (d, *J* = 10.4 Hz, 1H), 4.14 (s, 2H), 4.03 (s, 2H), 3.82 (s, 2H), 3.71 (d, *J* = 2.4 Hz, 3H). ^{13}C NMR (101 MHz, $CDCl_3$) δ 177.03, 170.11, 169.23, 155.12, 150.47, 138.02, 136.75, 129.85, 128.86, 124.36, 120.46, 110.63, 76.83, 52.23, 46.30, 40.84. HRMS (ESI-TOF) m/z: $[M+H]^+$ Calcd. For $C_{13}H_{16}N_2O_4$ 265.1183, found 265.1196.

Methyl-(4-methyl-2-((7-oxocyclohepta-1,3,5-trien-1yl)amino)pentanamido)propanoate ***(4g).*** *(tr-leu-β-ala-OMe)* The dipeptide was synthesized by the following general procedure .The Pure product was obtained as light yellow Viscous liquid (392 mg, 62% yield) ^{1}H NMR (400 MHz, $CDCl_3$) δ 7.36 – 7.31 (m, 1H), 7.29 (d, *J* = 4.7 Hz, 1H), 7.27 – 7.18 (m, 3H), 6.88 – 6.76 (m, 2H), 6.45 (d, *J* = 10.2 Hz, 1H), 3.99 – 3.95 (m, 1H), 3.54 – 3.44 (m, 5H), 2.49 (t, *J* = 6.1 Hz, 2H), 1.96 – 1.78 (m, 3H), 1.01 (d, *J* = 6.0 Hz, 1H), 0.91 (d, *J* = 6.0 Hz, 3H). ^{13}C NMR (176 MHz, $CDCl_3$) δ 177.32, 172.30, 172.01, 154.53, 137.86, 136.36, 130.63, 124.35, 110.17, 57.14,

51.79, 42.13, 35.07, 25.24, 23.14, 21.52. HRMS (ESI-TOF) m/z: $[M+H]^+$ Calcd. For $C_{17}H_{24}N_2O_4$ 321.1809, found 321.1820.

Methyl-(2-((7-oxocyclohepta-1,3,5-trien-1-yl)amino)propanamido)propanoate ***(4h).*** (*Tr-Ala-β-Ala-OMe*) The dipeptide was synthesized by the following general procedure. The Pure product was obtained as light red Viscous liquid (200 mg, 70% yield) ^{1}H NMR (400 MHz, $CDCl_3$) δ 7.34 – 7.28 (m, 1H), 7.24 – 7.16 (m, 3H), 6.84 (s, 1H), 6.78 (t, *J* = 9.5 Hz, 1H), 6.40 (d, *J* = 10.2 Hz, 1H), 4.05-3.99 (m, 1H), 3.56 – 3.42 (m, 5H), 2.49 (t, *J* = 6.1 Hz, 2H), 1.64 (d, *J* = 7.0 Hz, 3H). ^{13}C NMR (101 MHz, $CDCl_3$) δ 177.20, 172.18, 171.97, 154.12, 137.72, 136.12, 130.74, 124.27, 110.17, 77.37, 77.05, 76.74, 54.07, 51.70, 34.94, 33.70, 29.70, 19.11. HRMS (ESI-TOF) m/z: $[M+Na]^+$ Calcd. For $C_{14}H_{18}N_2O_4$ 301.1159, found 301.1184.

Methyl-((2S,3R)-3-methyl-2-((7-oxocyclohepta-1,3,5-trien-1-yl)amino)pentanamido)propanoate ***(4i).*** *(tr-Ile-β-ala-Ome)* The dipeptide was synthesized by the following general procedure . The Pure product was obtained as light red Viscous liquid (86 mg, 60% yield) ^{1}H NMR (400 MHz, $CDCl_3$) δ 7.41 (d, *J* = 20.5 Hz, 1H), 7.29 – 7.09 (m, 4H), 6.74 (t, *J* = 8.9 Hz, 1H), 6.46 (d, *J* = 9.4 Hz, 1H), 3.83 (s, 1H), 3.50 (s, 5H), 2.49 (s, 2H), 2.15 (s, 1H), 1.61 (s, 1H), 1.39 (ddd, *J* = 20.4, 13.4, 6.5 Hz, 1H), 1.08 – 0.83 (m, 7H). ^{13}C NMR (101 MHz, $CDCl_3$) δ 172.15, 170.65, 154.87, 137.64, 136.31, 130.02, 123.93, 110.08, 77.41, 77.10, 76.78, 63.16, 51.62, 37.60, 35.06, 33.77, 25.15, 15.98, 11.51. HRMS (ESI-TOF) m/z: $[M+Na]^+$ Calcd. For $C_{17}H_{24}N_2O_4$ 343.1628, found 343.1603,

Methyl-(2-((7-oxocyclohepta-1,3,5-trien-1-yl)amino)-3-phenylpropanamido)propanoate ***(4j).*** *(tr-Phe-β-ala-OMe)* The dipeptide was synthesized by the following general procedure . The Pure product was obtained as light-yellow solid (150 mg, 78% yield) ^{1}H NMR (400 MHz, $CDCl_3$) δ 7.45 (d, *J* = 4.2 Hz, 1H), 7.36 – 7.21 (m, 6H), 7.15 (dd, *J* = 20.5, 10.8 Hz, 1H), 6.75 (dd, *J* = 20.1, 10.3 Hz, 2H), 6.40 (d, *J* = 10.2 Hz, 1H), 4.20 (d, *J* = 5.3 Hz, 1H), 3.56 – 3.38 (m,

5H), 3.27 (dt, *J* = 13.9, 10.3 Hz, 2H), 2.51 – 2.37 (m, 2H), 2.07 (s, 1H). ^{13}C NMR (101 MHz, $CDCl_3$) δ 177.16, 172.04, 170.48, 154.19, 137.63, 136.05, 135.85, 130.50, 129.22, 128.92, 127.38, 124.19, 110.10, 59.27, 51.67, 38.68, 34.96, 33.66. HRMS (ESI-TOF) m/z:$[M+Na]^+$ Calcd. For $C_{20}H_{22}N_2O_4$ 377.1472, found 377.1476.

Methyl-methyl-2-((-5-(7-oxocyclohepta-1,3,5-trien-1-yl)pyrrolidine-2-carboxamido)butanoate ***(4k).*** *(tr-Pro-val-OMe)* The dipeptide was synthesized by the following general procedure. The Pure product was obtained as light red Viscous liquid (300 mg, 58% yield,) ^{1}H NMR (400 MHz, $CDCl_3$) δ 7.10 – 6.99 (m, 2H), 6.87 (d, *J* = 11.7 Hz, 1H), 6.70 (d, *J* = 8.5 Hz, 1H), 6.55 (t, *J* = 9.2 Hz, 1H), 6.47 (d, *J* = 10.5 Hz, 1H), 5.21 (d, *J* = 3.5 Hz, 1H), 4.50 – 4.43 (m, 1H), 3.75 (dd, *J* = 13.9, 8.4 Hz, 1H), 3.66 (s, 3H), 3.45 (dd, *J* = 16.7, 6.9 Hz, 1H), 2.29 – 1.90 (m, 6H), 0.91 (dd, *J* = 10.6, 7.3 Hz, 6H). ^{13}C NMR (101 MHz, $CDCl_3$) δ 180.30, 172.40, 172.09, 155.51, 135.69, 134.35, 132.48, 123.03, 113.97, 77.61, 77.29, 76.97, 63.54, 57.03, 51.94, 51.70, 31.35, 31.08, 23.23, 18.93, 17.76. HRMS (ESI-TOF) m/z: $[M+Na]^+$ Calcd. For $C_{18}H_{24}N_2O_4$ 355.1629, found 355.1627.

Methyl-(3-((7-oxocyclohepta-1,3,5-trien-1-yl)amino)propanoyl)pyrrolidine-2-carboxylate ***(4l).*** *(tr-β-ala-Pro-OMe)* The dipeptide was synthesized by the following general procedure. The Pure product was obtained as light red Viscous liquid (80 mg, 58% yield,) ^{1}H NMR (700 MHz, $CDCl_3$) δ 7.33 (s, 1H), 7.27 – 7.24 (m, 1H), 7.22 (t, *J* = 9.5 Hz, 1H), 7.13 (d, *J* = 11.5 Hz, 1H), 6.67 (t, *J* = 9.5 Hz, 1H), 6.61 (d, *J* = 10.4 Hz, 1H), 4.49 (dd, *J* = 8.5, 3.8 Hz, 1H), 3.77 – 3.71 (m, 4H), 3.71-3.69 (m, 1H), 3.65 – 3.60 (m, 1H), 3.49-3.46 (m, 1H), 2.79 – 2.66 (m, 2H), 2.19-2.16 (m, 1H), 2.11 – 2.03 (m, 1H), 2.03 – 1.94 (m, 2H), 1.82 (s, 1H). ^{13}C NMR (176 MHz, $CDCl_3$) δ 176.84, 172.76, 169.13, 155.46, 137.42, 136.42, 128.86, 122.53, 108.77, 77.32, 77.14, 76.96, 58.81, 52.42, 47.13, 38.38, 33.39, 29.28, 24.81. HRMS (ESI-TOF) m/z: $[M+H]^+$ Calcd. For $C_{18}H_{24}N_2O_4$ 305.1496, found 305.1519.

Methyl-(3-(2-((7-oxocyclohepta-1,3,5-trien-1-yl)amino)acetamido)propanamido)acetate ***(5a).*** *(tr-Gly-β-ala-Gly-OMe)* The Pure product was obtained as yellowish solid (155 mg, 75% yield,) ^{1}H NMR (700 MHz, MeOD) δ 7.41-7.44 (m, 4H), 7.14 (d, *J* = 11.5 Hz, 1H), 6.84 (t, *J* = 9.4 Hz, 1H), 6.69 (d, *J* = 10.3 Hz, 1H), 4.13 (s, 2H), 3.99 (d, *J* = 9.4 Hz, 1H), 3.93 – 3.88 (m, 3H), 3.81 (s, 2H), 3.74 – 3.68 (m, 4H), 3.54 (t, *J* = 6.4 Hz, 2H), 2.50 (t, *J* = 6.4 Hz, 2H). ^{13}C NMR (176 MHz, MeOD) δ 174.27, 172.00, 170.53, 169.06, 157.02, 149.86, 140.43, 139.38, 138.58, 136.41, 129.81, 129.30, 121.51, 46.64, 46.61, 46.57, 41.91, 41.87, 41.84, 41.03, 37.02, 36.29. HRMS (ESI-TOF) m/z: $[M+Na]^+$ Calcd. For $C_{15}H_{19}N_3O_5$ 344.1217, found 34401195.

Methyl-(3-(2-((7-oxocyclohepta-1,3,5-trien-1-yl)amino)propanamido)propanamido)propanoate ***(5b).*** *(tr-Ala-β-ala-Ala-OMe)* The Pure product was obtained as light red Viscous liquid (290 mg, 56% yield) ^{1}H NMR (700 MHz, $CDCl_3$) δ 7.38 – 7.23 (m, 3H), 7.19 (t, *J* = 10.1 Hz, 1H), 7.13 (d, *J* = 11.6 Hz, 1H), 6.85 – 6.69 (m, 2H), 6.45 (dd, *J* = 19.6, 10.3 Hz, 1H), 4.44 (td, *J* = 7.2, 3.3 Hz, 1H), 4.08 – 4.04 (m, 1H), 3.72 (s, 3H), 3.63 – 3.41 (m, 2H), 2.43 (dtd, *J* = 21.5, 14.9, 8.6 Hz, 2H), 1.61 (d, *J* = 7.0 Hz, 3H), 1.43 – 1.22 (m, 4H). ^{13}C NMR (176 MHz, $CDCl_3$) δ 176.95, 173.52, 172.38, 171.04, 154.32, 137.70, 136.39, 130.17, 123.96, 110.20, 110.11, 53.72, 52.53, 48.10, 35.77, 18.95, 17.87. HRMS (ESI-TOF) m/z: $[M+Na]^+$ Calcd. For $C_{17}H_{23}N_3O_5$ 372.1530, found 372.1518.

Methyl-methyl-2-(3-(-3-methyl-2-((7-oxocyclohepta-1,3,5-trien-1-yl)amino)butanamido)propanamido)butanoate ***(5c).*** *(tr-Val-β-ala-Val-OMe)* The Pure product was obtained as light red Viscous liquid (250 mg, 56% yield) ^{1}H NMR (700 MHz, $CDCl_3$) δ 7.43 (dd, *J* = 14.0, 6.5 Hz, 1H), 7.30 (dd, *J* = 19.6, 9.1 Hz, 1H), 7.24 – 7.17 (m, 2H), 7.06 (s, 5H), 6.75 (t, *J* = 9.5 Hz, 1H), 6.48 (t, *J* = 11.4 Hz, 1H), 6.25 (d, *J* = 8.0 Hz, 1H), 4.45 (dd, *J* = 8.1, 5.3 Hz, 1H), 3.79 (t, *J* = 5.3 Hz, 1H), 3.73 (d, *J* = 6.7 Hz, 3H), 3.61 (dq, *J* = 12.3, 6.0 Hz, 1H), 3.48 (td, *J* = 12.4, 5.9 Hz, 1H), 2.50 – 2.37 (m, 3H), 2.08 (mz, 1H), 1.06 (dd, *J* = 14.7, 6.8 Hz, 6H), 0.92 – 0.80 (m, 6H). ^{13}C NMR (176 MHz, $CDCl_3$) δ 176.99, 172.38, 171.10,

170.87, 154.91, 137.65, 136.25, 129.99, 123.94, 110.11, 77.16, 76.98, 76.80, 63.72, 57.13, 52.17, 35.57, 35.53, 31.18, 30.91, 19.49, 18.86, 18.08, 17.77. HRMS (ESI-TOF) m/z: $[M+H]^+$ Calcd. For $C_{21}H_{31}N_3O_5$ 406.2336, found 406.2340.

Methyl-methyl-2-(3-((-4-methyl-2-((7-oxocyclohepta-1,3,5-trien-1-yl)amino)pentanamido) propanamido) pentanoate ***(5d).*** *(tr-Leu-β-ala-Leu-OMe)* The Pure product was obtained as light red Viscous liquid (230 mg, 68% yield) ^{1}H NMR (400 MHz, $CDCl_3$) δ 7.39 – 7.10 (m, 5H), 6.74 (t, *J* = 9.4 Hz, 1H), 6.55 – 6.34 (m, 2H), 4.51 (s, 1H), 3.99 (d, *J* = 5.7 Hz, 1H), 3.73 (s, 3H), 3.52 (dddd, *J* = 35.2, 27.0, 13.2, 6.1 Hz, 2H), 2.43 (dt, *J* = 32.7, 11.3 Hz, 2H), 1.83 (dt, *J* = 11.5, 8.0 Hz, 3H), 1.61 (d, *J* = 6.2 Hz, 2H), 1.54 – 1.38 (m, 1H), 1.36 – 1.21 (m, 1H), 1.02 – 0.83 (m, 12H). ^{13}C NMR (101 MHz, $CDCl_3$) δ 177.07, 173.57, 172.25, 171.06, 154.62, 137.61, 136.30, 136.27, 130.22, 123.91, 109.90, 57.02, 52.35, 50.86, 41.13, 35.75, 25.09, 23.01, 22.76, 21.84, 21.48. HRMS (ESI-TOF) m/z: $[M+Na]^+$ Calcd. For $C_{23}H_{35}N_3O_5$ 456.2469, found 456.2441.

Methyl-methyl-2-(3-((-3-methyl-2-((7-oxocyclohepta-1,3,5-trien-1-yl)amino)pentanamido) propanamido)pentanoate ***(5e).*** *(tr-Ile-β-ala-Ile-OMe)* The Pure product was obtained as light red Viscous liquid (340 mg, 81% yield) ^{1}H NMR (400 MHz, $CDCl_3$) δ 7.49 (d, *J* = 6.5 Hz, 1H), 7.36 – 7.09 (m, 4H), 6.77 – 6.68 (m, 1H), 6.52 (dd, *J* = 20.0, 8.8 Hz, 2H), 4.54 – 4.45 (m, 1H), 3.85 (t, *J* = 6.0 Hz, 1H), 3.72 (s, 3H), 3.55 (dtd, *J* = 27.4, 13.3, 6.5 Hz, 2H), 2.55 – 2.38 (m, 2H), 2.10 (dd, *J* = 32.4, 6.0 Hz, 1H), 1.81 (s, 1H), 1.62 (d, *J* = 6.4 Hz, 1H), 1.47 – 1.07 (m, 3H), 1.06 – 0.79 (m, 12H). ^{13}C NMR (101 MHz, $CDCl_3$) δ 176.95, 172.43, 171.05, 170.84, 154.93, 137.55, 136.27, 129.85, 123.68, 109.92, 62.96, 56.46, 52.12, 37.70, 37.60, 35.63, 25.26, 25.19, 15.87, 15.45, 11.55, 11.47. HRMS (ESI-TOF) m/z: $[M+Na]^+$ Calcd. For $C_{23}H_{35}N_3O_5$ 456.2469, found 456.2441.

Methyl,2-dimethyl-4,7,11-trioxo-3-oxa-5,8,12-triazatetradecan-14-oate ***(6a).*** *(Boc-Gly-β-ala-Gly-OMe)* The pure product was obtained as white solid (300 mg, 91% yield) ^{1}H NMR (700 MHz, $CDCl_3$) δ 6.98 (d, *J* = 70.7 Hz, 2H), 5.45 (s, 1H), 4.00 (d, *J* = 5.8 Hz, 2H), 3.74 (d, *J* = 7.4 Hz, 5H), 3.56 (dd, *J* = 11.9, 6.1 Hz, 2H), 2.49 – 2.44 (m, 2H), 2.06 (s, 2H), 1.42 (s, 9H). 13C NMR (101 MHz, CDCl3) δ 170.95, 170.10, 156.19, 80.22, 77.35, 77.03, 76.71, 52.44, 44.39, 41.22, 35.97, 35.74 , 28.30. HRMS (ESI-TOF) m/z: $[M+Na]^+$ Calcd. For $C_{13}H_{23}N_3O_6$ 340.1479, found 340.1476.

Methyl-tetramethyl-4,7,11-trioxo-3-oxa-5,8,12-triazatetradecan-14-oate ***(6b).*** *(Boc-Al-β-ala-Ala-OMe)* The pure product was obtained as white solid (140 mg, 52% yield) ^{1}H NMR (700 MHz, $CDCl_3$) δ 7.20 (d, *J* = 44.7 Hz, 2H), 5.19 (s, 1H), 4.56 (m, 1H), 4.01 (t, *J* = 7.1 Hz, 1H), 3.85 (d, *J* = 5.3 Hz, 2H), 3.75 (s, 3H), 3.20 (s, 1H), 2.44 – 2.27 (m, 2H), 2.04 (d, *J* = 14.2 Hz, 1H), 1.41 (s, 2H), 1.41 (s, 9H), 1.33 (d, *J* = 7.0 Hz, 3H). 13C NMR (101 MHz, CDCl3) δ 174.81, 173.52, 172.38, 155.76, 80.12, 52.59, 50.89, 48.37, 36.73, 28.29, 17.88, 16.96. HRMS (ESI-TOF) m/z: $[M+Na]^+$ Calcd. For $C_{15}H_{27}N_3O_6$ 368.1792, found 368.1795.

Methyl-diisopropyl-2,2-dimethyl-4,7,11-trioxo-3-oxa-5,8,12-triazatetradecan-14-oate ***(6c).*** *(Boc-Val-β-ala-Val-OMe)* The pure product was obtained as white solid (250 mg, 89% yield) ^{1}H NMR (700 MHz, $CDCl_3$) δ 7.46 – 7.38 (m, 1H), 4.42 (d, *J* = 5.7 Hz, 1H), 3.84 (d, *J* = 5.5 Hz, 1H), 3.76 (d, *J* = 6.4 Hz, 3H), 3.72 – 3.65 (m, 1H), 3.36 (t, *J* = 18.2 Hz, 3H), 2.46-2.43 (m, 2H), 2.18 – 2.16 (m, 1H), 2.07-2.05 (m, 1H), 1.47 – 1.42 (m, 10H), 0.99 – 0.88 (m, 12H). ^{13}C NMR (176 MHz, $CDCl_3$) δ 173.29, 172.78, 156.31, 150.68, 129.14, 120.55, 80.01, 60.26, 58.00, 52.24, 36.11, 30.31, 29.67, 28.28, 19.23, 19.04, 18.12, 17.89. HRMS (ESI-TOF) m/z: $[M+H]^+$ Calcd. For $C_{19}H_{35}N_3O_6$ 402.2599, found 402.2565.

Methyl-diisobutyl-2,2-dimethyl-4,7,11-trioxo-3-oxa-5,8,12-triazatetradecan-14-oate ***(6d).*** *(Boc-Leu-β-ala-Leu-OMe)* The pure product was obtained as white solid (150 mg, 65% yield)

^{1}H NMR (700 MHz, $CDCl_3$) δ 7.50 (d, *J* = 6.5 Hz, 1H), 7.28 – 7.21 (m, 1H), 5.05 (d, *J* = 7.4 Hz, 1H), 4.60 (td, *J* = 10.8, 4.4 Hz, 1H), 4.02 – 3.91 (m, 2H), 3.73 (s, 3H), 3.09 (td, *J* = 11.4, 3.1 Hz, 1H), 2.36 – 2.24 (m, 2H), 1.70 – 1.57 (m, 4H), 1.40 (s, 10H), 0.98 – 0.88 (m, 12H). ^{13}C NMR (176 MHz, $CDCl_3$) δ 175.38, 173.57, 173.25, 156.27, 139.28, 114.08, 77.24,54.05, 52.52, 51.39, 40.80, 39.51, 37.48, 36.84, 29.70, 28.29, 24.93, 24.70, 22.98, 22.57, 22.26, 21.13. HRMS (ESI-TOF) m/z: $[M+Na]^+$ Calcd. For $C_{21}H_{39}N_3O_6$ 452.2731, found 452.2686.

Methyl-sec-butyl)-6-(sec-butyl)-2-methyl-4,7,11-trioxo-3-oxa-5,8,12-triazatetradecan-14-oate ***(6e).*** *(Boc-lle-β-ala-Ile-OMe)* The pure product was obtained as white solid (250 mg, 91% yield) ^{1}H NMR (700 MHz, $CDCl_3$) δ 6.59 (s, 1H), 5.11 (s, 1H), 3.94 – 3.88 (m, 1H), 3.70 (s, 3H), 3.60 – 3.46 (m, 2H), 2.56 (t, *J* = 6.1 Hz, 2H), 1.85 (s, 1H), 1.44 (s, 10H), 1.14 – 1.06 (m, 1H), 0.90 (t, *J* = 7.6 Hz, 6H). ^{13}C NMR (176 MHz, $CDCl_3$) δ 173.52, 172.43, 172.11, 156.09, 79.84, 77.22, 77.04, 76.86, 59.82, 57.07, 52.26, 36.86, 36.62, 36.19, 28.30, 25.32, 25.01, 15.68, 15.61 (d, *J* = 21.6 Hz), 11.42, 11.27. HRMS (ESI-TOF) m/z: $[M+Na]^+$ Calcd. For $C_{21}H_{39}N_3O_6$ 452.2731, found 452.2781.

2.6 References and Notes

1. Margulies, D.; Hamilton, A. D., Combinatorial protein recognition as an alternative approach to antibody-mimetics. *Curr. Opin. Chem. Biol.* **2010,** *14*, 705-712.

2. Fahs, S.; Patil-Sen, Y.; Snape, T. J., Foldamers as anticancer therapeutics: targeting protein–protein interactions and the cell membrane. *ChemBioChem* **2015,** *16*, 1840-1853.

3. Kendhale, A. M.; Gonnade, R.; Rajamohanan, P. R.; Hofmann, H.-J.; Sanjayan, G. J., Foldamers with unusual structural architecture from spirobi (indane) building blocks. *Chemical communications* **2008**, 2541-2543.

4. Hill, D. J.; Mio, M. J.; Prince, R. B.; Hughes, T. S.; Moore, J. S., A field guide to foldamers. *Chemical reviews* **2001,** *101*, 3893-4012.

5. Martinek, T. A.; Fülöp, F., Peptidic foldamers: ramping up diversity. *Chemical Society Reviews* **2012,** *41*, 687-702.

6. Horne, W. S.; Gellman, S. H., Foldamers with heterogeneous backbones. *Acc. Chem. Res.* **2008,** *41*, 1399-1408.

7. Gellman, S. H., Foldamers: a manifesto. *Acc. Chem. Res.* **1998,** *31*, 173-180.

8. Seebach, D.; Abele, S.; Gademann, K.; Jaun, B., Pleated sheets and turns of β-peptides with proteinogenic side chains. *Angew. Chem. Int. Ed.* **1999,** *38*, 1595-1597.

9. Kendhale, A. M.; Poniman, L.; Dong, Z.; Laxmi-Reddy, K.; Kauffmann, B.; Ferrand, Y.; Huc, I., Absolute control of helical handedness in quinoline oligoamides. *J. Org. Chem.* **2011,** *76*, 195-200.

10. Singh, P.; Misra, S.; Sepay, N.; Mondal, S.; Ray, D.; Aswal, V. K.; Nanda, J., Self-assembling behaviour of a modified aromatic amino acid in competitive medium. *Soft Matter* **2020,** *16*, 6599-6607.

11. Scheidt, H. A.; Das, A.; Korn, A.; Krueger, M.; Maiti, S.; Huster, D., Structural characteristics of oligomers formed by pyroglutamate-modified amyloid β peptides studied by solid-state NMR. *Physical Chemistry Chemical Physics* **2020,** *22*, 16887-16895.

12. Bag, S. S.; Jana, S.; Yashmeen, A.; De, S., Triazolo-β-aza-ε-amino acid and its aromatic analogue as novel scaffolds for β-turn peptidomimetics. *Chemical Communications* **2015,** *51*, 5242-5245.

13. Konda, M.; Kauffmann, B.; Rasale, D. B.; Das, A. K., Structural and morphological diversity of self-assembled synthetic γ-amino acid containing peptides. *Organic & Biomolecular Chemistry* **2016,** *14*, 4089-4102.

14. Tao, K.; Levin, A.; Adler-Abramovich, L.; Gazit, E., Fmoc-modified amino acids and short peptides: simple bio-inspired building blocks for the fabrication of functional materials. *Chemical Society Reviews* **2016,** *45*, 3935-3953.

15. Xue, S.; Zhang, N.; Hu, X.; Zeng, Y.; Zhang, J.; Xing, P.; Zhao, Y., Self-Assembly Evolution of N-Terminal Aromatic Amino Acids with Transient Supramolecular Chirality. *The Journal of Physical Chemistry Letters* **2020,** *11*, 1490-1496.

16. Bera, S.; Xue, B.; Rehak, P.; Jacoby, G.; Ji, W.; Shimon, L. J. W.; Beck, R.; Král, P.; Cao, Y.; Gazit, E., Self-Assembly of Aromatic Amino Acid Enantiomers into Supramolecular Materials of High Rigidity. *ACS Nano* **2020,** *14*, 1694-1706.

17. Yoo, B.; Kirshenbaum, K., Peptoid architectures: elaboration, actuation, and application. *Current opinion in chemical biology* **2008,** *12*, 714-21.

18. Yoo, B.; Kirshenbaum, K., Peptoid architectures: elaboration, actuation, and application. *Curr. Opin. Chem. Biol.* **2008,** *12*, 714-721.

19. Fowler, S. A.; Blackwell, H. E., Structure–function relationships in peptoids: recent advances toward deciphering the structural requirements for biological function. *Org. Biomol. Chem.* **2009,** *7*, 1508-1524.

20. Bautista, A. D.; Craig, C. J.; Harker, E. A.; Schepartz, A., Sophistication of foldamer form and function in vitro and in vivo. *Curr. Opin. Chem. Biol.* **2007,** *11*, 685-692.

21. Delsuc, N.; Massip, S.; Léger, J.-M.; Kauffmann, B.; Huc, I., Relative helix− helix conformations in branched aromatic oligoamide foldamers. *J. Am. Chem. Soc.* **2011,** *133*, 3165-3172.

22. Stringer, J. R.; Crapster, J. A.; Guzei, I. A.; Blackwell, H. E., Construction of peptoids with all trans-amide backbones and peptoid reverse turns via the tactical incorporation of N-aryl side chains capable of hydrogen bonding. *J. Org. Chem.* **2010,** *75*, 6068-6078.

23. Huang, M. L.; Ehre, D.; Jiang, Q.; Hu, C.; Kirshenbaum, K.; Ward, M. D., Biomimetic peptoid oligomers as dual-action antifreeze agents. *Proc. Natl. Acad. Sci. U S A* **2012,** *109*, 19922-19927.

24. Paul, B.; Butterfoss, G. L.; Boswell, M. G.; Huang, M. L.; Bonneau, R.; Wolf, C.; Kirshenbaum, K., N-naphthyl peptoid foldamers exhibiting atropisomerism. *Org. Lett.* **2012,** *14*, 926-929.

25. Paul, B.; Butterfoss, G. L.; Boswell, M. G.; Renfrew, P. D.; Yeung, F. G.; Shah, N. H.; Wolf, C.; Bonneau, R.; Kirshenbaum, K., Peptoid atropisomers. *J. Am. Chem. Soc.* **2011,** *133*, 10910-10919.

26. Butterfoss, G. L.; Yoo, B.; Jaworski, J. N.; Chorny, I.; Dill, K. A.; Zuckermann, R. N.; Bonneau, R.; Kirshenbaum, K.; Voelz, V. A., De novo structure prediction and experimental characterization of folded peptoid oligomers. *Proc. Natl. Acad. Sci. U S A* **2012,** *109*, 14320-14325.

27. Zhang, L.; Geng, Y.; Jin, Z., Transition-metal-free synthesis of N-aryl hydroxamic acids via insertion of arynes. *J. Org. Chem.* **2016,** *81*, 3542-3552.

28. Gan, J.; Ma, D., Synthesis of 1, 5-benzothiazepine dipeptide mimetics via two cui-catalyzed cross coupling reactions. *Organic letters* **2009,** *11*, 2788-2790.

29. Morejón, M. C.; Laub, A.; Westermann, B.; Rivera, D. G.; Wessjohann, L. A., Solution- and solid-phase macrocyclization of peptides by the Ugi–Smiles multicomponent reaction: synthesis of N-aryl-bridged cyclic lipopeptides. *Org. Lett.* **2016,** *18*, 4096-4099.

30. Bentley, R., A fresh look at natural tropolonoids. *Nat. Prod. Rep.* **2008,** *25*, 118-138.

31. Guo, H.; Roman, D.; Beemelmanns, C., Tropolone natural products. *Nat. Prod. Rep.* **2019,** *36*, 1137-1155.

32. Pauson, P. L., Tropones and tropolones. *Chem. Rev.* **1955,** *55*, 9-136.

33. Bryant, B. E.; Fernelius, W. C., Formation Constants of Metal Complexes of Tropolone and its Derivatives. II. Some Alkyltropolones1, 2. *J. Am. Chem. Soc.* **1954,** *76*, 1696-1697.

34. Bryant, B. E.; Fernelius, W. C., Formation Constants of Metal Complexes of Tropolone and its Derivatives. IV. α-Bromotropolone, Tribromotropolone and 2-Aminotropone1. *J. Am. Chem. Soc.* **1954,** *76*, 4864-4865.

35. Bryant, B. E.; Fernelius, W. C.; Douglas, B. E., Formation Constants of Metal Complexes of Tropolone and Its Derivatives. I. Tropolone1. *J. Am. Chem. Soc.* **1953,** *75*, 3784-3786.

36. Bryant, B. F.; Fernelius, W. C., Formation Constants of Some Metal Complexes of Tropolone and its Derivatives. III. The Benzotropolones and Purpurogallins1, 2. *J. Am. Chem. Soc.* **1954,** *76*, 3783-3784.

37. Balachandra, C.; Sharma, N. K., Direct/Reversible Amidation of Troponyl Alkylglycinates via Cationic Troponyl Lactones and Mechanistic Insights. *ACS Omega* **2018,** *3*, 997-1013.

38. Balachandra, C.; Sharma, N. K., Instability of Amide Bond Comprising the 2-Aminotropone Moiety: Cleavable under Mild Acidic Conditions. *Org. Lett.* **2015,** *17*, 3948-3951.

39. Balachandra, C.; Sharma, N. K., Synthesis and conformational analysis of new troponyl aromatic amino acid. *Tetrahedron* **2014,** *70*, 7464-7469.

40. Balachandra, C.; Sharma, N. K., Novel fluorophores: Syntheses and photophysical studies of boron-aminotroponimines. *Dyes Pigm.* **2017,** *137*, 532-538.

41. Palai, B. B.; Soren, R.; Sharma, N. K., BODIPY analogues: synthesis and photophysical studies of difluoro boron complexes from 2-aminotropone scaffolds through N, O-chelation. *Org. Biomol. Chem.* **2019,** *17*, 6497-6505.

42. Hovmöller, S.; Zhou, T.; Ohlson, T., Conformations of amino acids in proteins. *Acta. Cryst. D* **2002,** *58*, 768-776.

43. Kleywegt, G. J.; Jones, T. A., Phi/psi-chology: Ramachandran revisited. *Structure* **1996,** *4*, 1395-1400.

44. Greenfield, N. J., Analysis of circular dichroism data. In *Methods in enzymology*, Elsevier2004; Vol. 383, pp 282-317.

45. Greenfield, N. J., Analysis of the kinetics of folding of proteins and peptides using circular dichroism. *Nat. Protoc.* **2006,** *1*, 2891.

46. Bag, S. S.; Jana, S.; Yashmeen, A.; Senthilkumar, K.; Bag, R., Triazolyl-donor–acceptor chromophore-decorated unnatural amino acids and peptides: FRET events in a β-turn conformation. *Chem. Commun.* **2014,** *50*, 433-435.

2.7 Appendix

1. NMR (1H/13C) and HRMS spectra of Tr-Gly-Gly-OMe(**4a**) 75
2. NMR (1H/13C) and HRMS spectra of Tr-Gly-Aal-OMe(**4b**) 77
3. NMR (1H/13C) and HRMS spectra of Tr-Ala-Gly-OMe(**4c**) 79
4. NMR (1H/13C) and HRMS spectra of Tr-val-Gly-OMe(**4d**) 81
5. NMR (1H/13C) and HRMS spectra of Tr-val-β-Ala-OMe(**4e**) 83
6. NMR (1H/13C) and HRMS spectra of Tr-val-β-Ala-OMe (**4f**) 85
7. NMR (1H/13C) and HRMS spectra of Tr-Leu-β-Ala-OMe(**4g**) 87
8. NMR (1H/13C) and HRMS spectra of Tr-Ala-β-Ala-OMe (**4h**) 89
9. NMR (1H/13C) and HRMS spectra of Tr-Ile-β-Ala-OMe(**4i**) 91
10. NMR (1H/13C) and HRMS spectra of Tr-Phe-Gly-OMe(**4j**) 93
11. NMR (1H/13C) and HRMS spectra of Tr-Pro-Val-OMe(**4k**) 95
12. NMR (1H/13C) and HRMS spectra of Tr-β-Ala-Pro-OMe**(4l)** 97
13. NMR (1H/13C) and HRMS spectra of Tr-Gly-β-Ala-Gly-OMe**(5a)** 99
14. NMR (1H/13C) and HRMS spectra of Tr-Ala-β-Ala-OMe **(5b)** 101
15. NMR (^{1}H/^{13}C) and HRMS spectra of Tr-Val-β-Ala-Val-OMe **(5c)** 103
16. NMR (^{1}H/^{13}C) and HRMS spectra of Tr-Leu-β-Ala-Leu-OMe(**5d**) 105
17. NMR (^{1}H/^{13}C) and HRMS spectra of Tr-Ilu-β-Ala-Ilu-OMe(**5e**) 107
19. Crystal Structure determination: 109
20. Circular Dichroism (CD) Spectra. 112

1. NMR (1H/13C) and HRMS spectra of Tr-Gly-Gly-OMe(**4a**)

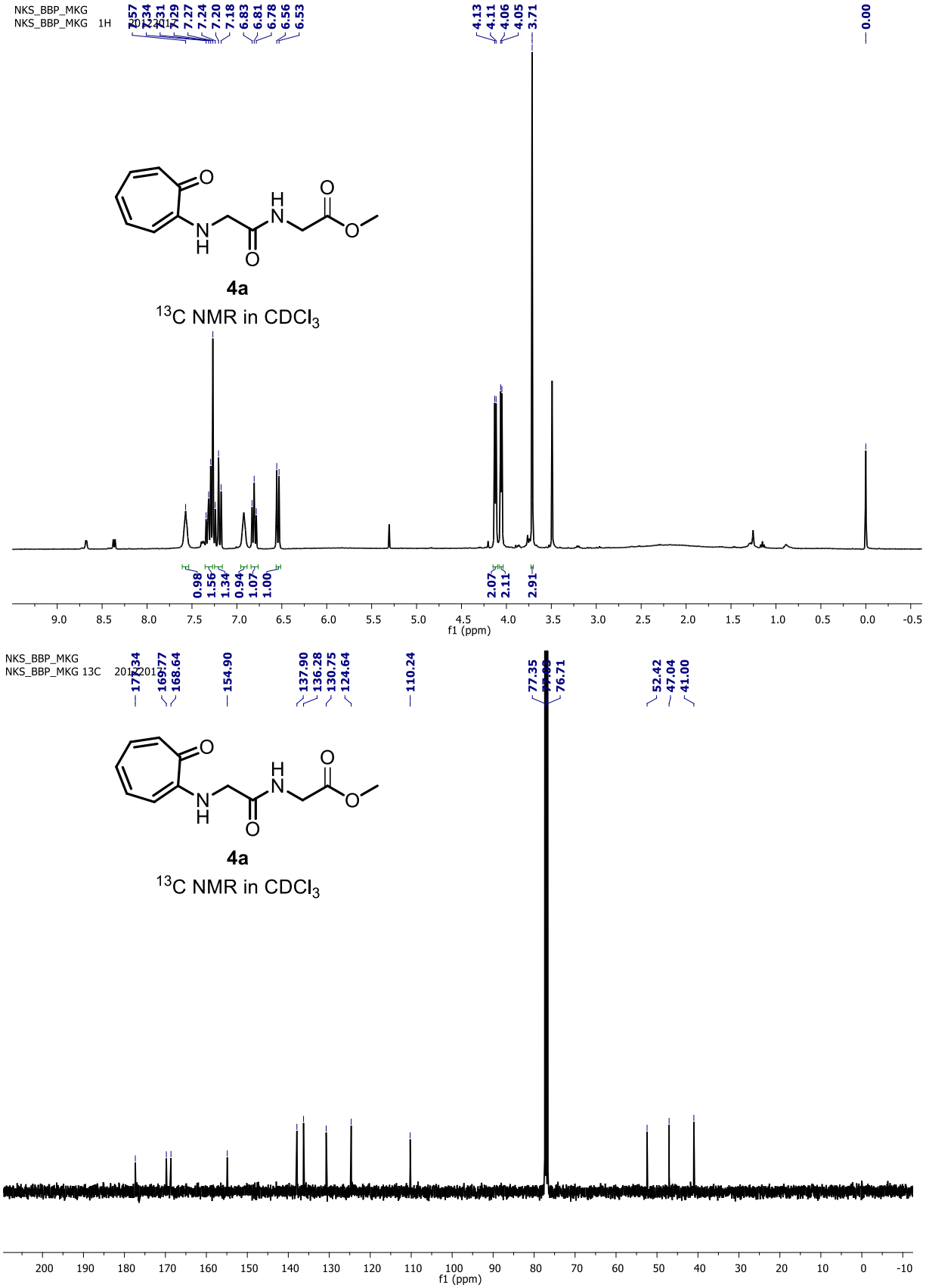

Figure. A1: $^{1}H,^{13}C$-NMR spectrum of Tr-Gly-Gly -OMe (**4a**) in $CDCl_3$

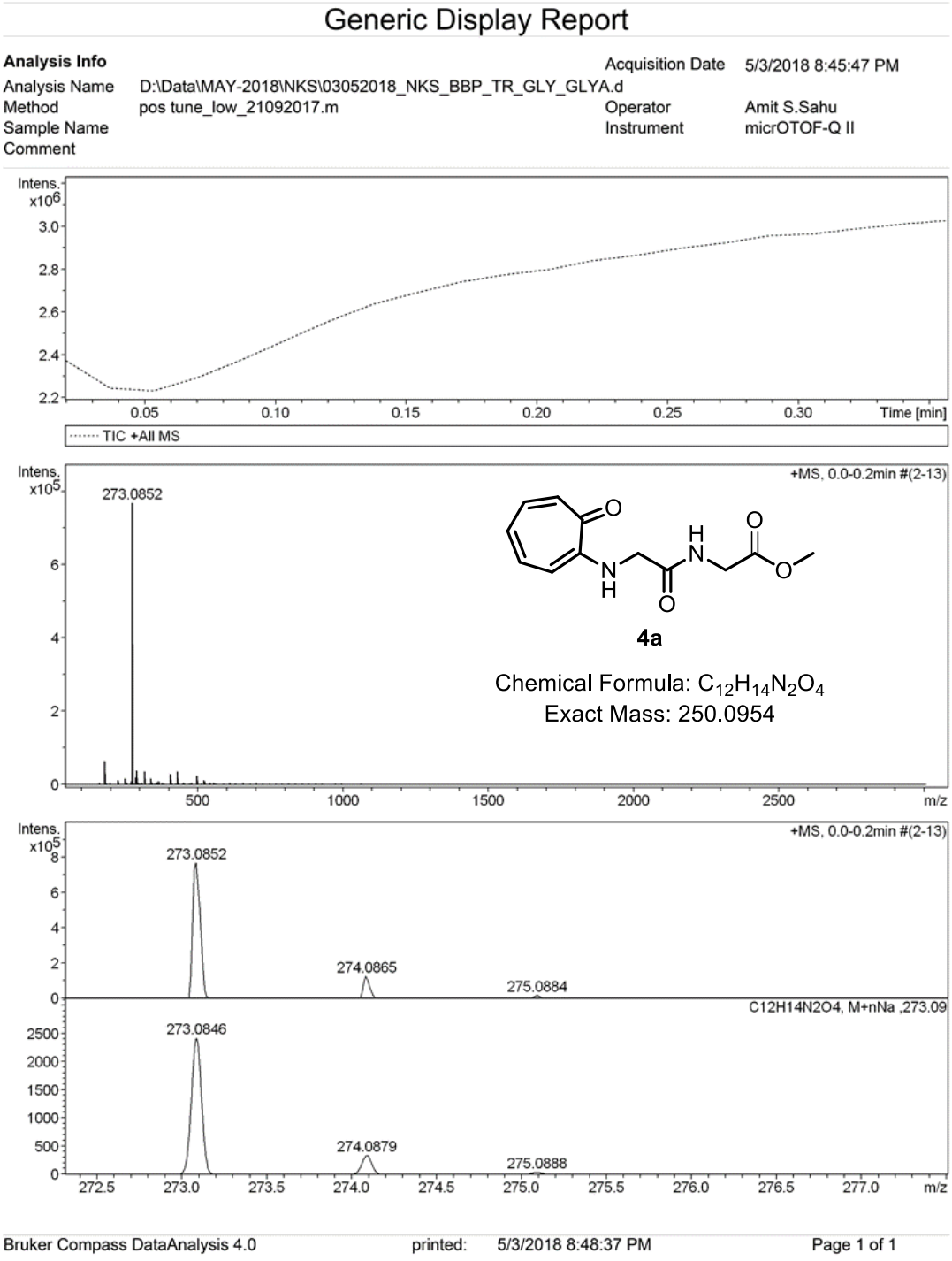

Figure. A2. ESI-MS/HRMS spectra of Tr-Gly-Gly -OMe (**4a**)

2. NMR (1H/13C) and HRMS spectra of Tr-Gly-Aal-OMe(**4b**)

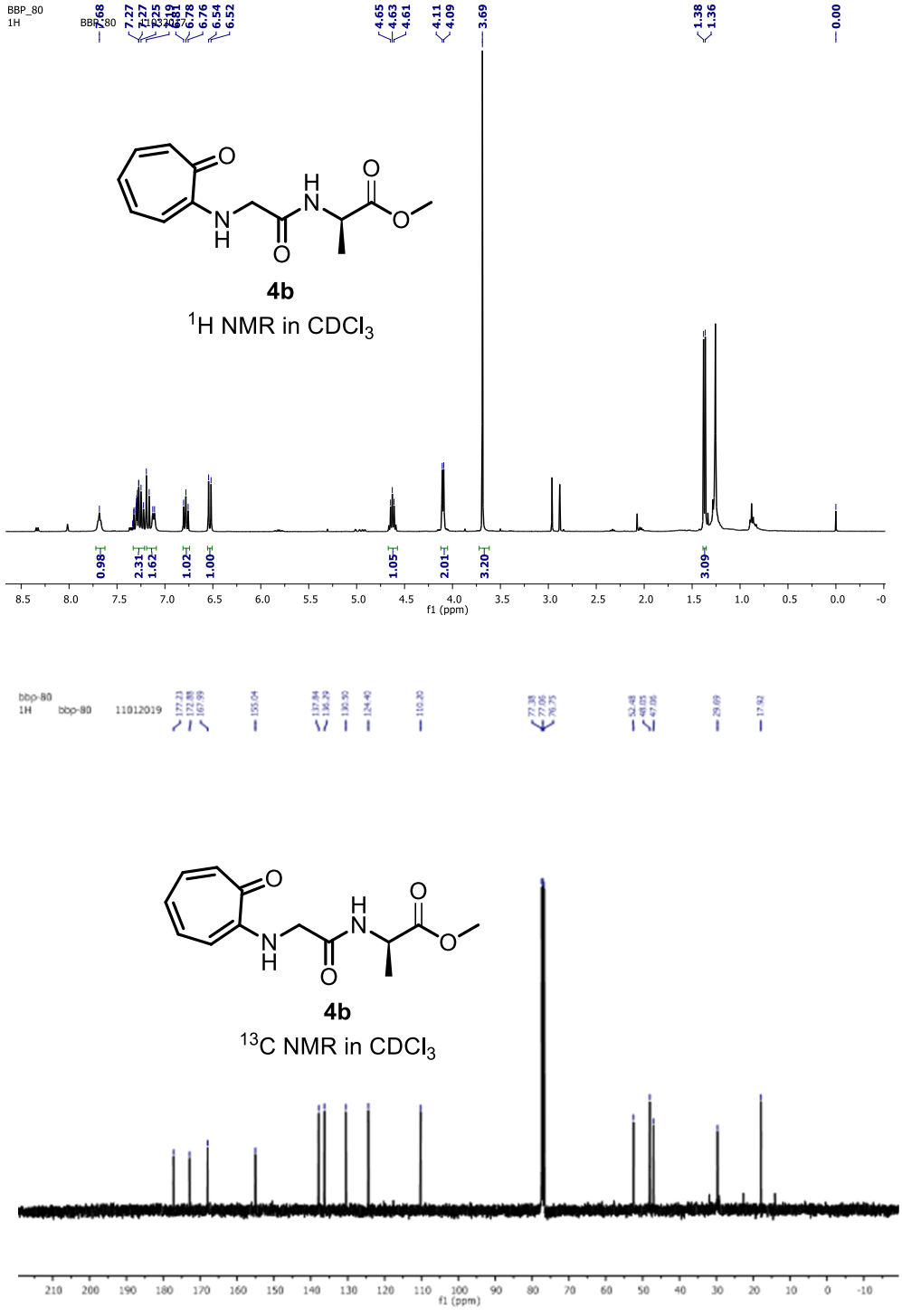

Figure. A3: $^{1}H,^{13}C$-NMR spectrum of Tr-Gly-Ala -OMe (**4b**) in $CDCl_3$ (*Impurites)

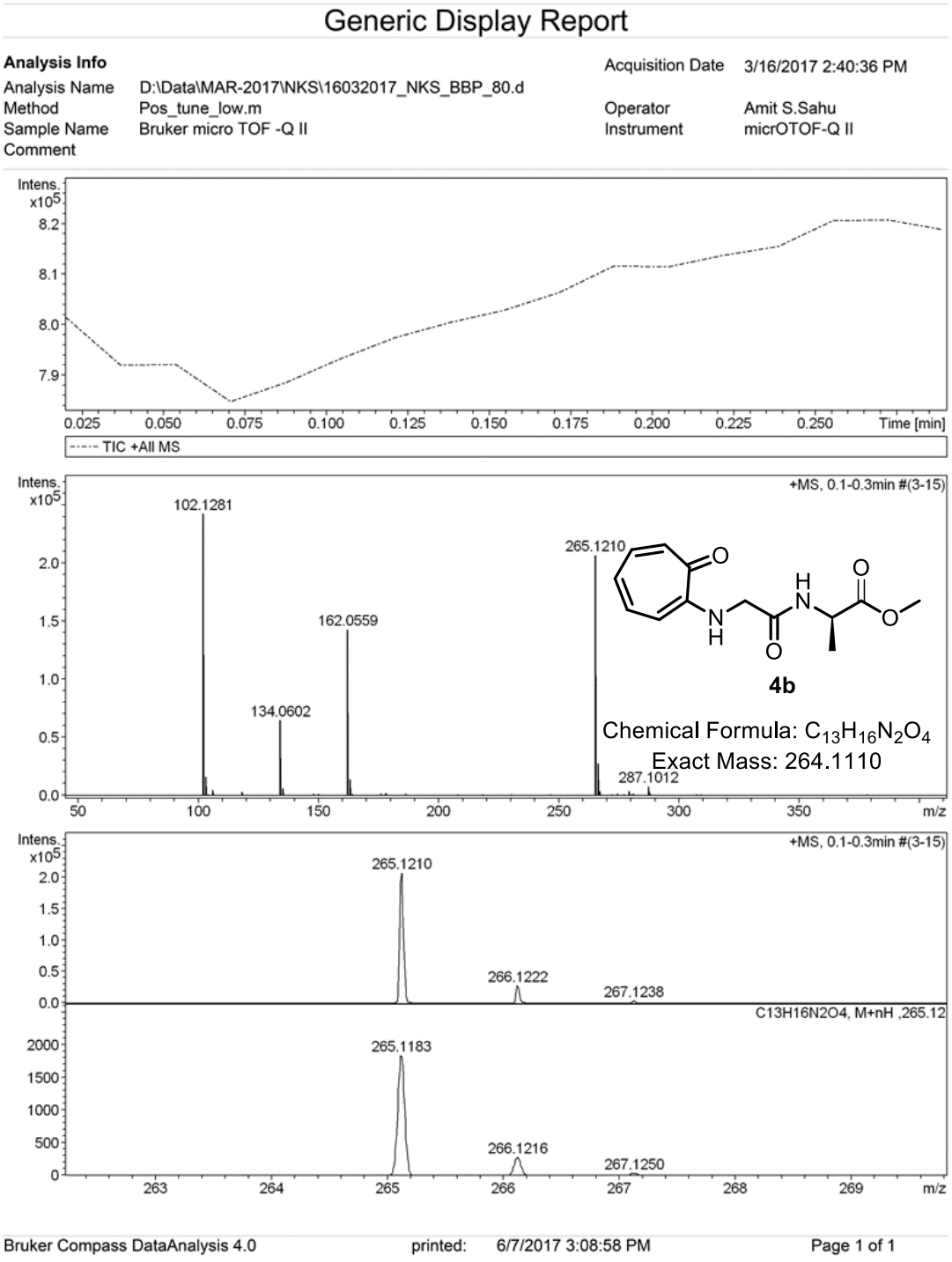

Figure. A4: ESI-MS/HRMS spectra of Tr-Gly-Ala -OMe (**4b**)

3. NMR (1H/13C) and HRMS spectra of Tr-Ala-Gly-OMe(**4c**)

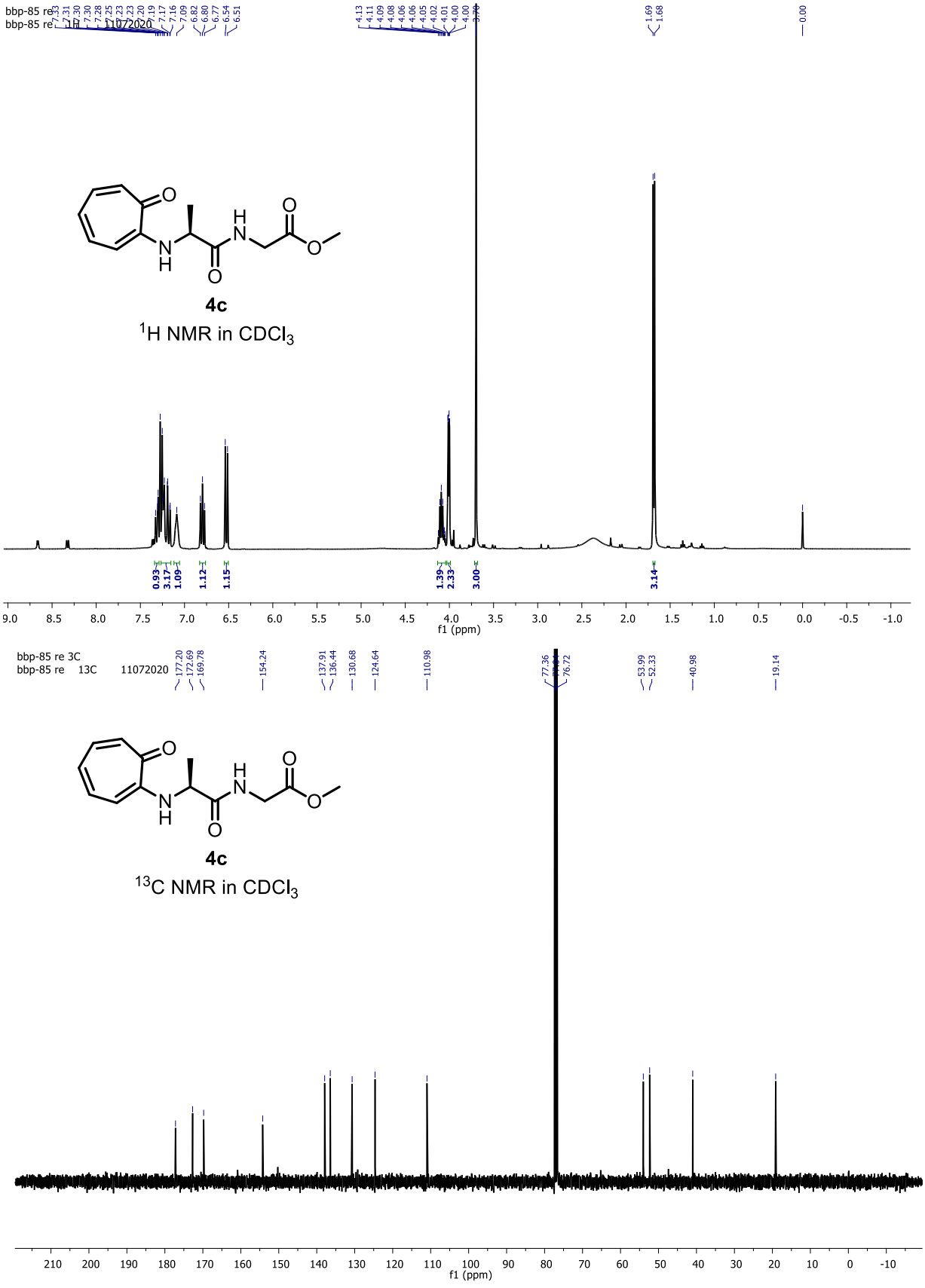

Figure. A5: Mass spectrum of Tr-Ala-Gly -OMe (**4c**) in $CDCl_3$

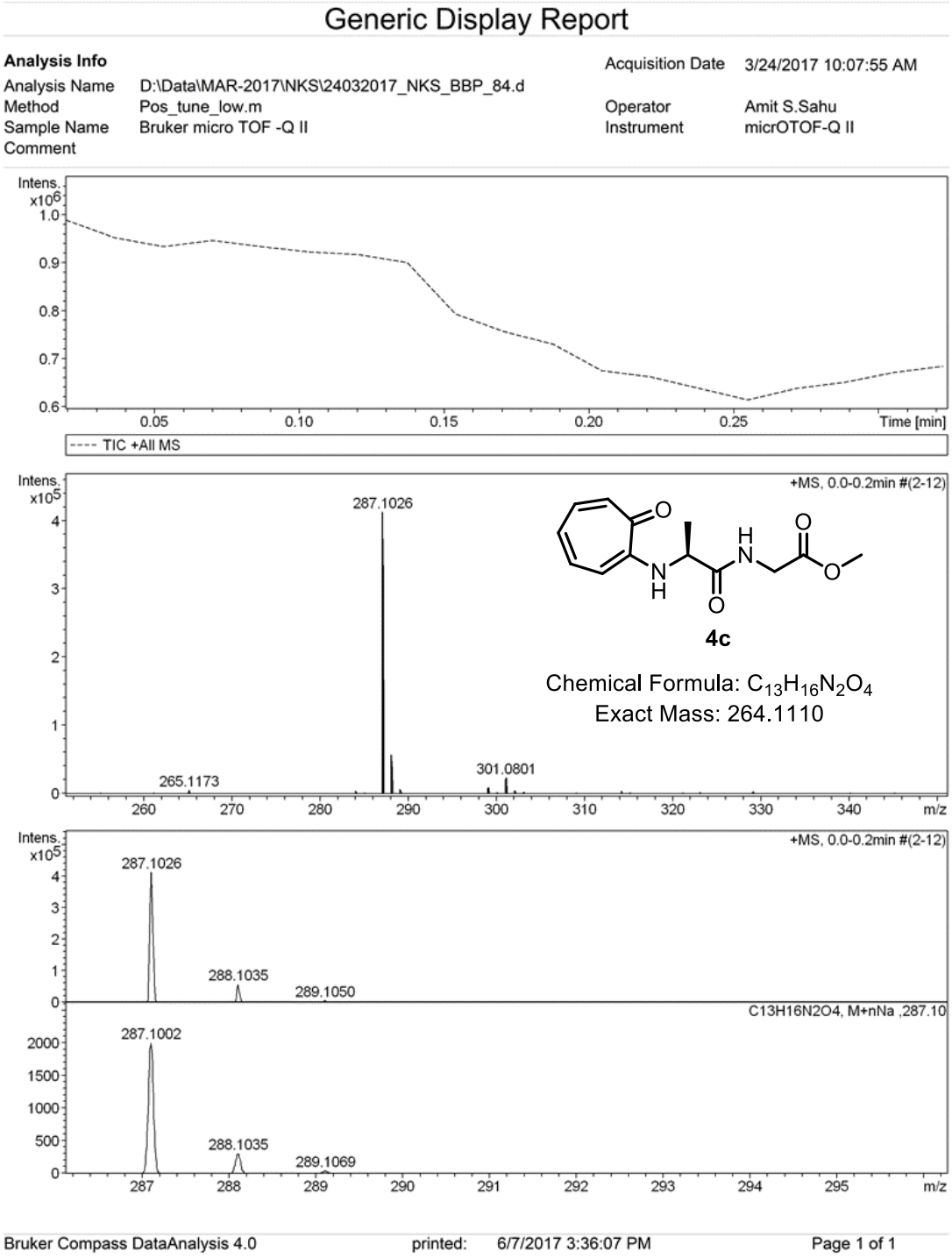

Figure. A6: ESI-MS/HRMS spectra of Tr-Ala-Gly -OMe (**4c**)

4. NMR (1H/13C) and HRMS spectra of Tr-val-Gly-OMe(**4d**)

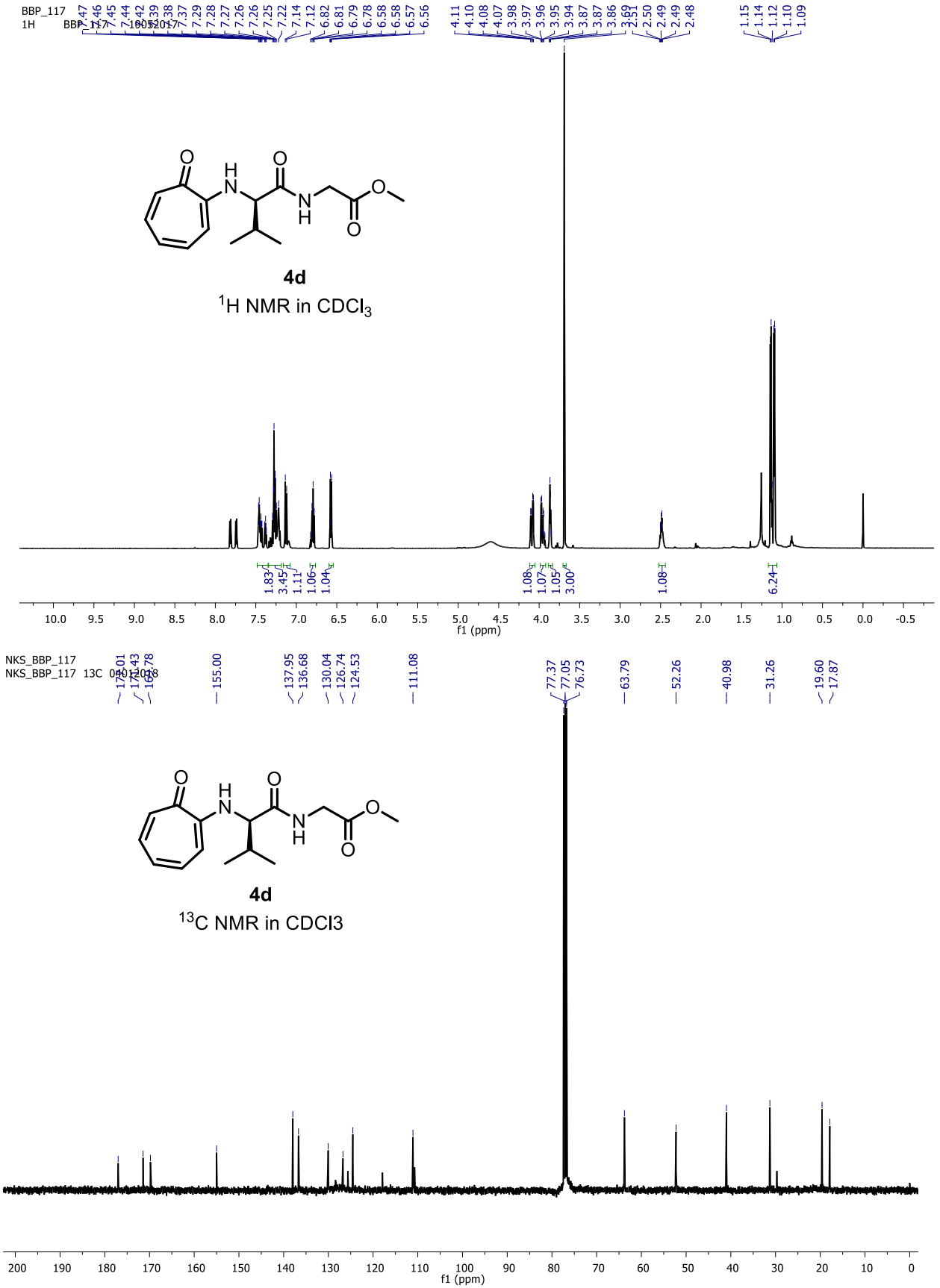

Figure. A7: Mass spectrum of Tr-Ala-Gly -OMe (**d**) in $CDCl_3$

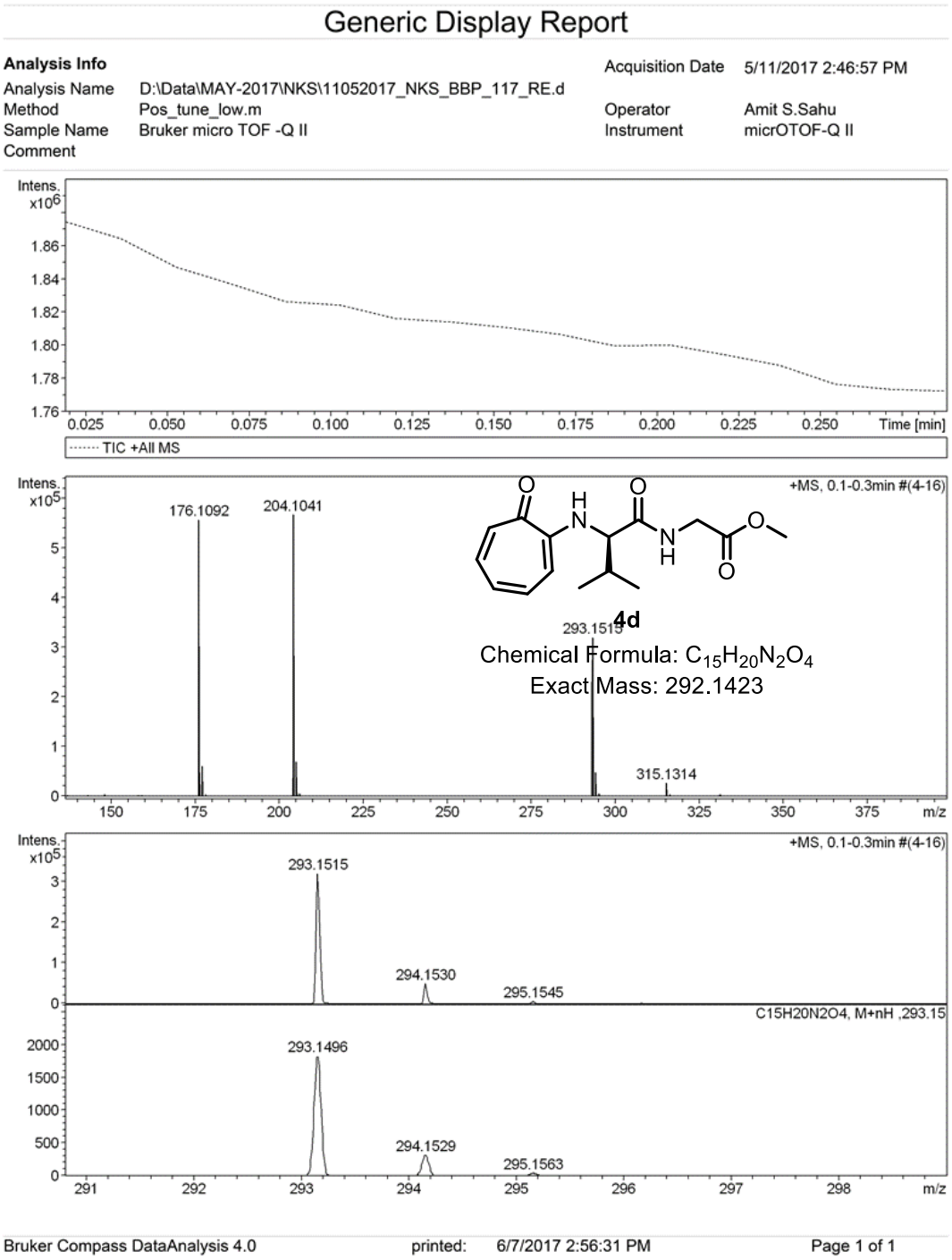

Figure. A8: ESI-MS/HRMS spectra of Tr-Val-Gly -OMe (**4d**)

5. NMR (1H/13C) and HRMS spectra of Tr-val-β-Ala-OMe(**4e**)

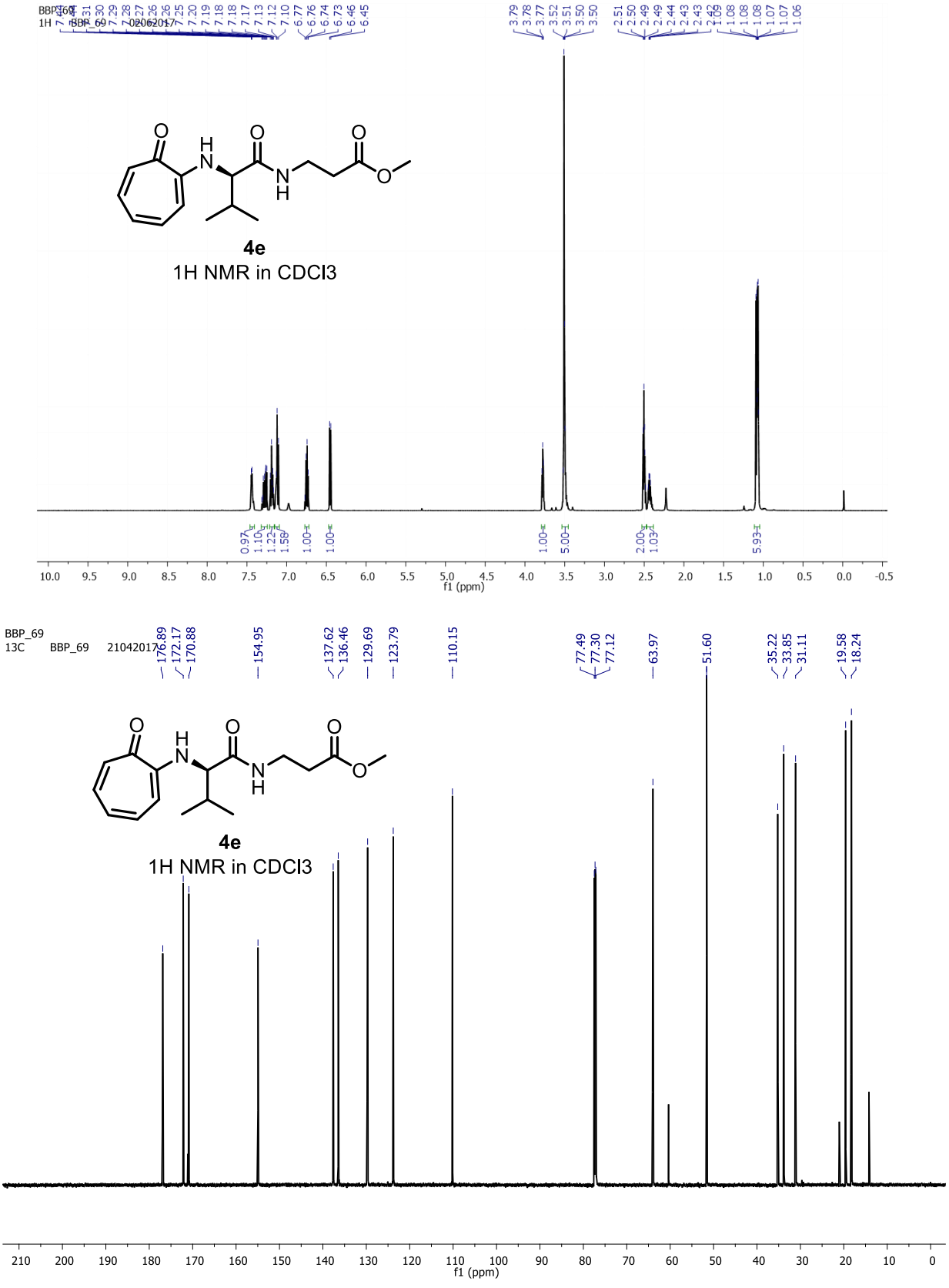

Figure. A9: $^{1}H,^{13}C$-NMR spectrum of Tr-val--β -OMe (**4e**) in $CDCl_3$

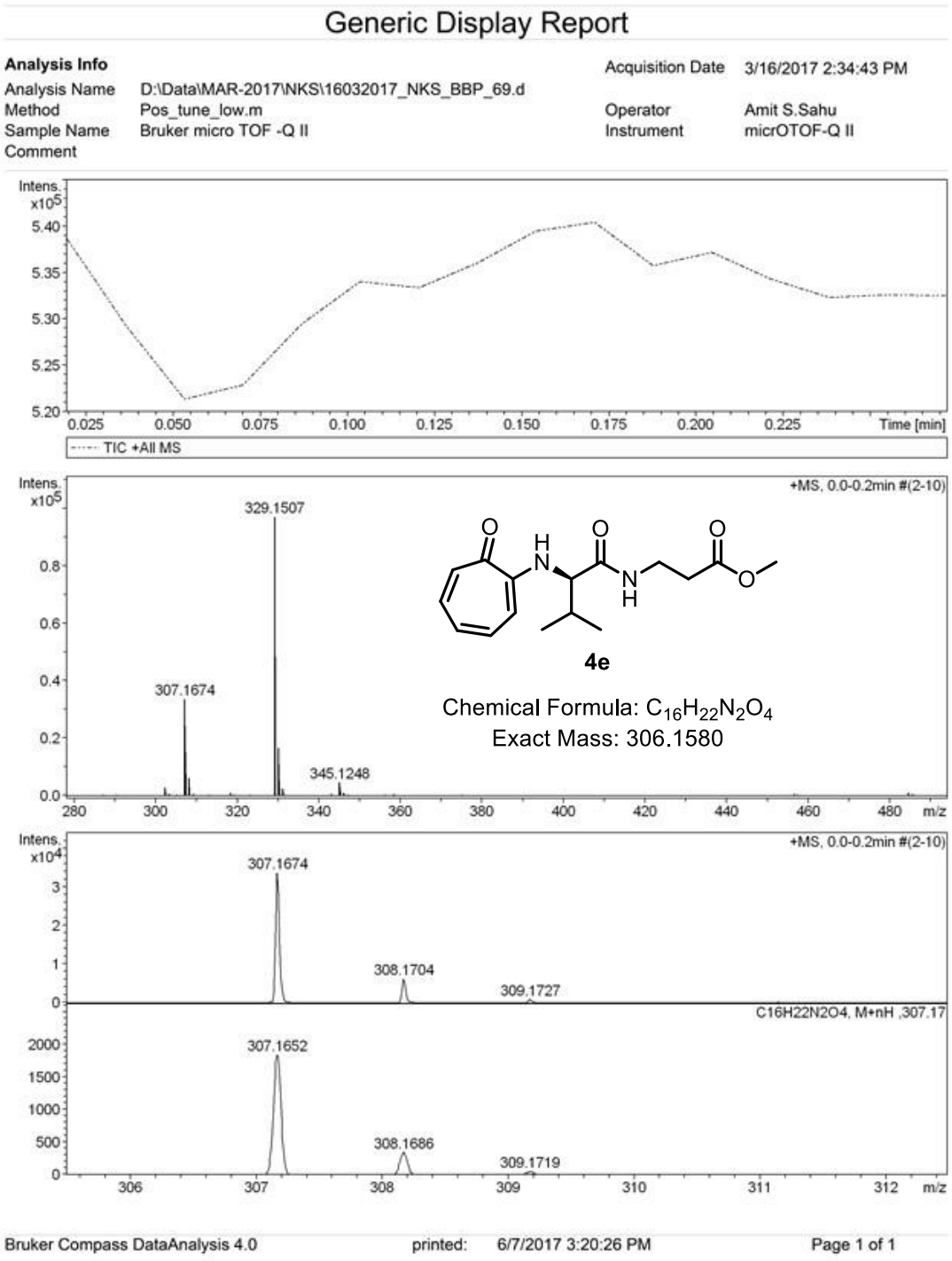

Figure. A10: ESI-MS/HRMS spectra of Tr-Val-β-Ala -OMe (**4d**)

6. NMR (1H/13C) and HRMS spectra of Tr-val-β-Ala-OMe (**4f**)

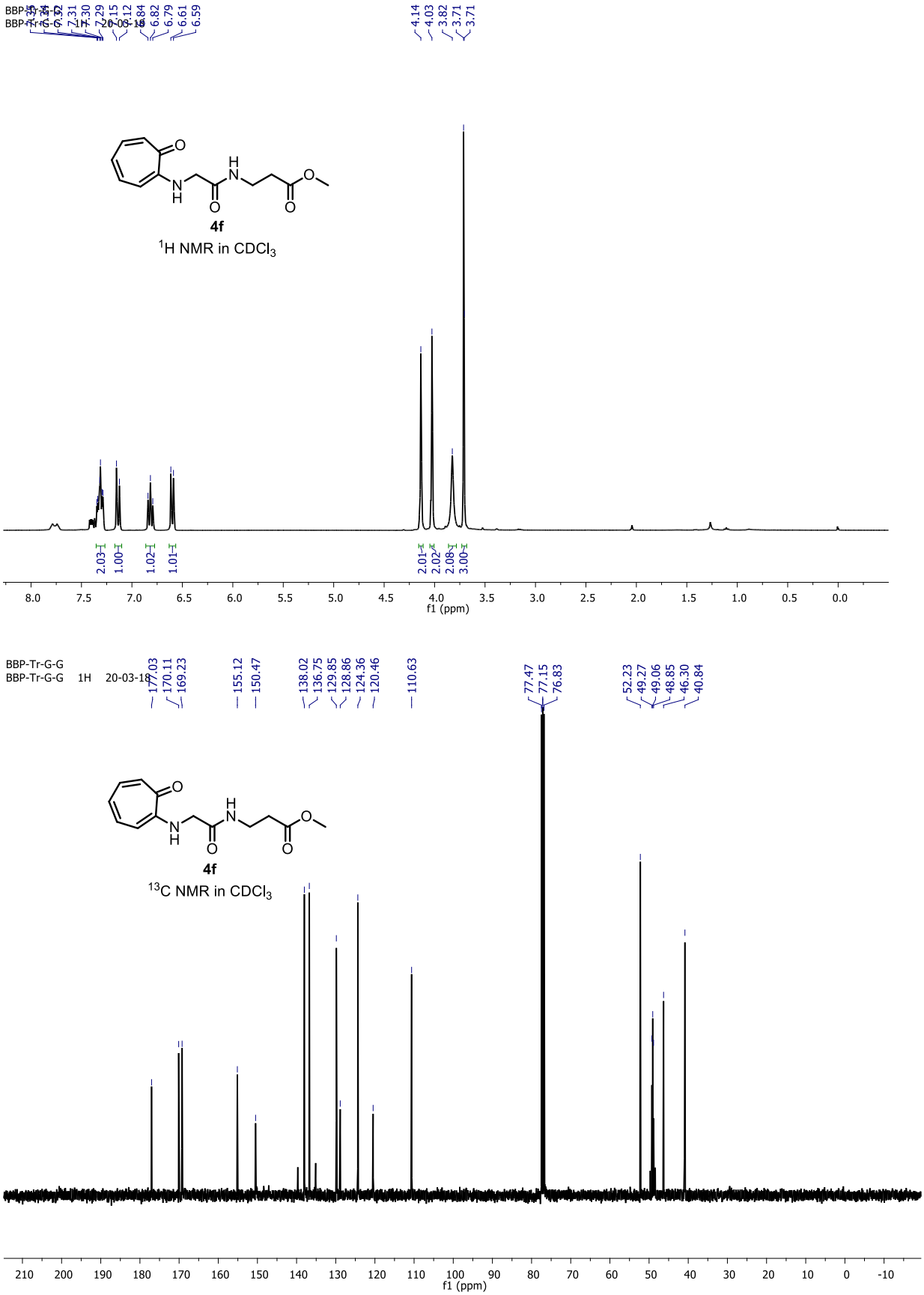

Figure. 11: $^{1}H,^{13}C$-NMR spectrum of Tr-Gly-β-Ala -OMe (**4f**) in $CDCl_3$

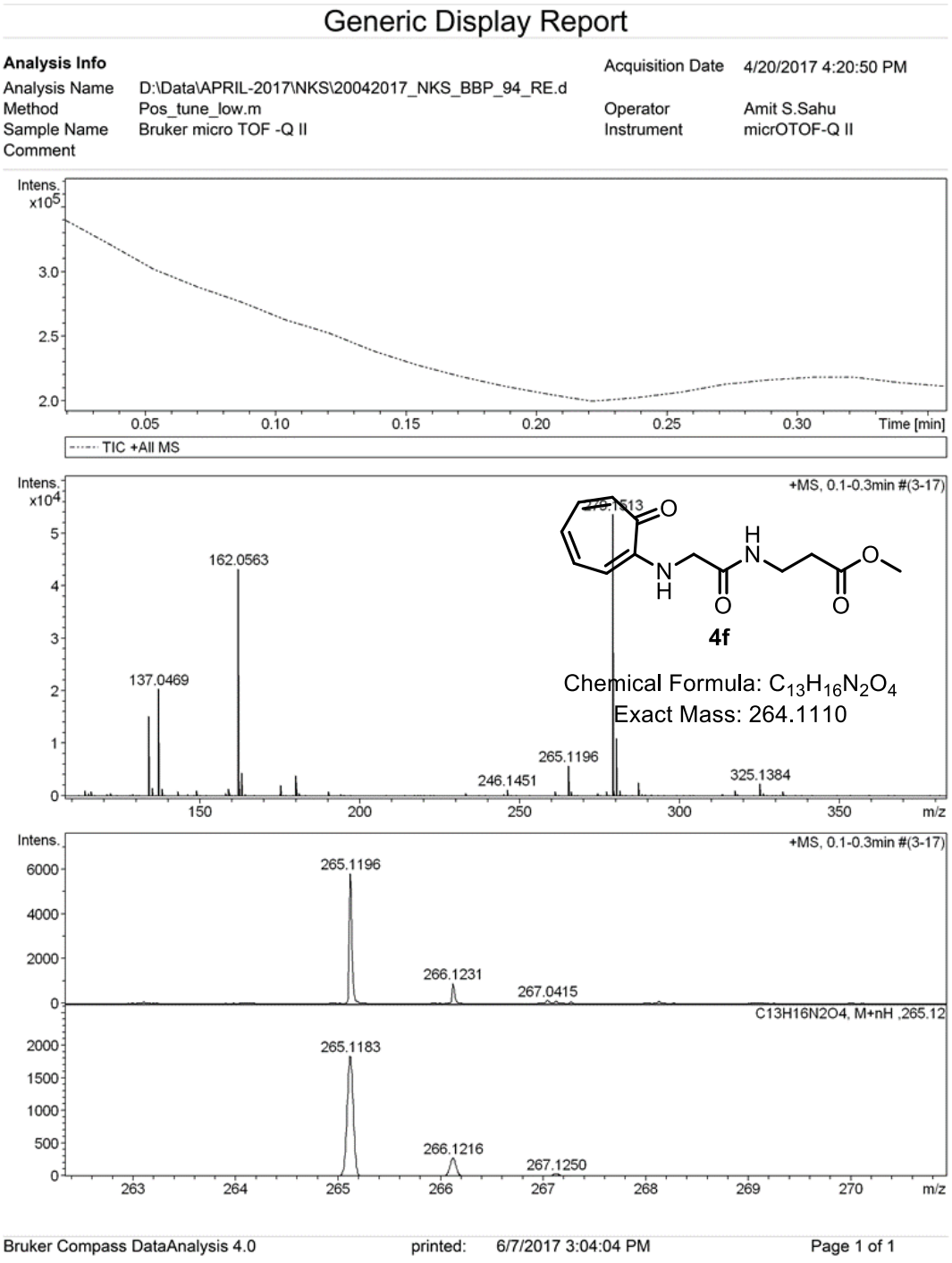

Figure. A12: ESI-MS/HRMS spectra of Tr-Gly-β-Ala -OMe (**4f**)

7. NMR (1H/13C) and HRMS spectra of Tr-Leu-β-Ala-OMe(**4g**)

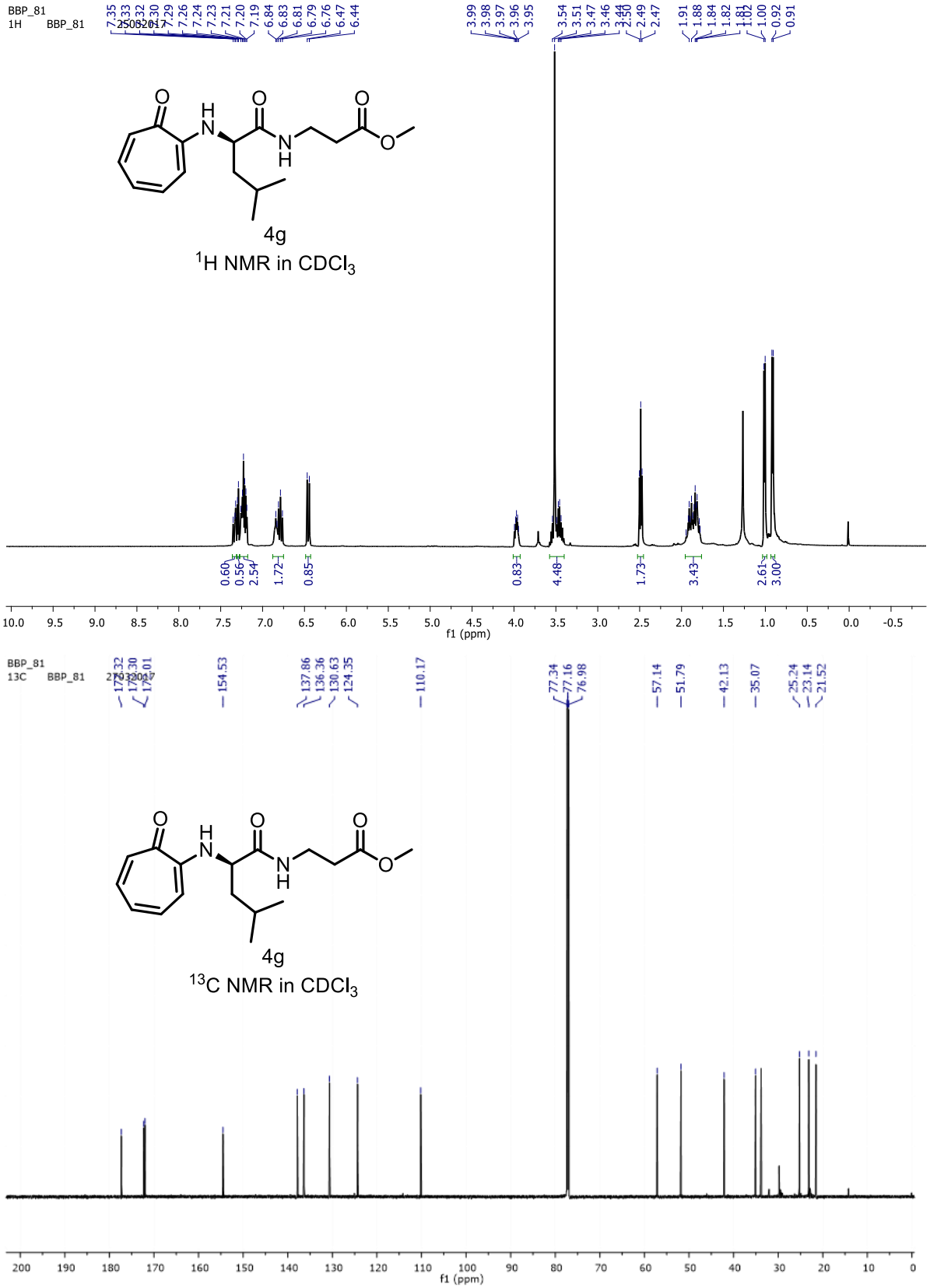

Figure. A13: $^{1}H,^{13}C$-NMR spectrum of Tr-Leu-β-Ala -OMe (**4g**) in $CDCl_3$

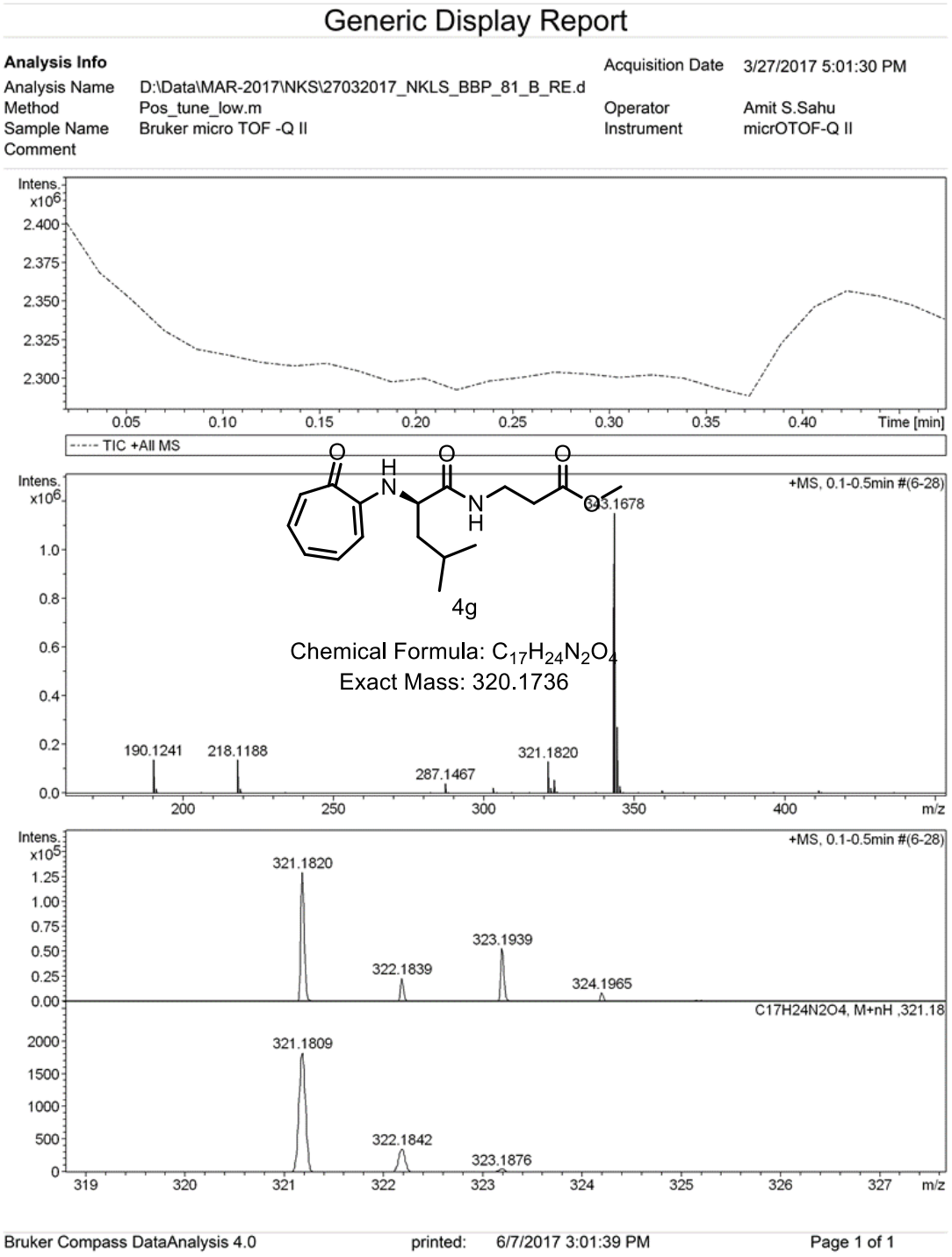

Figure. A14: ESI-MS/HRMS spectra of Tr-Leu-β-Ala -OMe (**4g**)

8. NMR (1H/13C) and HRMS spectra of Tr-Ala-β-Ala-OMe (**4h**)

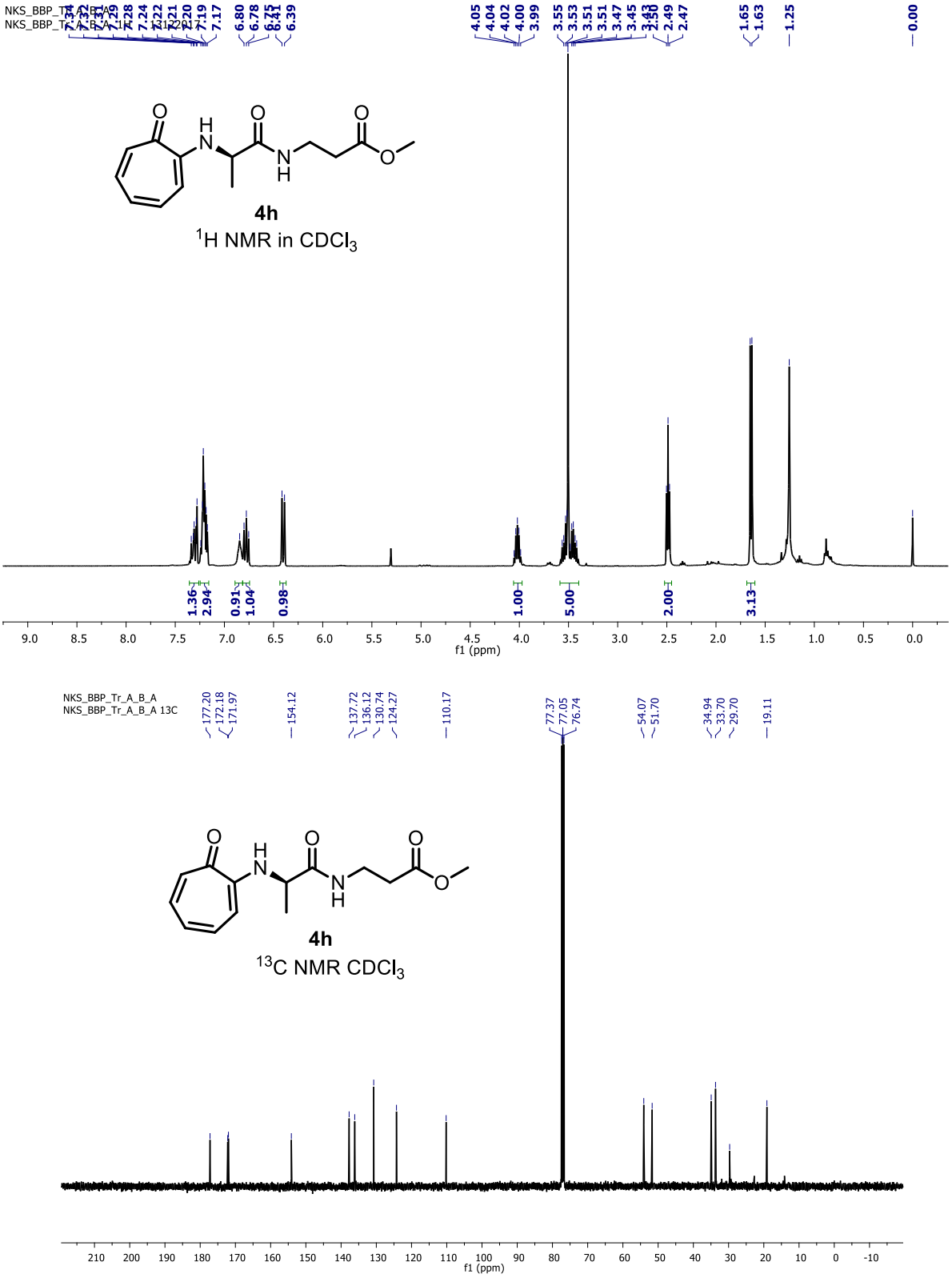

Figure. A15: $^{1}H,^{13}C$-NMR spectrum of Tr-Ala-β-Ala -OMe (**4h**) in $CDCl_3$

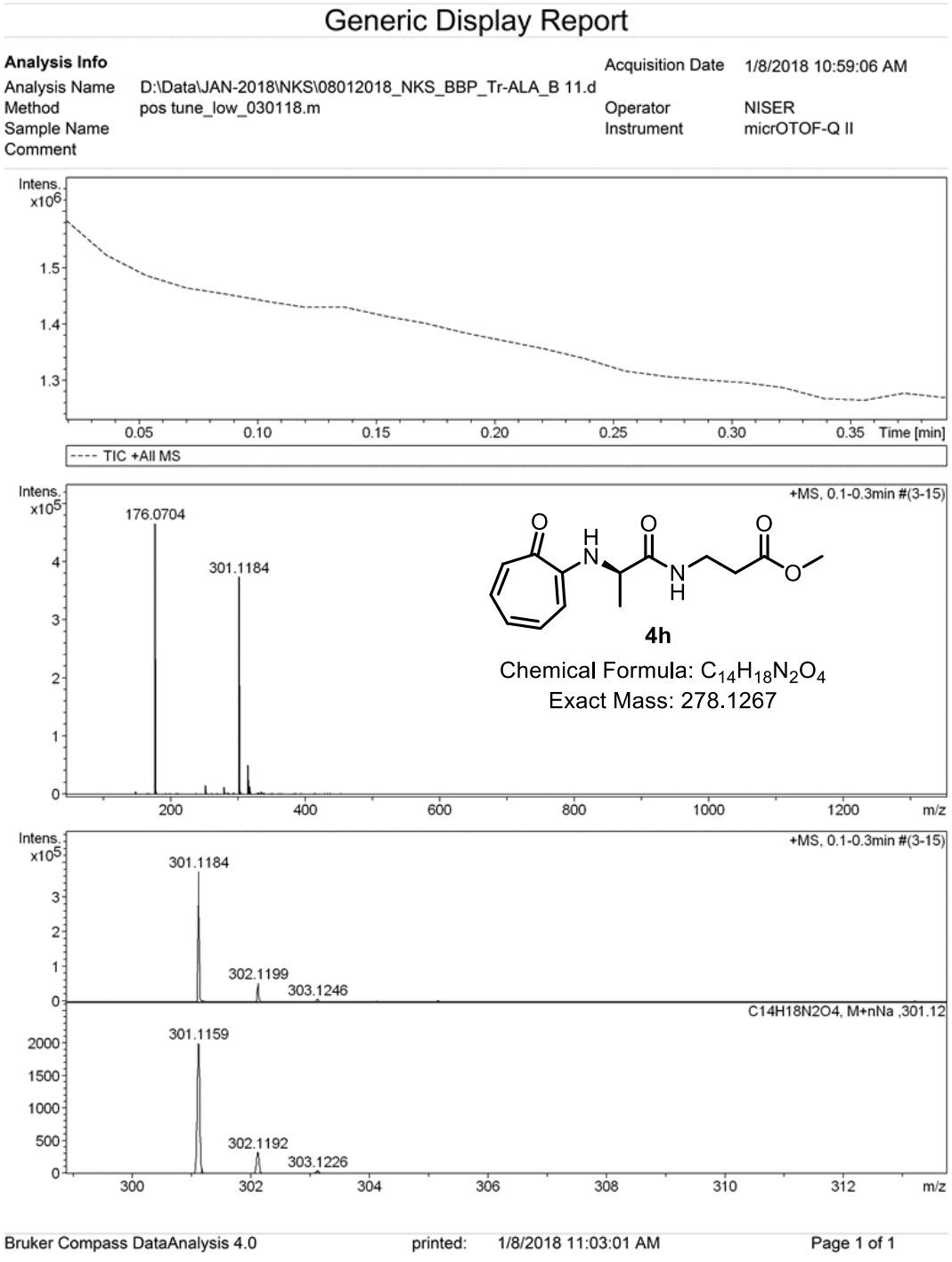

Figure. A16: ESI-MS/HRMS spectra of Tr-Gly-β-Ala -OMe (**4h**)

9. NMR (1H/13C) and HRMS spectra of Tr-Ile-β-Ala-OMe(**4i**)

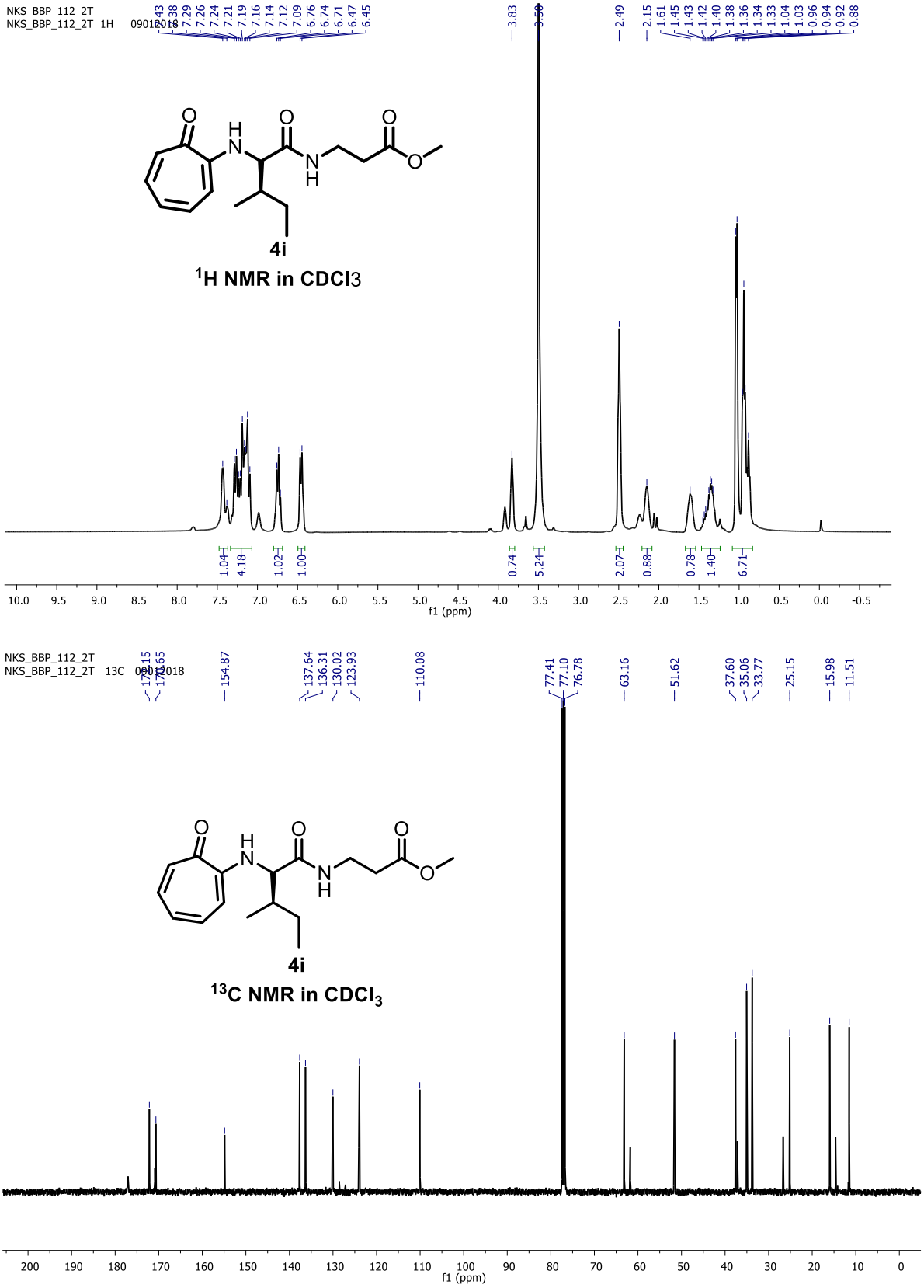

Figure. A17: $^{1}H,^{13}C$-NMR spectrum of Tr-Ile-β-Ala -OMe (**4i**) in $CDCl_3$

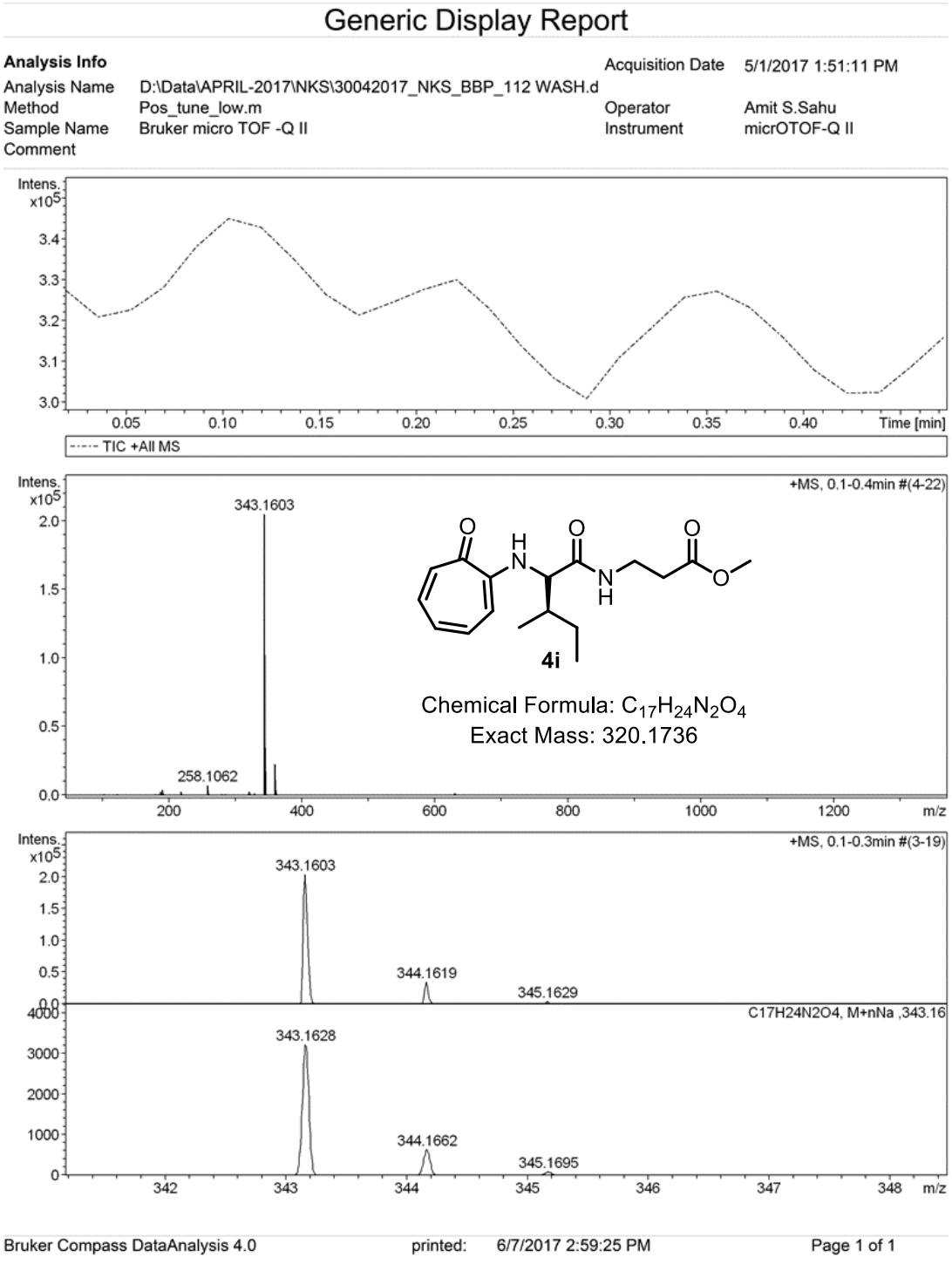

Figure. A18: ESI-MS/HRMS spectra of Tr-Ile-β-Ala -OMe (**4i**)

10. NMR (1H/13C) and HRMS spectra of Tr-Phe-Gly-OMe(**4j**)

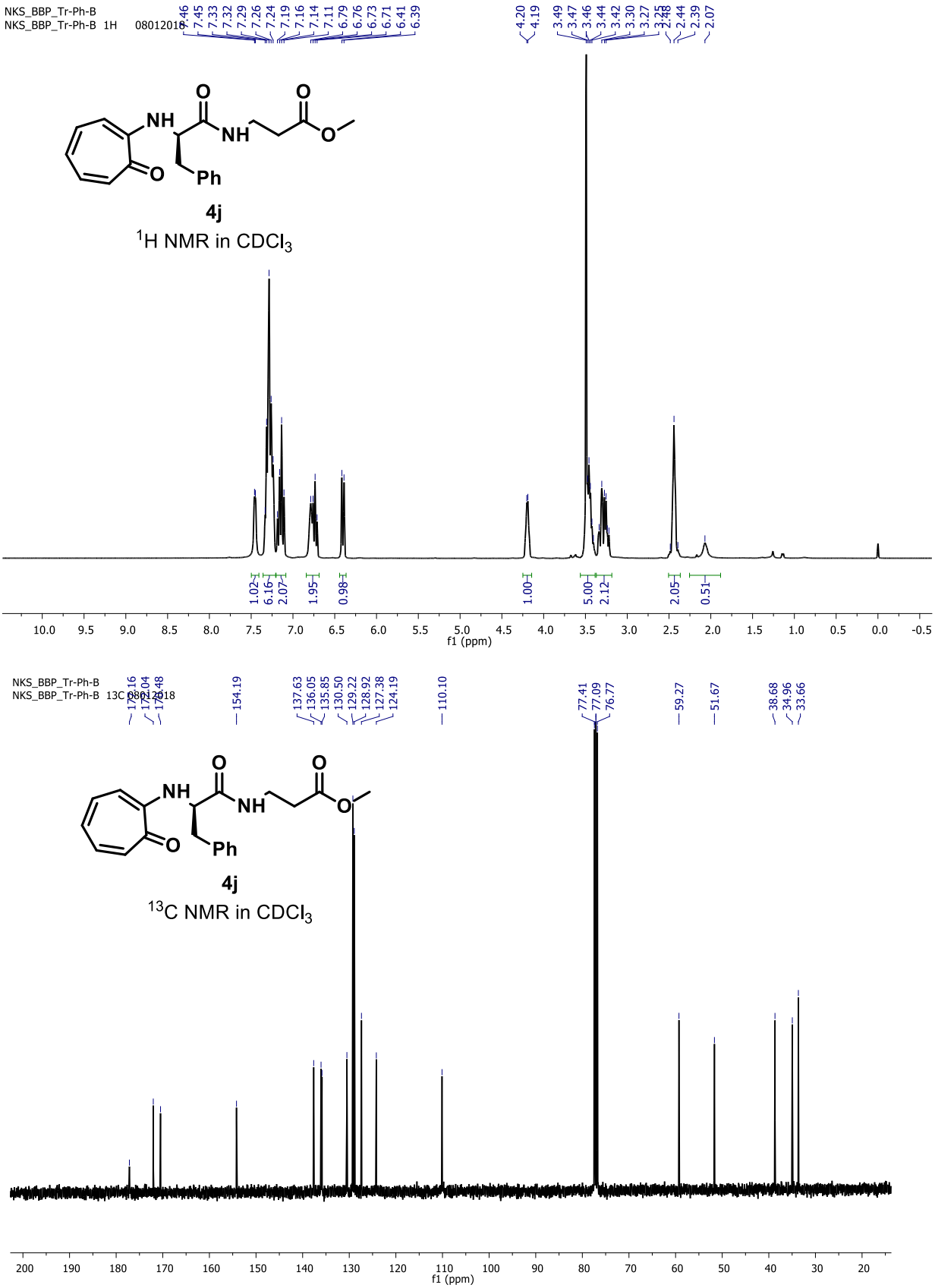

Figure. A19: $^{1}H,^{13}C$-NMR spectrum of Tr-Phe-β-Ala -OMe (**4j**) in $CDCl_3$

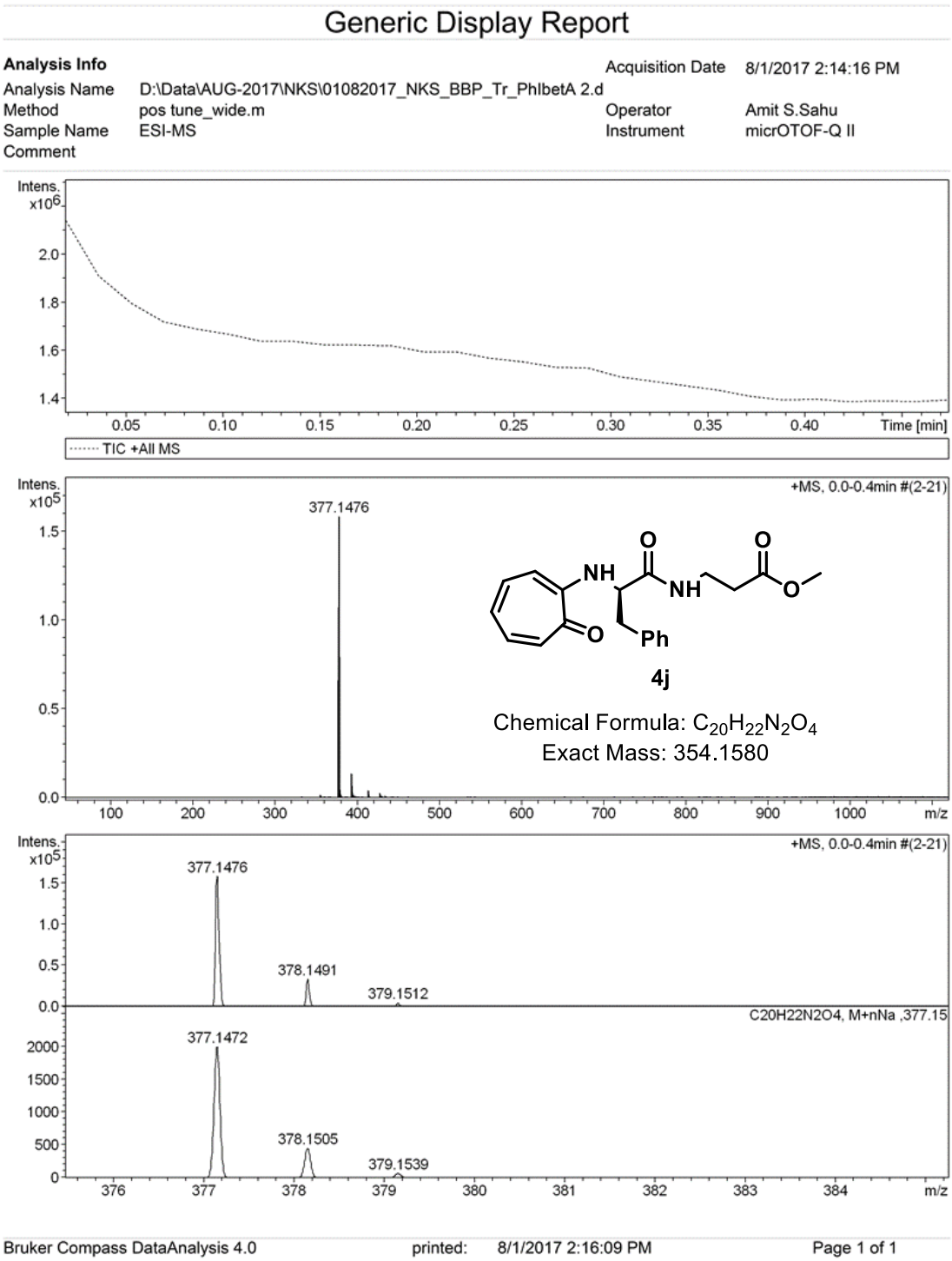

Figure. A20: ESI-MS/HRMS spectra of Tr-Phe-β-Ala -OMe (**4j**)

11. NMR (1H/13C) and HRMS spectra of Tr-Pro-Val-OMe(**4k**)

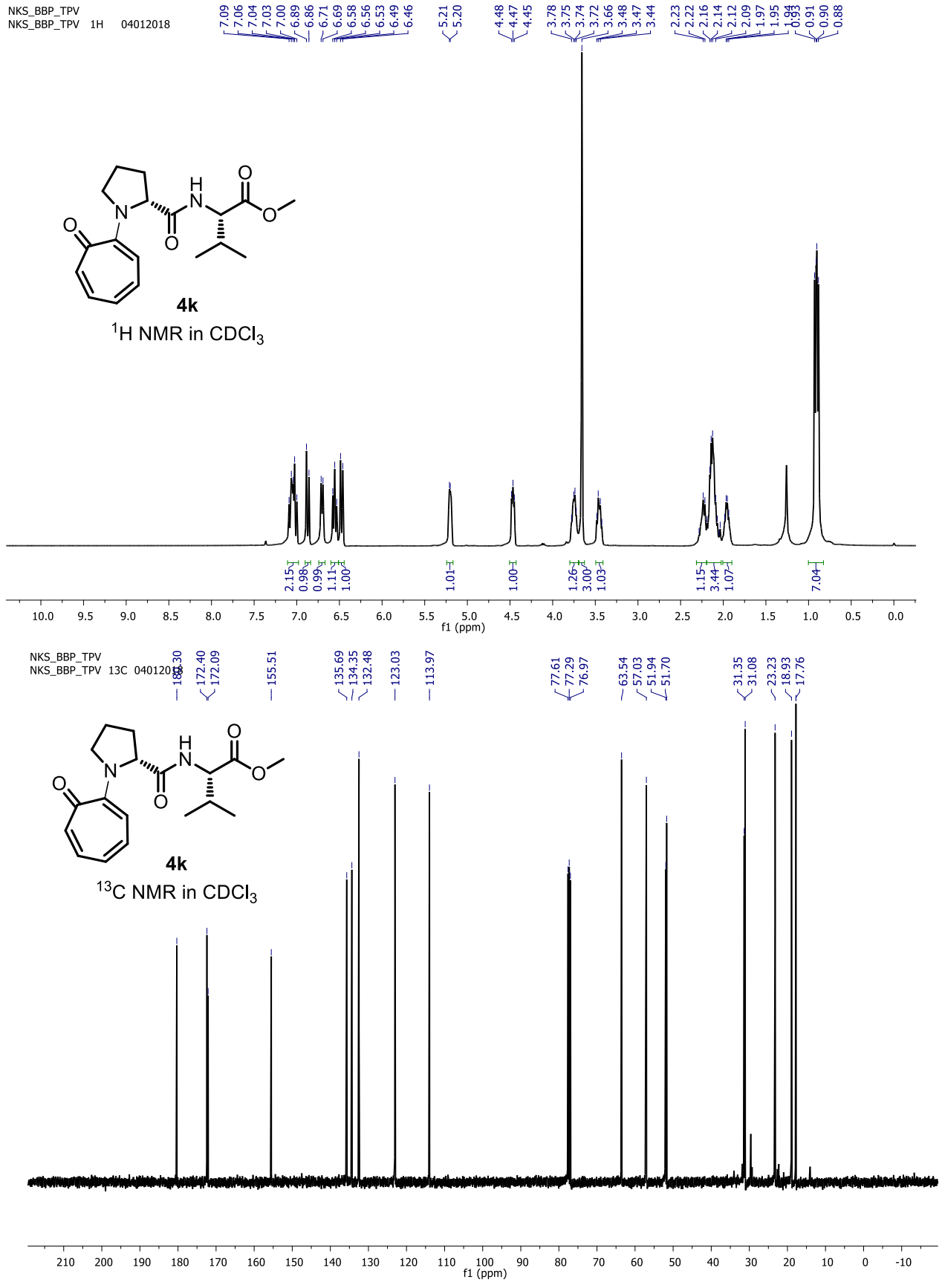

Figure. A21: $^{1}H,^{13}C$-NMR spectrum of Tr-Pro-Val -OMe (**4k**) in $CDCl_3$

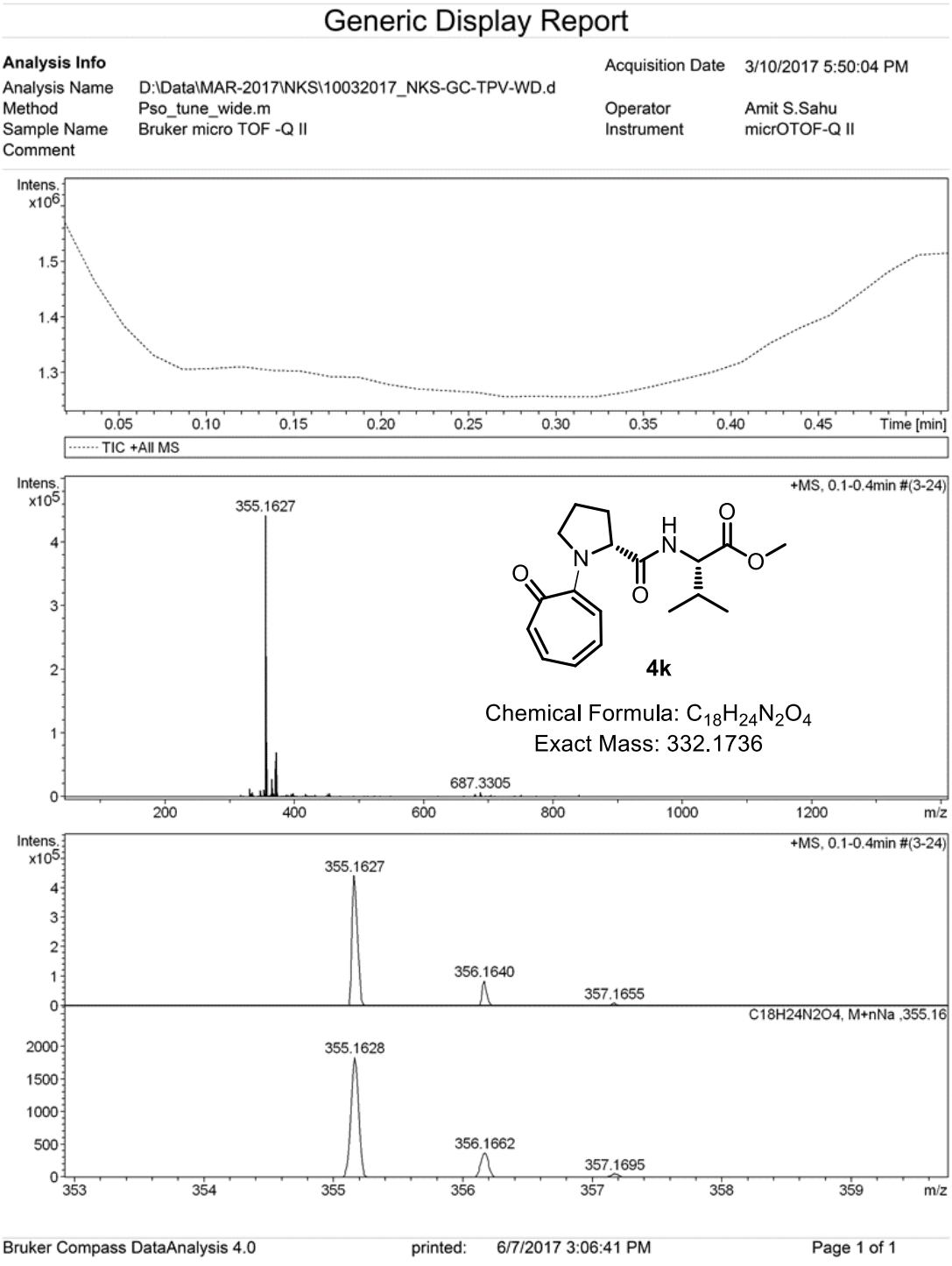

Figure. A22: ESI-MS/HRMS spectra of Tr-Pro-Val -OMe (**4k**)

12. NMR (1H/13C) and HRMS spectra of Tr-β-Ala-Pro-OMe(**4l**)

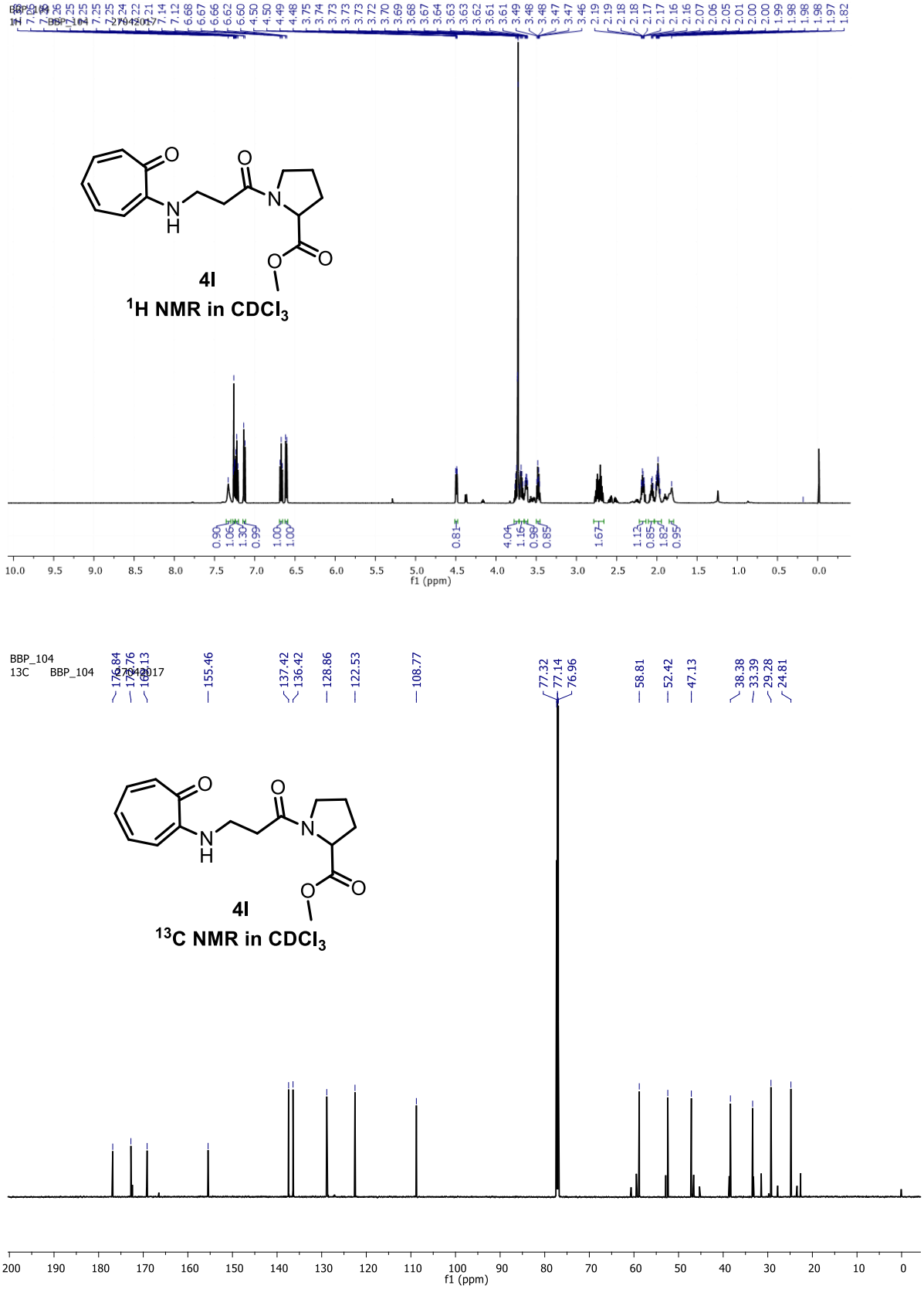

Figure. A23: $^{1}H,^{13}C$-NMR spectrum of Tr-β-Ala-Pro-OMe(**4l**) in $CDCl_3$

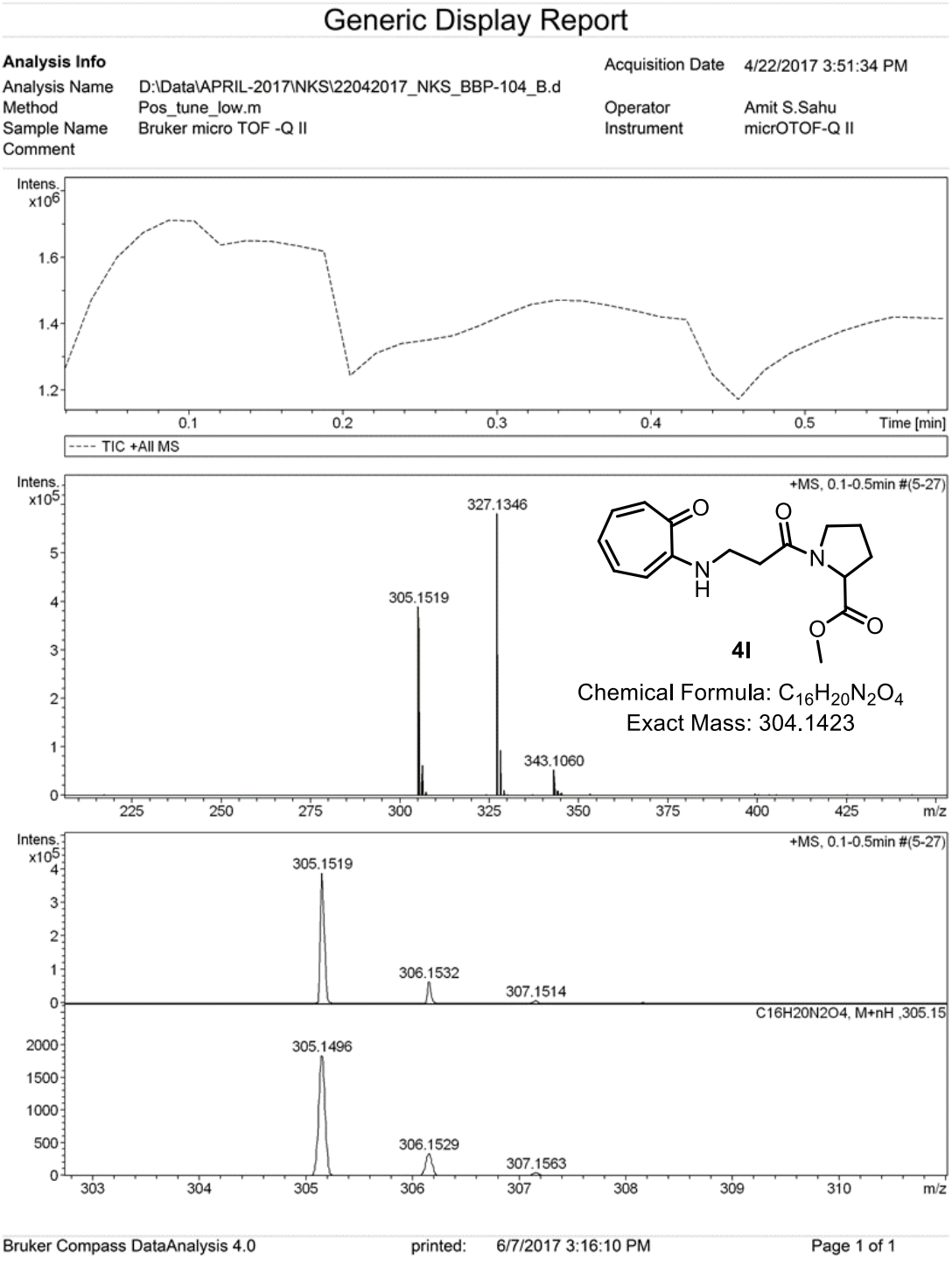

Figure. A24: ESI-MS/HRMS spectra of Tr-β-Ala-Pro-OMe(**4l**)

13. NMR (1H/13C) and HRMS spectra of Tr-Gly-β-Ala-Gly-OMe**(5a)**

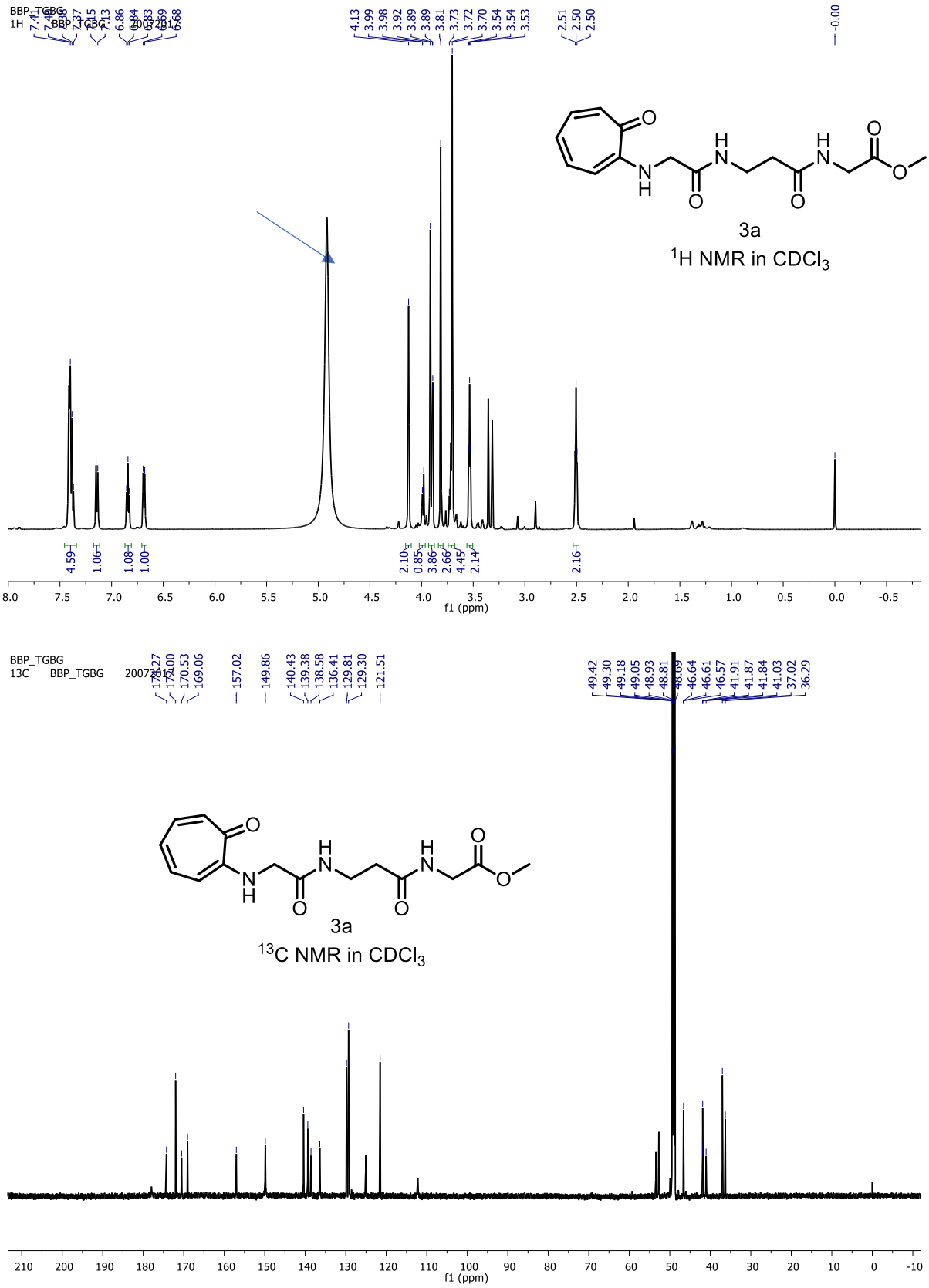

Figure. A25: $^{1}H,^{13}C$-NMR spectrum of Tr-Gly-β-Ala-Gly-OMe (**5a**) in $CDCl_3$

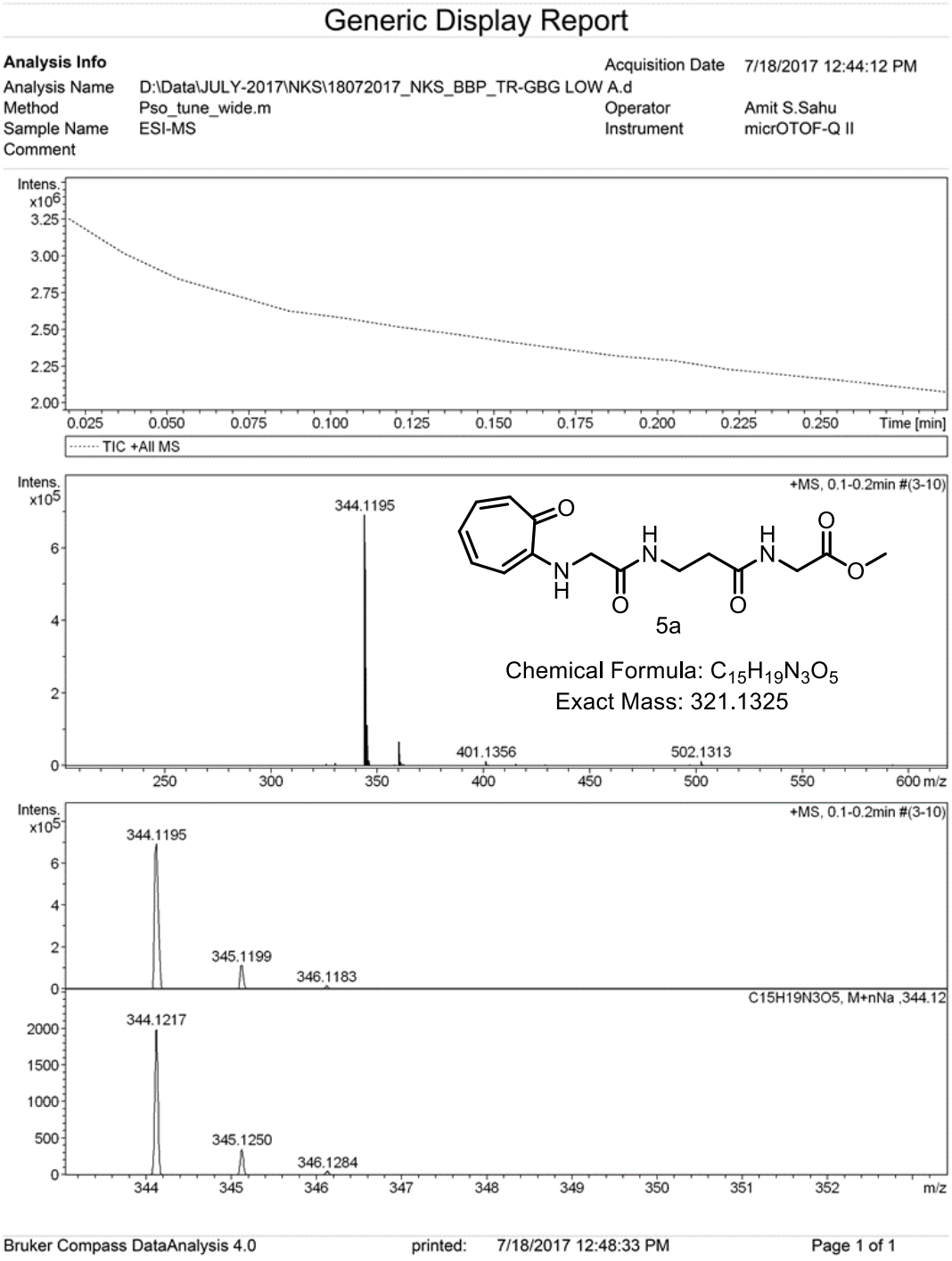

Figure. A26: ESI-MS/HRMS spectra of Tr-Gly-β-Ala-Gly-OMe (**5a**)

14. NMR (1H/13C) and HRMS spectra of Tr-Ala-β-Ala-OMe **(5b)**

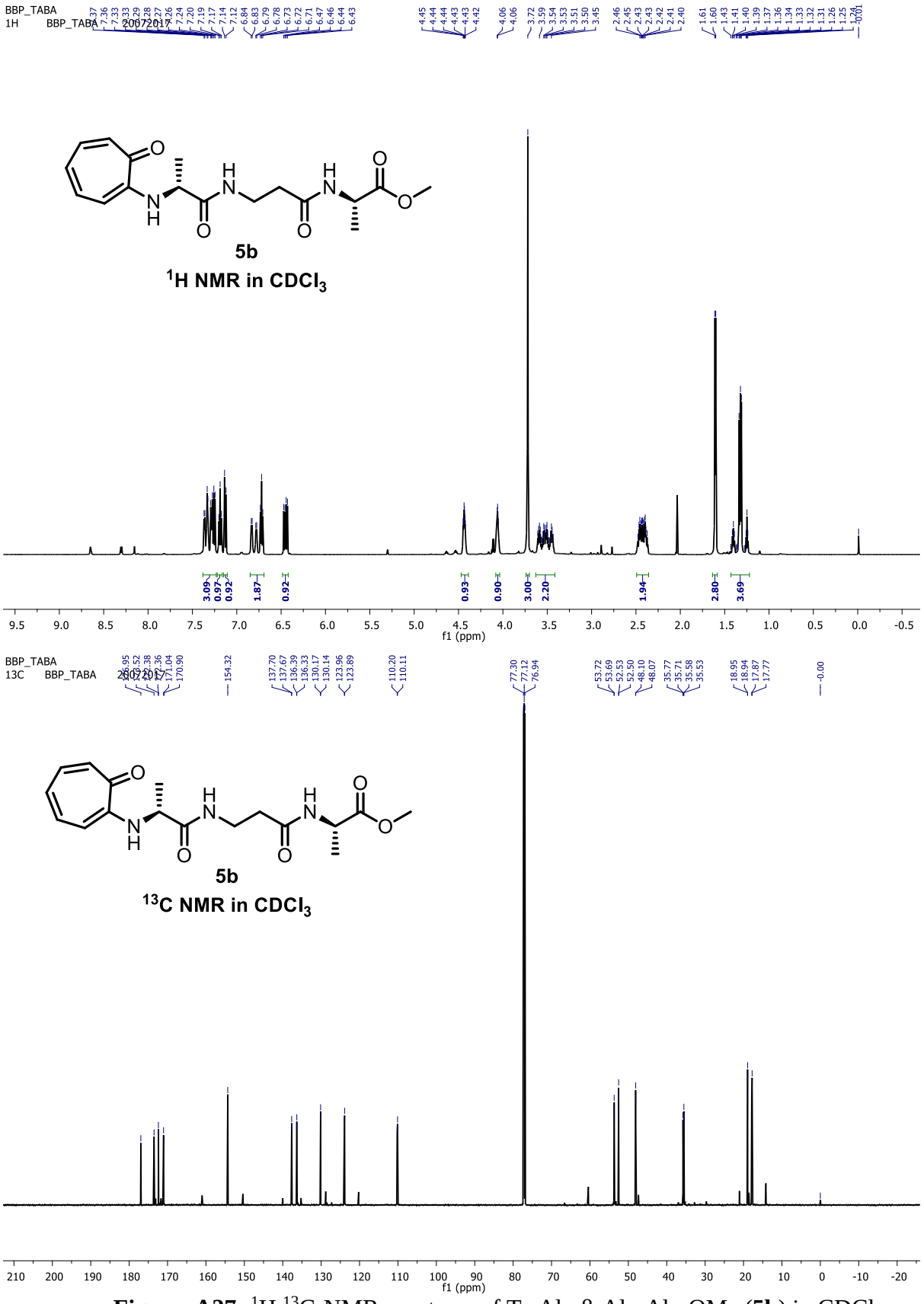

Figure. A27: $^{1}H,^{13}C$-NMR spectrum of Tr-Ala-β-Ala-Ala-OMe (**5b**) in $CDCl_3$

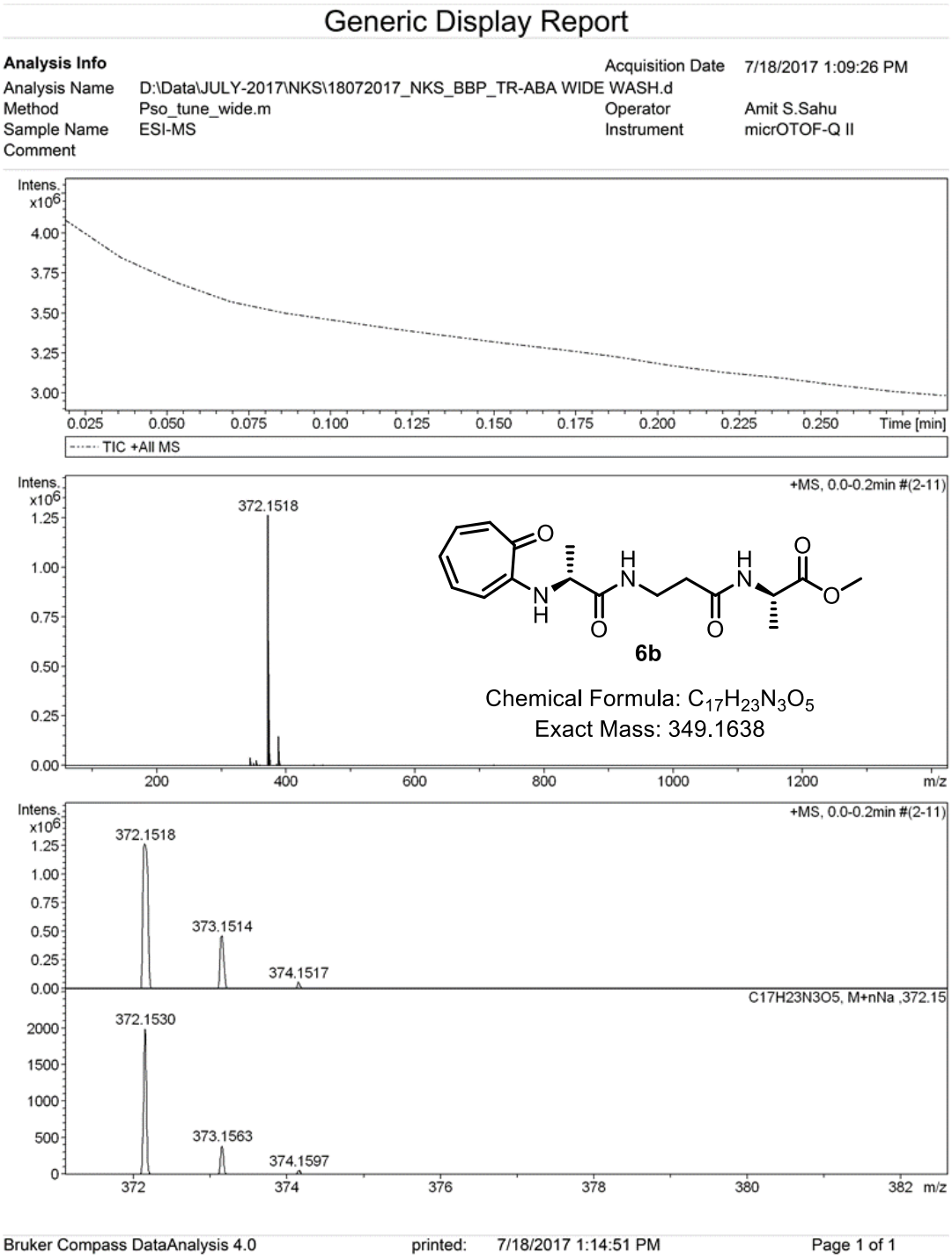

Figure. A28: ESI-MS/HRMS spectra of Tr-Ala-β-Ala-Ala-OMe (**5b**)

15. NMR ($^{1}H/^{13}C$) and HRMS spectra of Tr-Val-β-Ala-Val-OMe **(5c)**

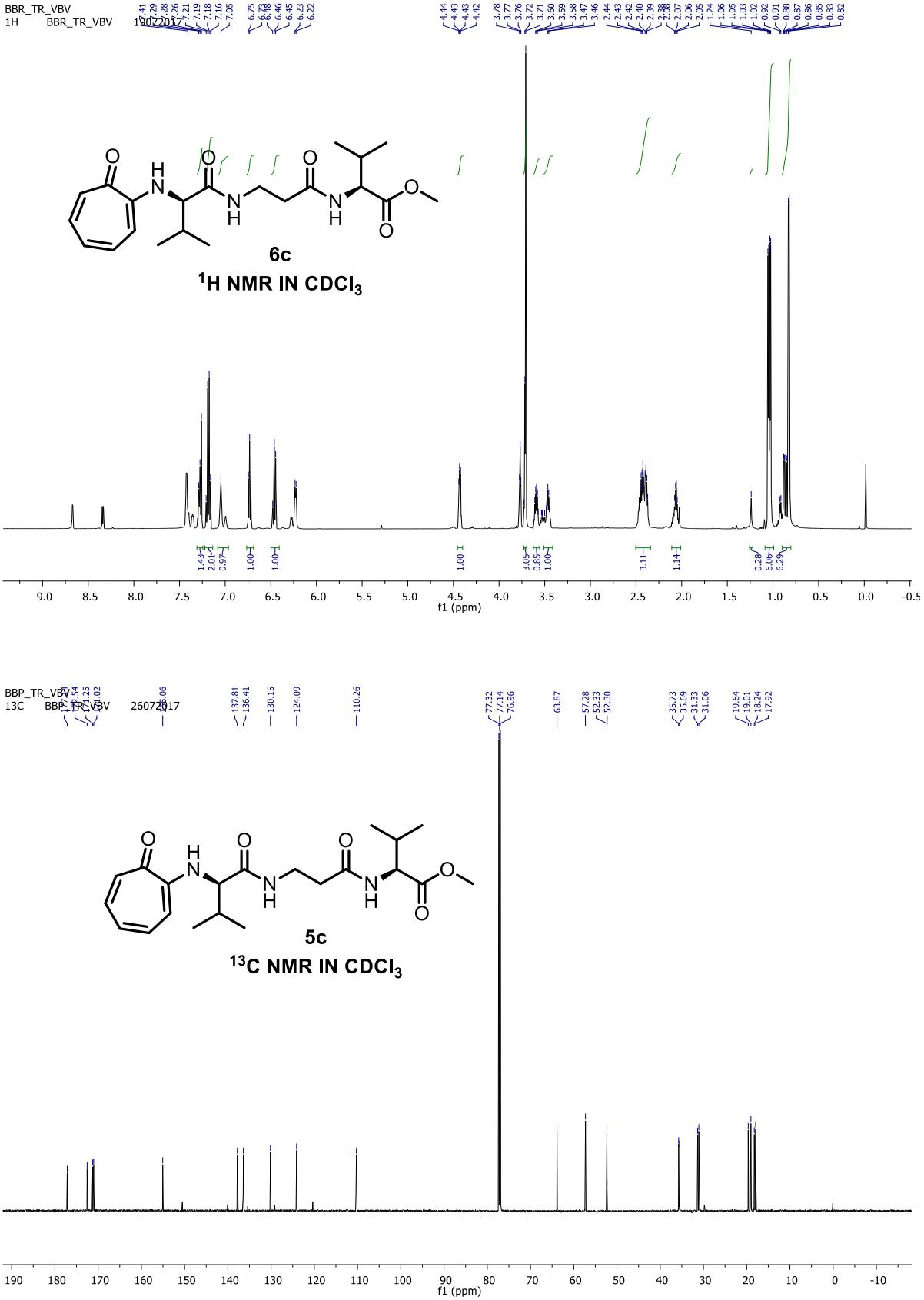

Figure. A29: $^{1}H,^{13}C$-NMR spectrum of Tr-Val-β-Ala-Val-OMe (**5c**) in $CDCl_3$

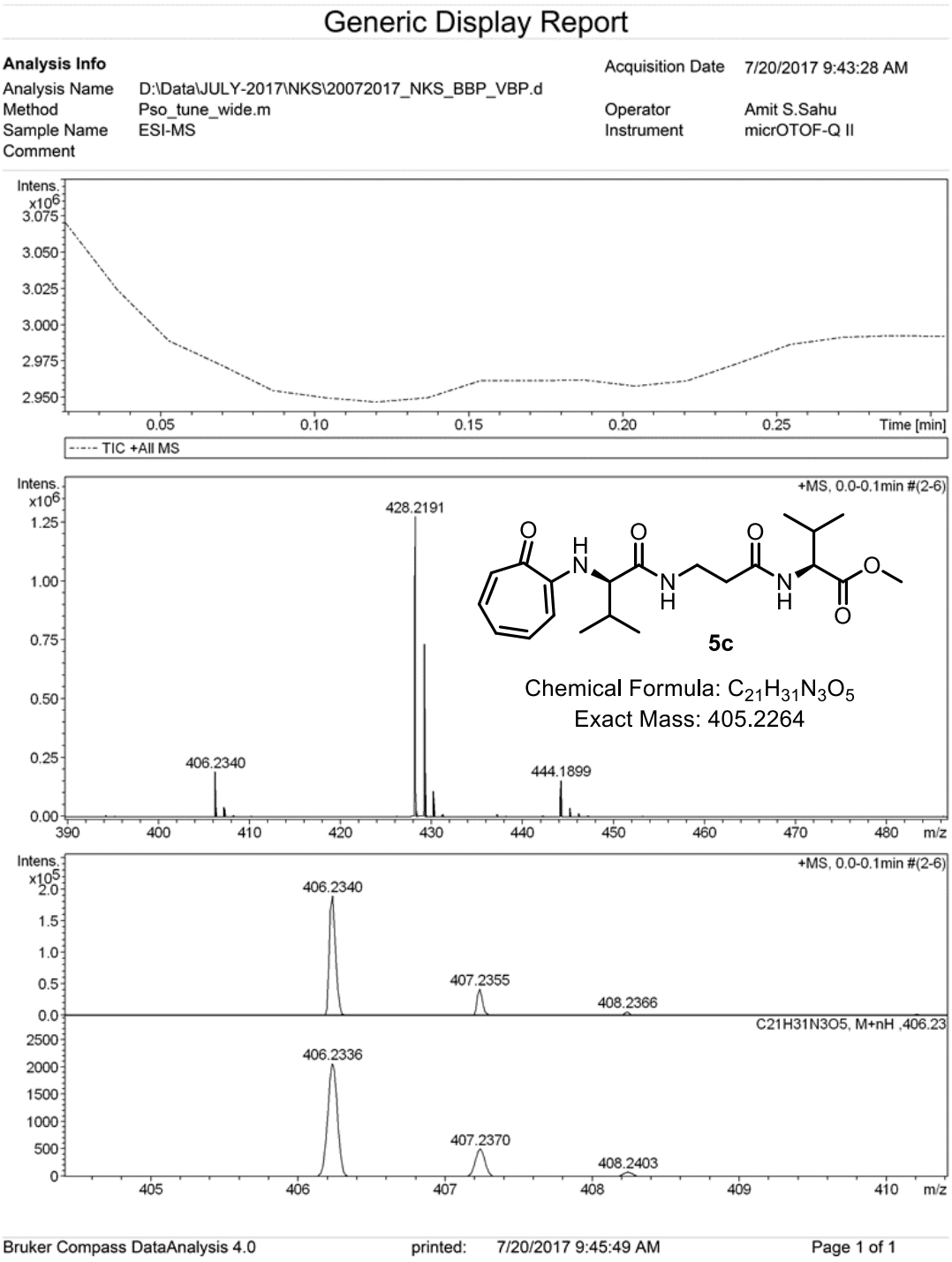

Figure. A30: ESI-MS/HRMS spectra of Tr-Val-β-Ala-Val-OMe (**5c**)

16. NMR ($^{1}H/^{13}C$) and HRMS spectra of Tr-Leu-β-Ala-Leu-OMe(**5d**)

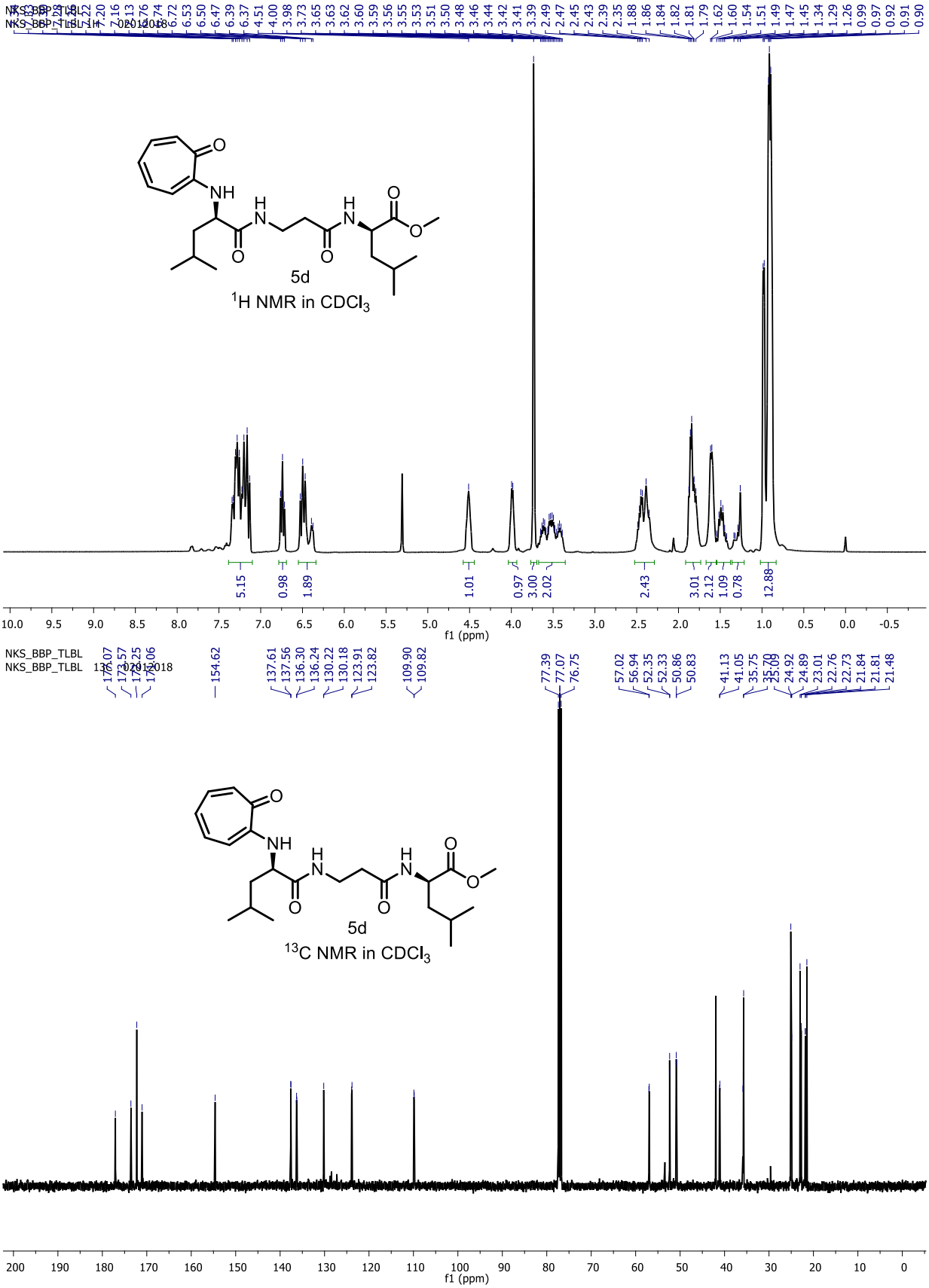

Figure. A31: $^{1}H,^{13}C$-NMR spectrum of Tr-Leu-β-Ala-Leu-OMe (**5d**) in $CDCl_3$

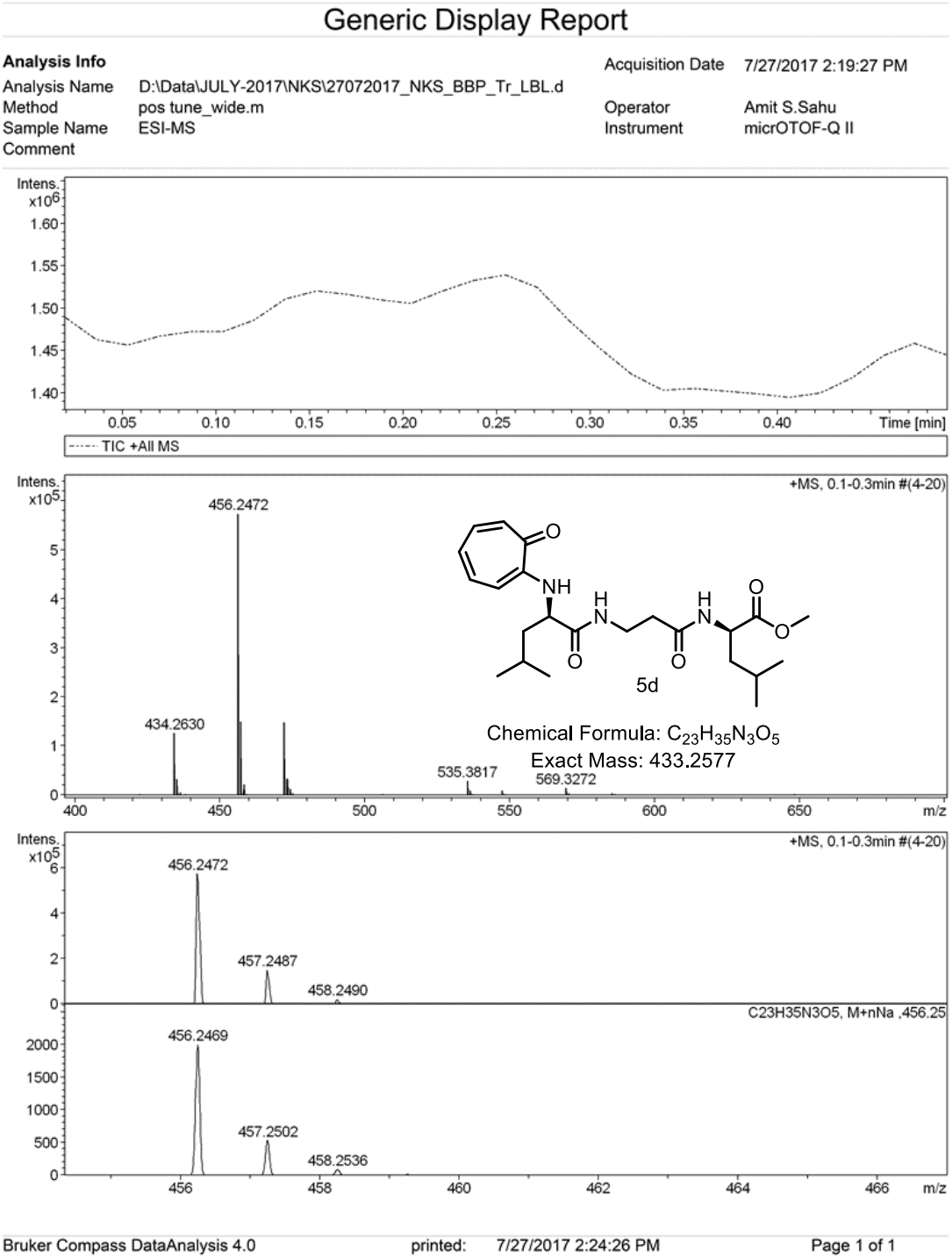

Figure. A32: ESI-MS/HRMS spectra of Tr-Leu-β-Ala-Leu-OMe (**5d**)

17. NMR ($^{1}H/^{13}C$) and HRMS spectra of Tr-Ilu-β-Ala-Ilu-OMe(**5e**)

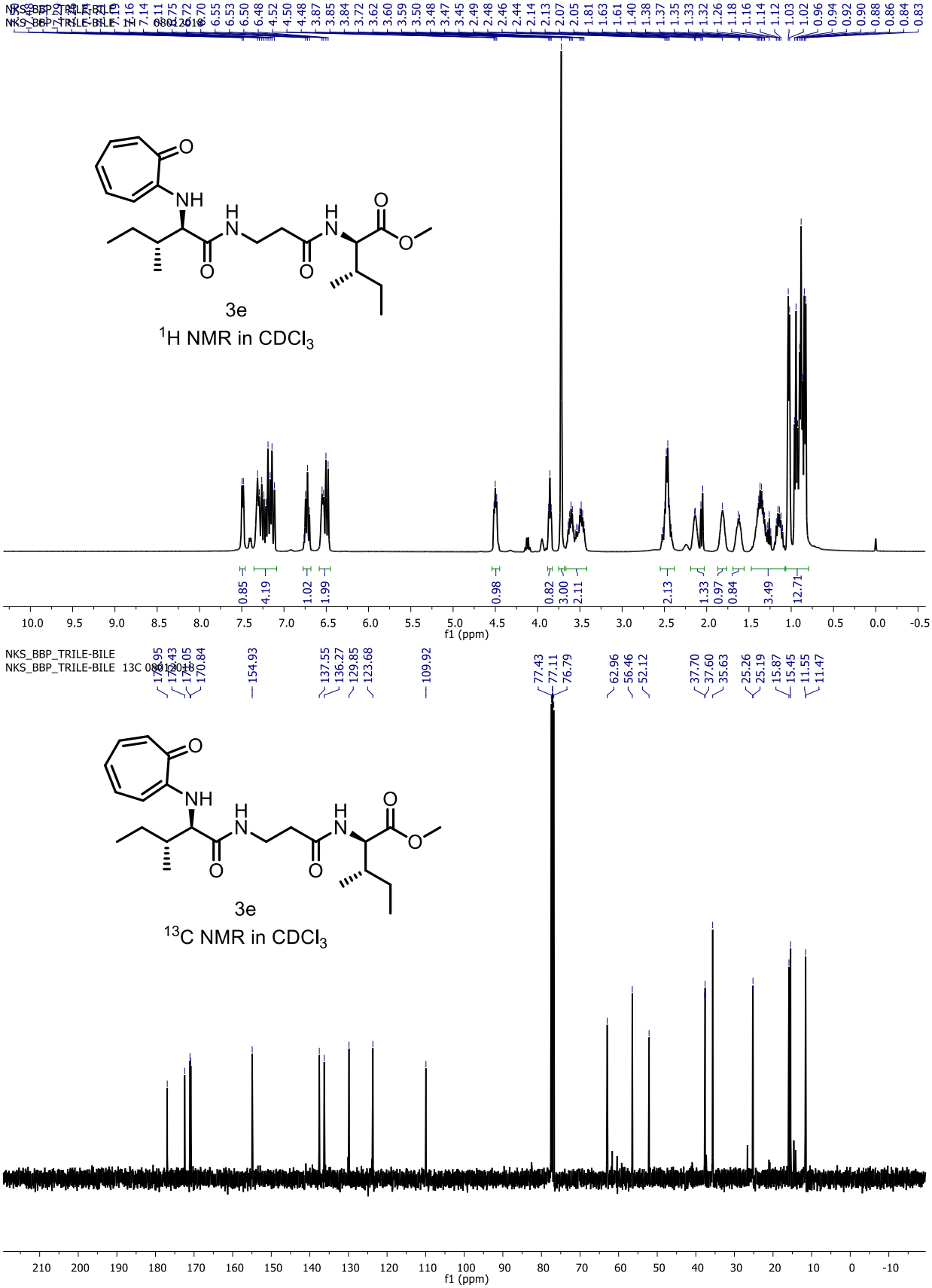

Figure. A33: $^{1}H,^{13}C$-NMR spectrum of Tr-Ile-β-Ala-Ile-OMe (**5e**) in $CDCl_3$

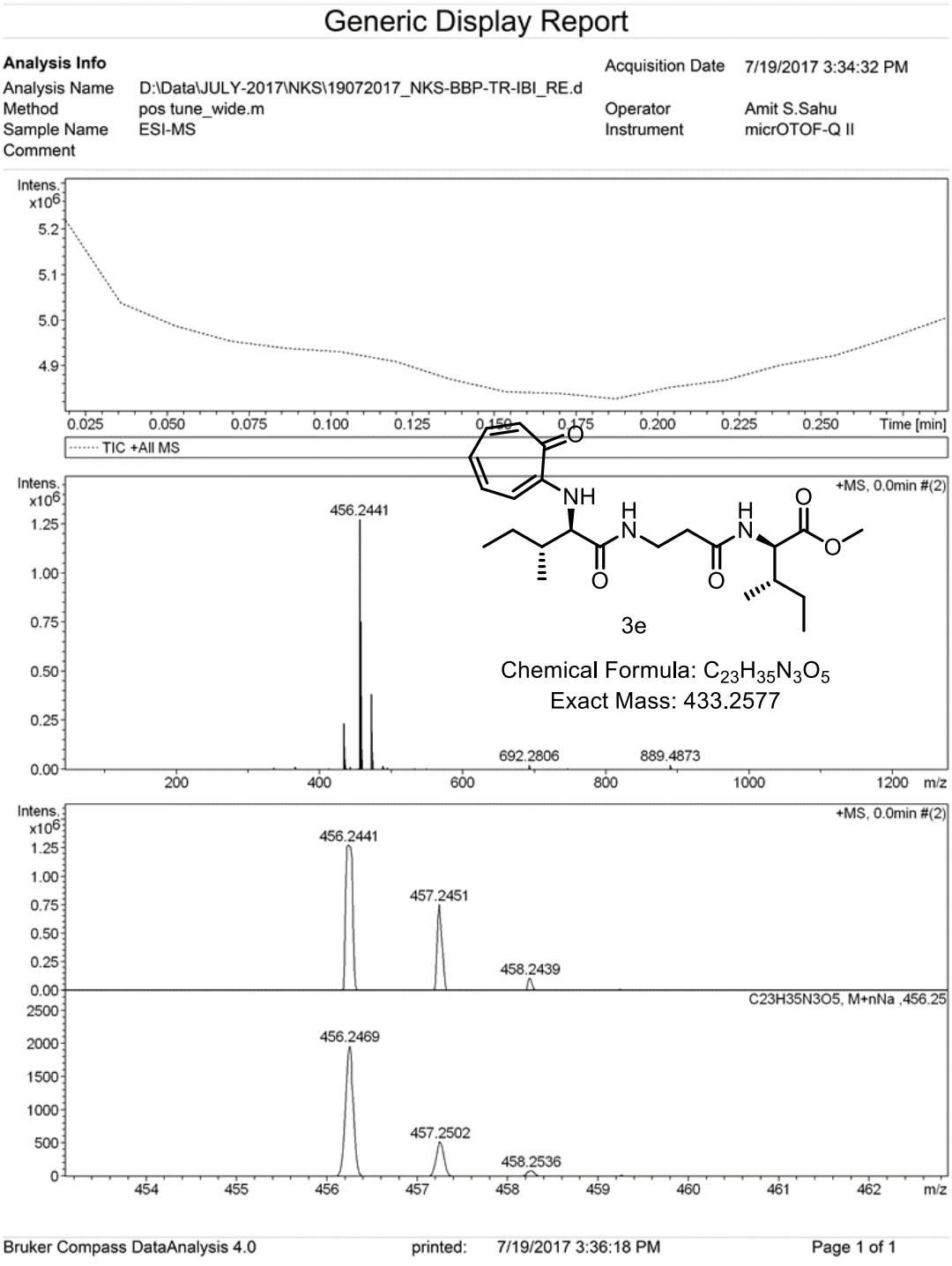

Figure. A34: ESI-MS/HRMS spectra of Tr-Ile-β-Ala-Ile-OMe (**5e**)

19. Crystal Structure determination:

Single crystals of (**4a/4b/4d/4e/4f/4j**) was grown by slow diffusion of solution in Dichloromethane into hexane, followed by evaporation under atmospheric conditions. The crystal data of all peptide were collected on a Bruker Kappa APEX II CCD diffractometer at 293 K and a Rigaku Oxford diffractometer at 293 K, respectively. Selected data collection parameters and other crystallographic results are summarized in SI. The program package SHELXTL[1] and Olex2 were used for structure solution, and packing diagram carried out by DIAMOND-3.2 software.

CCDC 1889029-1889034 contain the supplementary crystallographic data for **4a/4b/4d/4e/4f/4j**. These data can be obtained free of charge via https://www.ccdc.cam.ac.uk/data

Table S1: Crystallographic table

compounds	(**4a**)	(**4b**)	(**4d**)	(**4e**)	(**4f**)	(**4j**)
Identification code	CCDC 1889029	CCDC 1889030	CCDC 1889031	CCDC 1889033	CCDC 1889034	CCDC1889032
Empirical formula	$C_{12}H_{14}N_2O_4$	$C_{13}H_{16}N_2O_4$	$C_{15}H_{20}N_2O_4$	$C_{16}H_{22}N_2O_4$	$C_{13}H_{16}N_2O_4$	$C_{21}H_{27}N_5O_4$
Formula weight	250.25	264.28	292.33	306.35	264.28	357.48
Temperature/k	293(2)	296(2)	296(2)	296(2)	293(2)	293(2)
Crystal system	monoclinic	orthorhombic	triclinic	triclinic	monoclinic	triclinic
Space group	$P2_1/n$	$P2_12_12_1$	P-1	P-1	$P2_1/c$	P-1
A/å	13.8569(3)	6.8111(3)	7.8029(5)	8.2453(2)	13.8433(12)	9.5702(7)
B/å	4.87510(10)	7.3881(3)	10.6573(5)	9.1188(3)	11.6707(8)	9.7242(7)
C/å	18.1860(4)	27.5932(10)	10.8703(5)	11.2435(4)	8.3343(7)	11.5579(6)
α/°	90.00	90	115.740(4)	77.692(2)	90.00	72.878(6)
β/°	98.164(2)	90	99.231(3)	86.278(2)	100.376(7)	79.720(6)
γ/°	90.00	90	103.722(4)	86.449(2)	90.00	68.987(7)
Volume/å^3	1216.08(5)	1388.52(10)	754.32(7)	823.19(5)	1324.48(18)	956.37(11)
Z	4	4	2	2	4	2
ρ_{calc}g/cm^3	1.367	1.264	1.287	1.236	1.325	1.241
M/mm^{-1}	0.872	0.095	0.094	0.089	0.828	0.611
F(000)	528.0	560.0	312.0	328.0	560.0	384.0
Crystal size/mm^3	0.29 × 0.28 × 0.24	0.27 × 0.25 × 0.22	0.27 × 0.24 × 0.20	0.27 × 0.24 × 0.23	0.3 × 0.27 × 0.08	0.29 × 0.25 × 0.21
Radiation	CuKα (λ = 1.54184)	MoKα (λ = 0.71073)	MoKα (λ = 0.71073)	MoKα (λ = 0.71073)	CuKα (λ = 1.54184)	CuKα (λ = 1.54184)

2θ range for data collection/°	7.52 to 154.58	2.952 to 50.9	4.362 to 51.998	3.712 to 56.702	9.98 to 154.12	8.04 to 99.96
Index ranges	$-14 \leq h \leq 17$, $-5 \leq k \leq 5$, $-22 \leq l \leq 23$	$-8 \leq h \leq 8$, $-7 \leq k \leq 8$, $-33 \leq l \leq 33$	$-9 \leq h \leq 9$, $-13 \leq k \leq 12$, $-13 \leq l \leq 13$	$-10 \leq h \leq 11$, $-12 \leq k \leq 12$, $-15 \leq l \leq 14$	$-15 \leq h \leq 17$, $-13 \leq k \leq 14$, $-10 \leq l \leq 10$	$-9 \leq h \leq 9$, $-9 \leq k \leq 9$, $-11 \leq l \leq 11$
Reflections collected	9626	17437	10451	13278	9030	8659
Independent reflections	2482 [R_{int} = 0.0522, R_{sigma} = 0.0409]	2559 [R_{int} = 0.0561, R_{sigma} = 0.0396]	2967 [R_{int} = 0.0686, R_{sigma} = 0.0723]	4075 [R_{int} = 0.0203, R_{sigma} = 0.0198]	2695 [R_{int} = 0.0705, R_{sigma} = 0.0726]	1971 [R_{int} = 0.0847, R_{sigma} = 0.0770]
Data/restraints/parameters	2482/0/164	2559/0/173	2967/0/190	4075/0/202	2695/0/173	1971/0/237
Goodness-of-fit on f^2	1.067	1.015	0.969	1.040	1.067	1.188
Final r indexes [i>=2σ (i)]	R_1 = 0.0420, wR_2 = 0.1202	R_1 = 0.0420, wR_2 = 0.0923	R_1 = 0.0505, wR_2 = 0.1080	R_1 = 0.0437, wR_2 = 0.1170	R_1 = 0.0767, wR_2 = 0.2220	R_1 = 0.0747, wR_2 = 0.2141
Final r indexes [all data]	R_1 = 0.0480, wR_2 = 0.1240	R_1 = 0.0808, wR_2 = 0.1083	R_1 = 0.0993, wR_2 = 0.1226	R_1 = 0.0580, wR_2 = 0.1289	R_1 = 0.1142, wR_2 = 0.2996	R_1 = 0.0928, wR_2 = 0.2237
Largest diff. Peak/hole / e $å^{-3}$	0.17/-0.18	0.17/-0.14	0.18/-0.22	0.20/-0.16	0.24/-0.41	0.33/-0.22

20. Circular Dichroism (CD) Spectra.

CD experiments were recorded in degassed HPLC grade solvent CH_3OH And CH_3CN at 20 ^{0}C. CD spectra were recorded from 310-190 nm with peptide concentrations of 0.1 mM.CD data is collected with the following parameters, Data pitch 2 nm, DIT 2 sec, Bandwidth 2nm, Scanning speed 100 nm/min.

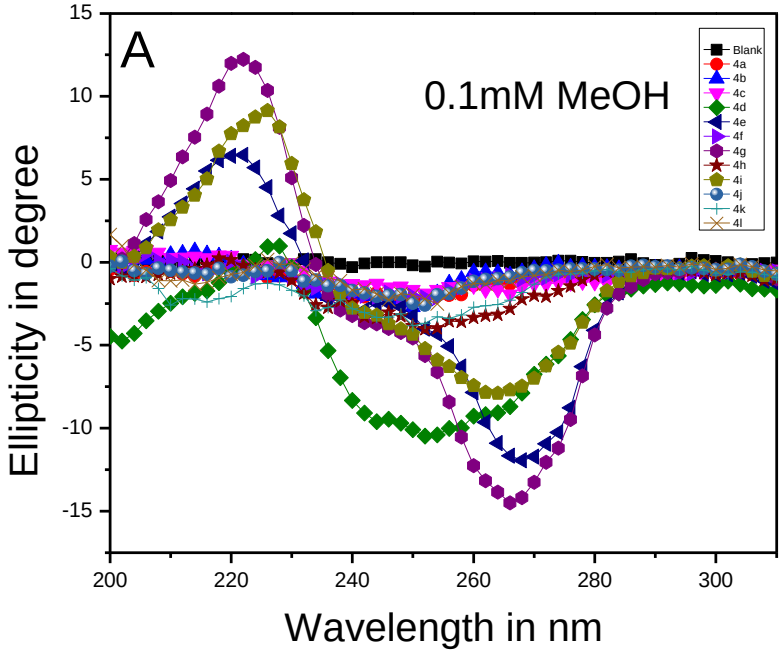

Figure. A35: CD spectra of peptide (**4a-4l**) in Methanol (MeOH)

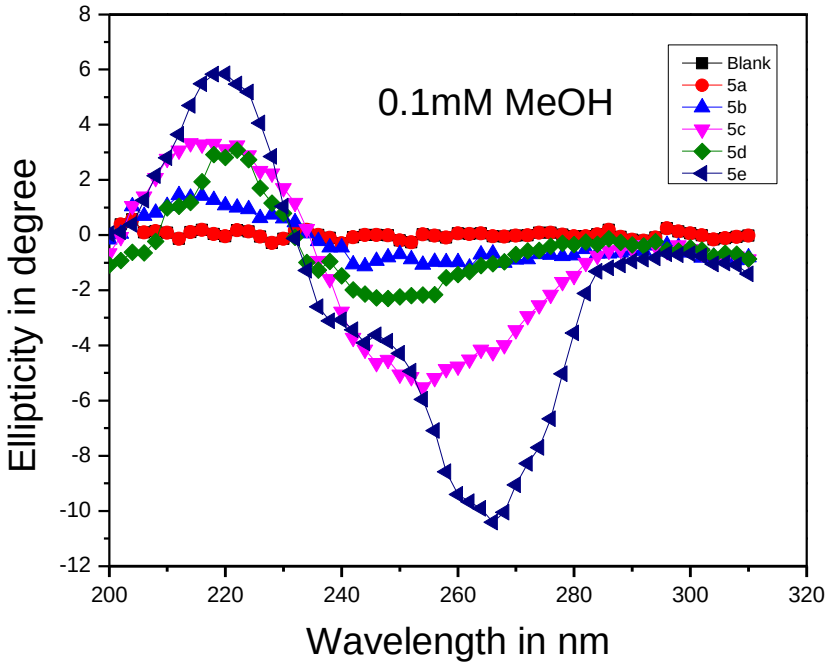

Figure. A36: CD spectra of *tri*-peptide (**5a-5e**) in Acetonitrile (MeOH)

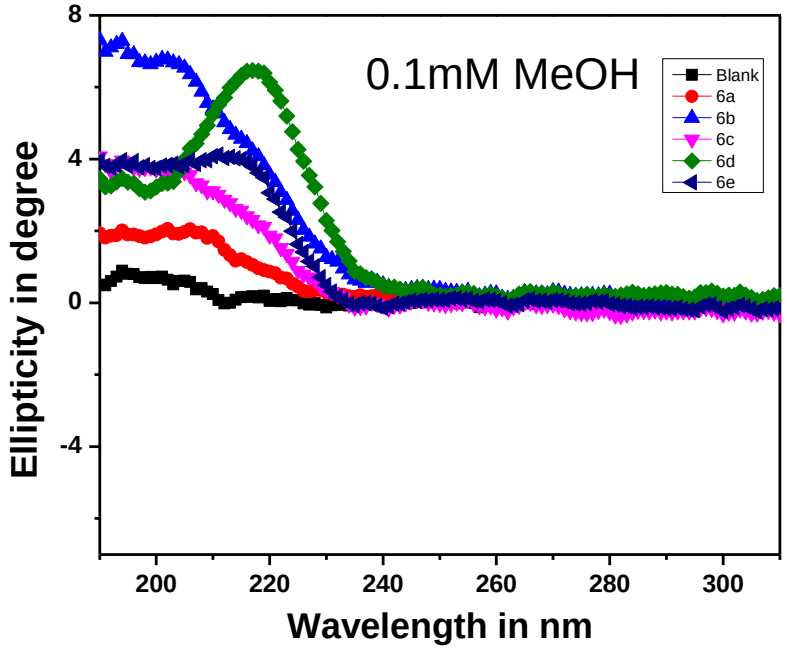

Figure. A37: CD spectra of peptide (**6a-6e**) in Methanol (MeOH

CHAPTER-3

PART-A

Title: Synthesis and Photophysical Studies of Functionalized *Troponyl*-BODIPY Analogues

3A.1 Introduction

3A.2 Objective of our work

3A.3 Result and discussion

3A.4 Conclusion

3A.5 Experimental Section

3A.6 Reference and Notes

3A.7 Appendix

3A.1 Introduction

Boron-Dipyrromethene (BODIPY) derivatives are versatile organic fluorescent dyes and enormously applied in syntheses of fluophore materials and excellent labeling agents of biomolecules for making chemical sensors, cell imaging agents and energy related cassette entities (**Figure 3A.1**).[1-4] Though few short comings such as solubility and functionality are persist with BODIPY dyes to use directly in practical applications. Recently, the functionalized BODIPY.[5] analogues are prepared from various dipyrromethene derived scaffolds and other related benzenoid aromatic ligands.[6] For examples, Alkenyl-BODIPY and C(sp^3) connected DYEmers are exhibited absorption peak for near infrared (NIR) region.[7] Dipyridylmethene (DIPYR) dyes, Pyridine-based BODIPY analoguesm, exhibits wide range of photophysical properties from non-emissive to green fluorescence with quantum yield 0.2-0.8.[8] BOIMPYs, benzimidazole containing analogue, have shown red-emmisve fluophores and considered as NIR-Dyes.[9, 10] Daniel Werz and Co-workers have prepared ethelene bridged oligo-BODIPYS which exhibit intramolecular J-aggregation and considered as superfluophores with quantum yield almost unity.[11] further the chlorinated dipyrromethene derivatives are desired for tuning their photophysical behaviors. Recently α-chlorinated-BODIPY analogues are prepared in one step directly from BODIPY using $CuCl_2$.[12] A new family of BODIPY dyes as *N*-BODIPYs (diaminoboron dipyrromethanes) are tested as smart photonic materials.[13] BOAHY, acyhydrozone containing BODIPY analogues has unique photophysical properties such as weak fluorescent in solution but emit brightly in powder form with maximum quantum yield 0.62. Most importantly, aggregation induced emission (AIE) and photoisomerization are noticed in BOAHY dye.[14] Moreover the application of BODIPY is expended to chemical transformation reaction. example Most recently, BODIPY analogue has been used as electron withdrawing

group for the activation of double bonds in asymmetric catalysis reaction which opens the door for the future transformation.[15] It would be interesting to prepare BODIPY analogues from naturally occurring small ligand. These reports encourage us to design biocompatible small fluorescent molecules for target specific biomolecules for various applications including the imaging in different cellular environments. In nature, the non-benzenoid aromatic derivatives occur as natural products which are biologically active and possessing valuable photophysical and chemical properties as like benzenoid derivatives. For example, Tropone and tropolone are non-benzenoid aromatic compounds containing seven-membered conjugated ring system, which are constituents of many natural products such as Colchicine, Thujaplicine, Manicoline, Theaflavin, and Isoimerubrin.[16-18] Tropolone and related derivatives, also called as tropolonoids, show distinctive electronic structure and exhibit characteristic photophysical behavior as excitation and emission.[19-21] Importantly, Tropolone and 2-Aminotropones show metal chelating properties with transition metal ions (Cu^{2+}, Zn^{2+}, Ni^{2+}) and lanthanides ions.[22-27] The UV absorption spectra of Tropolone exhibit more than one peak at different wavelength (λ) 265nm and 375nm (~$\lambda_{abs,265nm}$ & $\lambda_{abs,375nm}$) because of multiple transitions such as π-π*, n-π* and intramolecular charge transfer.[28, 29] Importantly, Tropolone is waek fluorescent molecule because of n-π* and intramolecular charge transfer, and exhibit fluorescence peak at $\lambda_{em,\ 410nm}$ 410nm at excitation $\lambda_{ex375nm}$. Owing to the intramolecular charge transfer, the fluorescence behavior of tropolone is sensitive to the polarity and pH conditions of environments. The fluorescence behavior of tropolone moiety has improved by changing the microenvironments in biological systems. For an example, Colchicine (tropolonoid natural product) has shown strong fluorescence characters after binding with the tubulin protein.[30, 31] Importantly, the substituted tropolone derivatives have shown strong fluorescence with enhanced

quantum yields.[32, 33] Other derivatives of tropolone as 2-aminotropone and 2-aminotroponimines also form complex with metal ions.[34, 35] Further aminotropones are modified as aminotroponimine derivatives and employed in complexation with various metal ions for various reasons including use as catalyst for selective organic transformation reactions.[36-40] In early sixties, Boron-aminotroponimine complexes were prepared but their photophysical properties were not explored (Figure 3A.1B).[41] Recently we have reported the syntheses of difluoroboron-aminotroponimine complexes (2-bora-l,3-diazaazulene derivatives) with various aryl/benzyme amine and demonstrated their fluorescence behavior with quantum yield upto 14-28%.[42].[42] repertoire of functional group bearing fluorophores from biocompatible 2-amintropone scaffold, we rationally designed carboxylate functionalized BODIPY analogues directly from aminotropone scaffold through *N,O*-chelation with Boron atom (**Figure 3A.1C**). In literature, aromatic scaffold-boron complexes are also explored through *N,O*-chelation in development of potential BODIPY analogues and have shown considerable impact.[43-45]

3A.2 Objective of our work

In this chapter, we have to explain the syntheses of various boron-aminotropones derivatives and examine their photo physical properties. *Tropolone* and α-amino acids which produce 2-Aminotropone scaffolds and form complex with *difluoro*-Boron through *N,O*-chelation. To studies the UV/Fluorescence behaviors in the different organic solvents.

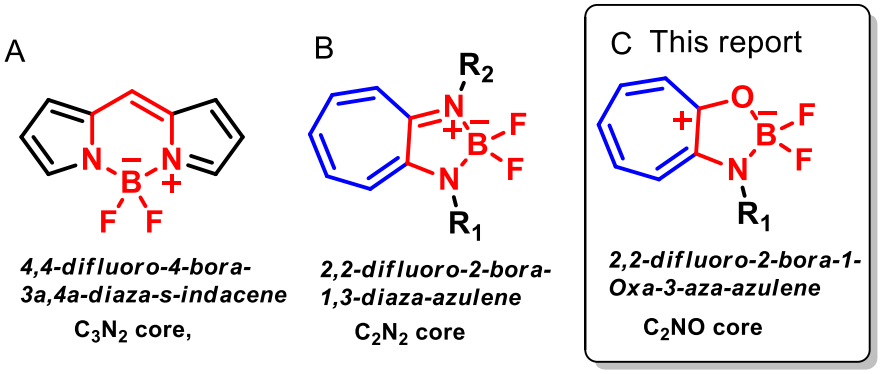

Figure 3A.1 Chemical structures of A) BODIPY complex; B) Boron-aminotroponimine complex; and C) Boron-aminotropone complex.

3A.3 Results and Discussions

We began the syntheses of boron-aminotropone complexes from commercially available tropolone (**1**) and naturally occurring L-amino acid by following synthetic route of Scheme 1. The amino acid ester derivatives were treated with 2-tosyloxytropone derivative by following our previously reported *N*-tropolonylation procedures.[42] We prepared 2-aminotropone glycine ethyl ester (**2a**) and its carboxylate acid (**3a-OH**) in good yield from glycine ester and 2-tosyloxytropone under reflux conditions. Similarly, other amino acid ester derivatives (Ala, Val, Leu, Phe, *β*-Ala) were *N*-troponylated and prepared as following: 2-aminotropone alanine ethyl ester (**2b**), 2-aminotropone valine methyl ester (**2c**), 2-aminotropone leucine methyl ester (**2d**) 2-aminotropone phenylalanine ethyl ester (**2e**), and 2-aminotropone-*β*-alanine methyl ester (**2f**). We also prepared *N*-troponylated dipeptide (**2g**) from dipeptide Gly-Val ester. To examine the superiority of aminotropone ligand (*N*,*O*-type) over non-tropone (*N*,*N*-types) in complexation with Boron, we synthesized *N*-troponyl picolylamine derivative (**2h**) and *N*-troponyl aminoquinoline (**2i**) from Picolylamine and 8-aminoquinoline respectively. These 2-aminotropone derivatives were treated with boronating reagent $BF_3.OEt_2$ under

mild basic conditions. As resultant, their respective boron-complexes were prepared such as difluoroboronyl aminotroponyl derivatives (**3a-3i**). NMR ($^{1}H/^{13}C/^{15}B/^{19}F$)/ESI-HRMS spectral data of ligands (**2a-2i**) and boron complexes (**3a-3i**) are provided in the Appendix.

Scheme 3A.1. Synthesis of difluoroboron-aminotropone complex

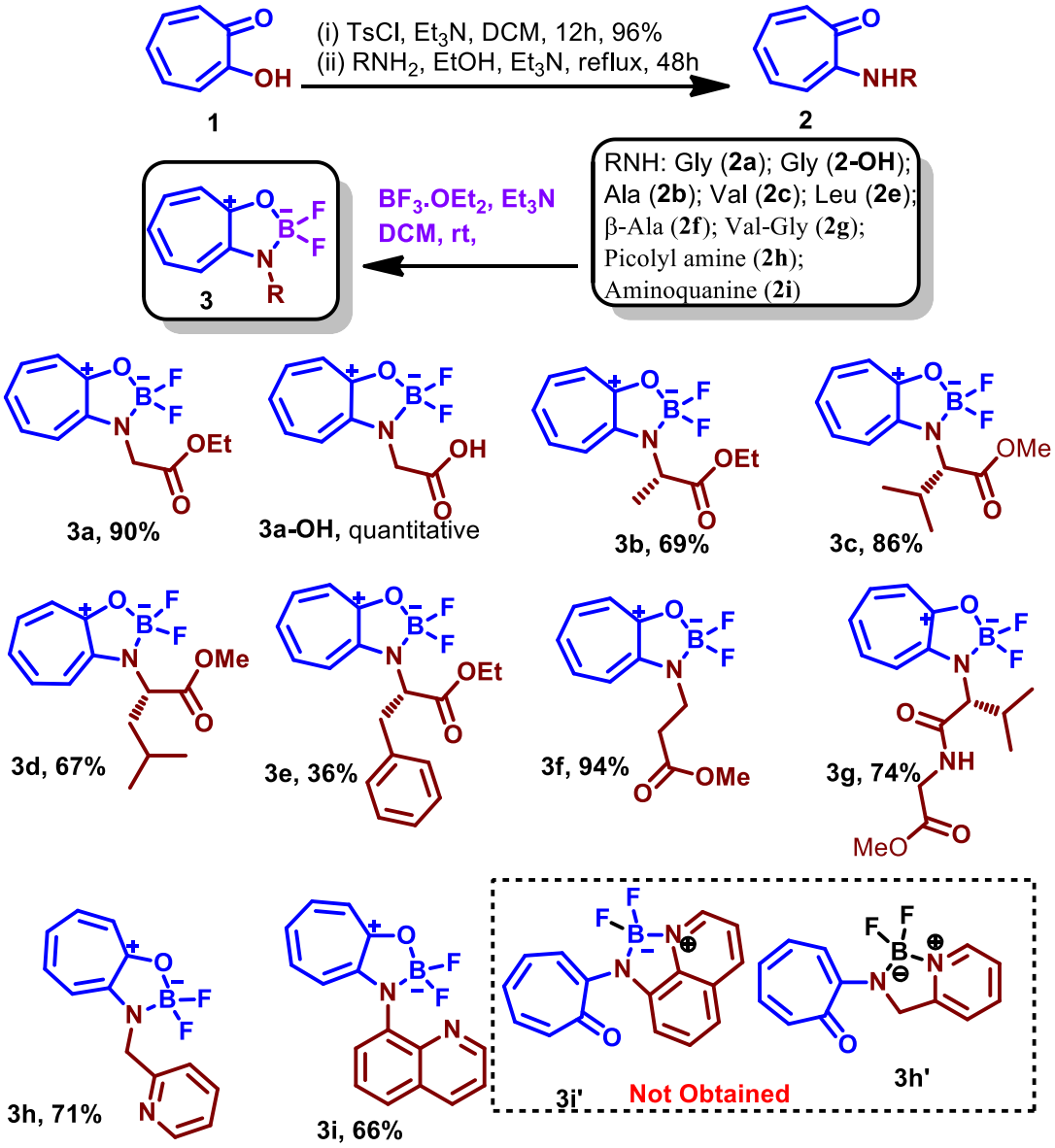

Pleasantly we crystalized the boron complexes in solvent system (DCM:MeOH). As resultant, we obtained the crystal of following six boron-aminotropone complexes in solid state: **3a-3c**, **3a-OH**, **3h-3i**. Their single crystals were diffracted by single crystal

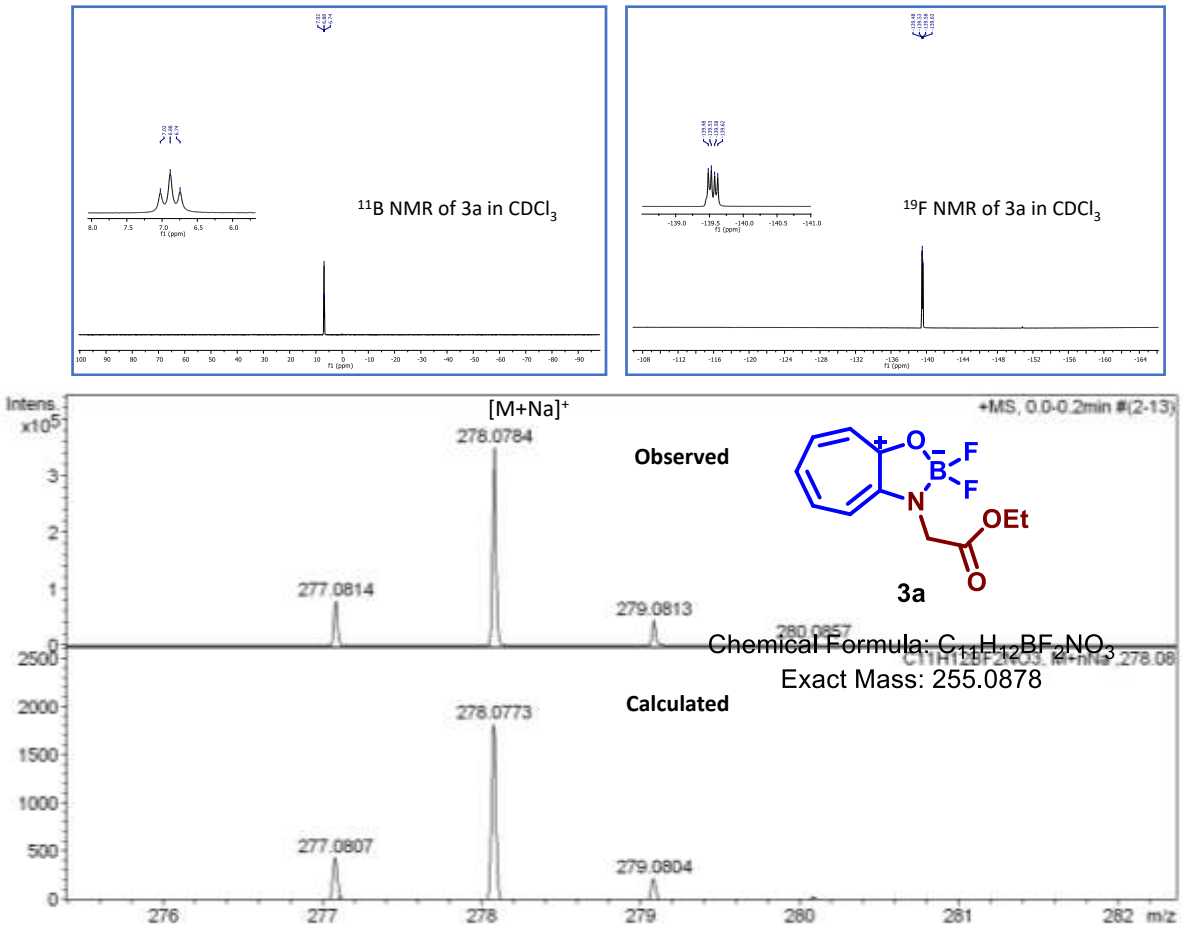

Figure 3A.2. 11B NMR and 19F NMR of **3a** in $CDCl_3$. HRMS spevtrum of **3a**.

diffractometer, then their data were analyzed which confirmed their chemical structures. Their solved X-ray data are deposited to Cambridge Crystallo-graphic Data Center (CCDC) with reference number CCDC 1888894-1888899. The crystal parameters of compound **3a-3c**, **3a-OH**, **3h-3i** are summarized in appendix Table A1. The ORTEP diagram of complex **3a-3c**, **3a-OH**, **3h-3i** is depicted in **Figure 3A.3** and **figure 3A.3**. **2a** alongwith bond length (N-B & O-B) and bond angles (N-B-O). The bond length and bond angles of solved structures are extracted and summarized in appendix **Table A2**. The crystal structure of aminotroponyl boron complexes (**3a**) reveal that. 2-aminotroponyl ligands form complex with

Boron through *N,O*-chelation with bond length N1-B (~1.5Å), O1-B (~1.4Å) and bond angle N1-B1-O1 (99.9^{o}). The crystal packing diagram of crysl **3a** (Glycine derivative) is depicted in Fig 2b which are packed due intermolecular troponyl C-H----F hydrogen bonding and π-π interaction between tilted troponyl ring of two parallel oriented molecules with distance 3.7Å (Figure 3A.4 C & Figure 3A.4 D). Similarly, ORTEP diagram of other crystals (**3a-OH, 3b**, **3c**, **3h** and **3i)** and their packing diagram are provided in **Figure 3A.3**. In crystal **3a-OH**, two molecules are oriented in antiparallel at distance 3.7Å and shows π-π interaction. The crystal packing diagram of crystal **3b** (Alanine derivatives) exhibit weak π-π interaction between two parallel orientation at distance 4.0 Å Importanly, crystal packing diagram of compound **3c** (Valine derivative) shows the formation of β-sheet by two types of π-π interactions at distance 4.0 Å and 4.3 Å. Most importantly, crystal structure of **3h** and **3i** are also formed with N,O type of chelation with B, though there are opportunity to form boron complexes via N,N chelation as **3h' and 3i'.** In contrast, the crystal packing of **3h** (Picolonyl derivative) and **3i** (Aminoquaninyl derivative) are different as tropone ring is not involved in intermolecular π-π interactions. Though pyridine ring of **3h** and benzene ring of **3i** are involved in inter molecular π-π interaction at distance 4.2 Å and 3.6 Å respectively. In all cases, boron realted bond length N1-B1 (~1.5Å) are lesser than and O1-B (~1.4Å) within the same range of bond angle N1-B1-O1 (~100^{o}). and nearly same with reported such other BODIPY analogues. Hence 2-aminotropone derivatives are excellent carboxylate functionalized scaffold for the formation of BODIPY analogues.

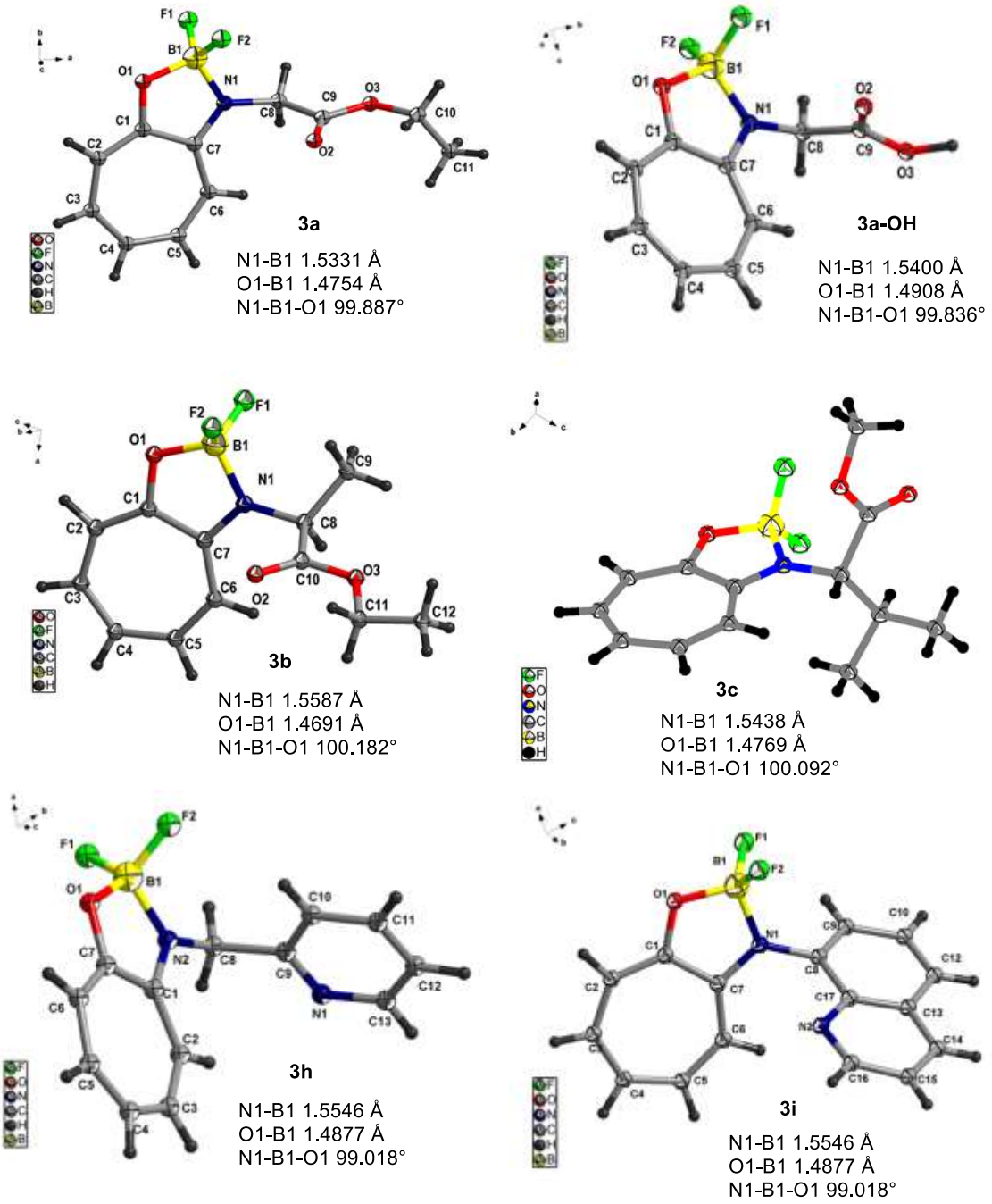

Figure 3A.3. ORTEP diagrams of boron complex **(3a, 3a-OH, 3b, 3c, 3h, and 3i**) with 50% probability of ellipsoids.

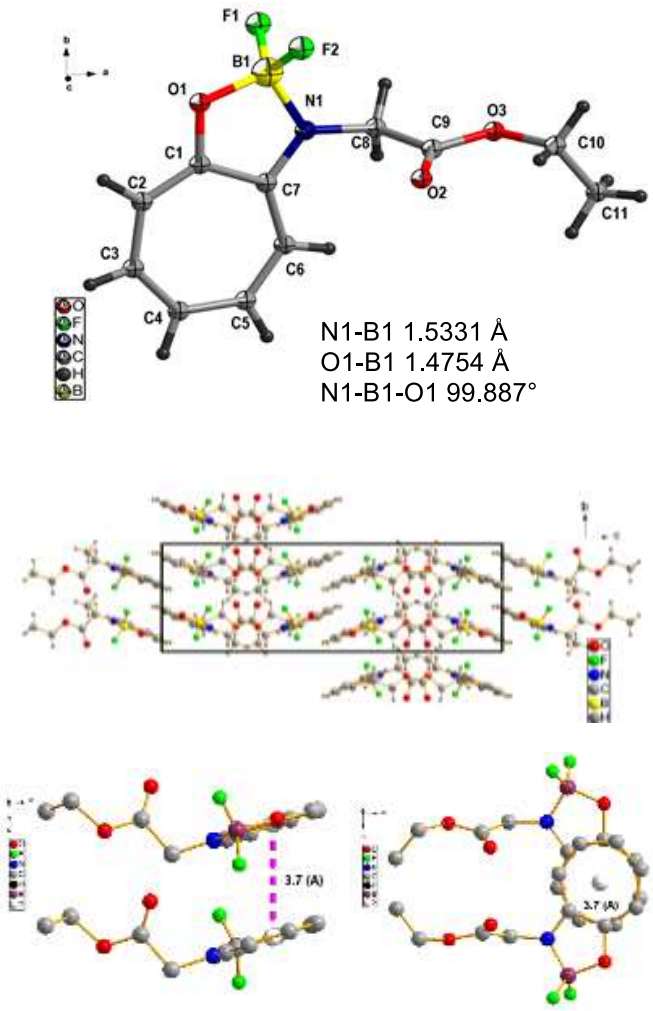

Figure 3A.4. Structural description of crystal BF_2-Aminotropone analogue **3a** (CCDC 1888899): a. ORTEP diagram with 50% probability of ellipsoids and important bond length; b. Packing diagram; π-π interaction (side view), c. interaction (top view); and d. ORTEP diagram with 50% probability of ellipsoids and important bond length.

Since BODIPY and related derivatives exhibit distinctive fluorescence characters which depends upon the nature of ligands, substituents of core structure dipyrromethene.[46] Herein we studied photophysical properties of difluoroboron-aminotropone complexes (**3a-3i**). We recorded UV/fluorescence spectra of complexes (**3a-3i**) in protic/aprotic

polar solvents (MeOH/CH_3CN) to investigate their UV/fluorescence characters. The UV-absorption spectra compounds (**3a-3i**) in MeOH is depicted in **Figure 3A.5A**, while other absorption and emission spectra are provided in appendix. The summary of UV-Vis absorption data of boron-aminotropones (**3a-3i**) are given in Table A3. The absorption spectra of those boron-aminotropone complexes (**3a-3h**), except aminoquinoline bearing complex (**3i**), exhibit three broad peaks nearly at wavelength (λ) 244nm, 330nm and 380nm in solvent MeOH/CH_3CN, which are almost like reported tropolone/aminotropone derivatives. These UV-absorption peaks are reportedly known in troplone due to π-π^*, n-π^* transitions and intramolecular charge transfer.[28] Aminoquinoline bearing boron complex (**3i**) exhibits prominently peak at λ_{380nm} with a shoulder peak at ~λ_{330nm}, possibly because of the delocalization of non-bonding electron over both tropone and Aminoquinoline rings. Importantly, phenylalanine bearing complex (**3e**) exhibit less structure peaks as prominently at λ_{330nm} with a shoulder peak at λ_{380nm} in compare to other α-amino acid bearing complexes (**3a-3d**). Presumably, the π-π interactions between tropone ring and phenyl ring perturbed the charge transfer of boron-complex (**3e**) and suppressed the absorption peak at λ_{380nm}. UV-Vis spectra of boron complexes (**3a-3i**) are almost similar in other solvent CH_3CN which support that no role solvent in their electronic transition. We also determined molar extinction coefficient of tropolonyl-boron complexes (**3a-3i**) at λ_{380nm} from respective spectra in solvent MeOH and their values are provided in Table A3 (Apppendix). For comparative studies, the bar diagram of extinction coefficient vs boron-complexes (**3a-3i**) is generated (**Figure 3A.5B**). The molar extinction coefficient of tropone-boron complexes is in following order 3e<3b<3c<3d~3g<3a<3f<3h<3i. The aminoquinoline containing tropone-boron complex (**3i**) is enhanced because of further delocalization of electrons which possibly lowered the energy difference of electronic transitions.

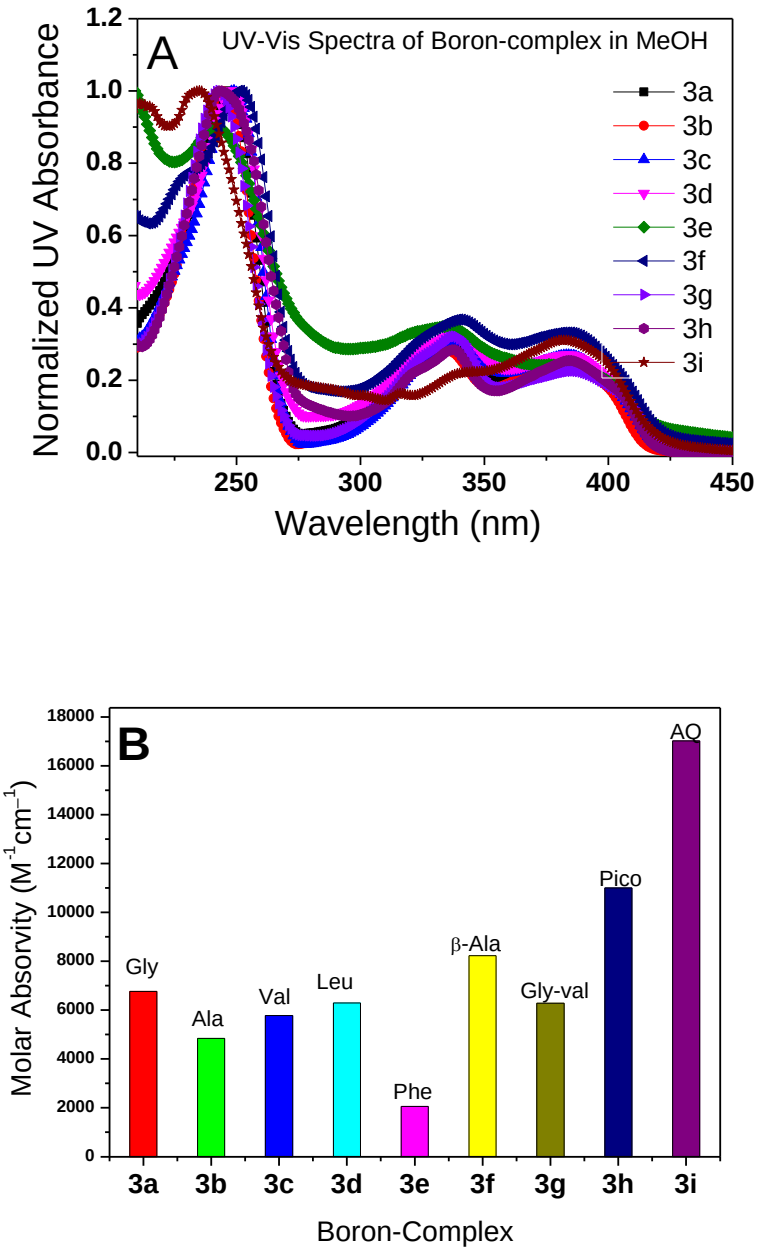

Figure 3A.5. Absorption spectra of boron-aminotropone complexes (**3a-i**) in methanol at $5x10^{-4}$M concentration (A); and Bar diagram of their molar extinction coefficient (B).

The normalized fluorescence spectra of difluoroboron complexes (**3a-3i**) at excitation wavelength ($\lambda_{ex.}$) 380nm along with respective UV spectra show that these complexes,

except complex **3i**, are fluorescent molecule in both solvents CH_3OH and CH_3CN (Appendix). Aminoquinoline tropon-boron complex (**3i**) is non-fluorescent molecule which does not exhibits emission spectra, though it exhibits UV absorption spectra at λ_{380nm} with high molar absorptivity. Further UV absorption and emission spectra of one complex **3a** in protic solvent MeOH are depicted in **Figure 3A.6A** which show strong emission peaks at $\lambda_{em,440\text{-}450nm}$ and secondary peaks at $\lambda_{em.410\text{-}420nm}$ with Stokes shift ~109nm. This spectra support that the fluorescence character of boron complex (**3a**) is due to intramolecular charge transfer and n-π^* transition. We noticed the appearance of almost similar UV/emission spectra in other fluorescent complexes **3b-3h** in both solvent MeOH/CH_3CN (Appendix). Further, we calculated their (**3a-3h**) quantum yield in both solvents using quinine sulfate in H_2SO_4 (0.1M) as reference (Appendix. Table A3). For comparative studies, we generated a bar diagram of quantum yield vs boron complexes (**Figure 3A.6B**) in solvent MeOH. This bar diagram shows quantum yield in following order **3a>3h>3c>3b>3d>3f~3g>>3e**. The simplest aminotropone boron complex as glycinatetropone-boron complex (**3a**) has quantum yield ca 0.15 which is maximum among others derivatives (**3b-3h**). We notice that quantum yield of aminotropone-boron complex decreases with branching α-position of amino acid as with **3c/3b/3d/3e**. The increasing the chain length of amino acid also decreases quantum yield as in **3f/3g**. The remarkable decrease in quantum yield in phenylalanine derivative (**3e**) is most probably due to the perturbation of charge transfer by π-π interaction between tropone and phenyl ring which supported by its UV spectra. Most importantly, quantum yield of picolylamine tropone complex (**3h**) is are nearly same as glycinate-tropone (**3a)** unlike non-fluorescent aminoquinolinenine derivative (**3i**). To examine the role of solvent in the fluorescence character of such boron-complex, we recorded the UV/emission spectra of complex **3a** in other solvents EtOH/THF and determined

photophysical parameters (Table A3). The quantum yield of **3a** is almost same in above mentioned solvents as like MeOH and CH_3CN. However substantial increased in quantum yield is noticed in THF. Our results show that the role of solvent's polarity is limited as like our previously reported Boron-aminotroponimine complexes.[42]

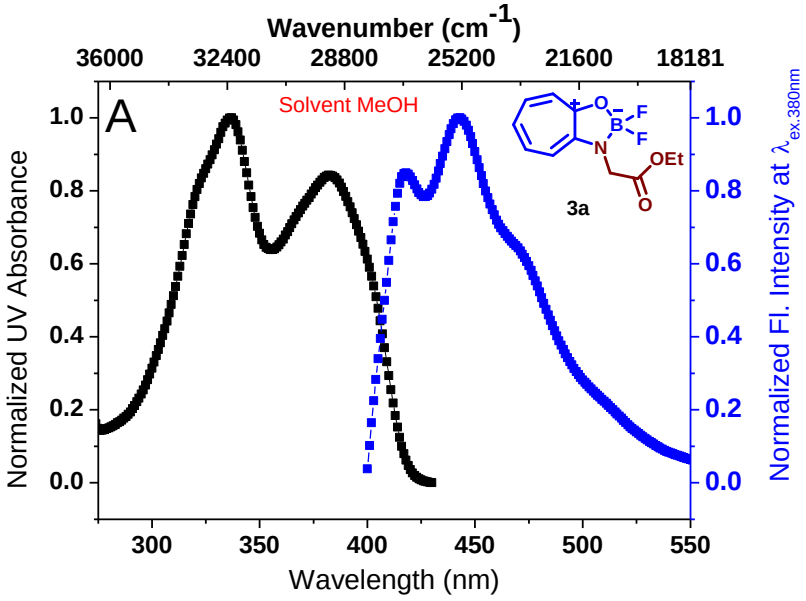

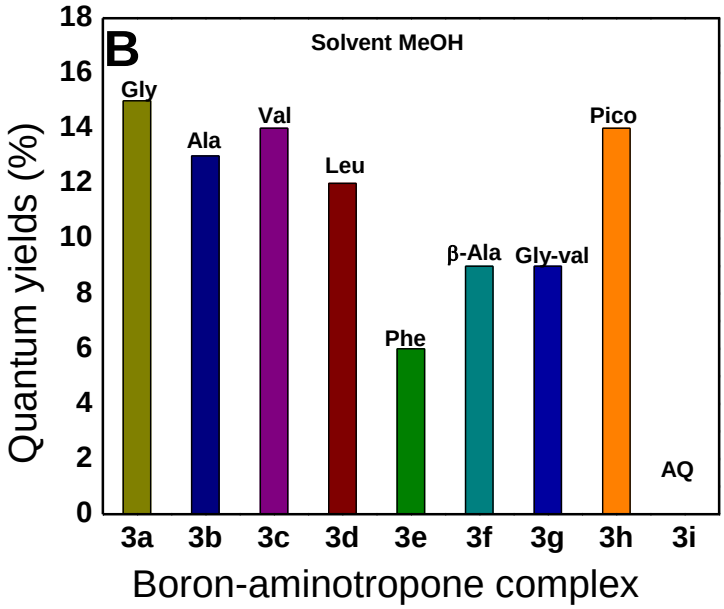

Figure 3A.6. (A) Absorption and Emission spectra of boron-aminotropone complexes (**3a**) in methanol at concentration ($5x10^{-4}$M). (B) Quantum yield bar diagram of boron-aminotropone complexes (**3a-3i**) in methanol.

Table 3A.1: Photophysical parameters of Boron-aminotropone complexes.

Entry	λ_{abs} [a] (nm)	Abs [a]	λ_{em} [a,c] (nm)	Σmax [a] ($M^{-1}cm^{-1}$)	Stoke's Shift (nm)	OD/Abs (nm)	Φ_f [b]
3a	333, 381	0.3383	417,438	6766	105	338	0.15
3b	336,382	0.2421	414,445	4842	109	339	0.13
3c	339,384	0.28905	418,446	5781	107	347	0.14
3d	339,384	0.3148	419,445	6296	106	343	0.12
3e	333,383	0.10306	418,446	2061	109	332	0.06
3f	339,384	0.4114	423,448	8228	109	341	0.09
3g	339,384	0.3144	424,448	6288	109	339	0.09
3h	337,384	0.5501	420,445	11002	108	357	0.14
3i	316,382	0.8510		17020		351	0.0

a. All measurements were carried out in methanol, b. Quantum yields were determined by considering quinine sulfate in 0.1 M H_2SO_4 as standard reference, c. λ_{ex} = 380 nm, d. boron complex **3i** has shown negligible fluorescence in methanol.

***Photostability*:** The photostability of any dye is important parameters suggest its stability in environment with time bound manner.[47, 48] We performed the photostability test of a lead BODIPY analogues **3a/3c/3h** in methanol (MeOH) by irradiation under 4W LED lamp with 265nm wavelength (Appendix). Their photostability plot (Amount % vs Time) are provided in Appendix. The amount of **3a** are significantly dropped down upto 20% after 3 h. While the amount of 3c and 3h are dropped by ~50% and 35 % respectively. The order photostability is 3h>3c>>3a. This test reveal picolonyl residue is more stable.

Solid Fluorescence. The fluorescence character of BODIPY analogues are sensitive to polarity of environment in solution and closeness of molecule in solid state.[14, 47] The fluorescence behaviour of a lead analogue (**3a**) was examined using solid probe. The emission spectra of spectra of solid analogue **3a** is provided in Suppl. Inform which exhibit the emission peak at wavelength 430 nm, narrow red-shift as compare to solution

in CH_3CN. Though the quantum yield of powder **3a** is depleted significantly as compare to solution state of **3a** in CH_3CN. This property may relate to the closeness of molecules (packing effect) in solid state by intermolecular interactions. Its crystal-packing structure also supports the presence of C-H---F (non-classical hydrogen bonding) and π-π interaction which give well-ordered structure in solid state.

***Cyclic voltammetry*.** We performed the cyclic voltammetry studies of lead BODIPY analogues, aminotropone-BF2 complex (**3a**, **3h** & **3i**), with or without reference sample Ferrocene in acetonitrile. Their cyclic voltammograms are shown in ESI (Fig. S82-S83). All three analogues (**3a**, **3h** & **3i**) undergo a irreversible electrochemical reduction at E_{pc} = -1.36 V (**3a**), -1.31 V (**3h**) and -1.29 V (**3i**) which correspond to single electron transfer to ligand tropolium cation. The irreversible chemical reduction are reported with many other BODIPY analogues.[49, 50] The electrochemical properties of monomeric BF2 formazanate complex are sensitive to the presence of carbon substituents (electron with drawing and electron donating). We therefore attribute the relative ease of reduction (less negative potential) associated with compound **3a** because of bearing the electron withdrawing ester group.

Finally, we carried out the DFT studies with B3LYP/6-31+G* level of theory in vacuum and calculated the HOMO and LUMO energies of crystalized complexes **3a/3a-OH/3b/3h/3i** to understand the role amino group substituents. Their (**3a/3a-OH/3b/3h/3i**) optimized structures were obtained from respective single crystal X-ray structure. Their structures show Cs symmetry and minima energy in potential energy surface curve. Their HOMO-LUMO of fluorescent complex (**3a)** and non-fluorescent complex (**3i)** are depicted with energy differences (E_{HOMO}-E_{LUMO}) in Figure 5, while HUMO and LUMO of other complexes are provided in the supporting Information. Herein, HOMO of boron complexes bearing amino

acid residue (**3a/3a-OH/3b/3h)** are mainly localized on aminotropone ring and difluoroboron residue, while their LUMO are localized only on aminotroponyl ring. However, HOMO of non-fluorescent boron complex (**3i**) is localized on both aromatic ring residues as troponyl and aminoquinoline, while it LUMO is mostly localized at tropone ring. Moreover, the energy difference ($\Delta E_{HOMO\text{-}ELUMO}$) for complex (**3i**) is ~3.8 eV relatively lower than others aminotropone-boron complexes **3a/3a-OH/3b/3h** (~3.9 eV). The localized electron density on the troponyl ring causes an electron deficiency in the fluorophore moiety, and a resulting nonradiative pathway with a concomitant fluorescence quenching. We assume that the excited state of tropone scaffold (half occupied-LUMO) of compound **3i** is quenched by electron hopping from aromatic quinoline system. It could also be possible by the complete charge transfer to the troponyl group, and very fast recombination pathways which quenched the radiative decay. The similar type of quenching is noticed in development of highly fluorescent nucleoside.[51]

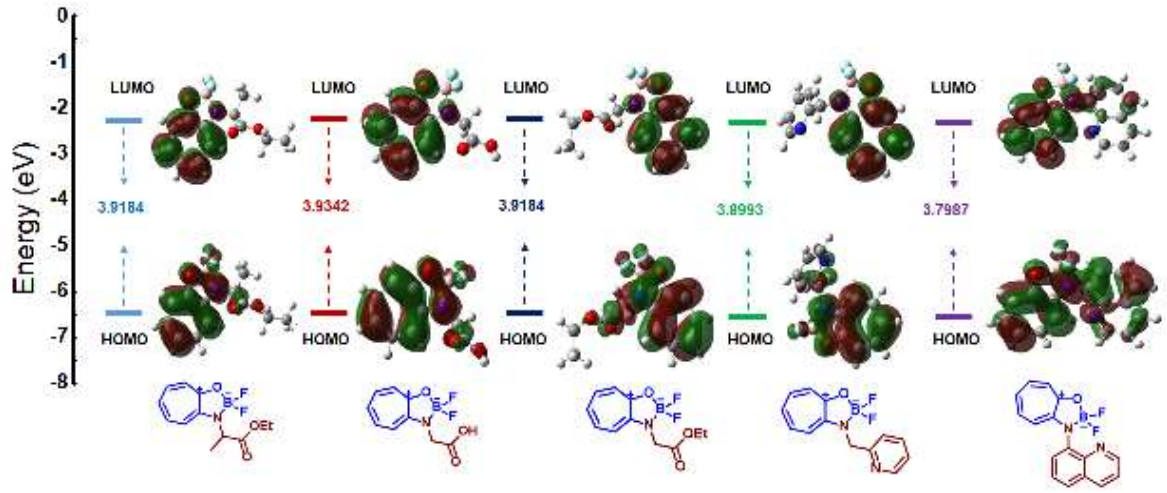

Figure 3A.7. Optimized structure and HOMO- LUMO energy gap (atomic unit in eV) of boron aminotropone (**3a, 3a-OH, 3b, 3h, 3i**) at B3LYP/6-31+G* level of theory in vacuum.

3A.4 Conlusions

In Conclusion, the synthesis of carboxylic acid functionalized difluoroboron-aminotropone compounds, new BODIPY analogues, are accomplished from biocompatible scaffolds, *N*-tropolonyl-L-amino acid derivatives. Importantly, structure of few lead compounds are confirmed by single crystal X-ray analyses of respective crystal. Their crystal packing diagrams reveal the presence of intermolecular hydrogen bonding as C-H----F and weak π-π interaction. Further, the photophysical properties of synthesized complexes are demonstrated by UV-Vis and fluorescence studies which support their fluorescence behavior with quantum yields range (~0.0-16.0%) and Stokes's shift ~109 nm. The fluorescence character of lead compound in solid state is described as weak fluorescent molecule as compare to solution state. The photostability of few complexes are noticed in solution for 3 h under UV-light. The electrochemical reaction of, at least, three compounds are studies in acetonitrile by cyclic voltammetry which confirms the irreversible type of reduction reaction. Finally, the theoretical studies (DFT) give the molecular orbitals (HOMO/LUMO) diagram/energy level for few lead compounds. Hence these functionalized BODIPY analogues are considered as potential carboxylic acid functionalized BODIPY analogues and could be useful in labelling of biomolecules.

3A.5 Experimental Procedure

General Information

All required materials and solvents were purchased from commercial suppliers and used without any further purification unless noted. Anhydrous dichloromethane was freshly prepared by distilling over Calcium hydride. Reactions were monitored by thin layer chromatography, visualized by UV and Ninhydrin. Column chromatography was performed in

100-200 mesh silica. FT-IR spectra were recorded on Thermo Scientific Nicolet iS5N FT-NIR spectrometer. Mass spectra were obtained from Bruker micrOTOF-Q II Spectrometer and the samples were prepared in methanol and injected in methanol and water mixture. NMR spectra were recorded on Bruker AV- 400 at room temperature (^{1}H: 400 MHz, ^{13}C: 100.6 MHz, ^{11}B:128 MHz, ^{19}F:377 MHz). ^{1}H, ^{13}C, ^{11}B and ^{19}F NMR chemical shifts were recorded in ppm, downfield from tetramethyl silane. Splitting patterns are abbreviated as: s, Singlet; d, doublet; dd, doublet of doublet; app d, apparent doublet; app dd, apparent doublet of doublet; t, triplet; q, quartet; dq, doublet of quartet; m, multiplet. The crystal data of all peptide were collected on a Rigaku Oxford diffractometer at 293 K respectively. Absorption spectra were obtained using Jasco V-730 spectrometer. Fluorescence spectra were obtained from Perkin-Elmer LS-55 using Xenon lamp. All spectroscopic measurements were carried out with spectroscopic grade, non-degassed solvents and at 20^{o}C. Relative fluorescence quantum yields were determined by comparing with quinine sulfate quantum yield in 0.1 M H_2SO_4 (0.54). The obtained values were substituted in the equation given below.

$$\phi_x = \phi_r \mathrm{x} \frac{F_x}{F_r} \mathrm{x} \frac{1-10^{-A_r}}{1-10^{A_x}} \mathrm{x} \frac{\eta_x^2}{\eta_x^2}$$

Absolute fluorescence quantum yields of **3a, 3c**, **3f, 3h** and **3i** in methanol (excited at 384 nm), of these dyes are measured by Edinburgh instrument FLS 920 using intergrating sphene according to the definition of fluorescence efficiency. The photostabilities of dyes **3a, 3c** and **3h** were studied by continuous irradiation with a UV lamp in 265 nm wavelength under 4W LED in methanol.

All reagents were purchased from commercial suppliers and used without further purification. The reaction was monitored by analytical TLC plates. The column chromatography was performed with Rankem silica gel (100-200 mesh). HRMS's were analyzed with Agilent Q-TOF 6500. All computational data for compound (**3a, 3a-OH, 3b, 3h, 3i**) has been calculated

using Gaussian 09 software and B3LYP/6-31+G* level of theory in vacuum.

Cyclic voltammograms of 1 mM **3a**, **3h** and **3i** were measured in acetonitrile solution, containing 0.1 M TBAPF6 as the supporting electrolyte, glassy carbon electrode as a working electrode, Pt wire as a counter electrode, and silver electrode as reference electrode at 100 mV s^{-1} of scanning rate at room temperature.

General Procedure for Synthesis of Aminotropone **2.** All aminotropones were synthesized by following the reported procedure. 2-tosyloxytropone and amines (1.2 *equiv*.) were dissolved in ethanol, to this Et3N (3.0) was added. The reaction mixture was allowed to reflux and monitored by TLC. The general reaction time observed for all the reactions is 24-36 h. All volatiles were evaporated under reduced pressure after reaction completion which was monitored by TLC. To the crude product 1.0 N HCl was added and extracted with dichloromethane (thrice), the combined organic layers were dried over Na_2SO_4 and evaporated under reduced pressure. The obtained crude product was purified by silica gel column chromatography by using ethyl acetate and hexane mixture as mobile phase.

Ethyl 2-oxocyclohepta-1,3,5-trienyl amino acetate **(2a):** The Pure product was obtained as light red Viscous liquid (59 mg, 66% yield,). **^{1}H NMR** (400 MHz, $CDCl_3$) δ 7.58 (s, 1H), 7.27 (dd, *J* = 12.0, 8.4 Hz, 1H), 7.19 (t, *J* = 9.8 Hz, 2H), 6.70 (t, *J* = 9.5 Hz, 1H), 6.37 (d, *J* = 10.2 Hz, 1H), 4.28 (q, *J* = 7.1 Hz, 2H), 4.08 (d, *J* = 5.6 Hz, 2H), 1.30 (t, *J* = 7.1 Hz, 3H). **^{13}C{^{1}H} NMR** (101 MHz, $CDCl_3$) δ 177.1, 168.5, 154.6, 137.3, 135.9, 130.0, 123.1, 108.7, 61.8, 44.7, 14.1. **HRMS** (ESI-TOF) m/z: $[M+H]^+$ Calcd. For $C_{11}H_{14}NO_3$ 208.0968, found 208.0983.

Ethyl 2-((7-oxocyclohepta-1,3,5-trien-1-yl)amino)propanoate **(2b):** The Pure product was obtained as light red Viscous liquid (50 mg, 69% yield,). **^{1}H NMR** (400 MHz,

$CDCl_3$) δ 7.47 (s, 1H), 7.27 (t, *J* = 4.3 Hz, 1H), 7.19 (dd, *J* = 10.6, 2 Hz, 2H), 6.71 (t, *J* = 9.4 Hz, 1H), 6.43 (d, *J* = 10.3 Hz, 1H), 4.29 (d, *J* = 7.2 Hz, 1H), 4.23 (dd, *J* = 14.3, 2 Hz, 2H), 3.77 (s, 1H), 1.62-1.60 (m, 3H), 1.29 – 1.25 (m, 3H).**^{13}C{^{1}H} NMR** (101 MHz, $CDCl_3$) δ 177.0, 137.4, 136.0, 130.0, 123.2, 108.9, 61.7, 51.2, 18.1, 18.0, 14.2. **HRMS** (ESI-TOF) m/z: $[M+H]^+$ Calcd. For $C_{12}H_{16}NO_3$ 222.1125, found 222.1127.

(*R*)-methyl 3-methyl-2-oxocyclohepta trienyl amino butanoate **(2c):** The Pure product was obtained as light red Viscous liquid (800 mg, 93% yield,) **^{1}H NMR** (400 MHz, $CDCl_3$) δ 7.38 (d, *J* = 8.3 Hz, 1H), 7.06-7.01 (m, 1H), 6.99-6.93(m, 1H), 6.47 (t, *J* = 9.6 Hz, 1H), 6.27 (d, *J* = 8.0 Hz, 1H), 3.87 (dd, *J* = 8.3, 6.0 Hz, 1H), 3.52 (s, 3H), 2.11-2.09 (m, 1H), 0.84 (dd, *J* = 24.4, 6.8 Hz, 6H). **^{13}C{^{1}H} NMR** (176 MHz, CDCl3) δ 176.7, 171.2, 154.6, 137.3, 136.0, 129.4, 123.1, 108.8, 61.1, 52.1, 31.3, 18.9, 18.5. **HRMS** (ESI-TOF) m/z: $[M+H]^+$ Calcd. For $C_{15}H_{21}N_2O_4$ 236.1281, found 236.1364.

Methyl 4-methyl-2-oxocyclohepta-1,3,5-trienyl amino pentanoate **(2d):** The Pure product was obtained as light red Viscous liquid (55 mg, 56% yield,). **^{1}H NMR** (400 MHz, $CDCl_3$) δ 7.36 (d, *J* = 6.3 Hz, 1H), 7.26 (t, *J* = 8.8 Hz, 1H), 7.17 (dd, *J* = 10.8, 2 Hz, 2H), 6.69 (t, *J* = 9.4 Hz, 1H), 6.47 (d, *J* = 10.2 Hz, 1H), 4.22 – 4.18 (m, 2H), 3.73 (s, 1H), 1.86 – 1.81 (m, 2H), 1.79 (dd, *J* = 13.2, 3 Hz, 1H), 1.25 (t, *J* = 7.1 Hz, 3H), 1.01 (d, *J* = 6.1 Hz, 3H), 0.93 (d, *J* = 6.0 Hz, 3H).**^{13}C{^{1}H} NMR** (101 MHz, $CDCl_3$) δ 177.0, 171.7, 154.5, 137.3, 136.0, 129.8, 123.1, 108.8, 61.4, 54.4, 41.3, 41.3, 24.9, 22.6, 14.1. **HRMS** (ESI-TOF) m/z: $[M+H]^+$ Calcd. For $C_{18}H_{20}NO_3$ 298.1438, found 298.1445.

Ethyl 2-oxocyclohepta-1,3,5-trienyl amino phenylpropanoate **(2e):** The Pure product was obtained as light red Viscous liquid (55 mg, 56% yield,). **^{1}H NMR** (400 MHz, $CDCl_3$) δ 7.92 (d, *J* = 7.4 Hz, 2H), 7.44 (d, *J* = 9.3 Hz, 1H), 7.35 (d, *J* = 7.9 Hz, 1H), 7.23 (ddd, *J* = 25.6, 21.1, 11.7 Hz, 1H), 7.09 (dd, *J* = 17.3, 6.6 Hz, 11H), 6.97 (t, *J* =

10.1 Hz, 8H), 4.23 – 4.07 (m, 6H), 2.45 (s, 25H), 2.04 (s, 5H), 1.30 – 1.21 (m, 15H).**^{13}C{^{1}H} NMR** (101 MHz, $CDCl_3$) δ 179.6, 155.3, 145.7, 141.3, 136.5, 134.8, 133.6, 131.0, 130.1, 129.8, 129.5, 128.7, 128.7, 60.5, 21.9, 21.2, 14.3. **HRMS** (ESI-TOF) m/z: $[M+H]^+$ Calcd. For $C_{18}H_{20}NO_3$ 298.1438, found 298.1422.

Methyl 3-((7-oxocyclohepta-1,3,5-trien-1-yl)amino)propanoate **(2f):** The Pure product was obtained as light red viscous liquid (50 mg, 73% yield,). **^{1}H NMR** (400 MHz, $CDCl_3$) δ 7.26 (dd, *J* = 21.4, 11.4 Hz, 2H), 7.16 (d, *J* = 11.5 Hz, 1H), 6.70 (t, *J* = 9.4 Hz, 1H), 6.59 (d, *J* = 10.3 Hz, 1H), 3.67 (dd, *J* = 12.9, 6.5 Hz, 2H), 2.74 (q, *J* = 6.8 Hz, 2H), 2.04 (s, 3H).**^{13}C{^{1}H} NMR** (101 MHz, $CDCl_3$) δ 171.6, 171.21, 155.3, 137.6, 136.4, 129.1, 129.0, 122.9, 122.8, 108.8, 61.1, 38.5, 33.4, 21.1. **HRMS** (ESI-TOF) m/z: $[M+H]^+$ Calcd. For $C_{11}H_{14}NO_3$ 208.0968, found 208.0977.

(*R*)-methyl-3-methyl-2-oxocyclohepta trienyl amino butanamido acetate **(2g):** The Pure product was obtained as yellowish solid (200 mg, 70% yield,). **^{1}H NMR** (700 MHz, $CDCl_3$) δ 7.48 – 7.44 (m, 1H), 7.44 – 7.36 (m, 1H), 7.29 – 7.20 (m, 3H), 7.15 – 7.07 (m, 1H), 6.80 (dd, *J* = 20.6, 11.1 Hz, 1H), 6.57 (d, *J* = 10.3 Hz, 1H), 4.59 (s, 1H), 4.09 (dd, *J* = 17.9, 6.0 Hz, 1H), 3.96 (dd, *J* = 17.9, 5.7 Hz, 1H), 3.87 (t, *J* = 5.7 Hz, 1H), 3.69 (s, 3H), 2.53 – 2.48 (m, 1H), 1.12 (dd, *J* = 30.4, 6.9 Hz, 6H). **^{13}C{^{1}H} NMR** (101 MHz, $CDCl_3$) δ 177.0, 171.4, 169.8, 155.0, 138.0, 136.7, 130.0, 126.7, 124.5, 111.1, 63.8, 52.3, 41.0, 31.3, 19.6, 17.9. **HRMS** (ESI-TOF) m/z: $[M+H]^+$ Calcd. For $C_{15}H_{21}N_2O_4$ 293.1496, found 293.1515.

2-((pyridin-2-ylmethyl)amino)cyclohepta-2,4,6-trienone **(2h):** The Pure product was obtained as yellowish solid (200 mg, 70% yield,). **^{1}H NMR** (400 MHz, $CDCl_3$) δ 8.61 (d, *J* = 4.3 Hz, 1H), 8.03 (s, 1H), 7.64 (t, *J* = 7.6 Hz, 1H), 7.31 – 7.11 (m, 5H), 6.66 (t, *J* = 9.3 Hz, 1H), 6.53 (d, *J* = 10.3 Hz, 1H), 4.67 (d, *J* = 5.9 Hz, 2H). **^{13}C{^{1}H} NMR** (101

MHz, $CDCl_3$) δ 177.2, 156.2, 155.3, 149.6, 137.2, 136.9, 136.1, 129.4, 122.7, 122.6, 121.2, 109.2, 48.3. **HRMS** (ESI-TOF) m/z: $[M+H]^+$ calcd. for $C_{13}H_{13}N_2O$ 213.1022, found 213.1021.

2-(quinolin-8-ylamino)cyclohepta-2,4,6-trienone (2i)**:** The Pure product was obtained as yellowish solid (200 mg, 70% yield,). **^{1}H NMR** (400 MHz, $CDCl_3$) δ 10.66 (s, 1H), 8.92 (d, *J* = 2.7 Hz, 1H), 8.13 (d, *J* = 7.6 Hz, 1H), 7.85 (t, *J* = 4.3 Hz, 1H), 7.68 (d, *J* = 10.3 Hz, 1H), 7.51 (d, *J* = 4.3 Hz, 2H), 7.45 (dd, *J* = 8.3, 4.2 Hz, 1H), 7.31 (d, *J* = 4.3 Hz, 2H), 7.18 (t, *J* = 10.2 Hz, 1H), 6.82 – 6.75 (m, 1H). **^{13}C{^{1}H} NMR** (101 MHz, $CDCl_3$) δ 178.3, 151.2, 149.4, 141.4, 137.3, 136.2, 135.8, 135.5, 131.7, 129.0, 126.4, 125.5, 122.4, 122.1, 115.9, 111.8. **HRMS** (ESI-TOF) m/z: $[M+H]^+$ calcd. for $C_{16}H_{13}N_2O$ 249.1022, found 249.1012.

General Procedure for Synthesis of Boron-aminotropone (3). Aminotropone **(2a)** (1eq.) was dissolved in anhydrous dichloromethane and Et_3N (15 eq.) was added. For further reaction $BF_3.OEt_2$ (15 eq.) was added to the resultant reaction mixture and stirred in room temperature. The completion of reaction was monitored by TLC, water was added to quench unreacted $BF_3.OEt_2$ and extracted with dichloromethane (thrice). The combined organic layer was dried over Na_2SO_4 and concentrated under reduced pressure. The crude product was purified through silica gel column chromatography by using 100% DCM as the mobile phase. Boron complex **3a** was obtained in 90% yield. Remaining all boron complexes were synthesized by following this general procedure.

Difluoromethoxy oxoethyl dihydrocyclohepta[d]oxazaborol-8a-ylium-2-uide **(3a):** The pure product was obtained as white solid (50.3mg, 90 % yield).M.p 112-115 °C. FT-IR (KBr plate) υ (cm^{-1}) = 2921, 2857, 1727, 1600, 1548, 1466, 1435, 1334, 1295, 1234, 1181, 1125, 1094, 1062, 732. **^{1}H NMR** (400 MHz, $CDCl_3$) δ 7.70 (t, *J* = 10 Hz, 1H),

7.61 (t, *J* = 12 Hz, 1H), 7.41 (d, *J* = 8 Hz, 1H), 7.18 (t, *J* = 8 Hz, 1H), 7.04 (d, *J* = 12 Hz, 1H), 4.35 (s, 2H), 4.24 (dd, *J* = 7.1, 2.0 Hz, 2H), 1.29 (td, *J* = 7.2, 2.1 Hz, 3H). **^{13}C{^{1}H} NMR** (101 MHz, CDCl3) δ 170.3, 141.6, 140.4, 130.7, 128.3, 120.6, 118.6, 62.0, 53.0, 15.1, 14.1. **^{11}B NMR** (128 MHz, $CDCl_3$) δ 6.88 (t, *J* = 17.92 Hz). **^{19}F NMR** (377 MHz, $CDCl_3$) δ -139.55 (dd, *J* = 35.7, 17.2 Hz). **HRMS** (ESI-TOF) m/z: $[M+Na]^+$ calcd. for $C_{11}H_{12}BF_2NO_3Na$ 278.0773, found 278.0784.

Difluoro methoxy oxopropan yldihydrocyclohepta[d]oxazaborol-8a-ylium-2-uide **(3b):** The pure product was obtained as white solid (49.5 mg, 69 % yield). FT-IR (KBr plate) υ (cm^{-1}) υ = 2919, 2856, 1737, 1608, 1556, 1474, 1449,1431, 1300, 1230, 1084, 1022, 733. **^{1}H NMR** (400 MHz, $CDCl_3$) δ 7.66 (t, *J*=10Hz, 1H), 7.60 (t, *J* = 11 Hz, 1H), 7.40 (d, *J* = 12 Hz, 1H), 7.18 (t, *J* = 8 Hz, 1H), 7.05(d,*J*=8Hz 1H), 4.53 (d, *J* = 4 Hz, 1H), 4.21 (q, *J* = 8 Hz, 2H), 1.82 (d, *J* = 8 Hz, 3H), 1.23 (t, *J* = 6 Hz, 3H). **^{13}C{^{1}H} NMR** (101 MHz, $CDCl_3$) δ 170.3, 141.5, 140.4, 128.3, 120.6, 118.6, 62.0, 53.0, 15.1, 14.1. **^{11}B NMR** (128 MHz, $CDCl_3$) δ 5.91 (t, *J* = 17.97 Hz). **^{19}F NMR** (377 MHz, $CDCl_3$) δ -131.34 (d, *J* = 84.9 Hz), -134.94 (ddd, *J* = 85.3, 37.1, 17.4 Hz). **HRMS** (ESI-TOF) m/z: $[M+Na]^+$ calcd. for $C_{12}H_{14}BF_2NO_3Na$ 292.0929, found 292.0925.

Difluoromethoxy methyloxobutanyl dihydrocyclohepta[d]oxazaborol-8a-ylium-2-uide **(3c):** The pure product was obtained as yellow solid (104.3mg, 86 % yield). M.p. 82-85 °C. FT-IR (KBr plate) υ (cm^{-1}) = 2961, 2875, 1749, 1601, 1584, 1463, 1435, 1333, 1283, 1250, 1204, 1073, 732. **^{1}H NMR** (400 MHz, $CDCl_3$) δ 7.69 (t, *J* = 10 Hz, 1H), 7.61 (t, *J* = 11 Hz 2H), 7.40 (d, *J* = 12 Hz, 1H), 7.21 (t, *J* = 10 Hz, 1H), 4.12 (d, *J* = 8 Hz, 1H), 3.76 (s, 3H), 2.83 – 2.72 (m, 1H), 1.11 (d, *J* = 8 Hz, 3H), 0.97 (d, *J* = 8 Hz, 3H). **^{13}C{^{1}H} NMR** (101 MHz, $CDCl_3$) δ 170.0, 141.6, 140.2, 128.8, 120.6, 119.6, 64.6, 52.55, 28.45, 20.30, 19.58. **^{11}B NMR** (128 MHz, $CDCl_3$) δ 5.80 (t, *J* = 18.56 Hz). **^{19}F NMR** (377

MHz, $CDCl_3$) δ -135.73, -135.82. **HRMS** (ESI-TOF) m/z: $[M+Na]^+$ calcd. for $C_{13}H_{17}BF_2NO_3Na$ 306.1086, found 306.1087.

Difluoromethoxy methyloxopentanyl dihydrocyclohepta[d]oxazaborol-8a-ylium-2-uide **(3d):** The pure product was obtained as yellow jelly type compound (20 mg, 67 % yield). FT-IR (KBr plate) υ (cm^{-1}) = 2959, 2871, 1738, 1602, 1548, 1463, 1434, 1369, 1333, 1233, 1070, 859, 756, 732. **^{1}H NMR** (400 MHz, $CDCl_3$) δ 7.71 – 7.64 (m, 1H), 7.59 (t, *J* = 9.7 Hz, 2H), 7.39 (d, *J* = 10.1 Hz, 1H), 7.19 (t, *J* = 9.7 Hz, 1H), 4.10 (d, *J* = 10.4 Hz, 1H), 3.75 (s, 3H), 2.79 (tt, *J* = 13.1, 6.5 Hz, 1H), 1.25 (s, 2H), 1.11 (d, *J* = 6.4 Hz, 3H), 0.95 (d, *J* = 6.7 Hz, 3H). **^{13}C{^{1}H} NMR** (101 MHz, $CDCl_3$) δ 170.0, 141.5, 140.2, 134.1, 128.7, 119.6, 64.6, 52.6, 29.7, 28.4, 20.3, 19.6.**^{11}B NMR** (128 MHz, $CDCl_3$) δ 5.80 (t, *J* = 17.8 Hz). **^{19}F NMR** (377 MHz, $CDCl_3$) δ -135.96 (dd, *J* = 35.6, 19.1 Hz). **HRMS** (ESI-TOF) m/z: $[M+Na]^+$ calcd. for $C_{15}H_{19}BF_2NO_3Na$ 306.1086, found 306.1096.

Difluoromethoxyoxo phenylpropanyl dihydrocyclohepta[d]oxazaborol-8a-ylium-2-uide **(3e):** The pure product was obtained as yellow jelly copmpound (53mg, 36 % yield). FT-IR (KBr plate) υ (cm^{-1}) = 2982, 1741, 1602, 1549, 1463, 1434, 1331, 1296, 1253, 1233, 1073, 752, 700. **^{1}H NMR (700 MHz, $CDCl_3$)** δ 7.53 (td, *J* = 10.2, 5.0 Hz, 2H), 7.32 (d, *J* = 10.2 Hz, 1H), 7.27 (d, *J* = 7.5 Hz, 2H), 7.22 (t, *J* = 7.5 Hz, 2H), 7.17 (t, *J* = 7.3 Hz, 1H), 7.13 (t, *J* = 9.8 Hz, 1H), 7.04 (d, *J* = 11.4 Hz, 1H), 4.69 (t, *J* = 7.1 Hz, 1H), 4.15 (ddq, *J* = 14.6, 7.4, 3.6 Hz, 2H), 3.56 (dd, *J* = 14.0, 7.6 Hz, 1H), 3.48 (dd, *J* = 14.0, 7.4 Hz, 1H), 1.15 (t, *J* = 7.2 Hz, 3H). **^{13}C{^{1}H} NMR** (176 MHz, $CDCl_3$) δ 169.04, 167.49, 160.35, 141.66, 140.32, 137.00, 129.44, 128.90, 128.58, 126.95, 120.67, 118.57, 61.93, 59.42, 35.89, 13.94. **^{11}B NMR** (128 MHz, $CDCl_3$) δ 6.07 (t, *J* = 18.3 Hz). **^{19}F NMR** (377 MHz, $CDCl_3$) δ -137.80 (dd, *J* = 36.6, 17.6 Hz). **HRMS** (ESI-TOF) m/z: $[M+Na]^+$ calcd. for $C_{18}H_{18}BF_2NO_3Na$ 368.1243, found 368.1253.

Difluoromethoxy oxopropyl dihydrocyclohepta[d]oxazaborol-8a-ylium-2-uide **(3f):** The pure product was obtained as yellow solid (58 mg, 94 % yield). M.p. 108-110 °C FT-IR (KBr plate) υ (cm^{-1}) = 2963, 2929, 2877, 1749, 1601, 1550, 1463, 1434, 1332, 1239, 1250, 1205, 1073, 732. **^{1}H NMR** (700 MHz, $CDCl_3$) δ 7.70 (t, *J* = 10.5 Hz, 1H), 7.54 (t, *J* = 10.5 Hz, 1H), 7.33 (t, *J* = 10.5 Hz, 2H), 7.15 (t, *J* = 7 Hz, 1H), 3.92 (t, *J* = 7 Hz, 2H), 3.71 (s, 3H), 2.91 (t, *J* = 7 Hz, 2H). **^{13}C{^{1}H} NMR** (176 MHz, $CDCl_3$) δ 172.0, 167.5, 160.1, 141.6, 139.8, 128.0, 119.5, 118.1, 52.0, 38.9, 32.3. **^{11}B NMR** (128 MHz, $CDCl_3$) δ 5.96 (t, *J* = 19.0 Hz). **^{19}F NMR** (377 MHz, $CDCl_3$) δ -137.42 (dd, *J* = 38.3, 18.9 Hz). **HRMS** (ESI-TOF) m/z: $[M+Na]^+$ calcd. for $C_{13}H_{17}BF_2NO_3Na$ 278.0773, found 278.0773.

Difluoromethoxy oxoethylaminomethyl oxobutanyl dihydrocyclohepta[d]oxazaborol-8a-ylium-2-uide **(3g):** The pure product was obtained as yellow jelly (48 mg, 74 % yield). FT-IR (KBr plate) υ (cm^{-1}) = 2984, 1731, 1600, 1555, 1514, 1478, 1445, 1431, 1294, 1232, 1088, 1004, 878, 753, 716. **^{1}H NMR** (400 MHz, $CDCl_3$) δ 7.72 – 7.64 (m, 1H), 7.58 (t, *J* = 10.4 Hz, 2H), 7.38 (d, *J* = 10.1 Hz, 1H), 7.20 (t, *J* = 9.6 Hz, 1H), 4.10 (d, *J* = 10.2 Hz, 1H), 3.74 (s, 3H), 2.78 (tt, *J* = 13.0, 6.6 Hz, 1H), 1.11 (d, *J* = 6.5 Hz, 3H), 0.95 (d, *J* = 6.7 Hz, 3H). **^{13}C {^{1}H} NMR** (101 MHz, $CDCl_3$) δ 170.0, 168.0, 141.6, 140.2, 128.8, 120.7, 119.6, 64.5, 52.5, 28.5, 20.3, 19.6. **^{11}B NMR** (128 MHz, $CDCl_3$) δ 5.79 (t, *J* = 18.3 Hz).**^{19}F NMR** (377 MHz, $CDCl_3$) δ -135.77 (d, *J* = 22.4 Hz). **HRMS** (ESI-TOF) m/z: $[M+Na]^+$ calcd. for $C_{15}H_{19}BF_2NO_3Na$ 263.1301, found 263.1310.

Difluoropyridinyl methyl dihydrocyclohepta[d] oxazaborol-8a-ylium-2-uide **(3h):** The pure product was obtained as yellow solid (130 mg, 71 % yield). M.p. 128-130 °C. FT-IR (KBr plate) υ (cm^{-1}) = 2923, 2860, 1606, 1547, 1460, 1455, 1434, 1385, 1329, 1256, 1082, 821, 789,731. **^{1}H NMR** (400 MHz, $CDCl_3$) δ 8.56 (s, 1H), 7.70 – 7.61 (m, 1H),

7.56 (dd, *J* = 19.0, 9.7 Hz, 2H), 7.48 (d, *J* = 7.0 Hz, 1H), 7.37 (d, *J* = 10.1 Hz, 2H), 7.22 (s, 1H), 7.13 (t, *J* = 9.2 Hz, 1H), 4.90 (s, 2H). **^{13}C{^{1}H} NMR** (101 MHz, $CDCl_3$) δ 167.9, 155.9, 149.1, 141.9, 140.0, 137.4, 128.3, 122.9, 122.6, 120.0, 119.1, 49.4. **^{11}B NMR** (128 MHz, $CDCl_3$) δ 6.07 (t, *J* = 18.3 Hz). **^{19}F NMR** (377 MHz, $CDCl_3$) δ -137.80 (dd, *J* = 36.6, 17.6 Hz). **HRMS** (ESI-TOF) m/z: $[M+Na]^+$ calcd. for $C_{15}H_{19}BF_2NO_3Na$ 283.0827, found 283.0844.

Difluoroquinolin dihydrocyclohepta[d] oxazaborol-8a-ylium-2-uide **(3i):** The pure product was obtained as white solid (120 mg, 66 % yield). M.p. 206-210 °C. FT-IR (KBr plate) υ (cm^{-1}) = 2923, 2860, 1606, 1547, 1474, 1455, 1434, 1385, 1229, 1295, 1256, 1082, 821, 789, 731. **^{1}H NMR** (400 MHz, $CDCl_3$) δ 8.78 (dd, *J* = 4.1, 1.6 Hz, 1H), 8.24 (dd, *J* = 8.3, 1.5 Hz, 1H), 7.90 (dd, *J* = 14.5, 7.4 Hz, 2H), 7.65 (dd, *J* = 13.7, 6.1 Hz, 1H), 7.59 (d, *J* = 10.2 Hz, 1H), 7.51 (d, *J* = 10.1 Hz, 1H), 7.44 (dd, *J* = 8.3, 4.2 Hz, 1H), 7.37 (d, *J* = 10.4 Hz, 1H), 7.15 (t, *J* = 9.7 Hz, 1H), 6.65 (d, *J* = 11.2 Hz, 1H). **^{13}C{^{1}H} NMR** (101 MHz, $CDCl_3$) δ 150.4, 142.7, 140.6, 139.5, 136.6, 134.9, 129.4, 128.9, 128.2, 126.9, 121.8, 121.2**. ^{11}B NMR** (128 MHz, $CDCl_3$) δ 6.10 (t, *J* = 16.9 Hz). **^{19}F NMR** (377 MHz, $CDCl_3$) δ -133.29 (s), -133.51 (ddd, *J* = 51.9, 36.1, 16.3 Hz), -138.91 (s), -138.91 – -139.69 (m). **HRMS** (ESI-TOF) m/z: $[M+Na]^+$ calcd. for $C_{15}H_{19}BF_2NO_3Na$ 319.0828, found 319.0838.

3A.6 References and Notes

1. Zaumseil, J.; Sirringhaus, H., Electron and ambipolar transport in organic field-effect transistors. *Chem Rev* **2007,** *107*, 1296-1323.

2. Bessette, A.; Hanan, G. S., Design, synthesis and photophysical studies of dipyrromethene-based materials: insights into their applications in organic photovoltaic devices. *Chem. Soc. Rev.* **2014,** *43*, 3342-3405.

3. Kim, H. N.; Guo, Z.; Zhu, W.; Yoon, J.; Tian, H., Recent progress on polymer-based fluorescent and colorimetric chemosensors. *Chem. Soc. Rev.* **2011,** *40*, 79-93.

4. Ulrich, G.; Ziessel, R.; Harriman, A., The Chemistry of Fluorescent Bodipy Dyes: Versatility Unsurpassed. *Angew. Chem. Int. Ed.* **2008,** *47*, 1184-1201.

5. Jokic, T.; Borisov, S. M.; Saf, R.; Nielsen, D. A.; Kühl, M.; Klimant, I., Highly photostable near-infrared fluorescent pH indicators and sensors based on BF2-chelated tetraarylazadipyrromethene dyes. *Analytical chemistry* **2012,** *84*, 6723-30.

6. Durantini, A. M.; Heredia, D. A.; Durantini, J. E.; Durantini, E. N., BODIPYs to the rescue: Potential applications in photodynamic inactivation. *Eur. J. Med. Chem.* **2018,** *144*, 651-661.

7. Ahrens, J.; Cordes, B.; Wicht, R.; Wolfram, B.; Bröring, M., Acidic Condensation of BODIPYs with Aldehydes: A Quick and Versatile Route to Alkenyl-BODIPYs and C (sp3)-Connected DYEmers. *Chem.: Eur. J.* **2016,** *22*, 10320-10325.

8. Golden, J. H.; Facendola, J. W.; Sylvinson MR, D.; Baez, C. Q.; Djurovich, P. I.; Thompson, M. E., Boron Dipyridylmethene (DIPYR) Dyes: Shedding Light on Pyridine-Based Chromophores. *J. Org. Chem.* **2017,** *82*, 7215-7222.

9. Patalag, L. J.; Jones, P. G.; Werz, D. B., BOIMPYs: Rapid Access to a Family of Red-Emissive Fluorophores and NIR Dyes. *Angew. Chem. Int. Ed.* **2016,** *55*, 13340-13344.

10. Patalag, L. J.; Jones, P. G.; Werz, D. B., Aza-BOIMPYs: A Tetrazole Auxochrome for Highly Red-Emissive Dipyrromethene-Based Fluorophores. *Chem.: Eur. J.* **2017,** *23*, 15903-15907.

11. Patalag, L. J.; Ho, L. P.; Jones, P. G.; Werz, D. B., Ethylene-bridged oligo-BODIPYs: access to intramolecular J-aggregates and superfluorophores. *J.Am. Chem. Soc.* **2017,** *139*, 15104-15113.

12. Zhou, X.; Yu, C.; Feng, Z.; Yu, Y.; Wang, J.; Hao, E.; Wei, Y.; Mu, X.; Jiao, L., Highly regioselective α-chlorination of the BODIPY chromophore with copper (II) chloride. *Org. Lett.* **2015,** *17*, 4632-4635.

13. Ray, C.; Díaz-Casado, L.; Avellanal-Zaballa, E.; Bañuelos, J.; Cerdan, L.; García-Moreno, I.; Moreno, F.; Maroto, B. L.; López-Arbeloa, Í.; de la Moya, S., N-BODIPYs Come into Play: Smart Dyes for Photonic Materials. *Chem.: Eur. J.* **2017,** *23*, 9383-9390.

14. Yu, C.; Hao, E.; Fang, X.; Wu, Q.; Wang, L.; Li, J.; Xu, L.; Jiao, L.; Wong, W.-Y., AIE-active difluoroboronated acylhydrozone dyes (BOAHY) emitting across the entire visible region and their photo-switching properties. *J. Mater.Chem. C* **2019,** *7*, 3269-3277.

15. Guerrero-Corellam, A. A.-P., J.; Pawar, T. J.; Díaz-Tendero, S.; Martín-Sómer, A.; Gómez, C . V.; Belmonte-Vázquez, J. L.; Ramírez-Ornelas, D. E.; Peña-Cabrera, E.; Frailem, A..; Cruz, D. C.; Alemán, J., BODIPY as electron withdrawing group for the activation of double bonds in asymmetric cycloaddition reactions. In *Chem. Sci.*. 2019; Vol. 10, pp 4346-4351.

16. Bentley, R., A fresh look at natural tropolonoids. *Nat. Prod. Rep.* **2008,** *25*, 118-138.

17. Crivat, G.; Taraska, J. W., Imaging proteins inside cells with fluorescent tags. *Trends Biotechnol.* **2012,** *30*, 8-16.

18. Liu, N.; Song, W.; Schienebeck, C. M.; Zhang, M.; Tang, W., Synthesis of Naturally Occurring Tropones and Tropolones. *Tetrahedron* **2014,** *70*, 9281-9305.

19. Hosoya, H.; Tanaka, J.; Nagakura, S., Ultra-violet absorption spectra of tropone, troponium ion, tropolone and 2, 4, 6-octatrienal. *Tetrahedron* **1962,** *18*, 859-874.

20. Yamaguchi, H.; Amako, Y.; Azumi, H., The electronic spectrum of the tropone molecule. *Tetrahedron* **1968,** *24*, 267-277.

21. Croteau, R.; Leblanc, R., Colchicine fluorescence measured with a laser spectrofluorimeter. *J. Lumin.* **1977,** *15*, 353-356.

22. Meyer, N.; Löhnwitz, K.; Zulys, A.; Roesky, P. W.; Dochnahl, M.; Blechert, S., Aminotroponate Zinc Complexes as Catalysts for the Intramolecular Hydroamination of Alkenes and Alkynes. *Organometallics* **2006,** *25*, 3730-3734.

23. Datta, S.; Roesky, P. W.; Blechert, S., Aminotroponate and Aminotroponiminate Calcium Amides as Catalysts for the Hydroamination/Cyclization Catalysis. *Organometallics* **2007,** *26*, 4392-4394.

24. Datta, S.; Gamer, M. T.; Roesky, P. W., Aminotroponiminate Complexes of the Heavy Alkaline Earth and the Divalent Lanthanide Metals as Catalysts for the Hydroamination/Cyclization Reaction. *Organometallics* **2008,** *27*, 1207-1213.

25. Kubisiak, M.; Zelga, K.; Justyniak, I.; Tratkiewicz, E.; Pietrzak, T.; Keeri, A. R.; Ochal, Z.; Hartenstein, L.; Roesky, P. W.; Lewiński, J., Catalytic Epoxidation of Enones Mediated by Zinc Alkylperoxide/tert-BuOOH Systems. *Organometallics* **2013,** *32*, 5263-5265.

26. Fullagar, J. L.; Garner, A. L.; Struss, A. K.; Day, J. A.; Martin, D. P.; Yu, J.; Cai, X.; Janda, K. D.; Cohen, S. M., Antagonism of a zinc metalloprotease using a unique metal-chelating scaffold: tropolones as inhibitors of P. aeruginosa elastase. *Chem. Commun.* **2013,** *49*, 3197-3199.

27. Muetterties, E.; Roesky, H.; Wright, C., Chelate Chemistry. V. Metal Chelates Based on Tropolone and Its Derivatives. *J. Am. Chem. Soc.* **1966,** *88*, 4856-4861.

28. Breheret, E.; Martin, M., Electronic relaxation of troponoids: tropolone fluorescence. *J. Lumin.* **1978,** *17*, 49-60.

29. Hojo, M.; Hasegawa, H.; Yoneda, H., Role of triple ion formation in the acid–base reaction between tropolone and triethylamine in acetonitrile. *J. Chem. Soc., Perkin Trans. 2* **1994**, 1855-1859.

30. Bhattacharyya, B.; Wolff, J., Promotion of fluorescence upon binding of colchicine to tubulin. *Proc. Natl. Acad. Sci. U.S.A.* **1974,** *71*, 2627-2631.

31. Bhattacharyya, B.; Wolff, J., Anion-induced increases in the rate of colchicine binding to tubulin. *Biochemistry* **1976,** *15*, 2283-2288.

32. De Sa, G.; Malta, O.; de Mello Donegá, C.; Simas, A.; Longo, R.; Santa-Cruz, P.; da Silva Jr, E., Spectroscopic properties and design of highly luminescent lanthanide coordination complexes. *Coord. Chem. Rev.* **2000,** *196*, 165-195.

33. Takagi, K.; Saiki, K.; Mori, K.; Yuki, Y.; Suzuki, M., Synthesis of tropolone-containing conjugated polymers and their optical properties. *Polym. J.* **2007,** *39*, 813.

34. Sayapin, Y. A.; Tupaeva, I. O.; Kolodina, A. A.; Gusakov, E. A.; Komissarov, V. N.; Dorogan, I. V.; Makarova, N. I.; Metelitsa, A. V.; Tkachev, V. V.; Aldoshin, S. M., 2-Hetaryl-1, 3-tropolones based on five-membered nitrogen heterocycles: synthesis, structure and properties. *Beilstein J. Org. Chem.* **2015,** *11*, 2179.

35. Zadeh, E. G.; Tang, S.; Woodward, A.; Liu, T.; Bondar, M.; Belfield, K., Chromophoric materials derived from a natural azulene: syntheses, halochromism and one-photon and two-photon microlithography. *J. Mater. Chem. C* **2015,** *3*, 8495-8503.

36. Dochnahl, M.; Loehnwitz, K.; Pissarek, J. W.; Biyikal, M.; Schulz, S. R.; Schoen, S.; Meyer, N.; Roesky, P. W.; Blechert, S., Intramolecular Hydroamination with Homogeneous Zinc Catalysts: Evaluation of Substituent Effects in N, N′-Disubstituted Aminotroponiminate Zinc Complexes. *Chem. Eur. j* **2007,** *13*, 6654-6666.

37. Roesky, P. W., The co-ordination chemistry of aminotroponiminatesDedicated to Professor Herbert W. Roesky on the occasion of his 65th birthday. *Chem. Soc. Rev.* **2000,** *29*, 335-345.

38. Zulys, A.; Dochnahl, M.; Hollmann, D.; Löhnwitz, K.; Herrmann, J. S.; Roesky, P. W.; Blechert, S., Intramolecular hydroamination of functionalized alkenes and alkynes with a homogenous zinc catalyst. *Angew. Chem. Int. Ed.* **2005,** *44*, 7794-7798.

39. Hussein, L.; Purkait, N.; Biyikal, M.; Tausch, E.; Roesky, P. W.; Blechert, S., Highly enantioselective hydroamination to six-membered rings by heterobimetallic catalysts. *Chem. Commun.* **2014,** *50*, 3862-3864.

40. Dochnahl, M.; Pissarek, J.-W.; Blechert, S.; Löhnwitz, K.; Roesky, P. W., A new homogeneous zinc complex with increased reactivity for the intramolecular hydroamination of alkenes. *Chem. Commun.* **2006**, 3405-3407.

41. Holmquist, H.; Benson, R., 2-Bora-and 2-Thia-1, 3-diazaazulenes. *J. Am. Chem. Soc.* **1962,** *84*, 4720-4722.

42. Balachandra, C.; Sharma, N. K., Novel fluorophores: Syntheses and photophysical studies of boron-aminotroponimines. *Dyes. Pigm.* **2017,** *137*, 532-538.

43. Hu, L.; Pan, J.; Zhang, X.; Hu, W.; Xiong, Y.; Zhu, X., Synthesis of N, O π-conjugated boron complexes and the reactivity of Suzuki cross-coupling. *Tetrahedron* **2017,** *73*, 223-229.

44. Lugovik, K. I.; Eltyshev, A. K.; Suntsova, P. O.; Smoluk, L. T.; Belousova, A. V.; Ulitko, M. V.; Minin, A. S.; Slepukhin, P. A.; Benassi, E.; Belskaya, N. P., Fluorescent boron complexes based on new N, O-chelates as promising candidates for flow cytometry. *Org. Biomol. Chem.* **2018,** *16*, 5150-5162.

45. Huang, J.; Wang, Y.; Van Hecke, K.; Pereshivko, O. P.; Peshkov, V. A., Studies on Functionalization of N, O-Chelated Isoquinoline-Enol Boron Complexes. *Eur. J. Org. Chem.* **2019,** *doi.org/10.1002/ejoc.201801872*.

46. Loudet, A.; Burgess, K., BODIPY dyes and their derivatives: syntheses and spectroscopic properties. *Chem Rev* **2007,** *107*, 4891-4932.

47. Yu, C.; Huang, Z.; Wang, X.; Miao, W.; Wu, Q.; Wong, W.-Y.; Hao, E.; Xiao, Y.; Jiao, L., A Family of Highly Fluorescent and Unsymmetric Bis (BF2) Chromophore Containing Both Pyrrole and N-Heteroarene Derivatives: BOPPY. *Org. Lett.* **2018,** *20*, 4462-4466.

48. Jokic, T.; Borisov, S. M.; Saf, R.; Nielsen, D. A.; Kühl, M.; Klimant, I., Highly photostable near-infrared fluorescent pH indicators and sensors based on BF2-chelated tetraarylazadipyrromethene dyes. *Anal. Chem.* **2012,** *84*, 6723-6730.

49. Barbon, S. M.; Price, J. T.; Yogarajah, U.; Gilroy, J. B., Synthesis and characterization of conjugated/cross-conjugated benzene-bridged boron difluoride formazanate dimers. *RSC Adv.* **2015,** *5*, 56316-56324.

50. Yu, C.; Jiao, L.; Zhang, P.; Feng, Z.; Cheng, C.; Wei, Y.; Mu, X.; Hao, E., Highly fluorescent BF2 complexes of hydrazine–Schiff base linked bispyrrole. *Org. Lett.* **2014,** *16*, 3048-3051.

51. Zilbershtein-Shklanovsky, L.; Weitman, M.; Major, D. T.; Fischer, B., Rules for the design of highly fluorescent nucleoside probes: 8-(substituted cinnamyl)-adenosine analogues. *J. Org. Chem.* **2013,** *78*, 11999-12008.

3A.7 Appendix

Table of contents

1. NMR (^{1}H, ^{13}C, ^{11}B, ^{19}F) and HRMS of Boron complex *tr-gly* **(3a)** 149

2. NMR (^{1}H, ^{13}C, ^{11}B, ^{19}F) and HRMS of Boron complex *tr-ala* **(3b)** 152

3. NMR (^{1}H, ^{13}C, ^{11}B, ^{19}F) and HRMS of Boron complex *tr-val* **(3c)** 155

4. NMR (^{1}H, ^{13}C, ^{11}B, ^{19}F) and HRMS of Boron complex *tr-lue* **(3d)** 158

5. NMR (^{1}H, ^{13}C, ^{11}B, ^{19}F) and HRMS of Boron complex *tr-phe* **(3e)** 161

6. NMR (^{1}H, ^{13}C, ^{11}B, ^{19}F) and HRMS of Boron complex *tr-beta ala* **(3f)** 164

7. NMR (^{1}H, ^{13}C, ^{11}B, ^{19}F) and HRMS of Boron complex *tr-dipep* **(3g)** 167

8. NMR (^{1}H, ^{13}C, ^{11}B, ^{19}F) and HRMS of Boron complex *tr-picolylamine* **(3h)** 170

9. NMR (^{1}H, ^{13}C, ^{11}B, ^{19}F) and HRMS of boron complex *tr-aminoquinoline* **(3i)** 173

10. Crystal structures and data 176

11. Photophysical studies 178

12. Theoretical data 184

13. Comparative N-B bond length studies 185

14. Cyclic Voltammetry studies 186

1. NMR (^{1}H, ^{13}C, ^{11}B, ^{19}F) and HRMS of Boron complex *tr-gly* **(3a)**

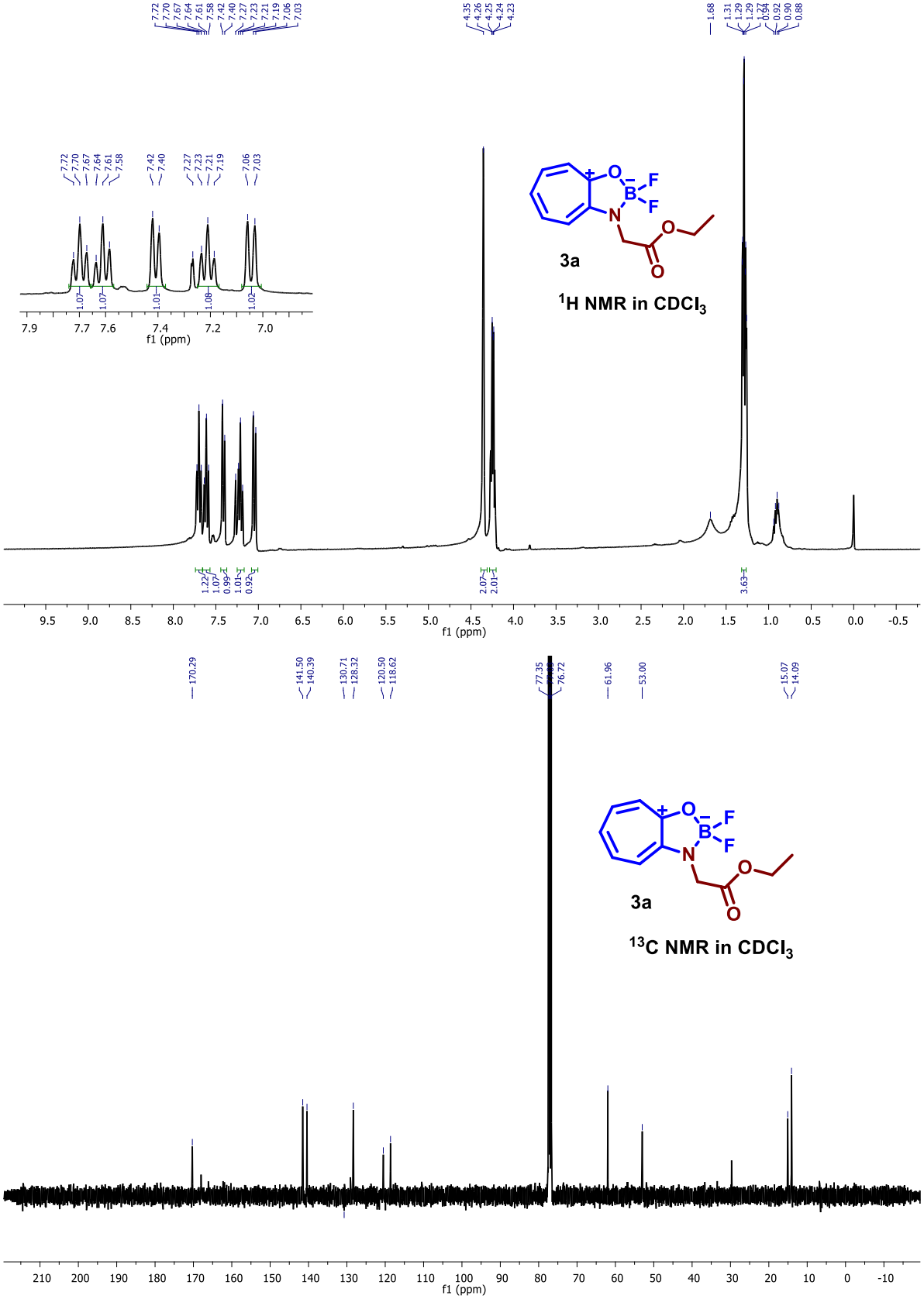

Figure A19. ^{1}H, ^{13}C NMR (400MHz, $CDCl_3$) spectra of Boron complex **(3a)** in $CDCl_3$

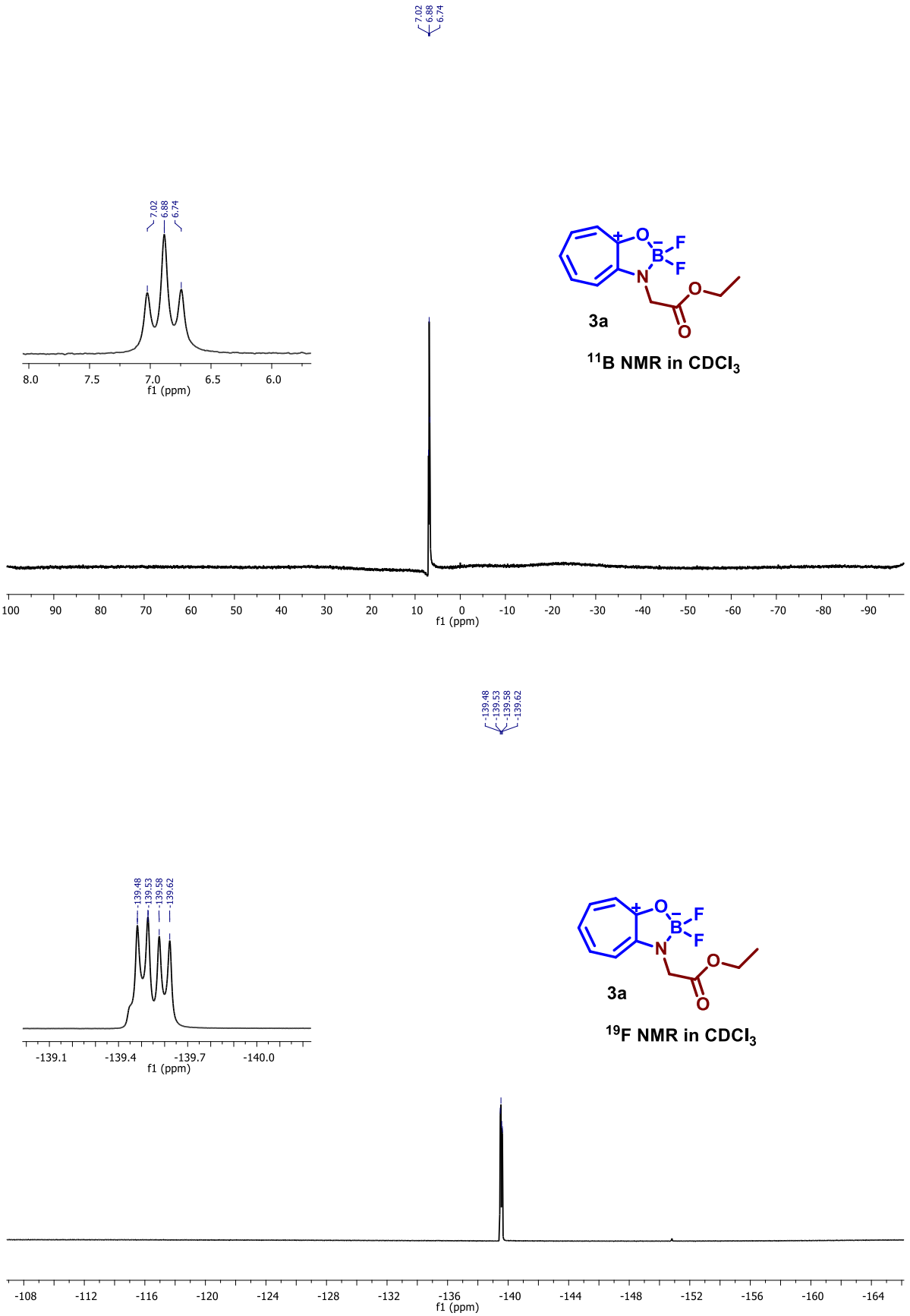

Figure A20. ^{11}B and ^{19}F NMR (400MHz, $CDCl_3$) spectra of Boron complex **(3a)** in $CDCl_3$

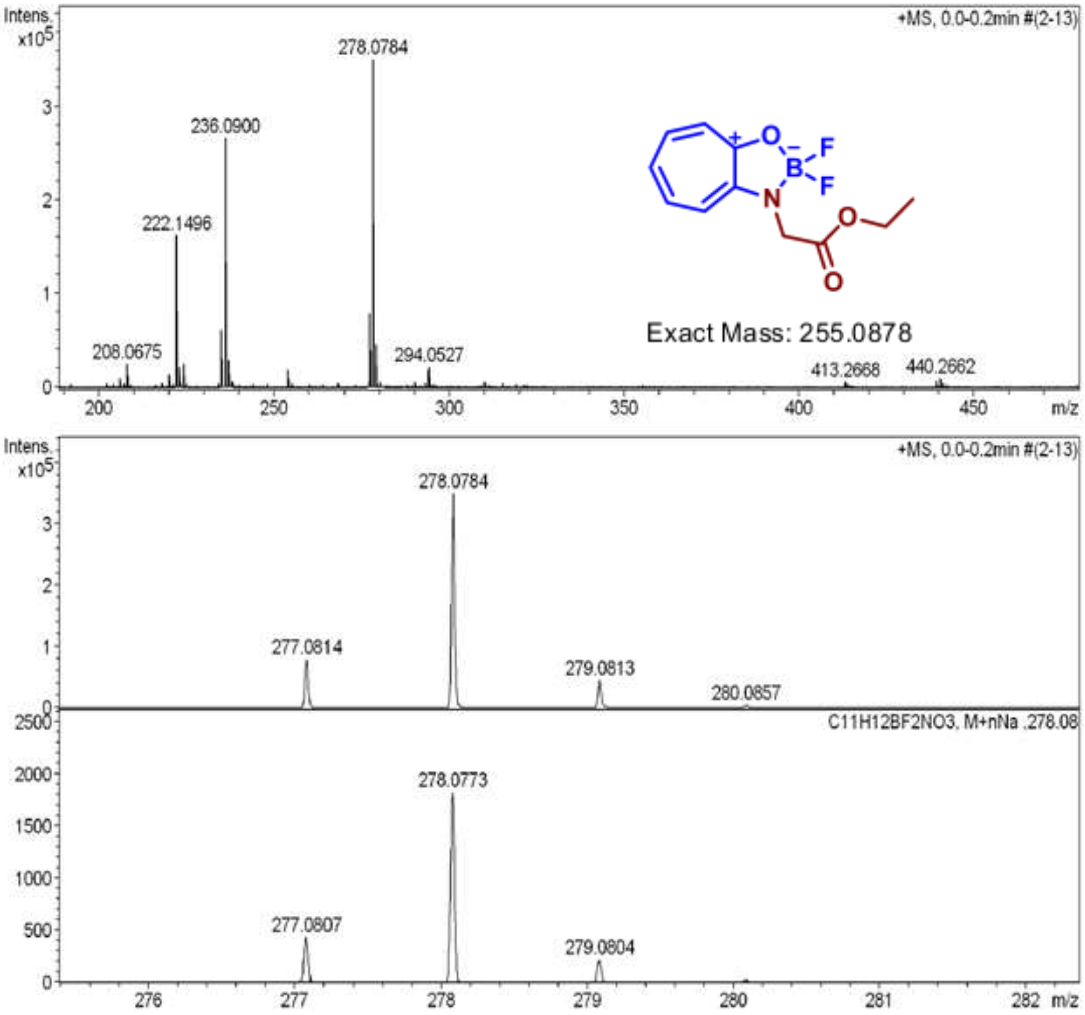

Figure A21. ESI-MS/HRMS spectra of Boron complex **(3a)**.

2. NMR (^{1}H, ^{13}C, ^{11}B, ^{19}F) and HRMS of Boron complex *tr-ala* **(3b)**

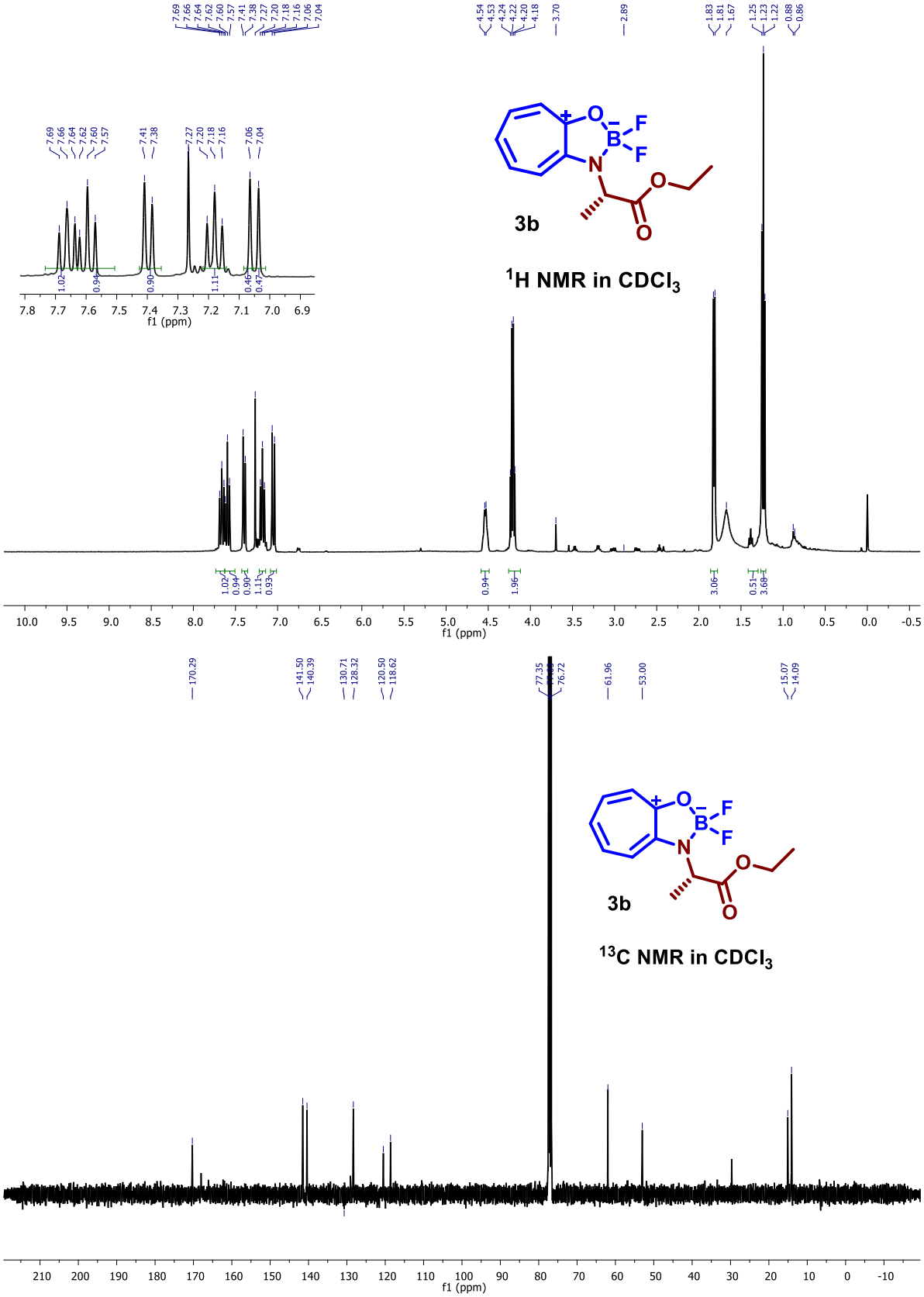

Figure A22. ^{1}H, ^{13}C NMR (400MHz, $CDCl_3$) spectra of Boron complex **(3b)** in $CDCl_3$

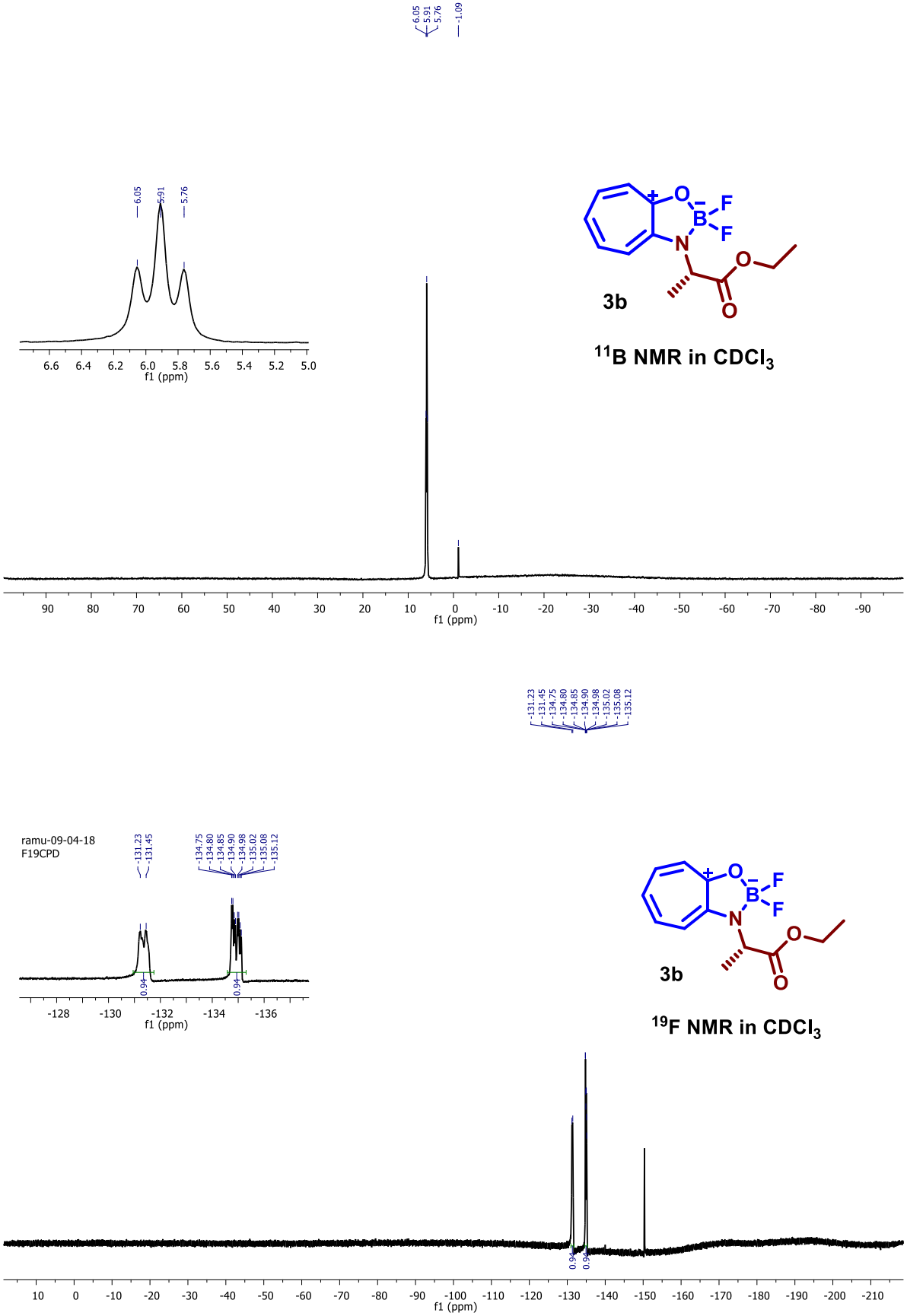

Figure A23. ^{11}B and ^{19}F NMR (400MHz, $CDCl_3$) spectra of Boron complex **(3b)** in $CDCl_3$

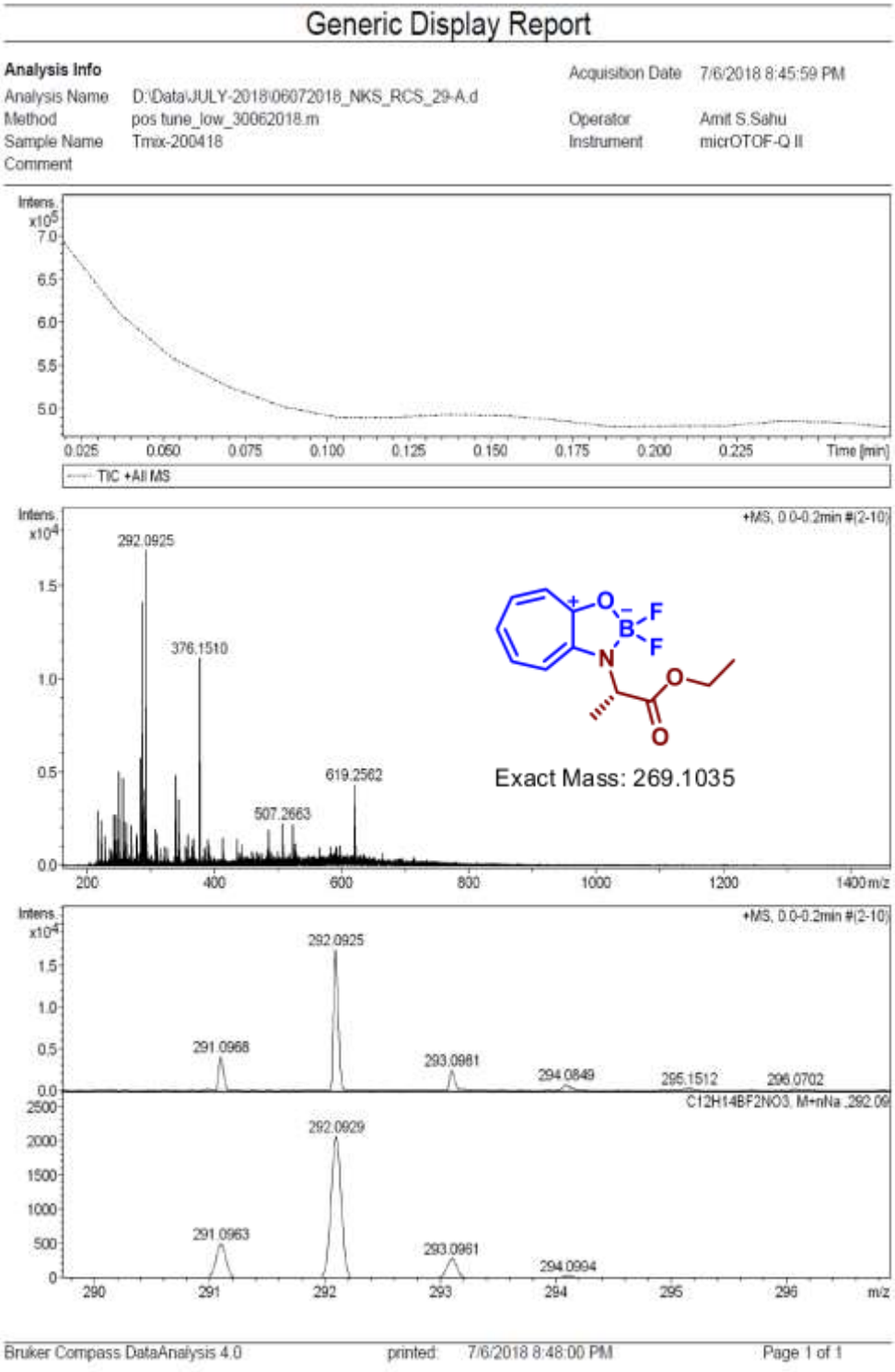

Figure A24. ESI-MS/HRMS spectra of Boron complex **(3b)**

3. NMR (^{1}H, ^{13}C, ^{11}B, ^{19}F) and HRMS of Boron complex *tr-val* **(3c)**

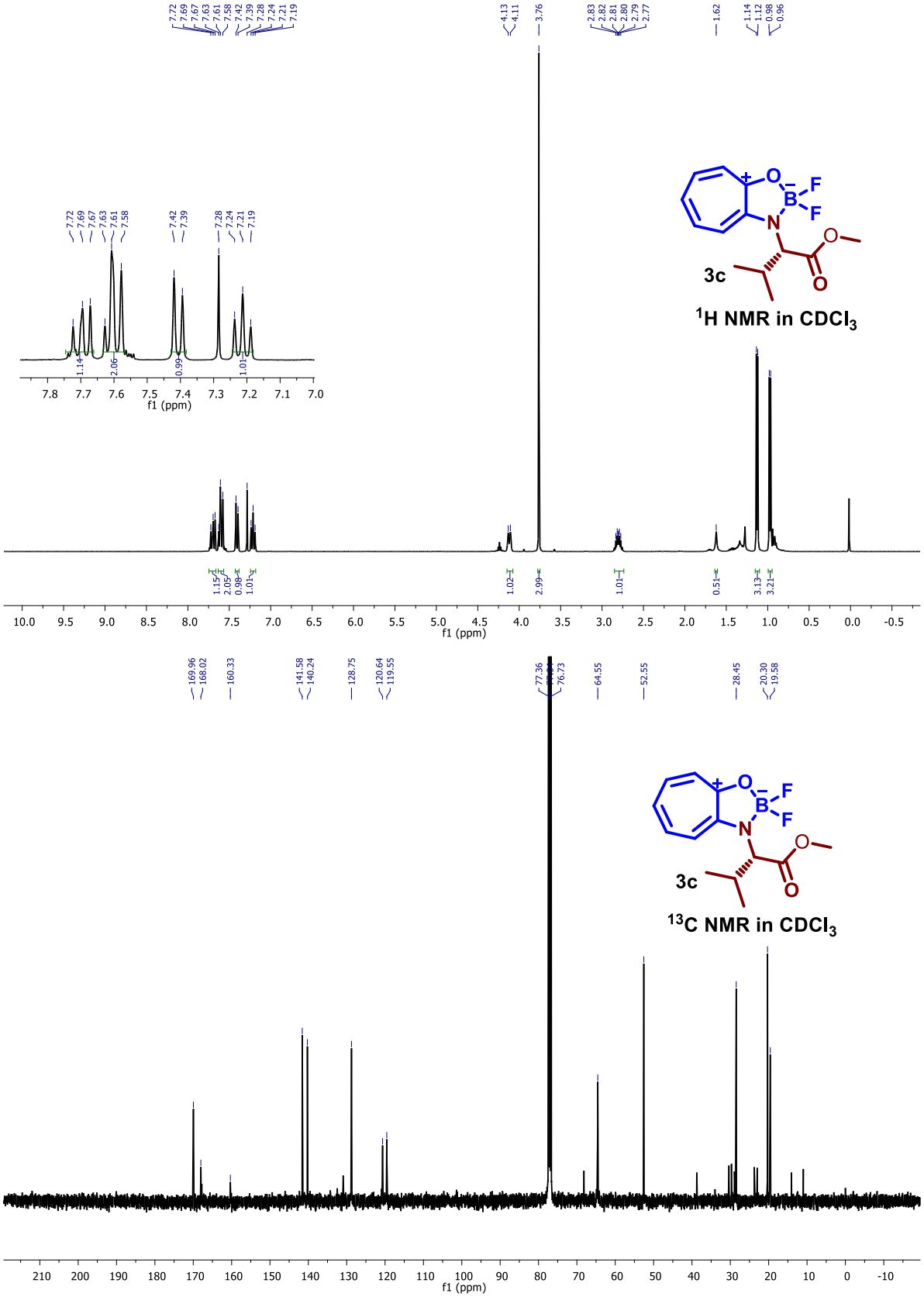

Figure A25. ^{1}H, ^{13}C NMR (400MHz, $CDCl_3$) spectra of Boron complex **(3c)** in $CDCl_3$

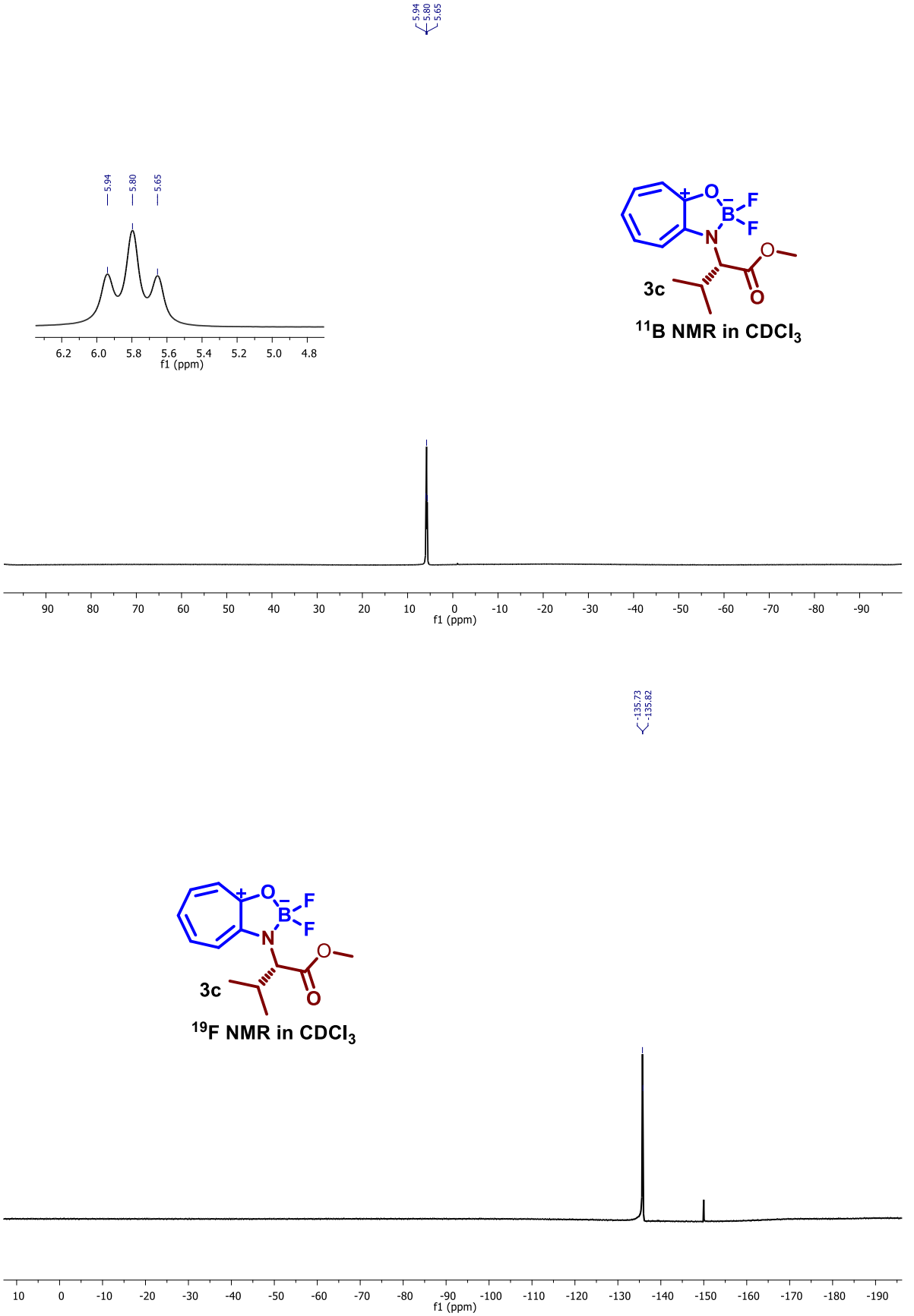

Figure A26. ^{11}B and ^{19}F NMR (400MHz, $CDCl_3$) spectra of Boron complex **(3c)** in $CDCl_3$

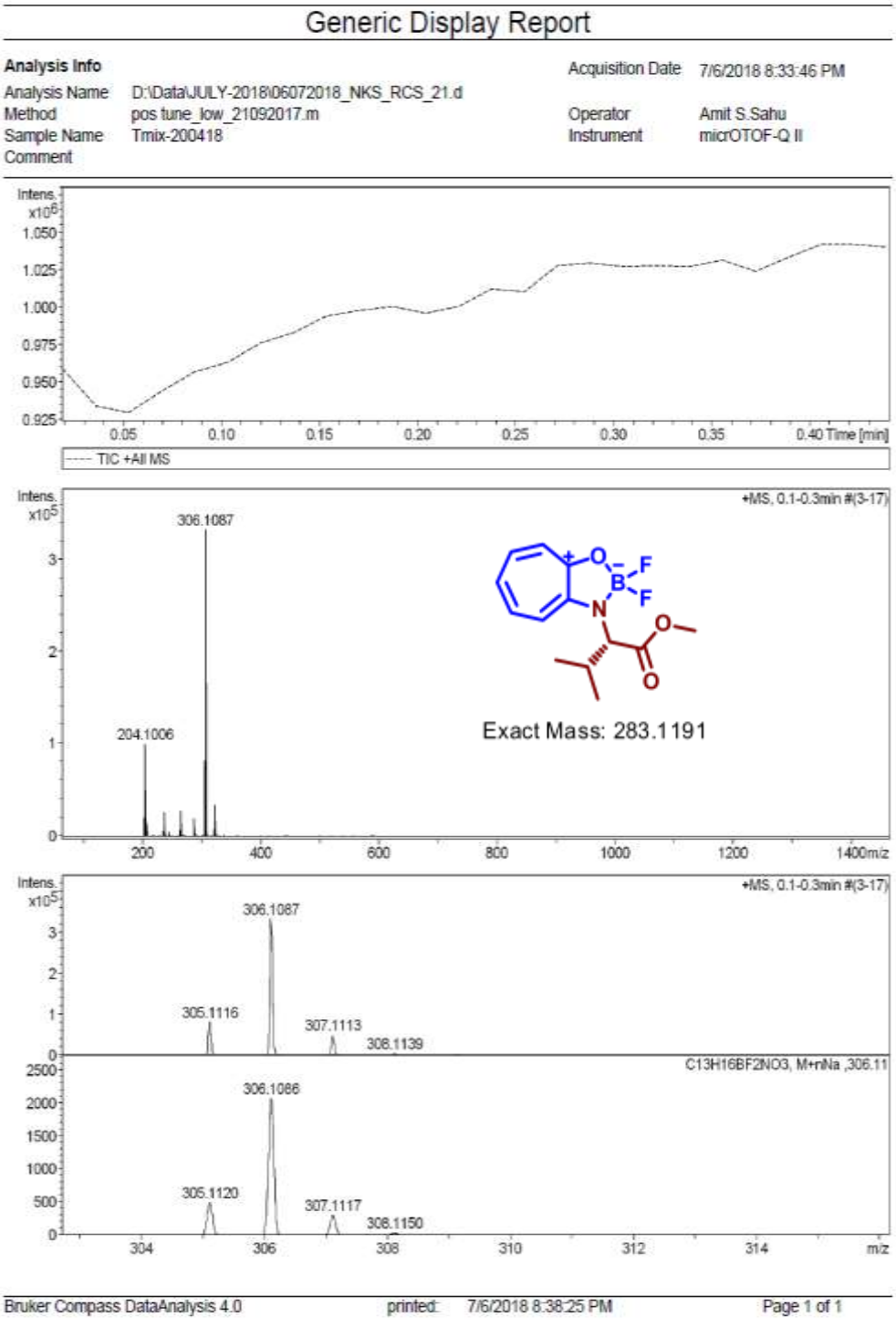

Figure A27. ESI-MS/HRMS spectra of Boron complex **(3c)**

4. NMR (^{1}H, ^{13}C, ^{11}B, ^{19}F) and HRMS of Boron complex *tr-lue* **(3d)**

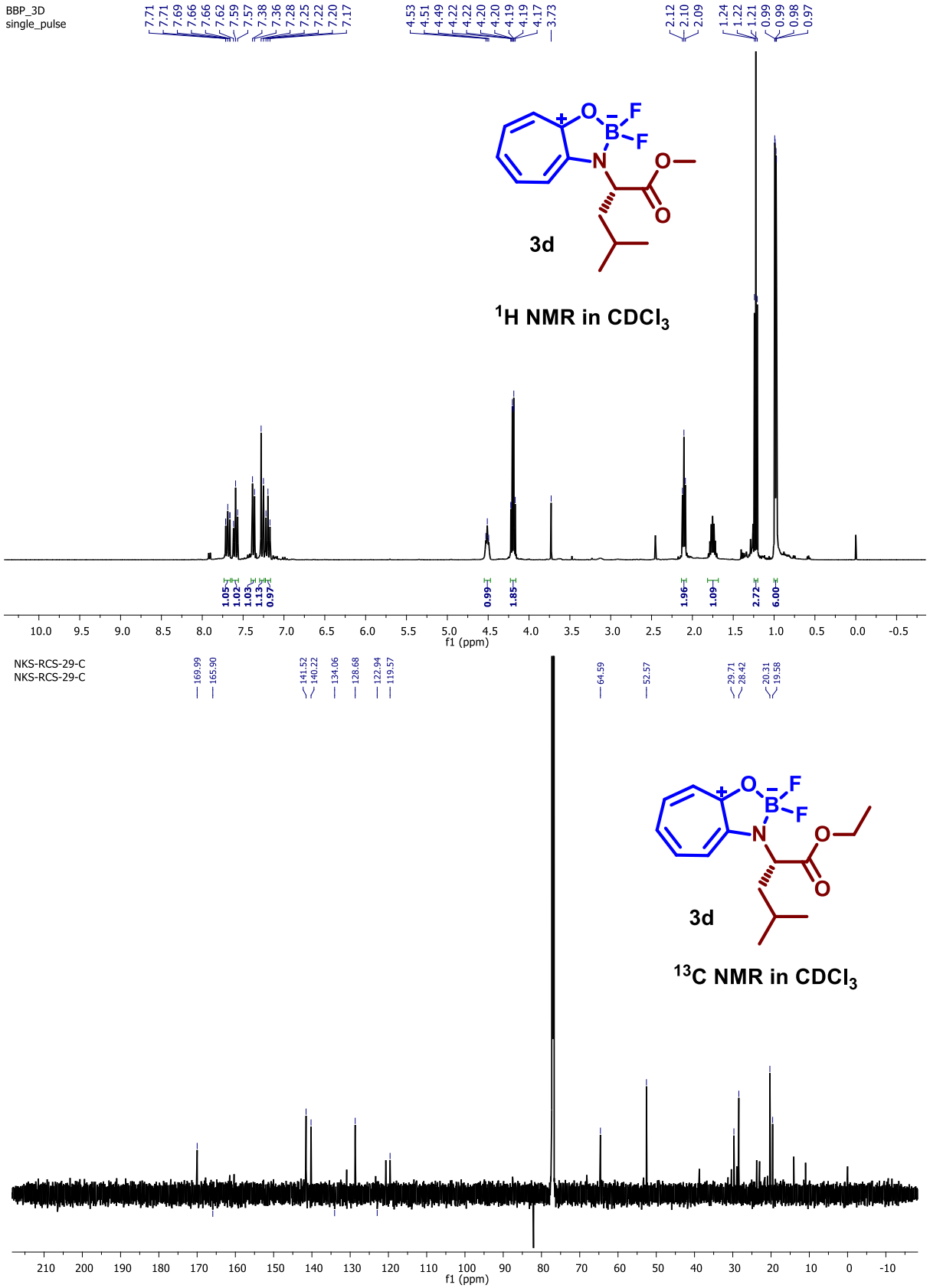

Figure A28. ^{1}H, ^{13}C NMR (400MHz, $CDCl_3$) spectra of Boron complex **(3d)** in $CDCl_3$

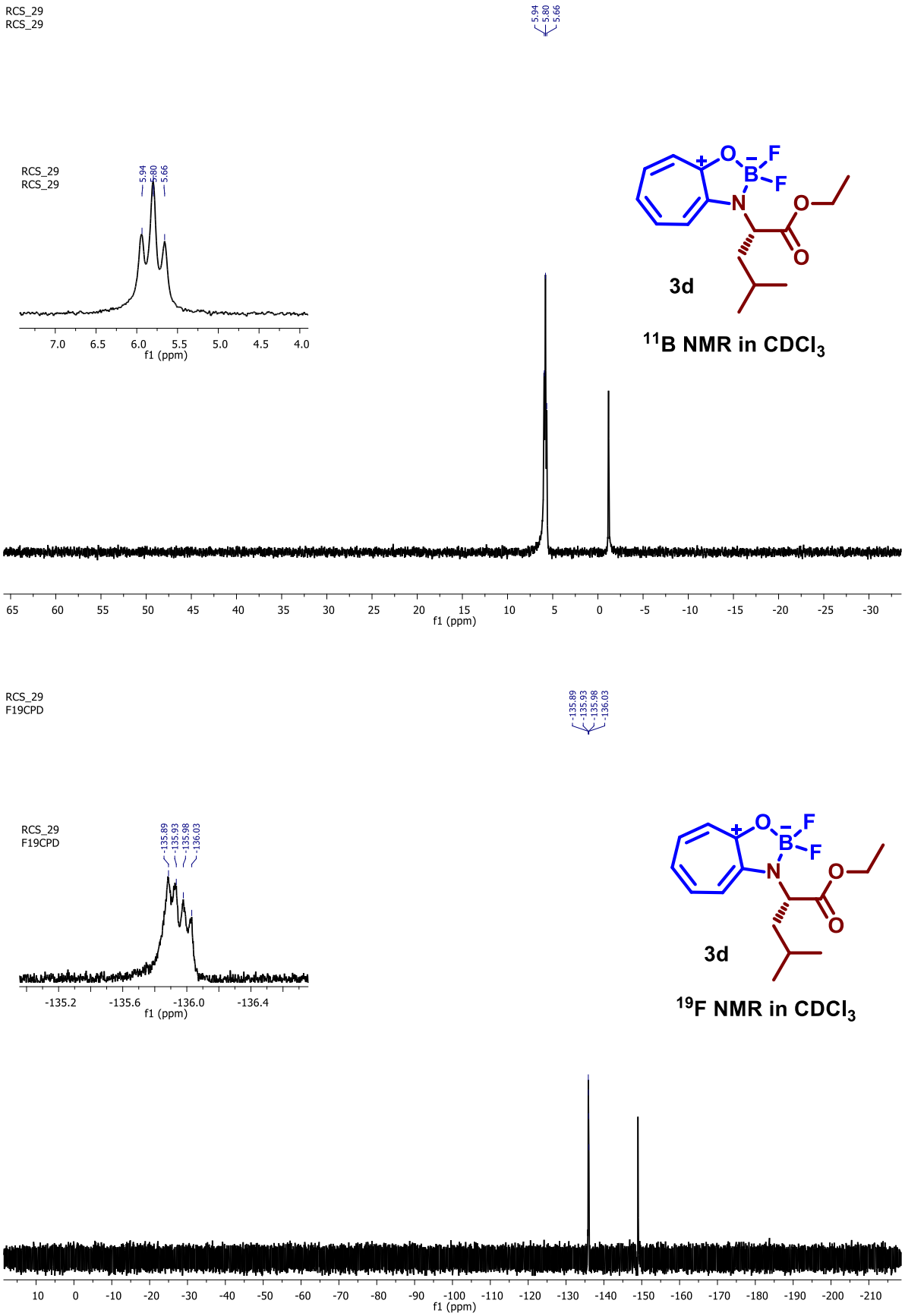

Figure A29. ^{11}B and ^{19}F NMR (400MHz, $CDCl_3$) spectra of Boron complex **(3d)** in $CDCl_3$

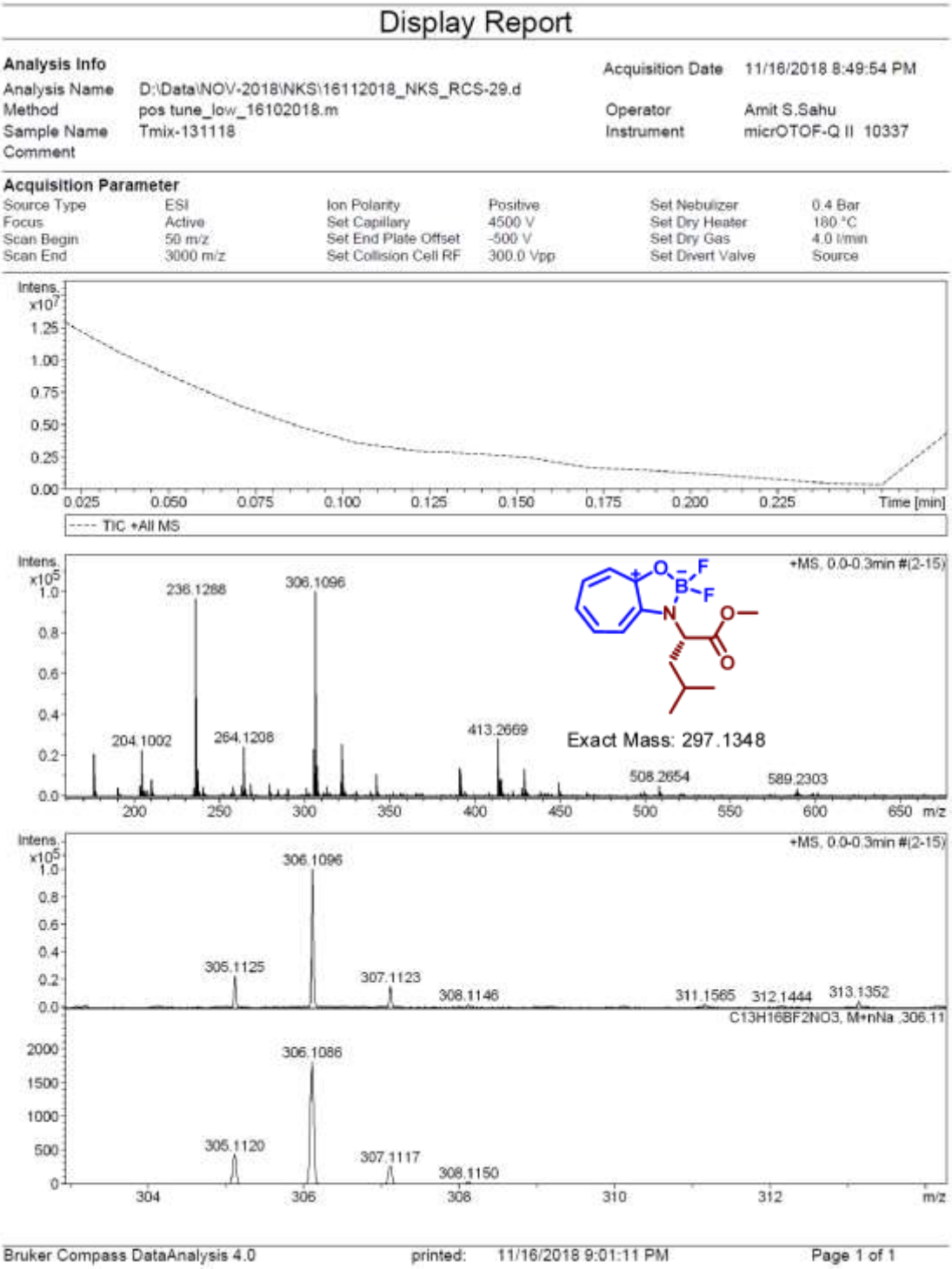

Figure A30. ESI-MS/HRMS spectra of Boron complex **(3d)**

5. NMR (^{1}H, ^{13}C, ^{11}B, ^{19}F) and HRMS of Boron complex *tr-phe* **(3e)**

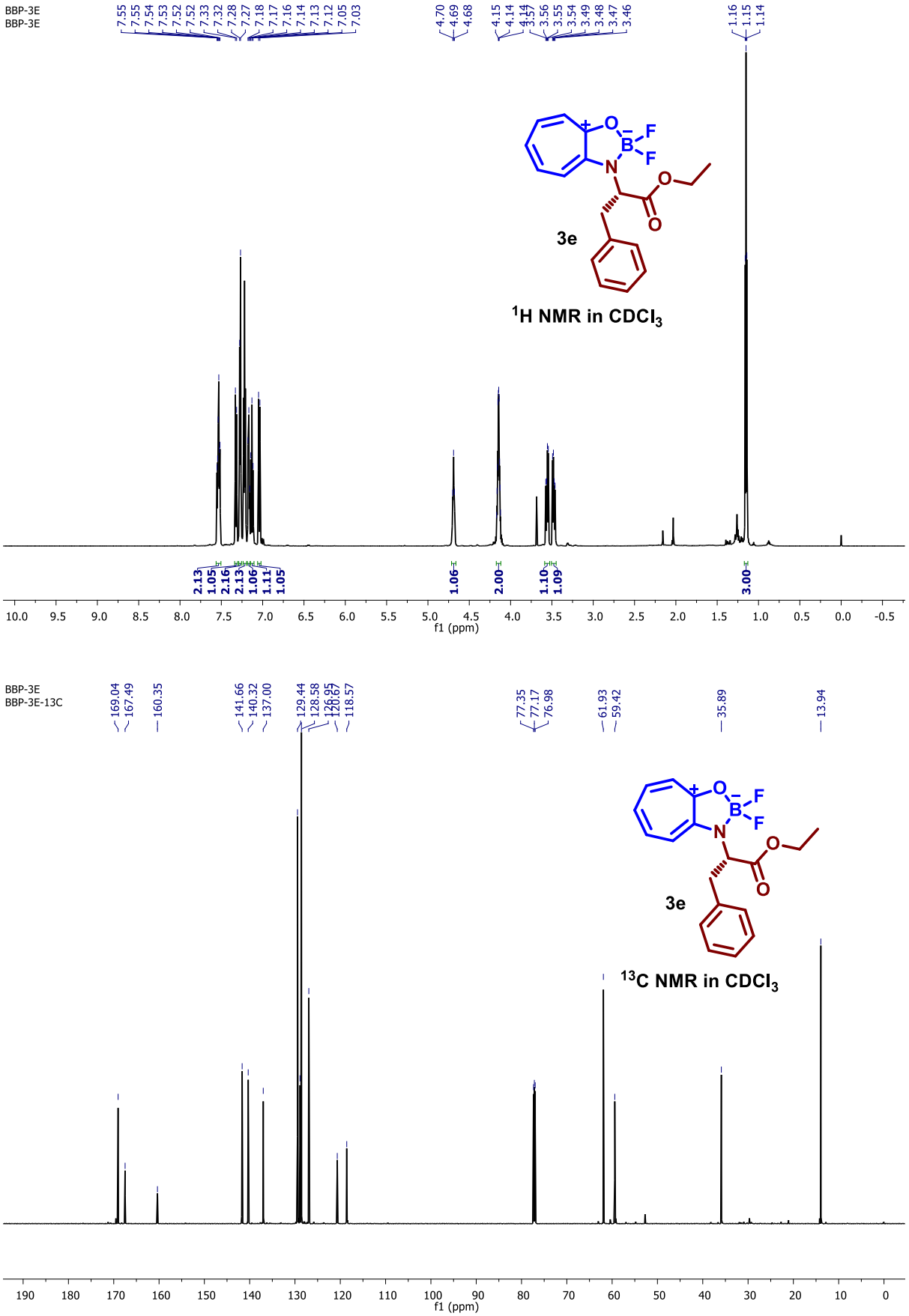

Figure A31. ^{1}H, ^{13}C NMR (700MHz, $CDCl_3$) spectra of Boron complex **(3e)** in $CDCl_3$

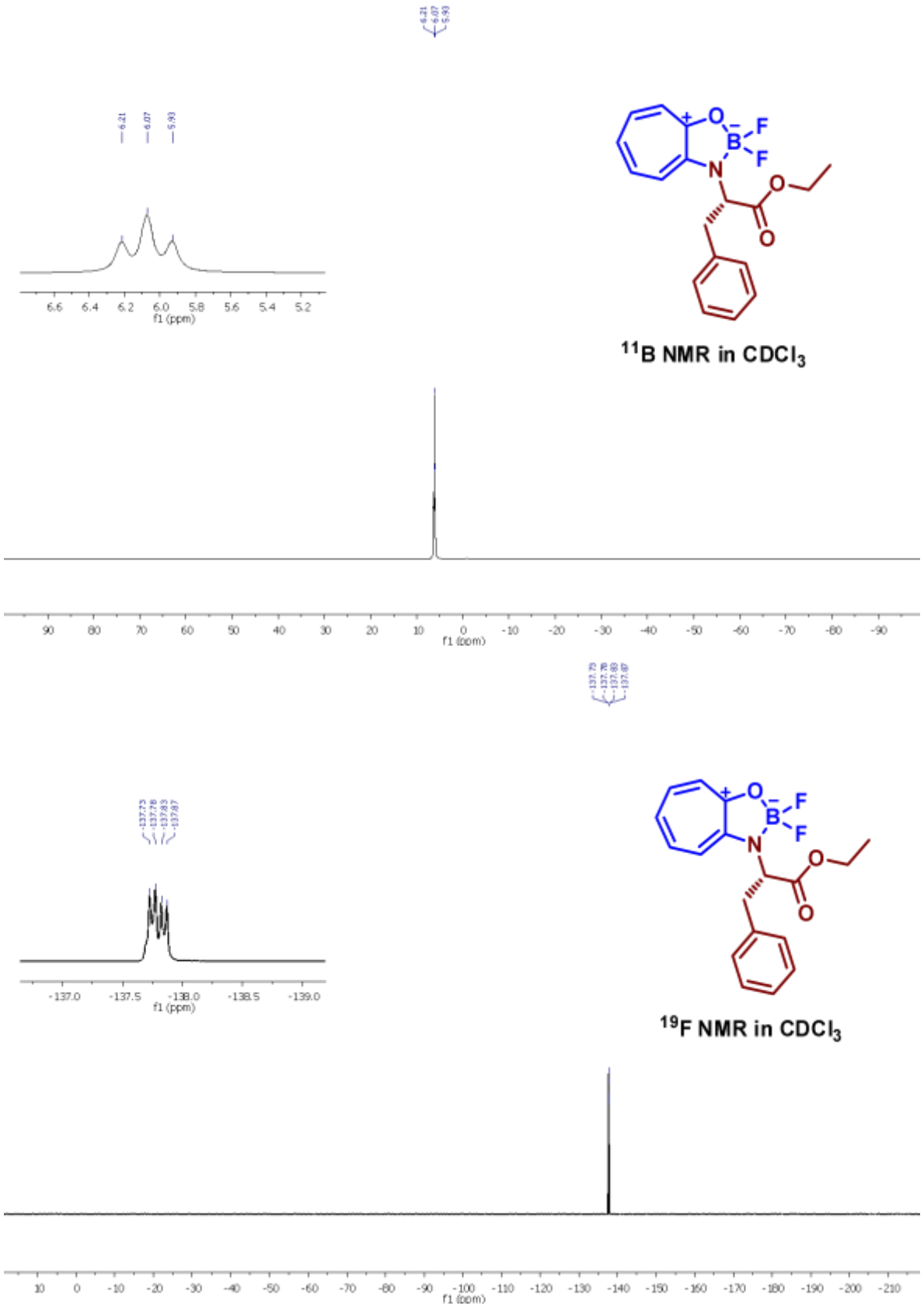

Figure A32. ^{11}B and ^{19}F NMR (400MHz, $CDCl_3$) spectra of Boron complex **(3e)** in $CDCl_3$

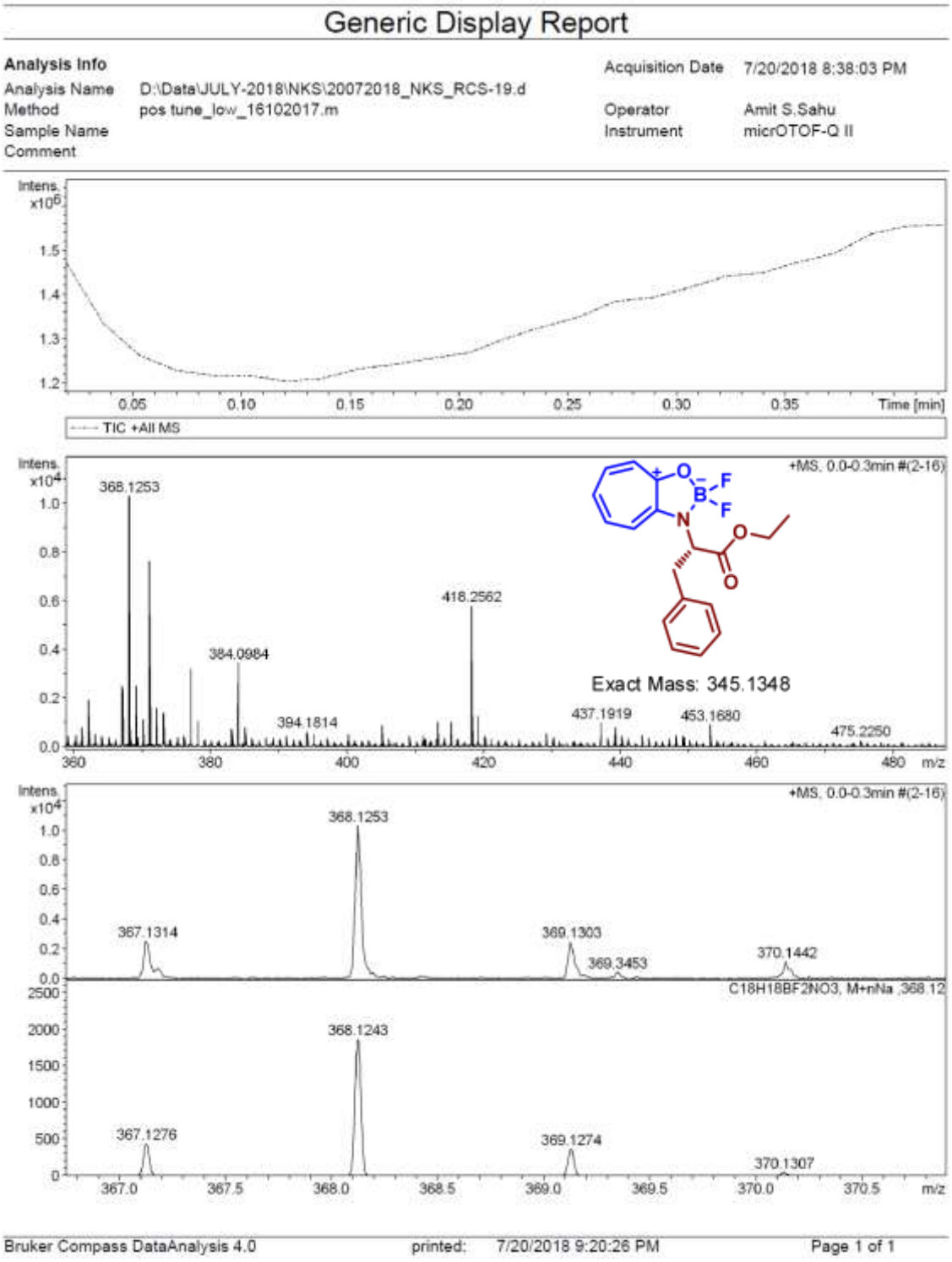

Figure A33. ESI-MS/HRMS spectra of Boron complex **(3e)**

6. NMR (^{1}H, ^{13}C, ^{11}B, ^{19}F) and HRMS of Boron complex *tr-beta ala* **(3f)**

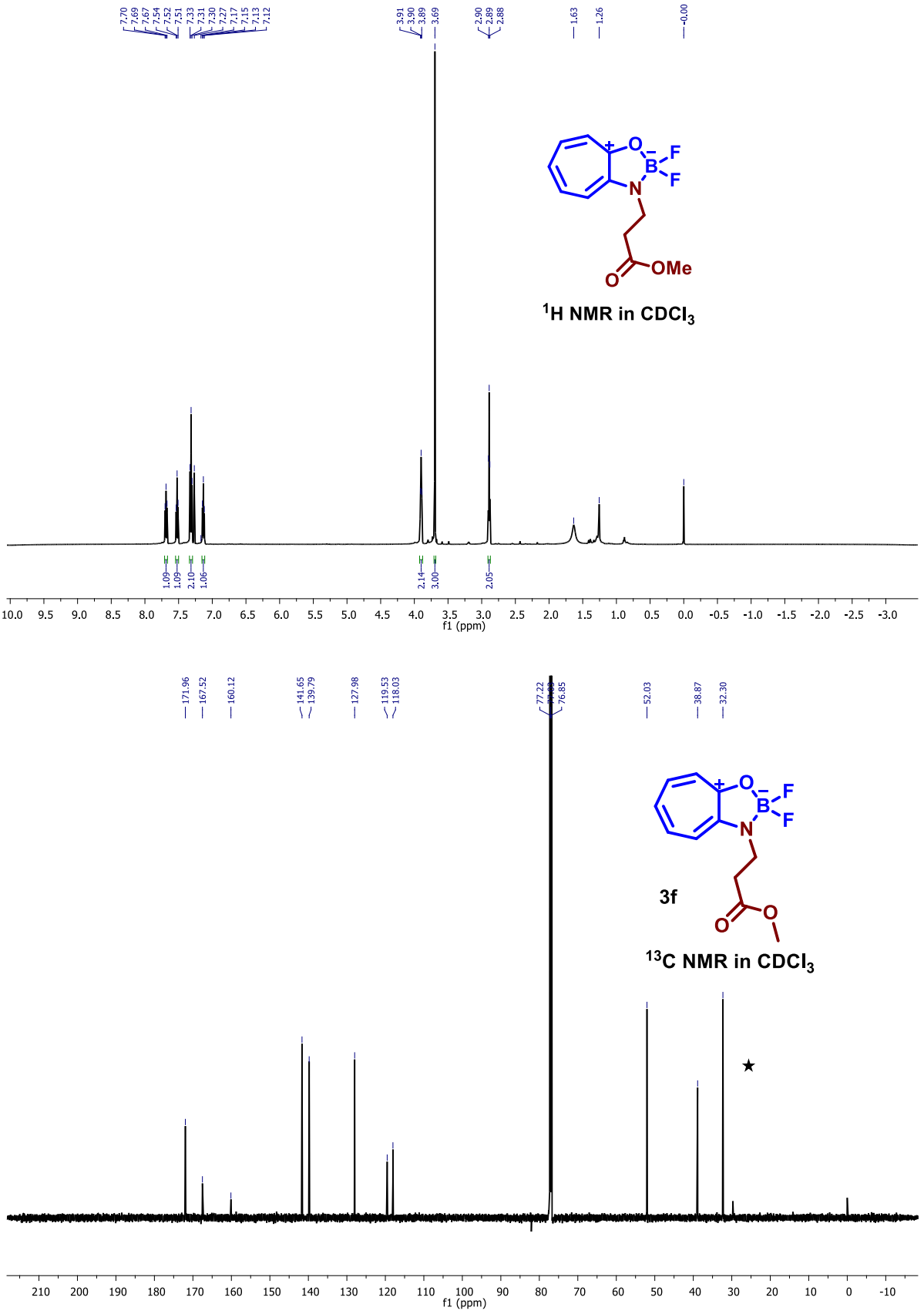

Figure A34. ^{1}H, ^{13}C NMR (700MHz, $CDCl_3$) spectra of Boron complex **(3f)** in $CDCl_3$

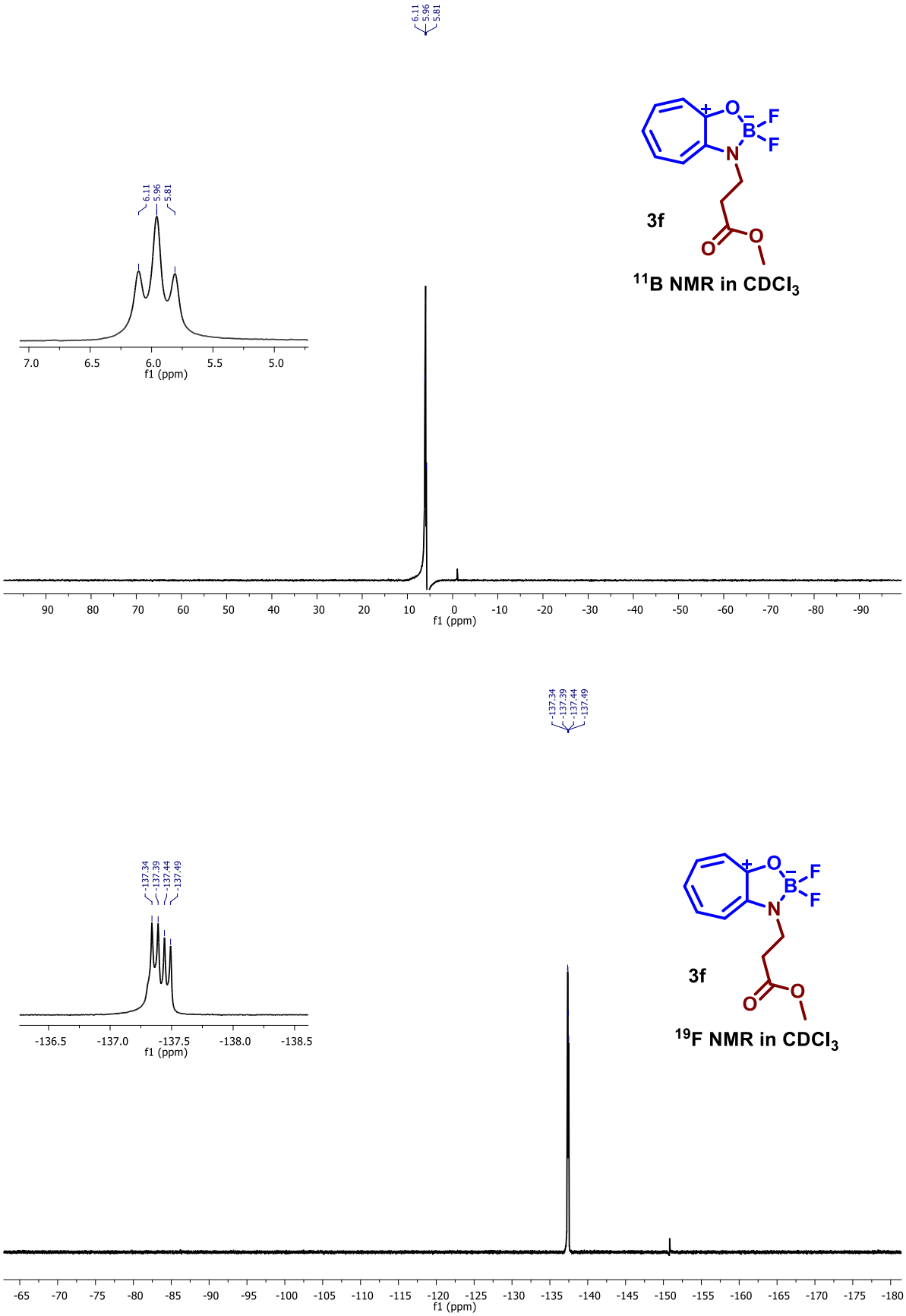

Figure A35. ^{11}B and ^{19}F NMR (400MHz, $CDCl_3$) spectra of Boron complex **(3f)** in $CDCl_3$

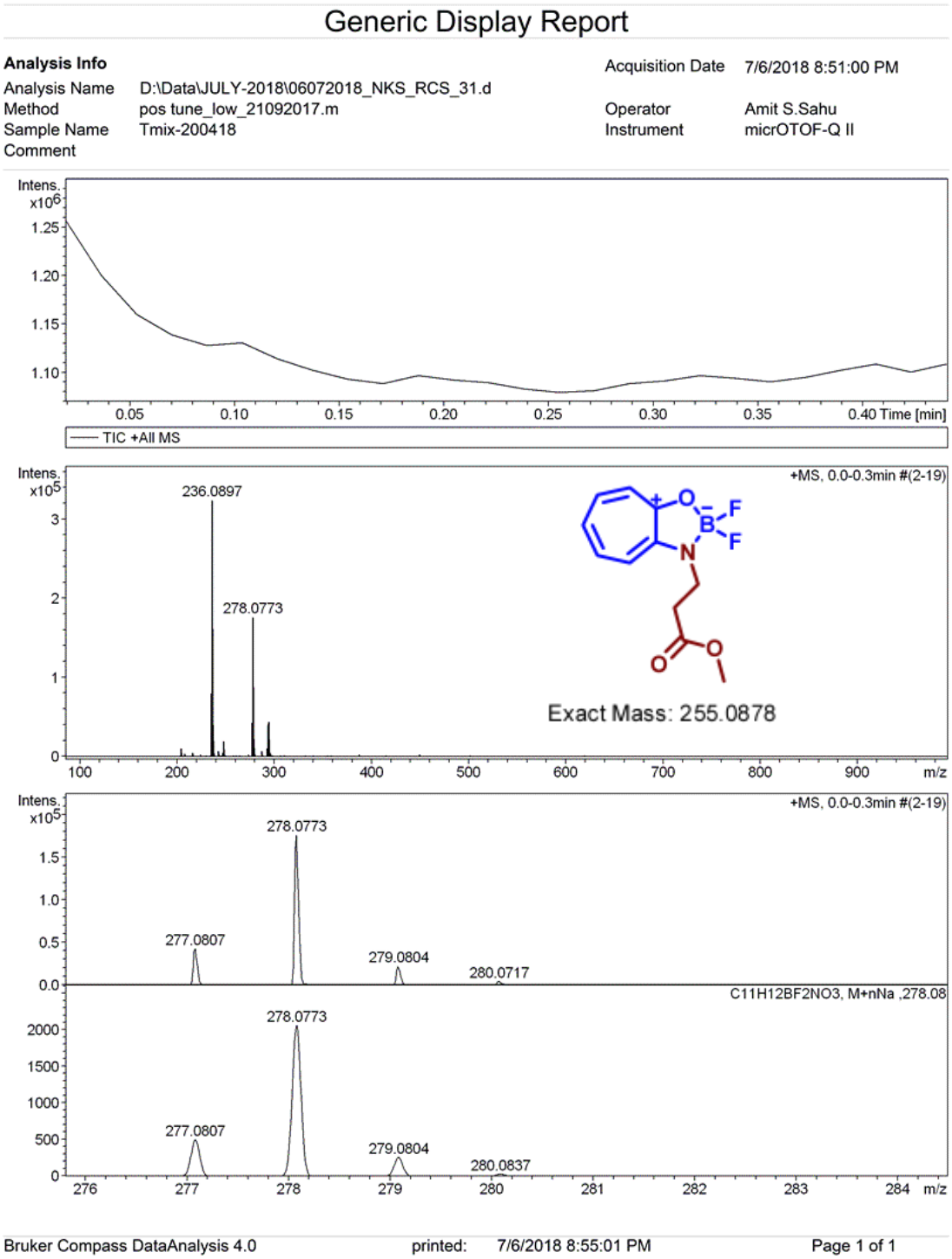

Figure A36. ESI-MS/HRMS spectra of Boron complex **(3f)**

7. NMR (^{1}H, ^{13}C, ^{11}B, ^{19}F) and HRMS of Boron complex *tr-dipep* **(3g)**

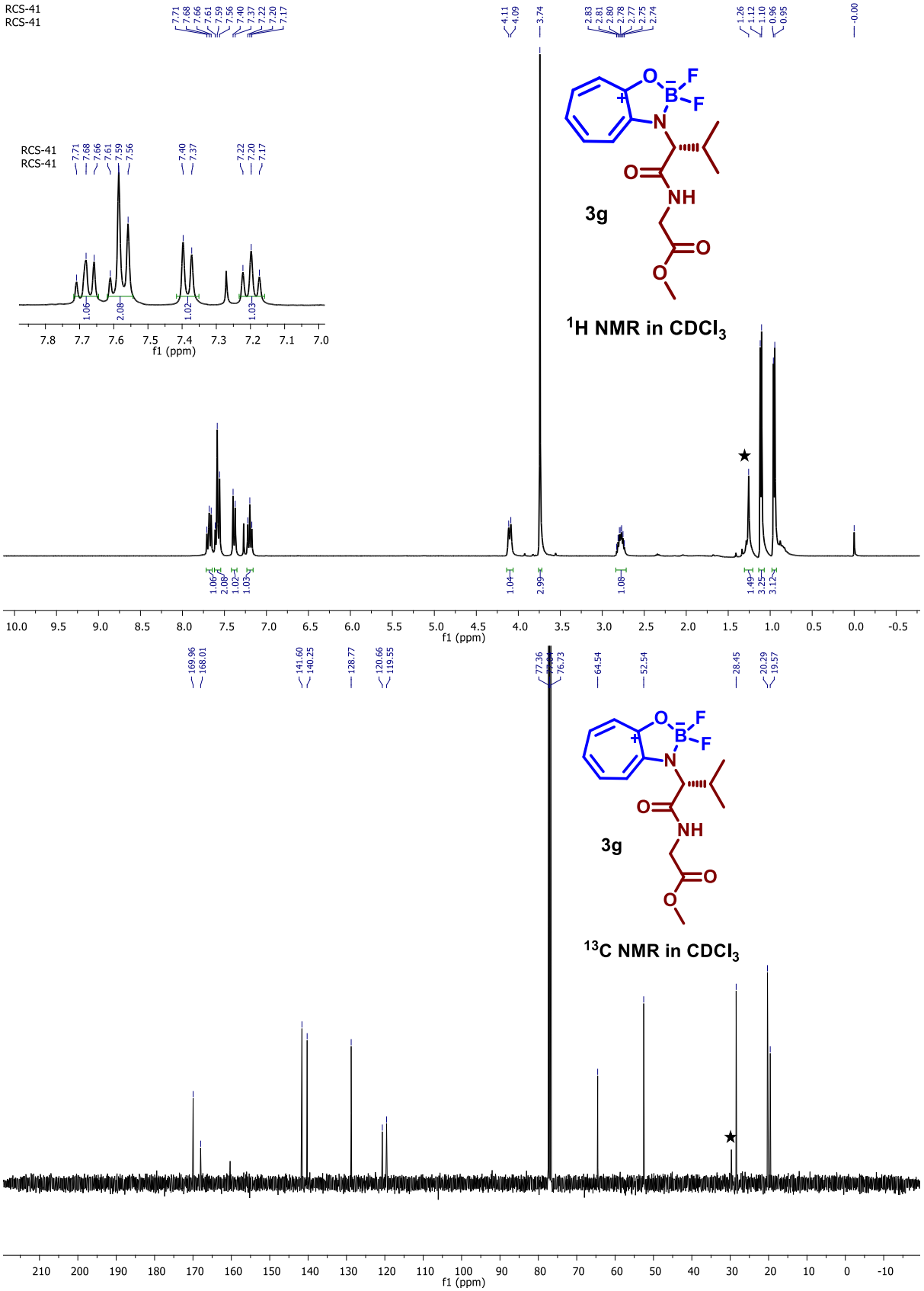

Figure A37. ^{1}H, ^{13}C NMR (400MHz, $CDCl_3$) spectra of Boron complex **(3g)** in $CDCl_3$

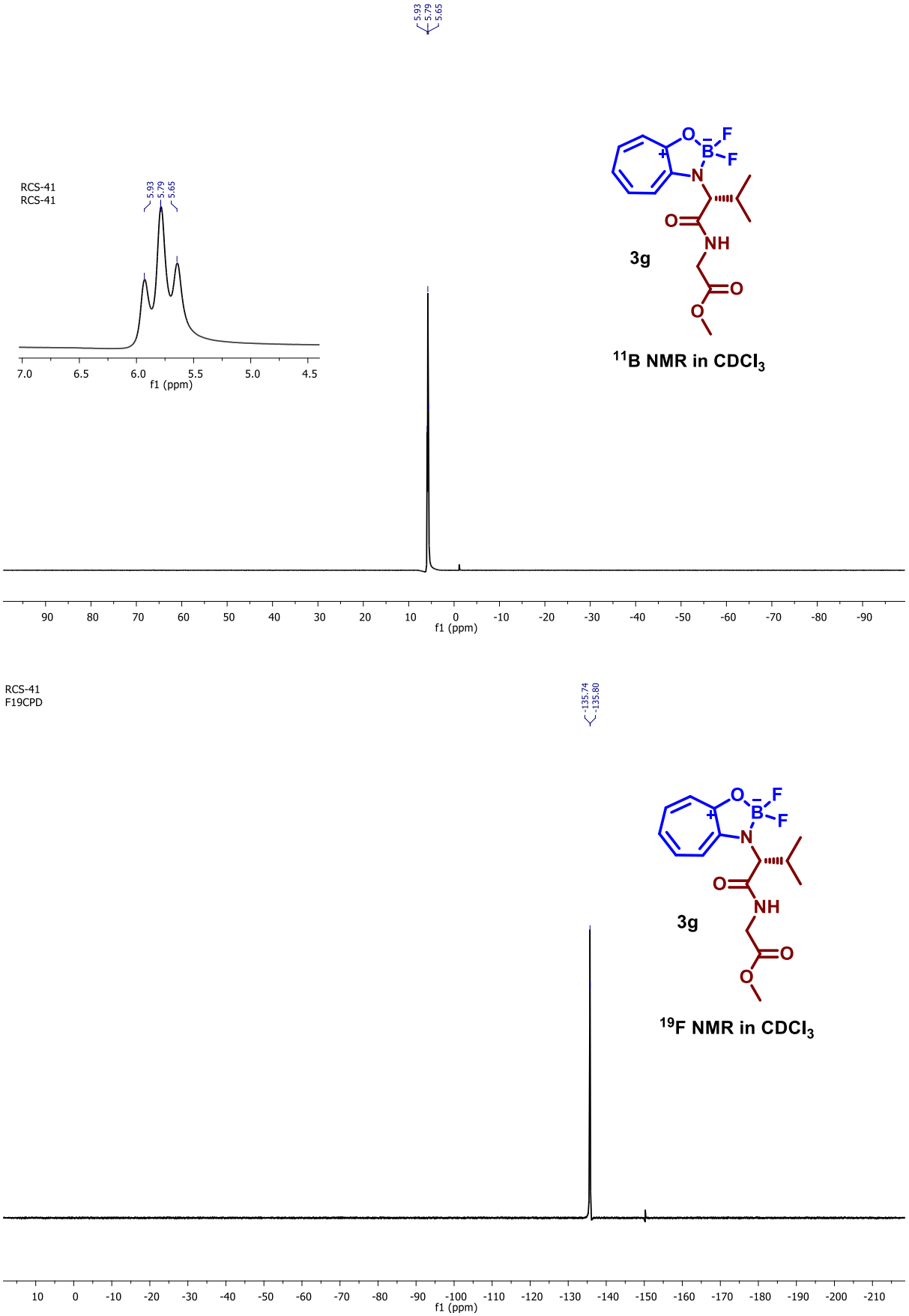

Figure A38. ^{11}B and ^{19}F NMR (400MHz, $CDCl_3$) spectra of Boron complex **(3g)** in $CDCl_3$

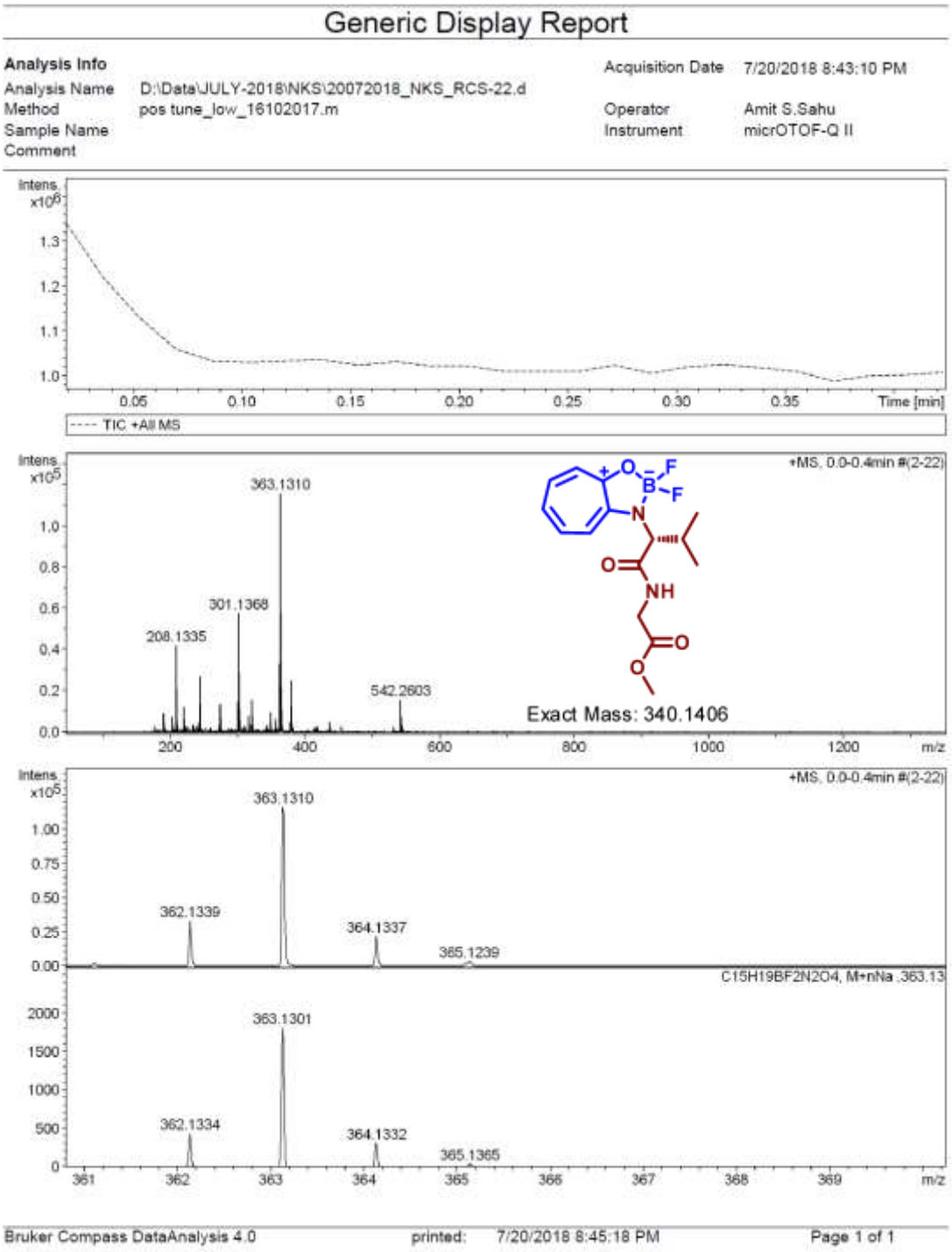

Figure A39. ESI-MS/HRMS spectra of Boron complex **(3g)**

8. NMR (^{1}H, ^{13}C, ^{11}B, ^{19}F) and HRMS of Boron complex *tr-picolylamine* **(3h)**

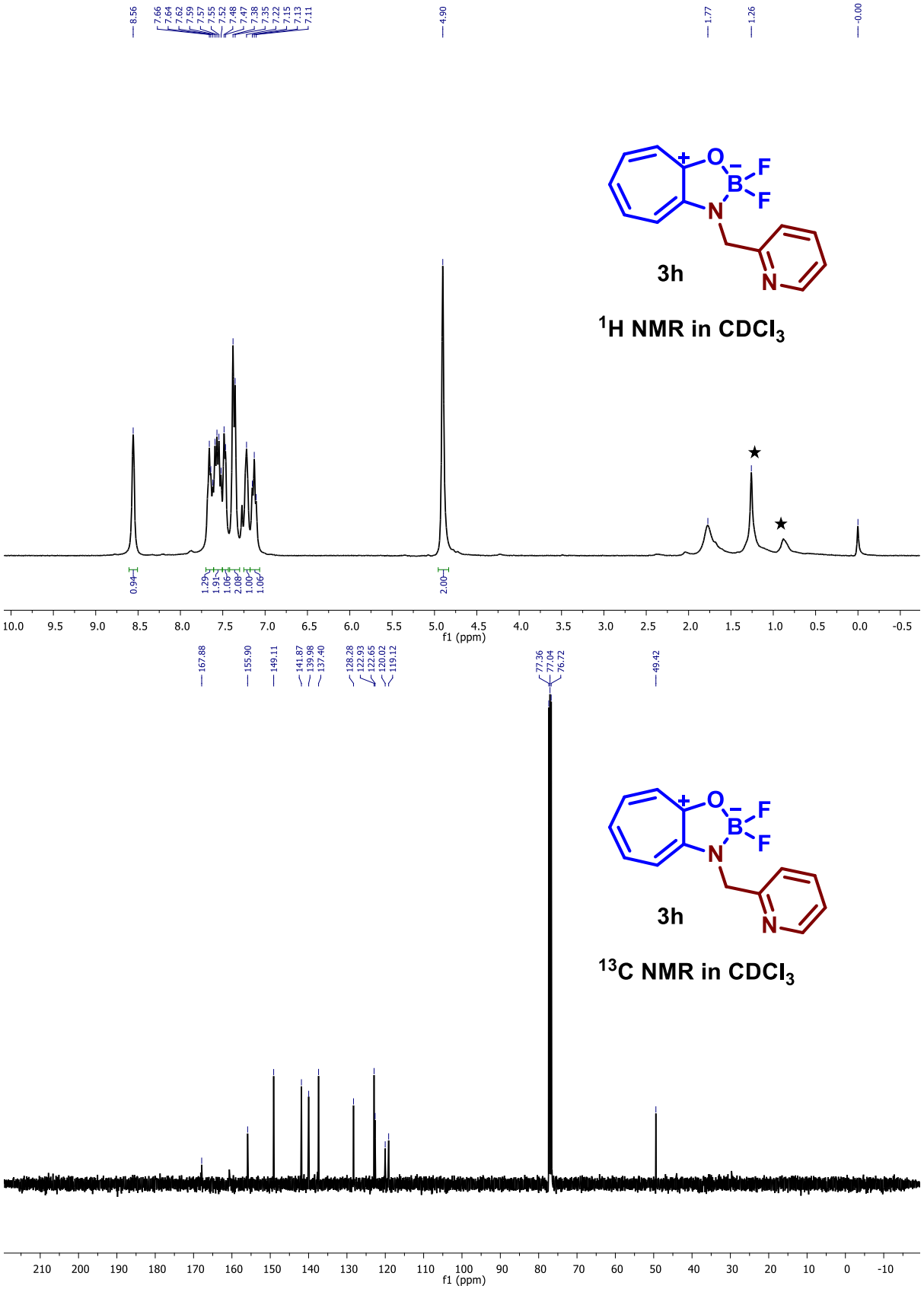

Figure A40. ^{1}H, ^{13}C NMR (400MHz, $CDCl_3$) spectra of Boron complex **(3h)** in $CDCl_3$

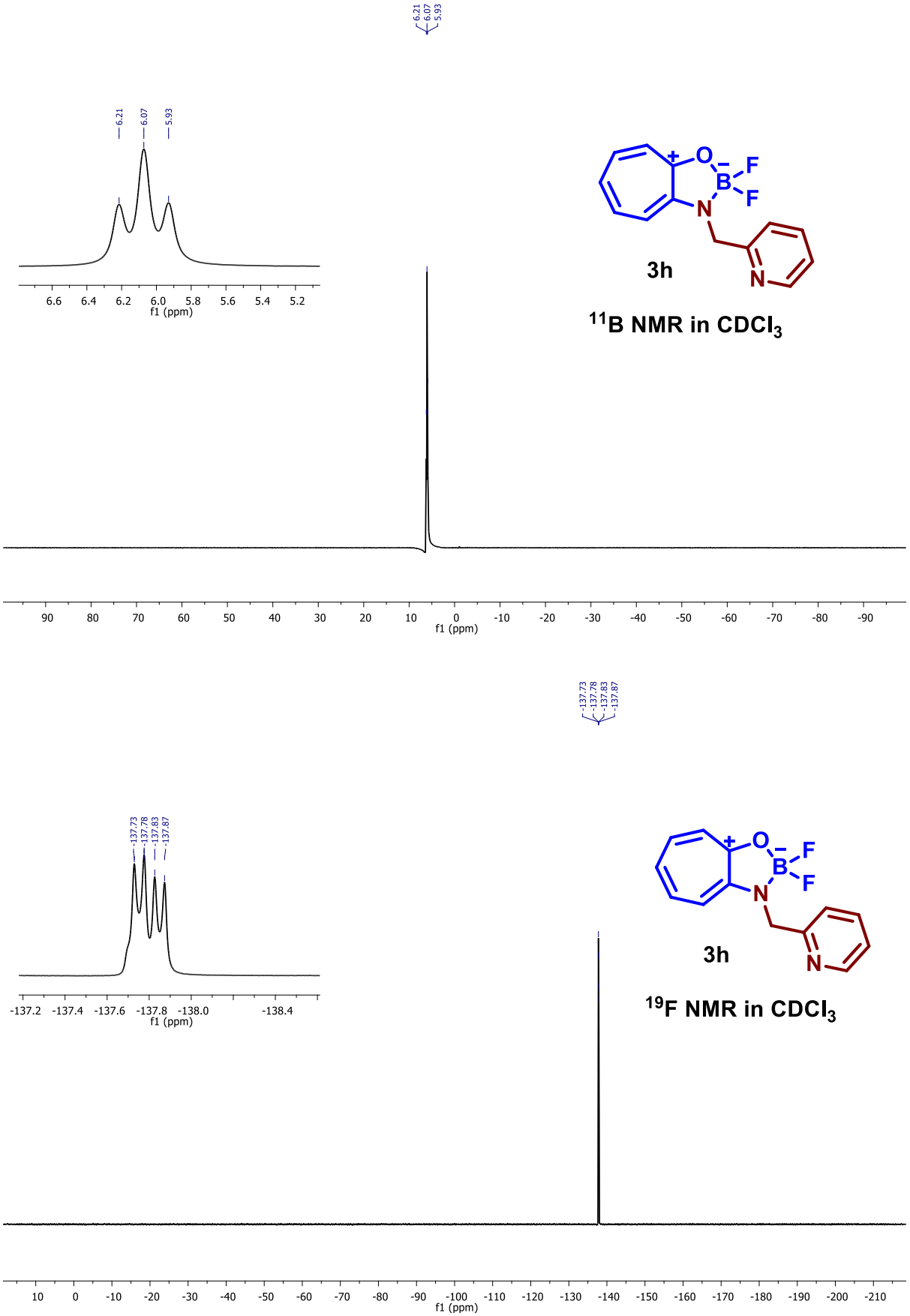

Figure A41. ^{11}B and ^{19}F NMR (400MHz, $CDCl_3$) spectra of Boron complex **(3h)** in $CDCl_3$

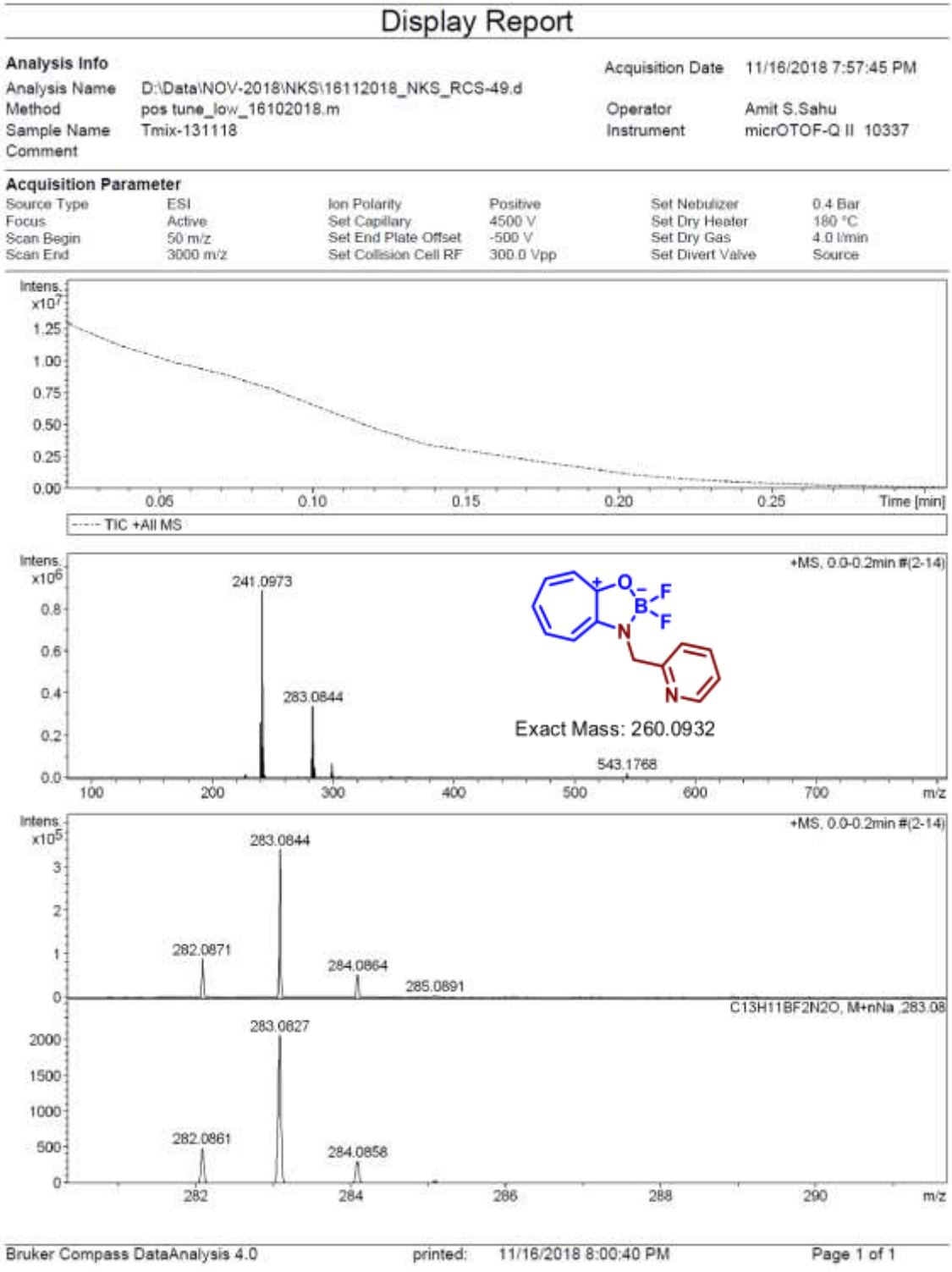

Figure A42. ESI-MS/HRMS spectra of Boron complex **(3h)**

9. NMR (^{1}H, ^{13}C, ^{11}B, ^{19}F) and HRMS of boron complex *tr-aminoquinoline* **(3i)**

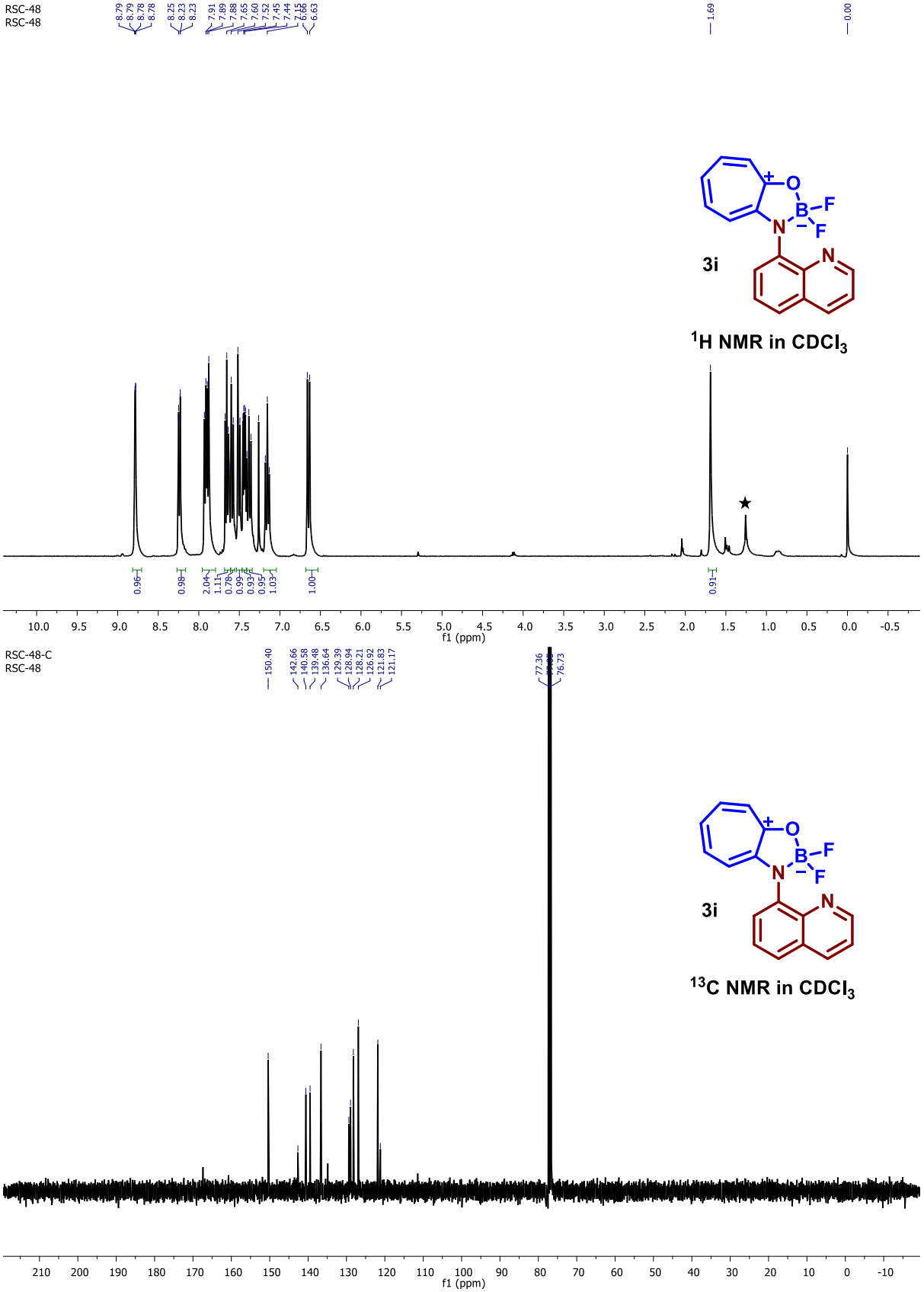

Figure A43. ^{1}H, ^{13}C NMR (400MHz, $CDCl_3$) spectra of Boron complex **(3i)** in $CDCl_3$

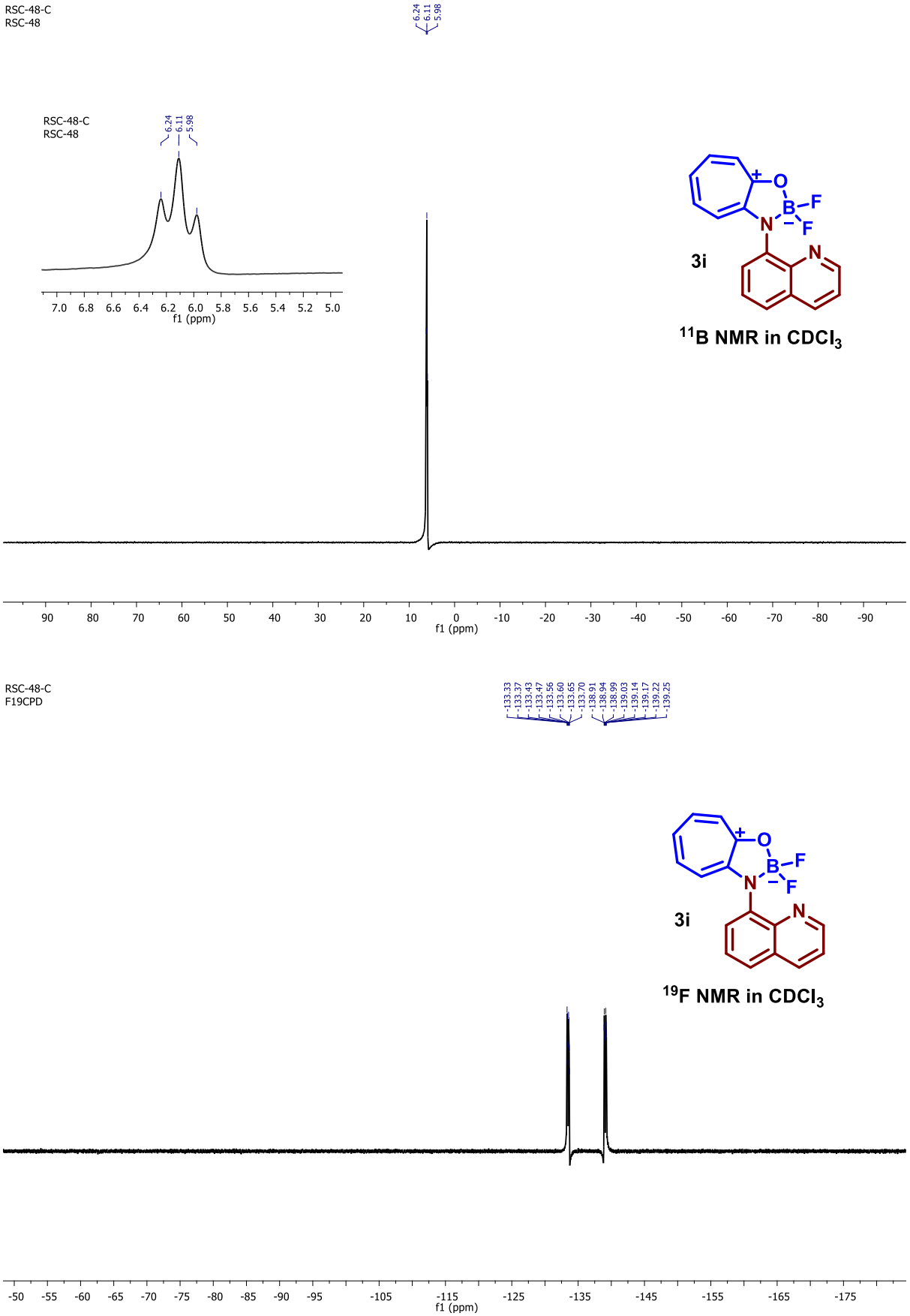

Figure A44. ^{11}B and ^{19}F NMR (400MHz, $CDCl_3$) spectra of Boron complex **(3i)** in $CDCl_3$

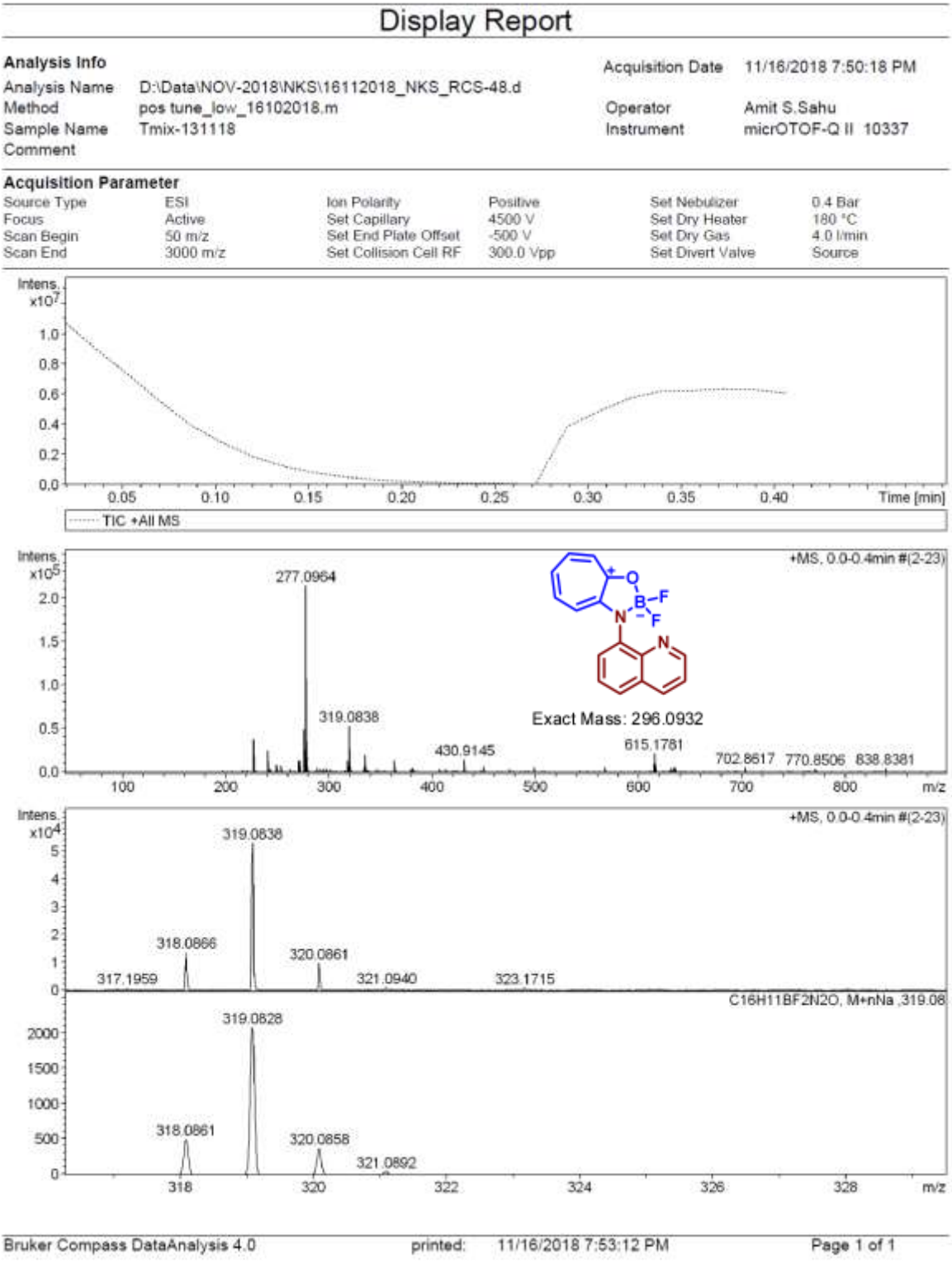

Figure A45. ESI-MS/HRMS spectra of Boron complex **(3i)**

10. Crystal structures and data

Good quality crystals of compounds were obtained in solvent mixture dichloromethane and hexane by slow evaporation method. The crystals data of all boron complexes were collected on a Rigaku Oxford diffractometer at 293 K respectively. Selected data collection parameters and other crystallographic results are summarized below. The program package SHELXTL[1] and Olex2 was used for structure solution and packing diagram carried out by DIAMOND-3.2 software.

CCDC 1888894-1888899 contain the supplementary crystallographic data for **3a,3a-OH,3b,3h** and **3i**. These data can be obtained free of charge via https://www.ccdc.cam.ac.uk/data

Table A1: Crystallographic table

compounds	(3a)	(3b)	(3c)	(3h)	(3i)	(3a-OH)
Identification code	**CCDC 1888899**	**CCDC 1888896**	**CCDC 1888897**	**CCDC 1888895**	**CCDC 1888898**	**CCDC1888894**
Empirical formula	$C_{11}H_{12}BF_2NO_3$	$C_{12}H_{14}BF_2NO_3$	$C_{26}H_{32}B_2F_4N_2O_6$	$C_{13}H_{11}BF_2N_2O$	$C_{16}H_{11}BF_2N_2O$	$C_9H_8BF_2NO_3$
Formula weight	255.04	269.07	566.20	260.07	296.10	226.97
Temperature/k	298.0	296(2)	293(2)	296.0	298	293(2)
Crystal system	monoclinic	Orthorhombic	triclinic	triclinic	monoclinic	monoclinic
Space group	$P2_1/c$	Pbca	P1	P-1	$P2_1/c$	$P2_1/n$
A/å	13.1705(7)	13.5273(5)	8.1582(2)	8.8495(2)	7.0792(4)	7.0433(4)
B/å	12.9185(4)	7.7581(4)	9.4094(2)	9.1023(2)	7.4313(4)	11.5620(8)
C/å	7.3648(2)	24.7812(15)	9.4305(2)	9.2653(2)	26.3653(14)	11.6118(8)
α/°	90	90	98.033(1)	62.940(2)	90	90
β/°	97.809(3)	90	94.918(2)	89.372(2)	96.772(5)	90.857(5)
γ/°	90	90	94.971(1)	69.175(2)	90	90
Volume/å^3	1241.45(8)	2600.7(2)	710.60(3)	610.93(3)	1377.34(13)	945.50(11)
Z	4	8	1	2	4	4
ρ_{calc}g/cm^3	1.3644	1.3742	1.3229	1.4136	1.4277	1.594
M/mm^{-1}	1.005	0.987	0.929	0.937	0.108	1.242
F(000)	530.2	1124.5	297.2	269.0	608.4	464.0
Crystal size/mm^3	0.001 × 0.0001 × 0.0001	0.001 × 0.0001 × 0.0001	0.21 × 0.21 × 0.2	0.001 × 0.0001 × 0.0001	0.001 × 0.0002 × 0.0001	0.01 × 0.01 × 0.01
Radiation	Cu Kα (λ = 1.54184)	Cu Kα (λ = 1.54184)	Cu Kα (λ = 1.54184)	Cu Kα (λ = 1.54184)	Mo Kα (λ = 0.71073)	CuKα (λ = 1.54184)
2θ range for data collection/°	6.78 to 148.96	7.14 to 148.92	9.52 to 148.94	10.88 to 150.68	6.9 to 52.74	10.798 to 148.932

Index ranges	-15 ≤ h ≤ 16, -16 ≤ k ≤ 16, -9 ≤ l ≤ 6	-17 ≤ h ≤ 16, -5 ≤ k ≤ 9, -30 ≤ l ≤ 29	-8 ≤ h ≤ 10, -11 ≤ k ≤ 11, -12 ≤ l ≤ 12	-8 ≤ h ≤ 11, -10 ≤ k ≤ 11, -11 ≤ l ≤ 11	-9 ≤ h ≤ 9, -9 ≤ k ≤ 9, -34 ≤ l ≤ 33	-8 ≤ h ≤ 8, -11 ≤ k ≤ 14, -14 ≤ l ≤ 14
Reflections collected	8441	10196	23106	9421	13111	6207
Independent reflections	2449 [R_{int} = 0.0828, R_{sigma} = 0.0590]	2546 [R_{int} = 0.0731, R_{sigma} = 0.0497]	5386 [R_{int} = 0.0504, R_{sigma} = 0.0278]	2469 [R_{int} = 0.0382, R_{sigma} = 0.0262]	2802 [R_{int} = 0.0177, R_{sigma} = 0.0158]	1880 [R_{int} = 0.0962, R_{sigma} = 0.0460]
Data/restraints/parameters	2449/0/164	2546/0/174	5386/3/367	2469/0/179	2802/0/199	1880/0/149
Goodness-of-fit on f^2	1.211	1.126	1.062	1.143	0.842	1.567
Final r indexes [i>=2σ (i)]	R_1 = 0.0974, wR_2 = 0.2898	R_1 = 0.0922, wR_2 = 0.2806	R_1 = 0.0594, wR_2 = 0.1735	R_1 = 0.0390, wR_2 = 0.1006	R_1 = 0.0391, wR_2 = 0.1750	R_1 = 0.1201, wR_2 = 0.3423
Final r indexes [all data]	R_1 = 0.1180, wR_2 = 0.3107	R_1 = 0.1296, wR_2 = 0.3336	R_1 = 0.0609, wR_2 = 0.1767	R_1 = 0.0423, wR_2 = 0.1034	R_1 = 0.0443, wR_2 = 0.1867	R_1 = 0.1295, wR_2 = 0.3485
Largest diff. Peak/hole / e $å^{-3}$	0.41/-0.36	0.29/-0.43	0.44/-0.25	0.12/-0.22	0.20/-0.22	0.64/-0.46

Table A2: Selected bond lengths and bond angles of boron complexes in solid state

compounds		3a	3b	3c	3h	3i	3a-OH
Selected bond lengths	C_1—C_7	1.4503 Å	1.4425 Å	1.4532 Å	1.4440 Å	1.4578 Å	1.4359 Å
	C_7—N_1	1.3252 Å	1.3394 Å	1.3317 Å	1.3250 Å	1.3273 Å	1.3257 Å
	C_1—O_1	1.3116 Å	1.3201 Å	1.3191 Å	1.3224 Å	1.3162 Å	1.3237 Å
	N_1—B_1	1.5331 Å	1.5587 Å	1.5438 Å	1.5453 Å	1.5546 Å	1.5400 Å
	O_1—B_1	1.4754 Å	1.4691 Å	1.4769 Å	1.4799 Å	1.4877 Å	1.4908 Å
	B_1—F_1	1.3800Å	1.3730 Å	1.3678 Å	1.3752 Å	1.3642 Å	1.3794 Å
	B_1—F_2	1.3790 Å	1.3783 Å	1.3700 Å	1.3821 Å	1.3754 Å	1.3878 Å
Selected bond angles	N_1—B_1—O_1	99.887°	100.182°	100.092°	99.688°	99.018°	99.836°
	O_1—B_1—F_1	111.216°	111.952°	110.796°	111.746°	111.616°	112.599°
	O_1—B_1—F_2	111.112°	110.886°	111.453°	111.092°	110.190°	112.566°
	N_1—B_1—F_1	111.417°	112.846°	113.098°	112.124°	112.744°	110.284°
	N_1—B_1—F_2	112.601°	111.091°	112.638°	112.609°	112.539°	112.401°
	F_1—B_1—F_2	109.349°	109.623°	108.610°	109.342°	110.291°	108.960°
	B_1—N_1—C_7	110.825°	109.191°	110.680°	110.607°	111.312°	110.641°
	B_1—O_1—C_1	111.621°	111.926°	111.200°	111.322°	111.839°	110.412°
	O_1—C_1—C_7	110.080°	110.144°	110.738°	110.323°	110.605°	108.537°
	N_1—C_7—C_1	107.553°	107.537°	107.242°	107.976°	107.209°	110.144°

11. Photophysical studies

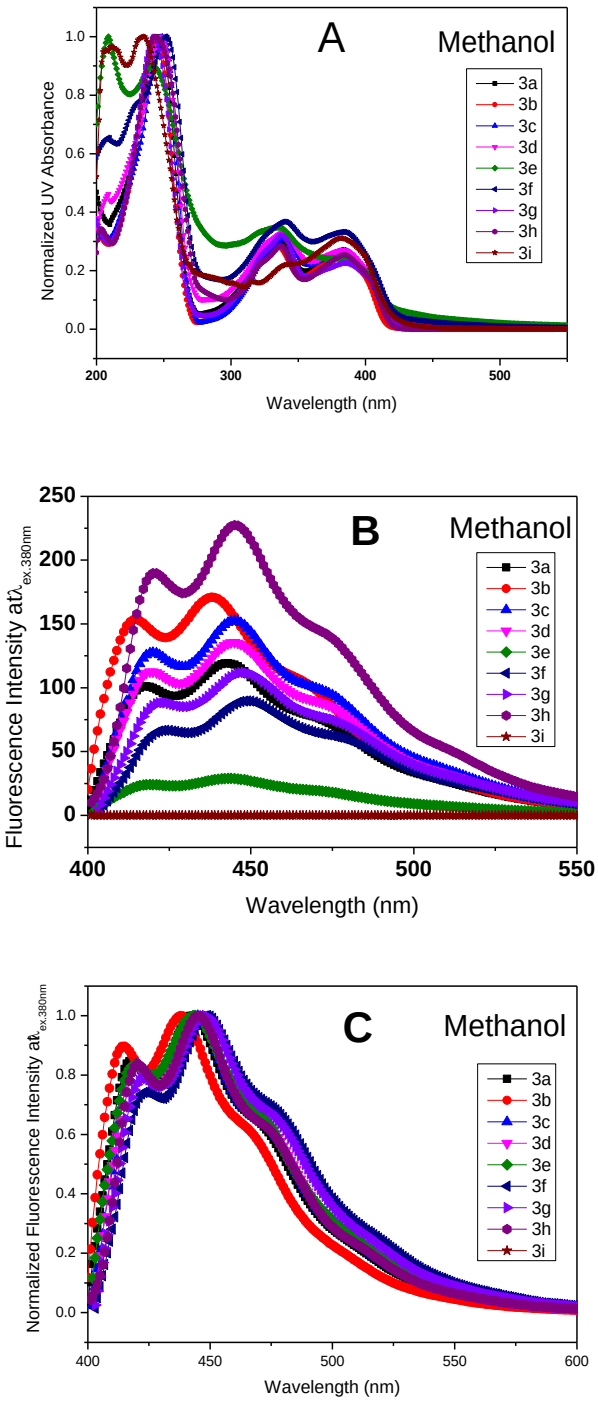

Figure A47: A) Normalized absorption B) Emission C) Normalized emission spectra of boron-aminotropone complexes (**3a-i**) in methanol at $50x10^{-5}$M concentration.

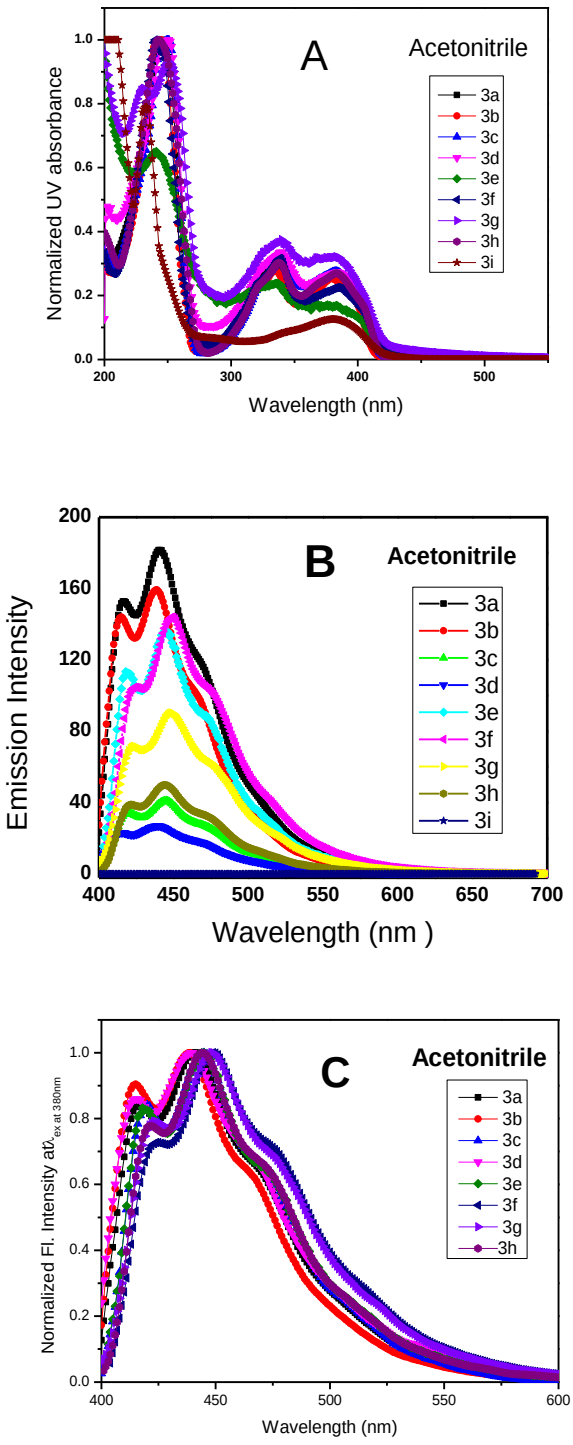

Figure A48: A) Normalized absorption B) Emission C) Normalized emission spectra of boron-aminotropone complexes (**3a-i**) in acetonitrile at $50x10^{-5}$M concentration.

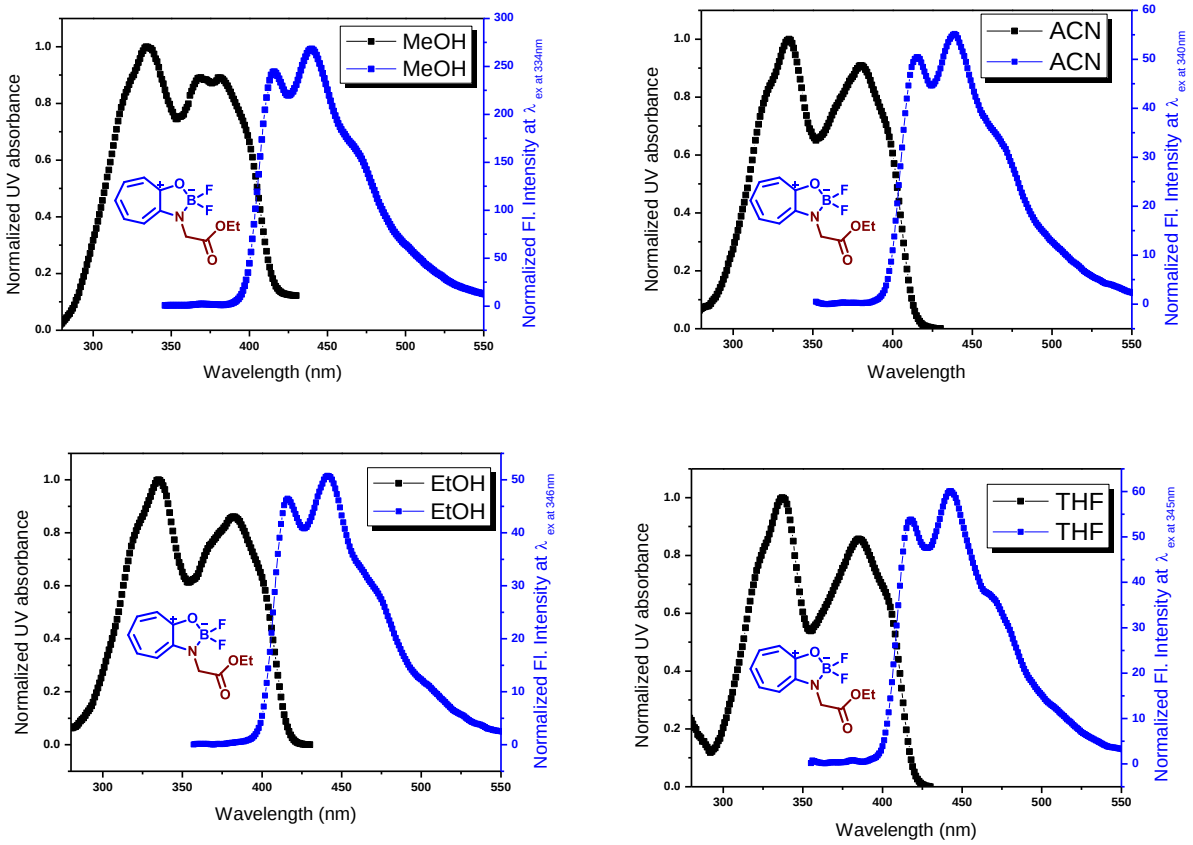

Figure A49: Normalized absorption-emission spectra of boron-aminotropone complexes (**3a)** in different solvent.

Table A4. Quantum yields of *boron-aminotropone* **(3a)**.

solvents	**λ_{abs} (nm)**	**Abs**	**λ_{em} (nm)**	**Stoke's Shift (nm)**	**OD/Abs (nm)**	**Φ_f**
Methanol	334, 380	0.06085	417,438	104	334	0.15
Acetonitrile	335,380	0.07202	415,441	106	340	0.14
Ethanol	335,382	0.08749	416,443	108	346	0.13
THF	337,385	0.08650	418,442	105	345	0.15

All measurements and quantum yields were determined for boron-complex **(4a)** by considering quinine sulfate in 0.1 M H_2SO_4 as standard reference.

Solid fluorescence of boron complexes

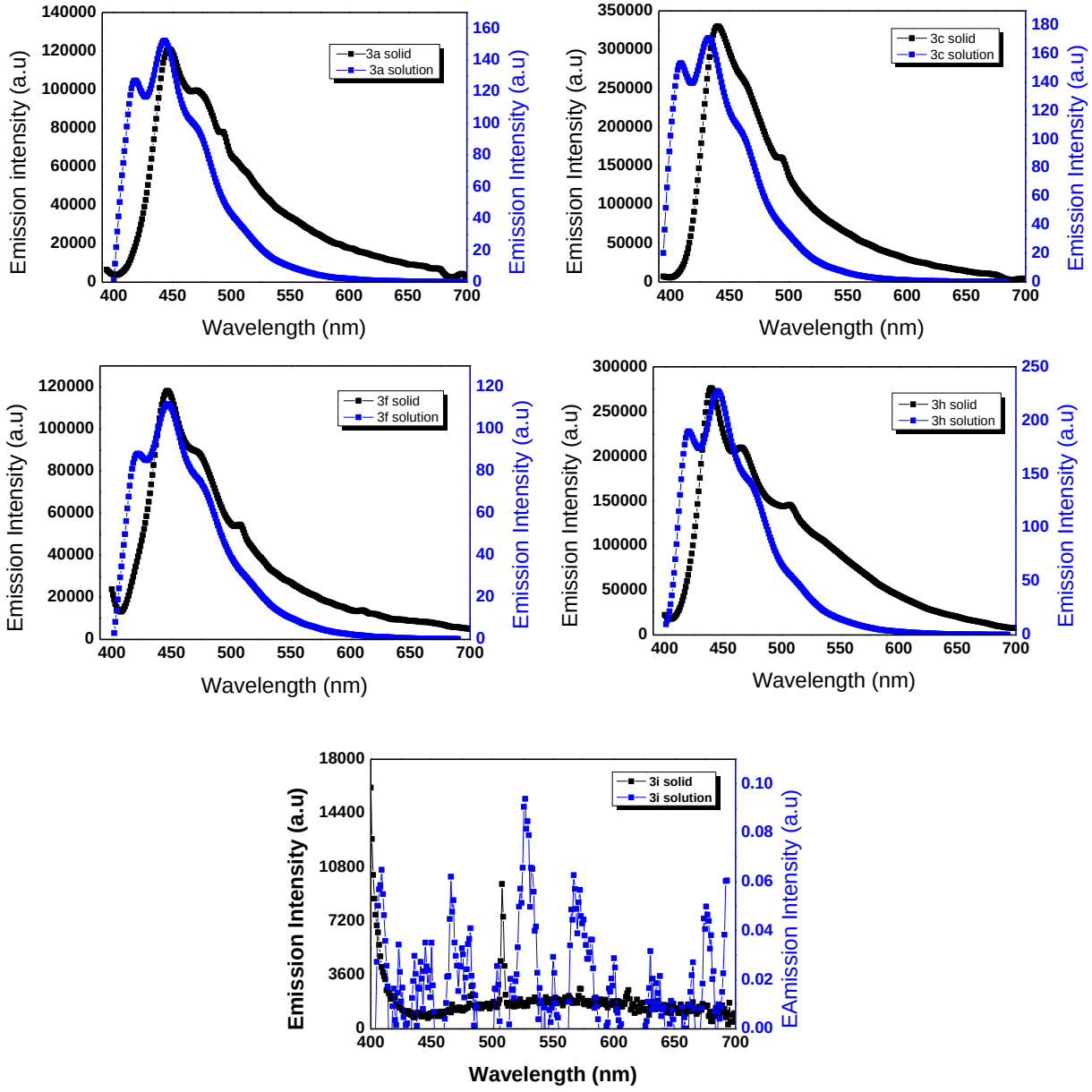

Figure A50: Comparision of Solid and Solution emission spectra of boron-aminotropone complexes (**3a, 3c, 3f, 3h, 3i)** in MeOH.

Table A5. Comparison of solid and solution fluorescence.

	MeOH			Solid	
Entry	λ_{abs} (nm)	λ_{em} (nm)	Φ_f (%)	λ_{em} (nm)	Φ_f (%)
1a	333, 381	417,438	15	447, 470, 492	4.94
1c	339,384	418,446	14	440, , 493	4.1
1f	339,384	423,448	9	447, 507,	0.73
1h	337,384	420,445	14	440, 465, 506	6.59
1i	381				0

Photostability of Boron complex **3a**:

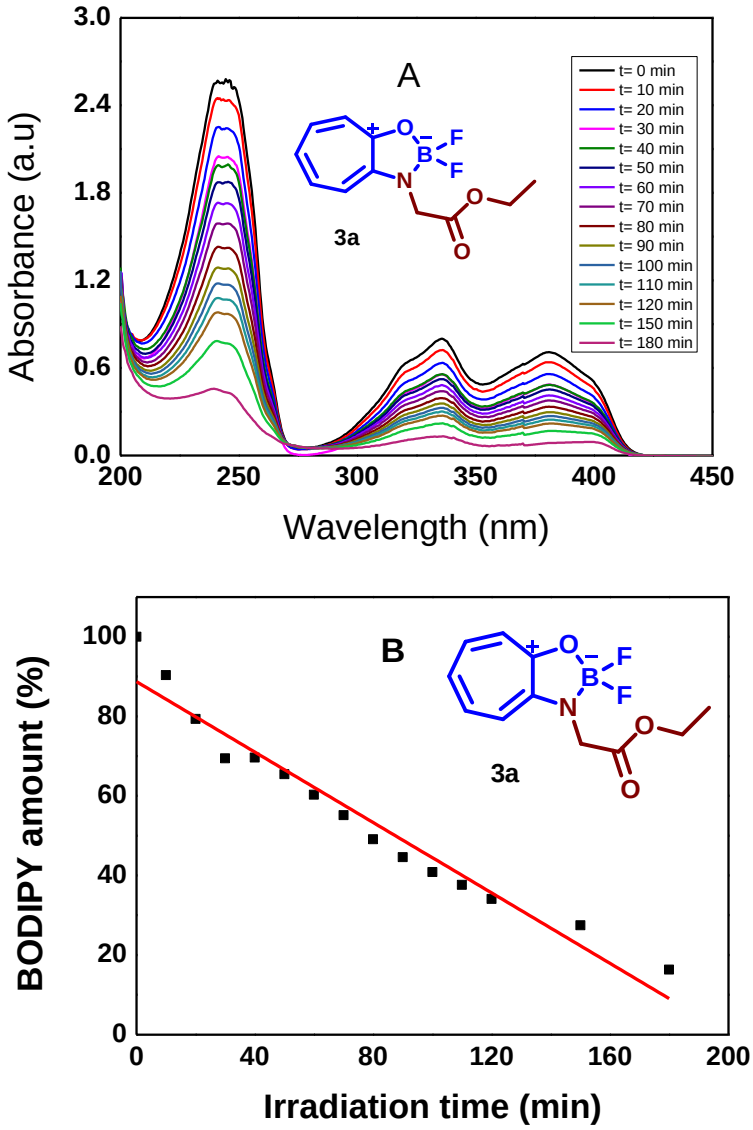

Figure A51: Photostability for boron-aminotropone complexes (**3a)** in MeOH A) Absorption spectra and B) Amount of decomposition with irradiation of UV ray at 265 nm.

Photostability of Boron complex **3c**:

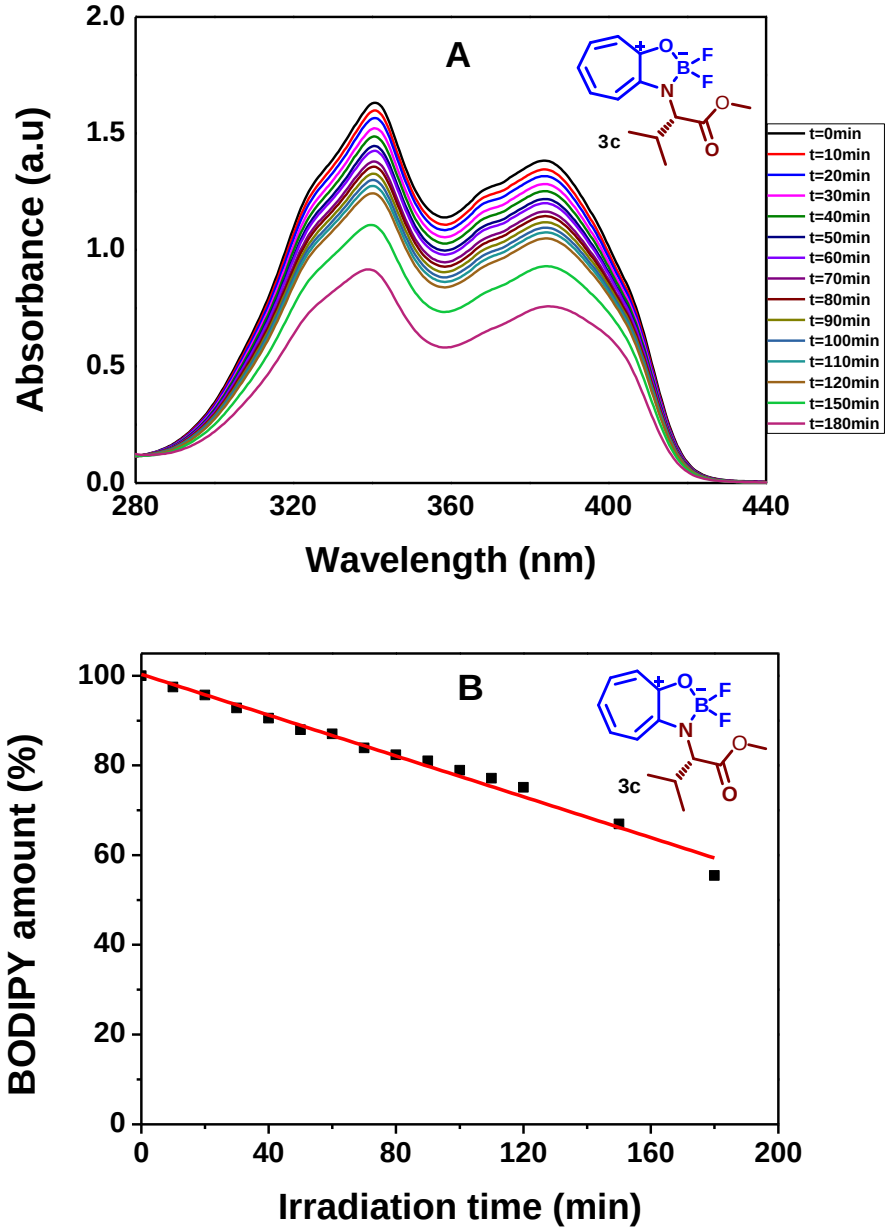

Figure A52: Photostability for boron-aminotropone complexes (**3c)** in MeOH A) Absorption spectra and B) Amount of decomposition with irradiation of UV ray at 265 nm.

Photostability of Boron complex **3h**:

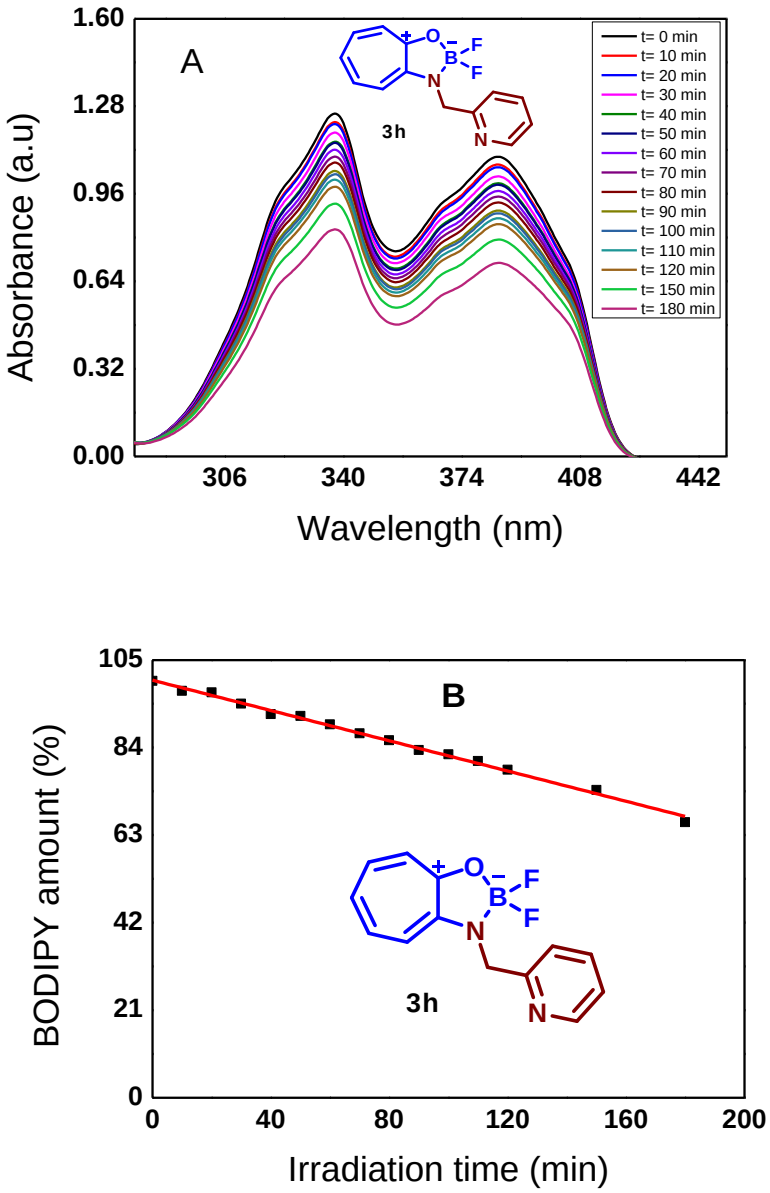

Figure A53: Photostability for boron-aminotropone complexes (**3c)** in MeOH A) Absorption spectra and B) Amount of decomposition with irradiation of UV ray at 265 nm.

12. Theoretical data

Cartesian coordinates of most sTable Atructure for compound (**3a, 3a-OH, 3b, 3h, 3i**) has been calculated using **Gaussian 09 software** and B3LYP/6-31+G* level of theory in vacuum. Since all molecules are in their minimum energy level, no imaginary frequency was observed.

Table-A6: Calculated HOMO and LUMO gap at B3LYP/6-31+G* level of theory in vacuum.

Analogue	Substituent	HOMO (eV)	LUMO (eV)	Δ (eV)	φ_f
3a	Gly	-6.5057	-2.5872	3.91844	0.15
3b	Ala	-6.4703	-2.5518	3.9184	0.13
3h	Picolylamine	-6.4831	-2.5837	3.8993	0.14
3i	AQ	-6.3048	-2.5061	3.7987	0
3j	Gly-OH	-6.6237	-2.6895	3.9342	0.02

13. Comparative N-B bond length studies

Table A7. Comparative bond length studies of compound 3a with reported BODIPY analogues.

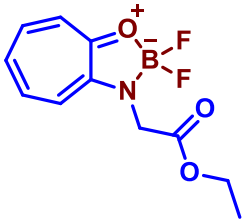

Synthesized compound

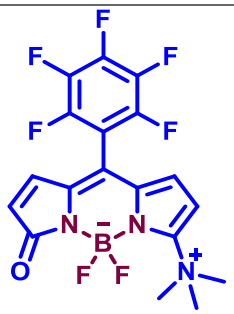

Model BODIPY

Chem. Commun., 2017, **53**, 1096-1099

3a	**Bond length(3a)**	**Model BODIPY**	**Bond length (M.B)**
N_1—B_1	1.5331Å	N_1—B_1	1.5265Å
O_1—B_1	1.4754Å	N_1—B_1	1.5797Å
B_1—F_1	1.3800Å	B_1—F_1	1.4046Å
B_1—F_2	1.3790Å	B_1—F_2	1.3808Å

14. Cyclic Voltammetry studies

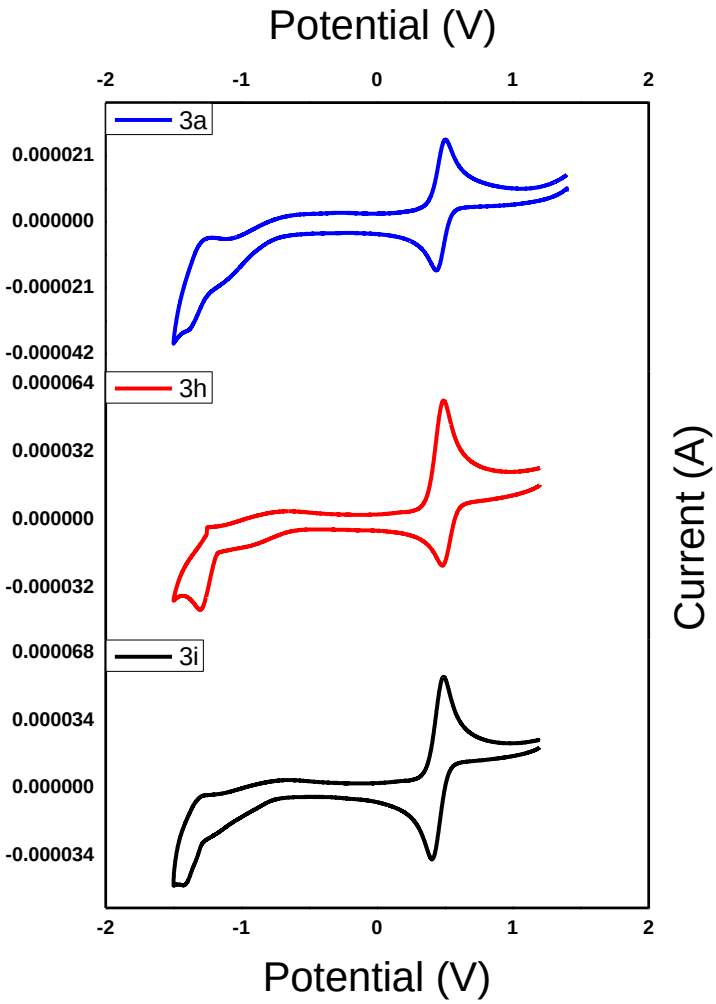

Figure A54. Cyclic voltammograms of 1mM (**3a**, **3h**, **3i**) measured in acetonitrile solution containing $TBPF_6$ as the supporting electrolyte and ferrocene as standard at room temperature. Glassy carbon electrode as a working electrode and scan rate 100mV.

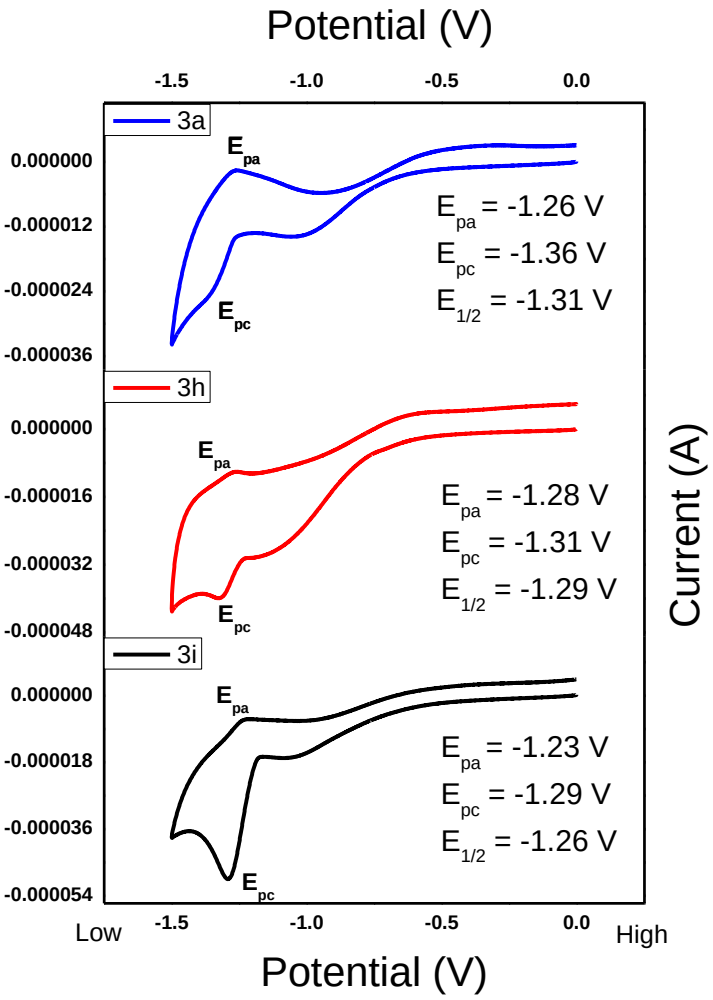

Figure A55. Cyclic voltammograms of 1mM (**3a**, **3h** & **3i**) measured in acetonitrile solution containing $TBPF_6$ as the supporting electrolyte at room temperature. Glassy carbon electrode as a working electrode and scan rate 100mV/s.

CHAPTER-3

PART-B

Title: **BODIPY Analogues: Synthesis and Photophysical Study of BODIPY Analogue from *Troponylalkyl Chain* via *N, O*-Chelation**

3B.1 Introduction

3B.2 Objective of our work

3B.3 Result and discussion

3B.4 Conclusion

3B.5 Experimental Section

3B.6 Reference and Notes

3B.7 Appendix

3B.1 Introduction

Boron-Dipyrromethene (BODIPY) derivatives are the most common organic fluorescent dyes for the development of fluophore materials, which are being used in the labeling of biomolecules and energy related cassette entities (Figure 1A).[1-4] Though these dyes have a few inadequacies such as solubility and functionality for practical applications. Thus various substituted dipyrromethene scaffolds are synthesized to improve the solubility, functionality, and dyes properties.[5] For examples, Alkenyl-BODIPY and C(sp^3) connected dimers are exhibited absorption peaks for near infrared (NIR) region.[6] Dipyridylmethene (DIPYR) dyes, Pyridine-based BODIPY analogues, exhibits a wide range of photophysical properties from non-emissive to green fluorescence with quantum yield 0.2-0.8.[7] BOIMPYs, benzimidazole containing analogue, have shown red-emissive fluorophores and considered as NIR-Dyes.[8, 9] Daniel Werz and Co-workers have synthesized prepared ethylene bridged oligo-BODIPYS which exhibit intramolecular J-aggregation and considered as super-fluorophores with quantum yield almost unity.[10] further the chlorinated dipyrromethene derivatives are desired for tuning their photophysical behaviors. Recently α-chlorinated-BODIPY analogues are prepared in one step directly from BODIPY using $CuCl_2$.[11] A new family of BODIPY dyes as *N*-BODIPYs (diaminoboron dipyrromethanes) are tested as smart photonic materials.[12] BOAHY, acyhydrozone containing BODIPY analogues has unique photophysical properties such as weak fluorescent in solution but emit brightly in powder form with maximum quantum yield 0.62. Most importantly, aggregation induced emission (AIE) and photoisomerization are noticed in BOAHY dye.[13] Moreover the application of BODIPY is expended to chemical transformation reaction. example Most recently, BODIPY analogue has been used as electron withdrawing group for the activation of double bonds in asymmetric catalysis reaction which opens the door for the future transformation.[14] These reports encourage us to design biocompatible small fluorescent molecules for target specific biomolecules for various

applications including imaging in different cellular environments. It would be interesting to prepare BODIPY analogues from naturally occurring small ligands. In nature, the non-benzenoid aromatic derivatives occur as natural products which are biologically active and possess valuable photophysical and chemical properties like benzenoid derivatives. For example, Tropone and tropolone are non-benzenoid aromatic compounds containing seven-membered conjugated ring system, which are constituents of many natural products such as Colchicine, Thujaplicine, Manicoline, Theaflavin, and Isoimerubrin.[15-17] Tropolone and related derivatives, also called as tropolonoids, show distinctive electronic structure and exhibit characteristic photophysical behavior as excitation and emission.[18-20] Importantly, Tropolone and 2-Aminotropones show metal chelating properties with transition metal ions (Cu^{2+}, Zn^{2+}, Ni^{2+}) and lanthanides ions.[21-26] The UV absorption spectra of Tropolone exhibit more than one peak at different wavelength (λ) 265nm and 375nm (~$\lambda_{abs,265nm}$ & $\lambda_{abs,375nm}$) because of multiple transitions such as π-π*, n-π* and intramolecular charge transfer.[27, 28] Importantly, Tropolone is weak fluorescent molecule because of n-π* and intramolecular charge transfer, and exhibit fluorescence peak at $\lambda_{em,\,410nm}$ 410nm at excitation $\lambda_{ex375nm}$. Owing to the intramolecular charge transfer, the fluorescence behavior of tropolone is sensitive to the polarity and pH conditions of environments. The fluorescence behavior of tropolone moiety has improved by changing the microenvironments in biological systems. For an example, Colchicine (tropolonoid natural product) has shown strong fluorescence characters after binding with the tubulin protein.[29, 30] Importantly, the substituted tropolone derivatives have shown strong fluorescence with enhanced quantum yields.[31, 32] Other derivatives of tropolone as 2-aminotropone and 2-aminotroponimines also form complex with metal ions.[33, 34] Further aminotropones are modified as aminotroponimine derivatives and employed in complexation with various metal ions for various reasons including use as catalyst for selective organic transformation reactions.[35-39] In early sixties, Boron-aminotroponimine complexes were prepared but their

photophysical properties were not explored (Figure. 3B. 1B).[40] Recently we have reported the syntheses of difluoroboron-aminotroponimine complexes (2-bora-l,3-diazaazulene derivatives) with various aryl/benzyme amine and demonstrated their fluorescence behavior with quantum yield upto ca.~0-15%.[41].[41] We have also prepared the carboxylate functionalized BODIPY analogues directly from aminotropone scaffold through *N*,*O*-chelation with Boron atom (**Figure. 3B. 1C**) In repertoire of troponoly BODIPY analogues, we rationally designed lipophilic aminotroponyl BODIPY analogues through *N*,*O*-chelation with Boron derivative (Figure 1D).

3B.2 Objective of our work

This Chapter describes the synthesis, structural analysis and photophysical properties of *N*-alkyl aminotroponyl difluoroboron complexes. contatining long chain hydrocarbon. To studies the UV/Fluorescence behaviors in the different organic solvents.

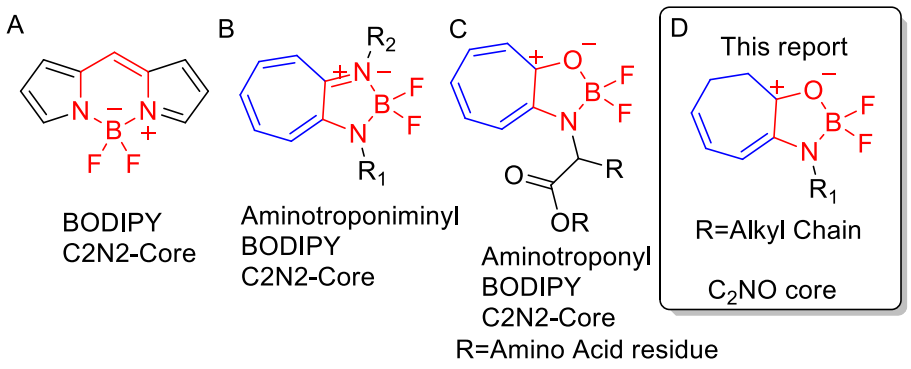

Figure. 3B. 1 Chemical structures of A) aminotroponimine ligand. B) boron dipyrromethene core. C) boronaminotroponimine core (this work).

3B.3 Result and discussion

we started the synthesis of boron-Aminotropone complexes from commercially available tropolone by adopting previous procedures (**scheme 3B.1**). In previously reported method, the tropolone was converted to 2-tosyltropone and treated with various alkyl chain amines to obtain N-substituted aminotropones. 2-aminotropone derivatives were treated with boronating reagent $BF_3.OEt_2$ under mild basic conditions. All the BF_2 complexes were purified by silica gel column chromatography by using Ethylacetate:Hexane (10:90). All the desire compounds was obtained good yields (80%). All the synthesized complexes are highly stable towards moister and air. All the N-substituted aminotropone and BF2 complexes were characterized by NMR (^{1}H, ^{13}C, ^{11}B, ^{19}F-NMR) and mass spectrometry (ESI-MS, HRMS) provided in the appendix. we crystalized the boron complexes in a DCM: MeOH solvent system. As a result, we obtained crystals of the following four boron–aminotropone complexes in the solid state**3a, 3b,3c and 3g**. Their single crystals were diffracted by single-crystal diffractometer, then their data were analysed and confirmed their chemical structures. Their solved X-ray data were deposited at the Cambridge Crystallographic Data Centre (CCDC).

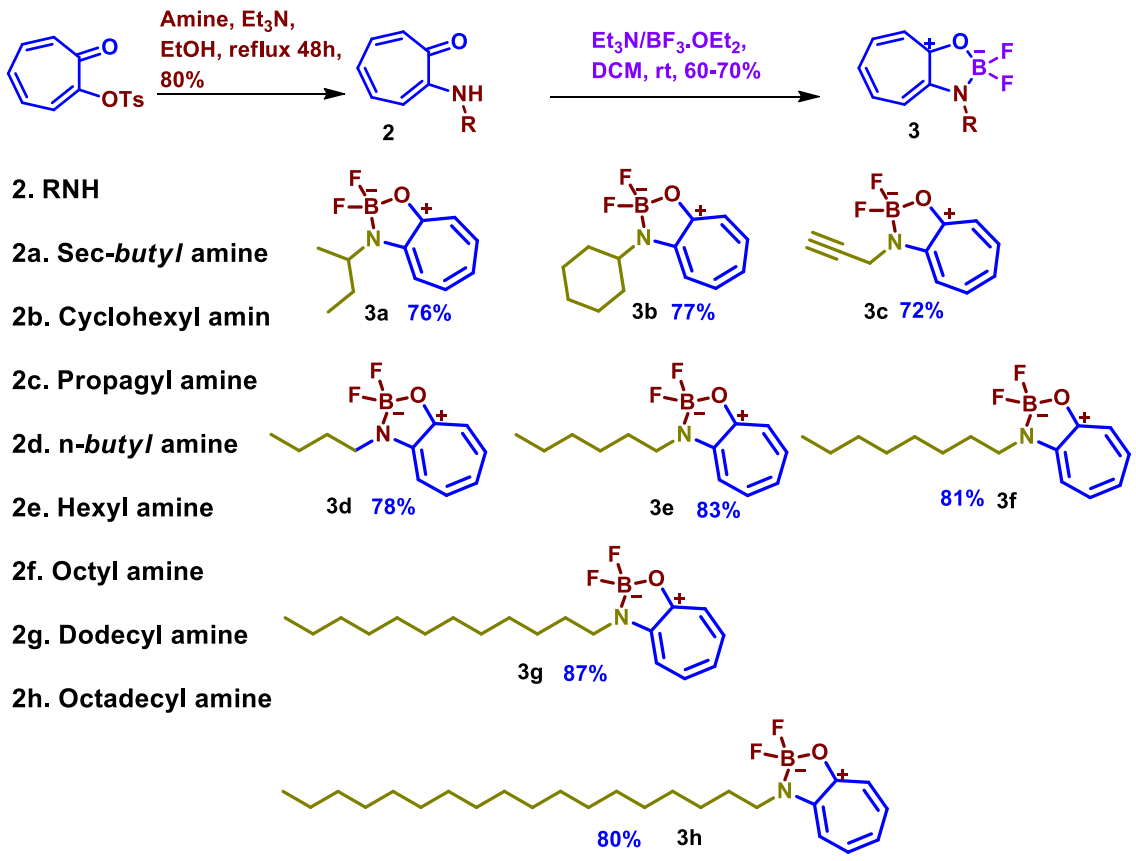

Scheme 3B. 1. Synthesis of boron-aminotroponimine complexes

Finally, the chemical structure of four boron complexes' **3a, 3b,3c, and 3g** was established by single X-ray crystal analysis, and its ORTEP diagram is showed (**Figure 3B.2)** the crystal analytical data of as cif file is despised in the Cambridge crystallography data center (CCDC) with CCDC number. the boron complex of all BF_2 complex exists in distorted-tetrahedral geometry. The selected bond length and bond angles are given in (**Table 3B.1**.) The crystal of all boron complexes was grown in a mixture solvent of DCM and MeOH.

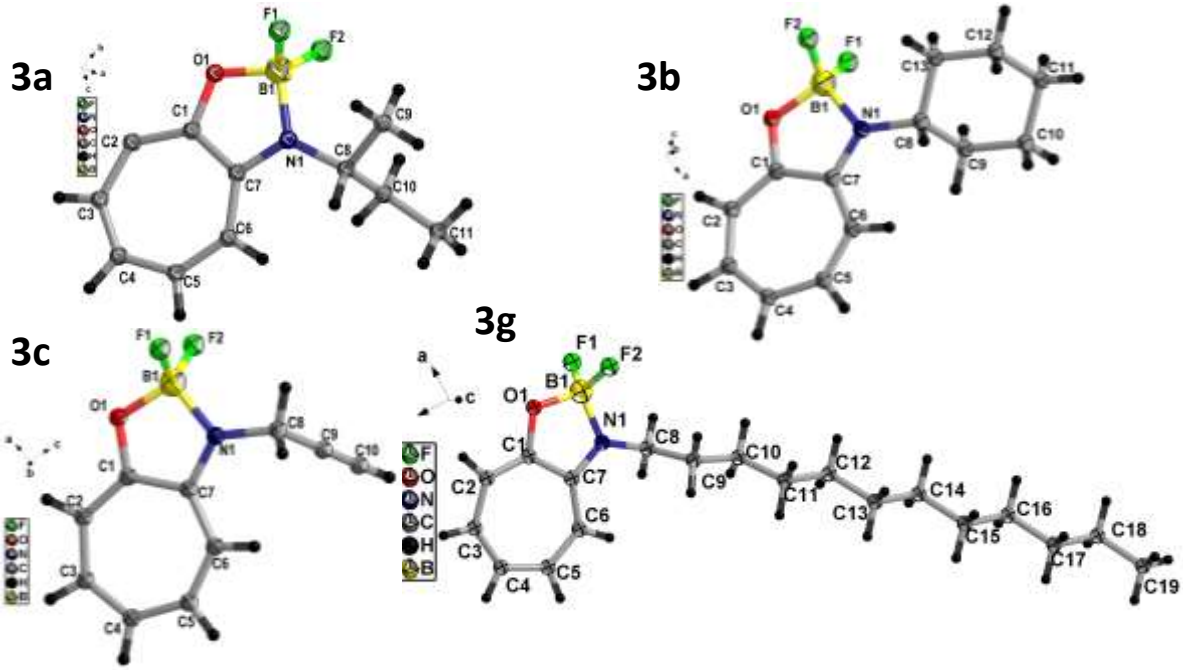

Figure. 3B. 2 ORTEP diagrams of boron complex (3a, 3b, 3c, and 3g) with 50% probability of ellipsoids.

Table. 3B. 1 Selected bond lengths and bond angles of Boron complexes **3a, 3b,3c and 3g** in solid state.

Selected bond lengths	Selected bond angles	Selected bond angles
3a. C1-C7 = 1.446 Å	O1-B1-N1 = 99.31°	B1-O1-C1 = 99.31°
C1-O1 = 1.313 Å	F1-B1-O1 = 109.92°	B1-N1-C7 = 110.68°
C7-N1 = 1.329 Å	F2-B1-N1 = 112.34°	O1-C1-C7 = 110.55°
O1-B1 = 1.487 Å	F1-B1-N1 = 113.67°	N1-C7-C1 = 107.79°
N1-B1 = 1.548 Å	F2-B1-O1 = 111.02°	F1-B1-F2 = 110.13°

Photophysical Studies. We recorded the absorption and emission spectra of newly synthesized lipophilic troponyl BODIPY analogues **3a-3h** in solvent methanol (MeOH) and acetonitrile (ACN). Their spectra are depicted in Figure 2. Their absorption spectra exhibit three peaks at wavelength (λ) ~245nm, ~340nm and ~390nm in both solvents, mainly due to the. π-π*, n-π* and charge transfer transition in aminotropone-difluoroboron residue. We also determined their extinction coefficients (ε) at λ_{390nm} in MeOH (Table 1, Col 5). The octadecyl aminotroponyl difluoroboron complex (**3h**) has lower ε value (~$5.8*10^3$ $M^{-1}cm^{-1}$) as compare to other analogues (~$9.0*10^3$ $M^{-1}cm^{-1}$). Their emission spectra exibit a intense peak at wavelength 455nm ($\lambda_{em,455nm}$) at extitaion wavelength 340nm ($\lambda_{ex,340nm}$) with Stock's shift ca. ~110nm in MeOH. Thus these analogues are fluorescent as like our previously reported aminoacid containing aminotroponyl difluoroboron complexes.[42] We measured their relative quantum yields in MeOH at temperature 20°C in comparesion to reference standard 0.1M quinine sulfate in H_2SO_4. Their quantum values are provided in **Table 3B.2** (Col 7). Importnatly, their quantum (**3a-3h**) yields are ca. 9-13%, varies with *N*-alkyl substituents, in MeOH. The bar diagram is shown in the following order of **3c>3a~3e~3g~3h>3d~3f>3b.** However, the quantum yield of alkyne substituted analogue (**3c**) has significantly high by ~3% as compare to other analogues (**3a/3b/3d-3h**) in MeOH. We also recorded their (**3a-3h**) quantum yield in the different solvents. of DCM, Cyclohexane, Chloroform and determined their photophysical parameters (Table S4). The quantum yield of **3h** slightly increased compared to solvents mentioned above as in MeOH .

Solid-state fluorescence

The fluorescence character of BODIPY analogues are sensitive to polarity of environment in solution and closeness of molecule in solid-state. The fluorescence behaviour of a lead analogue (**3f, 3g, 3h**) was examined using solid probe. The emission spectra of solid analogue

3f, 3g, 3h is provided in Suppl. Inform. The complex **3f, 3g, 3h** exhibits emission peak at wavelength 430 nm

Table. 3B. 2 Photophysical parameters of Boron-aminotropone complexes.

Entry	λ_{abs} [a] (nm)	Abs [a]	λ_{em} [a,b] (nm)	ε_{max} [a] ($M^{-1}cm^{-1}$)	Stoke's Shift (nm)	OD/Abs (nm)	Φ_f [b]
3a	342, 382	0.8620, 0.5615	431,455	8620	113	341	0.10
3b	343,382	0.8592, 0.5682	432,458	8592	115	350	0.08
3c	334,382	0.3220, 0.2968	418,440	3220	106	338	0.13
3d	341,388	0.9332, 0.6144	430,455	9332	114	345	0.09
3e	342,388	0.9931, 0.6558	430,455	9331	113	343	0.10
3f	342,388	0.9168, 0.6070	430,455	9168	113	348	0.09
3g	342,388	0.9520, 0.6321	430,455	9520	113	348	0.10
3h	342,380	0.5775, 0.3775	429,455	5775	113	351	0.10

a. All measurements were carried out in methanol with 10^{-4} M conc., b. λ_{ex} = 340 nm. Molar extinction coefficient (ε)

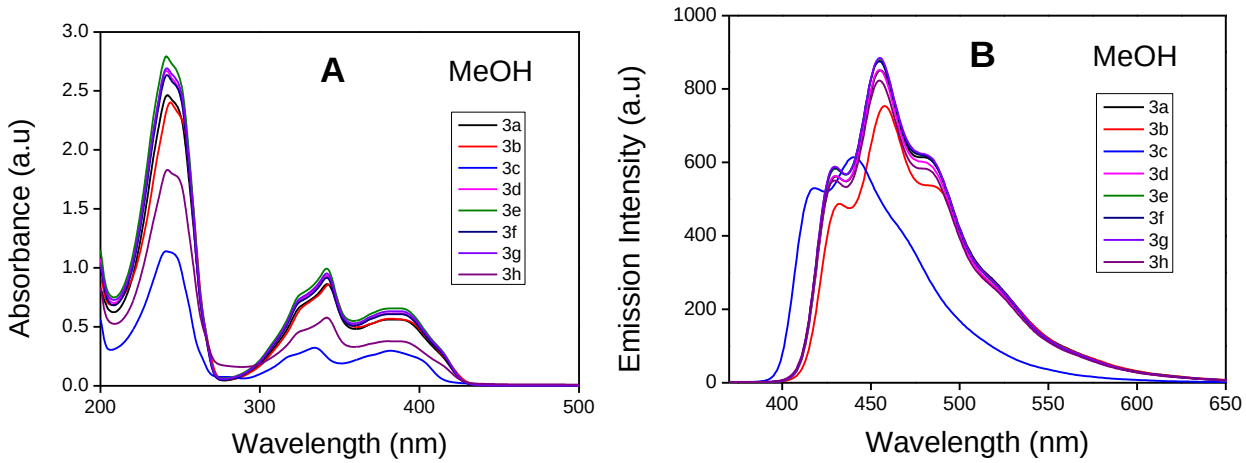

Figure. 3B. 3 (A) Absorption and (B) Emission spectra of boron-aminotropone complexes (**3a-h**) in methanol at $5x10^{-4}$M concentration.

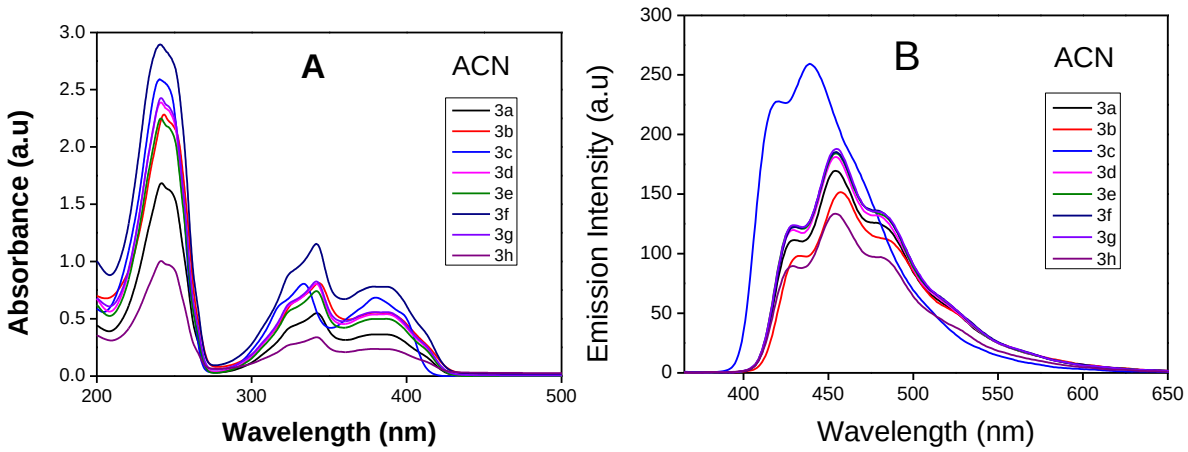

Figure. 3B. 4 (A) Absorption and (B) Emission spectra of boron-aminotropone complexes (**3a-h**) in Acetonitrile at $5x10^{-4}$M concentration.

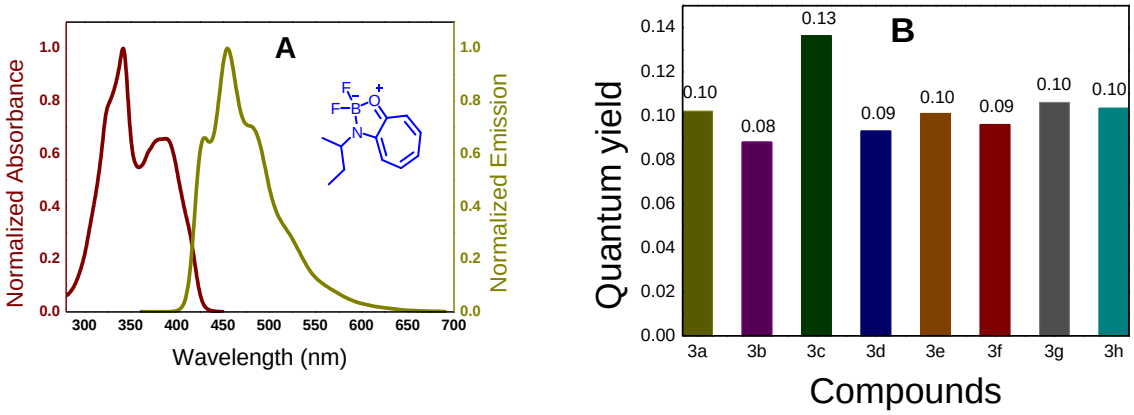

Figure. 3B. 5 (A) Absorption and Emission spectra of boron-aminotropone complexes (**3a**) in methanol at concentration ($5x10^{-4}$M). (B) Quantum yield bar diagram of boron-aminotropone complexes (**3a-3h**) in methanol.

The single cystal structure of few alkylated BODIPY analogues reveal the formation of self-assembly structure by intermolecular π-π interactions between troponyl residue and hydrophobic interactions between long chain residue. Thus we examined the morphology of long chain hydrocarbon containing BODIPY analogues (**3b/3f/3g/3h**) field emission scanning The FE-SEM image of analogue **3g/3h** shows the self-assembly nano-structure electron microscopy (FE-SEM). Boron complexes containing alkyl chain to access the information of structural features. The morphology of self-assembling was studied by field emission scanning electron microscopy (FE-SEM). Examining the SEM images reveals the formation of nanostructures varieties for self-assembly aggregates of **3b, 3f, 3g** and **3h**.

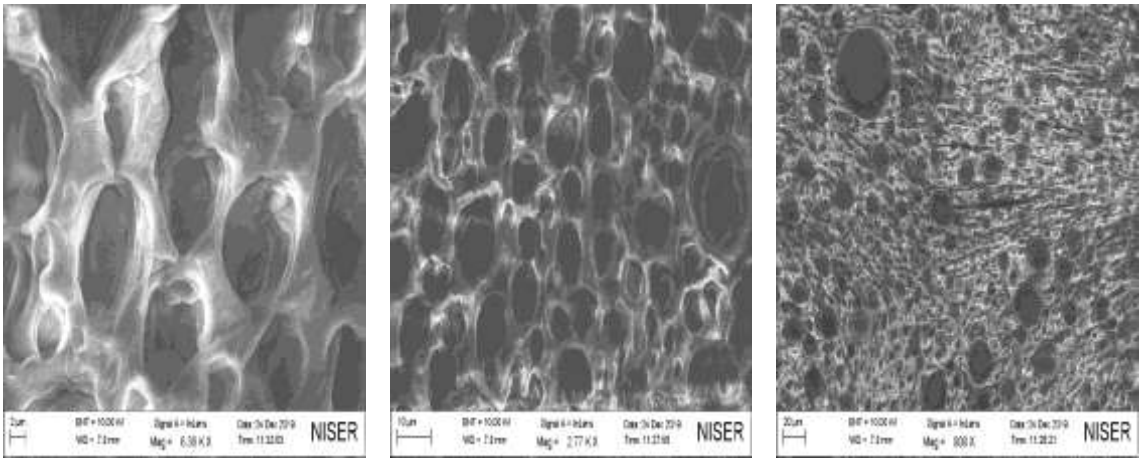

Figure. 3B. 6 FE-SEM images of **3f** 2µm, 10µm, 20µm

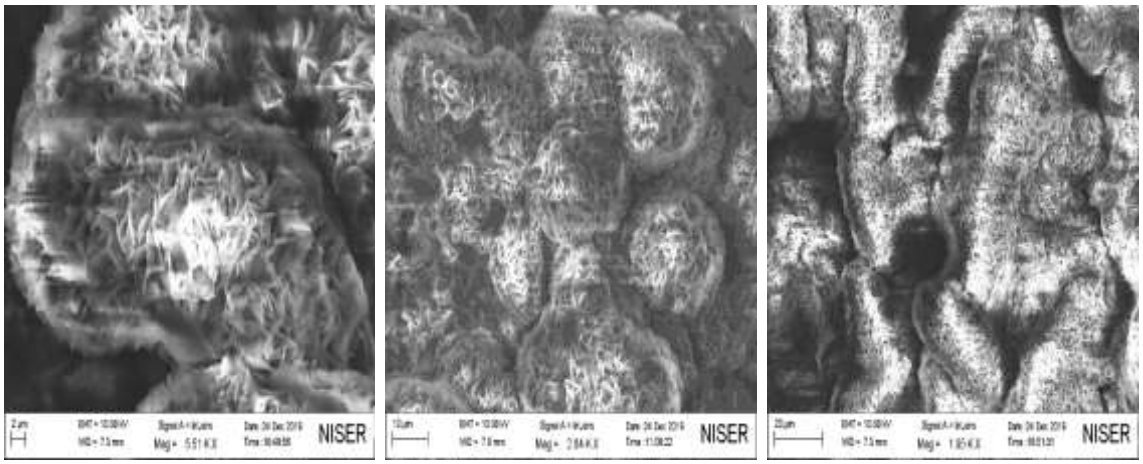

Figure. 3B. 7 FE-SEM images of **3g** 2µm, 10µm, 20µm

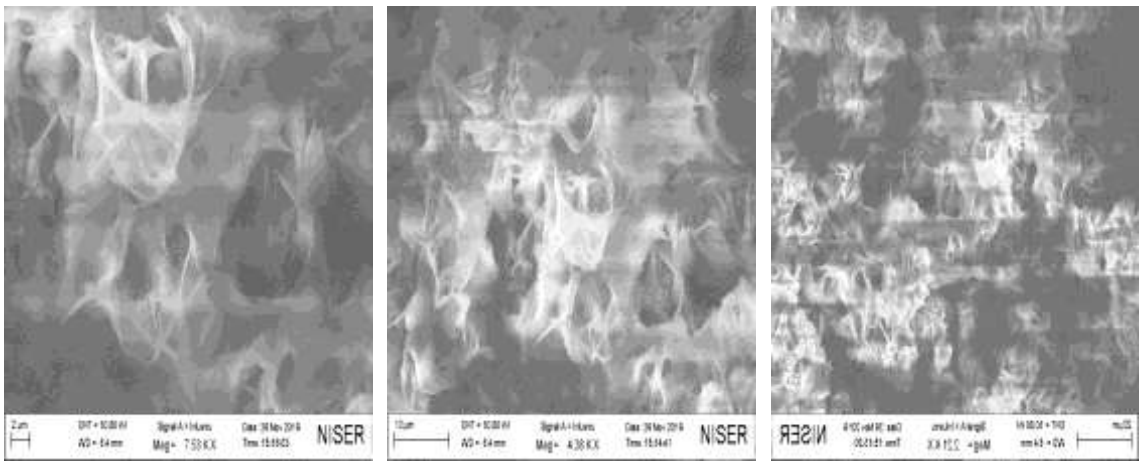

Figure. 3B. 8 FE-SEM images of **3g** 2µm, 10µm, 20µm

Since these BODIPY analogues are also fluorescent in nature. Their SEM-Morphologies confirm a uniqe supramolecular self-assembly structures. Thus we planed to visullize the morphologies of representative compounds **3f/3g** in oganic solvent DCM by the confocal fluorescence smicroscope. Their confocal images are provided in **Figure. 3B. 9.** The confocal image of compound **3f** at diferent scales also shows the formation of supramolecular self-assembled structures as ring type structures (Figure 3B.8a). The confocal image of compound **3g** shows the self assembled structure as the irregular polygonal type of structure (Figure 3B.8b). Both compounds (**3g/3f**) have long chain hydrocarbons (C8/12) which have specifically oriented in DCM because of lipophillic intractions and lead to the supramolecular structures. Hence these BODIPY analogues could be considered potential fluorescent bipolar nano materials.

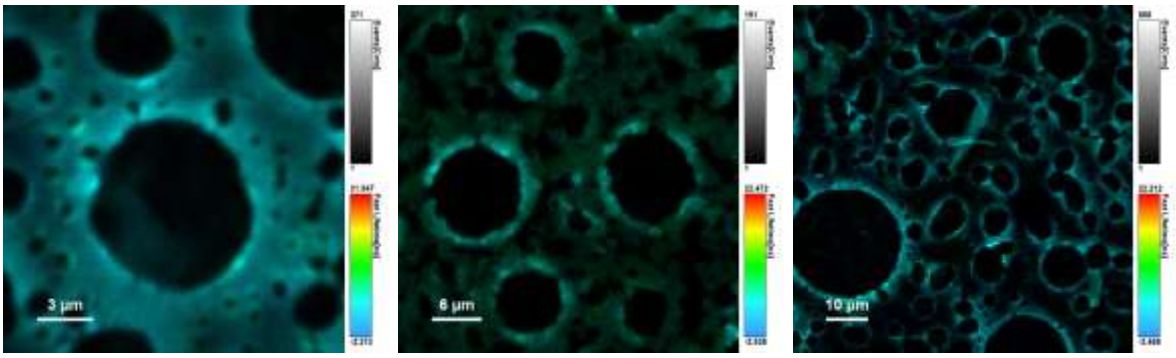

Figure. 3B. 9 (a) Confocal images of **3f** 3µm, 6µm, 10µm

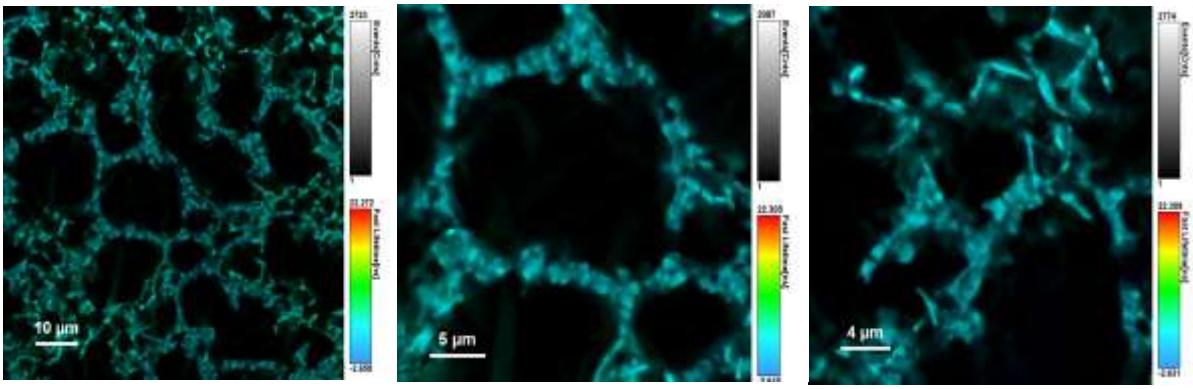

Figure. 3B. 9 (b) Confocal images of **3g** 4µm, 5µm, 10µm

3B.4 Conclusion

In conclusion, we have synthesized a library of amphiphilic Boronaminotopono complexes containing tropolonoid aromatic systems and explored their photophysical properties UV-Vis and fluorescence studies. The fluorescence quantum yield of BODIPY complexes reaches from 10-13% in MeOH and acetonitrile. Different solvent systems demonstrated photophysical properties. We also explored the chemical structure of the Alky chain containing the Boronaminotropone complex (**3a, 3b,3c, and 3g)** by crystal structures analysis. Further, the crystal packing diagram of supramolecular self-assembly revealed the presence of intermolecular hydrogen bonding between C-H....F. The Boronaminotropone complex's formation morphology of self-assembly networking confirmed SEM images. Moreover, all the BODIPY complexes indicate their potential future drug delivery.

3B.5 Experimental Section

All required materials and solvents were purchased from commercial suppliers and used without any further purification unless noted. Anhydrous dichloromethane was freshly prepared by distilling over Calcium hydride. Reactions were monitored by thin layer chromatography, visualized by UV and Ninhydrin. Column chromatography was performed in 100-200 mesh silica. Mass spectra were obtained from Bruker micrOTOF-Q II Spectrometer and the samples were prepared in methanol and injected in methanol and water mixture. NMR spectra were recorded on Bruker AV- 400 at room temperature (^{1}H: 400 MHz, ^{13}C: 100.6 MHz, ^{11}B:128 MHz, ^{19}F:377 MHz). ^{1}H, ^{13}C, ^{11}B and ^{19}F NMR chemical shifts were recorded in ppm, downfield from tetramethyl silane. Splitting patterns are abbreviated as: s, Singlet; d, doublet; dd, doublet of doublet; t, triplet; q, quartet; m, multiplet. The crystal data of all boron complex were collected on a Rigaku Oxford diffractometer at 293 K respectively. Absorption spectra were obtained using Jasco V-730 spectrometer. Fluorescence spectra were obtained from

Perkin-Elmer LS-55 using Xenon lamp. All spectroscopic measurements were carried out with spectroscopic grade, non-degassed solvents and at 20°C. Relative fluorescence quantum yields were determined by comparing with quinine sulfate quantum yield in 0.1 M H_2SO_4 (0.54). The obtained values were substituted in the equation given below.

$$\phi_x = \phi_r \mathrm{x} \frac{F_x}{F_r} \mathrm{x} \frac{1-10^{-A_r}}{1-10^{A_x}} \mathrm{x} \frac{\eta_x^2}{\eta_x^2}$$

Solid emission of boron complex **3f**, **3g** and **3h** (excited at 340nm and 380 nm), are measured by Edinburgh instrument FLS 920. HRMS's were analysed with Agilent Q-TOF 6500.

General Procedure for Synthesis of Aminotropone **2**. All aminotropones were synthesized by following the reported procedure. 2-tosyloxytropone and amines (1.2 *equiv*.) were dissolved in ethanol, to this Et3N (3.0 *equiv.*) was added. The reaction mixture was allowed to reflux for 24-36 h. The completion of the reaction was monitored by TLC. All volatiles were evaporated under reduced pressure after reaction completion. To the crude product, 1.0 N HCl was added and extracted with dichloromethane (thrice), the combined organic layers were dried over Na_2SO_4 and evaporated under reduced pressure. The obtained crude product was purified by silica gel column chromatography by using ethyl acetate and hexane mixture as mobile phase.

2-(sec-butylamino)cyclohepta-2,4,6-trienone (**2a**):

The pure product was obtained as yellowish solid (552 mg, 86%). ^{1}H NMR (400 MHz, $CDCl_3$) δ 7.27 – 7.12 (m, *J* = 28.0, 11.7 Hz, 3H), 6.65 (t, *J* = 9.4 Hz, 1H), 6.56 (d, *J* = 10.5 Hz, 1H), 3.66 – 3.60 (m, 1H), 2.00 (s, 1H), 1.75 – 1.60 (m, 2H), 1.28 (d, *J* = 6.4 Hz, 3H), 0.98 (t, *J* = 7.4 Hz, 3H). ^{13}C{H} NMR (101 MHz, $CDCl_3$) δ 176.51, 155.03, 137.16, 136.29, 128.03, 121.77,

108.82, 49.45, 29.10, 19.42, 10.40. HRMS (ESI-TOF) m/z: [M+Na] cal for $C_{11}H_{15}NO$ 200.1046, found 200.1046.

2-(cyclohexylamino)cyclohepta-2,4,6-trienone (**2b**):

The pure product was obtained as yellowish solid (352 mg, 95%). ^{1}H NMR (400 MHz, $CDCl_3$) δ 7.27 – 7.12 (m, 3H), 6.67 – 6.58 (m, 2H), 3.50 (t, *J*= 4 Hz, 1H), 2.05 (d, *J* = 12 Hz, 2H), 1.84 – 1.67 (m, 4H), 1.44 – 1.31 (m, 4H). ^{13}C{H} NMR (101 MHz, CDCl3) δ 176.53, 163.43, 154.63, 137.15, 136.28, 128.06, 121.78, 108.93, 51.06, 32.07, 25.57, 24.66. HRMS (ESI-TOF) m/z: [M+nH] cal for $C_{13}H_{17}NO$ 204.1383, found 204.1393.

2-(prop-2-yn-1-ylamino)cyclohepta-2,4,6-trienone (**2c**):

The pure product was obtained as yellowish solid (850 mg, 74%). ^{1}H NMR (400 MHz, $CDCl_3$) δ 7.33 – 7.27 (m, 2H), 7.21 (t, *J* = 12 Hz, 1H), 6.75 (t, *J* = 8 Hz, 1H), 6.62 (d, *J* = 8 Hz, 1H), 4.14 (dd, *J* = 5.9, 2.4 Hz, 2H), 2.30 (t, *J* = 2.4 Hz, 1H), 1.67 (s, 1H). ^{13}C{H} NMR (101 MHz, $CDCl_3$) δ 177.19, 154.49, 137.49, 136.05, 130.07, 123.40, 109.22, 77.87, 72.51, 32.50. HRMS (ESI-TOF) m/z: [M+nH] cal for $C_{10}H_9NO$ 160.0757, found 160.0759.

2-(butylamino)cyclohepta-2,4,6-trienone (**2d**):

The pure product was obtained as yellowish solid (327 mg, 94%). ^{1}H NMR (400 MHz, $CDCl_3$) δ 7.28 – 7.21 (m, 3H), 7.14 (d, *J* = 12 Hz, 1H), 6.66 (t, *J* = 12 Hz, 1H), 6.54 (d, *J* = 12 Hz, 1H), 3.33 – 3.28 (m, 2H), 1.75 – 1.70 (m, 2H), 1.47 (dd, *J* = 16, 8 Hz, 2H), 0.98 (t, *J* = 8 Hz, 3H). ^{13}C{H} NMR (101 MHz, $CDCl_3$) δ 176.58, 155.71, 137.27, 136.34, 128.28, 121.97, 108.65, 42.59, 30.47, 20.31, 13.75. HRMS (ESI-TOF) m/z: [M+nH] cal for $C_{11}H_{15}NO$ 178.1226, found 178.1237.

2-(hexylamino)cyclohepta-2,4,6-trienone (**2e**):

The pure product was obtained as yellowish solid (337 mg, 90%). ^{1}H NMR (400 MHz, $CDCl_3$) δ 7.24 (dd, *J* = 20.3, 10.4 Hz, 3H), 7.14 (d, *J* = 8 Hz, 1H), 6.66 (t, *J* = 8 Hz, 1H), 6.52 (d, *J* = 12 Hz, 1H), 3.29 (dd, *J* = 12, 6.5 Hz, 2H), 1.77 – 1.70 (m, 2H), 1.45 – 1.42 (m, 2H), 1.33 (d, *J* = 2.9 Hz, 4H), 0.90 (t, *J* = 5.9 Hz, 3H). ^{13}C{H} NMR (101 MHz, $CDCl_3$) δ 176.57, 155.68, 137.22, 136.31, 128.27, 121.93, 108.61, 42.89, 31.46, 28.41, 26.81, 22.53, 14.00. HRMS (ESI-TOF) m/z: [M+nH] cal for $C_{13}H_{19}NO$ 206.1539, found 206.1548.

2-(octylamino)cyclohepta-2,4,6-trienone (**2f**):

The pure product was obtained as yellowish solid (834mg, 98%).^{1}H NMR (400 MHz, $CDCl_3$) δ 7.09 (s, 1H), 6.97 – 6.84 (m, 3H), 6.37 – 6.29 (m, 1H), 6.23 – 6.18 (m, 1H), 2.98 – 2.91 (m, 2H), 1.43 – 1.36 (m, 2H), 1.11 – 1.00 (m, 10H), 0.63-0.59 (m, 3H). ^{13}C{H} NMR (101 MHz, $CDCl_3$) δ 176.19, 155.37, 136.77, 136.04, 127.88, 121.52, 108.24, 42.61, 31.57, 29.07, 28.98, 28.21, 26.94, 22.44, 13.89. HRMS (ESI-TOF) m/z: [M+nH] cal for $C_{16}H_{23}NO$ 234.1852, found 234.1843.

2-(dodecylamino)cyclohepta-2,4,6-trienone (**2g**):

The pure product was obtained as yellowish solid (448 mg, 85%). ^{1}H NMR (400 MHz, $CDCl_3$) δ 7.28 – 7.12 (m, 4H), 6.64 (t, *J* = 8 Hz, 1H), 6.51 (d, *J* = 12 Hz, 1H), 3.28 (d, *J* = 8 Hz, 2H), 1.76 – 1.69 (m, 2H), 1.42 – 1.26 (m, 20H), 0.87 (t, *J* = 8 Hz, 3H). ^{13}C{H} NMR (101 MHz, $CDCl_3$) δ 176.56, 155.67, 137.20, 136.29, 128.26, 121.90, 108.58, 42.89, 31.90, 29.62, 29.61, 29.56, 29.50, 29.33, 29.29, 28.45, 27.14, 22.68, 14.11. HRMS (ESI-TOF) m/z: [M+nH] cal for $C_{19}H_{31}NO$ 290.2478, found 290.2493.

2-(octadecylamino)cyclohepta-2,4,6-trienone (**2h**):

The pure product was obtained as yellowish solid (649 mg, 96%). ^{1}H NMR (400 MHz, $CDCl_3$) δ 7.28 – 7.20 (m, 3H), 7.14 (d, *J* = 12 Hz, 1H), 6.66 (t, *J* = 8 Hz, 1H), 6.53 (d, *J* = 12 Hz, 1H), 3.32 – 3.27 (m, 2H), 1.76 – 1.68 (m, 3H), 1.45 – 1.42 (m, 2H), 1.40 – 1.28 (m, 29H), 0.88 (t, *J*

= 6.7 Hz, 3H). $^{13}C\{H\}$ NMR (101 MHz, $CDCl_3$) δ 176.61, 155.70, 137.25, 136.30, 128.31, 121.93, 108.59, 42.92, 31.93, 29.71, 29.67, 29.58, 29.51, 29.37, 29.30, 28.47, 27.16, 22.70, 14.12. HRMS (ESI-TOF) m/z: [M+nH] cal for $C_{25}H_{43}NO$ 374.3417, found 374.3436.

*General Procedure for Synthesis of Boron-aminotropone (**3**).* Aminotropone **(2a)** (1 *equiv*.) was dissolved in anhydrous dichloromethane and Et_3N (15 *equiv*.) was added. For further reaction $BF_3.OEt_2$ (15 *equiv*.) was added to the resultant reaction mixture and stirred in room temperature. The completion of reaction was monitored by TLC, water was added to quench unreacted $BF_3.OEt_2$ and extracted with dichloromethane (thrice). The combined organic layer was dried over Na_2SO_4 and concentrated under reduced pressure. The crude product was purified through silica gel column chromatography by using 100% DCM as the mobile phase. Boron complex **3a** was obtained in 90% yield. Remaining all boron complexes were synthesized by following this general procedure.

NMR data of Boron-aminotropones

3-(sec-butyl)-2,2-difluoro-2,3-dihydrocyclohepta[d][1,3,2]oxazaborol-1-ium-2-uide (**3a**)

The pure product was obtained as reddish brown solid (290 mg, 76%).^{1}H NMR (400 MHz, $CDCl_3$) δ 7.63 – 7.58 (m, 1H), 7.46 (t, *J* = 12 Hz, 1H), 7.25 (t, *J* = 8 Hz, 1H), 7.15 (d, *J* = 12 Hz, 1H), 7.06 (t, *J* = 8 Hz, 1H), 3.83 (s, 1H), 1.98-1.91 (m, 1H), 1.81 – 1.74 (m, 1H), 1.44 (d, *J* = 4 Hz, 3H), 0.98 (t, *J* = 8 Hz, 3H). $^{13}C\{H\}$ NMR (101 MHz, $CDCl_3$) δ 167.33, 159.59, 141.10, 139.42, 127.23, 118.54, 117.92, 53.08, 28.02, 18.16, 11.33. ^{11}B NMR (128 MHz, $CDCl_3$) δ 6.08 (t, *J* = 20.0 Hz). ^{19}F NMR (377 MHz, $CDCl_3$) δ -130.88 (s), -130.93 (s), -130.99 (s), -131.04 (s), -131.11 (s), -131.16 (s), -131.22 (s), -131.27 (s), -132.59 (dd, *J* = 39.1, 19.1 Hz), -132.82 (dd, *J* = 39.1, 19.2 Hz). HRMS (ESI-TOF) m/z: [M+Na] cal for $C_{11}H_{14}BF_2NO$ 248.1031, found 248.1036.

3-cyclohexyl-2,2-difluoro-2,3-dihydrocyclohepta[d][1,3,2]oxazaborol-1-ium-2-uide (**3b**):

The pure product was obtained as reddish brown solid (180 mg, 77%). ^{1}H NMR (400 MHz, $CDCl_3$) δ 7.65 – 7.60 (m, 1H), 7.46 (t, *J* = 10 Hz, 1H), 7.21 (d, *J* = 12 Hz, 1H), 7.14 (d, *J* = 12 Hz, 1H), 7.06 (t, *J* = 10 Hz, 1H), 3.64 (s, 1H), 2.05-2.02 (m, 2H), 1.91 – 1.71 (m, 4H), 1.41 – 1.26 (m, 4H). ^{13}C{H} NMR (101 MHz, $CDCl_3$) δ 141.20, 139.38, 127.33, 118.51, 117.94, 55.17, 30.58, 25.56, 25.26. ^{11}B NMR (128 MHz, $CDCl_3$) δ 6.05 (t, *J* = 19.2Hz). ^{19}F NMR (377 MHz, $CDCl_3$) δ -131.55 (dd, *J* = 41.4 Hz, 19.2 Hz). HRMS (ESI-TOF) m/z: [M+Na] cal for $C_{13}H_{16}BF_2NO$ 274.1188, found 274.1193.

2,2-difluoro-3-(prop-2-yn-1-yl)-2,3-dihydrocyclohepta[d][1,3,2]oxazaborol-1-ium-2-uide (**3c**):

The pure product was obtained as yellowish solid (800 mg, 72%). ^{1}H NMR (400 MHz, $CDCl_3$) δ 7.78 (t, *J* = 10 Hz, 1H), 7.63 (t, *J* = 12 Hz, 1H), 7.38 (dd, *J* = 25.0, 10.6 Hz, 2H), 7.27 – 7.21 (m, 1H), 4.32 (s, 2H), 2.31 (s, 1H). ^{13}C{H} NMR (101 MHz, $CDCl_3$) δ 168.25, 159.89, 142.05, 140.54, 128.45, 120.59, 118.42, 73.00, 32.14, 29.70. ^{11}B NMR (128 MHz, $CDCl_3$) δ 5.76 (t, *J* = 17.8 Hz). ^{19}F NMR (377 MHz, $CDCl_3$) δ -139.06 (dd, *J* = 35.8, 17.6 Hz). HRMS (ESI-TOF) m/z: [M+Na] cal for $C_{10}H_8BF_2NO$ 230.0561, found 230.0563.

3-butyl-2,2-difluoro-2,3-dihydrocyclohepta[d][1,3,2]oxazaborol-1-ium-2-uide (**3d**):

The pure product was obtained as reddish brown solid (250 mg, 78%). ^{1}H NMR (400 MHz, $CDCl_3$) δ 7.65 – 7.59 (m, 1H), 7.47 (t, *J* = 10 Hz, 1H), 7.27 – 7.23 (m, 1H), 7.11 – 7.04 (m, 2H), 3.56 (t, *J* = 6 Hz, 2H), 1.79 – 1.75 (m, 2H), 1.47-1.41 (m, 2H), 0.98 (t, *J* = 8 Hz, 3H). ^{13}C{H} NMR (101 MHz, $CDCl_3$) δ 167.43, 159.89, 141.30, 139.48, 127.27, 118.65, 117.49, 43.44, 29.86, 20.57, 13.76. ^{11}B NMR (128 MHz, $CDCl_3$) δ 5.99 (t, *J* = 18.8 Hz). ^{19}F NMR (377 MHz, $CDCl_3$) δ -138.28 (dd, *J* = 37.5, 18.2 Hz). HRMS (ESI-TOF) m/z: [M+Na] cal for $C_{11}H_{14}BF_2NO$ 248.1031, found 248.1044.

2,2-difluoro-3-hexyl-2,3-dihydrocyclohepta[d][1,3,2]oxazaborol-1-ium-2-uide (**3e**):

The pure product was obtained as reddish brown solid (310 mg, 83%). ^{1}H NMR (400 MHz, $CDCl_3$) δ 7.66 – 7.61(m, 1H), 7.47 (t, *J* = 10 Hz, 1H), 7.23 (d, *J* = 12 Hz, 1H), 7.12 – 7.05 (m, 2H), 3.54 (t, *J* = 6 Hz, 2H), 1.81 – 1.73 (m, 2H), 1.42 – 1.31(m, 6H), 0.89 (t, *J* = 8 Hz, 3H). ^{13}C{H} NMR (101 MHz, $CDCl_3$) δ 167.31, 159.85, 141.40, 139.46, 127.40, 118.65, 117.56, 47.08, 43.66, 31.45, 27.79, 26.98, 22.53, 13.99, 8.71. ^{11}B NMR (128 MHz, $CDCl_3$) δ 5.97 (t, *J* = 18.7 Hz). ^{19}F NMR (377 MHz, $CDCl_3$) δ -138.17 (dd, *J* = 37.6, 18.0 Hz). HRMS (ESI-TOF) m/z: [M+Na] cal for $C_{13}H_{18}BF_2NO$ 276.1344, found 276.1354.

2,2-difluoro-3-octyl-2,3-dihydrocyclohepta[d][1,3,2]oxazaborol-1-ium-2-uide (**3f**):

The pure product was obtained as reddish brown solid (216 mg, 81%). ^{1}H NMR (400 MHz, $CDCl_3$) δ 7.65 – 7.60 (m, 1H), 7.47 (t, *J* = 10.2 Hz, 1H), 7.24(t, *J* = 11.0 Hz, 1H), 7.11 – 7.05 (m, 2H), 3.54 (t, *J* = 7.6 Hz, 2H), 1.81 – 1.74 (m, 2H), 1.40 – 1.27 (m, 10H), 0.88 (t, *J* = 8 Hz, 3H). ^{13}C{H} NMR (101 MHz, $CDCl_3$) δ 167.35, 159.86, 141.35, 139.45, 127.34, 118.62, 117.55, 43.68, 31.77, 29.25, 29.18, 27.84, 27.33, 22.61, 14.08. ^{11}B NMR (128 MHz, $CDCl_3$) δ 5.98 (t, *J* = 18.5 Hz). ^{19}F NMR (377 MHz, $CDCl_3$) δ -138.20 (dd, *J* = 36.7, 15.2 Hz).. HRMS (ESI-TOF) m/z: [M+Na] cal for $C_{15}H_{22}BF_2NO$ 304.1657, found 304.1659.

3-dodeyl-2,2-difluoro-2,3-dihydrocyclohepta[d][1,3,2]oxazaborol-1-ium-2-uide (**3g**):

The pure product was obtained as reddish brown solid (326 mg, 87%). ^{1}H NMR (400 MHz, $CDCl_3$) δ 7.62(t, J=10 Hz 1H), 7.48 (t, *J* = 10 Hz, 1H), 7.28 – 7.25 (m, 1H), 7.12 –7.06 (m, 2H), 3.56 (t, *J* = 8 Hz, 2H), 1.81 – 1.77(m, 2H), 1.42 – 1.28 (m, 18H), 0.90 (t, *J* = 6 Hz, 3H).^{13}C{H} NMR (101 MHz, $CDCl_3$) δ 167.49, 159.86, 141.27, 139.46, 127.24, 118.60, 117.48, 43.70, 31.91, 29.62, 29.57, 29.52, 29.33, 29.30, 27.84, 27.35, 22.68, 14.11. ^{11}B NMR (128 MHz, $CDCl_3$) δ 5.98 (t, *J* = 18.3 Hz). ^{19}F NMR (377 MHz, $CDCl_3$) δ -138.27 (dd, *J* = 37.1, 17.0 Hz). HRMS (ESI-TOF) m/z: [M+Na] cal for $C_{19}H_{30}BF_2NO$ 360.2284, found 360.2296.

2,2-difluoro-3-octadecyl-2,3-dihydrocyclohepta[d][1,3,2]oxazaborol-1-ium-2-uide (**3h**):

The pure product was obtained as white solid (270 mg, 80%).^{1}H NMR (400 MHz, $CDCl_3$) δ 7.61 (t, *J* = 10 Hz, 1H), 7.47 (t, *J* = 10 Hz, 1H), 7.26 – 7.23 (m, 1H), 7.09-7.04 (m, 2H), 3.54 (t, *J* = 8 Hz, 2H), 1.81 – 1.74 (m, 2H), 1.61 (s, 1H), 1.40 – 1.26(m, 30H), 0.88 (t, *J* = 6.4 Hz, 3H). ^{13}C NMR (101 MHz, $CDCl_3$) δ 167.46, 159.84, 141.24, 139.47, 127.21, 118.62, 117.48, 43.71, 31.93, 29.71, 29.67, 29.64, 29.58, 29.54, 29.37, 29.31, 27.84, 27.36, 22.70, 14.13. ^{11}B NMR (128 MHz, $CDCl_3$) δ 5.98 (t, *J* = 18.1 Hz). ^{19}F NMR (377 MHz, $CDCl_3$) δ -138.29 (dd, *J* = 36.8, 16.6 Hz). HRMS (ESI-TOF) m/z: [M+Na] cal for $C_{25}H_{42}BF_2NO$ 444.3224, found 444.3232.

3B.6 Reference and Notes

1. Zaumseil, J.; Sirringhaus, H., Electron and ambipolar transport in organic field-effect transistors. *Chem Rev* **2007,** *107*, 1296-1323.

2. Bessette, A.; Hanan, G. S., Design, synthesis and photophysical studies of dipyrromethene-based materials: insights into their applications in organic photovoltaic devices. *Chem. Soc. Rev.* **2014,** *43*, 3342-3405.

3. Kim, H. N.; Guo, Z.; Zhu, W.; Yoon, J.; Tian, H., Recent progress on polymer-based fluorescent and colorimetric chemosensors. *Chem. Soc. Rev.* **2011,** *40*, 79-93.

4. Ulrich, G.; Ziessel, R.; Harriman, A., The Chemistry of Fluorescent Bodipy Dyes: Versatility Unsurpassed. *Angew. Chem. Int. Ed.* **2008,** *47*, 1184-1201.

5. Durantini, A. M.; Heredia, D. A.; Durantini, J. E.; Durantini, E. N., BODIPYs to the rescue: Potential applications in photodynamic inactivation. *Eur. J. Med. Chem.* **2018,** *144*, 651-661.

6. Ahrens, J.; Cordes, B.; Wicht, R.; Wolfram, B.; Bröring, M., Acidic Condensation of BODIPYs with Aldehydes: A Quick and Versatile Route to Alkenyl-BODIPYs and C (sp3)-Connected DYEmers. *Chem.: Eur. J.* **2016,** *22*, 10320-10325.

7. Golden, J. H.; Facendola, J. W.; Sylvinson MR, D.; Baez, C. Q.; Djurovich, P. I.; Thompson, M. E., Boron Dipyridylmethene (DIPYR) Dyes: Shedding Light on Pyridine-Based Chromophores. *J. Org. Chem.* **2017,** *82*, 7215-7222.

8. Patalag, L. J.; Jones, P. G.; Werz, D. B., BOIMPYs: Rapid Access to a Family of Red-Emissive Fluorophores and NIR Dyes. *Angew. Chem. Int. Ed.* **2016,** *55*, 13340-13344.

9. Patalag, L. J.; Jones, P. G.; Werz, D. B., Aza-BOIMPYs: A Tetrazole Auxochrome for Highly Red-Emissive Dipyrromethene-Based Fluorophores. *Chem.: Eur. J.* **2017,** *23*, 15903-15907.

10. Patalag, L. J.; Ho, L. P.; Jones, P. G.; Werz, D. B., Ethylene-bridged oligo-BODIPYs: access to intramolecular J-aggregates and superfluorophores. *J.Am. Chem. Soc.* **2017,** *139*, 15104-15113.

11. Zhou, X.; Yu, C.; Feng, Z.; Yu, Y.; Wang, J.; Hao, E.; Wei, Y.; Mu, X.; Jiao, L., Highly regioselective α-chlorination of the BODIPY chromophore with copper (II) chloride. *Org. Lett.* **2015,** *17*, 4632-4635.

12. Ray, C.; Díaz-Casado, L.; Avellanal-Zaballa, E.; Bañuelos, J.; Cerdan, L.; García-Moreno, I.; Moreno, F.; Maroto, B. L.; López-Arbeloa, Í.; de la Moya, S., N-BODIPYs Come into Play: Smart Dyes for Photonic Materials. *Chem.: Eur. J.* **2017,** *23*, 9383-9390.

13. Yu, C.; Hao, E.; Fang, X.; Wu, Q.; Wang, L.; Li, J.; Xu, L.; Jiao, L.; Wong, W.-Y., AIE-active difluoroboronated acylhydrozone dyes (BOAHY) emitting across the entire visible region and their photo-switching properties. *J. Mater.Chem. C* **2019,** *7*, 3269-3277.

14. Guerrero-Corellam, A. A.-P., J.; Pawar, T. J.; Díaz-Tendero, S.; Martín-Sómer, A.; Gómez, C . V.; Belmonte-Vázquez, J. L.; Ramírez-Ornelas, D. E.; Peña-Cabrera, E.; Frailem, A..; Cruz, D. C.; Alemán, J., BODIPY as electron withdrawing group for the activation of double bonds in asymmetric cycloaddition reactions. In *Chem. Sci.*. 2019; Vol. 10, pp 4346-4351.

15. Bentley, R., A fresh look at natural tropolonoids. *Nat. Prod. Rep.* **2008,** *25*, 118-138.

16. Crivat, G.; Taraska, J. W., Imaging proteins inside cells with fluorescent tags. *Trends Biotechnol.* **2012,** *30*, 8-16.

17. Liu, N.; Song, W.; Schienebeck, C. M.; Zhang, M.; Tang, W., Synthesis of Naturally Occurring Tropones and Tropolones. *Tetrahedron* **2014,** *70*, 9281-9305.

18. Hosoya, H.; Tanaka, J.; Nagakura, S., Ultra-violet absorption spectra of tropone, troponium ion, tropolone and 2, 4, 6-octatrienal. *Tetrahedron* **1962,** *18*, 859-874.

19. Yamaguchi, H.; Amako, Y.; Azumi, H., The electronic spectrum of the tropone molecule. *Tetrahedron* **1968,** *24*, 267-277.

20. Croteau, R.; Leblanc, R., Colchicine fluorescence measured with a laser spectrofluorimeter. *J. Lumin.* **1977,** *15*, 353-356.

21. Meyer, N.; Löhnwitz, K.; Zulys, A.; Roesky, P. W.; Dochnahl, M.; Blechert, S., Aminotroponate Zinc Complexes as Catalysts for the Intramolecular Hydroamination of Alkenes and Alkynes. *Organometallics* **2006,** *25*, 3730-3734.

22. Datta, S.; Roesky, P. W.; Blechert, S., Aminotroponate and Aminotroponiminate Calcium Amides as Catalysts for the Hydroamination/Cyclization Catalysis. *Organometallics* **2007,** *26*, 4392-4394.

23. Datta, S.; Gamer, M. T.; Roesky, P. W., Aminotroponiminate Complexes of the Heavy Alkaline Earth and the Divalent Lanthanide Metals as Catalysts for the Hydroamination/Cyclization Reaction. *Organometallics* **2008,** *27*, 1207-1213.

24. Kubisiak, M.; Zelga, K.; Justyniak, I.; Tratkiewicz, E.; Pietrzak, T.; Keeri, A. R.; Ochal, Z.; Hartenstein, L.; Roesky, P. W.; Lewiński, J., Catalytic Epoxidation of Enones Mediated by Zinc Alkylperoxide/tert-BuOOH Systems. *Organometallics* **2013,** *32*, 5263-5265.

25. Fullagar, J. L.; Garner, A. L.; Struss, A. K.; Day, J. A.; Martin, D. P.; Yu, J.; Cai, X.; Janda, K. D.; Cohen, S. M., Antagonism of a zinc metalloprotease using a unique metal-chelating scaffold: tropolones as inhibitors of P. aeruginosa elastase. *Chem. Commun.* **2013,** *49*, 3197-3199.

26. Muetterties, E.; Roesky, H.; Wright, C., Chelate Chemistry. V. Metal Chelates Based on Tropolone and Its Derivatives. *J. Am. Chem. Soc.* **1966,** *88*, 4856-4861.

27. Breheret, E.; Martin, M., Electronic relaxation of troponoids: tropolone fluorescence. *J. Lumin.* **1978,** *17*, 49-60.

28. Hojo, M.; Hasegawa, H.; Yoneda, H., Role of triple ion formation in the acid–base reaction between tropolone and triethylamine in acetonitrile. *J. Chem. Soc., Perkin Trans. 2* **1994**, 1855-1859.

29. Bhattacharyya, B.; Wolff, J., Promotion of fluorescence upon binding of colchicine to tubulin. *Proc. Natl. Acad. Sci. U.S.A.* **1974,** *71*, 2627-2631.

30. Bhattacharyya, B.; Wolff, J., Anion-induced increases in the rate of colchicine binding to tubulin. *Biochemistry* **1976,** *15*, 2283-2288.

31. De Sa, G.; Malta, O.; de Mello Donegá, C.; Simas, A.; Longo, R.; Santa-Cruz, P.; da Silva Jr, E., Spectroscopic properties and design of highly luminescent lanthanide coordination complexes. *Coord. Chem. Rev.* **2000,** *196*, 165-195.

32. Takagi, K.; Saiki, K.; Mori, K.; Yuki, Y.; Suzuki, M., Synthesis of tropolone-containing conjugated polymers and their optical properties. *Polym. J.* **2007,** *39*, 813.

33. Sayapin, Y. A.; Tupaeva, I. O.; Kolodina, A. A.; Gusakov, E. A.; Komissarov, V. N.; Dorogan, I. V.; Makarova, N. I.; Metelitsa, A. V.; Tkachev, V. V.; Aldoshin, S. M., 2-Hetaryl-1, 3-tropolones based on five-membered nitrogen heterocycles: synthesis, structure and properties. *Beilstein J. Org. Chem.* **2015,** *11*, 2179.

34. Zadeh, E. G.; Tang, S.; Woodward, A.; Liu, T.; Bondar, M.; Belfield, K., Chromophoric materials derived from a natural azulene: syntheses, halochromism and one-photon and two-photon microlithography. *J. Mater. Chem. C* **2015,** *3*, 8495-8503.

35. Dochnahl, M.; Loehnwitz, K.; Pissarek, J. W.; Biyikal, M.; Schulz, S. R.; Schoen, S.; Meyer, N.; Roesky, P. W.; Blechert, S., Intramolecular Hydroamination with Homogeneous Zinc Catalysts: Evaluation of Substituent Effects in N, N′-Disubstituted Aminotroponiminate Zinc Complexes. *Chem. Eur. j* **2007,** *13*, 6654-6666.

36. Roesky, P. W., The co-ordination chemistry of aminotroponiminatesDedicated to Professor Herbert W. Roesky on the occasion of his 65th birthday. *Chem. Soc. Rev.* **2000,** *29*, 335-345.

37. Zulys, A.; Dochnahl, M.; Hollmann, D.; Löhnwitz, K.; Herrmann, J. S.; Roesky, P. W.; Blechert, S., Intramolecular hydroamination of functionalized alkenes and alkynes with a homogenous zinc catalyst. *Angew. Chem. Int. Ed.* **2005,** *44*, 7794-7798.

38. Hussein, L.; Purkait, N.; Biyikal, M.; Tausch, E.; Roesky, P. W.; Blechert, S., Highly enantioselective hydroamination to six-membered rings by heterobimetallic catalysts. *Chem. Commun.* **2014,** *50*, 3862-3864.

39. Dochnahl, M.; Pissarek, J.-W.; Blechert, S.; Löhnwitz, K.; Roesky, P. W., A new homogeneous zinc complex with increased reactivity for the intramolecular hydroamination of alkenes. *Chem. Commun.* **2006**, 3405-3407.

40. Holmquist, H.; Benson, R., 2-Bora-and 2-Thia-1, 3-diazaazulenes. *J. Am. Chem. Soc.* **1962,** *84*, 4720-4722.

41. Balachandra, C.; Sharma, N. K., Novel fluorophores: Syntheses and photophysical studies of boron-aminotroponimines. *Dyes. Pigm.* **2017,** *137*, 532-538.

42. Palai, B. B.; Soren, R.; Sharma, N. K., BODIPY analogues: synthesis and photophysical studies of difluoro boron complexes from 2-aminotropone scaffolds through N,O-chelation. *Org. Biomol. Chem.* **2019,** *17*, 6497-6505.

3B.7 Appendix

Table of contents

1. (^{1}H, ^{13}C, ^{11}B, ^{19}F)NMR and HRMS spectra of compound **3a**: 216
2. (^{1}H, ^{13}C, ^{11}B, ^{19}F)NMR and HRMS spectra of compound **3b**: 219
3. (^{1}H, ^{13}C, ^{11}B, ^{19}F)NMR and HRMS spectra of compound **3c**: 222
4. (^{1}H, ^{13}C, ^{11}B, ^{19}F)NMR and HRMS spectra of compound **3d**: 225
5. (^{1}H, ^{13}C, ^{11}B, ^{19}F)NMR and HRMS spectra of compound **3e**: 229
6. (^{1}H, ^{13}C, ^{11}B, ^{19}F)NMR and HRMS spectra of compound **3f**: 233
7. (^{1}H, ^{13}C, ^{11}B, ^{19}F)NMR and HRMS spectra of compound **3g**: 236
8. (^{1}H, ^{13}C, ^{11}B, ^{19}F)NMR and HRMS spectra of compound **3h**: 240
9. Crystal structures and data 244
10. Quantum Yield 245
11. Solid fluorescence 246

1. (^{1}H, ^{13}C, ^{11}B, ^{19}F)NMR and HRMS spectra of compound **3a**:

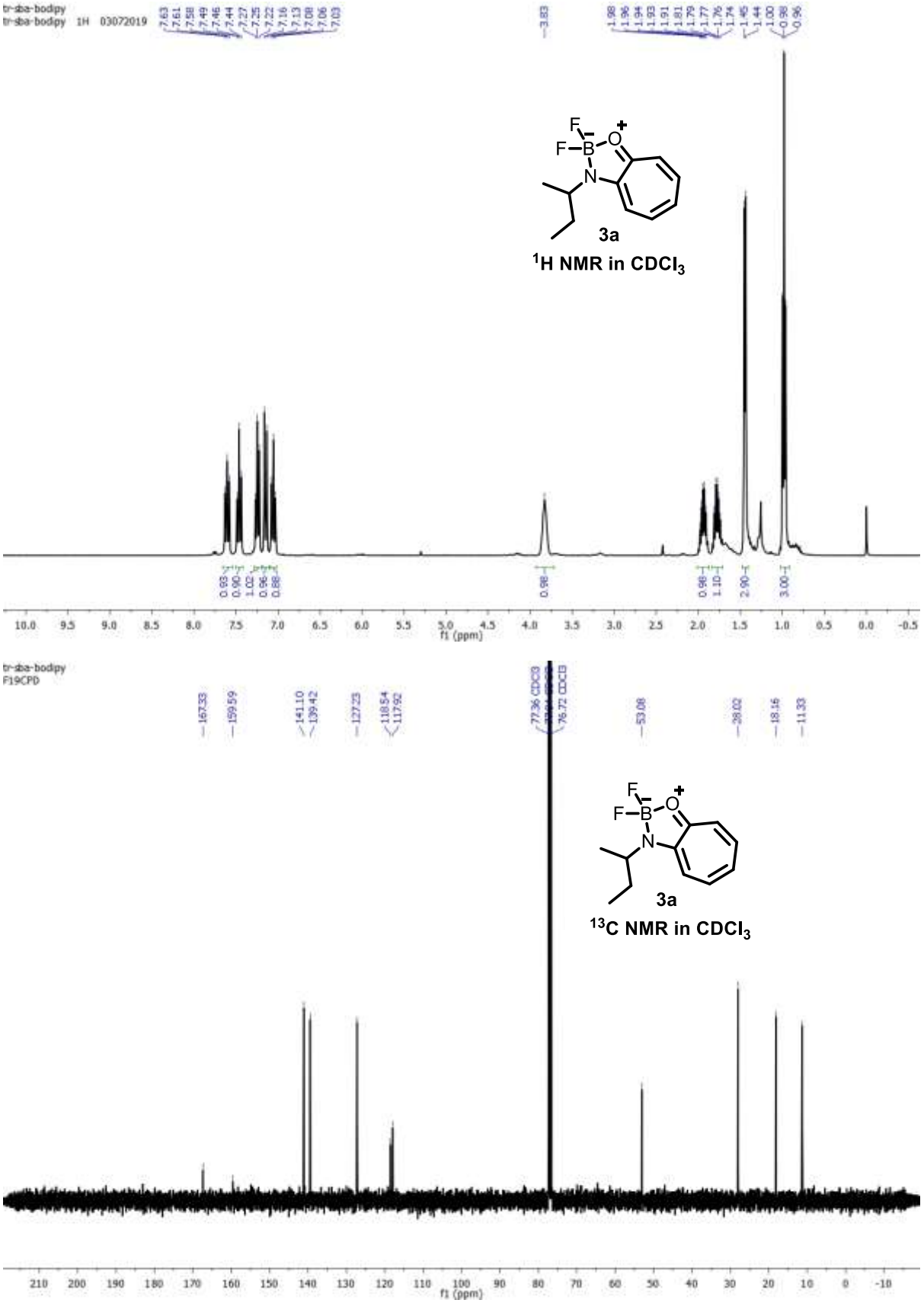

Figure A1. (^{1}H and ^{13}C) NMR spectra of Boron complex **3a** in $CDCl_3$.

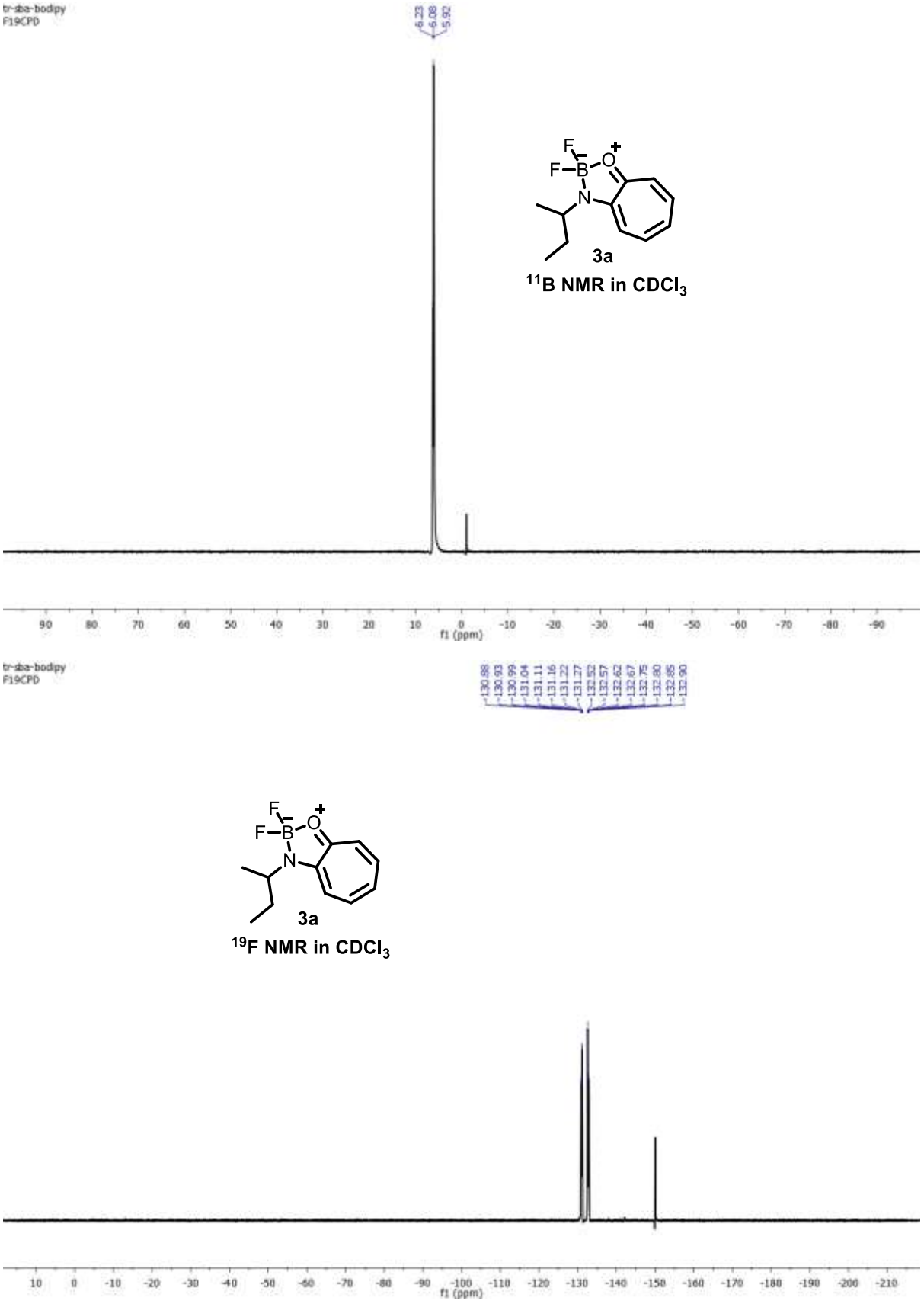

Figure A2. (^{11}B and ^{19}F) NMR spectra of Boron complex **3a** in $CDCl_3$.

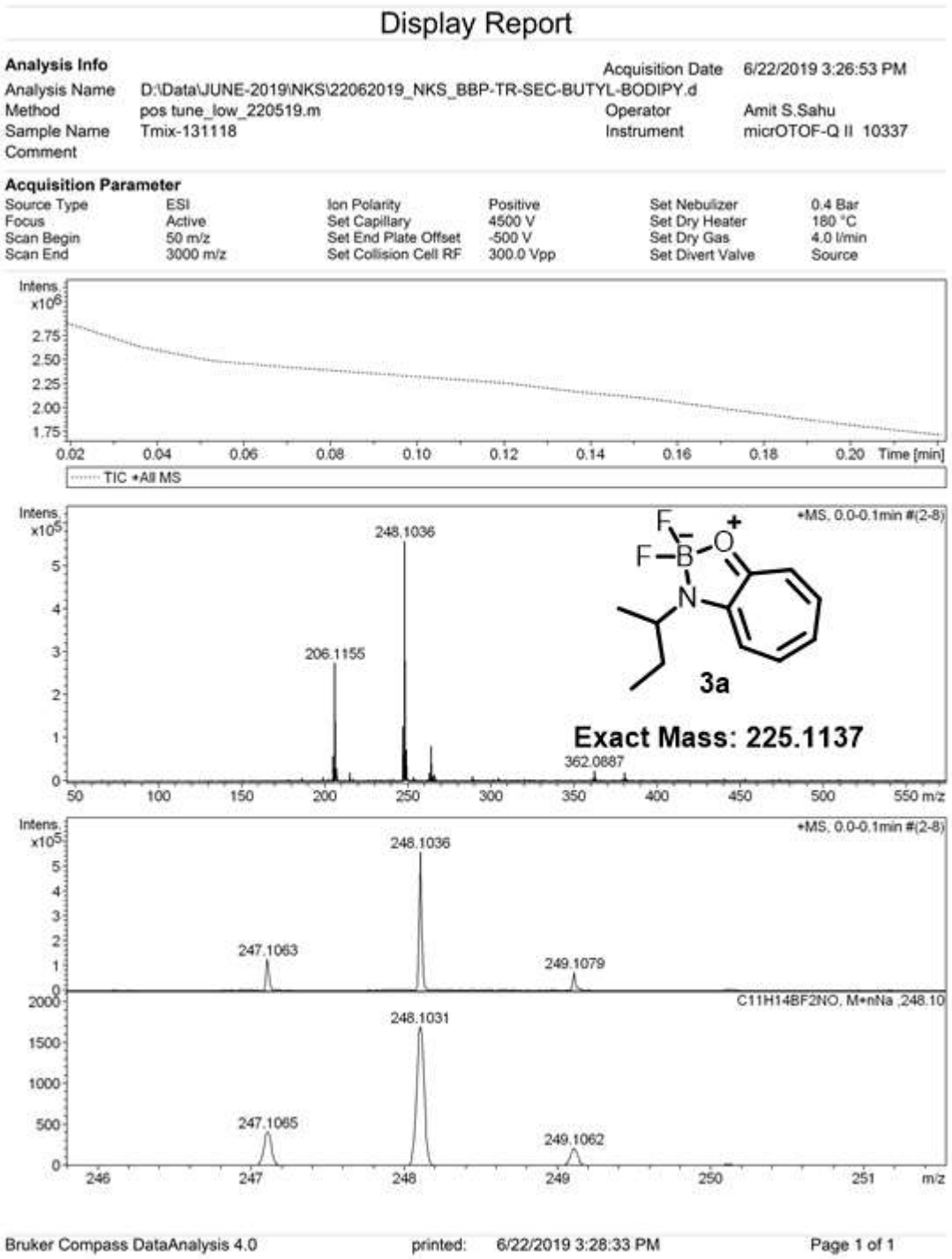

Figure A3. ESI/HRMS spectra of Boron complex **3a**.

2. (^{1}H, ^{13}C, ^{11}B, ^{19}F)NMR and HRMS spectra of compound **3b**:

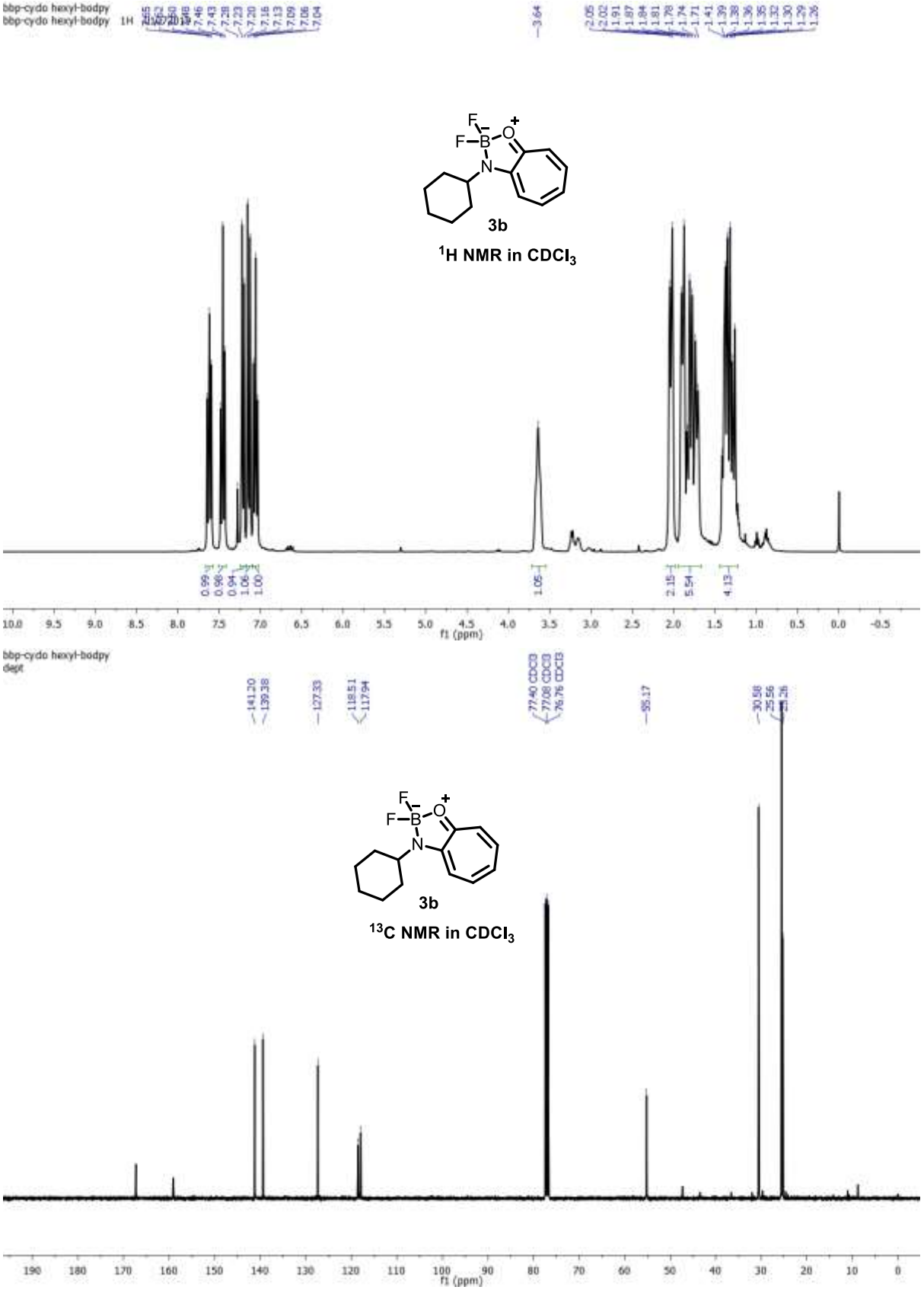

Figure A4. (^{1}H and ^{13}C) NMR spectra of Boron complex **3b** in $CDCl_3$.

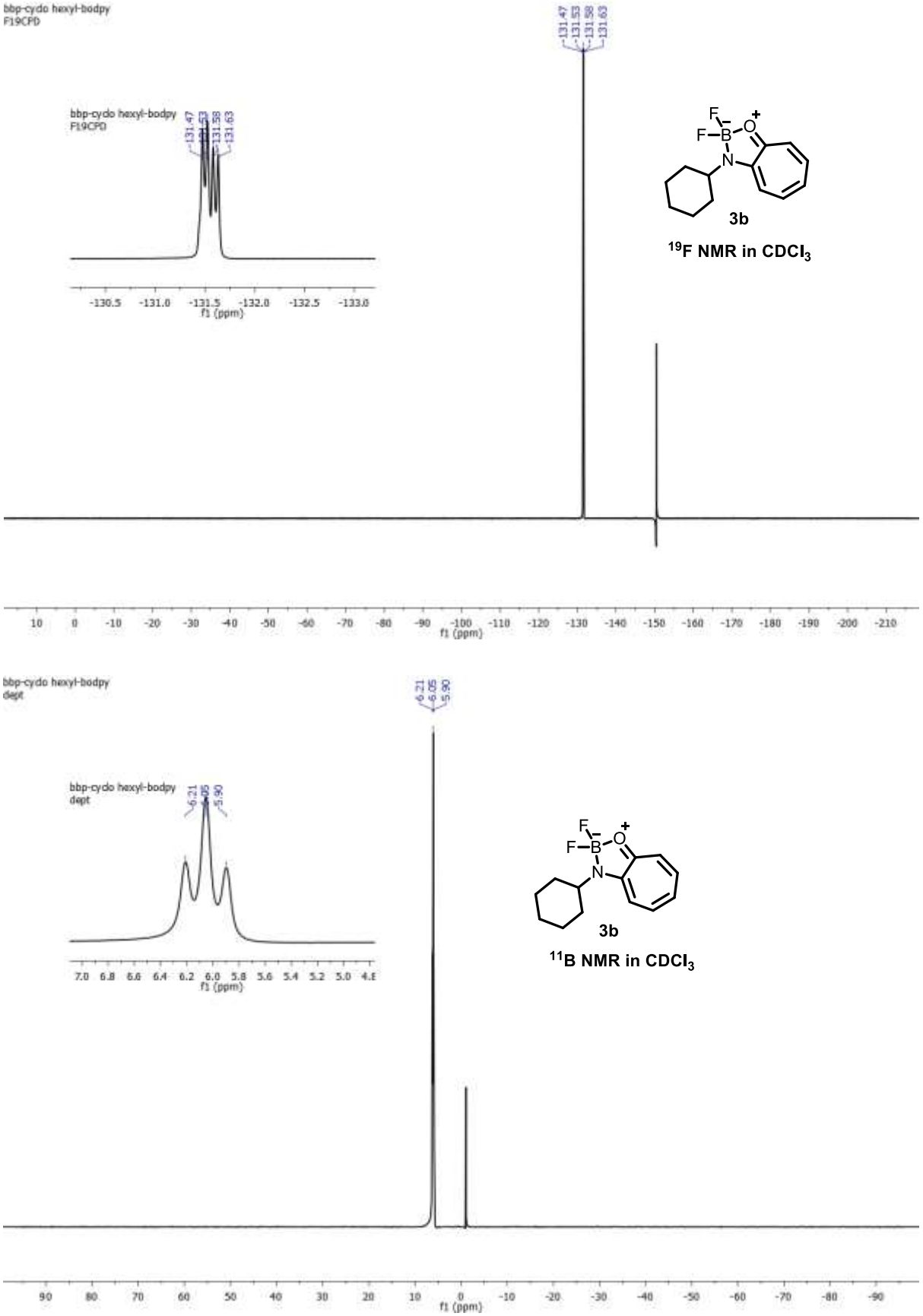

Figure A5. (^{11}B and ^{19}F) NMR spectra of Boron complex **3b** in $CDCl_3$.

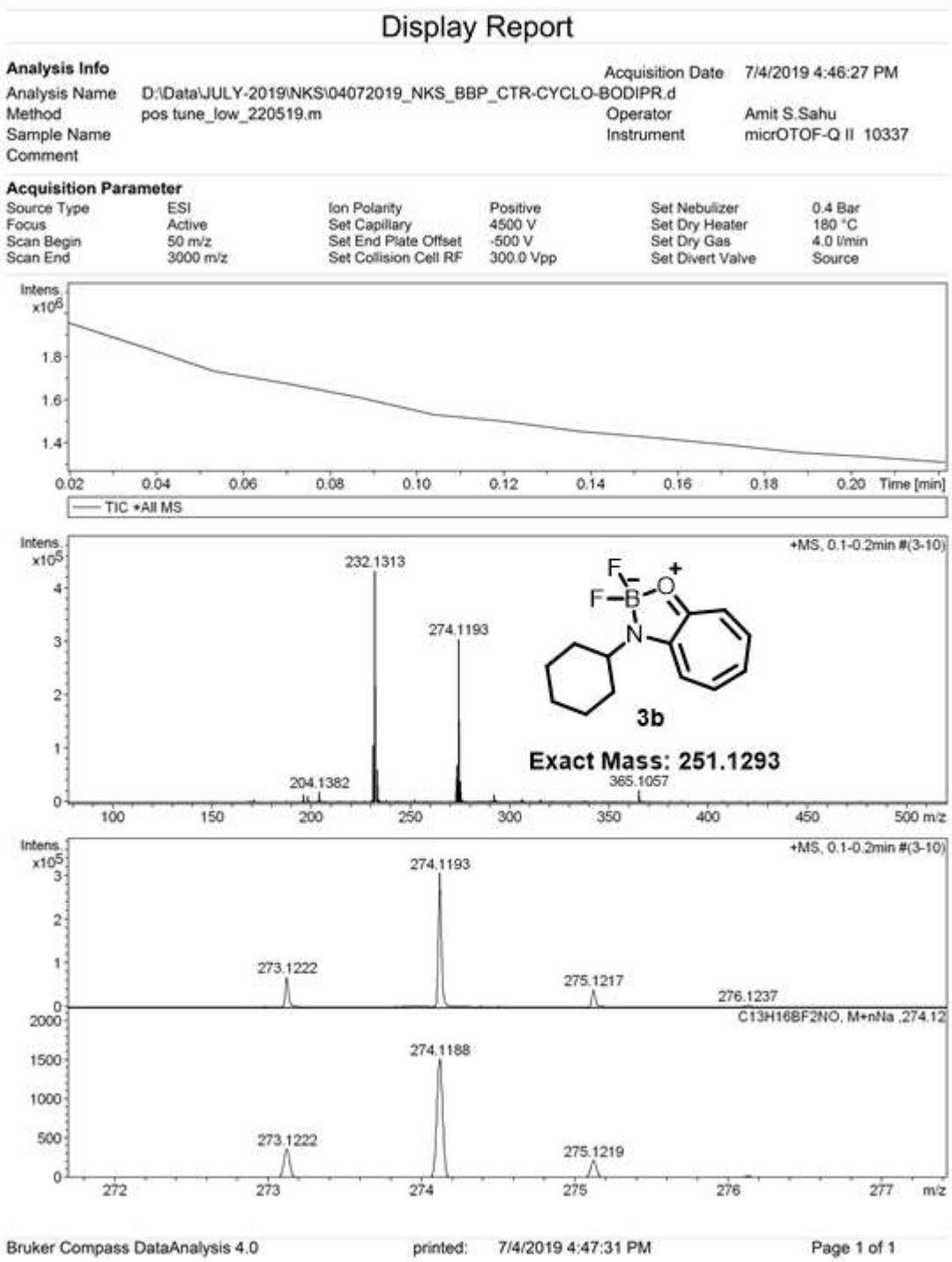

Figure A6. ESI/HRMS spectra of Boron complex **3b**.

3. (^{1}H, ^{13}C, ^{11}B, ^{19}F)NMR and HRMS spectra of compound **3c**:

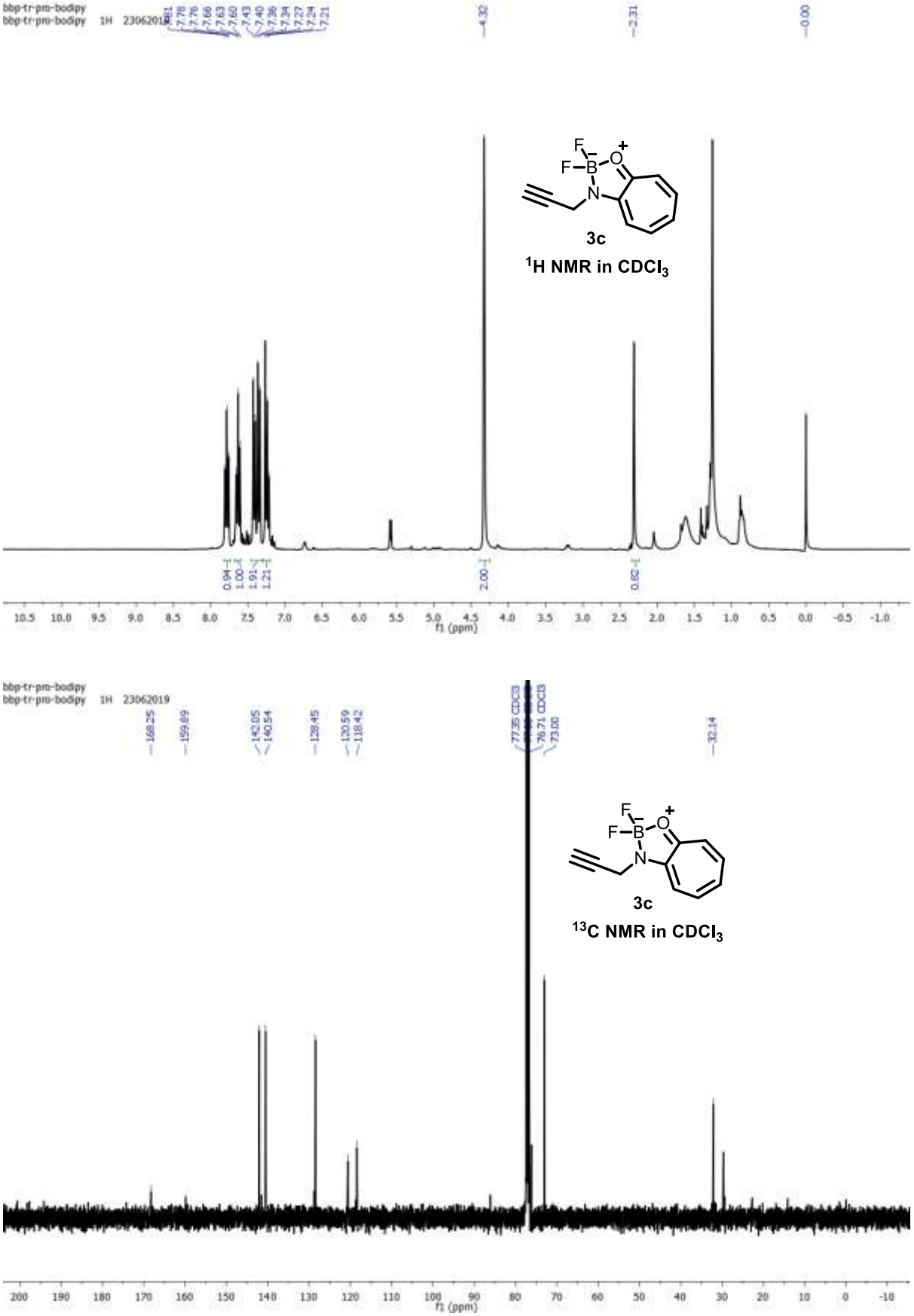

Figure A7. (^{1}H and ^{13}C) NMR spectra of Boron complex **3c** in $CDCl_3$.

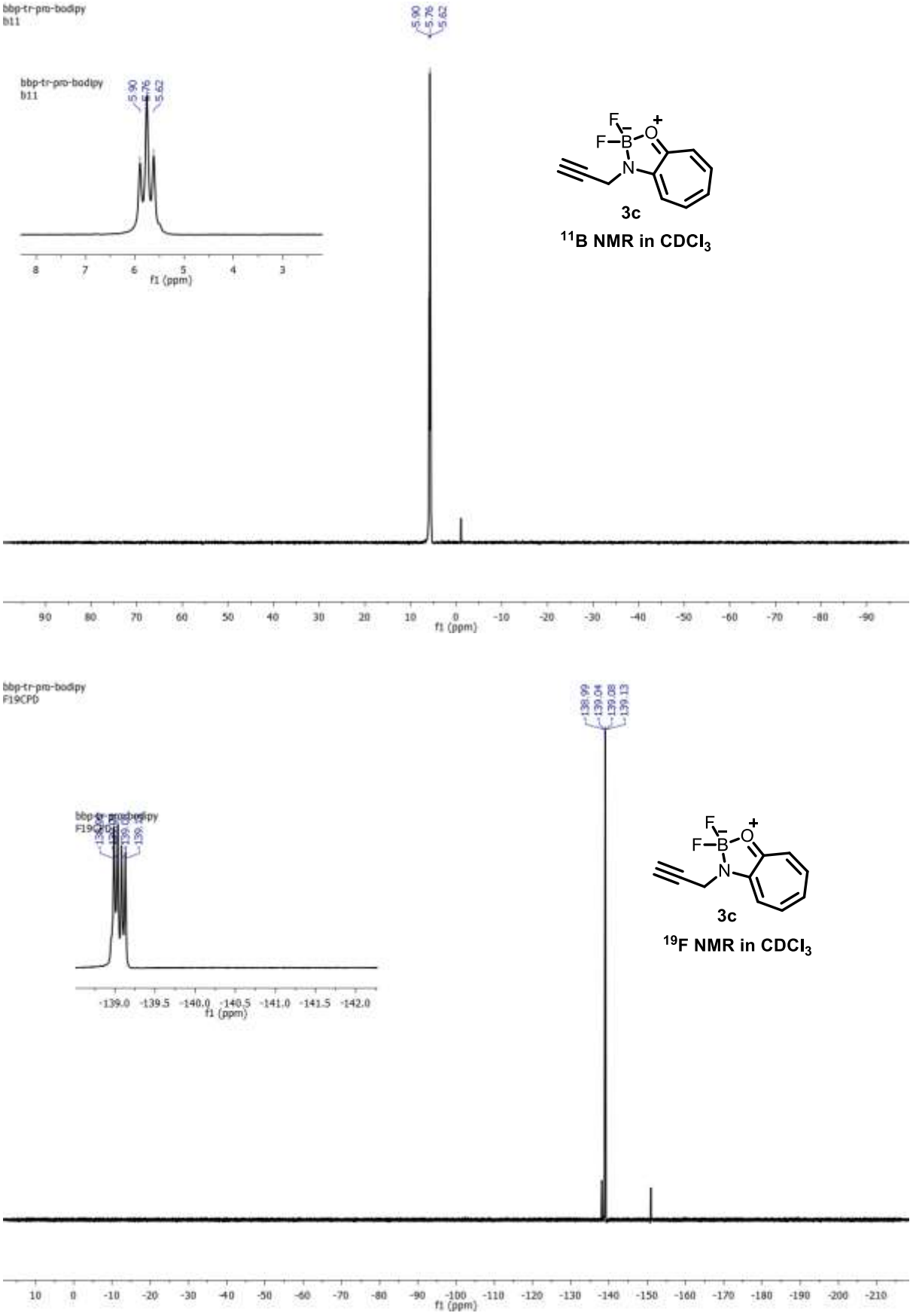

Figure A8. (^{11}B and ^{19}F) NMR spectra of Boron complex **3c** in $CDCl_3$.

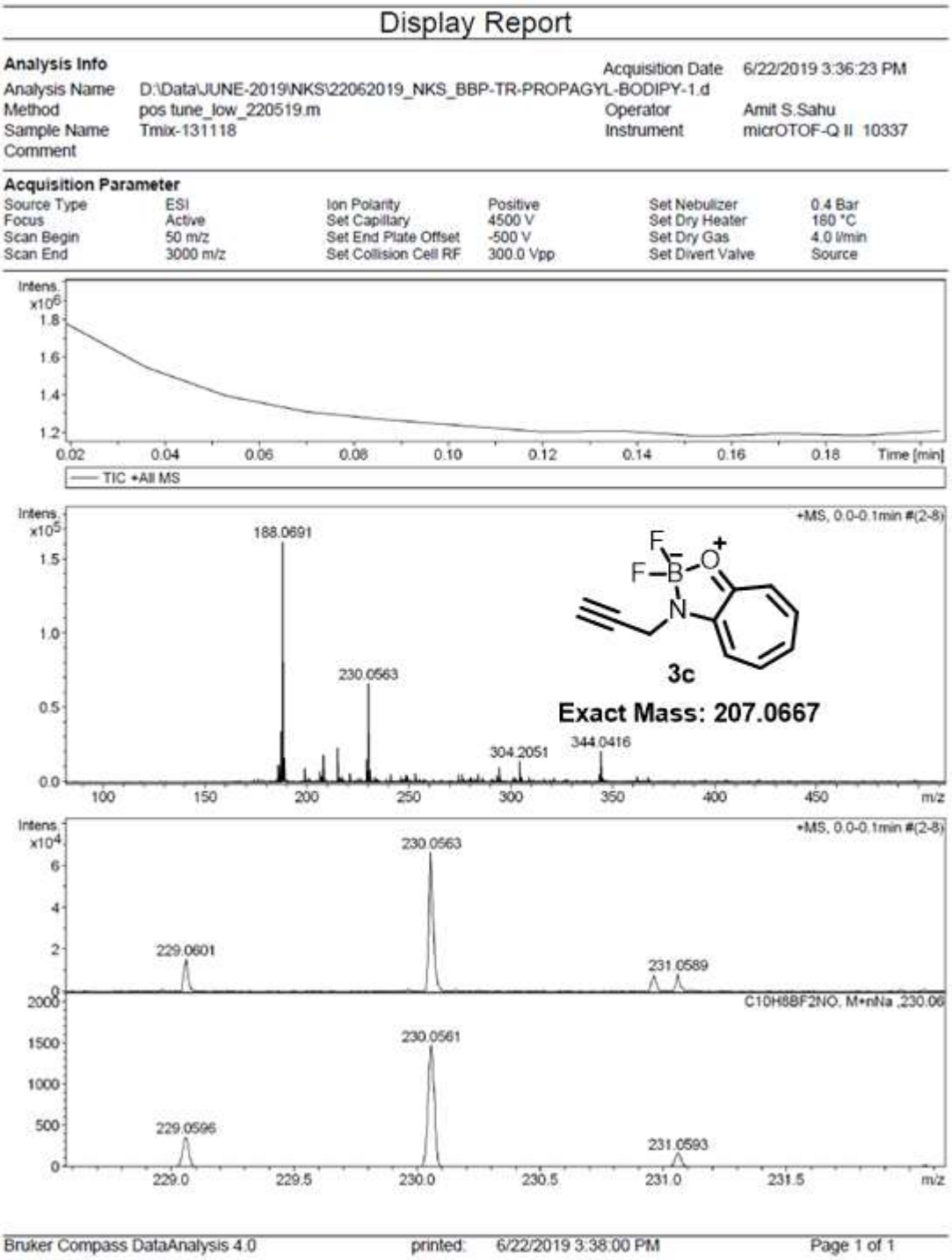

Figure A9. ESI/HRMS spectra of Boron complex **3c**.

4. (^{1}H, ^{13}C, ^{11}B, ^{19}F)NMR and HRMS spectra of compound **3d**:

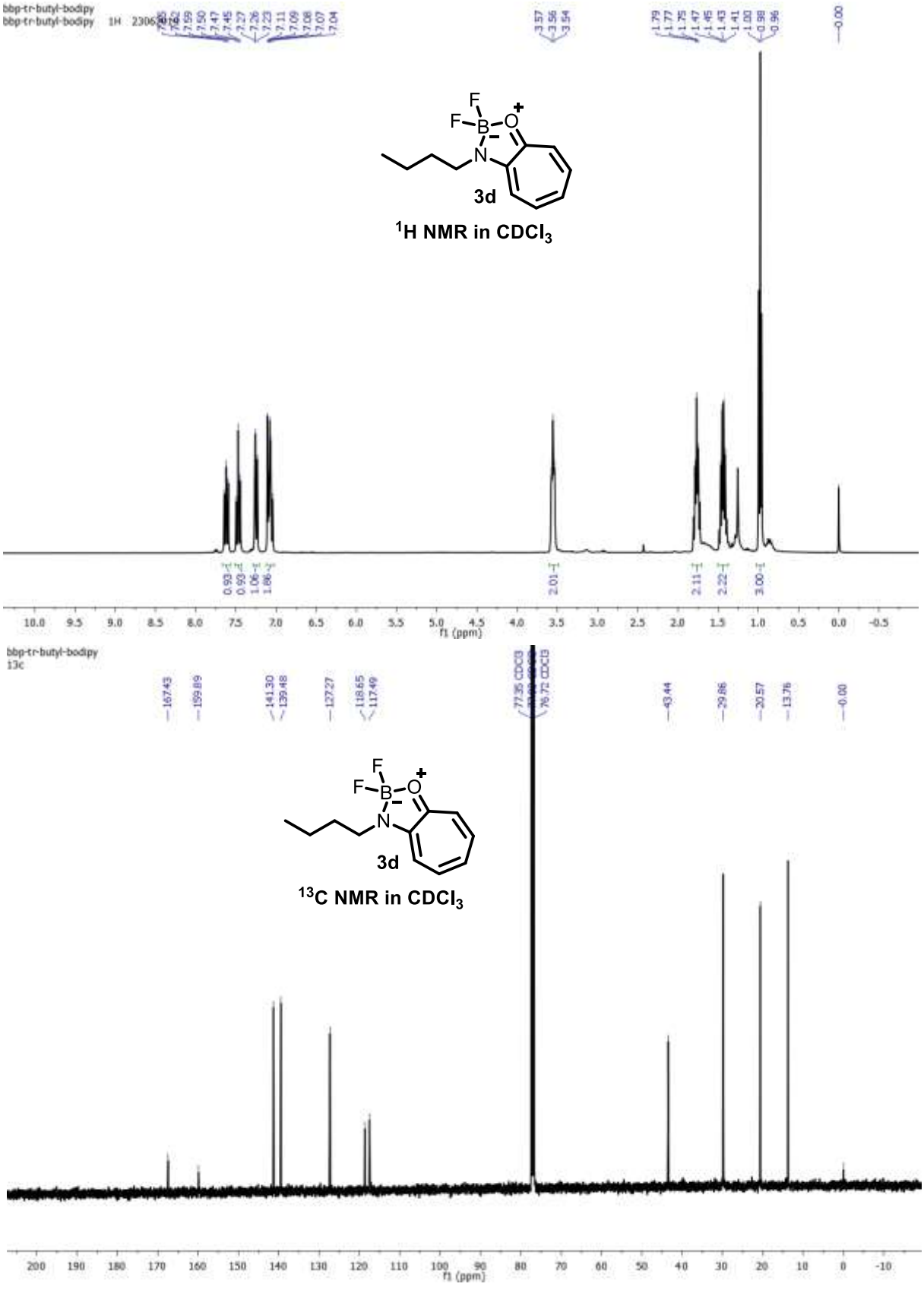

Figure A10. (^{1}H and ^{13}C) NMR spectra of Boron complex **3d** in $CDCl_3$.

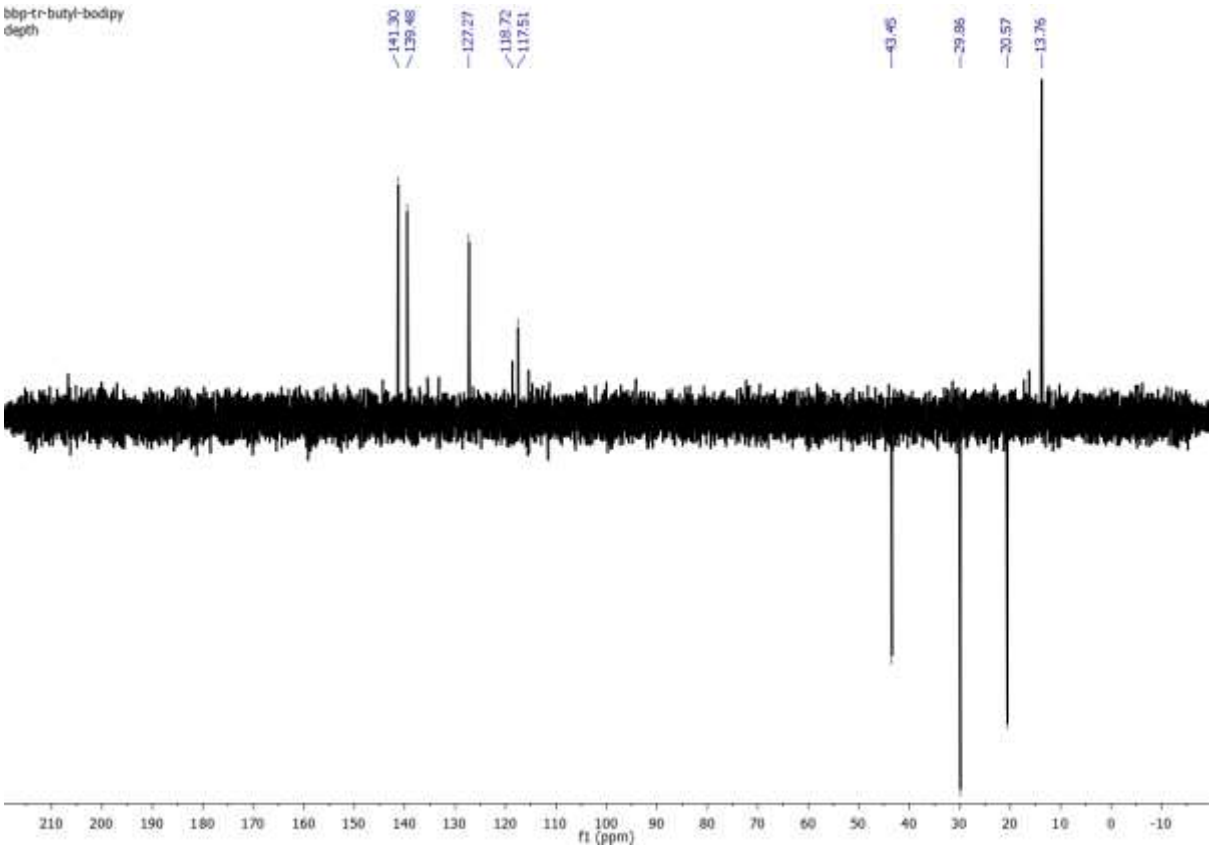
bbp-tr-butyl-bodipy
depth
141.30
139.48
127.27
118.72
117.51
43.45
29.86
30.57
13.76
210 200 190 180 170 160 150 140 130 120 110 100 90 80 70 60 50 40 30 20 10 0 -10
f1 (ppm)

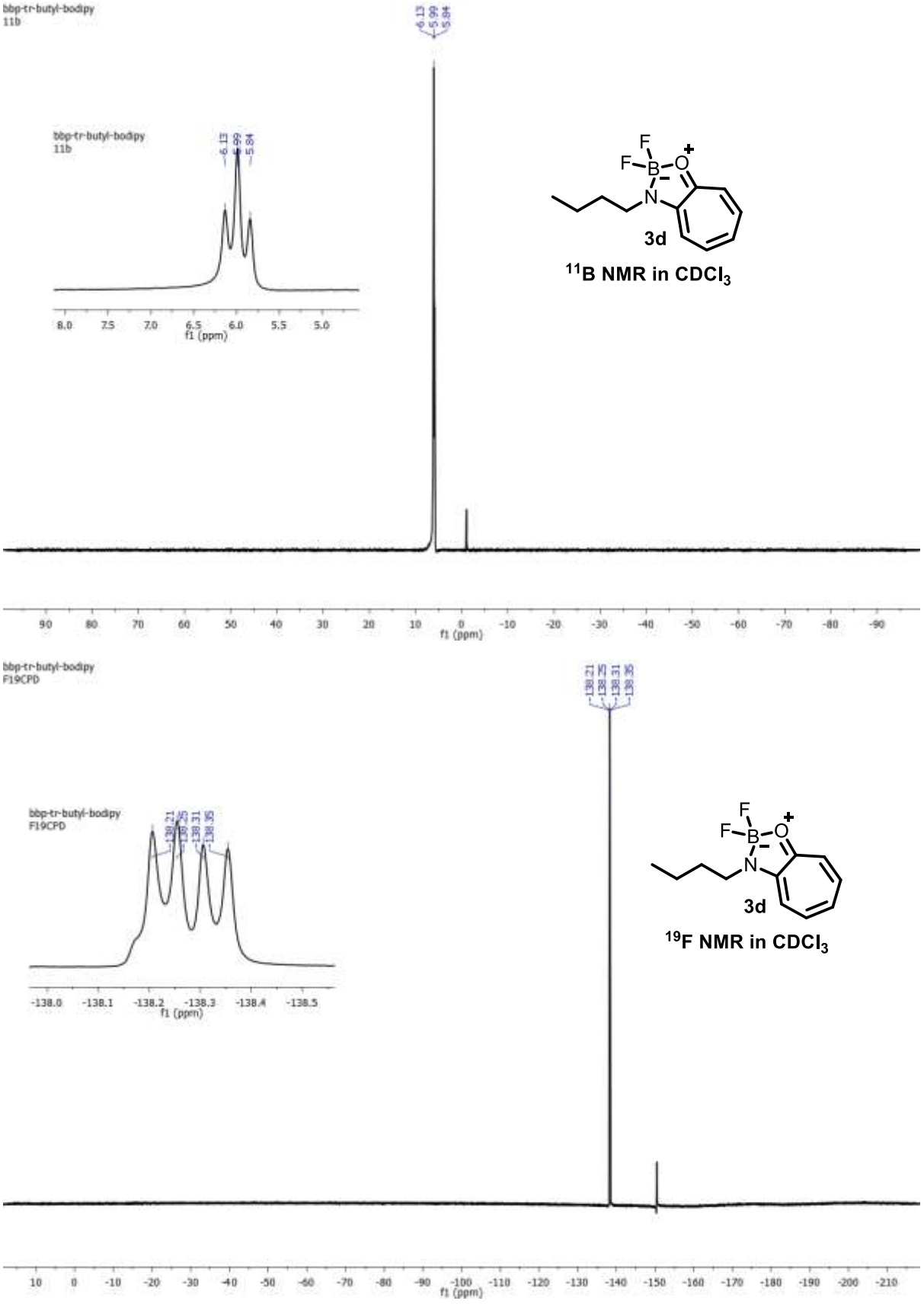

Figure A11. (^{11}B and ^{19}F) NMR spectra of Boron complex **3d** in $CDCl_3$.

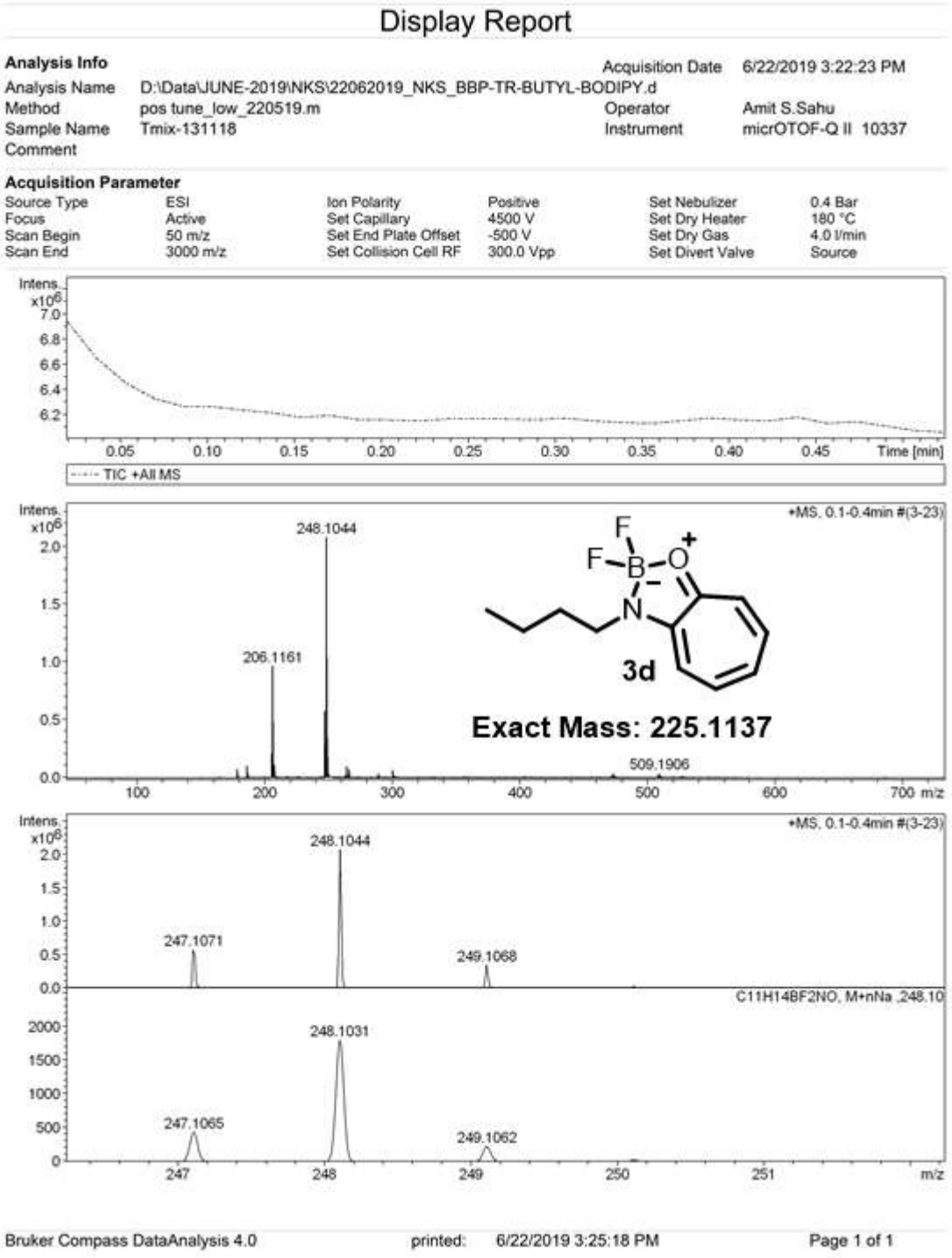

Figure A12. ESI/HRMS spectra of Boron complex **3d**.

5. (^{1}H, ^{13}C, ^{11}B, ^{19}F)NMR and HRMS spectra of compound **3e**:

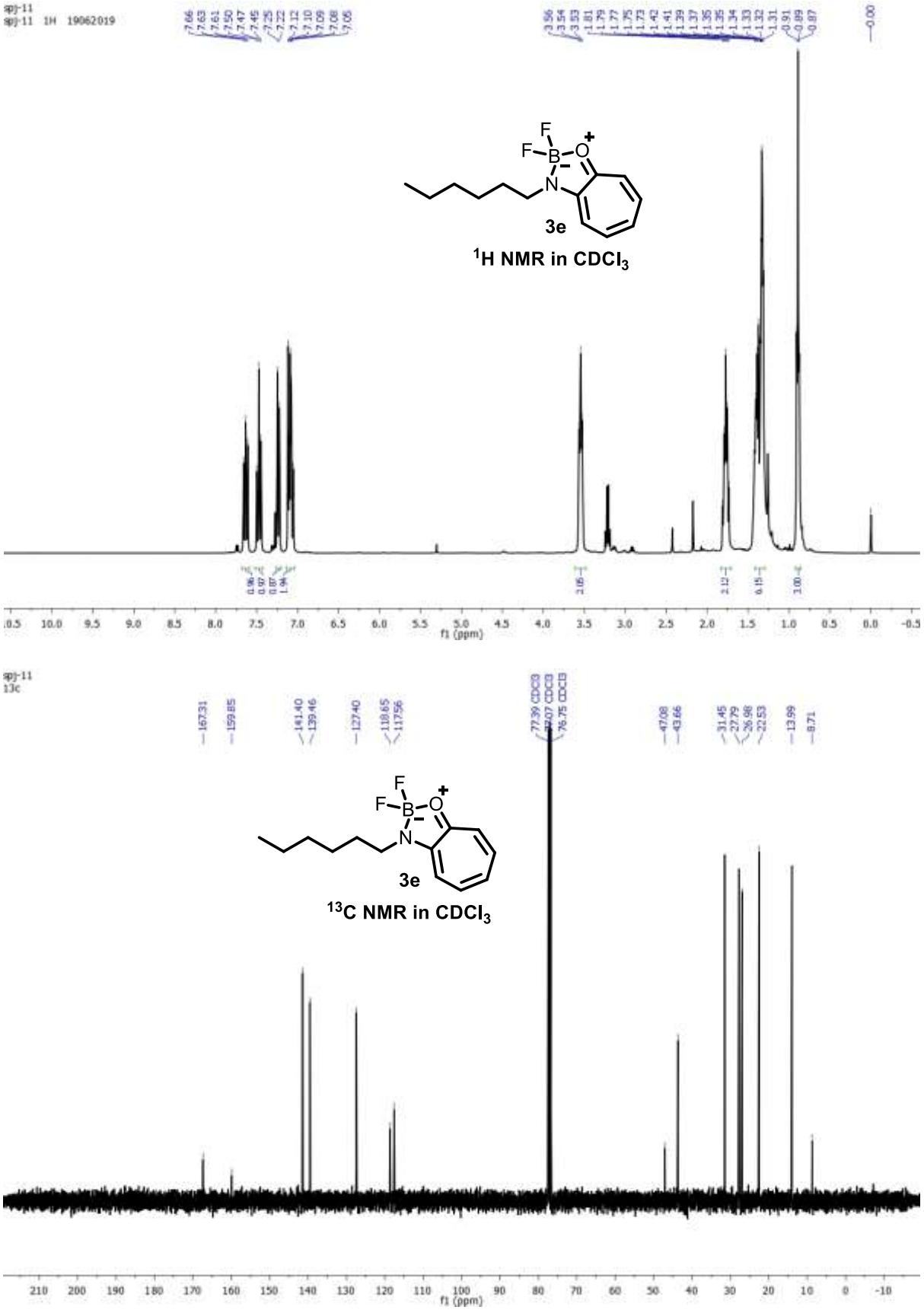

Figure A13. (^{1}H and ^{13}C) NMR spectra of Boron complex **3e** in $CDCl_3$.

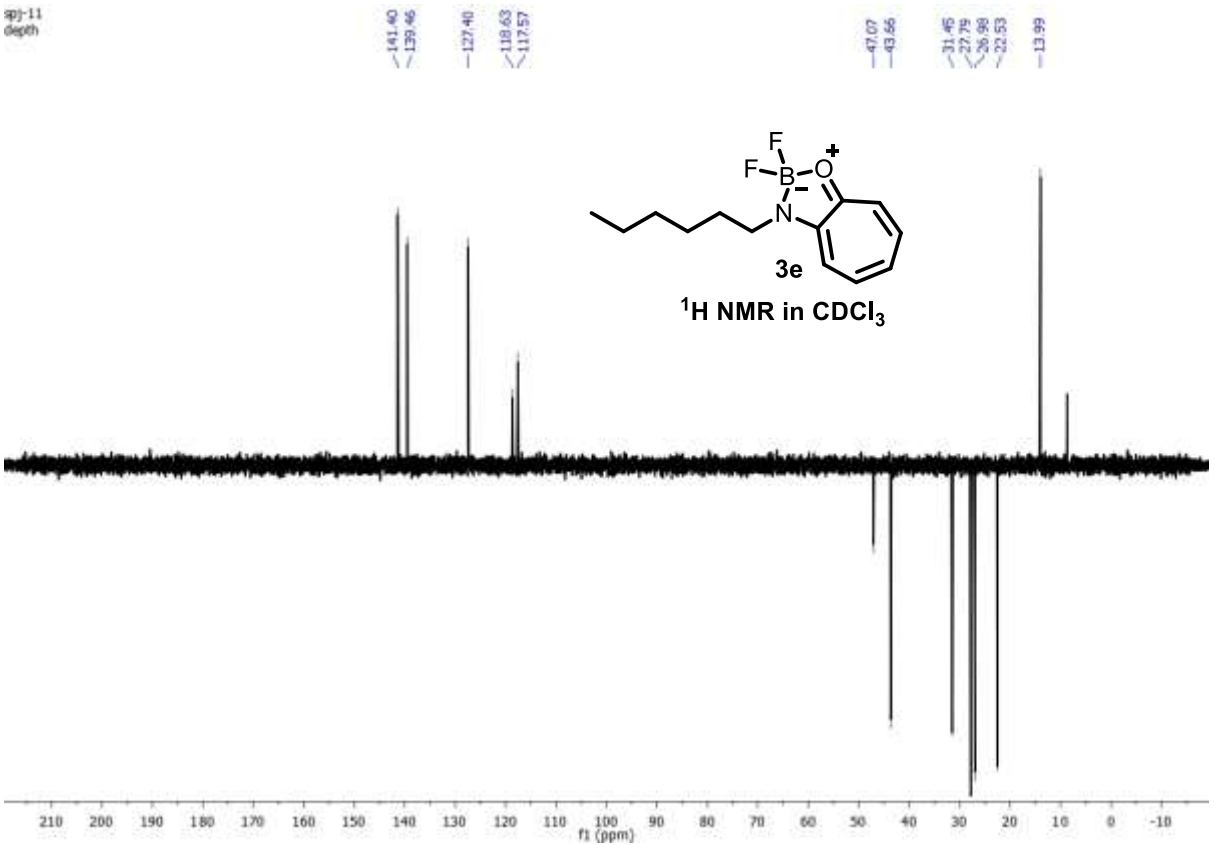
spj-11
depth
141.40
139.46
127.40
118.63
117.57
47.07
43.66
31.46
27.79
26.98
22.53
13.99
F
F
B
O
N
3e
^{1}H NMR in CDCl$_3$
210 200 190 180 170 160 150 140 130 120 110 100 90 80 70 60 50 40 30 20 10 0 -10
f1 (ppm)

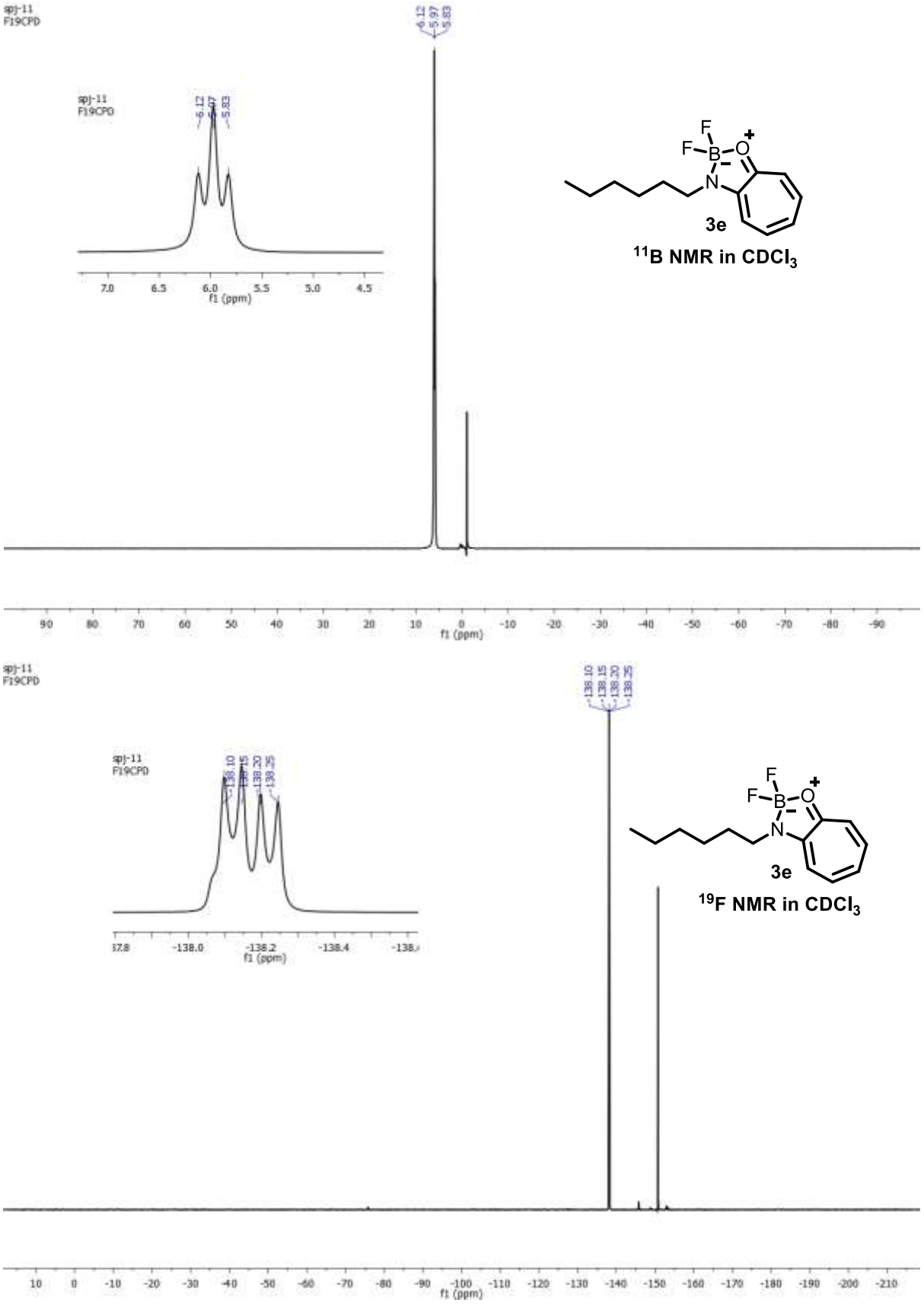

Figure 14. (^{11}B and ^{19}F) NMR spectra of Boron complex **3e** in $CDCl_3$.

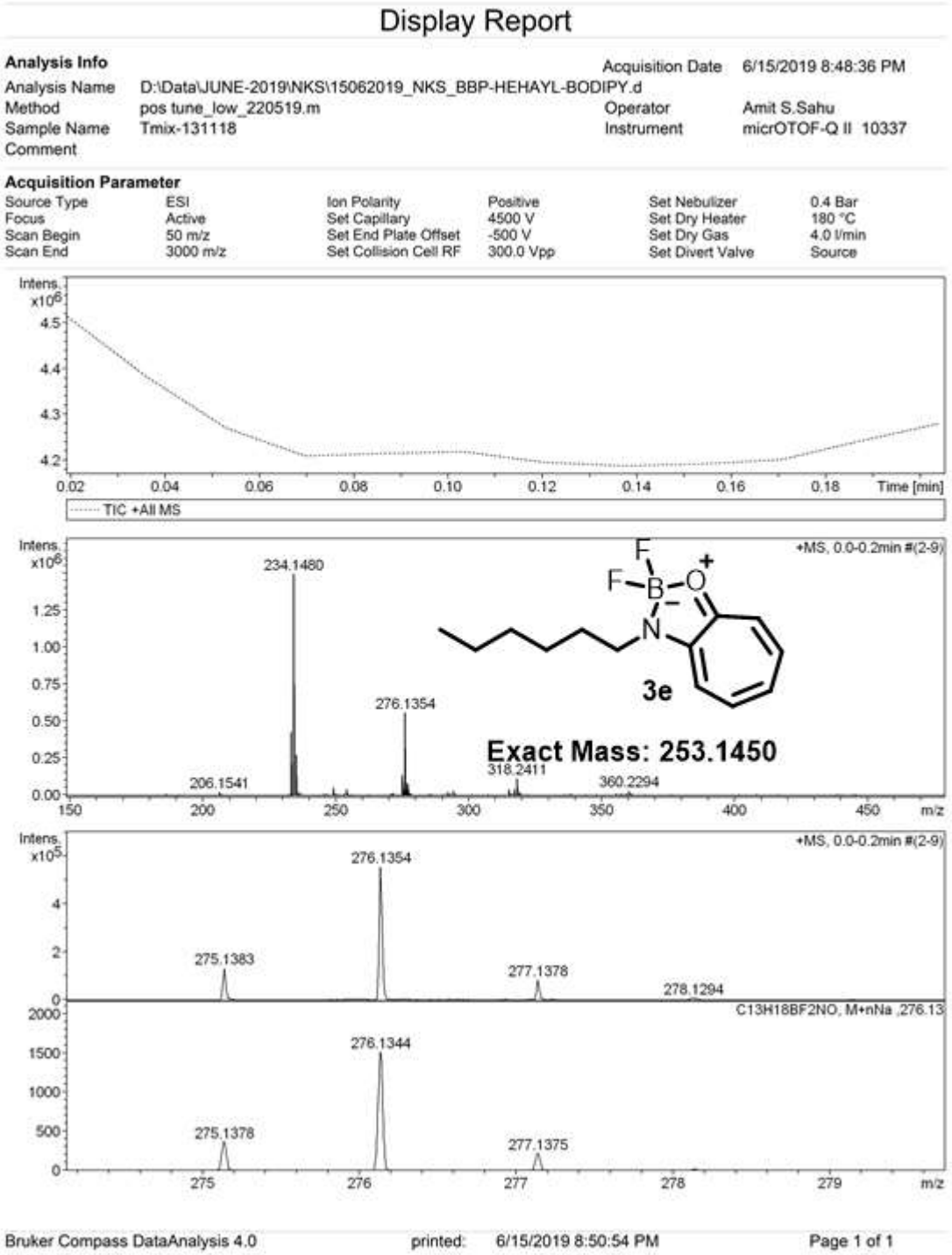

Figure A15. ESI/HRMS spectra of Boron complex **3e**.

6. (^{1}H, ^{13}C, ^{11}B, ^{19}F)NMR and HRMS spectra of compound **3f**:

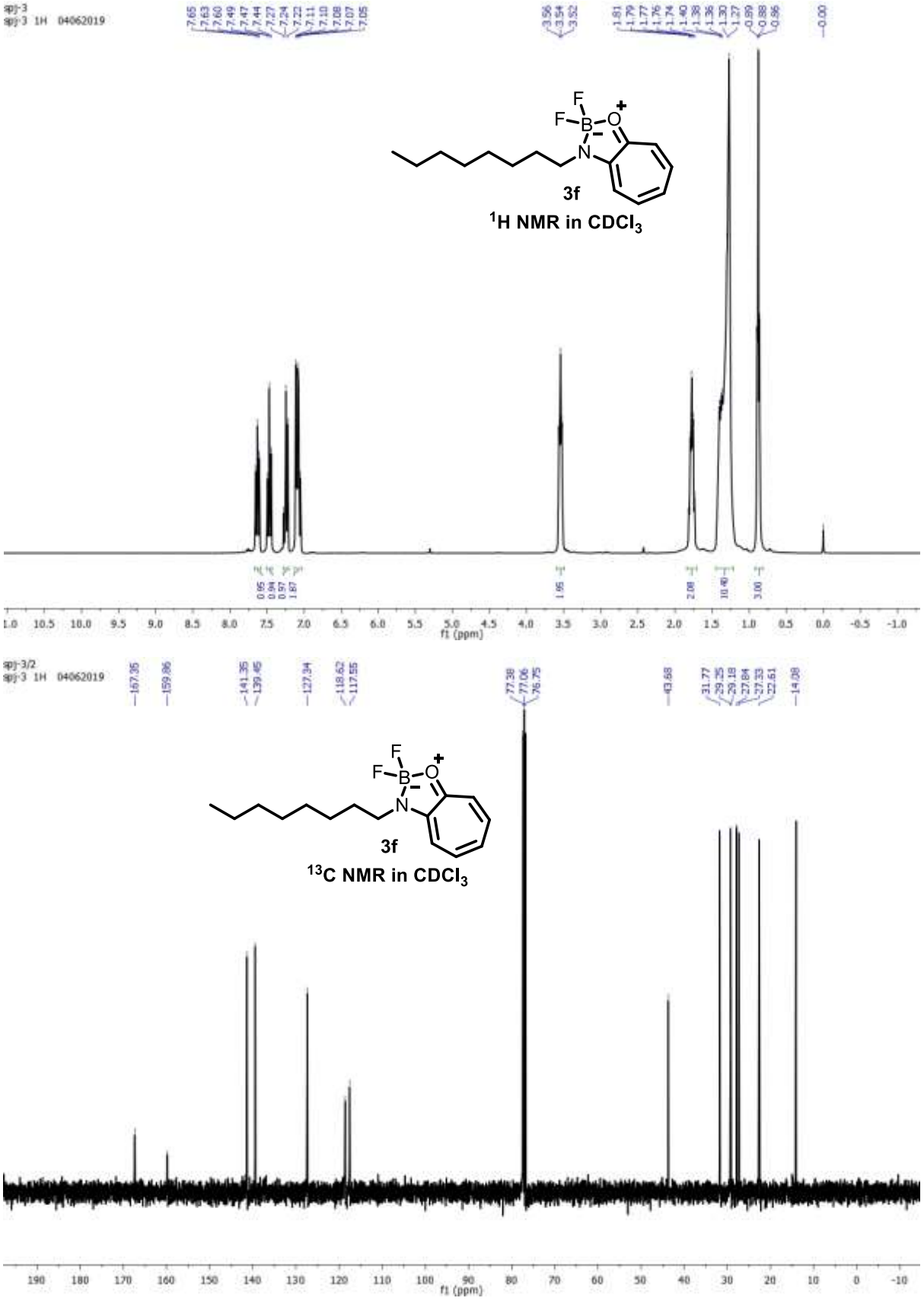

Figure A16. (^{1}H and ^{13}C) NMR spectra of Boron complex **3f** in $CDCl_3$.

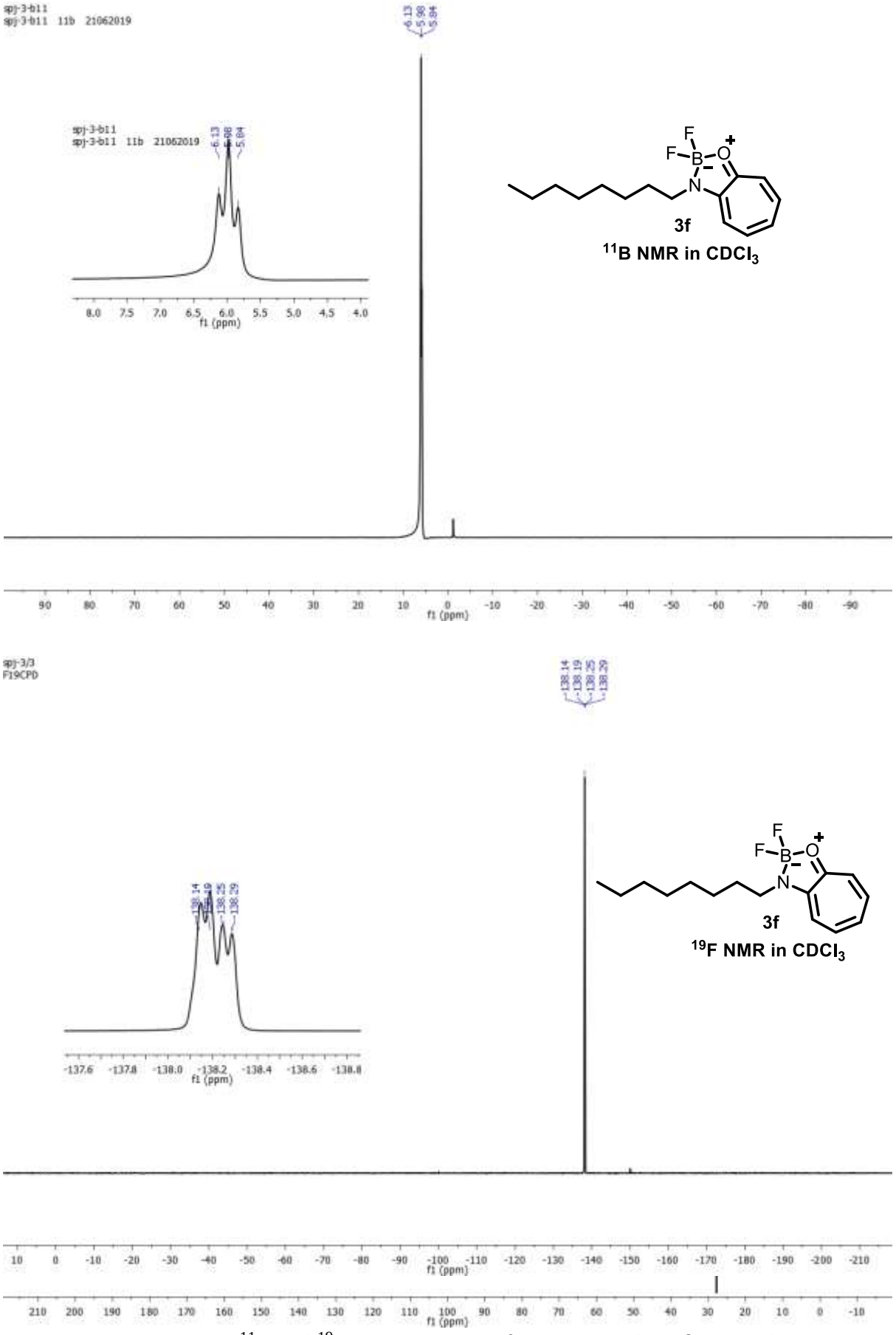

Figure A17. (^{11}B and ^{19}F) NMR spectra of Boron complex **3f** in $CDCl_3$.

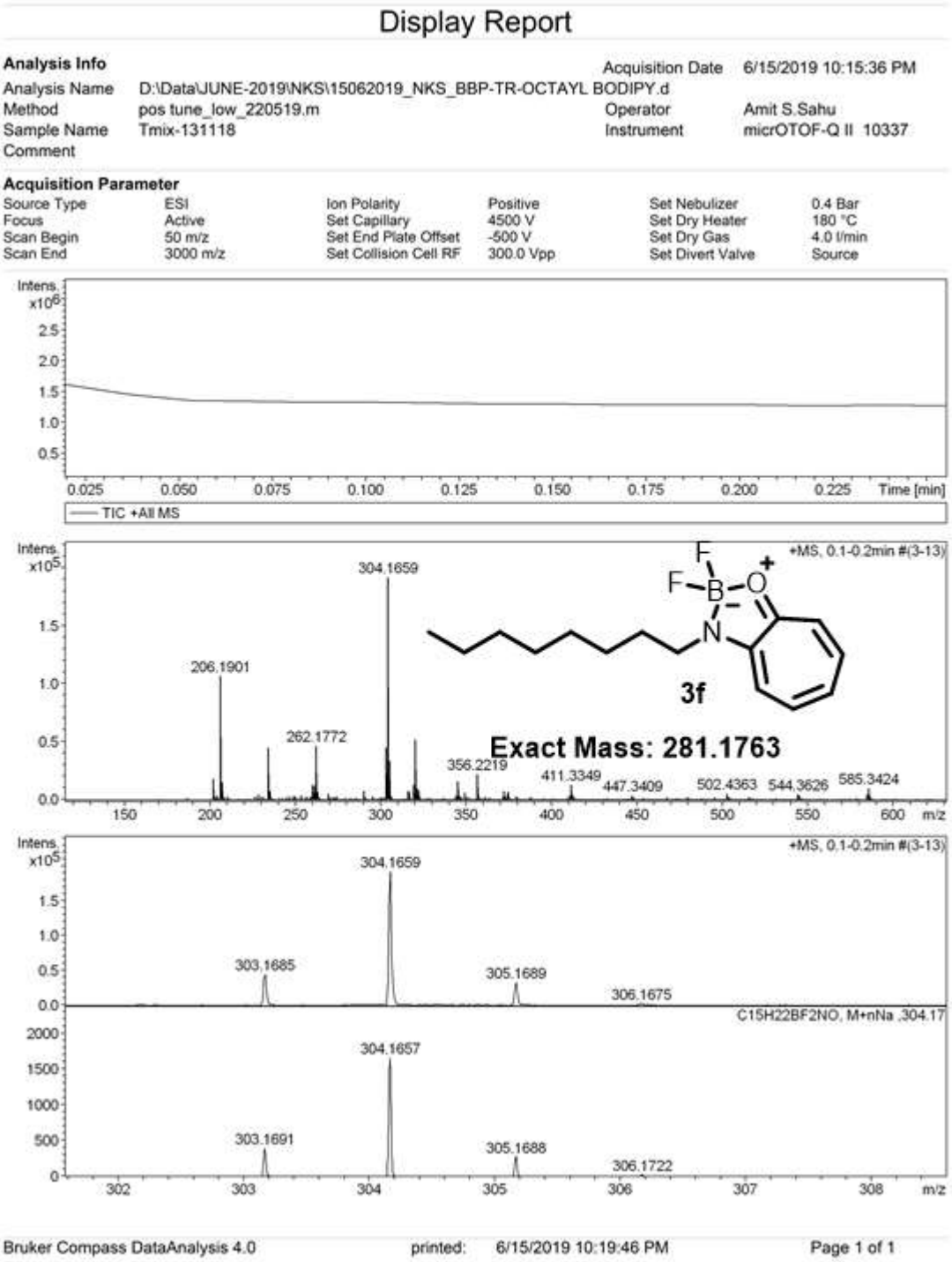

Figure A18. ESI/HRMS spectra of Boron complex **3f**.

7. (^{1}H, ^{13}C, ^{11}B, ^{19}F)NMR and HRMS spectra of compound **3g**:

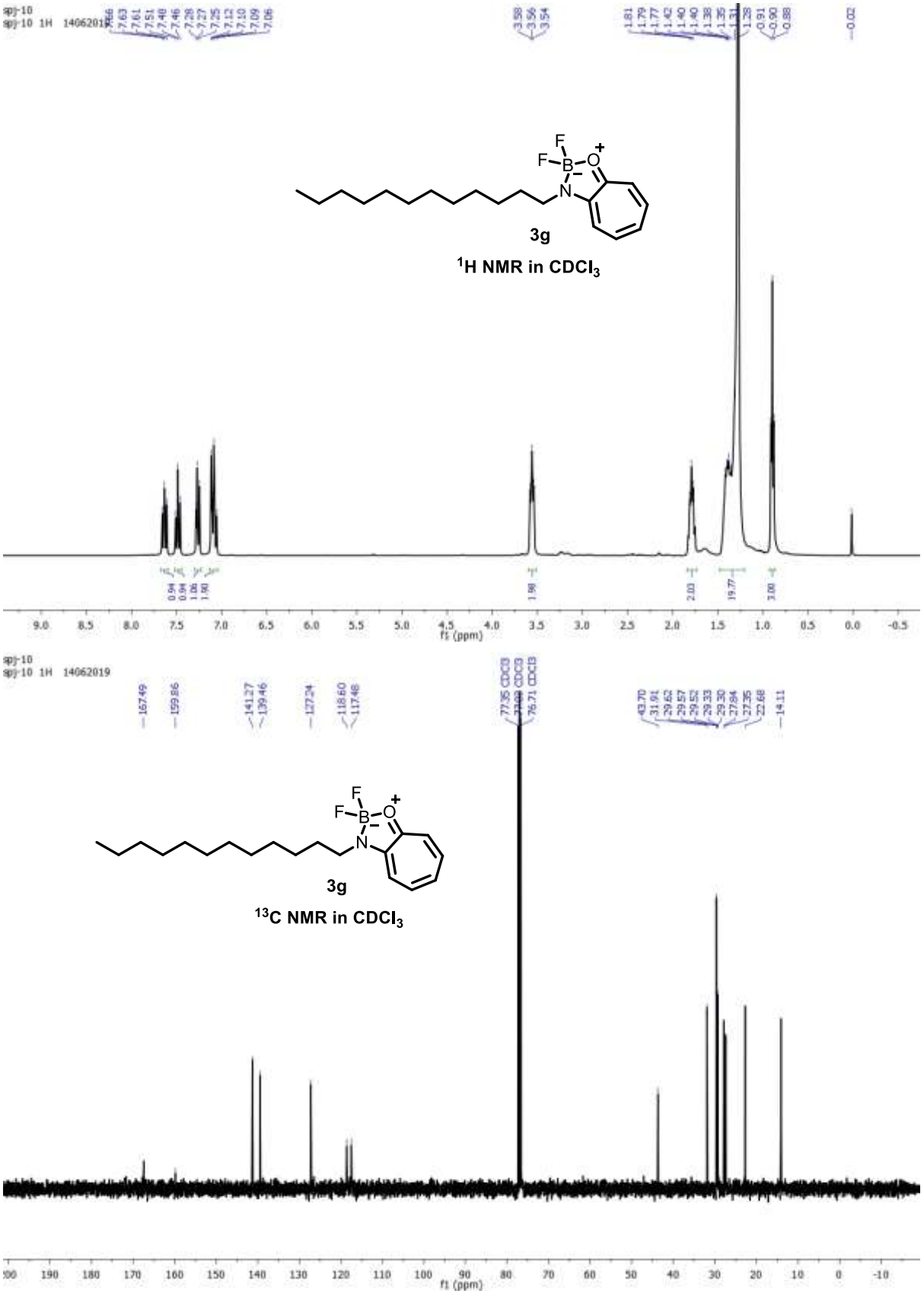

Figure A19. (^{1}H and ^{13}C) NMR spectra of Boron complex **3g** in $CDCl_3$.

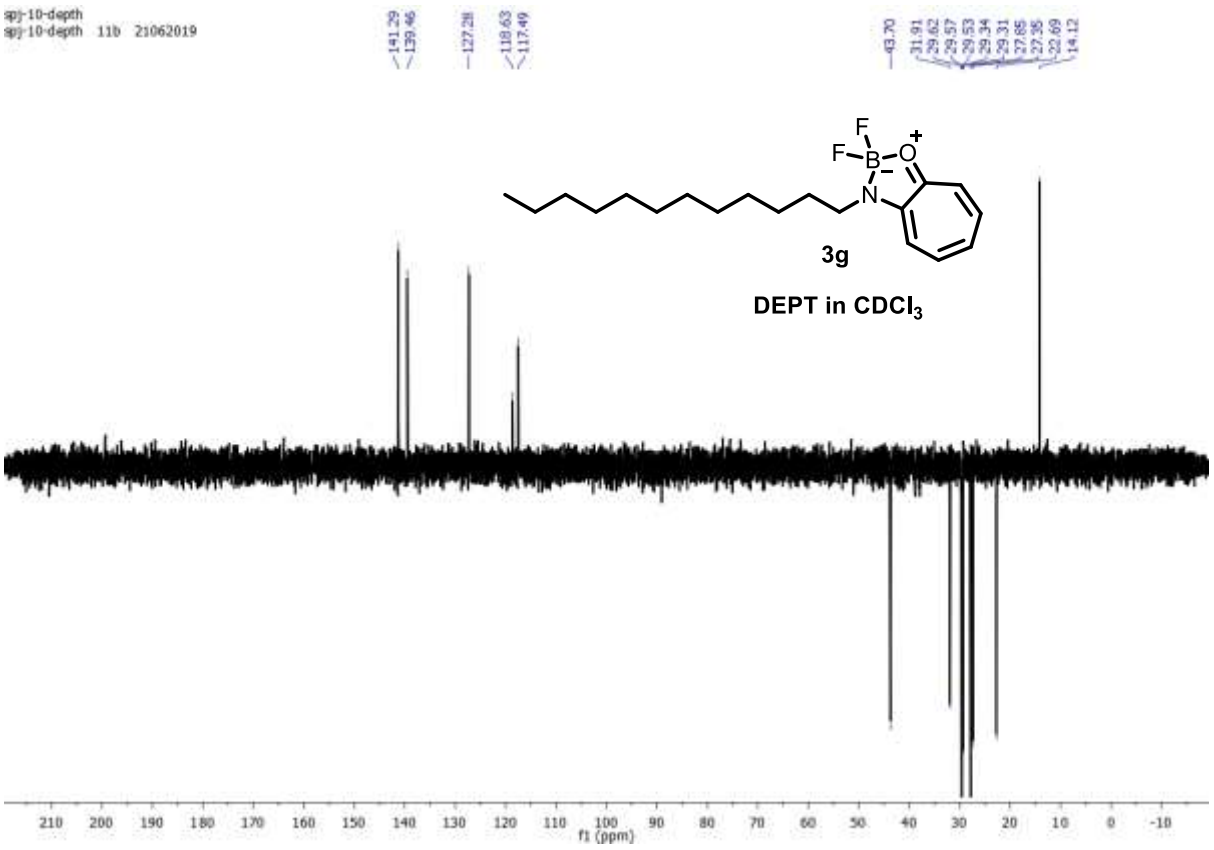
spj-10-depth
spj-10-depth 11b 21062019
141.29
139.46
127.28
118.63
117.49
63.70
31.91
29.62
29.57
29.53
29.34
29.31
27.85
27.35
22.69
14.12
F
F
B
O
N
3g
DEPT in CDCl3
210 200 190 180 170 160 150 140 130 120 110 100 90 80 70 60 50 40 30 20 10 0 -10
f1 (ppm)

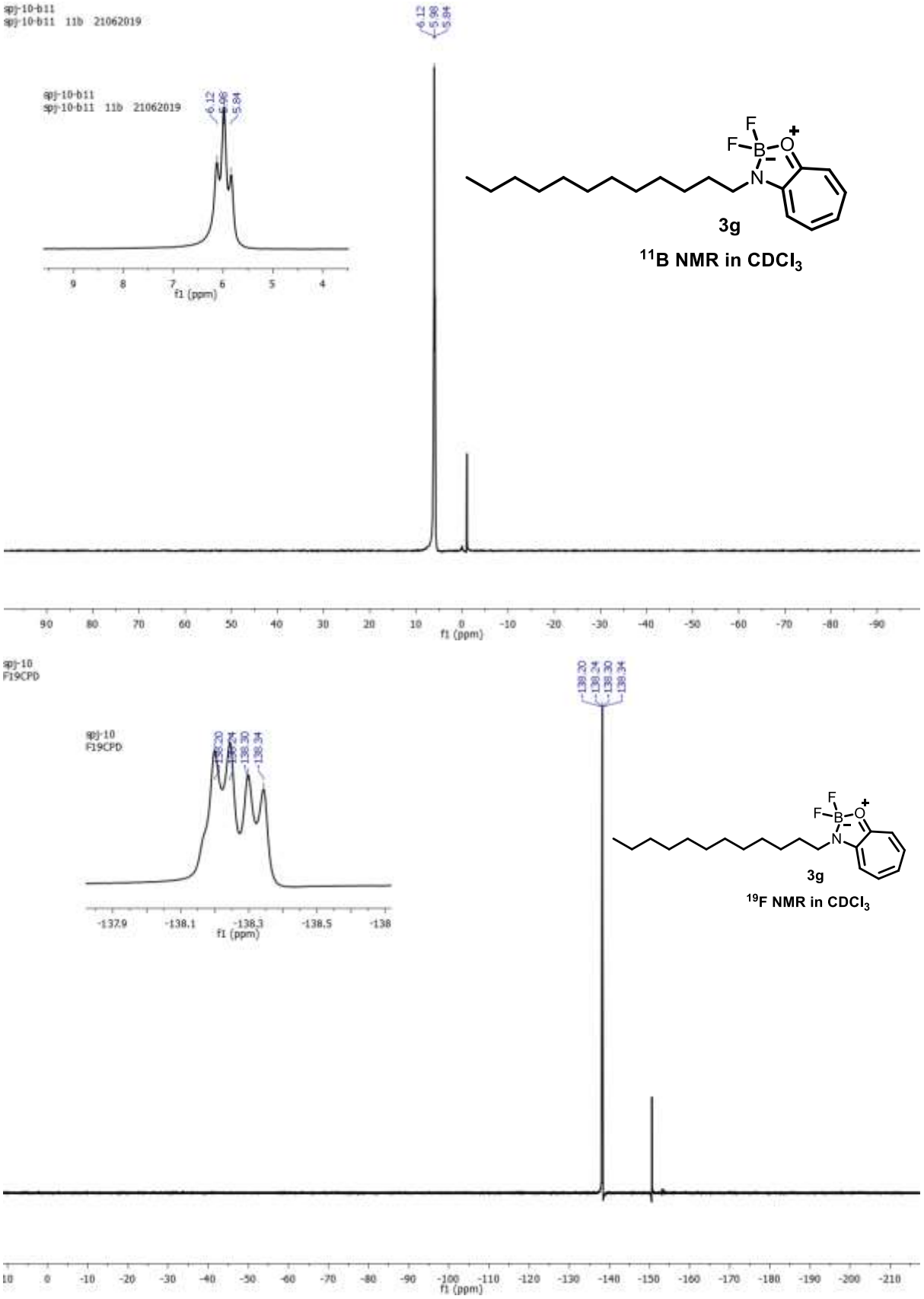

Figure A20. (^{11}B and ^{19}F) NMR spectra of Boron complex **3g** in $CDCl_3$.

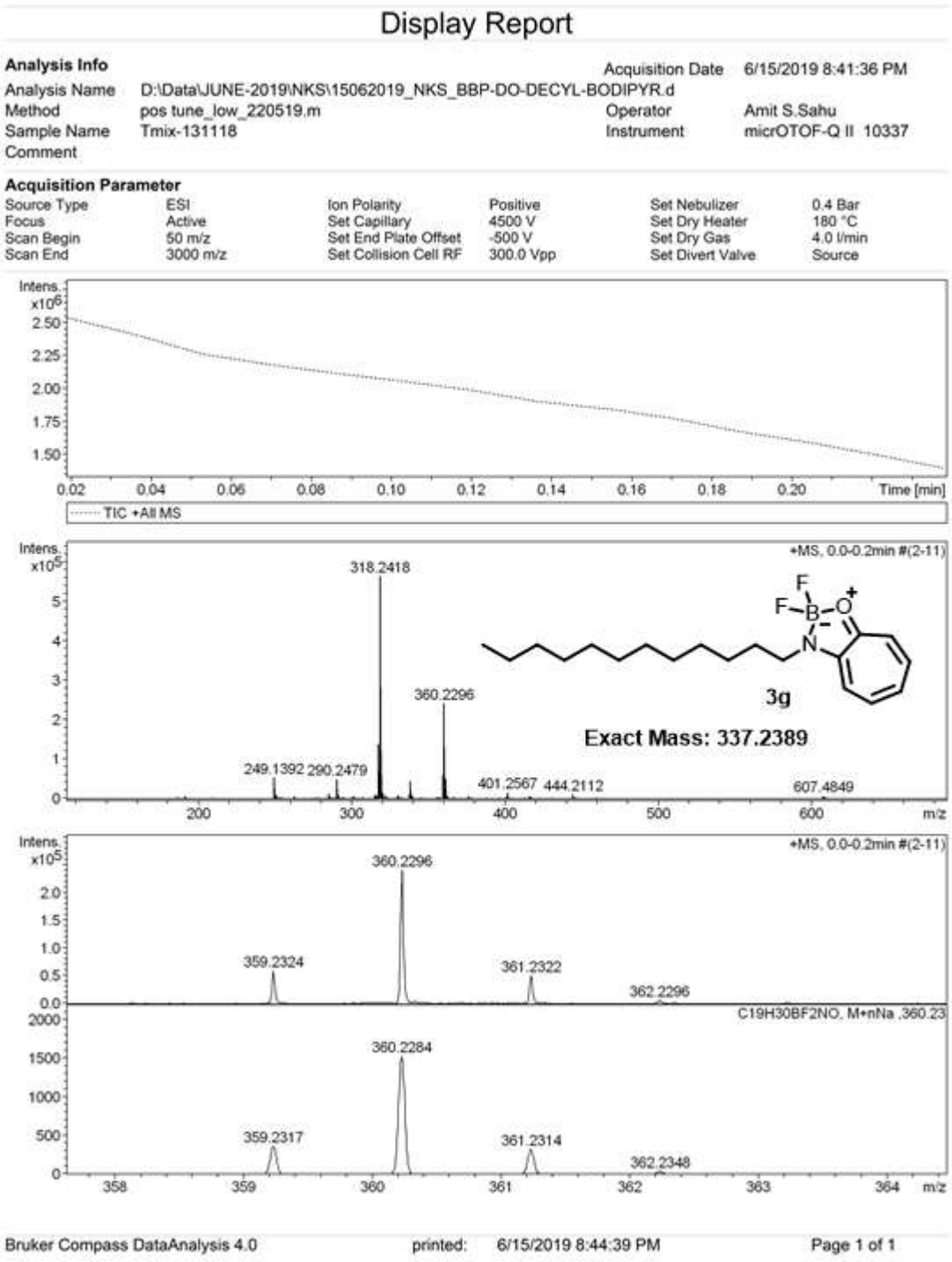

Figure A11. ESI/HRMS spectra of Boron complex **3g**.

8. (^{1}H, ^{13}C, ^{11}B, ^{19}F)NMR and HRMS spectra of compound **3h**:

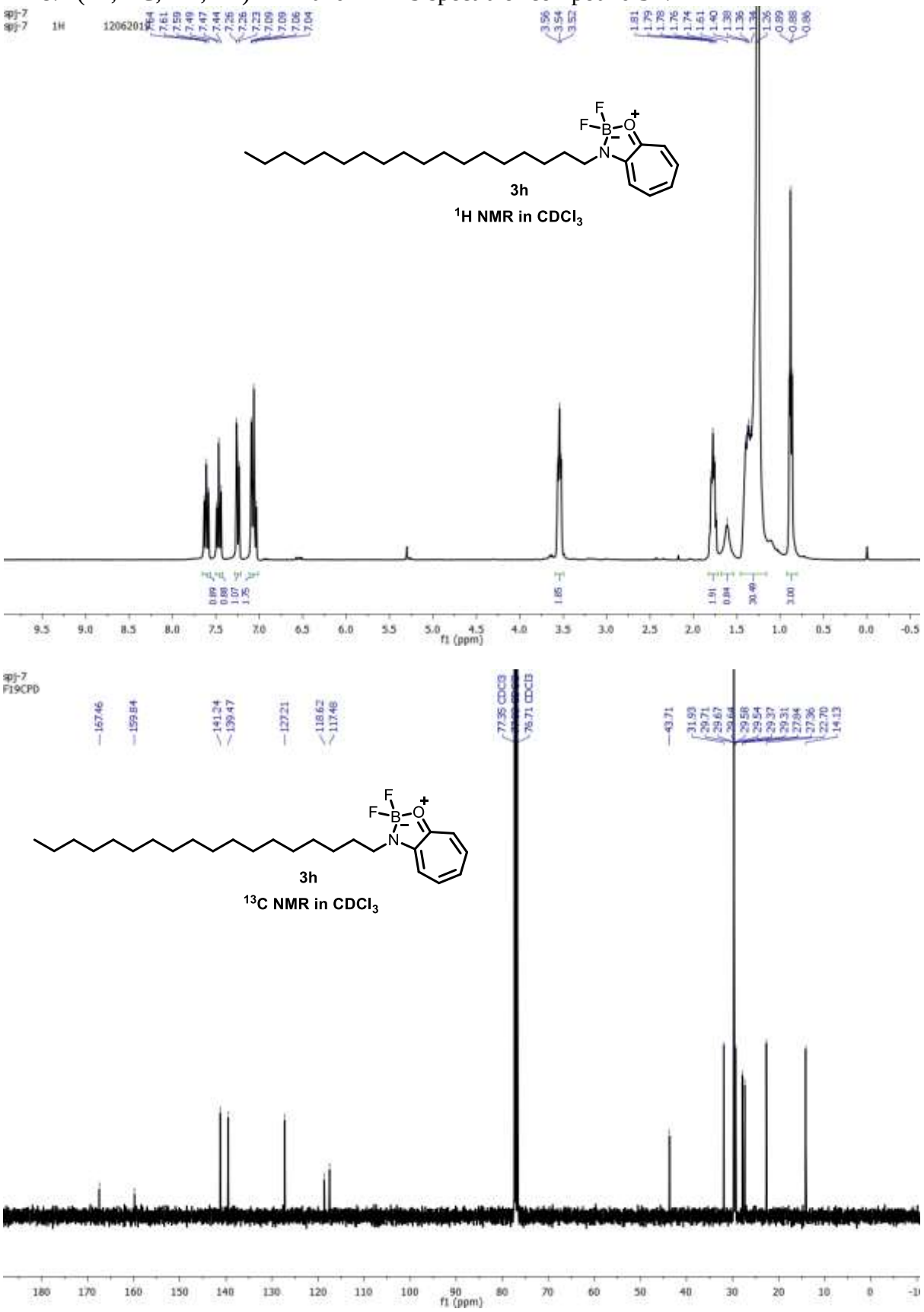

Figure A22. (^{1}H and ^{13}C) NMR spectra of Boron complex **3h** in $CDCl_3$.

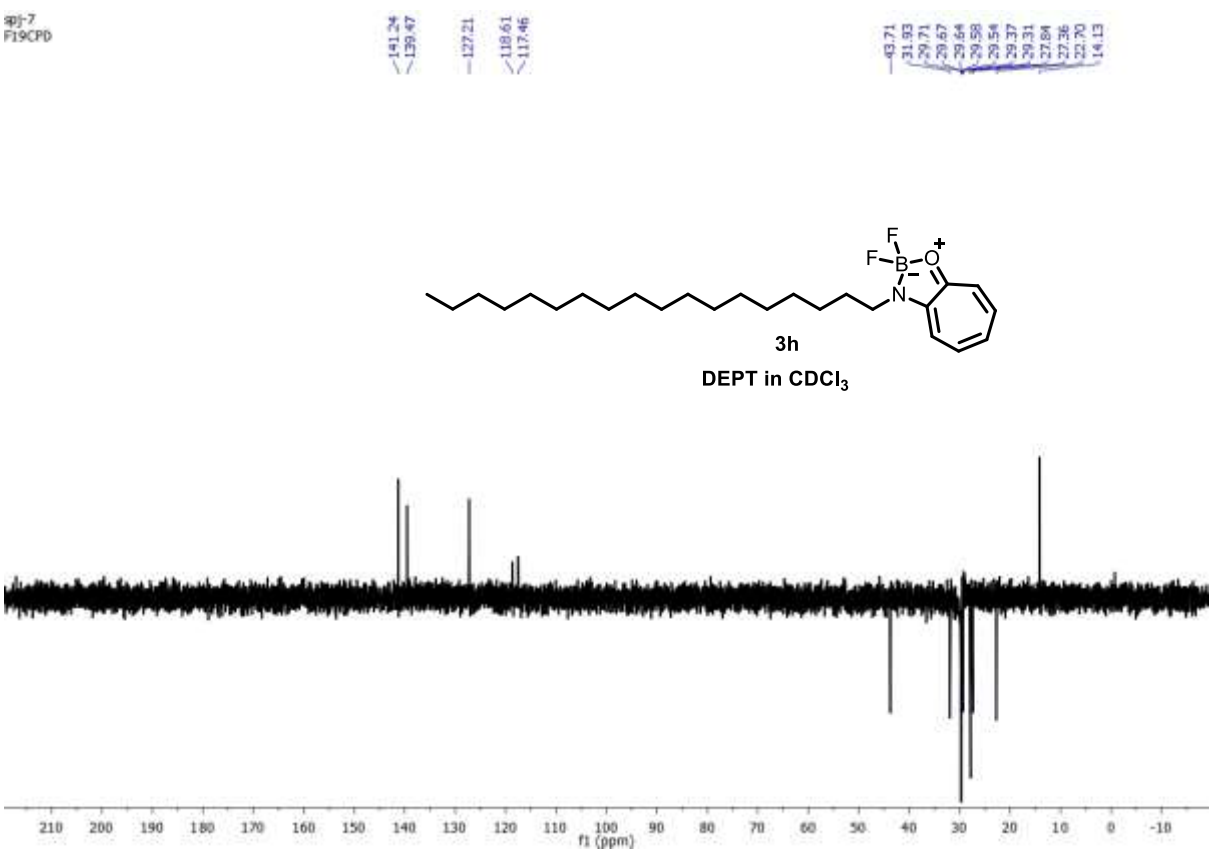
spj-7
F19CPD
141.24
139.47
127.21
118.61
117.46
63.71
31.93
29.71
29.67
29.64
29.58
29.54
29.37
29.31
27.84
27.36
22.70
14.13
F
F
B
O
N
3h
DEPT in CDCl3
210
200
190
180
170
160
150
140
130
120
110
100
90
80
70
60
50
40
30
20
10
0
-10
f1 (ppm)

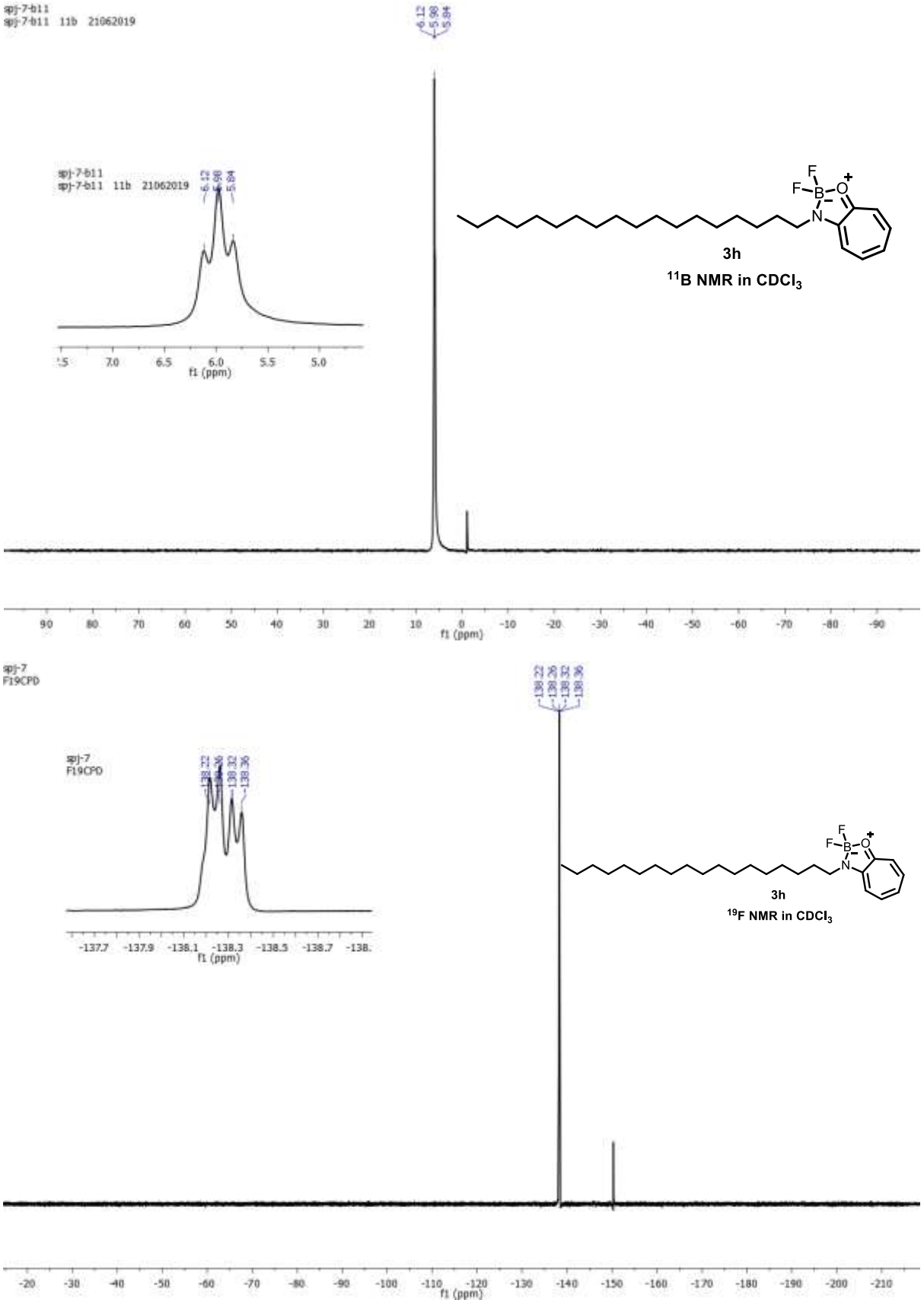

Figure A22. (^{11}B and ^{19}F) NMR spectra of Boron complex **3h** in $CDCl_3$.

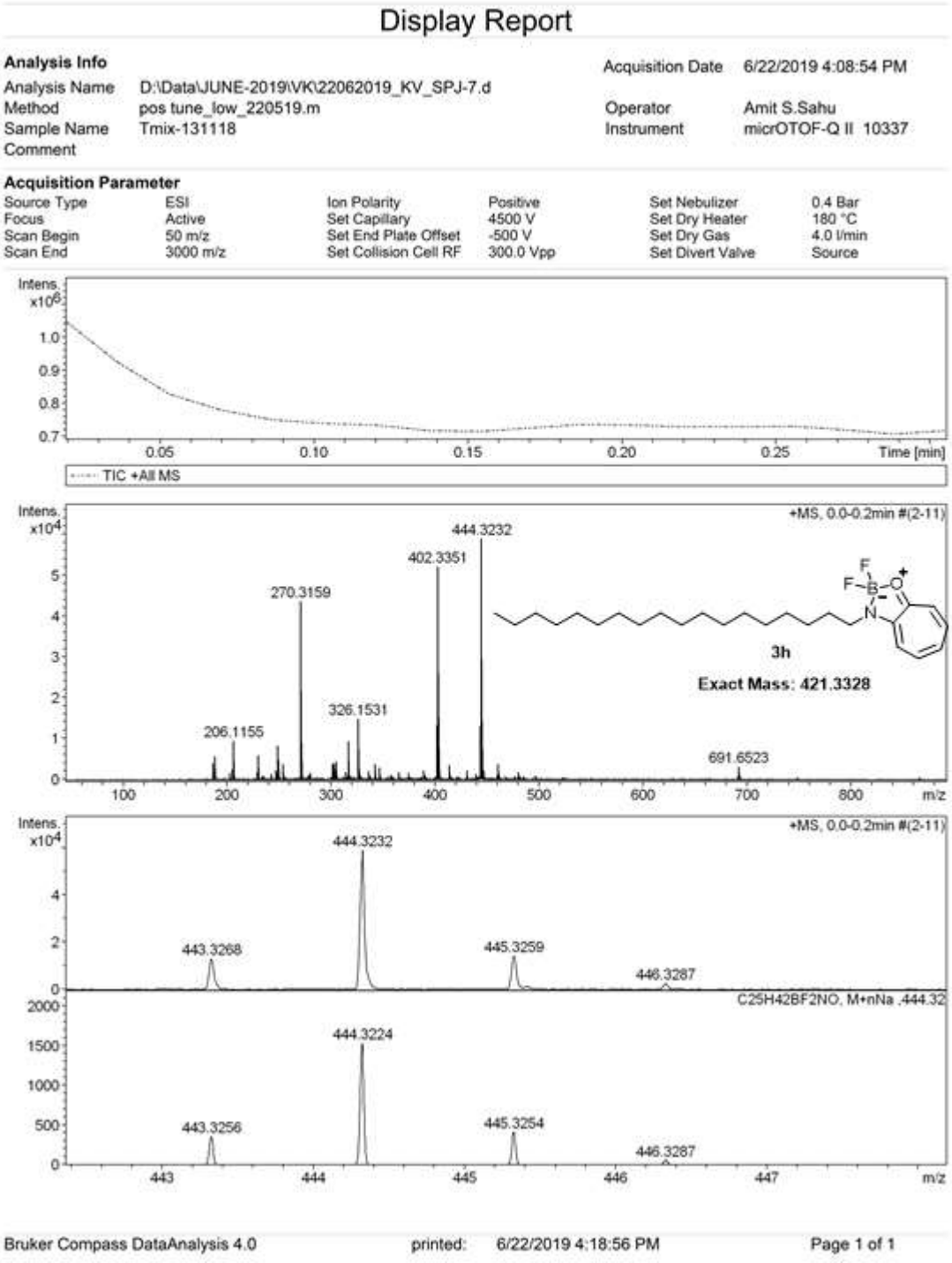

Figure A23. ESI/HRMS spectra of Boron complex **3h**.

9. Crystal structures and data

Good quality crystals of compounds were obtained in solvent mixture dichloromethane and hexane by slow evaporation method. The crystals data of all boron complexes were collected on a Rigaku Oxford diffractometer at 293 K respectively. Selected data collection parameters and other crystallographic results are summarized below. The program package SHELXTL1 and Olex2 was used for structure solution and packing diagram carried out by DIAMOND-3.2 software.

Table A1: Crystallographic table

compounds	**(3a)**	**(3b)**	**(3c)**	**(3g)**
Identification code	**3a**	**3b**	**3c**	**3g**
Empirical formula	$C_{11}H_{14}BF_2NO$	$C_{13}H_{16}BF_2NO$	$C_9H_7BF_2N_2O$	$C_{19}H_{30}BF_2NO$
Formula weight	225.04	251.08	207.98	337.25
Temperature/k	293(2)	293(2)	293(2)	293(2)
Crystal system	monoclinic	triclinic	triclinic	monoclinic
Space group	$P2_1/c$	P-1	P-1	$P2_1/c$
A/å	10.1369(9)	6.9250(2)	7.1208(4)	6.8771(4)
B/å	9.3670(8)	9.8929(4)	7.5780(7)	39.5578(19)
C/å	12.3745(11)	10.7904(6)	9.9731(7)	7.2722(3)
α/°	90	115.719(4)	92.671(7)	90
β/°	95.945(8)	105.120(4)	99.176(6)	100.825(5)
γ/°	90	93.044(3)	116.571(7)	90
Volume/$å^3$	1168.67(18)	631.08(5)	470.90(7)	1943.15(17)
Z	4	2	2	4
$\rho_{calc}g/cm^3$	1.279	1.321	1.467	1.153
M/mm^{-1}	0.102	0.102	0.123	0.082
F(000)	472.0	264.0	212.0	728.0
Crystal size/mm^3	0.002 × 0.002 × 0.001	0.002 × 0.001 × 0.001	0.002 × 0.001 × 0.0001	0.002 × 0.001 × 0.001
Radiation	MoKα (λ = 0.71073)	MoKα (λ = 0.71073)	MoKα (λ = 0.71073)	MoKα (λ = 0.71073)
2θ range for data collection/°	6.59 to 52.742	7.014 to 52.742	6.89 to 52.736	7.038 to 60.77
Index ranges	$-12 \le h \le 12$, $-11 \le k \le 11$, $-15 \le l \le 13$	$-8 \le h \le 8$, $-12 \le k \le 12$, $-13 \le l \le 13$	$-8 \le h \le 8$, $-8 \le k \le 9$, $-12 \le l \le 12$	$-8 \le h \le 9$, $-49 \le k \le 50$, $-9 \le l \le 9$
Reflections collected	10434	11895	8480	22042

Independent reflections	2387 [R_{int} = 0.0357, R_{sigma} = 0.0287]	2572 [R_{int} = 0.0218, R_{sigma} = 0.0170]	1920 [R_{int} = 0.0305, R_{sigma} = 0.0221]	4672 [R_{int} = 0.0349, R_{sigma} = 0.0256]
Data/restraints/parameters	2387/0/147	2572/0/163	1920/0/140	4672/0/218
Goodness-of-fit on f^2	1.231	1.173	1.050	1.030
Final r indexes [i>=2σ (i)]	R_1 = 0.0836, wR_2 = 0.2849	R_1 = 0.0517, wR_2 = 0.1367	R_1 = 0.0345, wR_2 = 0.0865	R_1 = 0.0540, wR_2 = 0.1343
Final r indexes [all data]	R_1 = 0.0997, wR_2 = 0.3071	R_1 = 0.0575, wR_2 = 0.1393	**3c**	R_1 = 0.0761, wR_2 = 0.1444
Largest diff. Peak/hole / e $å^{-3}$	0.99/-0.35	0.26/-0.19	$C_9H_7BF_2N_2O$	0.19/-0.14

10. Quantum Yield

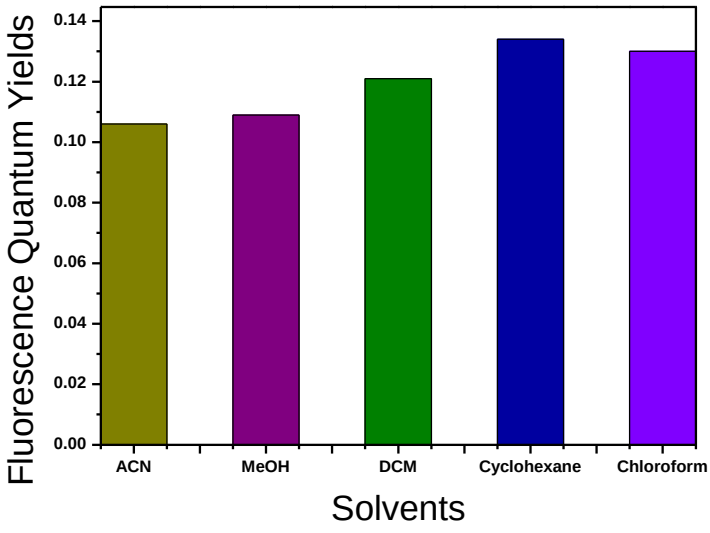

Figure A24. Bar diagram of quantum yield A) Boron complex (3a-h) and B) with difference solvent.

Table A4. Quantum yields of *boron-aminotropone* (3h).

solvents	λ_{abs} (nm)	Abs	λ_{em} (nm)	Stoke's Shift (nm)	OD/Abs (nm)	Φ_f
Methanol	334, 380	0.06085	417,438	104	334	0.10
Acetonitrile	335,380	0.07202	415,441	106	340	0.10
DCM	335,382	0.08749	416,443	108	346	0.12
Cyclohexane	337,385	0.08650	418,442	105	345	0.13
Chloroform	343,394	0.06974	431,556	113	346	0.13

All measurements and quantum yields were determined for boron-complex **(3h)** by considering quinine sulfate in 0.1 M H_2SO_4 as standard reference.

11. Solid fluorescence

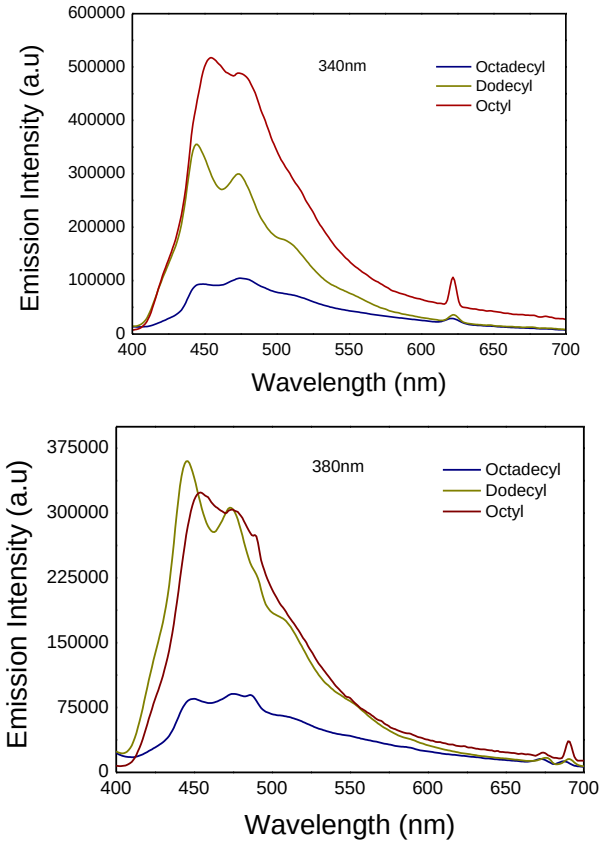

Figure A25. Solid emission spectra of born complex **3f**, **3g**, **3i**.

CHAPTER-4

Title: Synthesis and Biochemical Evaluation of *Troponyl* dihydropyrazine Molecules as DNA Binding Agents

4.1 Introduction

4.2 Objective of our work

4.3 Result and discussion

4.4 Conclusion

4..5 Experimental Section

4.6 Reference and Notes

4. 7 Appendix

4.1 Introduction

Pyrazine is a six-membered heterocyclic molecule, and its related derivatives are known bioactive natural products.[1] Pyrazine derivatives are extensively explored in the development of small molecule therapeutic drugs, including antiviral. For example, an antiviral drug Favipiravir has also been recommended as a drug for the recent pandemic viral disease COVID-19.[2, 3] Other pyrazine derivatives such as the benzopyrazine related molecules show unique physiochemical properties and have been employed for the generation of therapeutics drugs, dyes, and polymers. The benzopyrazine analogues are synthesized from tropolone as 2,3-dihydro-cycloheptapyrazine derivatives and these have not been much explored (Figure 1a). Tropolone is a non-benzenoid aromatic molecule that occurs in plants as a natural product.[4, 5]Tropolone related products have shown significant pharmacophoric behaviour as antimicrobial,[6] antifungal,[7] cytotoxicity on the tumor cells,[8] and inhibitory effect on metalloprotease.[9-11] Other derivatives of tropolone such as the 2-aminotropone analogues, cycloheptapyrazine derivatives, troponyl dihydrapyrazine molecules, have also shown remarkable biochemical activities such as tumor-specific cytotoxicity and type of cell death (Fig 1a).[12, 13] The synthesis of cycloheptapyrazine derivatives are accomplished from 2-aminotroponyl ethylamine under reflux conditions.[14, 15] Recently tropolone scaffold has been explored into unnatural peptides and DNA biomolecules which exhibit unique hydrogen bonding into peptides and pH-dependent fluorescence properties into DNA (Fig 1b).[16, 17] We have further improved the fluorescence properties by derivatizing tropolone into difluoro derivative as BODIPY analogues.[18, 19] Usually amide bonds are stable under mild acidic conditions. However, the amide bond containing N-troponyl alkyl glycinate residue is cleavable under mild acidic condition, even with 6% TFA in acetonitrile.[20, 21] The cleavage of such amides are demonstrated by the formation of cationic troponium lactone followed by

ketene intermediate. The formation of such ketene intermediate is previously reported from N-troponyl-N-alkyl glycinate (trag) ester derivative.[21]

4.2 Objective of our work

This chapter explains the unprecedented synthesis of carboxylate functionalized aryl troponyl dihydropyrazine molecule. In literature, the ketene intermediate is reportedly known to react with imine derivative via [2+2] cycloaddition under mild acidic conditions, leading to a β-Lactam adduct.[22-24] We attempted to trap that troponyl ketene intermediate of trag ester with imine through [2+2] cycloaddition reactions under acidic conditions. Interestingly all the newly synthesized dihyropyrazine compounds are fluorescent in nature. We have further studied their photophysical properties.

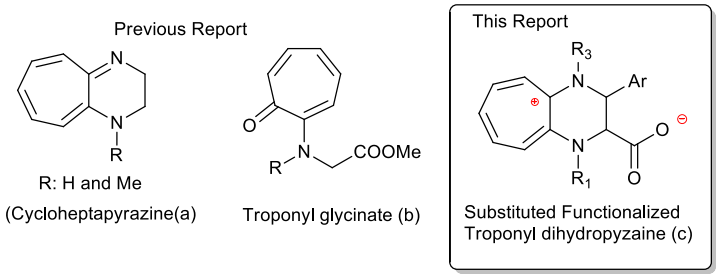

Figure. 4.1 Chemical structure of troponyl derivatives

Interestingly, herein, we have isolated a new adduct as aryl-substituted troponyl dihydropyrazine derivatives from N-troponyl alkyl glycinate and imine derivative under acidic conditions (Fig 1c). So far there is no such report about the formation of dihydropyrazine from imine derivatives. This report describes the synthesis, mechanistic studies of product formation, and structural features of newly synthesized dihydropyrazine derivatives. For biological importance, we examined the inhibition of cancerous cell proliferation with

representative troponyl dihydropyrazine molecule by MTT-assay. Thus, these pyrazine derivatives are potential fluorescent therapeutic drug candidates.

4.3 Result and discussion

We began the synthesis of unnatural amino acid derivative as N-troponyl-N-alkyl glycinate derivative from commercially available Tropolone molecule (Scheme 1). The tropolone (**1**) was derivatized into tropolonyl tosylate, and then employed for N-troponylation with N-Phenylethyl glycinate ester under reflux condition by following the reported procedure to produce an unnatural troponyl amino acid derivative as N-troponyl-N-phenylethyl glycinate (**tr-pheneg**) methyl ester (**2**).[21] We also prepared imine derivatives (**5**) from substituted benzaldehydes (**3**) and N-alkyl amines (**4**) by using the reported procedure.[25] These imines were purified and characterized by ^{1}H-NMR/ESI-Mass before using in the next steps. In our previous report, troponyl alkyl glycinate ester forms ketene intermediate through the formation of cationic troponium lactone (CTL) under mild acidic conditions (5% TFA in ACN).[21] Herein we also treated tr-pheneg ester (**2**) with TFA (5.0% in ACN) to generate troponyl ketene intermediate as **2-OEt**, by elimination of ethanol (EtOH) through the formation of CTL. The freshly prepared imine derivatives were added to that ketene (**2-OEt**) containing reaction mixture. After completion of the reaction, we isolated new compounds after column purification and characterized them by ^{1}H-/^{13}C-NMR/ESI-HRMS techniques. Their analytical data are provided in the Supporting Information (Figure A1-S36). In the case of imine **5a**, prepared from benzaldehyde (**3a**) and benzylamine (**4a**), we isolated a new compound from that ketene (**2-OEt**)**,** and their NMR/Mass analytical data support the formation of an adduct containing phenyl and benzyl residues of imine (**5a**). It could be β-Lactam derivative (**6***) because of [2+2] cycloaddition reaction between ketene (**2-OEt**) and imine (**5a**). However, the characteristic ^{13}C-NMR peak of troponyl carbonyl, tr-C=O (~δ182.0ppm) disappeared in the

new product **6a**. Importantly, its ^{13}C-NMR exhibit two new peaks at ~δ150.0 ppm & ~δ152.0 ppm along with carboxylate carbonyl (-COO) at ~δ170ppm (Table A1, Entry 1). In the previous report, **tr-pheneg**) methyl ester (**2**) forms cationic troponium lactone (CTL) intermediate under similar acidic conditions which have characteristic ^{13}C-NMR peaks of troponyl residue at ~δ150.0ppm & ~δ152.0ppm, at expense of troponyl carbonyl tr-C=O peak at ~δ182.0ppm.[21] Thus, our isolated product is not a β-lactam derivative (**6***). We repeated a similar reaction with **tr-pheneg** methyl ester (**2**) with different imines (**5**) under similar conditions and then isolated respective compounds as N-alkyl-N-phenylethyl aryl substituted troponyl dihydrapyrazine derivatives. Their purified products were characterized by NMR/Mass as dihydrapyrazine derivatives **6b-6o** (Scheme 4.1) from respective imines (**5**). N-Benzyl-N-phenylethyl aryl troponyl dihydropyrazine compounds (**6b/6d-6g/6m-6o**) are prepared from benzyl amine containing imines of different arylaldehydes. N,N'-biphenylethyl aryl troponyl dihydropyrazine compounds (**6c**) are prepared from imine (5) containing phenylethy amine and 4-nitrobenzaldehyde. N-alkyl-N-phenylethyl aryl troponyl dihydropyrazine compounds (**6h-6l)** are prepared from respective imines (**5**) containing alkyl amine and arylaldehydes. Their ^{13}C-NMR spectra also exhibit the disappearance of troponyl carbonyl like **6a**. Their comparative ^{13}C-NMR are provided in Appendix Table A1 (Entry 2-16).

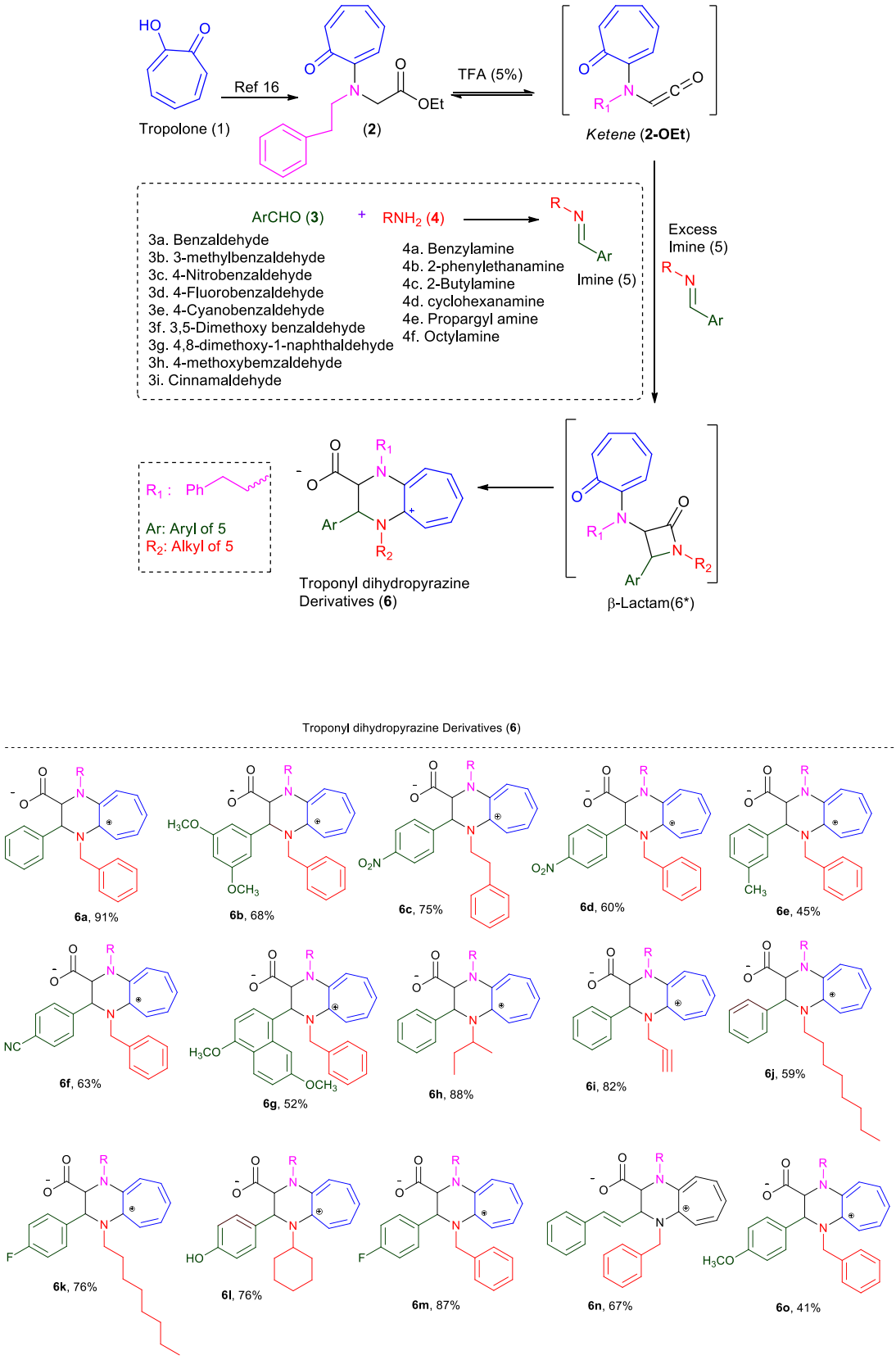

Scheme 4.1. Syntheses of aryl substituted troponyl dihydropyrazine compounds

Herein we have obtained the single crystal of *tr-pheneg* ester (**2)** and studied them by X-ray diffractometer. Its ORTEP diagram is depicted in below (Figure. 2A), while other crystal parameters are provided in Appendix (Table A1). We also submitted its X-ray data to Cambridge crystallographic data centre (CCDC) with number 2035166. This X-ray analysis confirms the structure of *tr-pheneg* ester (**2)** for comparative structural studies of troponyl ring with troponylated derivatives. We have also obtained the single crystal of troponyl dihydropyrazine derivative **6a/6d/6k** and studied by X-ray diffractometer analyses**.** Their ORTEP diagrams are depicted in **Figure 4.2**, and other crystal parameters are provided in Appendix (Table A3/A4/A5). We also submitted their X-ray data to CCDC with number 1889119 for compound **6a**, 2035165 for compound **6d** and 2035167 for compound **6k.** Their X-ray analysis confirm their structure as carboxylate functionalized aryl substituted troponyl dihydrapyrazine derivatives- **Figure 4.2 B** for compound **6a**, Figure 4.2C for compound **6d** and Figure 4.2C for compound **6k.** These crystal structure reveal that the orientation of carboxylate is *trans* (opposite) to the aryl group (aryl aldehyde residue) in troponyl dihydropyrazine ring. For comparative studies of troponyl ring in *tr-pheneg* ester (**2)** and troponyl dihydropyrazine derivatives **(6),** we extracted C-C bond lengths of troponyl ring for both compound **2** and compound **6a/6k/6d** (Figure 4.2e & Figure A40). The C6-C7 bond length of troponyl ring of troponyl dihydropyrazine derivative (**6a**) are relatively longer than *tr-pheneg* ester (**2)**'s C6-C7 bond length while other C-C bond lengths are almost same (Figure 4.2E). The increase in bond length could be possible due to the accumulation of positive charge that occur on C1 and C7 of troponyl residue in troponyl dihydropyrazine derivative **6a**. In literature, the increase in bond length is attributed to the accumulation of high positive residual charges at vicinal carbons and it has been theoretically calculated in aminotroponiminium derivative.[26] The C-C bond length of troponyl ring is consistent with the other two troponyl dihydropyrazine derivative **6d/6k** crystal structure.

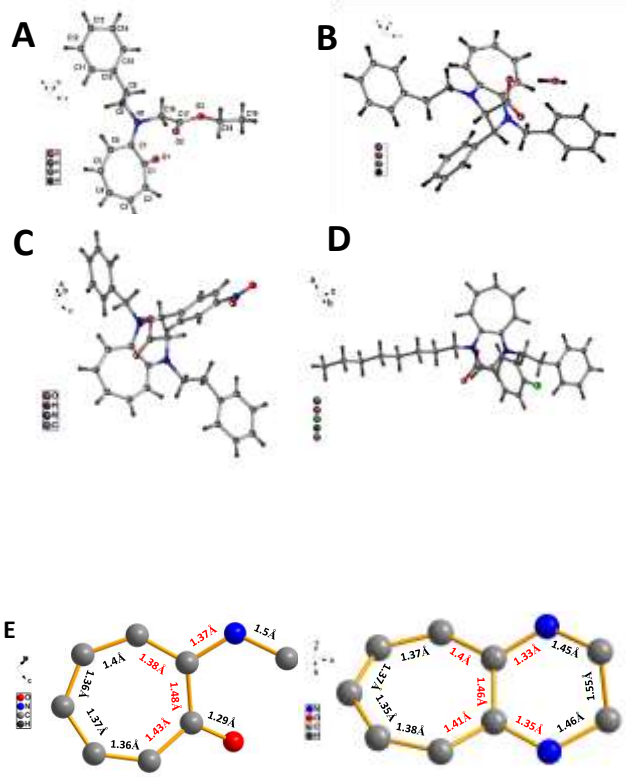

Figure 4.2 ORTEP diagram of cyclohetapyrazine derivatives: A. Compound 2; B. Compound 6a; C. Compound 6d; D. Compound 6k; and E. C-C bond length comparison of troponyl ring ester and dihydrapyrazine

For mechanistic studies, we monitored the progress of pyrazine derivative formation by ^{1}H-NMR (Figure A41-42). We recorded time-dependent ^{1}H-NMR spectra of tr-pheneg ester (**2**) after addition of TFA (6% in $CDCl_3$)) and then imine. We noticed the α-CH_2 of compound **2** (δ4.3ppm, singlet)) is shifted to downfield at δ4.5 ppm (singlet) after the addition of TFA. After the addition of imine, we noticed the appearance of an additional peak at δ4.6ppm (singlet) just after 30 minutes, and its peak intensity progressively increased with respect to time at the expense of other peaks (δ4.5ppm, singlet) depletion. Apparently, the remarkable downfield

shift of α-CH_2 occurs due to the formation of a new intermediate with TFA and then the formation of troponyl dihydrapyrazine adduct with imine.

Further, this reaction was monitored by UV-Vis studies to propose the mechanism. Since tropolone derivative and imines are excellent chromophores. Thus we monitored the reaction progress by UV-Vis spectrophotometer (Fig S43/S44). The Trag ester (**2a**) exhibits characteristic peaks at ~$\lambda_{250nm,}$ ~λ_{360nm} & ~λ_{420nm} while aryl imine shows a peak at ~λ_{260nm}. The UV-spectra of isolated characterized product (**6a**, dhydroipyrazine derivative) exhibit peaks at λ_{270nm}, λ_{370nm} & λ_{460nm}, significantly red-shift to tr-pheneg ester (**2)**. Time-dependent UV spectra of tr-pheneg ester (**2)**, and imine were recorded in the presence of TFA (6%) (Fig S43). Like the previous report, new peaks appeared at ~λ_{380nm} after treatment with TFA, possibly because of the formation of reactive troponium cation lactone (CTL), and ketene.[21] After mixing with imine (**5a**), the new additional peak appeared at λ_{270nm}, and their intensities decreased with the progress of time. We assume that CTL intermediate forms ketene and further reacts with imine through 2+2 cycloaddition reaction as β-lactam. This lactam further rearranges into stable troponyl dihydropyrazine derivative (**6a**).

Herein, we propose the reaction mechanism for the formation of carboxylate functionalized aryl-substituted troponyl dihydrapyrazine derivative from troponyl amino acid derivative (2) and freshly prepared imine (benzaldehyde-amine) under mild acidic conditions (Figure. 3). We assume that tr-pheneg ester (2) forms cationic tropolium lactone (CTL) reactive species (2') and then ketene (2") under mild acidic conditions (6% TFA in ACN). The formation of such lactone and ketene are previously demonstrated from troponyl alkyl glycinate derivative under mild acidic conditions (6% TFA in ACN).[21] In literature, the ketene intermediate is reportedly known to react with imine derivative to produce new adduct via [2+2] cycloaddition under mild acidic conditions.[22-24] We propose that ketene (2") reacts with imine (5) via [2+2] cycloaddition reaction and produces β-lactam derivative (6'). In next step, this β-lactam

derivative (6') forms α-substituted CTL-reactive species (6") by cleavage of lactam amide bond. This intermediate reacts with the amine group intramolecularly and leads to the stable dihydrapyrazine compound (6) after rearrangement **Fiure4.3**.

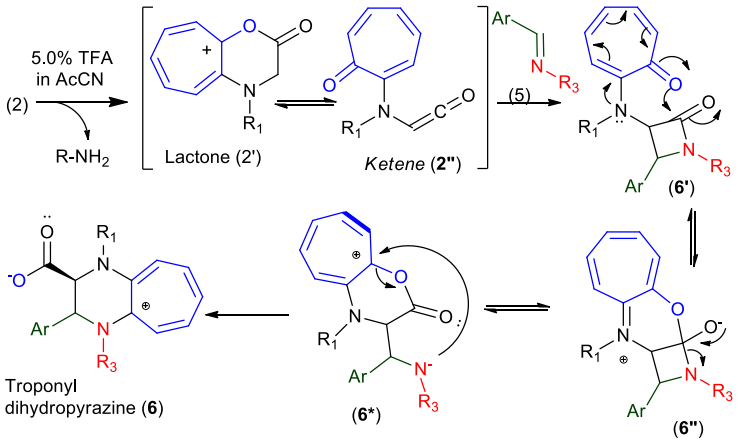

Figure 4.3. Plausible mechanism for synthesis of dihydropyrazine derivatives.

We recorded the absorption and emission spectra of representative compounds (**6a**/**6e**/**6j**/**6n)** with different concentration of *ct*-DNA near physiological conditions (pH 7.1 at room temperature). Their spectra are provided in **Figure 4.4**. The absorption spectra of compound **6a** exhibits hyperchromicity at wavelength 260nm (λ_{260nm}) with isosbestic point λ_{300nm} by increasing the concentration of *ct*-DNA (**Figure 4.4 A**). The emission spectra of compound **6a,** at excitation wavelength 440nm ($\lambda_{ex.440nm}$), exhibit the enhancement of compound **6a** fluorescence intensity at emission wavelength 520nm ($\lambda_{em.520nm}$) with increasing the concentration of DNA (**Figure 4.4 B**). Other compounds 6**e/6j/6n** also exhibit the similar absorption hyperchromicity (~λ_{260nm}) and fluorescence enhancement (~$\lambda_{em.520nm}$) with increasing the concentration of *ct*-DNA at pH7.0 (**Figure 4.4**). These result support the significant interactions of troponyl dihydropyrazine derivatives with DNA duplex structure.

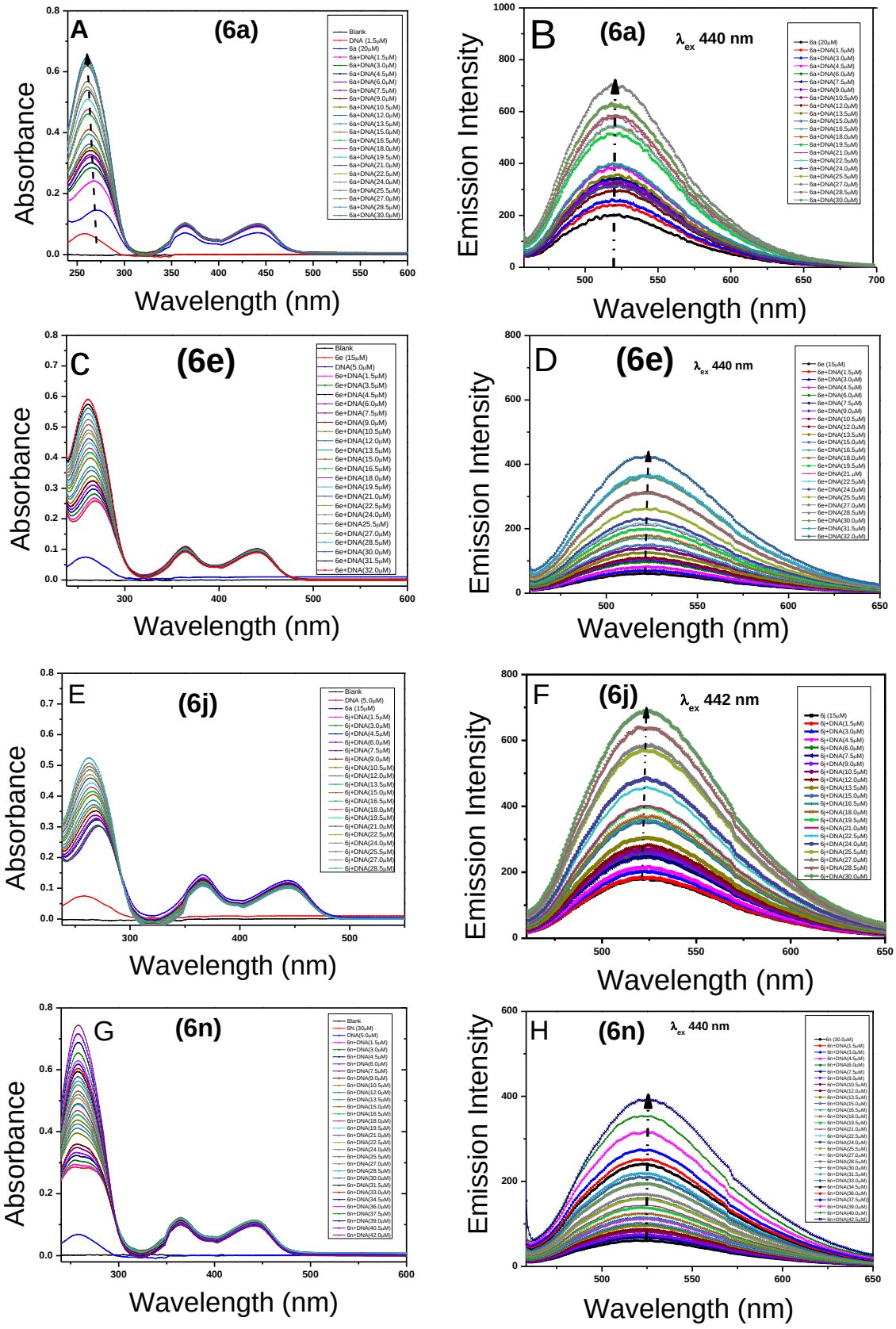

Figure 4.4. UV-Vis and Fluorescence spectra of *Troponyl dihydropyrazine* derivatives (**6a/6e/6j/6n)** under different concentration of DNA at pH 7.0 (Room temperature).

Generally small molecules bind with DNA duplex mainly through two modes: (1) Intercalation by planer molecules and (2) Groove binding by non-planer molecules. For example, ethidium bromide (EtBr) bind with DNA duplex through nucleobase intercalation while Hoecst dye binds through groove binding modes. Importantly, both complexes DNA:EtBr and DNA:Hoecst complexes exhibit enhanced fluorescence characters after binding with DNA duplexes, and considered as DNA markers, though their binding modes are quite different. Herein, the crystal structures of representative troponyl dihydropyrazine derivative shows that their structures are the non-planer, so they may bind with DNA duplex through the grove binding mode. For comparative studies, we recorded the absorption and emission spectra of *ct*-DNA:EtBr and *ct*-DNA:Hoecst complexes with or without troponyl dihydropyrazine derivative (**6a**). We notice that the fluorescence intensity of DNA:EtBr and *ct*-DNA:Hoecst complexes enhances with increasing the concentration of compound **6a**. These studies reveal the strong interaction of compound **6a** with *ct*-DNA even in presence of EtBr and Hoecst in respective binding sites (intercalation/minor groove) of *ct*-DNA duplex. Hence, troponyl dihydopyrazine derivatives presumably bind with the major groove of *ct*-DNA duplex.

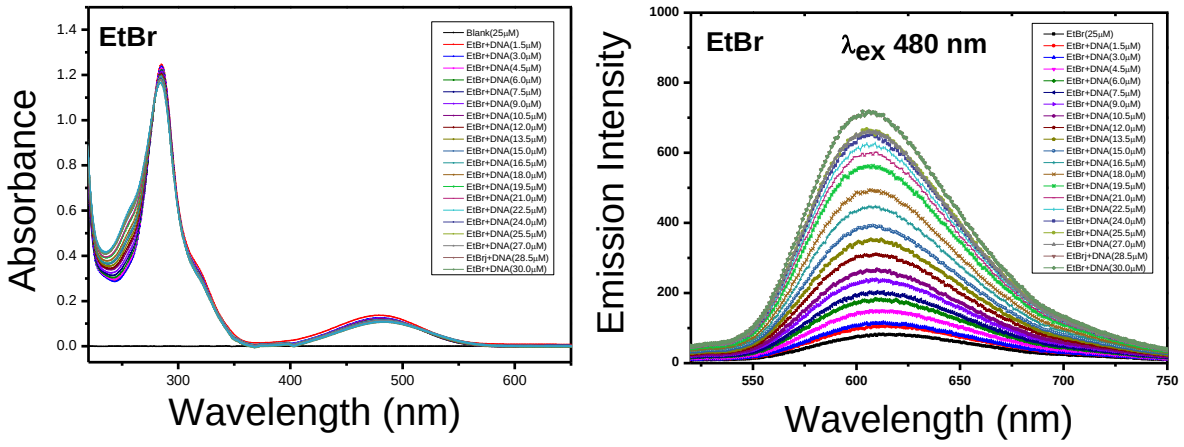

Figure 4.5. UV-Vis and Fluorescence spectra of EtBr under different concentration of with ct-DNA.

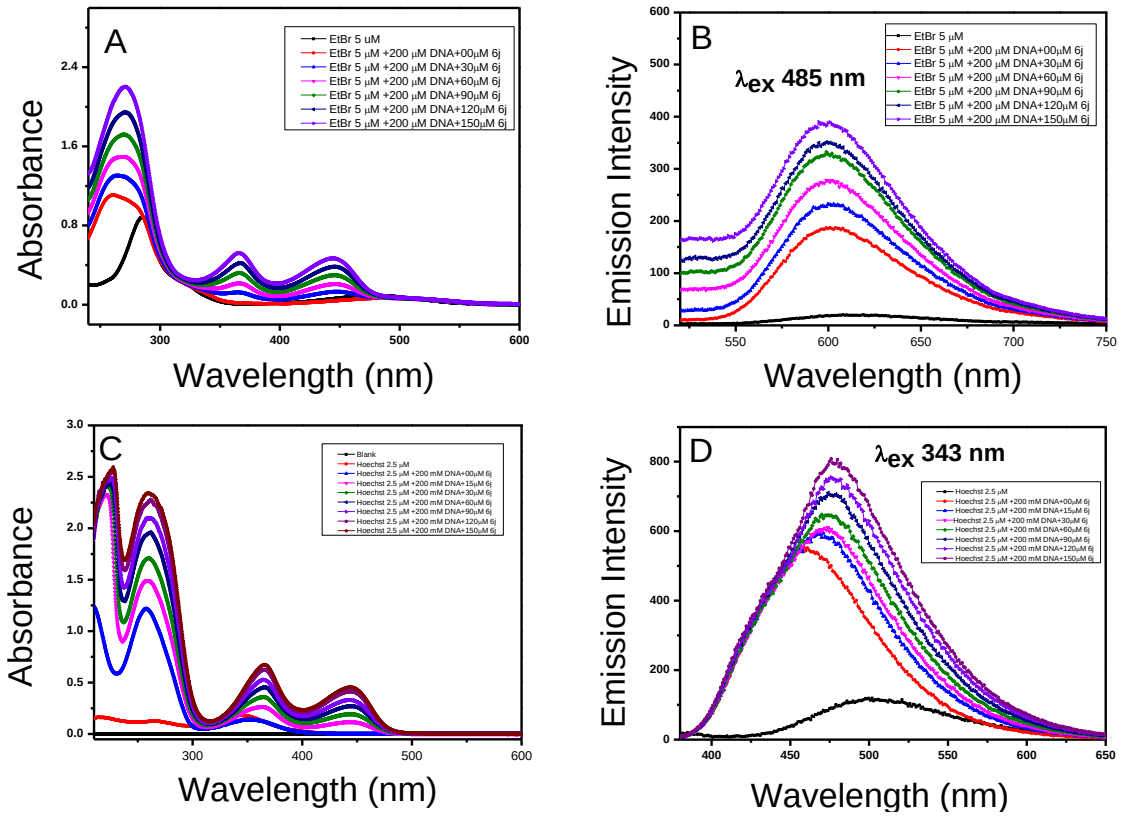

Figure 4.6. UV-Vis and Fluorescence spectra of ct-DNA under different concentration of *Troponyl dihydraopyrazine* derivatives (**6a/6e/6j/6n)** with EtBr and Hoechst dyes.

We also studied the impact of *Troponyl dihydropyrazine* derivatives (**6a/6e/6j/6n)** in the *ct*-DNA duplex structure by circular dichroism (CD) spectral analyses. We recorded CD spectra of ct-DNA near physiological conditions at pH 7.0 (room temperature) with different concentration of compounds. Their CD spectra are provided in Figure Sxx. The CD spectra of *ct*-DNA exhibit the characteristic CD-signal of B-type DNA duplex structure that almost remain unchanged with increasing the concentration of compound **6a/6e/6j/6n**. In fact, compound **6j** stabilized the *ct*-DNA duplex structure. Thus there is no significant perturbation in the native DNA duplex structure after binding with *Troponyl dihydropyrazine* derivatives.

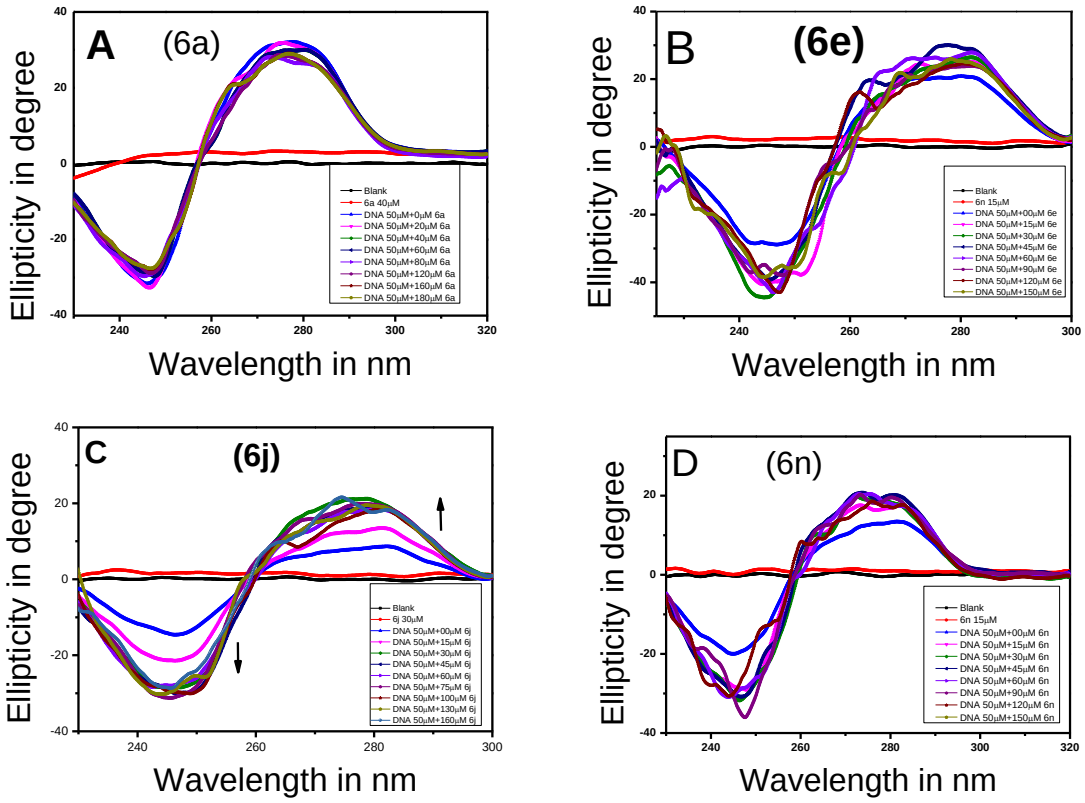

Figure 4.7. CD-spectra *Troponyl dihydraopyrazine* derivatives **6a/6e/6j/6n** under different concentration of DNA at pH 7.0 (Room temperature)

For practical utility, we attempted to evaluate their biological application in vivo through MTT Assay, known for assessing the cellular metabolic activities.[27, 28] We performed MTT Assay in Hela cells with the representative troponyl dihydropyrazine compound (**6a**). MTT assay profile is provided in the (Figure 4.8). Our result shows that compound **6a** significantly inhibits the cancer HeLa cell proliferation with IC_{60} (~26nM). Hence, troponyl dihydropyrazine derivatives are potential anti-cancer therapeutic drug candidates.

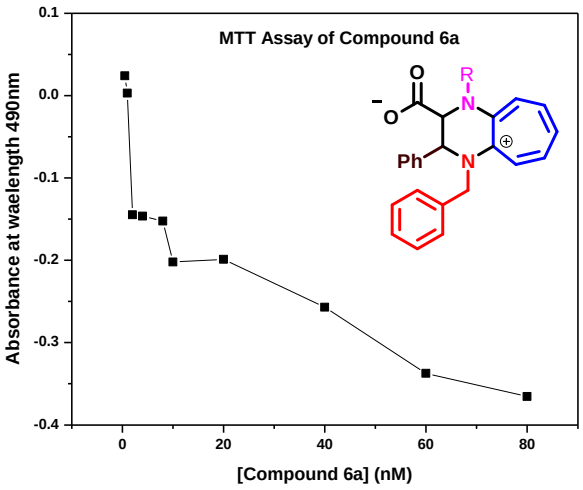

Figure 4.8 MTT assay profile of compound **6a**

4.4 Conclusion

Herein, we have accomplished the synthesis of new carboxylate functionalized aryl-substituted troponyl dihydropyrazine derivatives from unnatural amino acid ester derivative as troponyl alky glycinate in presence of aryl-imine under mild acidic conditions. The chemical structure of three representative compounds are confirmed by X-ray data analyses of respective single crystal state along with their NMR. The formations of such troponyl dihydropyrazine derivatives are established mechanistically via the formation of ketene followed by its [2+2] cycloaddition reaction with imine under mild acidic conditions. However, these cycloaddition reactions are non-stereospecific. Notably, the representative troponyl dihydropyrazine derivative exhibits the inhibition of HeLa-cells. Overall the substituted troponyl dihydropyrazine carboxylate derivatives are novel heterocyclic compounds possessing therapeutic properties.

Material and Instrumentation: All required materials were obtained from commercial and used without purification. Anhydrous Acetonitrile was freshly prepared by distilling over calcium hydride. Reaction were monitored by thin layer chromatography, visualized by UV and Ninhydrin. Column chromatography was performed in 230-400 and 100-200 mesh silica. Mass spectra were obtained from Bruker MicrOTOF-Q II Spectometer.NMR spectra were recorded on Bruker AV-700MHz and Bruker AV-400 (1H:400MHz ,13C:100.6 MHz).1H and 13C NMR chemical shift were recorded in ppm downfield from tetramethyl silane, splitting patterns are abbreviated as: s, singlet; d, doublet; dd, doublet of doublet; t, triplet; q, quartet; dq, doublet of quartet; m, multiplet. The crystal data of two compund were collected on a Rigaku Oxford diffractometer at 293 K respectively. Absorption spectra were obtained using Jasco V-730 spectrometer. Fluorescence spectra were obtained from Perkin-Elmer LS-55 using Xenon lamp. All spectroscopic measurements were carried out with spectroscopic grade, nondegassed solvents and at 20^{o}C. Relative fluorescence quantum yields were determined by comparing with Cumarine quantum yield in methanol.

4..5 Experimental Section

***Synthesis of Trag monomer and peptide*:** Previously we reported the synthesis of Troponyl ester and amide[1]; Here, we followed the same procedure for synthesis of monomer and peptides. In this study we are reporting the trapped ketene intermediate [2+2] cycloaddition reaction under mild acidic condition to form a Troponyl six member cyclic compound with novel pyrazine derivatives.

General Procedure of Schiff Base Synthesis: Schiff bases were prepared by condensation of aldehyde (1 eq.) with amines (1 eq.). Different aldehydes (1 eq.) and amines (1 eq.) were dissolved in MeOH, anhydrous Na_2SO_4 was added as a drying agent and the mixture was

refluxed for 6 h. The completion of reaction was monitored by TLC. After complete conversion the reaction mixture was filtered using glass funnel. Then the filtrate was dried under reduced pressure and the crude products were used for the next step of synthesis without any purification[2].

Trapping Ketene Intermediate via [2+2] Cycloaddition reaction with Imine: The *N*-troponyl-*N*-phenylethyl glycinate (*tr-pheneg*) ester (**2**) (1 eq.) was taken in a round bottom flask under Argon atmosphere in dry Acetonitrile and treated with 5% TFA at 0 °C .After 5 min of stirring, imine (**5**) (4 eq.) was added and the reaction mixture was allowed to stir for 6-12h at rt. The reaction mixture was monitored by TLC, and after completion of the reaction, the reaction mixture was concentrated under reduced pressure. Concentrated reaction mixture was dissolved in DCM (30ml) and washed with water thrice(3*30ml) followed by saturated sodium bicarbonate(20ml) and brine(20ml). The organic layers were combined, dried over sodium sulphate and concentrated under vacuum. The crude reaction mixture was purified by column chromatography using DCM:MeOH (95:5) and the desired product was obtained. The obtained product was well characterised by $^{1}H/^{13}C$-NMR and HRMS. The characterisation data of all new synthesized compounds are provided bellow.

Analytical Data

Benzyl phenethyl phenyldihydro cyclohepta[b]pyrazinium carboxylate (**6a**)

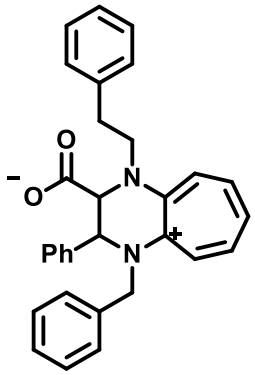

6a

The *dihydrocyclohepta[b]pyrazine* compound (**6a**) was synthesised by according to general procedures **(2.3)**. The crude reaction was purified by column chromatography using silica gel (100-200 mesh size), giving a yellow viscous liquid 60mg (**91%** yield in 4% MeOH/DCM)

^{1}H NMR (400 MHz, $CDCl_3$) δ 7.45 – 7.13 (m, 16H), 6.89-6.82 (dd, *J* = 12.0, 8.3 Hz, 4H), 6.72-6.769 (d, *J* = 11.5 Hz, 1H), 5.95 (s, 1H), 4.78 – 4.58 (m, 3H), 3.86 (dt, *J* = 15.6, 8.0 Hz, 1H), 3.69 (ddd, *J* = 14.4, 9.2, 5.2 Hz, 1H), 3.44 (s, 1H), 2.51 (dt, *J* = 16.2, 8.3 Hz, 1H), 2.35 (ddd, *J* = 14.1, 8.9, 5.4 Hz, 1H). ^{13}C NMR (101 MHz, $CDCl_3$) δ 167.39 , 152.07, 151.00, 139.28, 139.10 , 138.21, 136.95, 132.44, 129.61, 129.45, 128.85, 128.70, 128.54, 128.25, 127.08, 126.92, 126.39, 125.97, 116.68, 116.54, 71.38, 67.63, 56.86, 55.71, 50.61, 31.31. HRMS (ESI-TOF) m/z :$[M+H]^+$ Calcd. For $C_{38}H_{28}N_2O_2$ 461.2224, found 461.2200.

Benzyl-dimethoxyphenyl phenethyl dihydro cyclohepta[b]pyrazinium carboxylate **(6b)**

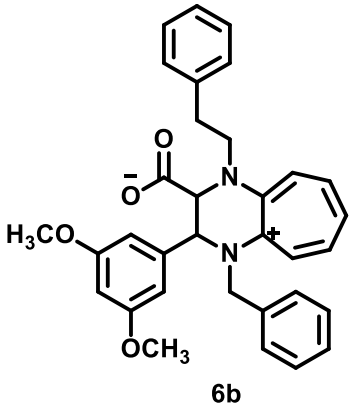

6b

The *dihydrocyclohepta[b]pyrazine* compound (**6b**) was synthesised by according to general procedures **(2.3)**. The crude reaction was purified by column chromatography using silica gel (100-200 mesh size), giving a yellow viscous liquid 150mg (**68%** yield in 3% MeOH/DCM)

^{1}H NMR (400 MHz, $CDCl_3$) δ 7.43 (dd, *J* = 13.9, 7.3 Hz, 2H), 7.32-7.20 (m, 5H), 6.90 – 6.82 (m, 3H), 6.63 (d, *J* = 11.5 Hz, 1H), 6.46 (s, 1H), 6.32 (d, *J* = 1.8 Hz, 1H), 5.85 (s, 1H), 4.76 – 4.54 (m, 1H), 3.95 – 3.77 (m, 5H), 3.48 (s, 1H), 2.71 – 2.53 (m, 1H). ^{13}C NMR (176 MHz,

$CDCl_3$) δ 167.06, 161.66, 150.96, 140.78, 139.15, 132.26, 129.67, 128.91, 128.27, 127.02, 126.21, 116.51, 104.23, 99.90, 71.03, 67.61, 56.73, 55.98, 55.69, 55.55, 53.45, 31.73. HRMS (ESI-TOF) m/z: $[M+H]^+$ Calcd. For $C_{32}H_{30}N_2O_4$ 507.2278, found 507.2269.

Nitrophenyl diphenethyldihydro cyclohepta[b]pyrazinium carboxylate (**6c**)

The *dihydrocyclohepta[b]pyrazine* compound (**6c**) was synthesised by according to general procedures **(2.3)**. The crude reaction was purified by column chromatography using silica gel (230-400 mesh size), giving a black viscous liquid 100mg (**75%** yield in 6% MeOH/DCM).100mg (75% yield) of the pure product was isolated as black viscous liquid.

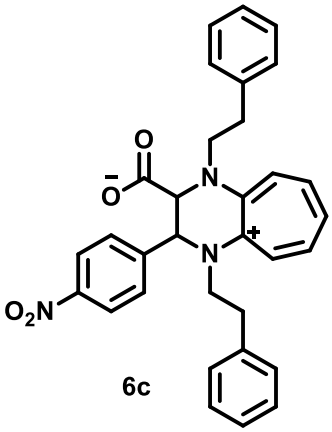

6c

^{1}H NMR (400 MHz, $CDCl_3$) δ 8.19 (d, *J* = 8.6 Hz, 1H), 7.57 – 7.48 (m, 1H), 7.45 – 6.96 (m, 13H), 6.92 – 6.85 (m, 1H), 6.71 (d, *J* = 11.3 Hz, 1H), 6.07 (s, 1H), 5.91 (s, 1H), 4.19 (dt, *J* = 14.8, 7.4 Hz, 1H), 4.10 – 4.00 (m, 1H), 3.71 – 3.55 (m, 1H), 3.28 (m, 1H), 3.11 (t, *J* = 7.4 Hz, 1H), 2.95 (t, *J* = 7.4 Hz, 1H), 2.58 (t, *J* = 7.4 Hz, 1H), 1.41 (d, *J* = 12.7 Hz, 1H). ^{13}C NMR (101 MHz, $CDCl_3$) δ 151.12, 149.47, 148.19, 141.30, 140.27, 139.67, 138.14, 136.72, 136.58, 129.12, 128.93, 128.65, 128.54, 127.30, 126.62, 124.59, 117.80, 83.41, 69.13, 54.57, 53.71, 42.27, 36.62, 32.59, 31.82, 29.70, 22.70. HRMS (ESI-TOF) m/z: $[M+H]^+$ Calcd. For $C_{32}H_{30}N_2O_4$ 520.2231, found 520.2259.

Benzyl nitrophenyl phenethyl dihydro cyclohepta[b]pyrazinium carboxylate **(6d)**

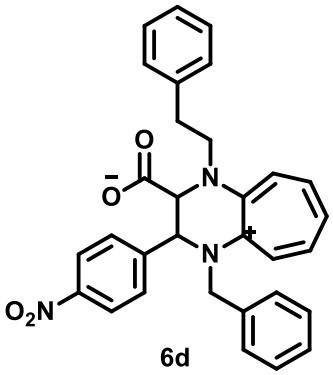

6d

The *dihydrocyclohepta[b]pyrazine* compound (**6d**) was synthesised by according to general procedures **(2.3)**. 170mg (60%) of pure product obtained as a yellow viscous.

^{1}H NMR (400 MHz, $CDCl_3$) δ 8.24 (t, *J* = 8.1 Hz, 3H), 7.63-7.52 (m, 3H), 7.38 – 7.18 (m, 12H), 7.04 (d, *J* = 11.4 Hz, 1H), 6.92 – 6.91 (m, 2H), 5.87 (s, 1H), 4.86 – 4.69 (m, 3H), 4.25 (dd, *J* = 19.5, 8.4 Hz, 1H), 3.90 – 3.69 (m, 3H), 3.62 – 3.49 (m, 2H), 2.64-2.52 (m, 2H). ^{13}C NMR (176 MHz, $CDCl_3$) δ 151.91, 150.85, 147.93, 147.84, 144.30, 140.11, 139.94, 136.12, 131.54, 129.39, 129.15, 129.01, 128.75, 128.54, 128.50, 128.40, 128.18, 127.07, 127.03, 126.47, 124.43, 123.94, 118.23, 117.88, 66.09, 57.16, 56.41, 55.35, 31.35. HRMS (ESI-TOF) m/z: $[M+H]^+$ Calcd. For $C_{31}H_{27}N_3O_4$ 506.2074, found 506.2079.

Benzyl phenethyl (m-tolyl) dihydro cyclohepta[b]pyrazinium carboxylate (**6e**)

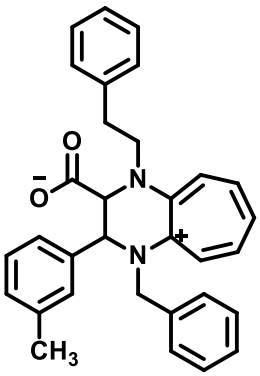

6e

The *dihydrocyclohepta[b]pyrazine* compound (**6e**) was synthesised by according to general procedures **(2.3)**. 170mg (45% yield) of the pure product was isolated as yellow viscous liquid. ^{1}H NMR (400 MHz, $CDCl_3$) δ 7.49 – 7.43 (m, 4H), 7.35-7.28 (m, 3H), 7.25 – 7.19 (m, 5H), 7.09 (d, *J* = 8.0 Hz, 2H), 6.90 – 6.84 (m, 3H), 6.70 (d, *J* = 11.5 Hz, 1H), 5.92 (s, 1H), 4.78-4.56 (m, 3H), 3.94 – 3.86 (m, 1H), 3.80-3.73 (m, 1H), 2.61 – 2.54 (m, 1H), 2.50-2.43 (m, 1H), 2.39 (s, 3H), 2.21 (s, 2H). ^{13}C NMR (101 MHz, $CDCl_3$) δ 167.21, 152.16, 152.12, 139.13, 139.09, 138.63, 137.18, 137.00, 135.14, 132.34, 130.09, 129.65, 128.85, 128.55,128.26, 126.97, 126.84, 126.26, 125.90, 116.51, 116.34, 71.46, 67.45, 56.73, 55.83, 31.40, 21.13. HRMS (ESI-TOF) m/z: $[M+H]^+$ Calcd. For $C_{32}H_{30}N_2O_2$ 475.2380, found 475.2368.

cyanobenzyl-phenethyl-phenyl-dihydro-cyclohepta[b]pyrazinium carboxylate **(6f)**

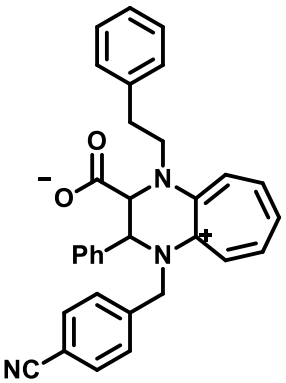

6f

The *dihydrocyclohepta[b]pyrazine* compound (**6f**) was synthesised by according to general procedures **(2.3)**. 60mg (88% yield) of the pure product was isolated as yellow viscous ^{1}H NMR (400 MHz, CD_3CN) δ 7.76 (d, *J* = 7.0 Hz, 2H), 7.60 (dt, *J* = 20.2, 10.1 Hz, 2H), 7.41 (dd, *J* = 17.2, 6.8 Hz, 3H), 7.34 – 7.15 (m, 10H), 7.07 (d, *J* = 6.1 Hz, 2H), 4.98 (d, *J* = 17.0 Hz, 1H), 4.72 (d, *J* = 17.0 Hz, 1H), 4.25 (d, *J* = 13.1 Hz, 1H), 3.98 (d, *J* = 13.0 Hz, 1H), 3.81 (d, *J* = 5.7 Hz, 2H), 2.67 (d, *J* = 5.6 Hz, 1H), 2.47 (s, 1H). ^{13}C NMR (101 MHz, CD_3CN) δ 161.50, 151.44, 150.11, 141.98, 139.85, 139.73, 137.16, 133.03, 132.94, 129.22, 129.17, 128.79, 128.73, 128.20, 127.54, 126.93, 126.76, 120.80, 118.96, 118.38, 118.20, 117.91, 115.02, 112.33, 63.07, 55.34, 55.32, 54.89, 30.81. HRMS (ESI-TOF) m/z: $[M+H]^+$ Calcd. For $C_{32}H_{37}N_3O_2$ 486.2176, found 486.2190.

Benzyl-dimethoxynaphthalen-yl phenethyl dihydro cyclohepta[b]pyrazinium carboxylate (**6g**)

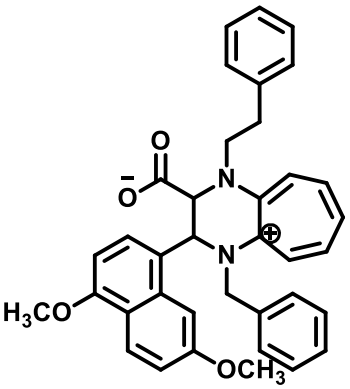

6g, 52%

The *dihydrocyclohepta[b]pyrazine* compound (**6g**) was synthesised by according to general procedures **(2.3)**. 35mg (52%) of pure product obtained as a yellow viscous.

^{1}H NMR (400 MHz, $CDCl_3$) δ 8.27 (dd, *J* = 9.2, 6.2 Hz, 1H), 7.53 – 6.91 (m, 16H), 6.80 – 6.63 (m, 2H), 6.59 (d, *J* = 8.1 Hz, 1H), 4.92 – 4.69 (m, 2H), 4.12 (dd, *J* = 24.7, 6.6 Hz, 1H), 3.93 (dd, *J* = 47.2, 29.6 Hz, 6H), 3.48 (s, 1H), 3.24 (s, 1H), 3.04 (s, 1H), 2.32 (s, 1H). ^{13}C NMR (101 MHz, $CDCl_3$) δ 159.59, 156.78, 150.41, 139.65, 139.24, 136.73, 132.81, 132.08, 129.67, 128.80, 128.76, 126.95, 126.54, 125.15, 124.19, 122.74, 121.40, 120.80, 117.77, 117.06, 101.20, 100.80, 62.28, 56.23, 55.61, 37.11, 31.59, 29.71, 22.70, 13.90. HRMS (ESI-TOF) m/z: $[M]^+$ Calcd. For $C_{37}H_{35}N_2O_4$ 571.2591, found 571.2556.

Sec-butylphenethyphenyl dihydro cyclohepta[b]pyrazinium carboxylate(**6h**):

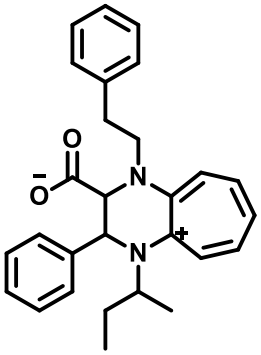

6h

The *dihydrocyclohepta[b]pyrazine* compound (**6h**) was synthesised by according to general procedures **(2.3)**53mg (88% yield) of the pure product was isolated as yellow viscous solid. ^{1}H NMR (400 MHz, $CDCl_3$) δ 7.46 – 7.31 (m, 5H), 7.19 (s, 5H), 6.82 (s, 3H), 6.56 (dd, *J* = 20.0, 10.6 Hz, 1H), 5.92 (s, 1H), 4.54 (d, *J* = 12.7 Hz, 1H), 4.04 (s, 1H), 3.69 (s, 2H), 2.65 (s, 3H), 2.35 (s, 1H), 2.20 (s, 1H), 2.01 (d, *J* = 26.2 Hz, 1H), 1.53 (s, 2H), 1.26 (s, 1H), 1.05 (d, *J* = 8.5 Hz, 3H), 0.80 (s, 2H). ^{13}C NMR (101 MHz, $CDCl_3$) δ 166.72, 150.82, 150.72, 149.97, 139.49, 138.56, 138.36, 138.31, 136.95, 129.23, 129.18, 128.84, 128.41, 126.91, 125.64, 125.47, 125.24, 113.93, 113.88, 113.59, , 72.64, 54.86, 30.85, 27.54, 24.99, 17.56, 14.59, 11.47, 10.86. HRMS (ESI-TOF) m/z: $[M+H]^+$ Calcd. For $C_{28}H_{30}N_2O_2$ 427.2380, found 427.2368.

Phenethyl phenyl prop-yn-1-yl dihydro cyclohepta[b]pyrazinium carboxylate (**6i**)

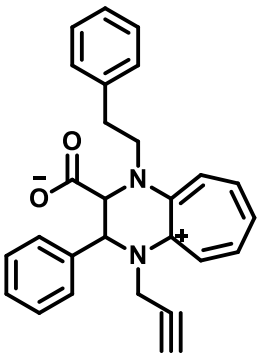

6i

The *dihydrocyclohepta[b]pyrazine* compound (**6i**) was synthesised by according to general procedures **(2.3)**. 95mg (82%) of pure product obtained as a yellow viscous. ^{1}H NMR (700 MHz, Chloroform-*d*) δ 7.51 (t, *J* = 10.1 Hz, 1H), 7.42 – 7.33 (m, 4H), 7.21 – 7.13 (m, 6H), 6.99 (t, *J* = 9.3 Hz, 1H), 6.82 – 6.78 (m, 2H), 6.70 (d, *J* = 11.5 Hz, 1H), 5.96 (s, 1H), 4.61 – 4.49 (m, 2H), 4.23 (dd, *J* = 18.4, 1.9 Hz, 1H), 3.81 (dt, *J* = 15.7, 7.8 Hz, 1H), 3.73 (ddd, *J* = 14.8, 9.3, 5.5 Hz, 1H), 3.45 – 3.24 (m, 2H), 2.47 (h, *J* = 8.4, 7.6 Hz, 2H), 2.37 (ddd, *J* = 14.2, 8.8, 5.5 Hz, 1H). ^{13}C NMR (176 MHz, $CDCl_3$) δ 152.08, 149.93, 148.64, 139.71, 139.47, 139.28, 138.93, 137.39, 136.92, 129.30, 128.86, 128.66, 128.47, 127.65, 126.95, 125.87, 117.51, 116.98, 76.30, 74.50, 72.01, 68.64, 55.73, 43.26, 31.28.HRMS (ESI-TOF) m/z :$[M+H]^+$ Calcd. For $C_{27}H_{24}N_2O_2$ 409.1911, found 409.1955.

Octyl phenethyl phenyl dihydro cyclohepta[b]pyrazinium carboxylate (**5j**):

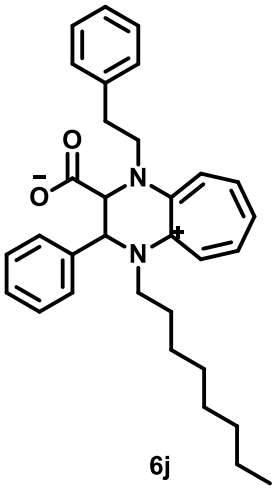

The *dihydrocyclohepta[b]pyrazine* compound (**6j**) was synthesised by according to general procedures **(2.3)**.160mg (59%) of pure product obtained as a yellow viscous. ^{1}H NMR (400 MHz, $CDCl_3$) δ 7.44 – 7.38 (m, 4H), 7.30 – 7.11 (m, 7H), 6.89-6.84 (m, 2H), 6.78-6.74 (m, 2H), 6.52 (d, *J* = 12.0 Hz, 1H), 5.90 (s, 1H), 4.53 (s, 1H), 3.79 (t, *J* = 7.2 Hz, 2H), 3.58 – 3.51 (m, 1H), 3.32 (td, *J* = 14.1, 4.8 Hz, 1H), 2.67 (s, 2H), 2.53 – 2.35 (m, 2H), 2.05 (s, 1H), 1.86 – 1.84 (m, 1H), 1.32 – 1.26 (m, 10H), 0.87 (t, *J* = 6.3 Hz, 3H). ^{13}C NMR (176 MHz, $CDCl_3$) δ 166.65, 151.07, 150.01, 138.76, 138.61, 137.53, 136.97, 129.32, 128.76, 128.56, 128.48, 128.33, 126.82, 125.90, 125.68, 115.10, 114.69, 71.31, 67.04, 63.56, 55.50, 52.91, 31.6, 31.18, 29.16, 28.89, 26.85, 25.65, 24.70, 22.49, 13.99. HRMS (ESI-TOF) m/z: $[M+H]^+$ Calcd. For $C_{38}H_{38}N_2O_2$ 483.3006, found 483.3015.

4-fluorophenyl octyl phenethyl dihydro cyclohepta[b]pyrazinium-carboxylate **(5k)**

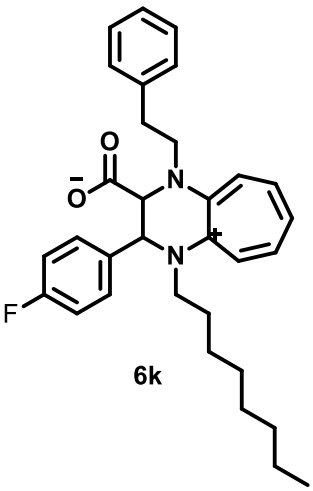

The *dihydrocyclohepta[b]pyrazine* compound (**6k**) was synthesised by according to general procedures **(2.3)**.110mg (76% yield) of the pure product was obtained as light-yellow viscous liquid. ^{1}H NMR (400 MHz, $CDCl_3$) δ 7.59 (t, *J* = 10.1 Hz, 1H), 7.48 – 7.38 (m, 1H), 7.36 – 7.20 (m, 5H), 7.17 – 6.91 (m, 4H), 6.79 (d, *J* = 11.3 Hz, 1H), 4.24 (d, *J* = 14.0 Hz, 1H), 4.07 – 3.92 (m, 1H), 3.77 – 3.57 (m, 1H), 2.63 (t, *J* = 7.1 Hz, 1H), 1.87 (m, 2H), 1.42 (t, *J* = 9.6 Hz, 2H), 1.29 (d, *J* = 12.5 Hz, 12H), 0.88 (t, *J* = 6.1 Hz, 3H). ^{13}C NMR (101 MHz, $CDCl_3$) δ 164.10, 161.63, 149.72, 139.14, 138.90, 136.62, 128.99, 128.64, 127.26, 127.21, 117.06, 116.49, 115.78, 63.24,

55.59, 53.49, 31.67, 29.67, 29.14, 26.87, 25.82, 22.58, 14.06, HRMS (ESI-TOF) m/z: $[M+H]^+$ Calcd. For $C_{31}H_{38}N_2O_2F$ 457.3014, found 457.3033.

cyclohexyl-hydroxyphenyl phenethyl dihydro cyclohepta[b]pyrazinium-carboxylate (**6l**)

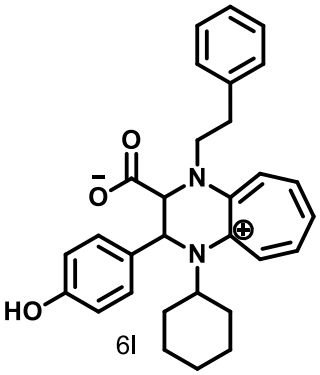

6l

The *dihydrocyclohepta[b]pyrazine* compound (**6l**) was synthesised by according to general procedures **(2.3)**. 80mg (76% yield) of the pure product was isolated as yellow viscous solid. ^{1}H NMR (400 MHz, $CDCl_3$) δ 7.65 (dd, *J* = 15.8, 14.1 Hz, 1H), 7.50 – 7.28 (m, 4H), 7.24 – 7.13 (m, 4H), 6.97 – 6.77 (m, 4H), 6.55 (dd, *J* = 20.3, 11.2 Hz, 1H), 5.90 (d, *J* = 4.8 Hz, 1H), 4.53 (d, *J* = 13.0 Hz, 1H), 4.12 – 3.97 (m, 1H), 3.80 – 3.54 (m, 2H), 2.39 – 2.29 (m, 1H), 2.21 (ddd, *J* = 12.4, 8.8, 4.2 Hz, 1H), 1.96 (ddd, *J* = 23.4, 18.5, 10.8 Hz, 3H), 1.68 (s, 1H), 1.50 (s, 1H), 1.22 (s, 2H), 1.09 – 0.97 (m, 4H), 0.93 – 0.76 (m, 4H). ^{13}C NMR (101 MHz, $CDCl_3$) δ 190.67, 150.83, 150.04, 139.39, 138.62, 138.34, 136.92, 129.25, 129.20, 128.86, 128.40, 128.31, 126.95, 125.50, 125.33, 113.92, 113.73, 54.94, 30.88, 29.71, 25.00, 24.71, 17.57, 11.46, 10.86,HRMS (ESI-TOF) m/z: $[M+H]^+$ Calcd. For $C_{30}H_{32}N_2O_3$ 469.2471, found 469.2486.

Fluorobenzyl phenethyl phenyl dihydrocyclohepta[b]pyrazinium carboxylate(**6m**)

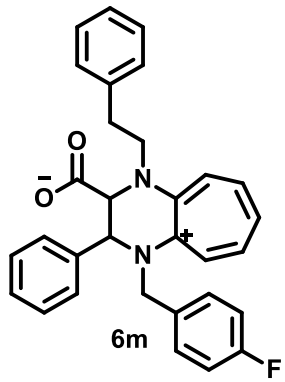

6m

The *dihydrocyclohepta[b]pyrazine* compound (**6m**) was synthesised by according to general procedures **(2.3)**. 105mg (87% yield) of the pure product was isolated as yellow viscous liquid ^{1}H NMR (400 MHz, Methanol-d_4) δ 7.74 – 6.96 (m, 20H), 5.91 (d, *J* = 1.7 Hz, 1H), 4.86 (s, 2H), 3.98 (ddd, *J* = 15.6, 9.7, 6.6 Hz, 1H), 3.74 (ddd, *J* = 15.0, 9.9, 5.5 Hz, 1H), 3.37 – 3.27 (m, 2H), 2.61 (ddd, *J* = 20.2, 10.7, 5.7 Hz, 1H), 2.34 (ddd, *J* = 14.2, 9.7, 5.5 Hz, 1H). ^{13}C NMR (176 MHz, MeOD) δ 170.04, 163.24, 161.83, 151.80, 150.77, 139.81, 138.56, 138.22, 137.37, 137.18, 129.10, 128.99, 128.71, 128.54,

128.47, 128.43, 128.33, 126.49, 125.93, 121.71, 120.07, 119.58, 118.93, 117.71, 71.74, 69.77, 65.69, 55.31, 47.98, 47.86, 47.74, 47.61, 47.49, 47.37, 47.25, 30.76. HRMS (ESI-TOF) m/z: $[M+H]^+$ Calcd. For $C_{30}H_{25}FN_2O_2$ 465.1973, found 465.1973.

benzyl-phenethy-styryl--dihydro-cyclohepta[b]pyrazin-ium-carboxylate(**6n**)

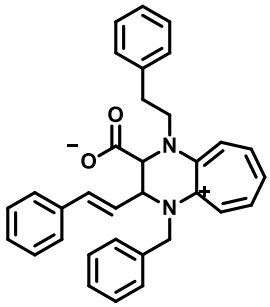

6n

The *dihydrocyclohepta[b]pyrazine* compound (**6n**) was synthesised by according to general procedures **(2.3)**. 105mg (67% yield) of the pure product was isolated as yellow viscous solid. ^{1}H NMR (400 MHz, $CDCl_3$) δ 7.43 (s, 5H), 7.34 (s, 5H), 7.18 (s, 7H), 6.95 – 6.73 (m, 4H), 6.49 (d, *J* = 15.6 Hz, 1H), 6.23 – 6.11 (m, 1H), 5.33 (d, *J* = 29.0 Hz, 1H), 4.90 (d, *J* = 16.5 Hz, 1H), 4.64 (dd, *J* = 40.0, 23.2 Hz, 2H), 4.50 (s, 1H), 4.13 – 3.84 (m, 2H), 3.65 (d, *J* = 33.1 Hz, 1H), 3.02 (s, 2H). ^{13}C NMR (101 MHz, $CDCl_3$) δ 167.22, 152.11, 151.62, 139.34, 139.23, 139.12, 139.02, 138.24, 136.99, 136.91, 135.17, 133.93, 132.54, 132.37, 129.63, 129.59, 129.48, 128.95, 128.86, 128.77, 128.53, 128.26, 127.12, 127.09, 126.93, 126.76, 126.44, 126.28, 125.93, 123.99, 117.22, 117.09, 116.58, 71.46, 68.80, 67.62, 66.00, 56.52, 55.97, 32.10, 31.31. HRMS (ESI-TOF) m/z: $[M+Na]^+$ Calcd. For $C_{33}H_{30}N_2O_2Na$ 509.2199, found 509.2216.

benzyl-methoxyphenylphenethyl-dihydro- cyclohepta[b]pyrazinum-carboxylate **(6o):**

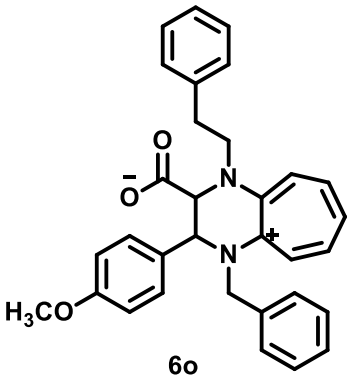

6o

The *dihydrocyclohepta[b]pyrazine* compound (**6o**) was synthesised by according to general procedures **(2.3)**. 52mg (41% yield) of the pure product was isolated as yellow viscous liquid. ^{1}H NMR (400 MHz, $CDCl_3$) δ 7.42 (s, 5H), 7.36 – 7.31 (m, 1H), 7.18 (d, *J* = 5.0 Hz, 5H), 7.13 – 7.01 (m, 4H), 6.96 – 6.84 (m, 4H), 5.71 (d, *J* = 30.2 Hz, 1H), 5.07 (s, 1H), 4.72 (t, *J* = 15.8 Hz, 2H), 4.14 (d, *J* = 6.9 Hz, 1H), 3.84 – 3.71 (m, 3H), 3.64 (s, 1H), 3.27 (s, 11H), 3.06 (s, 1H),

2.53 (s, 1H). ^{13}C NMR (101 MHz, $CDCl_3$) δ 160.32, 151.95, 151.71, 140.12, 139.99, 136.57, 131.56, 129.79, 129.73, 129.42, 128.95, 128.66, 128.61, 127.33, 127.13, 126.25, 126.20, 125.96, 118.12, 117.45, 114.98, 77.37, 76.74, 65.68, 56.31, 55.45, 31.53, 22.67, 14.15. HRMS (ESI-TOF) m/z: $[M+H]^+$ Calcd. For $C_{33}H_{30}N_2O_3$ 491.2329, found 491.2312.

N-troponyl-N-phenylethyl glycinate (tr-pheneg) ester (**2**)

^{1}H NMR (400 MHz, CD_3CN) δ 7.33 (q, *J* = 6.4 Hz, 4H), 7.28 – 7.21 (m, 1H), 7.16 – 7.05 (m, 2H), 6.76 (dd, *J* = 20.8, 11.3 Hz, 2H), 6.66 – 6.59 (m, 1H), 4.31 (s, 2H), 4.15 (q, *J* = 7.1 Hz, 2H), 3.73 – 3.65 (m, 2H), 3.00 (dd, *J* = 8.9, 7.0 Hz, 2H), 1.24 (t, *J* = 7.1 Hz, 3H).

N-benzylidene-phenylmethaneamine (**5a**)

^{1}H NMR (400 MHz, $CDCl_3$) δ 8.40 – 8.29 (m, 1H), 7.89 – 7.79 (m, 3H), 7.50 (ddd, *J* = 9.8, 5.7, 1.8 Hz, 1H), 7.43 (s, 2H), 7.41 – 7.36 (m, 3H), 7.34 – 7.27 (m, 1H), 4.82 (d, *J* = 5.7 Hz, 2H). Mass (ESI-TOF) m/z: $[M+H]^+$ found 196.1293.

4.6 Reference and Notes

1. Kosuge, T.; Kamiya, H., Discovery of a pyrazine in a natural product: tetramethylpyrazine from cultures of a strain of Bacillus subtilis. *Nature* **1962,** *193*, 776-776.

2. Ahsan, W.; Javed, S.; Al Bratty, M.; Alhazmi, H. A.; Najmi, A., Treatment of SARS-CoV-2: How far have we reached? *Drug Discov Ther.* **2020**.

3. Du, Y. X.; Chen, X. P., Favipiravir: pharmacokinetics and concerns about clinical trials for 2019-nCoV infection. *Clin. Pharmacol. Ther.* **2020**.

4. Bentley, R., A fresh look at natural tropolonoids. *Nat. Prod. Rep.* **2008,** *25*, 118-138.

5. Guo, H.; Roman, D.; Beemelmanns, C., Tropolone natural products. *Nat. Prod. Rep.* **2019,** *36*, 1137-1155.

6. Nakano, K.; Chigira, T.; Miyafusa, T.; Nagatoishi, S.; Caaveiro, J. M.; Tsumoto, K., Discovery and characterization of natural tropolones as inhibitors of the antibacterial target CapF from Staphylococcus aureus. *Sci. Rep.* **2015,** *5*, 1-10.

7. Silber, J.; Ohlendorf, B.; Labes, A.; Wenzel-Storjohann, A.; Näther, C.; Imhoff, J. F., Malettinin E, an antibacterial and antifungal tropolone produced by a marine Cladosporium strain. *Front. Mar. Sci.* **2014,** *1*, 35.

8. Balsa, L. M.; Ruiz, M. C.; de la Parra, L. S. M.; Baran, E. J.; León, I. E., Anticancer and antimetastatic activity of copper (II)-tropolone complex against human breast cancer cells, breast multicellular spheroids and mammospheres. *J. Inorg. Biochem.* **2020,** *204*, 110975.

9. Ononye, S. N.; VanHeyst, M. D.; Oblak, E. Z.; Zhou, W.; Ammar, M.; Anderson, A. C.; Wright, D. L., Tropolones as lead-like natural products: the development of potent and selective histone deacetylase inhibitors. *ACS Med. Chem. Lett.* **2013,** *4*, 757-761.

10. Morita, Y.; Matsumura, E.; Okabe, T.; Shibata, M.; Sugiura, M.; Ohe, T.; Tsujibo, H.; Ishida, N.; Inamori, Y., Biological activity of tropolone. *Biol. Pharm. Bull.* **2003,** *26*, 1487-1490.

11. Fullagar, J. L.; Garner, A. L.; Struss, A. K.; Day, J. A.; Martin, D. P.; Yu, J.; Cai, X.; Janda, K. D.; Cohen, S. M., Antagonism of a zinc metalloprotease using a unique metal-chelating scaffold: tropolones as inhibitors of P. aeruginosa elastase. *Chem. Commun.* **2013,** *49*, 3197-3199.

12. Narita, T.; Suga, A.; Kobayashi, M.; Hashimoto, K.; Sakagami, H.; Motohashi, N.; Kurihara, T.; Wakabayashi, H., Tumor-specific cytotoxicity and type of cell death induced by benzo [b] cyclohept [e][1, 4] oxazine and 2-aminotropone derivatives. *Anticancer Res.* **2009,** *29*, 1123-1130.

13. Wakabayashi, H.; Narita, T.; Suga, A.; Sakagami, H., Hormetic response of cultured normal and tumor cells to 2-aminotropone derivatives. *in vivo* **2010,** *24*, 39-44.

14. Nozoe, T.; Ishikawa, S.; Shindo, K., Synthesis and reactions of 2, 3-dihydrocyclohepta [b][1, 4]-thiazines and 2, 3-dihydro-1H-cyclohepta [b] pyrazines. *Heterocycles* **1989,** *28*, 733-744.

15. Kawamata, Y.; Imafuku, K.; Li, D. H.; Jin, Z. T.; Li, Z. H.; Xiao, Y. W., Reactions of 2, 3-dihydro-1H-cyclohepta [b] pyrazines with acyl halides. *J. Heterocycl. Chem.* **1994,** *31*, 1553-1556.

16. Balachandra, C.; Sharma, N. K., Synthesis and conformational analysis of new troponyl aromatic amino acid. *Tetrahedron* **2014,** *70*, 7464-7469.

17. Bollu, A.; Sharma, N. K., Tropolone-Conjugated DNA: Fluorescence Enhancement in the Duplex. *ChemBioChem* **2019,** *20*, 1467-1475.

18. Ito, Y.; Amimoto, K.; Kawato, T., Prototropic tautomerism and solid-state photochromism of N-phenyl-2-aminotropones. *Dyes and Pigm.* **2011,** *89*, 319-323.

19. Palai, B. B.; Soren, R.; Sharma, N. K., BODIPY analogues: synthesis and photophysical studies of difluoro boron complexes from 2-aminotropone scaffolds through N, O-chelation. *Org. Biomol. Chem.* **2019,** *17*, 6497-6505.

20. Balachandra, C.; Sharma, N. K., Instability of Amide Bond Comprising the 2-Aminotropone Moiety: Cleavable under Mild Acidic Conditions. *Org. Lett.* **2015,** *17*, 3948-3951.

21. Balachandra, C.; Sharma, N. K., Direct/Reversible Amidation of Troponyl Alkylglycinates via Cationic Troponyl Lactones and Mechanistic Insights. *ACS Omega* **2018,** *3*, 997-1013.

22. Cossio, F. P.; Arrieta, A.; Sierra, M. A., The Mechanism of the Ketene− Imine (Staudinger) Reaction in Its Centennial: Still an Unsolved Problem? *Acc. Chem. Res.* **2008,** *41*, 925-936.

23. Fu, N.; Tidwell, T. T., Preparation of β-lactams by [2+ 2] cycloaddition of ketenes and imines. *Tetrahedron* **2008,** *46*, 10465-10496.

24. Jiao, L.; Liang, Y.; Xu, J., Origin of the Relative Stereoselectivity of the β-Lactam Formation in the Staudinger Reaction. *J. Am. Chem. Soc.* **2006,** *128*, 6060-6069.

25. Pesek, J. J.; Frost, J. H., Synthesis of Imines from Aromatic Aldehydes and Aliphatic Amines in Aqueous Solution. *Synth. Commun.* **1974,** *4*, 367-372.

26. Balasubrahmanyam, S. N.; Namboothiri, I. N.; Pius, K., A Computational Evaluation of Bond Order and Charge Distributions in Isomeric Aminotroponiminiums and Their Benzo-Fused Derivatives. **2012**.

27. Stockert, J. C.; Horobin, R. W.; Colombo, L. L.; Blázquez-Castro, A., Tetrazolium salts and formazan products in Cell Biology: Viability assessment, fluorescence imaging, and labeling perspectives. *Acta Histochem.* **2018,** *120*, 159-167.

28. Mosmann, T., Rapid colorimetric assay for cellular growth and survival: application to proliferation and cytotoxicity assays. *J. Immunol. Methods* **1983,** *65*, 55-63.

4. 7 Appendix

1. NMR($^{1}H/^{13}C$) and HRMS of Aryl Troponyl dihydro pyrazine (**6a)** 278
2. NMR($^{1}H/^{13}C$) and HRMS of Aryl Troponyl dihydro pyrazine (**6b**) 280
3. NMR($^{1}H/^{13}C$) and HRMS of Aryl Troponyl dihydro pyrazine **(6c)** 282
4. NMR($^{1}H/^{13}C$) and HRMS of Aryl Troponyl dihydro pyrazine (**6d**) 284
5. NMR($^{1}H/^{13}C/^{13}$CDEPT -135) and HRMS of Aryl Troponyl dihydro pyrazine (**6e**) 286
6. NMR(1H/13C) and HRMS of Aryl Troponyl dihydro pyrazine **(6f)** 289
7. NMR($^{1}H/^{13}C$) and HRMS of Aryl Troponyl dihydro pyrazine **(6g)** 291
8. NMR($^{1}H/^{13}C/^{13}$CDEPT) and HRMS of Aryl Troponyl dihydro pyrazine **(6h)** 293
9. NMR($^{1}H/^{13}C$) and HRMS of Aryl Troponyl dihydro pyrazine **(6i)** 296
10. NMR($^{1}H/^{13}C$) and HRMS of Aryl Troponyl dihydro pyrazine **(6j)** 298
11. NMR($^{1}H/^{13}C/^{13}$CDEPT) and HRMS of Aryl Troponyl dihydro pyrazine **(6k)** 300
12. NMR(1H/13C) and HRMS of Aryl Troponyl dihydro pyrazine **(6l)** 303
13. NMR($^{1}H/^{13}C$) and HRMS of Aryl Troponyl dihydro pyrazine **(6m)** 305
14. NMR($^{1}H/^{13}C$) and HRMS of Aryl Troponyl dihydro pyrazine **(6n)** 307
15. NMR($^{1}H/^{13}C$) and HRMS of Aryl Troponyl dihydro pyrazine **(6o)** 309
16. Crystal structures and data 314
17. Comparative studies of C-C bond length of Troponyl ring 316
18. Time-dependent 1H-NMR spectra In CD_3CN 317
19. MTT Assay 319

1. NMR(^{1}H/^{13}C) and HRMS of Aryl Troponyl dihydro pyrazine (**6a)**

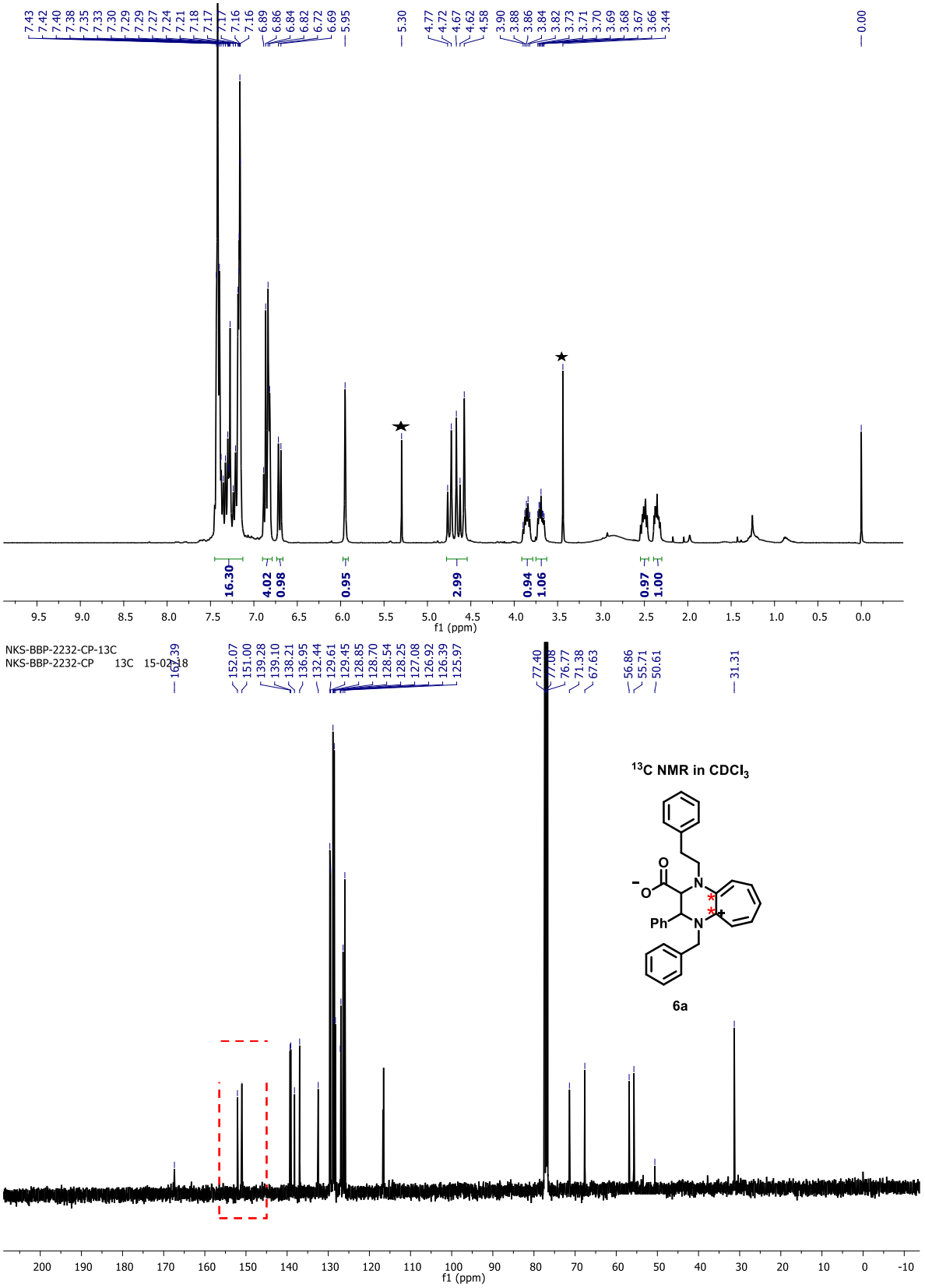

*Residual solvents and impurity grease

Figure A1. ^{1}H-/^{13}C-NMR spectra of **(6a)** in $CDCl_3$

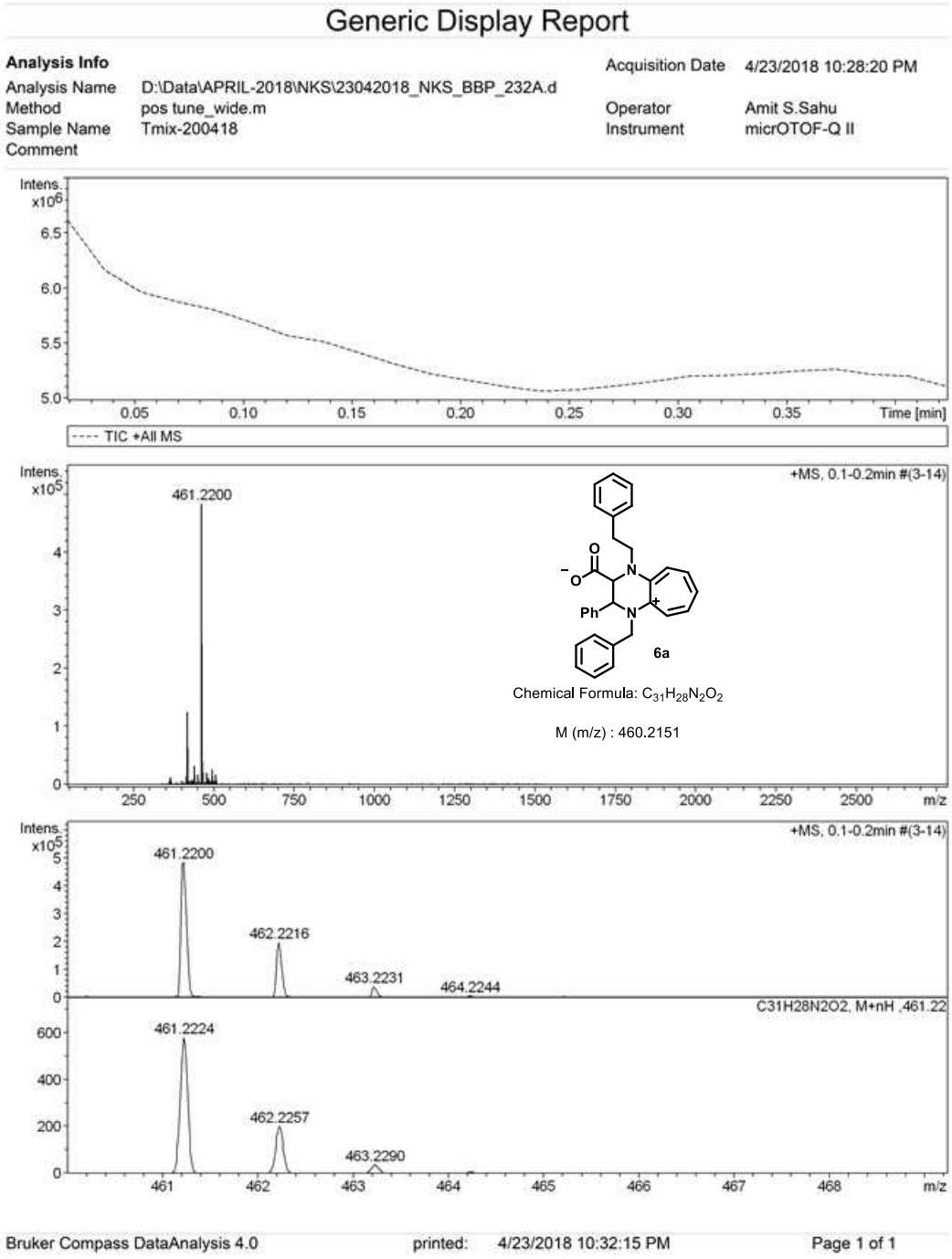

Figure A2. ESI/HRMS spectra of compound **(6a)**

2. NMR($^{1}H/^{13}C$) and HRMS of Aryl Troponyl dihydro pyrazine (**6b**)

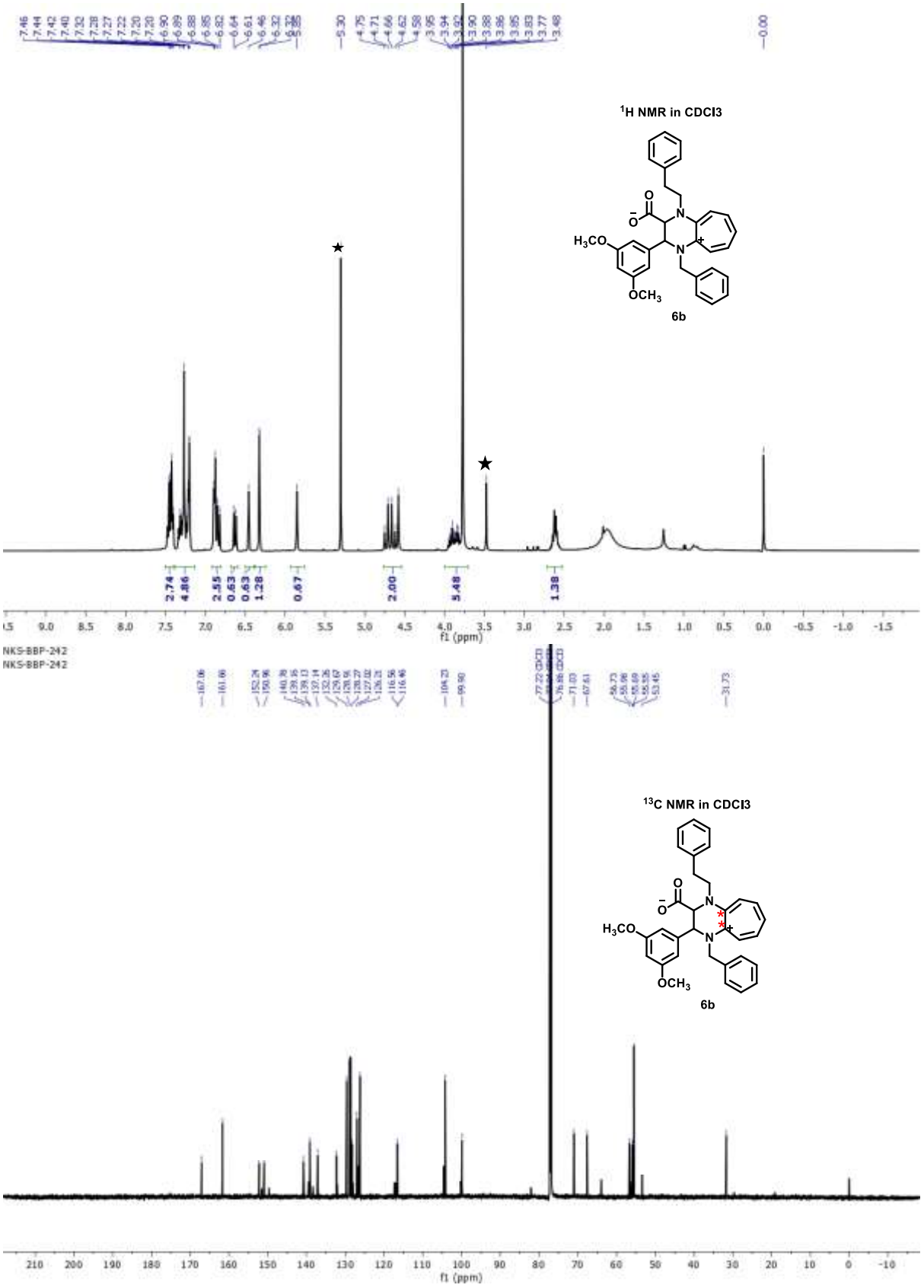

(*Residual solvents and impurity grease)

Figure A3. ^{1}H-/^{13}C-NMR spectra of **(6b)** in $CDCl_3$

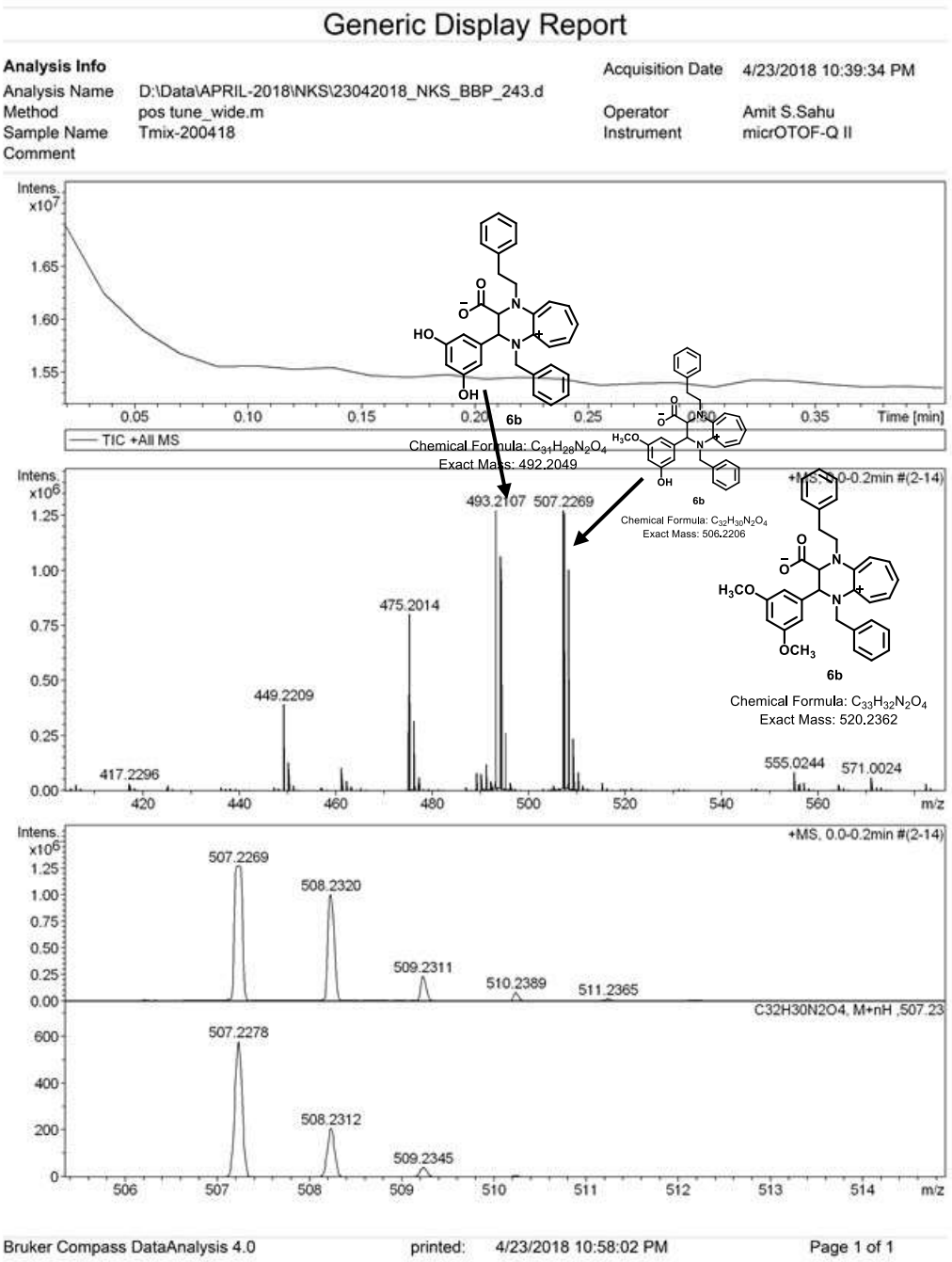

Figure A4. ESI/HRMS spectra of compound **(6b)**

3. NMR(^{1}H/^{13}C) and HRMS of Aryl Troponyl dihydro pyrazine **(6c)**

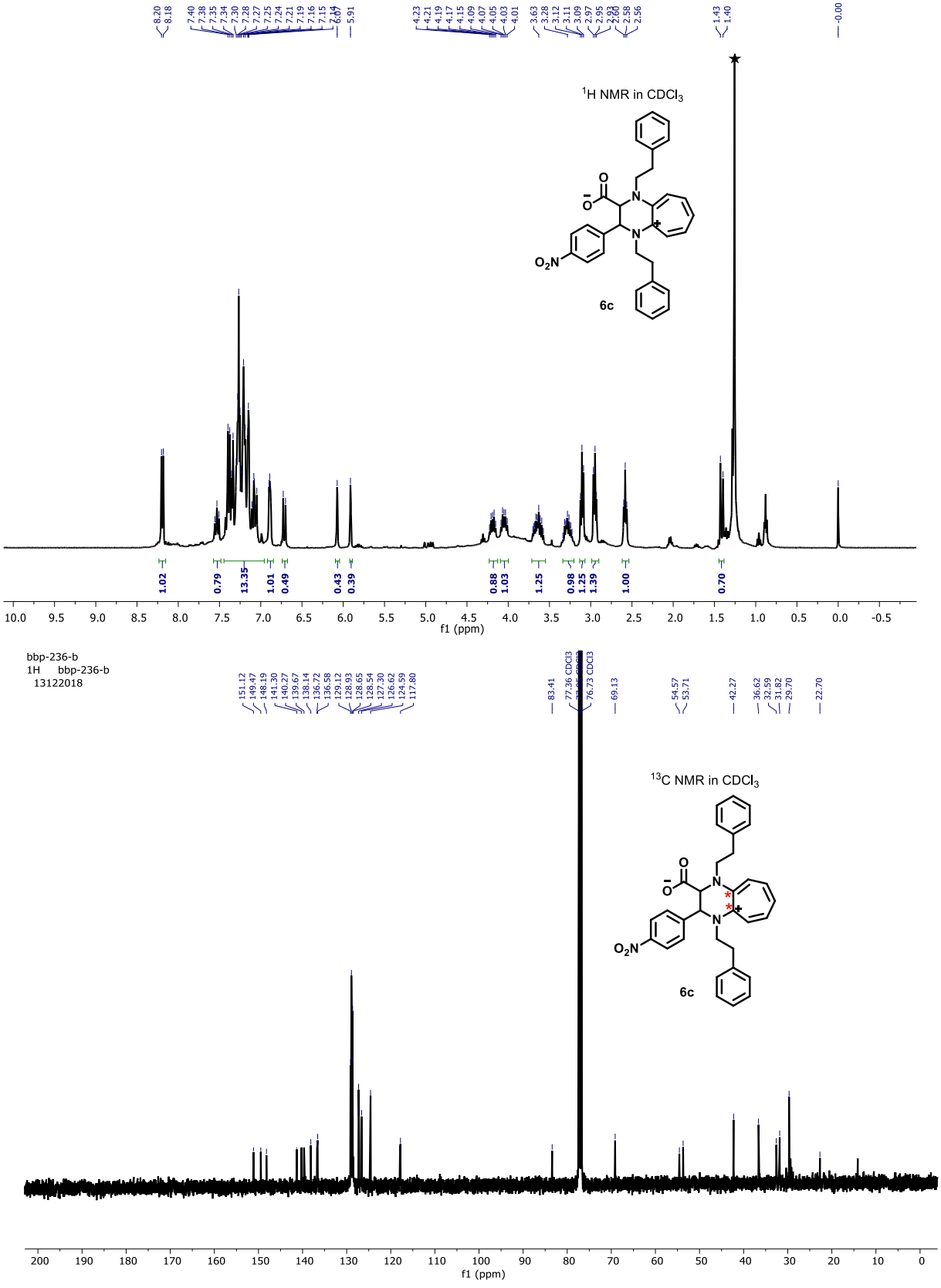

Figure A5. ^{1}H-/^{13}C-NMR spectra of **(6c)** in $CDCl_3$

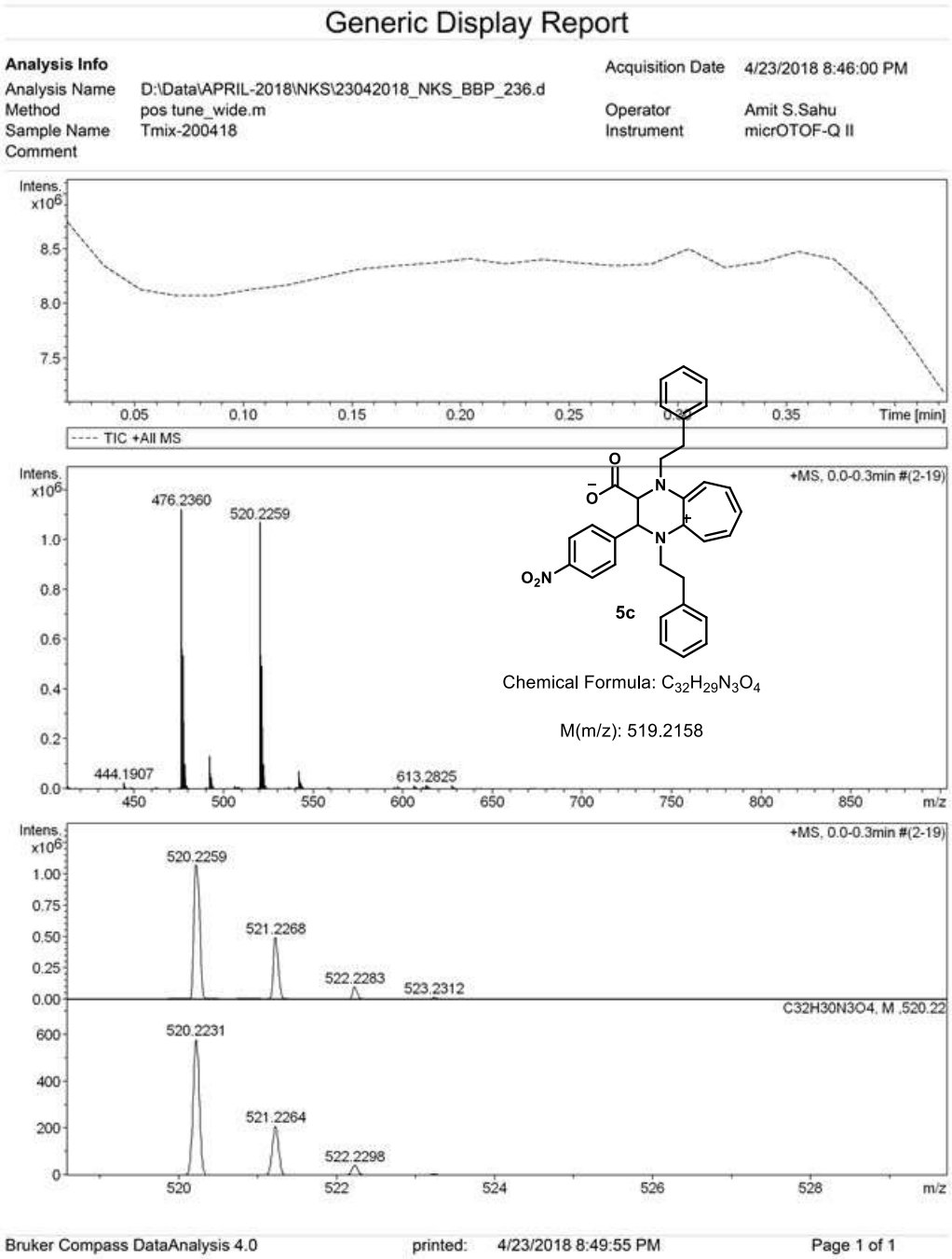

Figure A6. ESI/HRMS spectra of compound **(6c)**

4. NMR($^{1}H/^{13}C$) and HRMS of Aryl Troponyl dihydro pyrazine (**6d**)

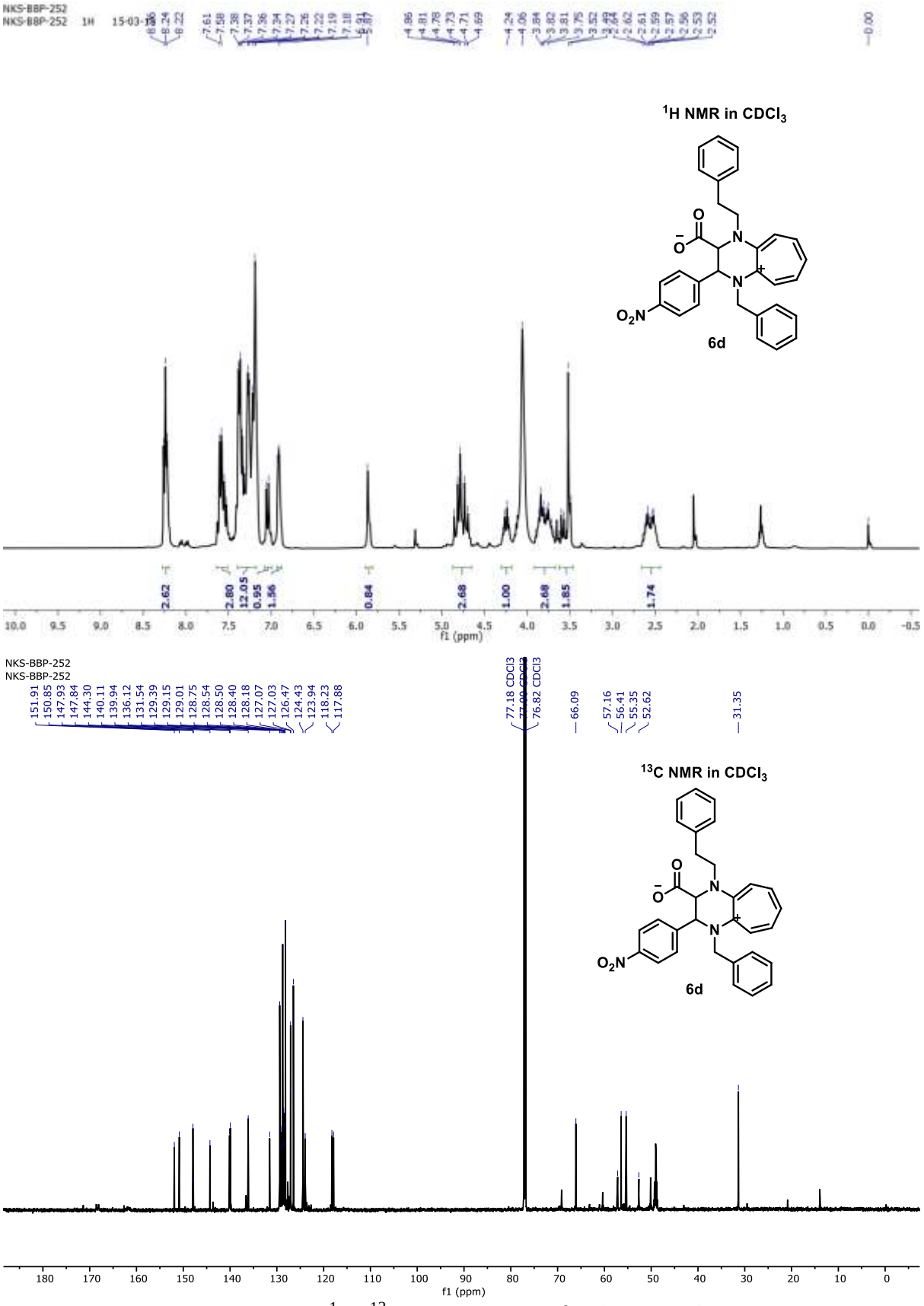

Figure A7. ^{1}H-/^{13}C-NMR spectra of **(6d)** in $CDCl_3$

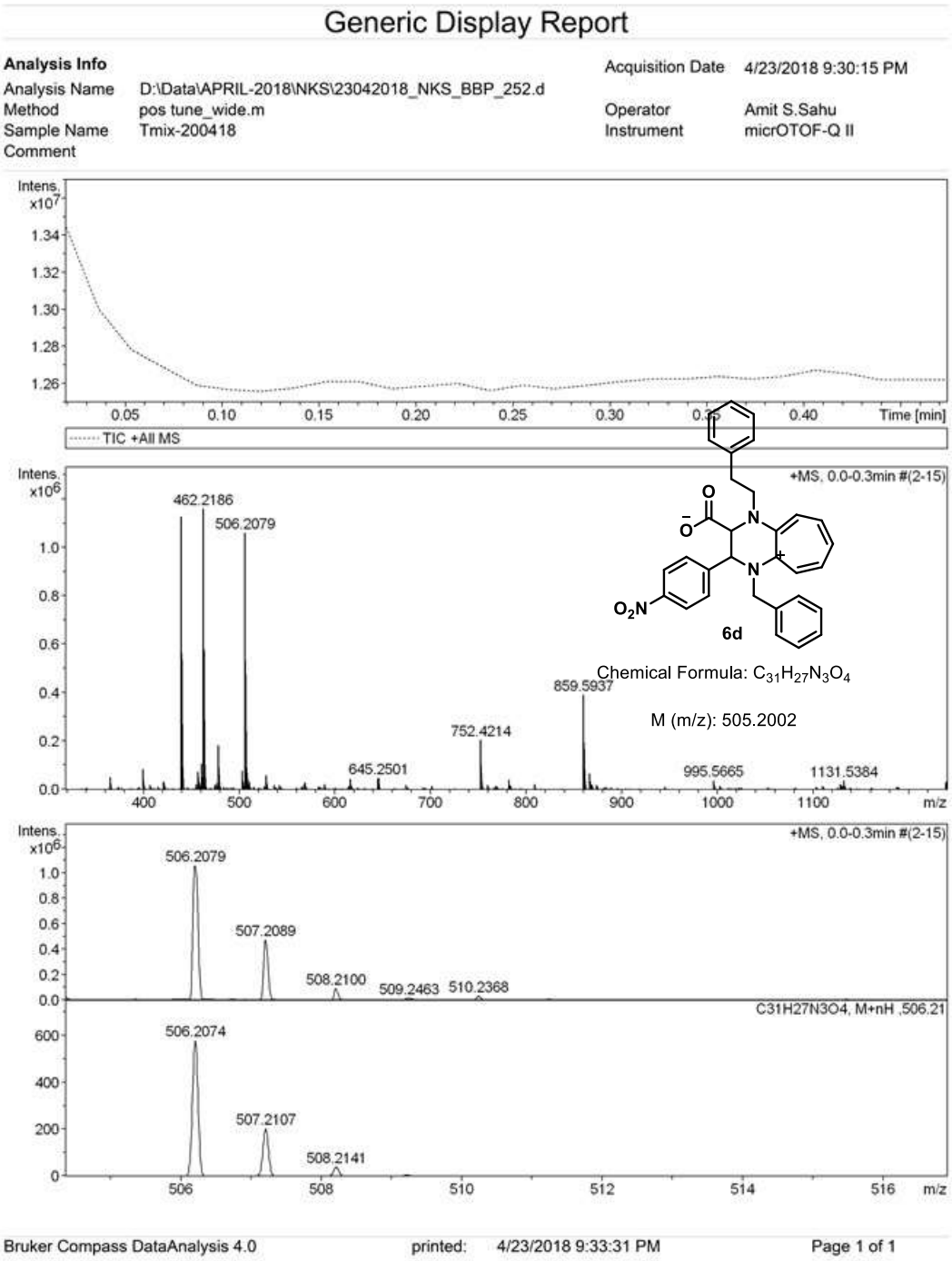

Figure A8. ESI/HRMS spectra of compound **(6d)**

5. NMR(^{1}H/^{13}C/^{13}CDEPT -135) and HRMS of Aryl Troponyl dihydro pyrazine (**6e**)

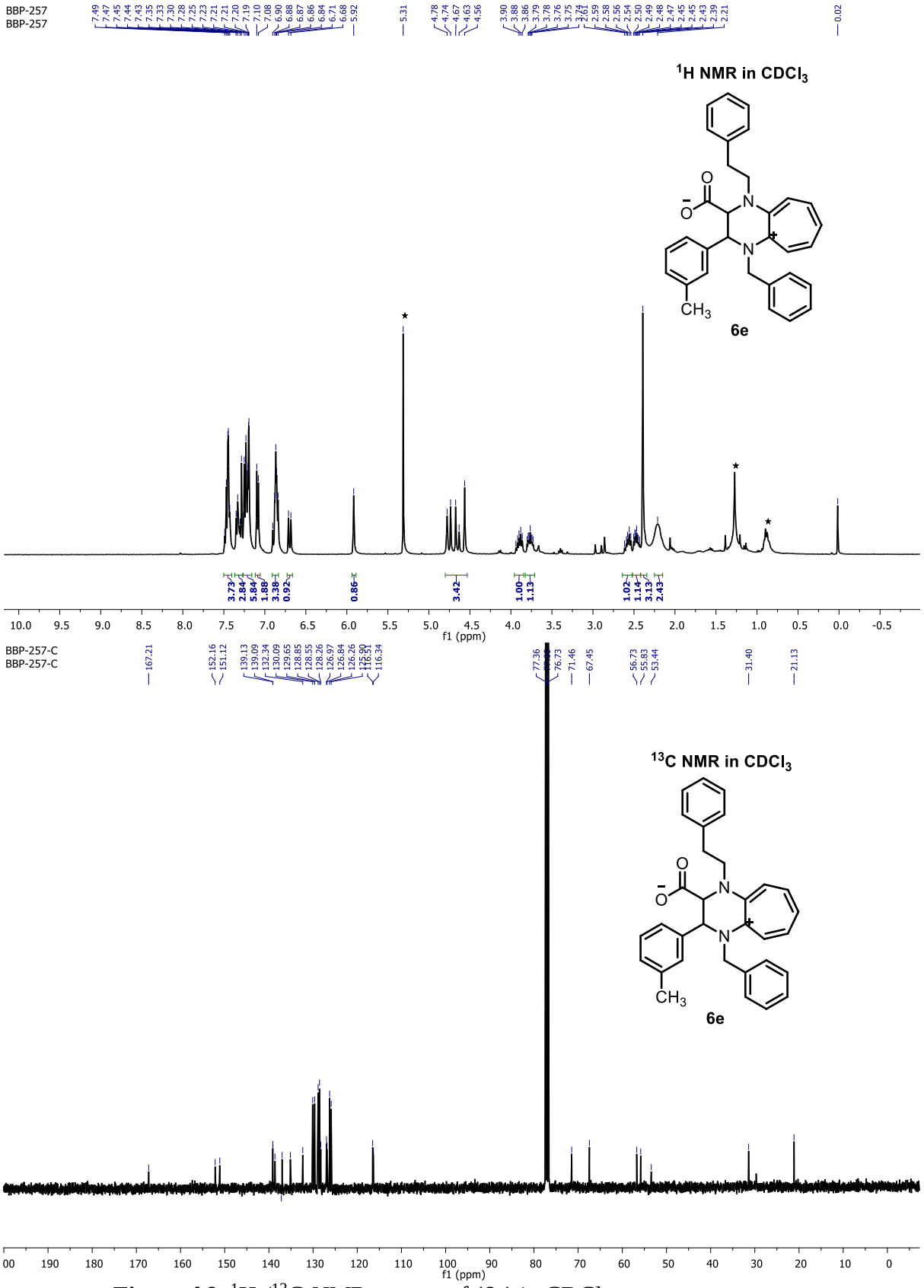

Figure A9. ^{1}H-/^{13}C-NMR spectra of **(6e)** in $CDCl_3$

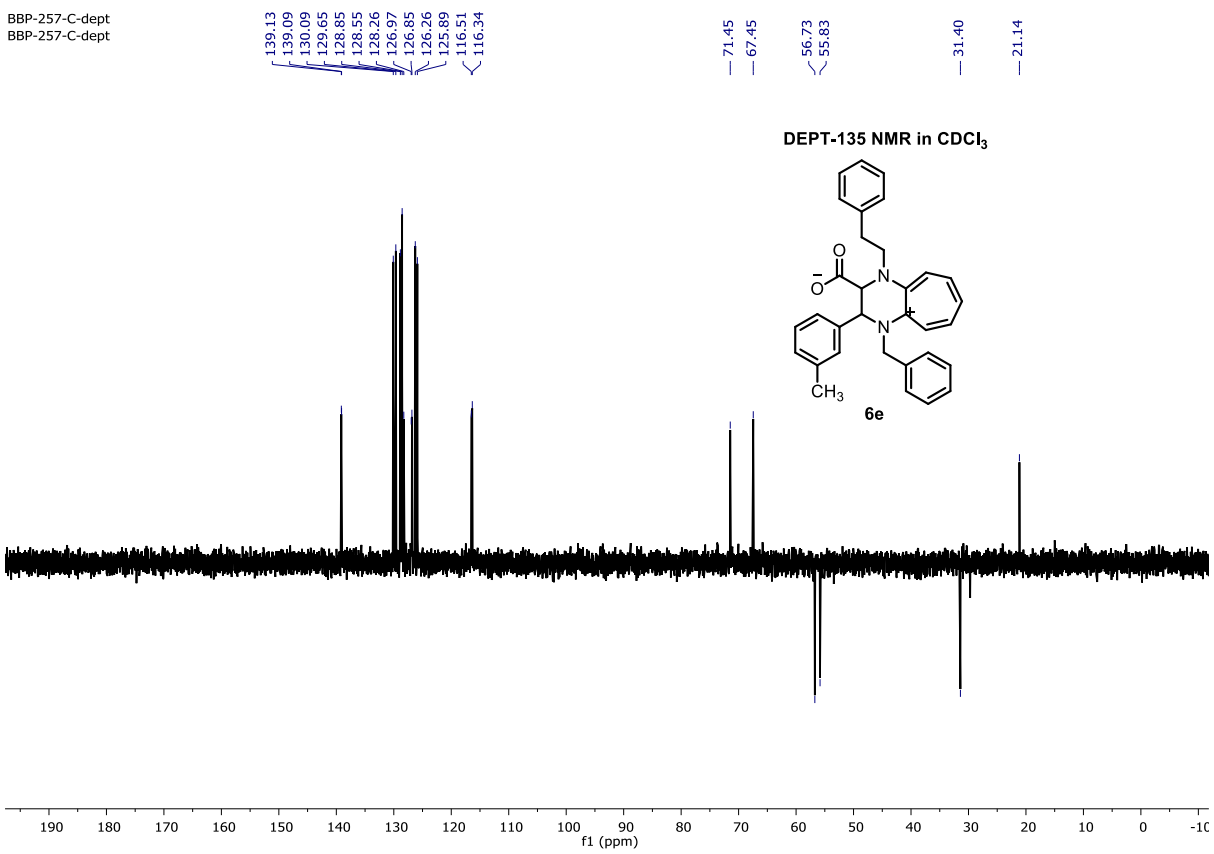

Figure A10. ^{13}CDEPT-135 NMR spectra of **(6e)** in $CDCl_3$

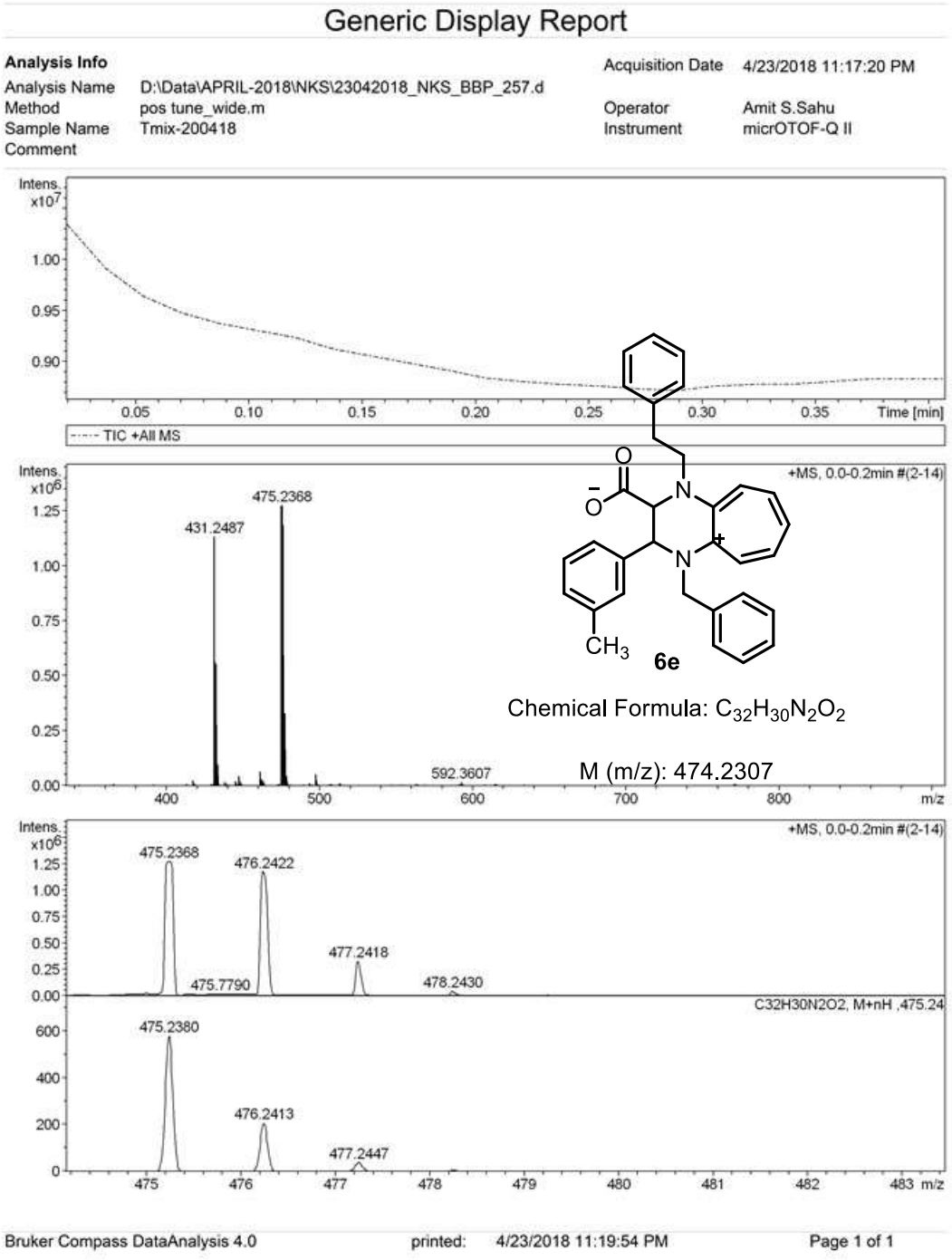

Figure A11. ESI/HRMS spectra of compound **(6e)**

6. NMR(1H/13C) and HRMS of Aryl Troponyl dihydro pyrazine **(6f)**

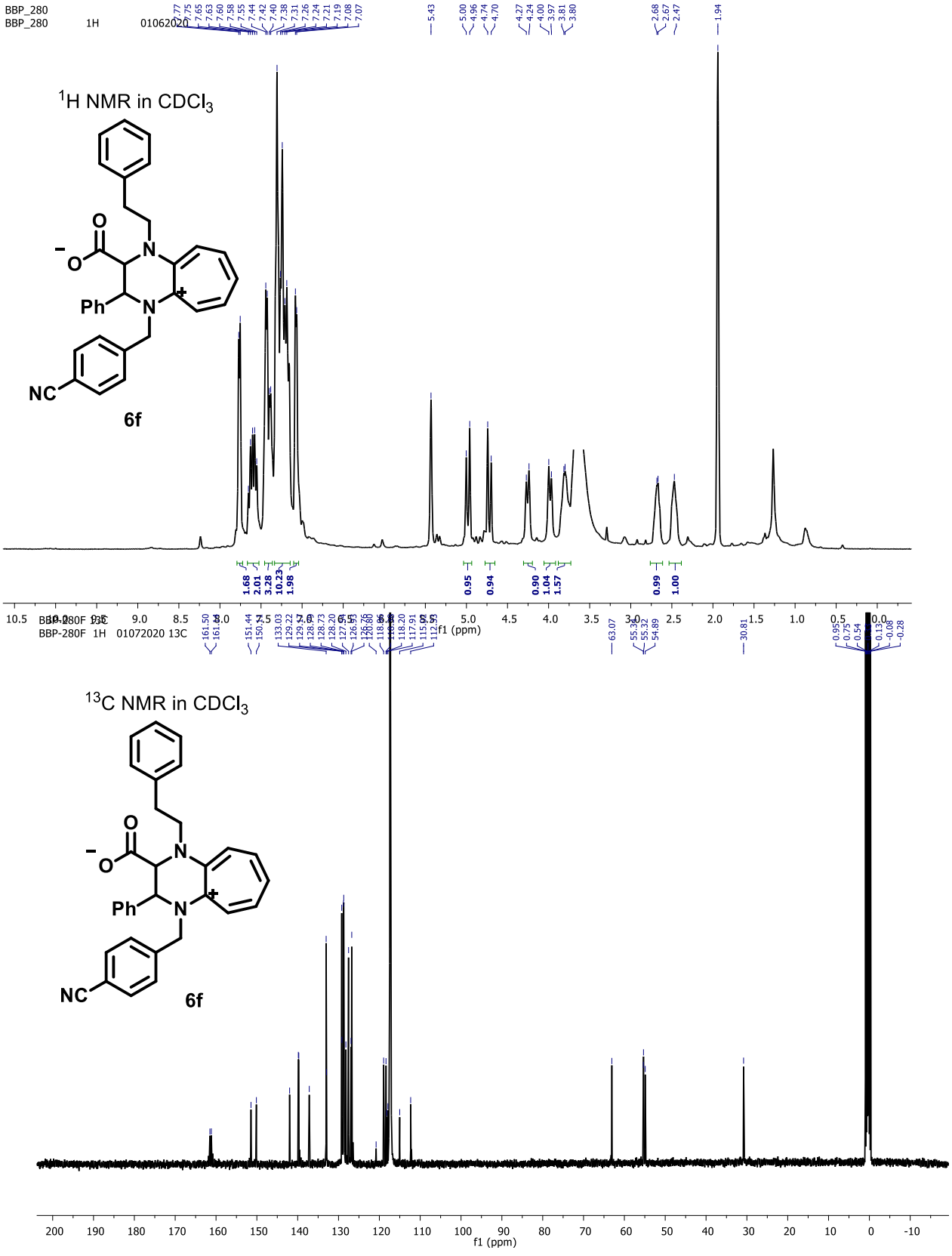

Figure A12. ^{1}H-/^{13}C- NMR spectra of **(6f)** in $CDCl_3$

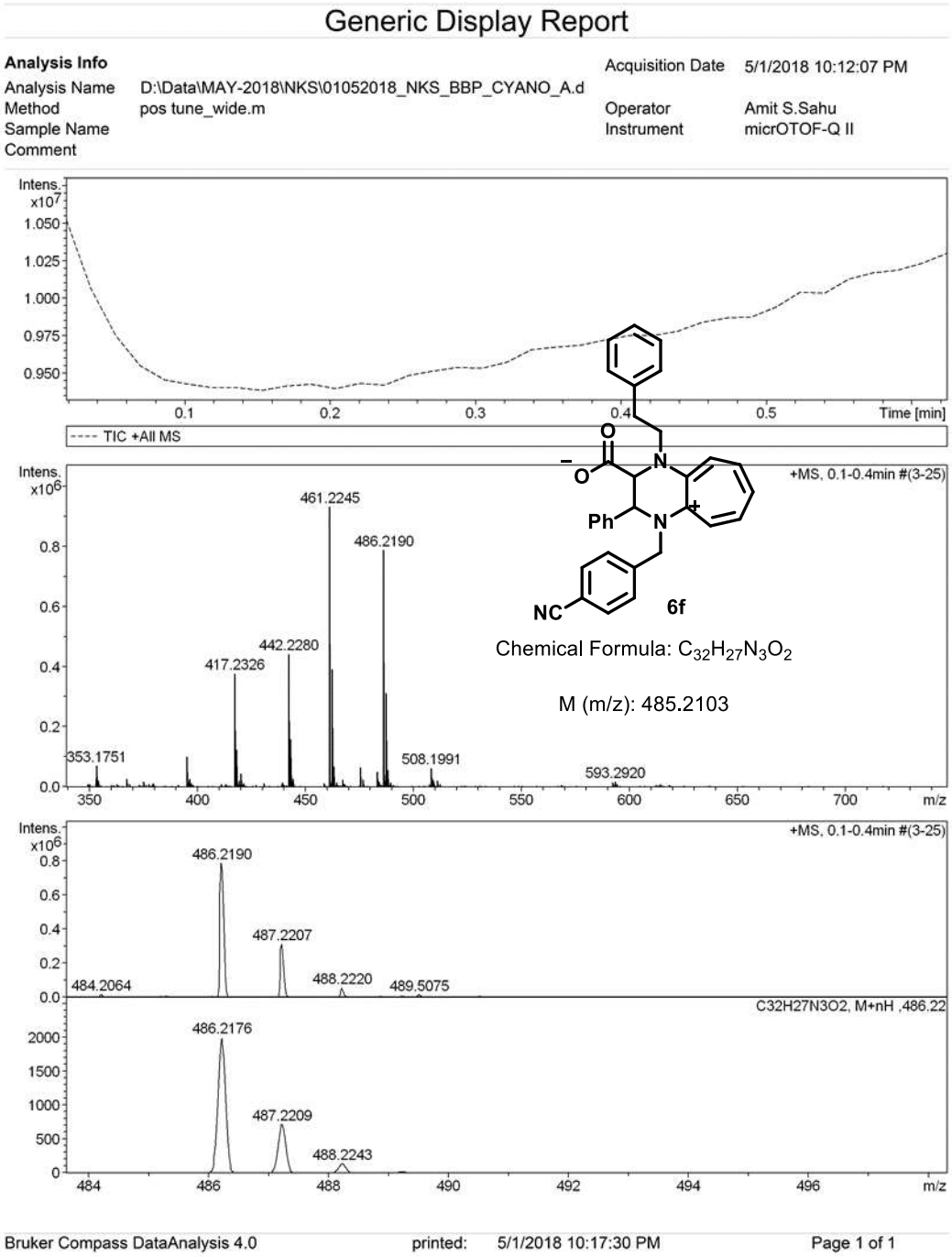

Figure A13. ESI/HRMS spectra of compound **(6f)**

7. NMR(^{1}H/^{13}C) and HRMS of Aryl Troponyl dihydro pyrazine **(6g)**

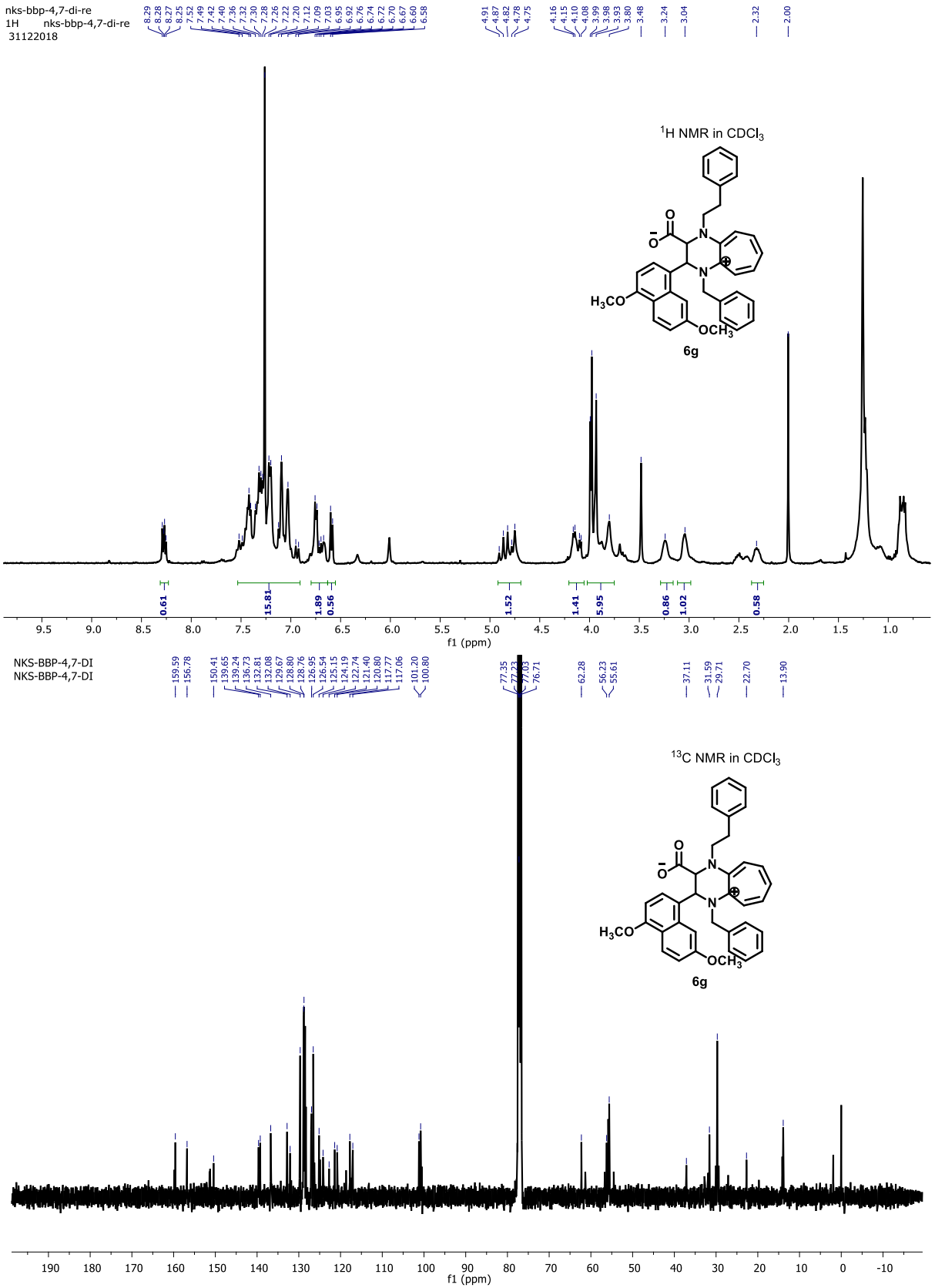

Figure A14. ^{1}H-/^{13}C-NMR spectra of **(6g)** in $CDCl_3$

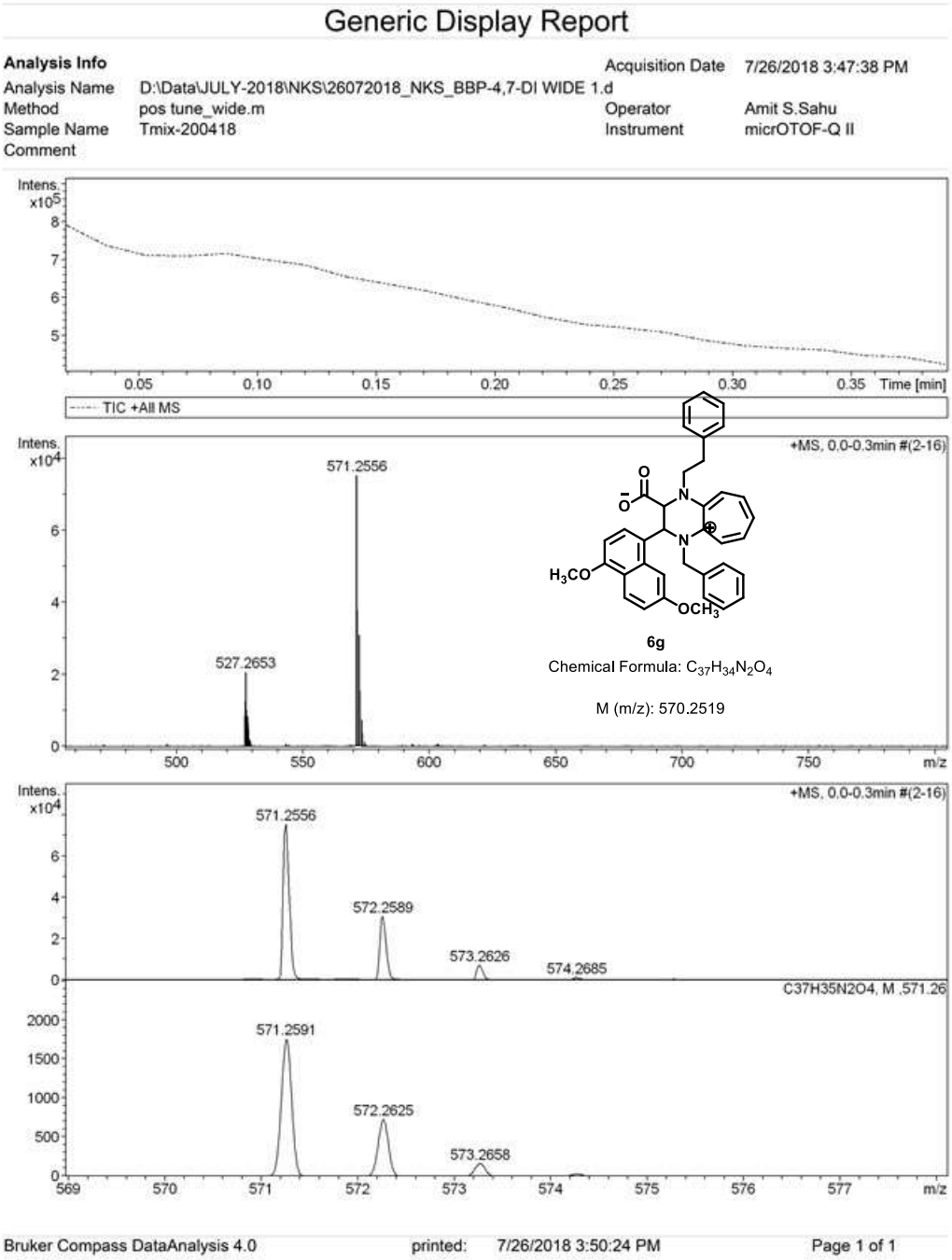

Figure A15. ESI/HRMS spectra of compound **(6g)**

8. NMR(^{1}H/^{13}C/^{13}CDEPT) and HRMS of Aryl Troponyl dihydro pyrazine **(6h)**

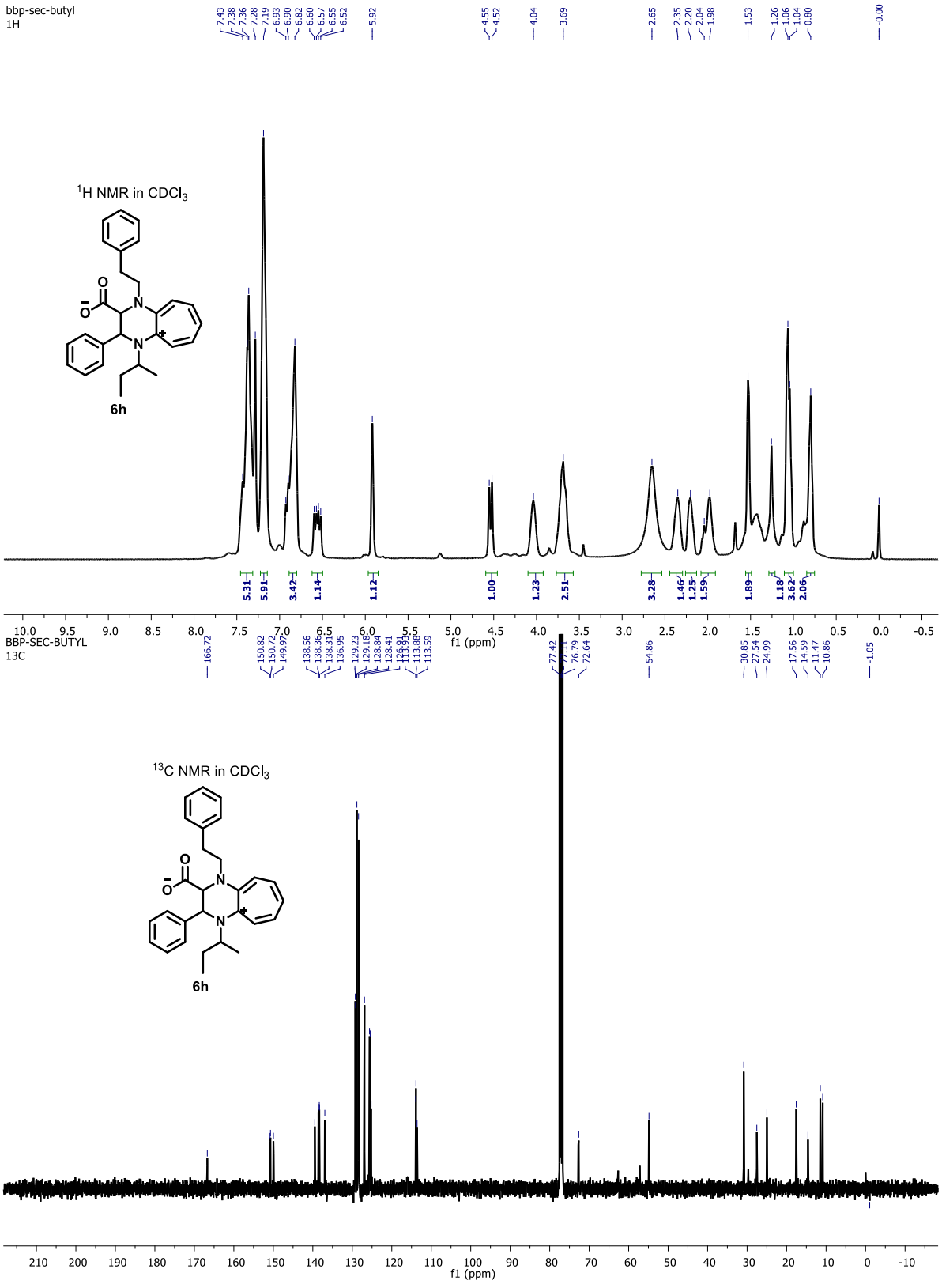

Figure A16. ^{1}H-/^{13}C-NMR spectra of **(6h)** in $CDCl_3$

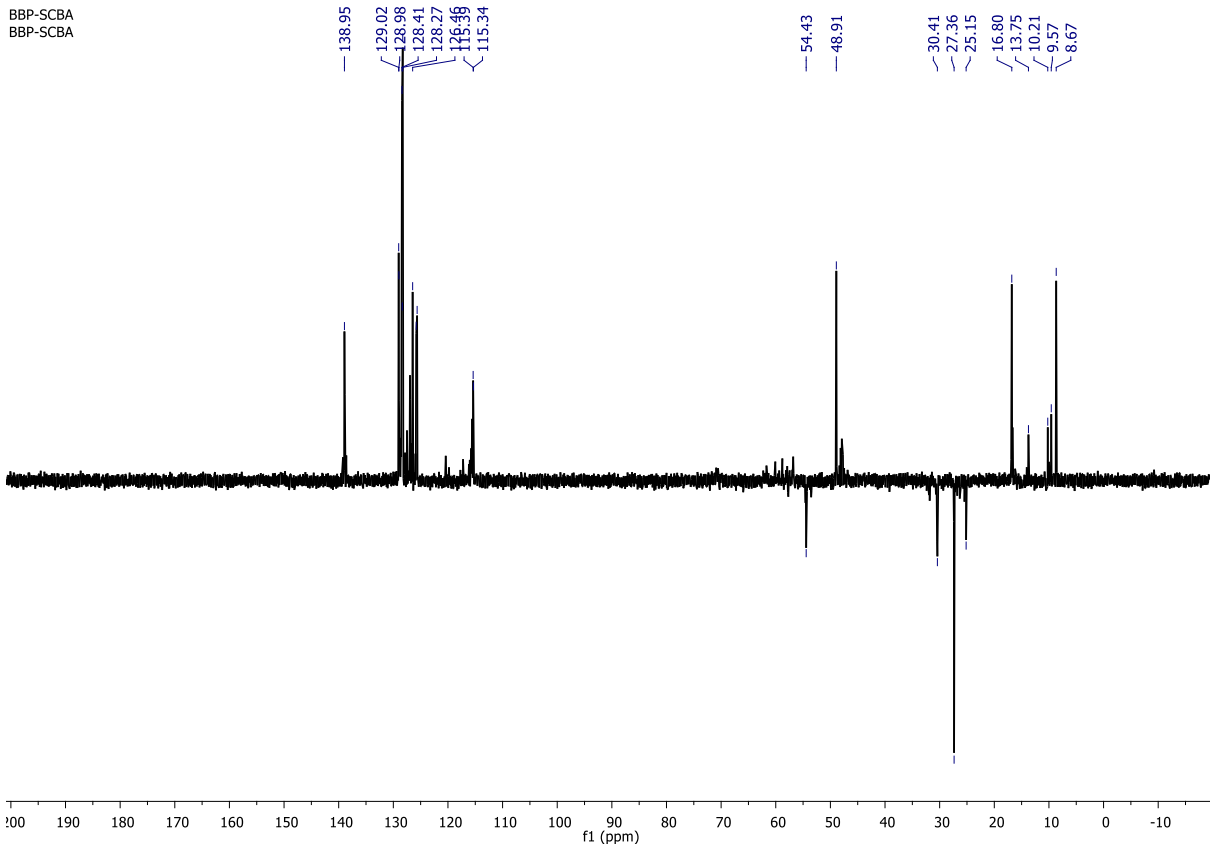

Figure A17. ^{13}CDEPT -135 NMR spectra of **(6h)** in $CDCl_3$

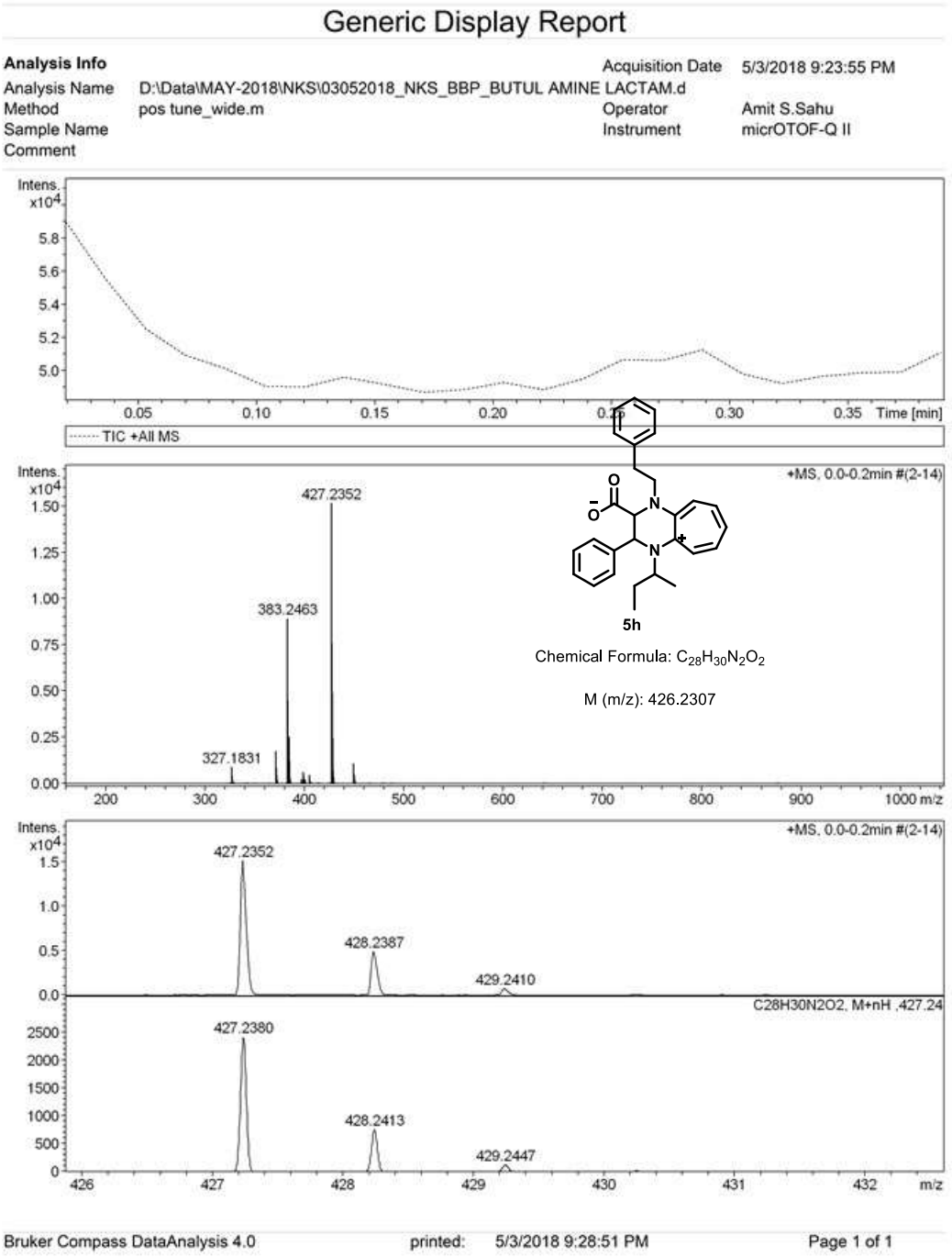

Figure A18. ESI/HRMS spectra of compound **(6h**

9. NMR($^{1}H/^{13}C$) and HRMS of Aryl Troponyl dihydro pyrazine **(6i)**

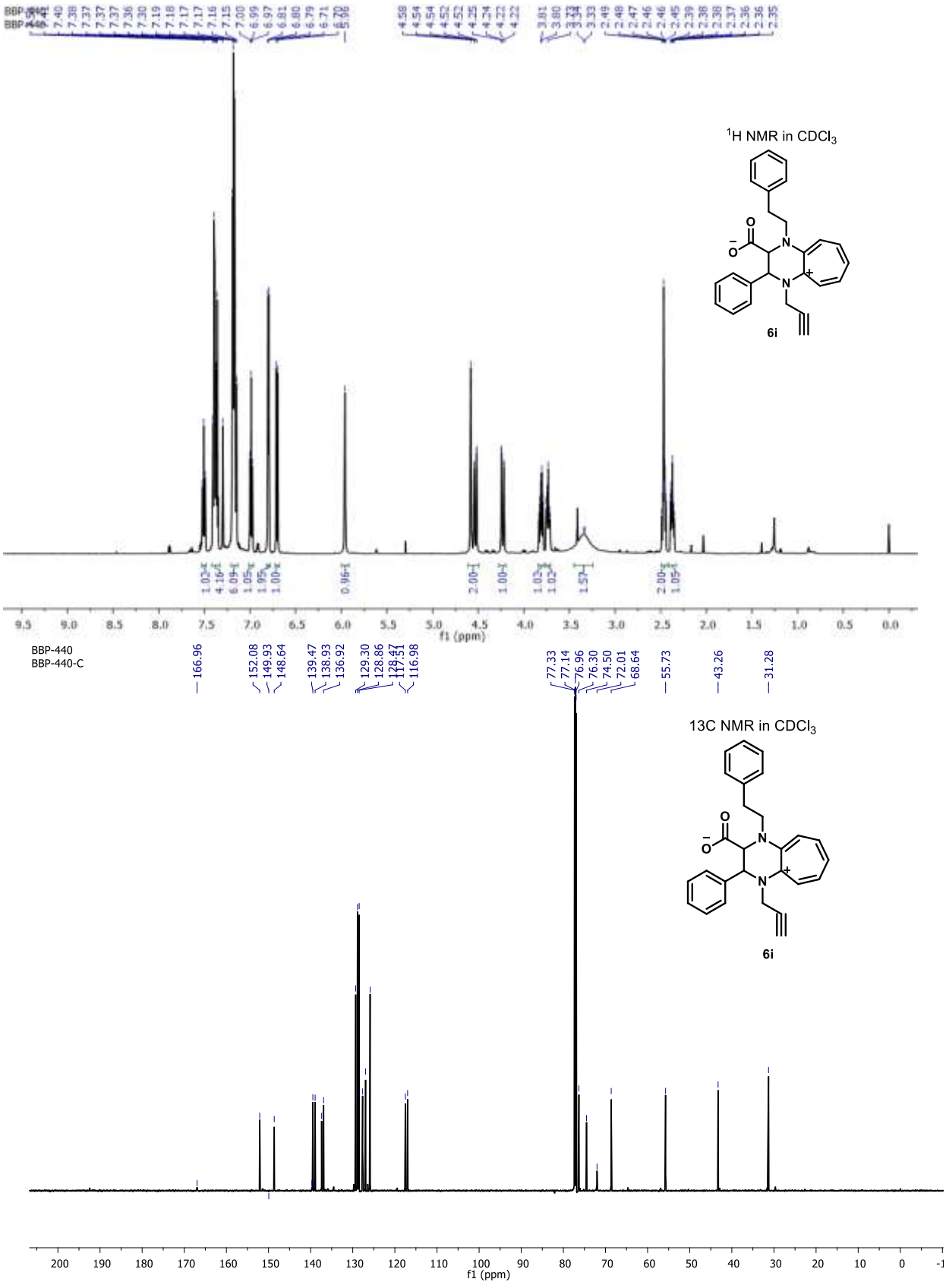

Figure A19. ^{1}H-/^{13}C NMR spectra of **(6i)** in $CDCl_3$

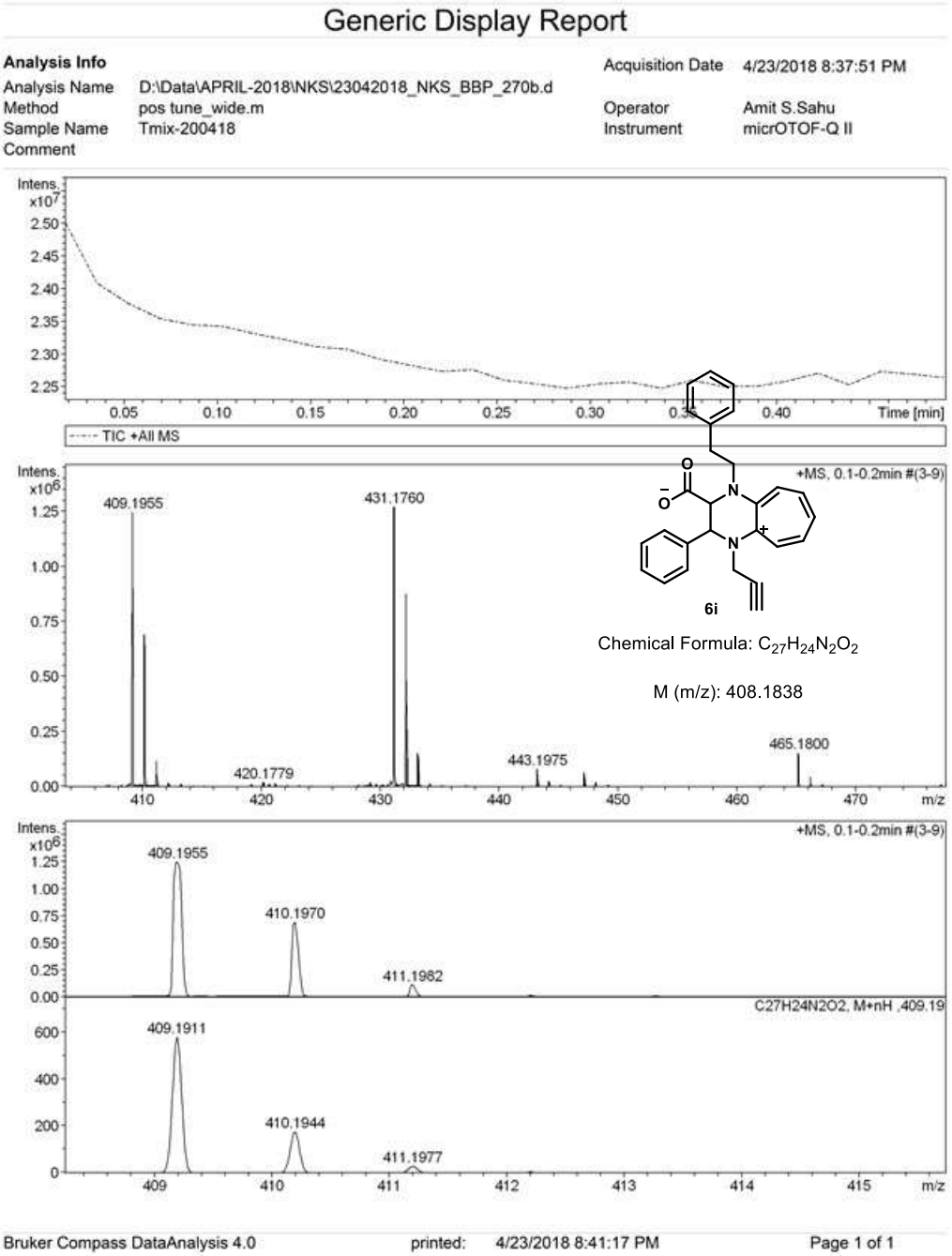

Figure A20. ESI/HRMS spectra of compound **(6i)**

10. NMR(^{1}H/^{13}C) and HRMS of Aryl Troponyl dihydro pyrazine **(6j)**

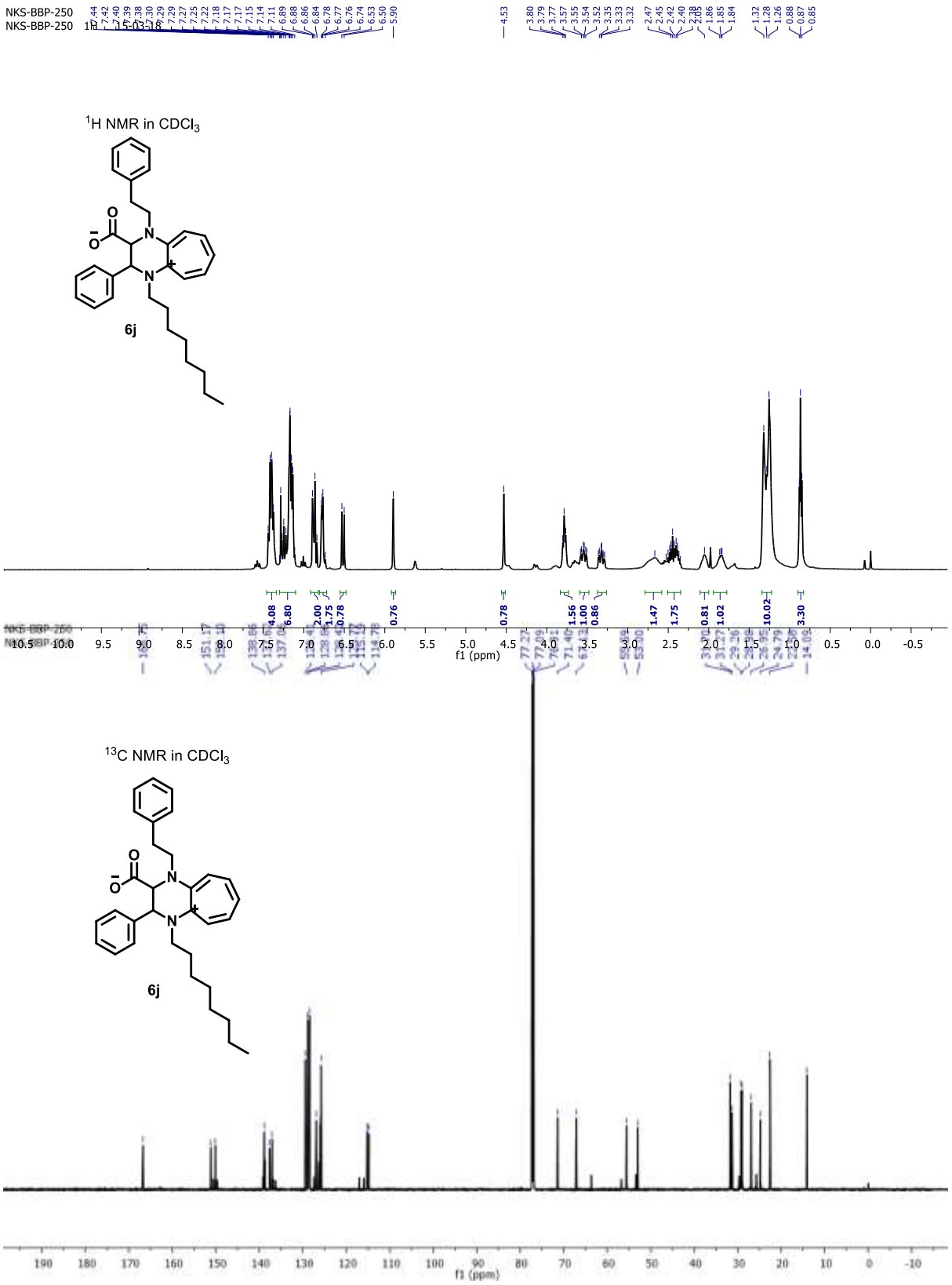

Figure A21. ^{1}H-/^{13}C- NMR spectra of **(6j)** in $CDCl_3$

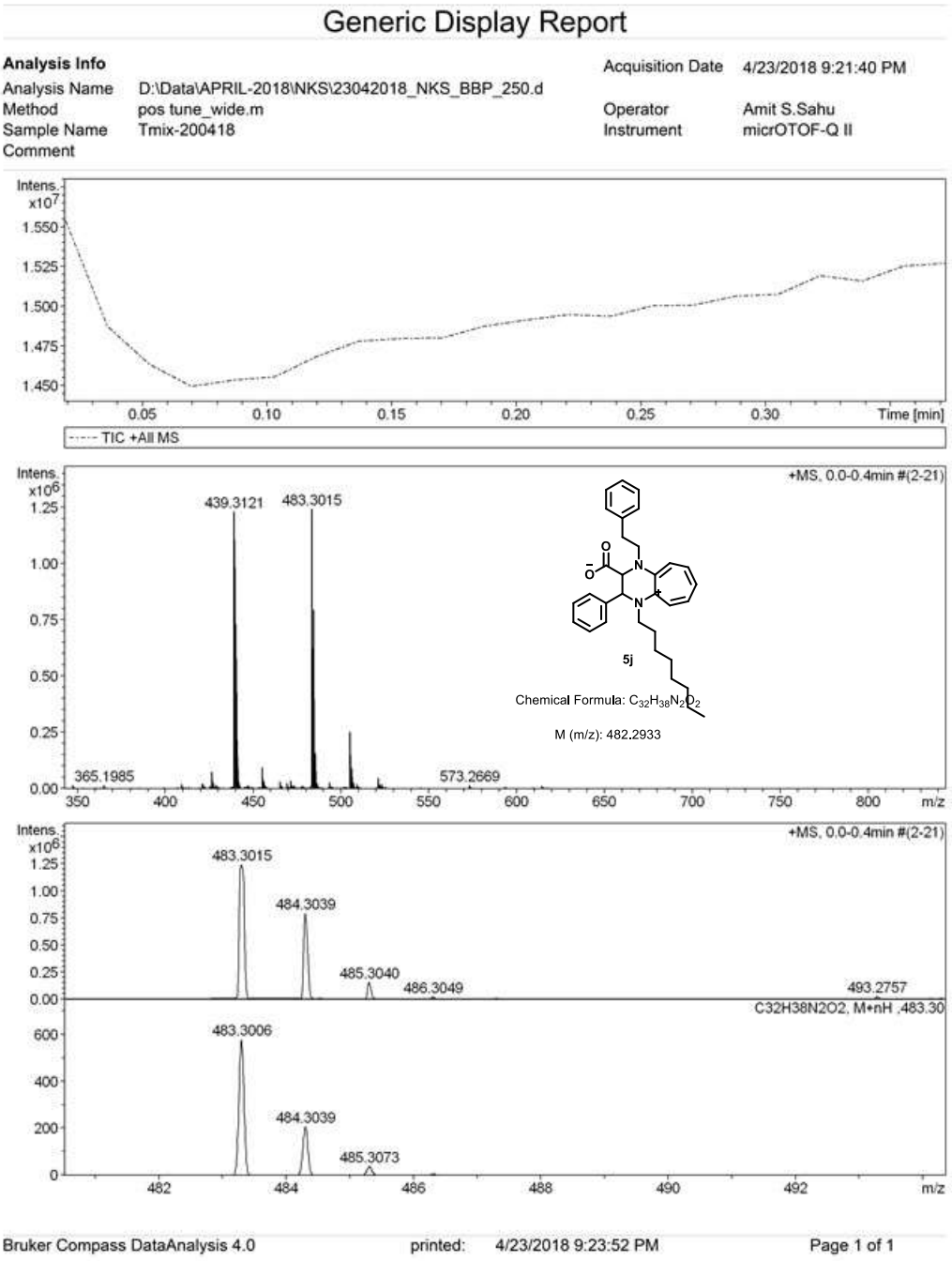

Figure A22. ESI/HRMS spectra of compound **(6j)**

11. NMR(^{1}H/^{13}C/^{13}CDEPT) and HRMS of Aryl Troponyl dihydro pyrazine **(6k)**

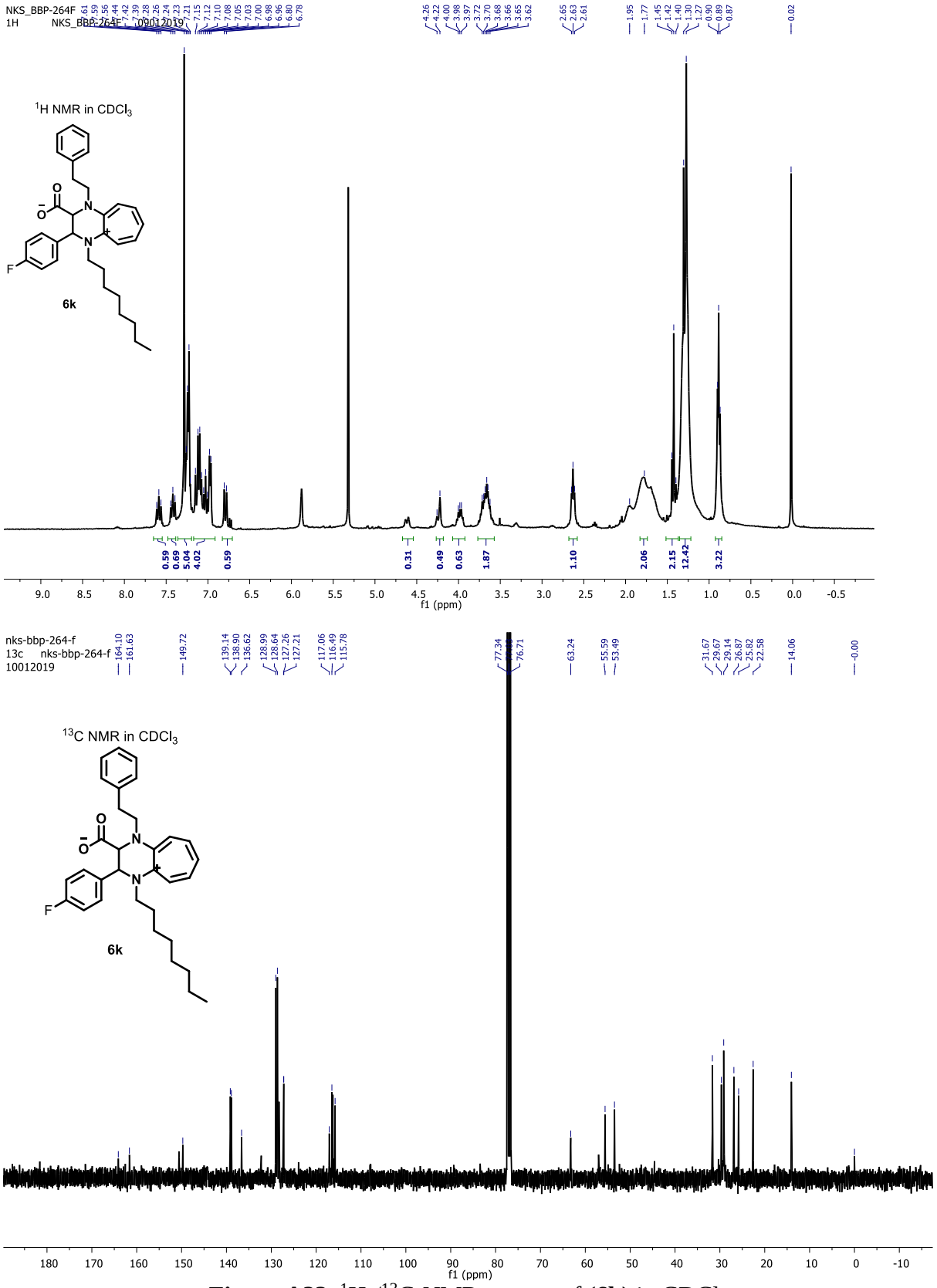

Figure A23. ^{1}H-/^{13}C-NMR spectra of **(6k)** in $CDCl_3$

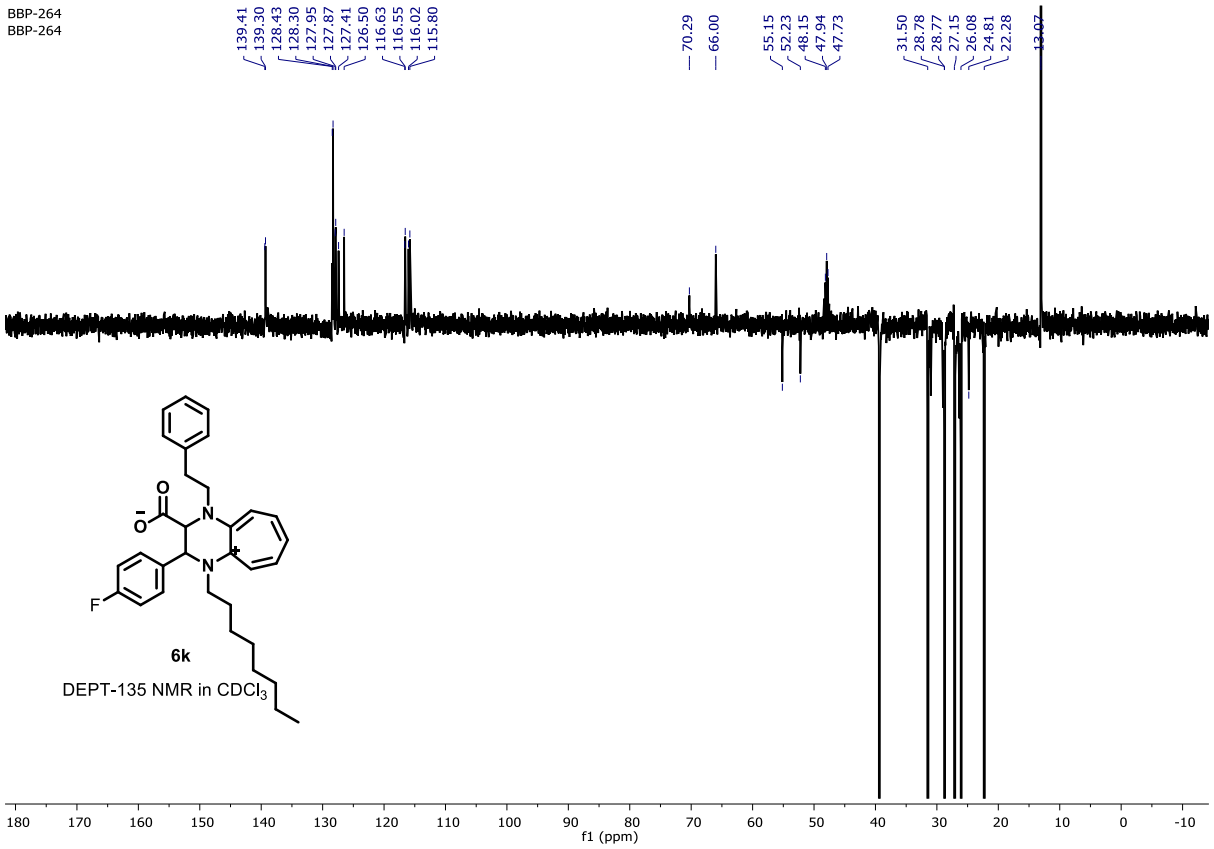

Figure A24. ^{13}CDEPT NMR spectra of **(6k)** in $CDCl_3$

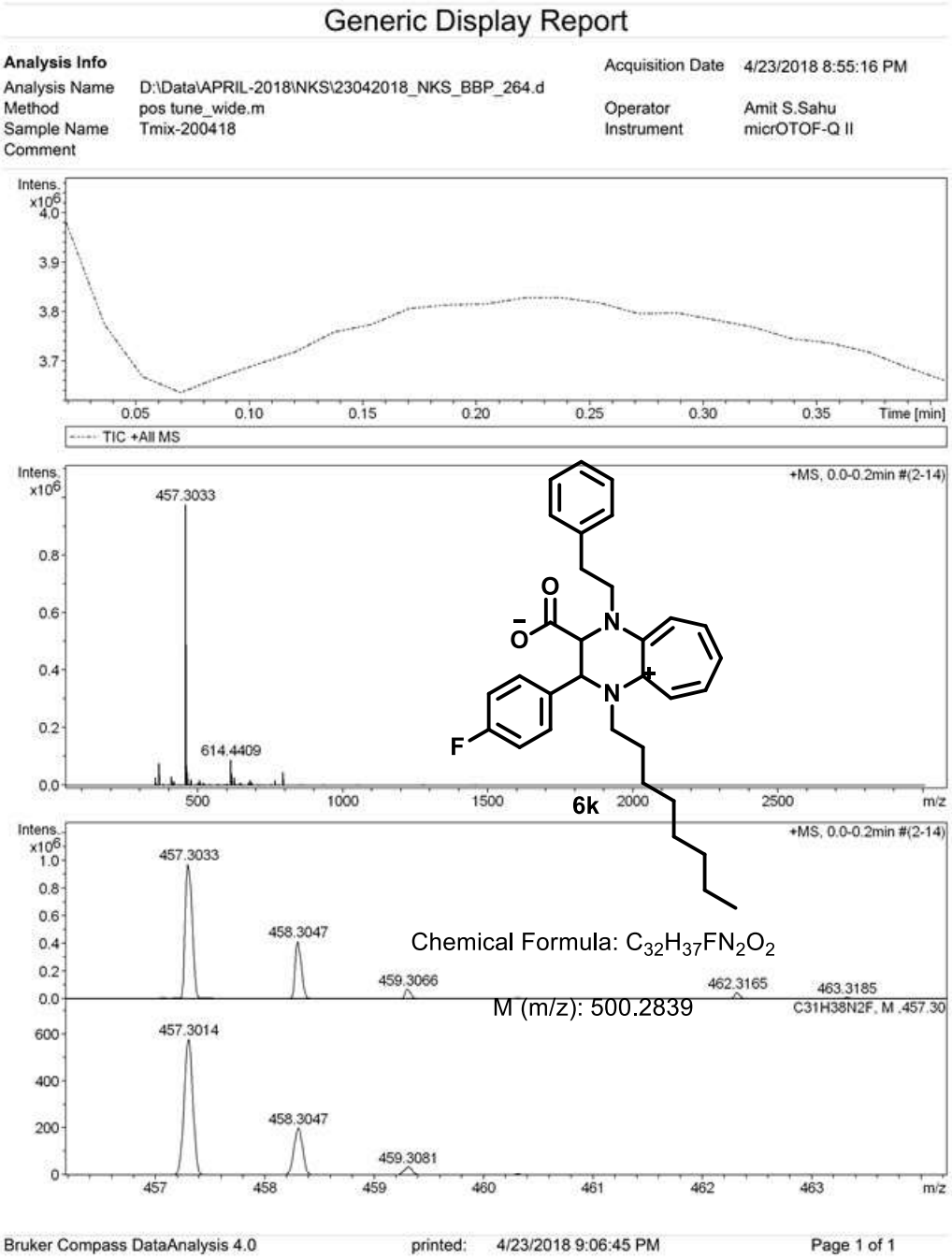

Figure A25. ESI/HRMS spectra of compound **(6k)**

12. NMR(1H/13C) and HRMS of Aryl Troponyl dihydro pyrazine **(6l)**

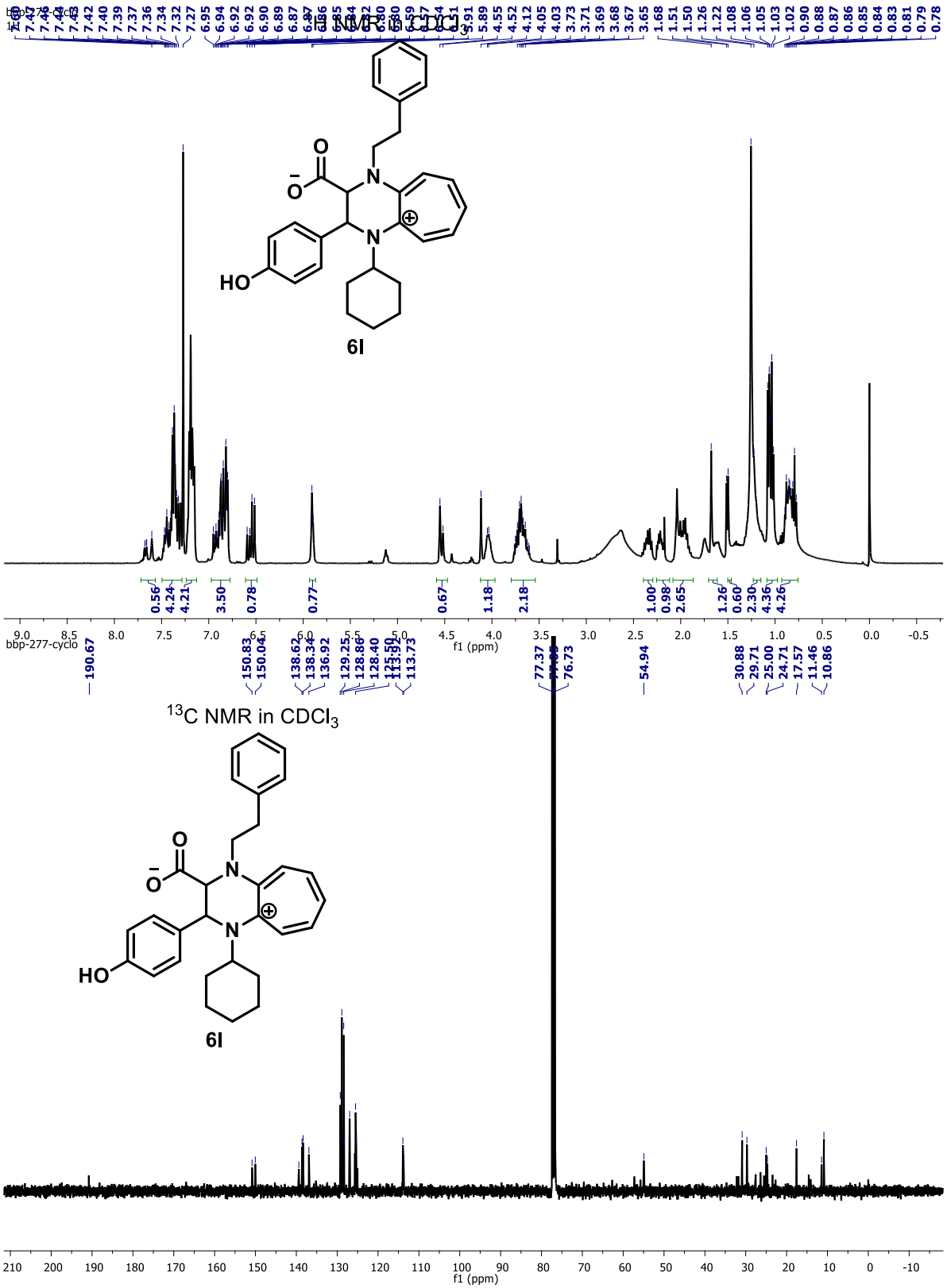

Figure A26. ^{1}H-/^{13}C NMR spectra of **(6m)** in $CDCl_3$

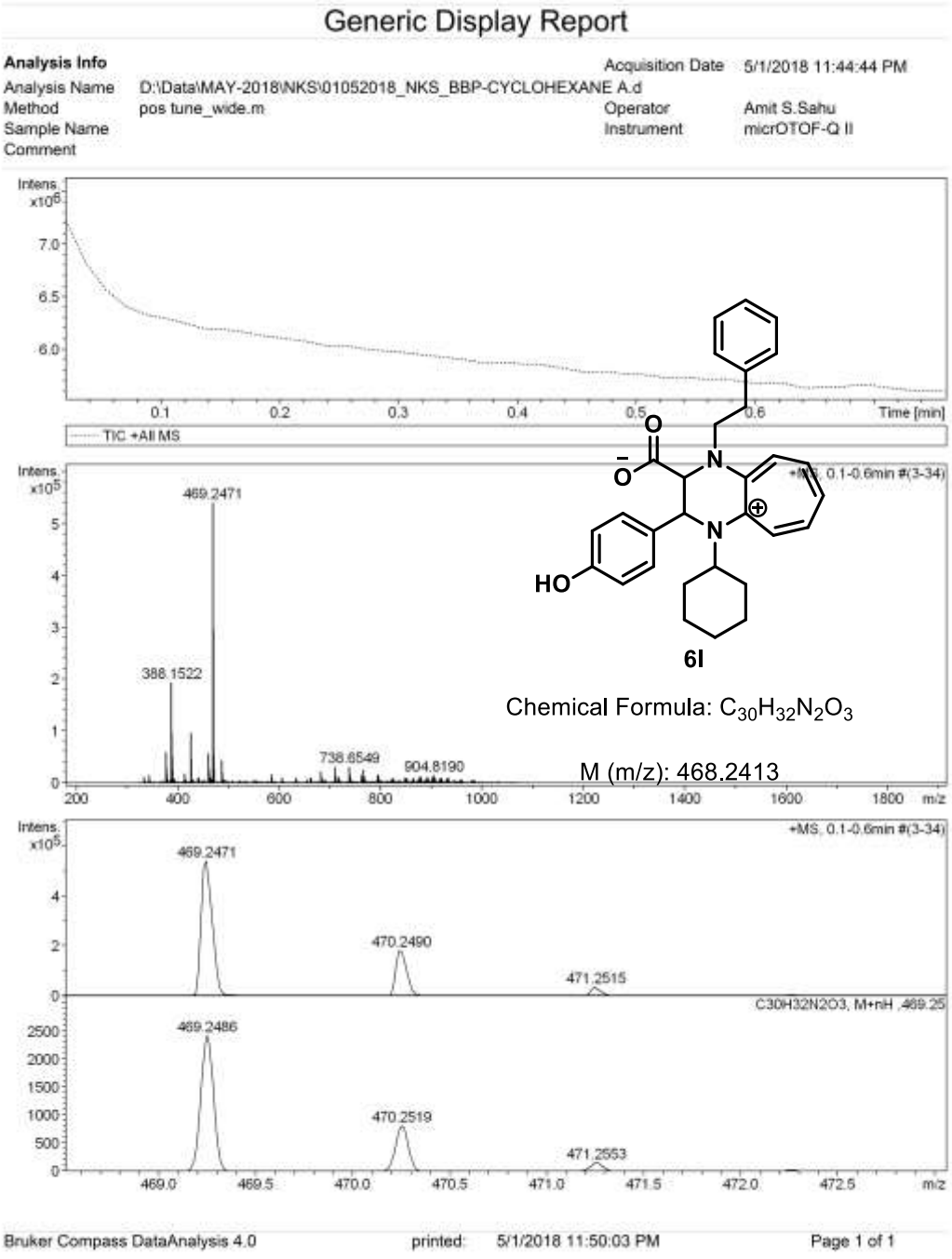

Figure A27. ESI/HRMS spectra of compound **(6l)**

13. NMR(^{1}H/^{13}C) and HRMS of Aryl Troponyl dihydro pyrazine **(6m)**

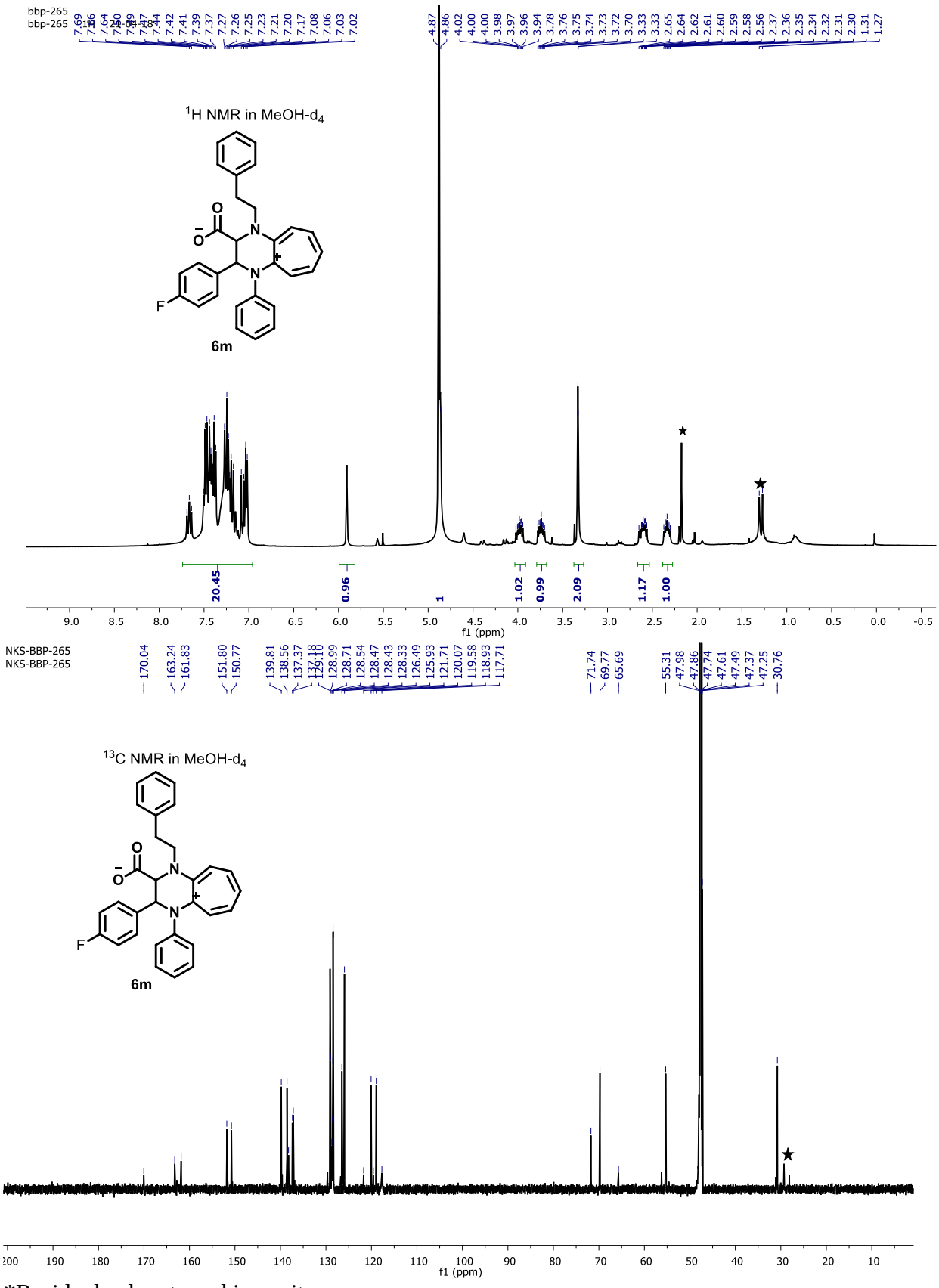

*Residual solvents and impurity grease

Figure A28. ^{1}H-/^{13}C-NMR spectra of **(6m)** in MeOH-d$_4$

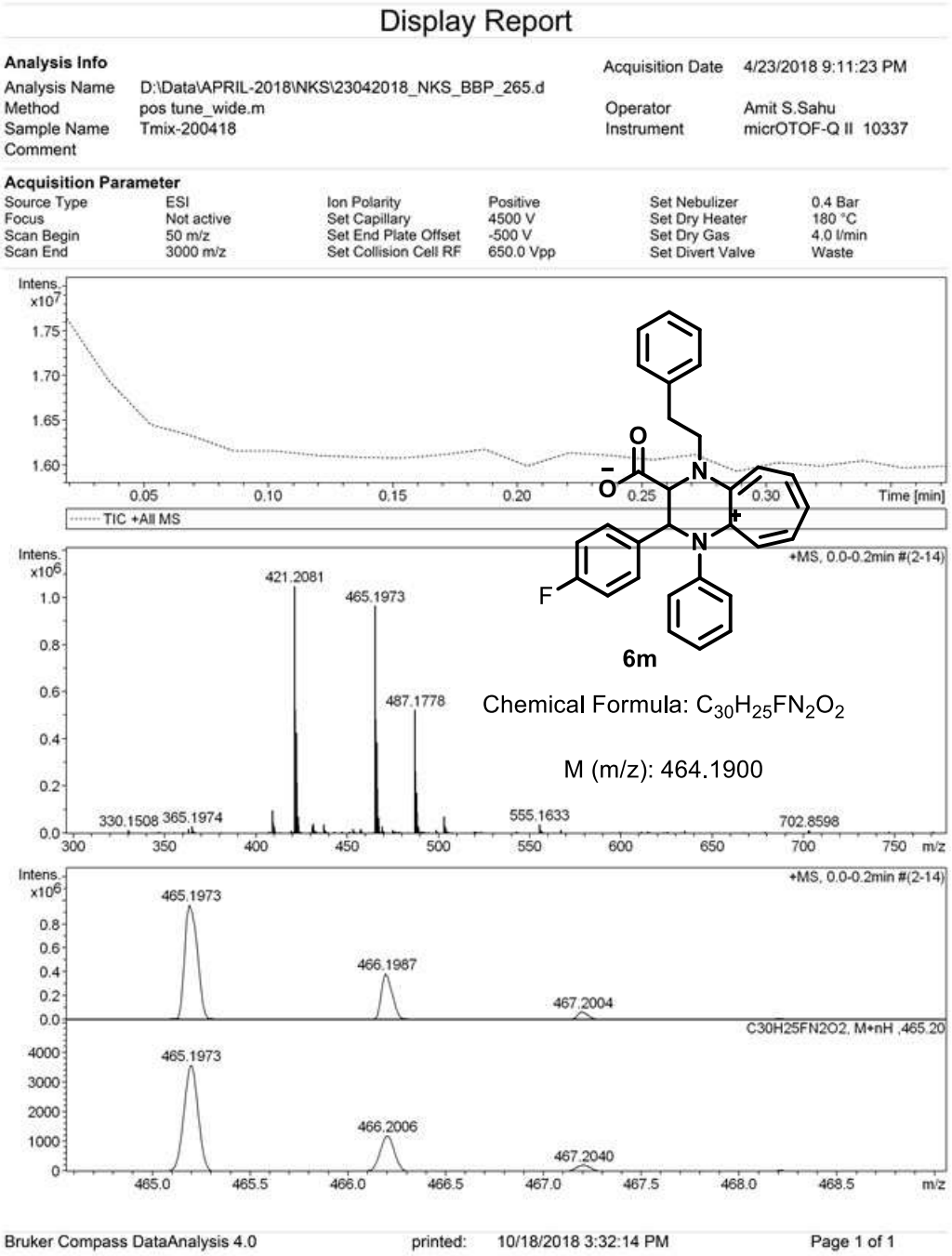

Figure A29. ESI/HRMS spectra of compound **(6m)**

14. NMR(^{1}H/^{13}C) and HRMS of Aryl Troponyl dihydro pyrazine **(6n)**

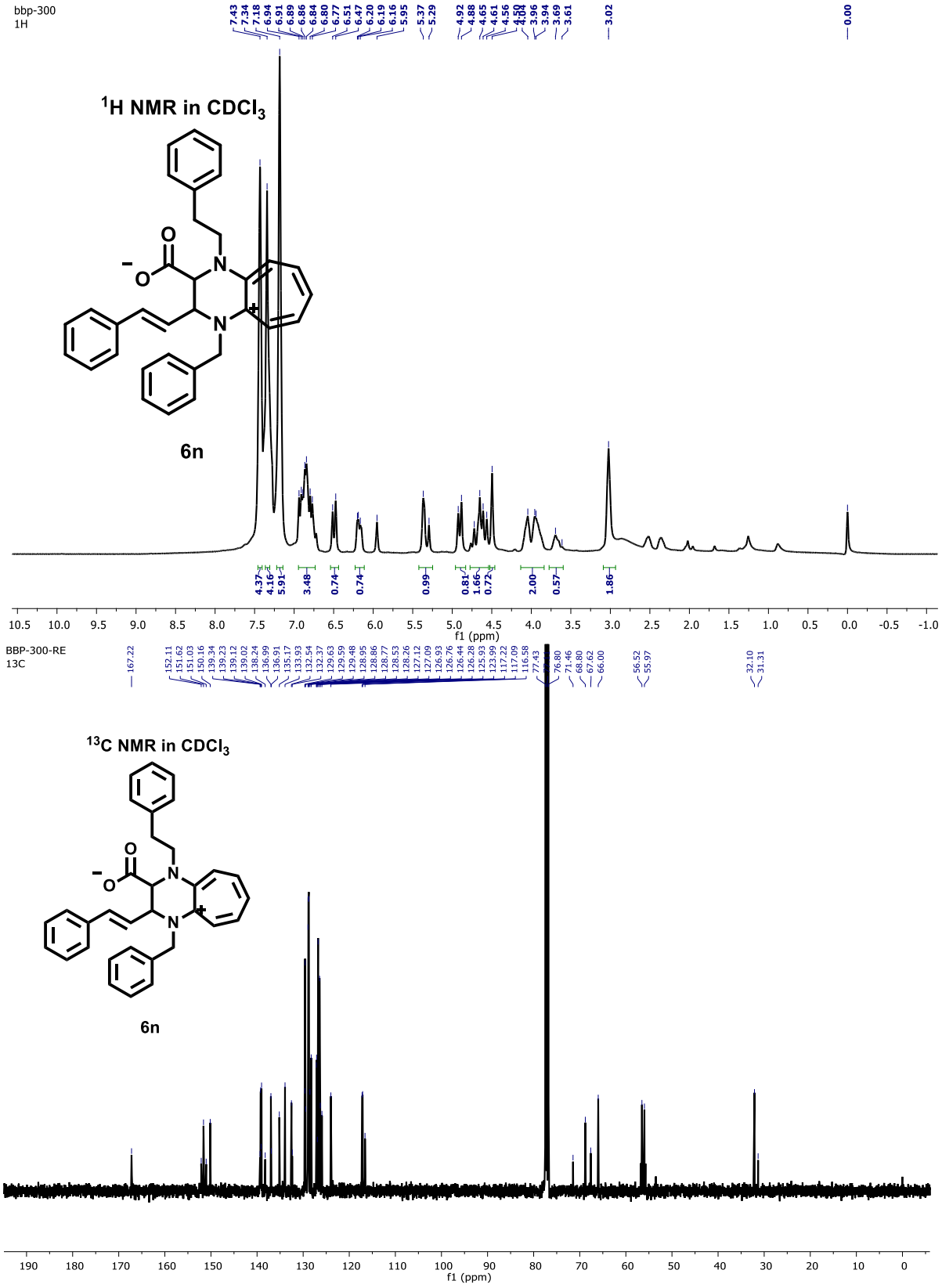

Figure A30. ^{1}H-/^{13}C-NMR spectra of **(6n)** in $CDCl_3$.

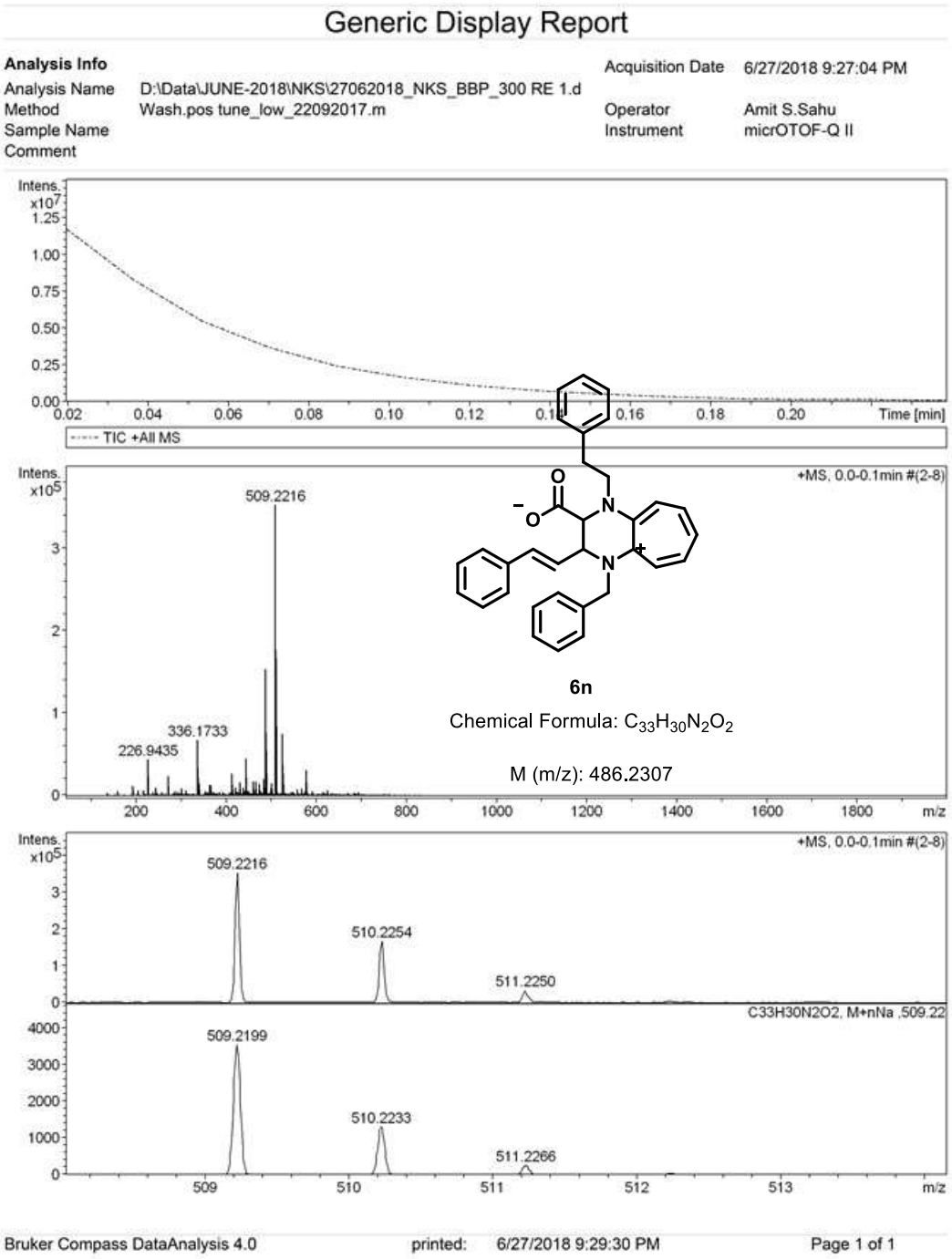

Figure A31. ESI/HRMS spectra of compound **(6n)**

15. NMR(^{1}H/^{13}C) and HRMS of Aryl Troponyl dihydro pyrazine **(6o)**

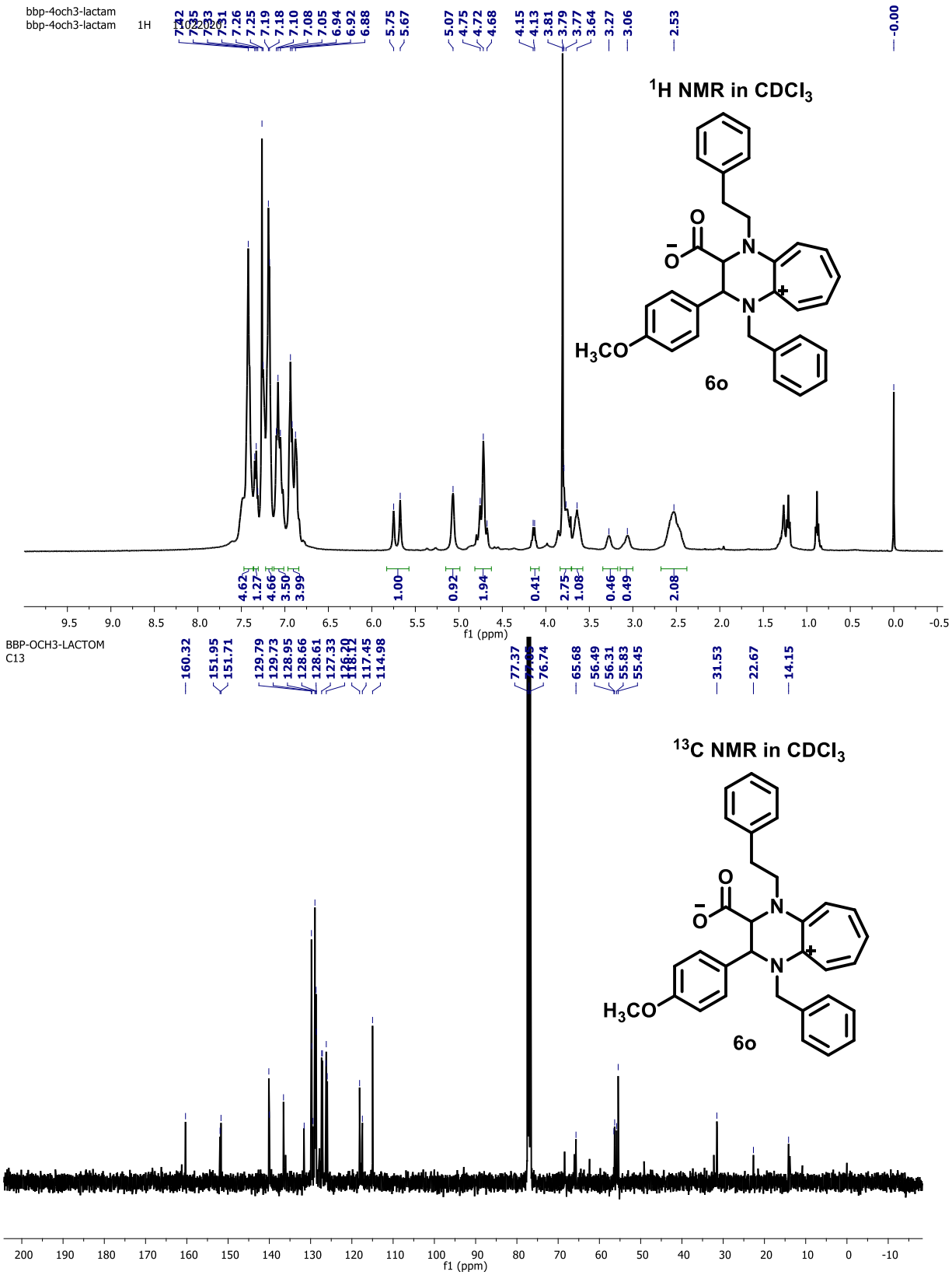

*Residual solvents and impurity grease

Figure A32. ^{1}H-/^{13}C- NMR spectra of **(6n)** in $CDCl_3$

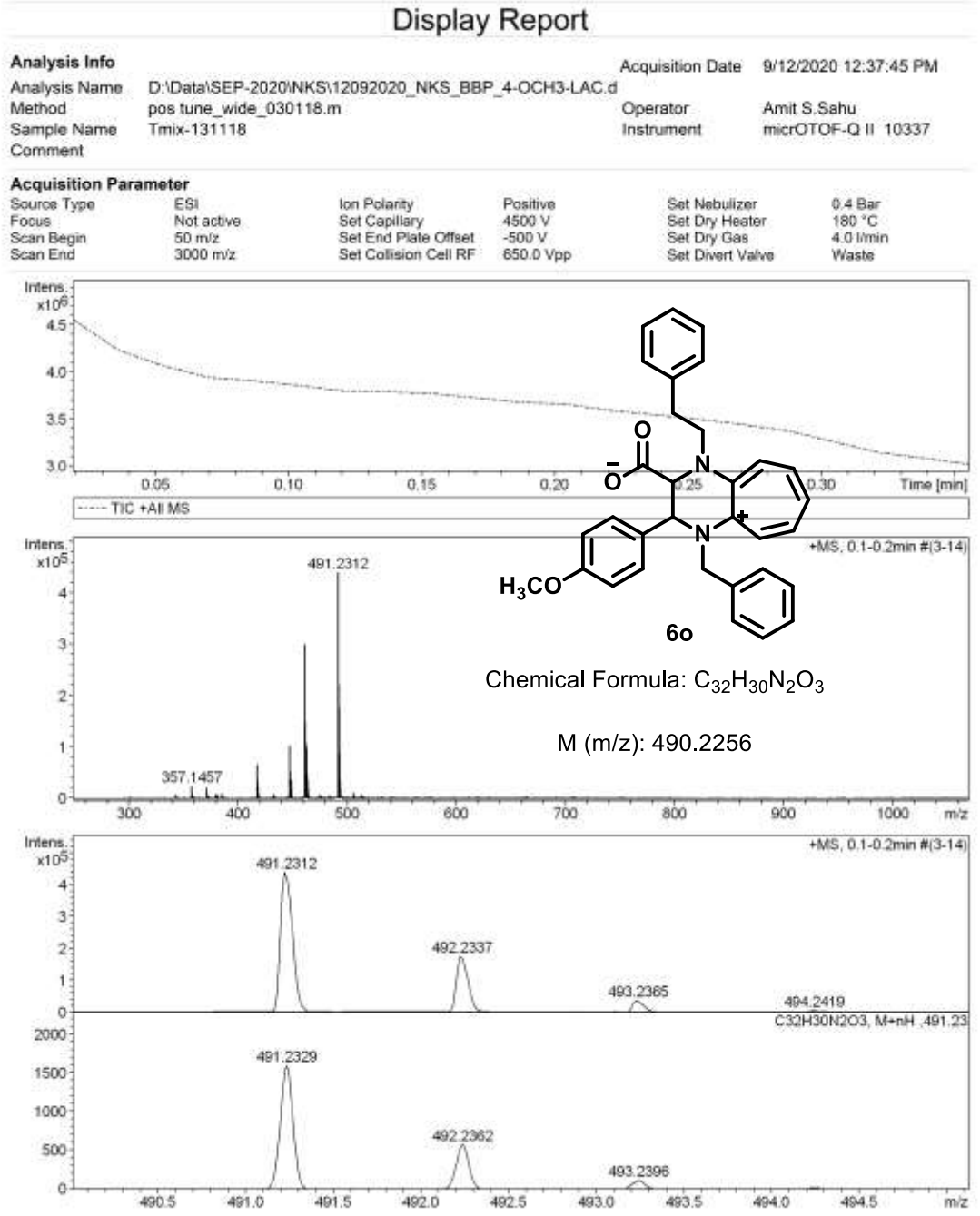

Figure A33. ESI/HRMS spectra of compound **(6o)**

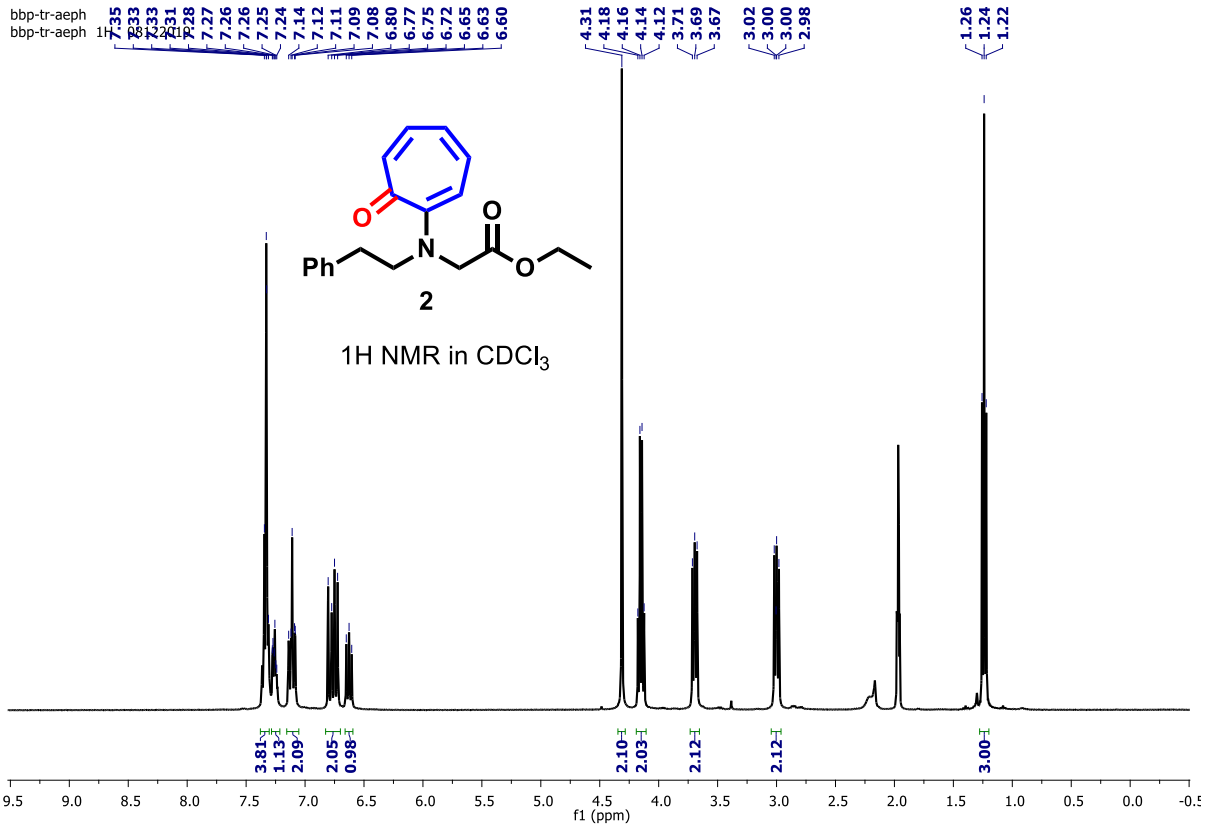

Figure A34. ^{1}H- NMR spectra of **(2)** in $CDCl_3$

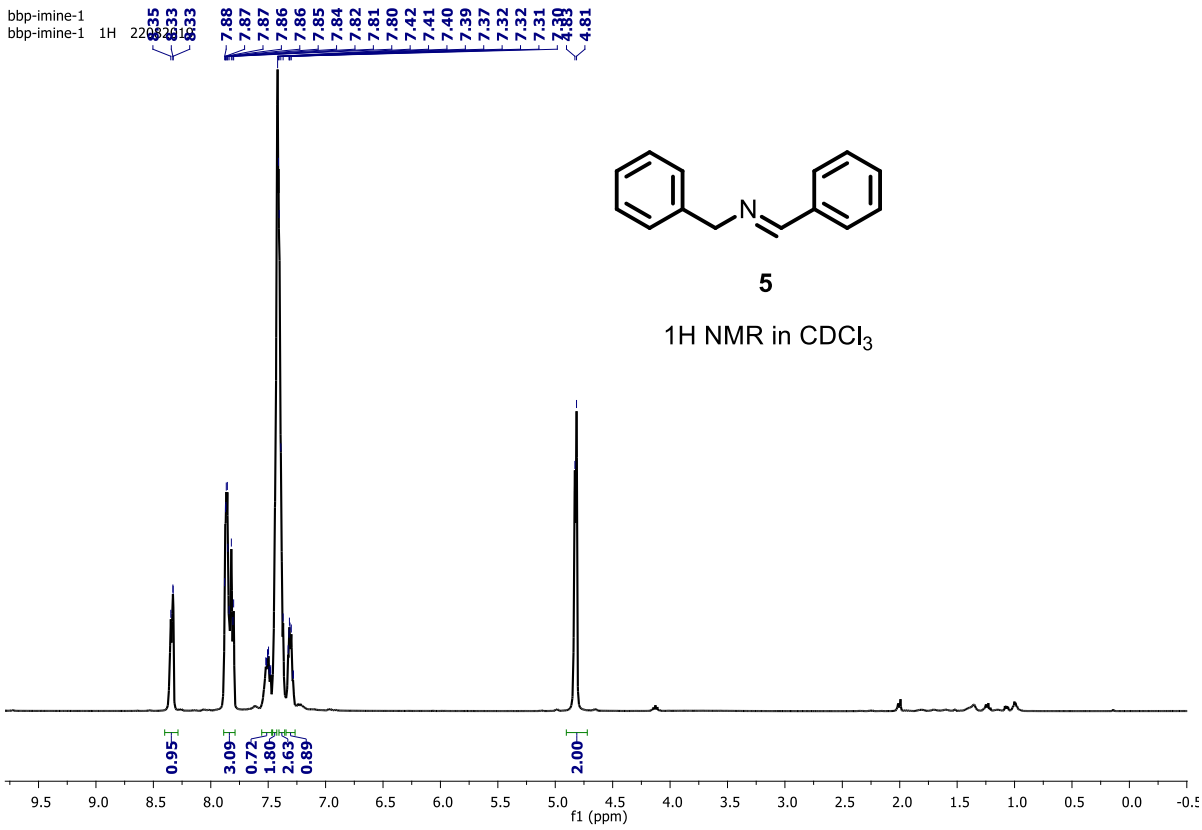

Figure A35. ^{1}H- NMR spectra of **(5)** in $CDCl_3$

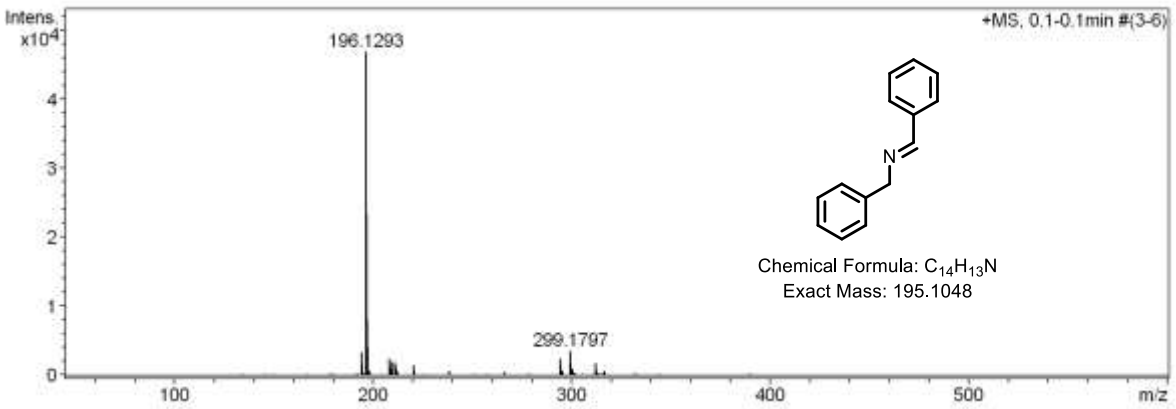

Figure A36. Mass spectra of compound **(5).** Other imines are characterized similarly

Table A1. Comparison of selective ^{13}C peaks of hydrapyrazine (**6a-6o**) and *tr-pheneg* methyl ester (**2**)

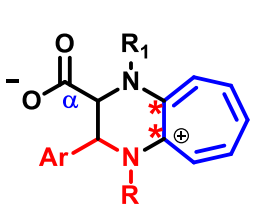

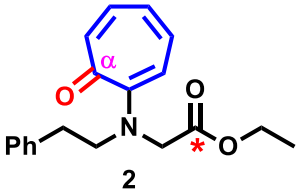

2

Entry No.	Compounds	α	**
01	6a	167.3	151.0, 150.0
02	6b	167.0	152.4, 150.9
03	6c	no	151.1, 148.9
04	6d	no	151.9, 150.8
05	6e	167.2	151.1, 151.0
06	6f	161.5	151.4, 150.3
07	6g	no	150.5, 150.4
08	6h	166.7	150.8, 150.0
09	6i	167.0	152.0, 149.9
10	6j	167.7	151.1, 150.1
11	6k	164.1	150.0, 149.7
12	6l	no	150.8, 150.0
13	6m	170.0	151.8, 150.7
14	6n	167.7	151.6, 150.1
15	6o	no	151.9, 151.7
16	2	181.8	170.9 ACS Omega **2018**, *3*, 997−1013

no= not observed/ very small possibly because of steric effect of bulky aryl group.

16. Crystal structures and data

Good quality crystals of compounds were obtained in solvent mixture dichloromethane and hexane by slow evaporation method. The crystals data of two compounds were collected on a Rigaku Oxford diffractometer at 293 K respectively. Selected data collection parameters and other crystallographic results are summarized below. The program package SHELXTL[1] and Olex2 was used for structure solution and packing diagram carried out by DIAMOND-3.2 software.

CCDC deposition number of **2** (2035166)**, 6a** (1889119), **6d** (2035165) and **6k** (2035167) contain the supplementary crystallographic data, these data can be obtained free of charge via https://www.ccdc.cam.ac.uk/data.

Crystal data of Phenylethyl glycinate (*pheneg*) ester **(2)**

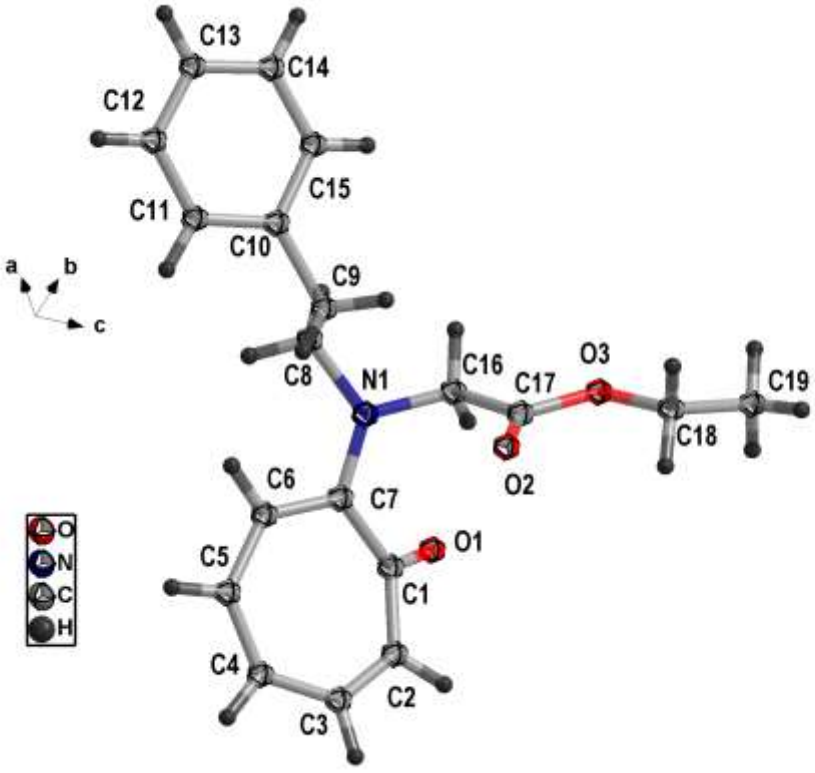

Figure A37. ORTEP Diagram of pyrazin-4-ium compound **(2)** [ellipsoid contour probability: 50%].

Table A1: Crystallographic table

compounds	(2)	(6a)	(6d)	(6k)
Identification code	**CCDC 2035166**	**CCDC 1889119**	**CCDC 2035165**	**CCDC 2035167**
Empirical formula	$C_{19}H_{21}NO_3$	$C_{31}H_{30}N_2O_3$	$C_{31}H_{28}N_3O_4$	C32H37FN2O2
Formula weight	311.37	478.57	506.56	37.20
Temperature/k	293(2)	293(2)	297(1)	295(2)
Crystal system	monoclinic	monoclinic	monoclinic	triclinic
Space group	$P2_1/c$	$P2_1/n$	$P2_1/n$	P-1
A/å	5.4825(3)	9.1107(3)	9.6632(8)	10.5590(3)
B/å	23.8368(16)	16.5195(9)	22.944(4)	15.1481(3)
C/å	13.0746(8)	17.0838(5)	16.041(2)	15.2096(4)
α/°	90	90	90	111.565(2)
β/°	95.892(5)	99.724(3)	101.653(12)	105.940(2)
γ/°	90	90	90	95.356(2)
Volume/å^3	1699.63(18)	2534.24(18)	3483.3(9)	2123.51(10)
Z	4	4	4	40
ρ_{calc}g/cm^3	1.217	1.254	0.966	1.163
M/mm^{-1}	0.082	0.642	0.521	0.710
F(000)	664.0	1016.0	1068.0	796.0
Crystal size/mm^3	0.021 × 0.0111 × 0.003	0.14 × 0.12 × 0.1	0.3 × 0.2 × 0.1	0.12 × 0.1 × 0.02
Radiation	MoKα (λ = 0.71073)	CuKα (λ = 1.54184)	CuKα (λ = 1.54184)	CuKα (λ = 1.54184)
2θ range for data collection/°	6.838 to 52.744	7.496 to 149.002	6.818 to 136.5	6.628 to 148.996
Index ranges	-6 ≤ h ≤ 6, -27 ≤ k ≤ 29, -16 ≤ l ≤ 16	-11 ≤ h ≤ 11, -20 ≤ k ≤ 20, -21 ≤ l ≤ 20	-11 ≤ h ≤ 7, -27 ≤ k ≤ 27, -19 ≤ l ≤ 19	-13 ≤ h ≤ 13, -18 ≤ k ≤ 14, -19 ≤ l ≤ 18
Reflections collected	15011	19921	35399	28676
Independent reflections	3463 [R_{int} = 0.0692, R_{sigma} = 0.0470]	5056 [R_{int} = 0.0896, R_{sigma} = 0.0730]	6151 [R_{int} = 0.2125, R_{sigma} = 0.1301]	8486 [R_{int} = 0.0499, R_{sigma} = 0.0414]
Data/restraints/parameters	3463/0/209	5056/0/328	6151/0/344	8486/3/510
Goodness-of-fit on f^2	1.050	1.059	1.192	1.732
Final r indexes [i>=2σ (i)]	R_1 = 0.0771, wR_2 = 0.2111	R_1 = 0.0842, wR_2 = 0.2280	R_1 = 0.1592, wR_2 = 0.3887	R_1 = 0.1211, wR_2 = 0.3988
Final r indexes [all data]	R_1 = 0.1018, wR_2 = 0.2297	R_1 = 0.1141, wR_2 = 0.2509	R_1 = 0.2473, wR_2 = 0.4536	R_1 = 0.1488, wR_2 = 0.4366
Largest diff. Peak/hole / e å$^{-3}$	0.41/-0.19	0.47/-0.32	0.56/-0.54	1.39/-0.47

17. Comparative studies of C-C bond length of Troponyl ring

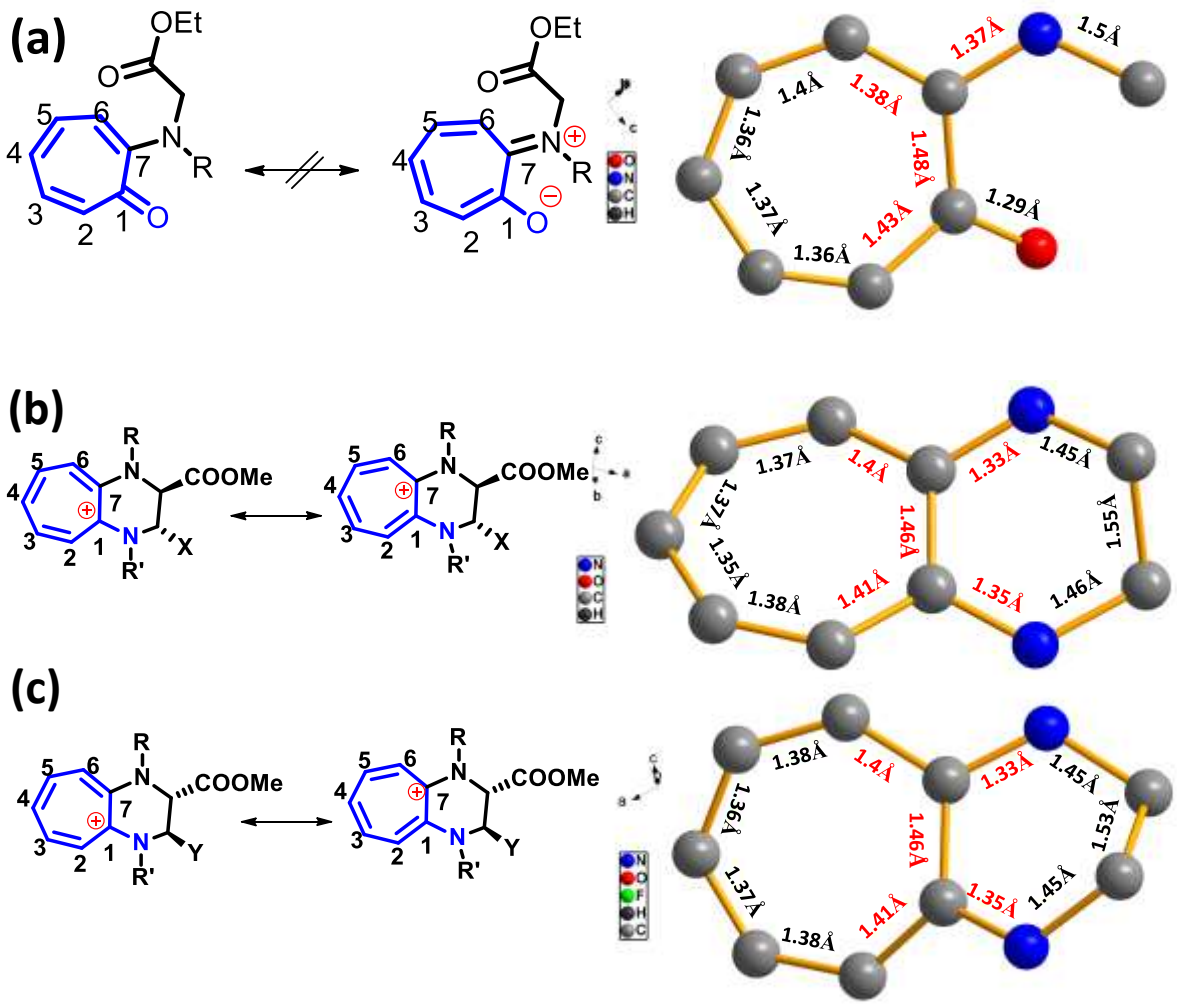

Figure A38. C-C bond length of Troponyl ring of troponyl dihydropyrazine

18. Time-dependent 1H-NMR spectra In CD_3CN

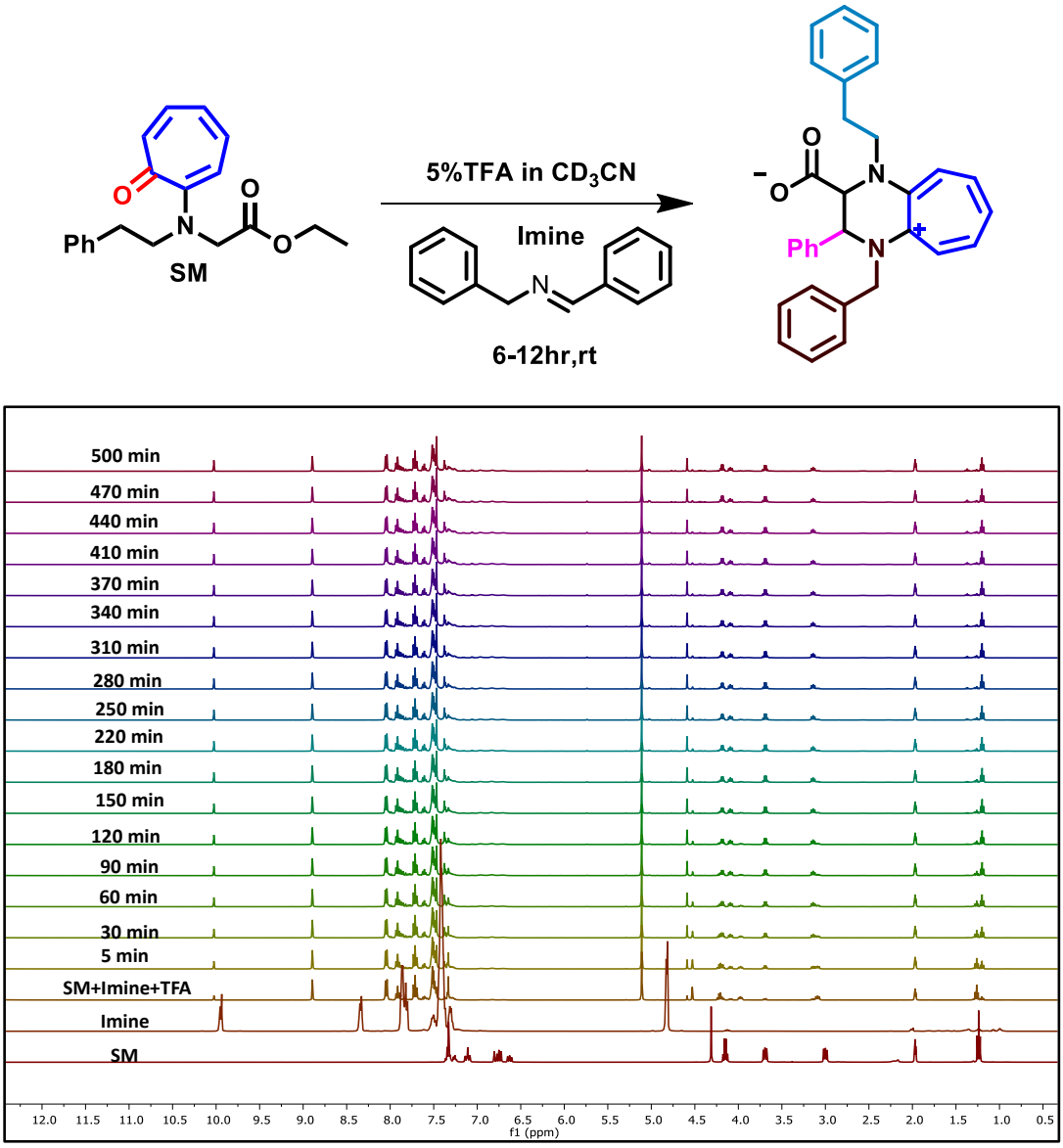

Figure A39: Time depended NMR in CD_3C UV-Visible Spectroscopic Studies formation of Aryl troponyl dihydra pyrazine

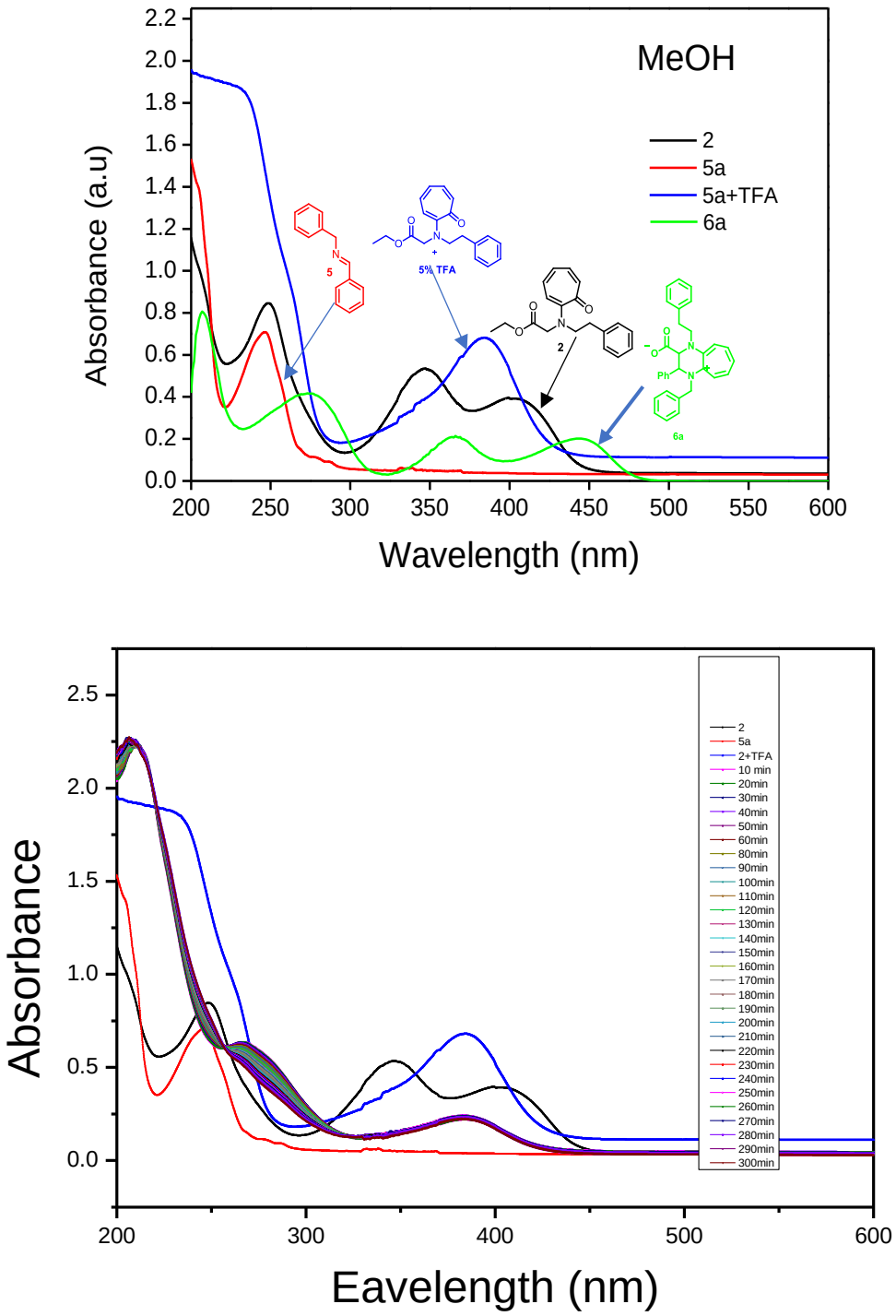

Figure A40: Time-dependent UV-Vis spectra in 5% TFA (CH_3CN)

19. MTT Assay

General Info

Run information

Session name	MTT assay bibhu bhaiya
Session creator	admin
Run name	MTT assay bibhu bhaiya
Run creator	admin
Run started	12/11/2019 12:38:15 PM+05:30
Total warnings	0
Total errors	0

Instrument parameters

Instrument name	VarioskanFlash
Instrument version	4.00.53
Instrument serial number	3001-2135
Actual instrument temperature	36.9 36.8 36.8
Dispenser	1 2
LumiSens module	1446-05
LumiSens scaling factor	1

SW Parameters

Run Software Version	SkanIt Software 2.4.5 RE for Varioskan Flash
Current Software Version	SkanIt Software 2.4.5 RE for Varioskan Flash

RunLog

2019-12-11 12:38:28+05:30 - Execution started
2019-12-11 12:38:34+05:30 - Shake1 started
2019-12-11 12:39:34+05:30 - Shake1 completed
2019-12-11 12:39:34+05:30 - Photometric1 started
2019-12-11 12:39:41+05:30 - Current temperature : 36.9
2019-12-11 12:39:47+05:30 - Photometric1 completed
2019-12-11 12:39:47+05:30 - Execution completed

Steps Data

Protocol properties

Protocol name	MTT assay 6a

Protocol description	
Plate template	96-well Corning, flat bottom plate
Execution block	
type	plate
Execution order	7
Settle delay [ms]	0
Well interval [ms]	0

Shake1

Step duration	0:01:00.0
ON time	0:00:02.0
OFF time	0:00:59.100
Speed [rpm]	600
Diameter [mm]	1
Shaking mode	Start with ON time

Photometric1

Measurement technology	Photometric
Measurement type	Normal
Step duration	0:00:00.0
Lag time	0:00:00.0
Measurement time [ms]	100
Bandwidth [nm]	5
Multipoint	Not in use
Wavelength [nm]	490

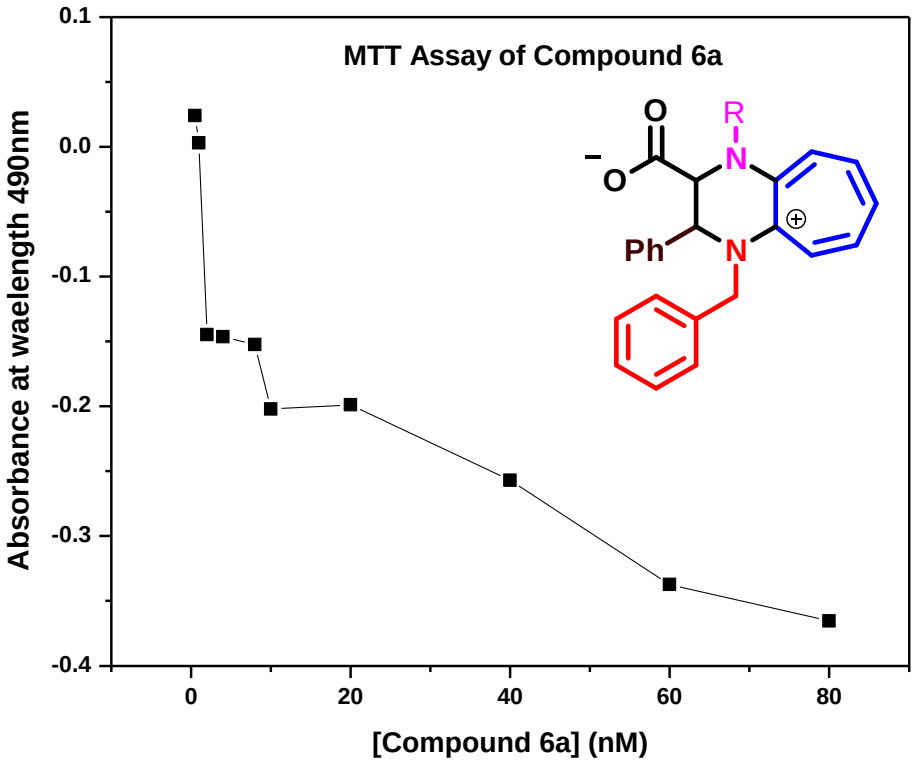

Figure A41. MTT asaay profile f compound **6a**

CHAPTER-5

Title: Synthesis of *Troponylated*-Uridinyl Nucleoside Analogues

5.1 Introduction

5.2 Objective of our work

5.3 Result and discussion

5.4 Conclusion

5.5 Experimental Section

5.6 References and Notes

5.7 Appendix

5.1 Introduction

Nucleic acids are the biopolymers which carries genetic information of living system.[1] There are mainly two types of nucleic acids: (a) Deoxyribonucleic acid (DNA) and (b) Ribonucleic acid (RNA). These biopolymers are prepared from nucleoside monomers through phosphate diester bonds.[2] The chemical structure of nucleosides contain pentose sugar ring (ribose and deoxyribose) and nitrogenous nucleobases (A/T/G/C/U). Modified nucleoside, nucleotide, and oligonucleotide have become the backbone of modern science.[3,4] The modified nucleic acids are also called Xeno nucleic acids (XNAs). It gives varieties of advantages for biochemical and biophysical tools as well as drug discovery assays applications.[5, 6] The synthetic chemists have modified the nucleosides to explore the structure and function of modified DNA/RNA. For examples, the synthesis of florescencent DNA/RNA are accomplished by the conjugation of chromophore and fluorophores.[7-9] The chemically functionalized DAN/RNA are also achieved by introducing the functional group moieties at their sugar ring and nucleobases. In literature, the fluorescent-DNA/RNA analogues are mostly derived benzenoid aromatic scaffolds.[1, 10-13] However, non-benzenoid aromatic scaffolds are also occurred in nature as various metabolites. Tropolone is a non-benzenoid seven-member aromatic compound.[14] [15]Tropolone and its naturally occurring derivatives exhibit various biological activities.[16] For example, tropolone and its related derivatives as tropolonoid are found in plants and fungi.[17] Tropolone and related derivatives possess various biological activities such as antibacterial,[18] antifungal,[19] antitumor,[20] and antiviral[21] agents. Troponylted are biologically active compounds such as Zinc dependent metalloprotein inhibitors, including carboxypeptidase-A inhibitors.[18, 22-24] This chapter describes the synthesis of rationally designed tropolonlyted uridine and deoxyuridine analogues.

5.2 Objective of our work

(a) The synthesis of *aminotroponyl*-BODIPY conjugated modified deoxyuridine nucleoside analogues for DNA.

(b) The synthesis of *troponyl* conjugated uridine modified nucleoside analogues for RNA.

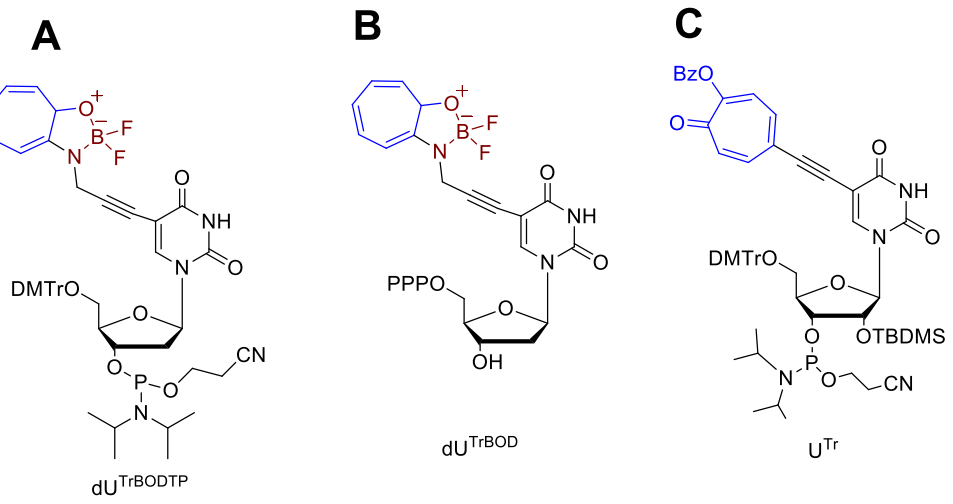

Figure 5.1. (a)*Troponylated*-BODIPY deoxyuridine phosphorsmidite, **(b)** *Troponylated*-BODIPY deoxyuridine Triphosphate **(c)** *Troponylated*-uridine Phoshpramidite.

5.3 Results and discussion

Synthesis of the phosphoramidites dU^{TrBOD} and nucleoside and triphosphate dU^{TrBOD}TP

We began the synthesis of *troponyl*-BODIPY deoxyuridine nucleoside analogue from commercially available 2'-deoxy 5-iodouridine and Tropolone (**Scheme 5.1**). In chapter-3B, tropolone was tosylated as compound (**1**) and used for the *N*-arylation of propargyl amine that produced alkyne functionalized 2-aminotroponyl derivative (**2**). This derivative (**2**) was treated

with boronating reagent $BF_3.OEt_2$ under mild basic conditions that formed the difluroboron complex (**3**).

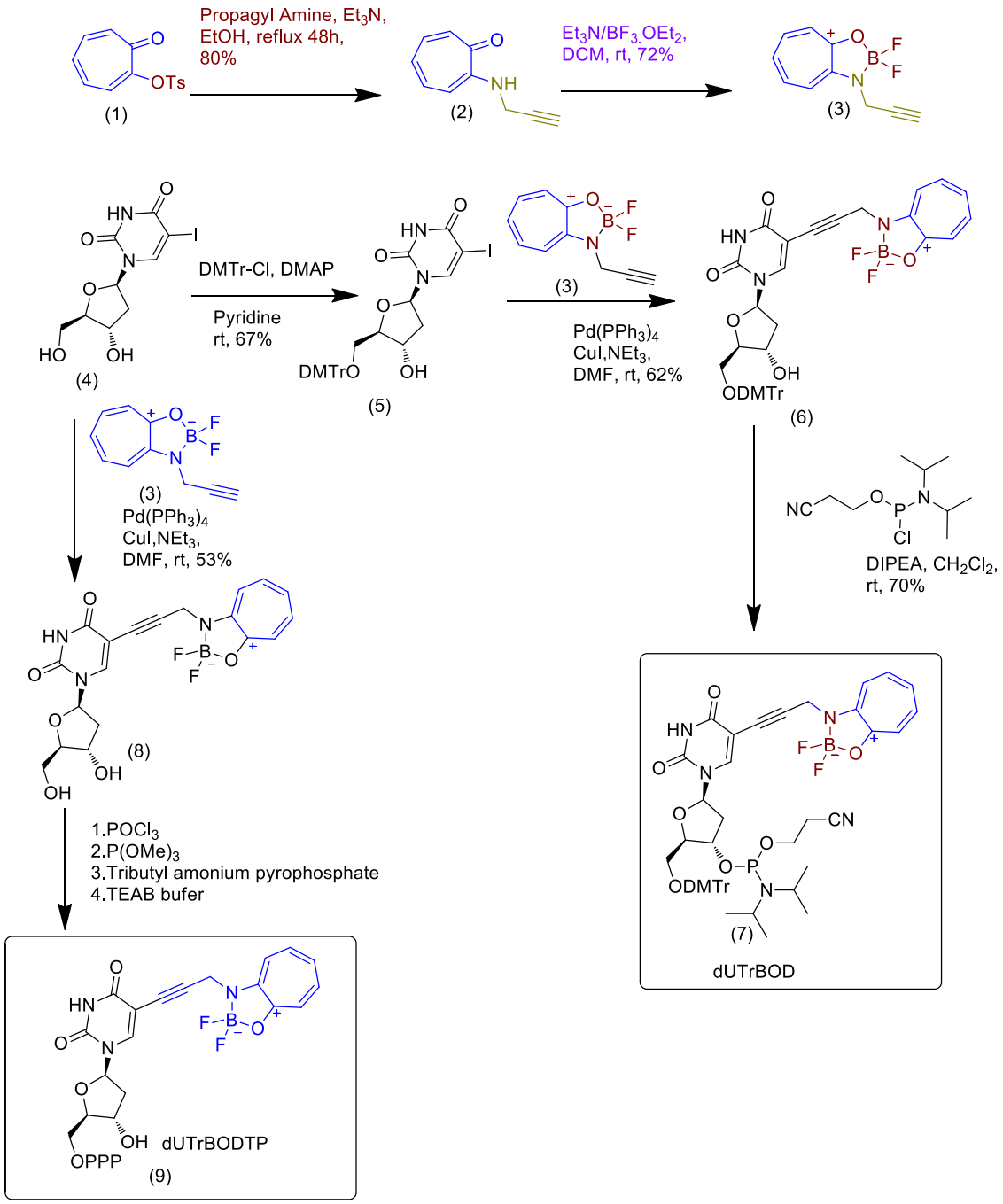

Scheme 5.1 Synthesis of Trpoponylated BODIPY thymidine phoshporamdities **dU^{TrBO}** and Triphosphate **dU^{TrBOD}TP**

Next, 5-Iodouridine nucleoside (**4**) was derived into 5'-*O*-DMTr protected derivative (**5**), and used for the conjuation of *toponyl*-BODIPY derivative (**3**) through Pd-catalysed Sonagasira coupling conditions that produced the desired *troponyl*-BODIPY uridine (dU^{TrBOD}) nucleoside analogue (**6**). This nucleoside (**6**) was converted into modified uridine phosphoramidite (**7**) by using the versatile phosphoralating reagent 2-(Cyanoethyl N,N-diisopropylchlorophosphoramidite). The unprotected dU^{TrBOD} nucleoside (**8**) was also prepared from 5-Iodouridine (**4**) and *troponyl*-BODIPY derivative (**3**) for the synthesis of triphosphate nucleoside analogue. Then the nucleoside (**8**) was treated with phoshporelating reagents and the product was isolated as *Troponyl*-BODIPY uridine triphosphate (**9**). All synthetic derivatives characterized by NMR(^{1}H, ^{13}C, ^{11}B, ^{19}F-NMR) and ESI-Mass, HRMS techniques. Their characterization data are provided in the Appendix.

Further we attempt to synthesis of troponyl-uridine phoshoramidities.We started the synthesis of designed *Troponyl*-Uridine phosphoramidite from commercially available nucleoside (**1)**. The synthesis is described in **Scheme 5.2**, Uridine (1) was converted into 5'-Iodo-Uridine (**2)**, following previously reported procedure.[25] 5'-Iodo-uridine was converted into 5-Ethynyl-uridine (**3**) in two steps by following literature procedures [26]. the alkyl nucleoside the 5'-OH group protected by 4,4'-dimethoxytriryl (DMTr), nucleoside was prepared *via* standard DMTr protection of 5'-Ethynyl-uridine to generate product (**6).** The DMTr protected Ethynyl-uridine were coupled with benzoyl protected 5-Iodotroolone under sonogashira cross coupling reaction conditions using Pd catalyst which produce 5'-DMTr-*troponyled* Ethnyl-uridine nucleoside (**7**). For the synthesis of phosphoramidites, 2'-OH of troponylated uridine nucleoside was protected with TBDMS as compound (**8**), and employed for phosphorylation, at 3'-OH with phosphorylating agent diisopropylchlorophosoramidities under basic conditions which produced the desired troponylated uridine phophoramidite (**9**) in good yield. The

characterization data (1H-/13C-NMR/^{31}P-NMR/ESI-HRMS) of compound (**9**) are provided in appendix.

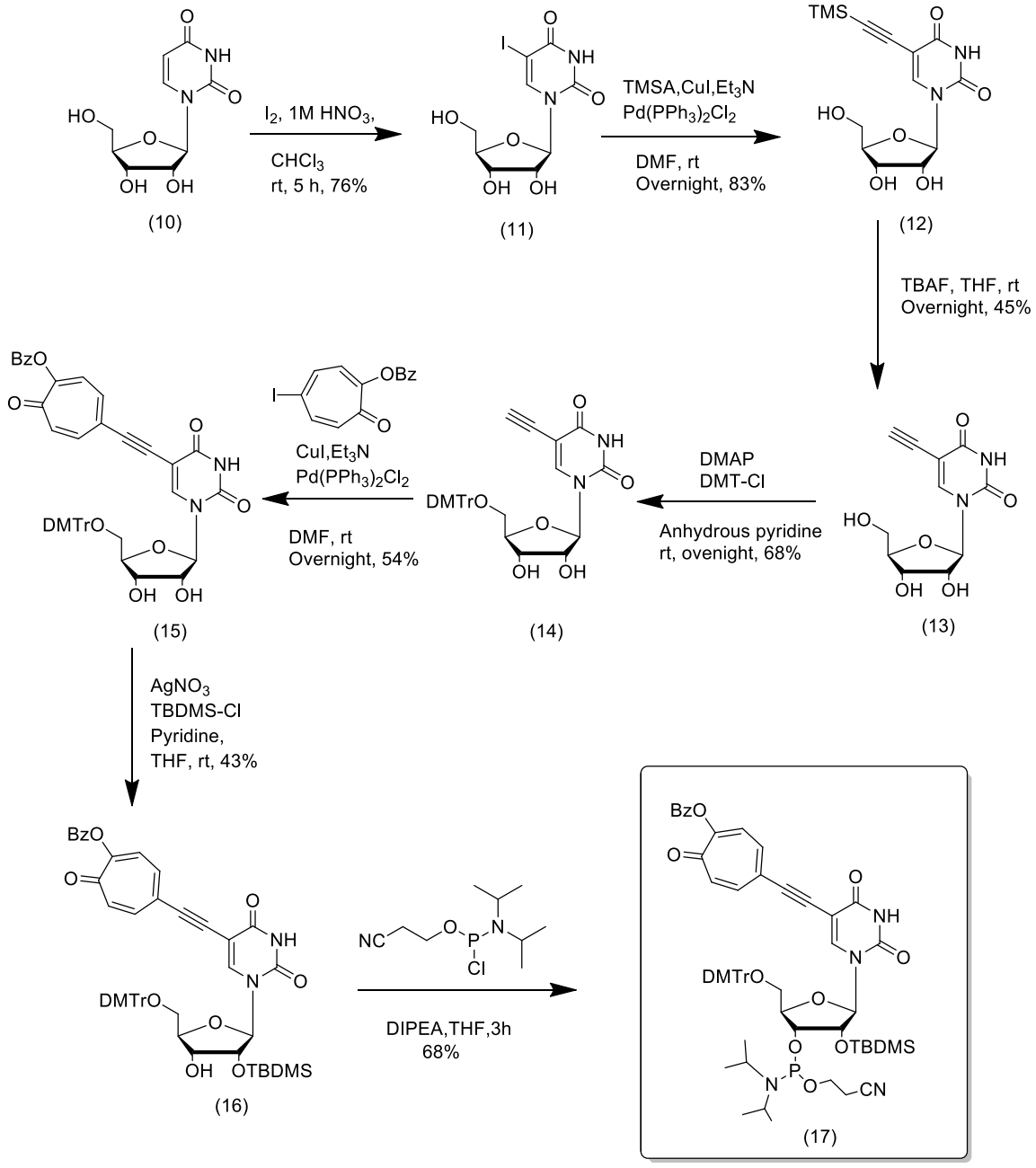

Scheme 5.2 Synthesis of *Trpoponylated* uridine phosphoramidite

Cell proliferation assay

In order to analyse the effect of Compound (**8**) **dU^{TrBOD}** on cell viability, cell proliferation assay was conducted. Human embryonic kidney derived cell line Hek293T and human cervical carcinoma derived cell line Hela cells were used for the assay. $2*10^4$ cells/ mL in 10% DMEM were seeded in 96 well microtiter plate and incubated for 10 h. After incubation cells were observed for its shape and confluency and media as carefully aspirated. Different concentrations of respective compounds (**8**) were prepared in DMEM medium and each concentration was added in triplicate along with only media and DMSO (exact concentration used for making the compound solution) control. The 96 well plate was incubated under standard conditions (humidified incubator with 5% CO_2 under 37°C) for 24 h. The CellTiter 96® AQ_{ueous} One Solution as used to analyse the cell proliferation ability in presence of different compounds. 10µl of CellTiter 96® AQueous One Solution Reagent into each well of the 96-well assay plate containing the samples in 190µl of culture medium followed by incubation for 1h at standard condition. After incubation absorbance was recorded using Variouscan (**8**) at 490 nm. The cytotoxicity of **dU^{TrBOD}** was assessed that both Hek293T and Hela cells are proving non-cytotoxicity.

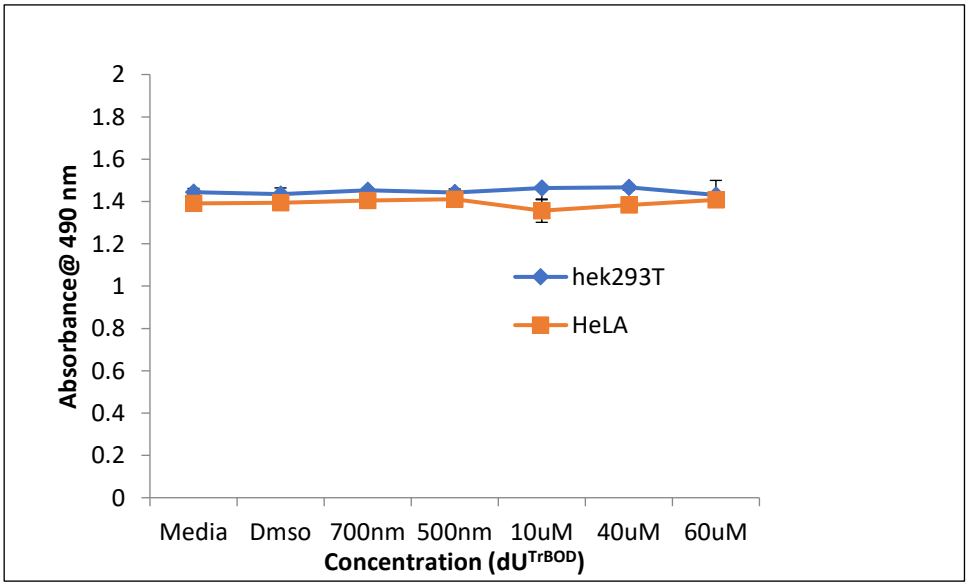

Figure 00. Cell viability o Hek293T and Hela cell after incubation with **dU^{TrBOD}** of dfferent concentrations.

5.4 Conclusion

We have successfully synthesized 2'-deoxyuridine *Troponylted*-BODIPY nucleoside and 5'-O-triphosphate bearing *Troponylted*-BODIPY and *troponyl* uridine phosphoramidites. The cell viability of test of **dU^{TrBOD}** were carried out Human embryonic kidney derived cell line Hek293T and human cervical carcinoma derived cell line Hela cells were used for the assay.

5.5 Experimental Section

Material and Instrumentation: All required chemicals were purchased from commercial and used without purification. Anhydrous DMF, DCM, was freshly prepared by distilling over calcium hydride. Reaction were monitored by thin layer chromatography, visualized by UV and Ninhydrin. Column chromatography was performed in 230-400 and 100-200 mesh silica. Mass spectra were obtained from Bruker MicrOTOF-Q II Spectrometer. NMR spectra were recorded on Bruker AV-700MHz and Bruker AV-400 (1H:400MHz ,13C:100.6 MHz).1H and 13C NMR chemical shift were recorded in ppm downfield from tetramethyl silane, splitting patterns are abbreviated as: s, singlet; d, doublet; dd, doublet of doublet; t, triplet; q, quartet; dq, doublet of quartet; m, multiplet.

Trop-Propargyl amine (2)

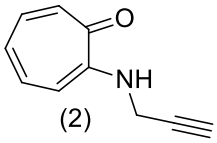

(2)

The propagylaminotropons were synthesized in our previous reported procedures. 2-tosyloxytropone (1.0 *quiv*.) and propargyl amines (1.2 *equiv*.) were dissolved in ethanol; to this, Et_3N (3.0 *equiv*.) were added. The reaction mixture was allowed to reflux for 24-36h. the reaction mixture was evaporated under reduced pressure after reaction completion. The obtained crude product was purified

column chromatography to get pure popagylaminotropone (**2**). The pure product was obtained as yellowish solid (850 mg, 74%). ^{1}H NMR (400 MHz, $CDCl_3$) δ 7.33 – 7.27 (m, 2H), 7.21 (t, *J* = 12 Hz, 1H), 6.75 (t, *J* = 8 Hz, 1H), 6.62 (d, *J* = 8 Hz, 1H), 4.14 (dd, *J* = 5.9, 2.4 Hz, 2H), 2.30 (t, *J* = 2.4 Hz, 1H), 1.67 (s, 1H). ^{13}C{H} NMR (101 MHz, $CDCl_3$) δ 177.19, 154.49, 137.49, 136.05, 130.07, 123.40, 109.22, 77.87, 72.51, 32.50. HRMS (ESI-TOF) m/z: [M+nH] cal for $C_{10}H_9NO$ 160.0757, found 160.0759.

Trop-Propargyl amine BODIPY (3)

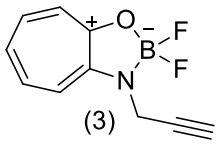

(3)

Compound **2** was dissolved in anhydrous dichloromethane, and Et_3N (15 *equiv.*) was added for further reaction $BF_3.OEt_2$ (15 *equiv.*) was added to the resultant reaction mixture and stirred at room temperature. The completion of reaction was monitored by TLC, and water was added to quench unreacted $BF_3.OEt_2$ and extracted with dichloromethane (thrice). The combined organic layer was dried over Na_2SO_4 and concentrated under reduced pressure. The crude product was purified through silica gel column chromatography by using 50% EtOAc/Hexane as the mobile phase. The pure product Boron complex (**3)** was yellowish solid (800 mg, 72%). ^{1}H NMR (400 MHz, $CDCl_3$) δ 7.78 (t, *J* = 10.2 Hz, 1H), 7.63 (t, *J* = 10.3 Hz, 1H), 7.38 (dd, *J* = 25.0, 10.6 Hz, 2H), 7.27 – 7.21 (m, 1H), 4.32 (s, 2H), 2.31 (s, 1H). $^{13}C^{27}$ NMR (101 MHz, $CDCl_3$) δ 168.25, 159.89, 142.05, 140.54, 128.45, 120.59, 118.42, 73.00, 32.14, 29.70. ^{11}B NMR (128 MHz, $CDCl_3$) δ 5.76 (t, *J* = 17.8 Hz). ^{19}F NMR (377 MHz, $CDCl_3$) δ -139.06 (dd, *J* = 35.8, 17.6 Hz). HRMS (ESI-TOF) m/z: [M+Na] cal for $C_{10}H_8BF_2NO$ 230.0561, found 230.0563.

2′-Deoxy-5′-O-DMT-5-iodouridine (5):

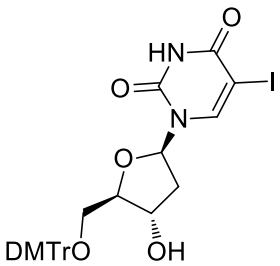

(5)

A mixture of commercially 2'-Deoxy-5-iodouridine **4** (2.0 g, 5.6492 mmol, 1.0equiv), DMAP (0.68mg, 0.5649 mmol, 0.1equiv), DMTr-Cl (2.8 g, 8.4738 mmol, 1.5equiv) and anhydrous pyridine (20mL) was stirred at room temperature 12h under N_2 atmosphere. Then the reaction mixture was evaporated under vacuum and the resulting residue was purified by silica gel column chromatography (3%MeOH in DCM containing 1% Et_3N).to afford compound 2 as an of white foam (2.1 g, 67%).^{1}H NMR (400 MHz, $CDCl_3$) δ 8.67 – 8.60 (m, 1H), 8.17 (s, 1H), 7.46 – 7.41 (m, 2H), 7.37 – 7.23 (m, 8H), 6.87 (d, *J* = 8.9 Hz, 3H), 6.35 (dd, *J* = 7.8, 5.7 Hz, 1H), 4.63 – 4.52 (m, 1H), 4.14 (q, *J* = 2.8 Hz, 1H), 3.80 (s, 6H), 3.40 (qd, *J* = 10.7, 3.2 Hz, 2H), 2.53 (ddd, *J* = 13.5, 5.6, 2.3 Hz, 1H), 2.31 (ddd, *J* = 13.7, 7.7, 6.1 Hz, 1H). ^{13}C NMR (101 MHz, $CDCl_3$) δ 160.17, 158.67, 150.05, 149.34, 144.32, 135.46, 135.35, 130.12, 130.09, 129.16, 128.14, 128.06, 127.12, 124.01, 113.41, 113.18, 87.07, 86.57, 85.68,76.74, 72.47, 68.71, 63.50, 55.31, 41.48.

2′-Deoxy-5′-O-DMT-5-Trop-propargyl amine BODIPY modified deoxyuridine (6):

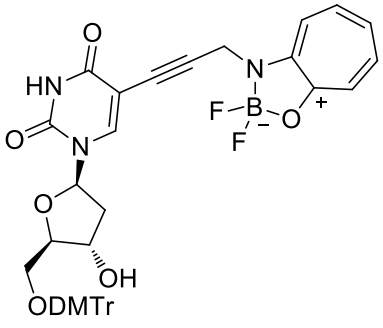

(6)

A mixture of 2′-Deoxy-5′-O-DMT-5-iodouridine **1** (1.0 g., 1.52 mmol, 1.0 equiv), Trop-propagyl amine BODIPY **3** (0.378 g, 1.82 mmol, 1.2 equiv), tetrakis(triphenylphosphine)palladium (0.176 g, 0.152 mmol, 0.1 equiv), copper (I) iodide (0.057 g, 0.3048 mmol, 0.2 equiv), and triethylamine (1.0 mL, 1.58 mmol, 5 equiv) was dissolved in anhydrous DMF (10 ml). The reaction mixture was stirred at room temperature overnight under N_2 atmosphere. After completion of reaction, the reaction mixture was evaporated under vacuum and the resulting crude residue was purified by column chromatography (50% EtOAC in DCM with few drop of Et_3N) to afford a yellow solid (0.700 g, 62%). ^{1}H NMR (400 MHz, $CDCl_3$) δ 8.74 (s, 1H), 7.79 – 7.71 (m, 1H), 7.64 (t, *J* = 10.2 Hz, 1H), 7.47 – 7.35 (m, 4H), 7.29 – 7.14 (m,

9H), 6.83 (d, *J* = 8.5 Hz, 4H), 6.31 (dd, *J* = 6.1, 4.8 Hz, 1H), 5.79 (s, 1H), 4.61 (d, *J* = 5.4 Hz, 1H), 4.17 (d, *J* = 4.6 Hz, 1H), 3.80 (d, *J* = 2.3 Hz, 6H), 3.57 – 3.41 (m, 2H), 2.82 – 2.72 (m, 1H), 2.43 – 2.29 (m, 1H). ^{13}C NMR (101 MHz, $CDCl_3$) δ 171.43, 168.02, 162.67, 158.78, 158.74, 158.64, 154.59, 151.70, 147.34, 144.58, 142.45, 140.56, 139.48, 137.89, 135.09, 134.99, 130.15, 130.07, 129.14, 128.11, 127.90, 127.86, 127.78, 127.09, 120.84, 118.46, 113.37, 113.18, 106.54, 102.94, 88.24, 87.08, 86.37, 81.45, 70.15, 62.30, 60.42, 55.30, 55.27, 42.23, 39.65, 21.06, 14.20 ^{11}B NMR (128 MHz, $CDCl_3$) δ 5.84 (s). ^{19}F NMR (377 MHz, $CDCl_3$) δ -138.08 (d, *J* = 26.4 Hz), -138.29 (s), -138.36 (s). HRMS (ESI-TOF) m/z: $[M + Na]^+$ calcd For $C_{40}H_{36}BF_2N_3O_8$ 758.2463, found 758.2444.

Tropolonylated Containing BODIPY thymidine phosphoramidite (7):

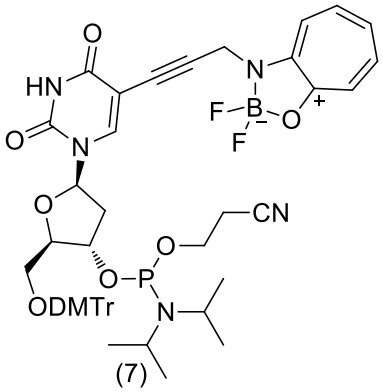

(7)

To the solution of compound **4** (0.482 g, 0.653 mmol, 1 equiv) in anhydrous dichloromethane (6 ml) was added *N*,*N*-diisopropylethylamine (0.340 ml, 1.959 mmole, 3 equiv) and stirred for 10 min. To the solution slowly added 2-cyano *N*,*N*-diisopropylchlrophosphoramidie (0.271 ml, 0.979mmol, 1.5 equiv) and the reaction mixture for 2 h. After compaction of reaction the solvent was evaporated to dryness and the residue was purified by column chromatography (60% EtOAC in Hexane with few drop of Et_3N) to afford a yellow solid (0.426 g, 70%). ^{1}H NMR (400 MHz, $CDCl_3$) δ 8.78 (s, 1H), 7.79 – 7.57 (m, 3H), 7.45 – 7.12 (m, 12H), 6.82 (d, *J* = 6.8 Hz, 4H), 6.30 (d, *J* = 2.4 Hz, 1H), 6.21 – 6.10 (m, 1H), 5.65 (s, 1H), 4.67 (s, 2H), 4.25 – 4.10 (m, 3H), 3.79 (s, 6H), 3.63 – 3.42 (m, 7H), 3.35 – 3.21 (m, 1H), 2.76 (dd, *J* = 8.4, 3.6 Hz, 3H), 2.73 – 2.57 (m, 1H), 2.51 – 2.33 (m, 2H), 1.40 – 1.34 (m, 6H), 1.16 (d, *J* = 4.8 Hz, 9H). ^{13}C NMR (101 MHz, $CDCl_3$) δ 171.51, 168.05, 167.27, 160.14, 158.80, 154.44, 151.49, 144.45, 142.36, 140.52, 137.82, 134.88, 130.26, 130.21, 128.85, 128.10, 128.00, 127.21, 120.79, 118.75, 118.46, 117.49, 113.35, 106.45, 103.01, 88.16, 87.07, 77.35, 71.87,

61.97, 58.08, 55.32, 55.28, ^{11}B NMR (128 MHz, $CDCl_3$) δ 5.87 (s). 43.33, 43.21, 39.65, 24.58, 22.34, 20.17, 14.07. ^{19}F NMR (377 MHz, $CDCl_3$) δ -138.28 (d, *J* = 61.9 Hz), -138.59 (s). ^{31}P NMR (162 MHz, $CDCl_3$) δ 149.62 (s), 149.01 (s). HRMS (ESI-TOF) m/z: $[M + nCl]^+$ calcd For $C_{49}H_{53}BF_2N_5O_9P$ 758.2463, found 758.2444.

Tropolonylated Containing BODIPY Thymidine Nucleoside (8):

A mixture of 2′-Deoxy-5′-iodouridine **4** (0.250 g., 0.706 mmol, 1.0 equiv.), Trop-propargyl amine BODIPY **3** (0.75 g, 0.847 mmol, 1.2 equiv.), tetrakis(triphenylphosphine)palladium (0.8 g, 0.070 mmol, 0.1 equiv.), copper (I) iodide (0.026 g, 0.141 mmol, 0.2 equiv.), and triethylamine (0.480 mL, 3.531 mmol, 5 equiv.) was dissolved in anhydrous DMF (10 ml). The reaction mixture was stirred at room temperature overnight under N_2 atmosphere. After completion of reaction, the reaction mixture was evaporated under vacuum and the resulting crude residue was purified by column chromatography (5% MeOH in DCM) to afford a yellow solid 53% yield product **8**. ^{1}H NMR (400 MHz, DMSO-d_6) δ 11.66 (s, 1H), 8.40 (s, 1H), 7.85 – 7.68 (m, 1H), 6.12 (dt, *J* = 15.7, 6.3 Hz, 2H), 5.26 (dd, *J* = 11.7, 4.3 Hz, 2H), 5.14 (t, *J* = 4.8 Hz, 1H), 4.91 (s, 1H), 4.23 (tt, *J* = 10.5, 4.3 Hz, 2H), 3.80 (q, *J* = 3.3 Hz, 1H), 3.68 – 3.53 (m, 3H), 2.12 (ddd, *J* = 6.7, 5.0, 2.2 Hz, 2H). ^{13}C NMR (101 MHz, DMSO) δ 171.02, 166.10, 160.37, 153.51, 151.13, 149.98, 144.92, 142.97, 140.68, 138.47, 129.83, 120.47, 119.56, 105.37, 102.84, 88.09, 87.50, 87.40, 84.53, 69.89, 69.51, 69.15, 60.70, 60.64, 48.49, 45.67, 40.08, 40.04, 39.88, 39.83, 39.67, 39.62, 39.41, 39.20, 39.00, 38.79. ^{11}B NMR (128 MHz, $CDCl_3$) δ 5.85 (s). . ^{19}F NMR (377 MHz, $CDCl_3$) δ -138.28 (d, *J* = 8.0 Hz), -138.59 (s). HRMS (ESI-TOF) m/z: $[M + Na]^+$ calcd For $C_{19}H_{18}BF_2N_3$ 758.2463, found 758.2444.

Tropolonylated Containing BODIPY thymidine Triphosphate (7):

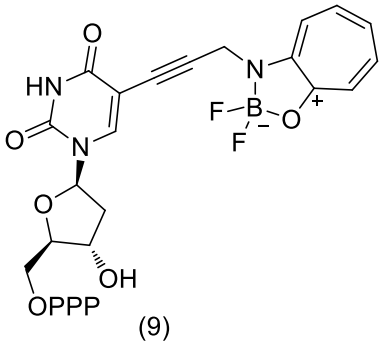

(9)

To the solution of Tropolonylated Containing BODIPY Thymidine Nucleoside (**8**) (70 mg, 1.161 mmol, 1.0 equiv) in trimethyl phosphate, diissilled $POCl_3$ (61uL, 0.4041 mmol, 2.5 equiv) as added in ice cold conditions. The solution as stirred or 24 h at ~ 4° C. after 24 h, a turbid solution of Bis(tributylamine) pyrophasphate (310 mg, 1153 mmole, 7 equiv.) and tributyl amine in dry DMF (2 mL) was added. The reaction mixture was stirred for another hour at 0-4 °C and then quenched 1 M triehyl ammonium bicaboonate buffer (TABF, pH 7.5, 15 mL) and stirred for another 20 min . and then the reaction mixture concentrated to dryness and purified by using an DEAE spehasex-A25 anione exchange coloumn (10 mM-1M TEAB, pH 7.5) folloed by revrese phase plash chromatoraphy. ^{1}H NMR (400 MHz, Deuterium Oxide) δ 7.93 – 7.84 (m, 1H), 7.73 (t, *J* = 10.3 Hz, 1H), 7.53 (dd, *J* = 22.2, 10.5 Hz, 2H), 7.41 (d, *J* = 10.1 Hz, 1H), 6.68 (d, *J* = 18.2 Hz, 1H), 6.24 (q, *J* = 6.1 Hz, 1H), 4.58 (s, 2H), 4.50 – 4.19 (m, 1H), 4.17 – 3.86 (m, 1H), 3.86 – 3.67 (m, 1H), 2.65 – 2.53 (m, 1H), 2.29 (ddd, *J* = 22.9, 14.2, 7.0 Hz, 1H), 1.28 (d, *J* = 4.2 Hz, 1H). ^{11}B NMR (128 MHz, Deuterium Oxide) δ 5.78. ^{19}F NMR (377 MHz, Deuterium Oxide) δ -136.78. ^{31}P NMR (162 MHz, Deuterium Oxide) δ 8.16, 7.83, 6.54, 3.03. HRMS (ESI-TOF) m/z: $[M + Na]^+$ calcd For $C_{19}H_{17}BF_2N_3O_{15}P_3$ 6700.0010, found 670.2332.

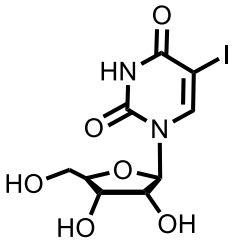

(11)

Compound **(11)**: In a round bottom flask, uridine 2.0 g and iodine powder 2.3 g were dissolved in a mixture of chloroform 100 ml and 1M nitric acid 20 ml. The reaction mixture was heated at reflux condition for 5-6h. The reaction progress was monitored by TLC(20 % MeoH in DCM). After Colling of the reaction mixture the precipitate was collected by filtration and dried under vacuumed for 2h. to provide 5-Iodo uridine (2.2 g,73%) . ^{1}H NMR (400 MHz, DMSO) δ 11.68 (s, 1H), 8.48 (s, 1H), 5.72 (d, *J* = 3.4 Hz, 1H), 4.01 (d, *J* = 21.5 Hz, 2H), 3.86 (s, 1H), 3.68 (d, *J* = 11.4 Hz, 1H), 3.57 (d, *J* = 11.5 Hz, 1H).

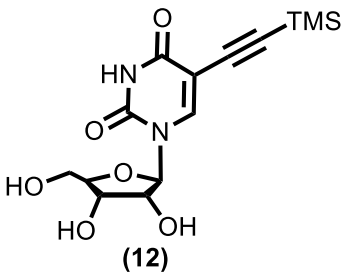

(12)

Compound **(12)**: under the nitrogen conditions 5-Iodouridine (2.92g, 1eq), CuI (205mg, 0.2eq) and $Pd(PPh_3)_4$(624mg,0.1eq) were dissolved in dry DMF and Et_3N (3.6ml, 5eq). then TMSA (3.7ml, 5eq) was slowly added and the reaction mixture was heated 55^0 C and left the stir overnight. The reaction progress was monitored by TLC (10% MeOH in DCM), After completion of reaction mixture evaporated and the residue was treated with methanol and filtered pass through the Celite. The filtrate was concentrated and the residue was purified by silica gel column chromatography (1.47g, 83%). ^{1}H NMR (400 MHz, DMSO) δ 11.66 (s, 1H), 8.35 (s, 1H), 5.74 (d, *J* = 4.6 Hz, 1H), 5.42 (d, *J* = 5.3 Hz, 1H), 5.21 (t, *J* = 4.7 Hz, 1H), 5.07 (d, *J* = 5.4 Hz, 1H), 4.05 (d, *J* = 5.0 Hz, 1H), 3.98 (d, *J* = 5.0 Hz, 1H), 3.86 (d, *J* = 4.3 Hz, 1H), 3.67 (s, 1H), 3.59 (s, 1H), 0.19 (s, 9H). ^{13}C NMR (101 MHz, DMSO) δ 160.97, 148.91, 144.23, 97.80, 97.48, 96.57, 87.12, 84.35, 69.48, 60.34, 45.20, 8.16, -0.51.HRMS (ESI-TOF) m/z: $[M+Na]^+$ Calcd. For $C_{15}H_{20}N_2O_6Si$ 363.0974, found 363.0983.

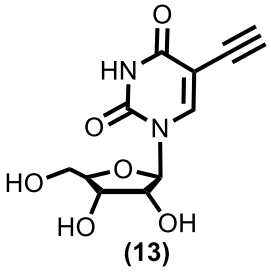

(13)

Compound **(13)**: under nitrogen conditions Compound **3** (1.47gm, 1eq.) was dissolved in dry THF (10ml) followed by dropwise addition of TBAF (2.5ml, 2eq). The reaction was allowed to stir overnight at room temperature. After completion of reaction the reaction mixture concentrated under reduced pressure and the residue was purified by silica gel column chromatography (15%MeOH in DCM). The yield of the product compound **4** as an off white solid (500mg, 45%). ^{1}H NMR (400 MHz, DMSO) δ 11.64 (s, 1H), 8.38 (s, 1H), 5.74 (d, *J* = 4.5 Hz, 1H), 5.42 (d, *J* = 5.3 Hz, 1H), 5.24 (t, *J* = 4.6 Hz, 1H), 5.07 (d, *J* = 5.3 Hz, 1H), 4.09 (s, 1H), 4.05 (dd, *J* = 9.8, 4.9 Hz, 1H), 4.01 – 3.96 (m, 1H), 3.90 – 3.84 (m, 1H), 3.68 (dd, *J* = 9.0, 5.9 Hz, 1H), 3.62 – 3.54 (m, 1H). ^{13}C NMR (101 MHz, DMSO) δ 162.09, 151.85, 150.13, 147.63, 145.13, 98.09, 88.86, 85.21, 84.10, 76.77, 74.44, 69.78, 60.66, 40.35, 40.14, 39.93,

39.72, 39.51. HRMS (ESI-TOF) m/z: $[M+Na]^+$ Calcd. For $C_{11}H_{12}N_2O_6$ 291.0606, found 291.0588.

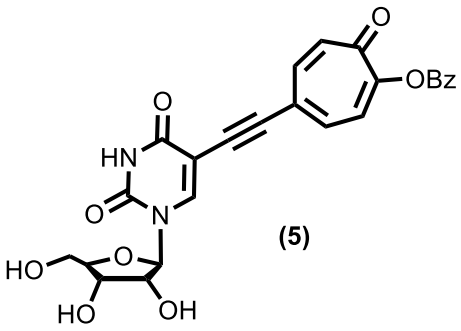

(5)

Compound **(14):** Deoxy-5-ethynyluridine (**4**, 1eq), 2-benzoyloxy-5-iodotropone (1.2eq), tetrakis(triphenylphosphine)palladium (0.1eq), copper(I) iodide (0.2e), and triethylamine (5eq) was dissolved in dry DMF and stirred overnight under nitrogen. The solvent were evaporated under pressure, and the reaction mixture was purified by silica gel column chromatography(10% MeOH in DCM), to give yellow solid, ^{1}H NMR (400 MHz, $CDCl_3$) δ 11.80 (s, 1H), 9.18 (s, 1H), 8.10 (d, *J* = 7.5 Hz, 2H), 7.78 (t, *J* = 7.4 Hz, 2H), 7.70 – 7.59 (m, 3H), 7.41 (s, 1H), 5.86 (s, 5H), 5.75 (s, 1H), 5.65 (d, *J* = 4.2 Hz, 1H), 5.37 (dd, *J* = 10.4, 5.5 Hz, 1H), 5.04 (d, *J* = 5.7 Hz, 1H), 4.03 (dd, *J* = 13.3, 6.9 Hz, 3H), 3.88 (d, *J* = 11.8 Hz, 1H), 3.69 (d, *J* = 10.4 Hz, 1H). ^{13}C NMR (101 MHz, DMSO) δ 163.88 (s), 141.02 (s), 134.74 (s), 133.34 (s), 130.37 (s), 129.47 (s), 105.51 (s), 92.33 (s), 84.54 (s), 75.33 (s), 68.27 (s), 59.77 (s), 55.26 (s), 46.21 (s), 40.26 (d, *J* = 21.0 Hz), 39.95 (s), 39.74 (s), 39.43 (d, *J* = 21.0 Hz), 39.11 (s), 39.06 – 38.82 (m), 8.99 (s). HRMS (ESI-TOF) m/z: $[M+Na]^+$ Calcd. For $C_{25}H_{20}N_2O_9$ 515.1051, found 515.1061.

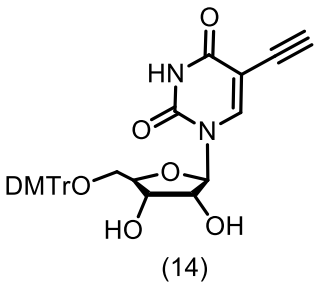

(14)

Compound (**14)**: A mixture of Deoxy-5-ethynyluridine (**5,** 1gm, 3.73mmol, 1eq), DMAP (45mg, 4.85mmol, .01eq), DMT-Cl (1.63gm, 4.85mmole, 1.3eq) and anhydrous pyridine (20ml) was stirred at room temperature for 12h under nitrogen atmosphere. Then the pyridine was evaporated under reduced pressure and the resulting residue was purified

by column chromatography (3% MeOH/0.1 %Et_3N/DCM) to afford compound **8** as an off white foam solid (1.44gm, 68%).^{1}H NMR (400 MHz, DMSO) δ 7.95 (s, 1H), 7.47 – 7.16 (m, 9H), 6.89 (d, *J* = 8.6 Hz, 4H), 5.75 (d, *J* = 5.8 Hz, 1H), 5.48 (s, 1H), 5.15 (s, 1H), 4.19 (s, 1H), 4.05 (s, 1H), 3.98 (d, *J* = 2.4 Hz, 1H), 3.89 (s, H), 3.20 – 3.12 (m, 1H), ^{13}C NMR (101 MHz, DMSO) δ 162.00, 161.57, 158.57, 150.06, 147.06, 145.20, 144.86, 144.57, 136.00, 135.95, 135.77, 132.04, 130.18, 128.87, 128.40, 128.23, 128.09, 127.65, 127.17, 113.75, 98.60, 89.44, 89.23, 86.32, 84.87, 84.21, 83.88, 83.50, 82.59, 76.04, 74.45, 73.74,73.09, 70.30, 69.04, 63.89, 55.51, 46.32, 46.19, 12.01. HRMS (ESI-TOF) m/z: $[M+Na]^+$ Calcd. For $C_{11}H_{12}N_2O_6$ 593.1925, found 593.1984.

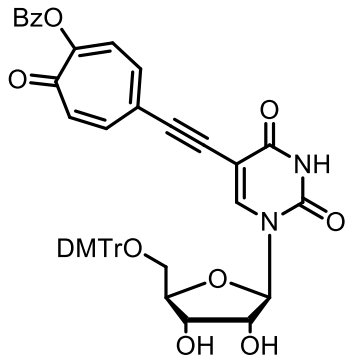

(15)

Compound (**15**): 5-ethynyluridinre 2'-DMTr **8** (0.200 g, 0.350 mmol), 2-benzoyloxy-iodotropon (0.184 g, 0.5263mmol), tetrakis(triphenylphosphine)palladium (0.040 g, 0.035 mmol), copper(I)iodide (0.013g, 0.072 mmol), and triethyl amine (0.238 ml, 1.755 mmol) was dissolved in 10ml dry DMF and stirred overnight under nitrogen conditions. After completion of the reaction was monitored by TLC. Then the solvent was evaporated under pressure, and the reaction mixture was purified by mesh 230-400 silica gel column chromatography (5% MeOH in DCM), to give yellow solid (0.147 g,54% yield). ^{1}H NMR (400 MHz, $CDCl_3$) δ 10.28 (s, 1H), 8.58 (s, 1H), 8.09 (d, *J* = 7.5 Hz, 2H), 7.59 (t, *J* = 7.4 Hz, 1H), 7.44 (dd, *J* = 15.2, 7.6 Hz, 4H), 7.38 – 7.23 (m, 7H), 7.13 (t, *J* = 7.0 Hz, 1H), 6.79 (t, *J* = 13.6 Hz, 6H), 6.33 (d, *J* = 11.0 Hz, 2H), 6.04 (s, 1H), 5.07 (s, 1H), 4.49 (d, *J* = 34.4 Hz, 2H), 4.22 (s, 1H), 3.68 (d, *J* = 3.5 Hz, 7H), 3.20 (d, *J* = 10.1 Hz, 1H), 1.94 (s, 2H). ^{13}C NMR (101 MHz, $CDCl_3$) δ 163.8, 161.63, 158.72, 150.11, 144.61, 143.83, 136.37, 135.74, 133.78, 130.48, 130.35, 129.86, 128.64, 128.53, 128.07, 127.22, 113.51, 99.88, 95.31, 90.28, 87.12, 84.68,70.23, 62.50, 55.29.

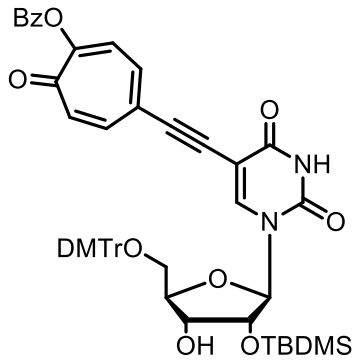

(16)

Compound (**16)**: A mixture of compound **7** (250mg, 0.314mmol, 1eq) and silver nitrate (140mg., 0.818mmol, 2.6eq) were dissolved in anhydrous pyridine (5.0ml) and the above solution was added dry THF (20ml). After stirring for 10 min TBDMS-Cl (47mg, 0.818mmole, 2.6eq) was added. The reaction mixture was stirred for additional 3h and filtrate through celite pad, and washed with two times EtOAC and the combine organic solution was the washed with sodium bicarbonate followed by brine, the organic extract was dried over sodium sulphate and evaporated. The resulting crude residue was purified by silica gel column chromatography to afford the product **8** as a yellowish solid (120mg, 43% yield). 1H NMR (400 MHz, CDCl3) δ 9.09 (s, 1H), 8.69 (s, 1H), 8.16 (d, J = 7.4 Hz, 2H), 7.64 (dd, J = 9.2, 5.6 Hz, 1H), 7.50 (dd, J = 10.2, 6.3 Hz, 4H), 7.40 – 7.25 (m, 7H), 7.20 (t, J = 7.3 Hz, 1H), 6.89 – 6.77 (m, 6H), 6.31 (d, J = 11.4 Hz, 2H), 6.09 (d, J = 4.8 Hz, 1H), 4.57 (t, J = 4.8 Hz, 1H), 4.27 (d, J = 3.9 Hz, 1H), 4.24 – 4.20 (m, 1H), 3.76 – 3.73 (m, 6H), 3.72 (d, J = 1.5 Hz, 1H), 3.22 (dd, J = 11.1, 1.6 Hz, 1H), 2.66 (d, J = 4.1 Hz, 1H), 0.97 – 0.91 (m, 9H), 0.18 (d, J = 14.1 Hz, 6H). 13C NMR (101 MHz, CDCl3) δ 171.23, 163.80, 160.75, 158.84, 158.81, 158.63, 149.09, 147.35, 145.05, 144.63, 143.67, 139.49, 135.71, 135.17, 130.48, 129.92, 129.81, 129.16, 128.70, 128.57, 128.24, 127.85, 127.79, 127.34, 127.08, 113.52, 113.47, 113.17, 99.88, 95.09, 94.78, 88.85, 87.41, 85.53, 85.05, 84.56, 84.31, 81.45, 77.37, 77.05, 76.74, 75.74, 71.11, 69.90, 62.91, 60.43, 55.30, 55.26, 25.70, 25.64, 21.07, 18.03, 14.21, 0.01, -4.65, -4.68, -5.11, -5.14.

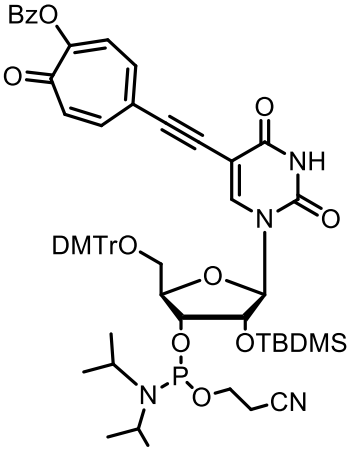

(17)

To the solution of compound (**17) (**0.096 g , 0.155mmol, 1.0 equiv) in dry THF (4.0ml) was added *N*,*N*-diisopropylethylamine(0.035ml, 0.2643, 2.5 equiv) and stirred for 15 min under ice cold conditions. To the reaction mixture was added slowly 2-cyano *N*,*N*-diisopropylchlrophosphoramidite (0.046ml, 0.264 mmol, 2.5 equiv) and the reaction mixture was stirred for 2 h., the completion of reaction was monitored by TLC. The reaction mixture was evaporated to dryness and the crude reaction mixture was purified by column chromatography (50% EtOAC in Hexane) to afford the yellow coloured solid (0.080 g, 68%). ^{1}H NMR (400 MHz, $CDCl_3$) δ 8.72 (d, *J* = 16.4 Hz, 2H), 8.16 (d, *J* = 7.3 Hz, 3H), 7.64 (t, *J* = 7.4 Hz, 2H), 7.50 (t, *J* = 7.7 Hz, 8H), 7.40 – 7.29 (m, 13H), 7.21 (dd, *J* = 8.0, 6.0 Hz, 2H), 6.88 – 6.80 (m, 9H), 6.26 (dd, *J* = 18.1, 11.5 Hz, 3H), 6.05 (dd, *J* = 40.8, 5.3 Hz, 1H), 4.68 – 4.62 (m, 1H), 4.59 (t, *J* = 4.7 Hz, 1H), 4.39 (d, *J* = 3.8 Hz, 1H), 4.31 – 4.21 (m, 3H), 3.96 (td, *J* = 13.2, 6.6 Hz, 1H), 3.74 (d, *J* = 0.9 Hz, 10H), 3.61 – 3.50 (m, 4H), 3.15 (d, *J* = 11.2 Hz, 2H), 2.67 (d, *J* = 6.1 Hz, 2H), 2.32 (dt, *J* = 10.3, 6.3 Hz, 2H), 1.35 – 1.27 (m, 7H), 1.18 – 1.14 (m, 17H), 0.97 – 0.92 (m, 17H), 0.91 (s, 8H), 0.17 – 0.11 (m, 11H).

5.6 References and Notes

1. McKenzie, L. K.; El-Khoury, R.; Thorpe, J. D.; Damha, M. J.; Hollenstein, M., Recent progress in non-native nucleic acid modifications. *Chemical Society Reviews* **2021,** *50*, 5126-5164.

2. McKenzie, L. K.; El-Khoury, R.; Thorpe, J. D.; Damha, M. J.; Hollenstein, M., Recent progress in non-native nucleic acid modifications. *Chem. Soc. Rev.* **2021,** *50*, 5126-5164.

3. Wolk, S. K.; Mayfield, W. S.; Gelinas, A. D.; Astling, D.; Guillot, J.; Brody, E. N.; Janjic, N.; Gold, L., Modified nucleotides may have enhanced early RNA catalysis. *Proceedings of the National Academy of Sciences* **2020,** *117*, 8236-8242.

4. Perrone, D.; Marchesi, E.; Preti, L.; Navacchia, M. L., Modified Nucleosides, Nucleotides and Nucleic Acids via Click Azide-Alkyne Cycloaddition for Pharmacological Applications. *Molecules* **2021,** *26*, 3100.

5. Duffy, K.; Arangundy-Franklin, S.; Holliger, P., Modified nucleic acids: replication, evolution, and next-generation therapeutics. *BMC Biol.* **2020,** *18*, 112.

6. Ochoa, S.; Milam, V. T., Modified Nucleic Acids: Expanding the Capabilities of Functional Oligonucleotides. *MDPI* **2020,** *25*, 4659.

7. Xu, W.; Chan, K. M.; Kool, E. T., Fluorescent nucleobases as tools for studying DNA and RNA. *Nature Chemistry* **2017,** *9*, 1043-1055.

8. Sinkeldam, R. W.; Greco, N. J.; Tor, Y., Fluorescent Analogs of Biomolecular Building Blocks: Design, Properties, and Applications. *Chemical Reviews* **2010,** *110*, 2579-2619.

9. Seo, T. S.; Bai, X.; Kim, D. H.; Meng, Q.; Shi, S.; Ruparel, H.; Li, Z.; Turro, N. J.; Ju, J., Four-color DNA sequencing by synthesis on a chip using photocleavable fluorescent nucleotides. *Proceedings of the National Academy of Sciences* **2005,** *102*, 5926-5931.

10. Leone, D.-L.; Hubalek, M.; Pohl, R.; Sykorova, V.; Hocek, M., 1, 3-Diketone-Modified Nucleotides and DNA for Cross-Linking with Arginine-Containing Peptides and Proteins. *Angewandte Chemie International Edition* **2021**.

11. Matyašovský, J.; Tack, L.; Palágyi, A.; Kuba, M.; Pohl, R.; Kraus, T.; Güixens-Gallardo, P.; Hocek, M., Nucleotides bearing aminophenyl-or aminonaphthyl-3-methoxychromone solvatochromic fluorophores for the enzymatic construction of DNA probes for the detection of protein–DNA binding. *Organic & Biomolecular Chemistry* **2021,** *19*, 9966-9974.

12. George, J. T.; Srivatsan, S. G., Bioorthogonal chemistry-based RNA labeling technologies: evolution and current state. *Chemical Communications* **2020,** *56*, 12307-12318.

13. Hocek, M., Enzymatic synthesis of base-functionalized nucleic acids for sensing, cross-linking, and modulation of protein–DNA binding and transcription. *Acc. Chem. Res.* **2019,** *52*, 1730-1737.

14. Pauson, P. L., Tropones and tropolones. *Chemical Reviews* **1955,** *55*, 9-136.

15. Bentley, R., A fresh look at natural tropolonoids. *Natural product reports* **2008,** *25*, 118-138.

16. Chung, S.; Himmel, D. M.; Jiang, J.-K.; Wojtak, K.; Bauman, J. D.; Rausch, J. W.; Wilson, J. A.; Beutler, J. A.; Thomas, C. J.; Arnold, E.; Le Grice, S. F. J., Synthesis, Activity, and Structural Analysis of Novel α-Hydroxytropolone Inhibitors of Human Immunodeficiency Virus Reverse Transcriptase-Associated Ribonuclease H. *J. Med. Chem.* **2011,** *54*, 4462-4473.

17. Cox, R. J.; Al-Fahad, A., Chemical mechanisms involved during the biosynthesis of tropolones. *Curr. Opin. Chem. Biol.* **2013,** *17*, 532-536.

18. Fullagar, J. L.; Garner, A. L.; Struss, A. K.; Day, J. A.; Martin, D. P.; Yu, J.; Cai, X.; Janda, K. D.; Cohen, S. M., Antagonism of a zinc metalloprotease using a unique metal-

chelating scaffold: tropolones as inhibitors of P. aeruginosa elastase. *Chemical communications* **2013,** *49*, 3197-3199.

19. Angawi, R. F.; Swenson, D. C.; Gloer, J. B.; Wicklow, D. T., Malettinin A: a new antifungal tropolone from an unidentified fungal colonist of Hypoxylon stromata (NRRL 29110). *Tetrahedron Lett.* **2003,** *44*, 7593-7596.

20. Yang, P.-S.; Wang, M.-J.; Jayakumar, T.; Chou, D.-S.; Ko, C.-Y.; Hsu, M.-J.; Hsieh, C.-Y., Antiproliferative activity of hinokitiol, a tropolone derivative, is mediated via the inductions of p-JNK and p-PLCγ1 signaling in PDGF-BB-stimulated vascular smooth muscle cells. *Molecules* **2015,** *20*, 8198-8212.

21. Lomonosova, E.; Daw, J.; Garimallaprabhakaran, A. K.; Agyemang, N. B.; Ashani, Y.; Murelli, R. P.; Tavis, J. E., Efficacy and cytotoxicity in cell culture of novel α-hydroxytropolone inhibitors of hepatitis B virus ribonuclease H. *Antiviral research* **2017,** *144*, 164-172.

22. Morita, Y.; Matsumura, E.; Okabe, T.; Shibata, M.; Sugiura, M.; Ohe, T.; Tsujibo, H.; Ishida, N.; Inamori, Y., Biological activity of tropolone. *Biol. Pharm. Bull.* **2003,** *26*, 1487-90.

23. Jacobsen, F. E.; Lewis, J. A.; Heroux, K. J.; Cohen, S. M., Characterization and evaluation of pyrone and tropolone chelators for use in metalloprotein inhibitors. *Inorg. Chim. Acta* **2007,** *360*, 264-272.

24. Jacobsen, J. A.; Fullagar, J. L.; Miller, M. T.; Cohen, S. M., Identifying chelators for metalloprotein inhibitors using a fragment-based approach. *J. Med. Chem.* **2011,** *54*, 591-602.

25. Vohtancev, I. P.; Sherstyuk, Y. V.; Silnikov, V. N.; Abramova, T. V., Effective Synthesis of 5-Iodo Derivatives of Pyrimidine Morpholino Nucleosides. *Org. Prep. Proced. Int.* **2018,** *50*, 332-342.

26. Bollu, A.; Sharma, N. K., Tropolone-Conjugated DNA: Fluorescence Enhancement in the Duplex. *ChemBioChem* **2019,** *20*, 1467-1475.

27. Cobb, A. J. A., Recent highlights in modified oligonucleotide chemistry. *Org. Biomol. Chem.* **2007,** *5*, 3260-3275.

5.7 Appendix

Table of Contents

1. NMR (^{1}H, ^{13}C) and HRMS spectra of compound **2**: 346
2. NMR (^{1}H, ^{13}C, ^{11}B, ^{19}F) and HRMS spectra of compound **3**: 348
3. NMR (^{1}H, ^{13}C) and HRMS spectra of compound **5**: 351
4. NMR (^{1}H, ^{13}C, ^{11}B, ^{19}F) and HRMS spectra of compound **6**: 352
5. NMR (^{1}H, ^{13}C, ^{11}B, ^{19}F, ^{31}P) and HRMS spectra of phosphonamidites **7**: 355
6. NMR (^{1}H, ^{13}C, ^{11}B, ^{19}F, ^{31}P) and HRMS spectra of Trpoponylated BODIPY thymidine **8**: 359
7. NMR (^{1}H, ^{11}B, ^{19}F, ^{31}P) and HRMS spectra of Triphosphate **9**: 362
8. NMR (1H, 13C) and HRS spectra of compound 11 365
9. NMR (^{1}H, ^{13}C) and HRS spectra of compound **12**: 366
10. NMR (^{1}H, ^{13}C) and HRMS spectra of compound **13**: 368
11. NMR (^{1}H, ^{13}C) and HRMS spectra of compound **14**: 370
12. NMR (^{1}H, ^{13}C) and HRMS spectra of compound **15**: 372
13. NMR (^{1}H, ^{13}C) and HRMS spectra of compound **16**: 374
14. NMR (^{1}H, ^{13}C) and HRMS spectra of compound **17**: 376

1. NMR (^{1}H, ^{13}C) and HRMS spectra of compound **2**:

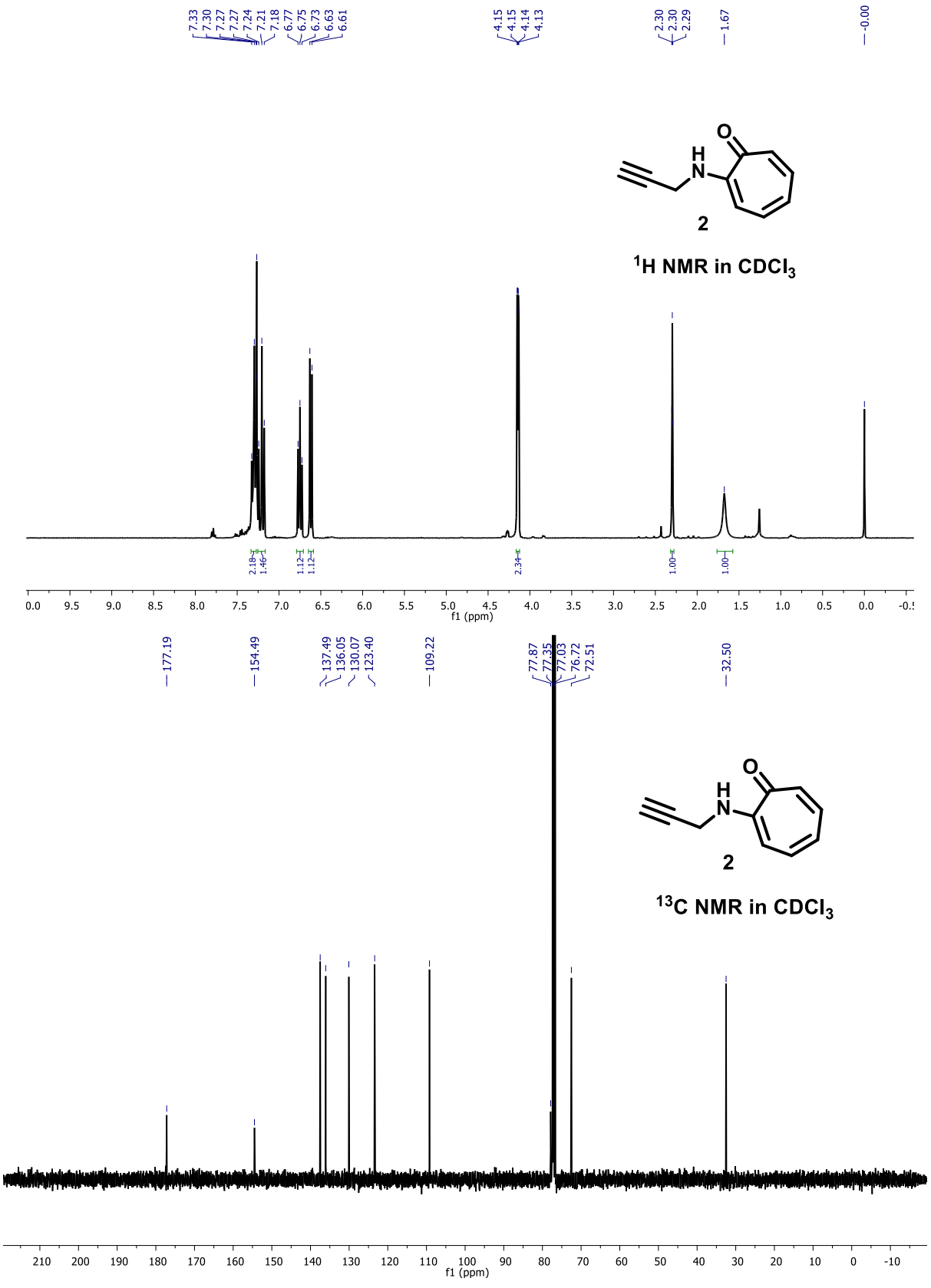

Figure A1. (^{1}H and ^{13}C) NMR spectra of Aminotropone **2** in $CDCl_3$.

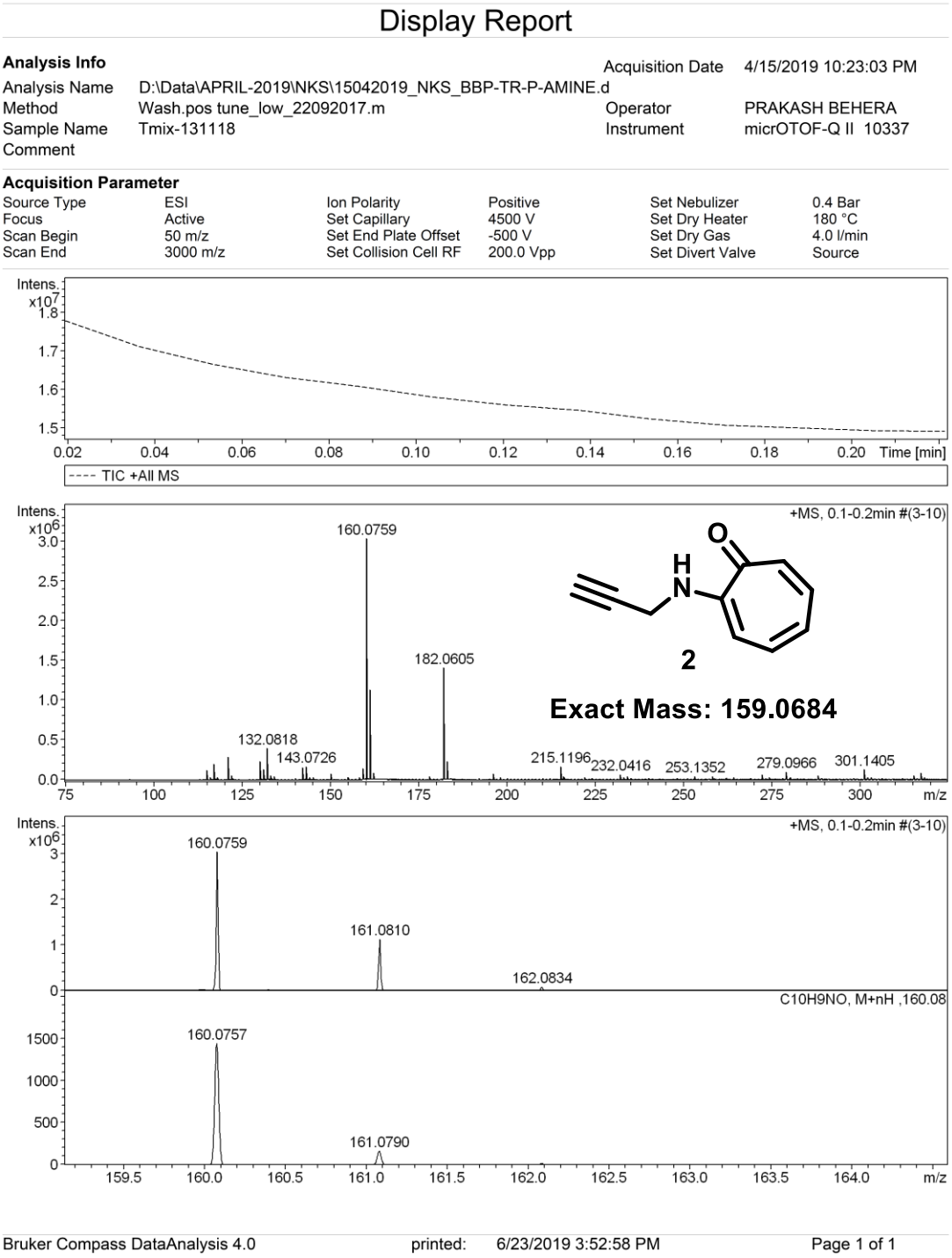

Figure A2. ESI/HRMS spectra of Aminotropone **2**.

2. NMR (^{1}H, ^{13}C, ^{11}B, ^{19}F) and HRMS spectra of compound **3**:

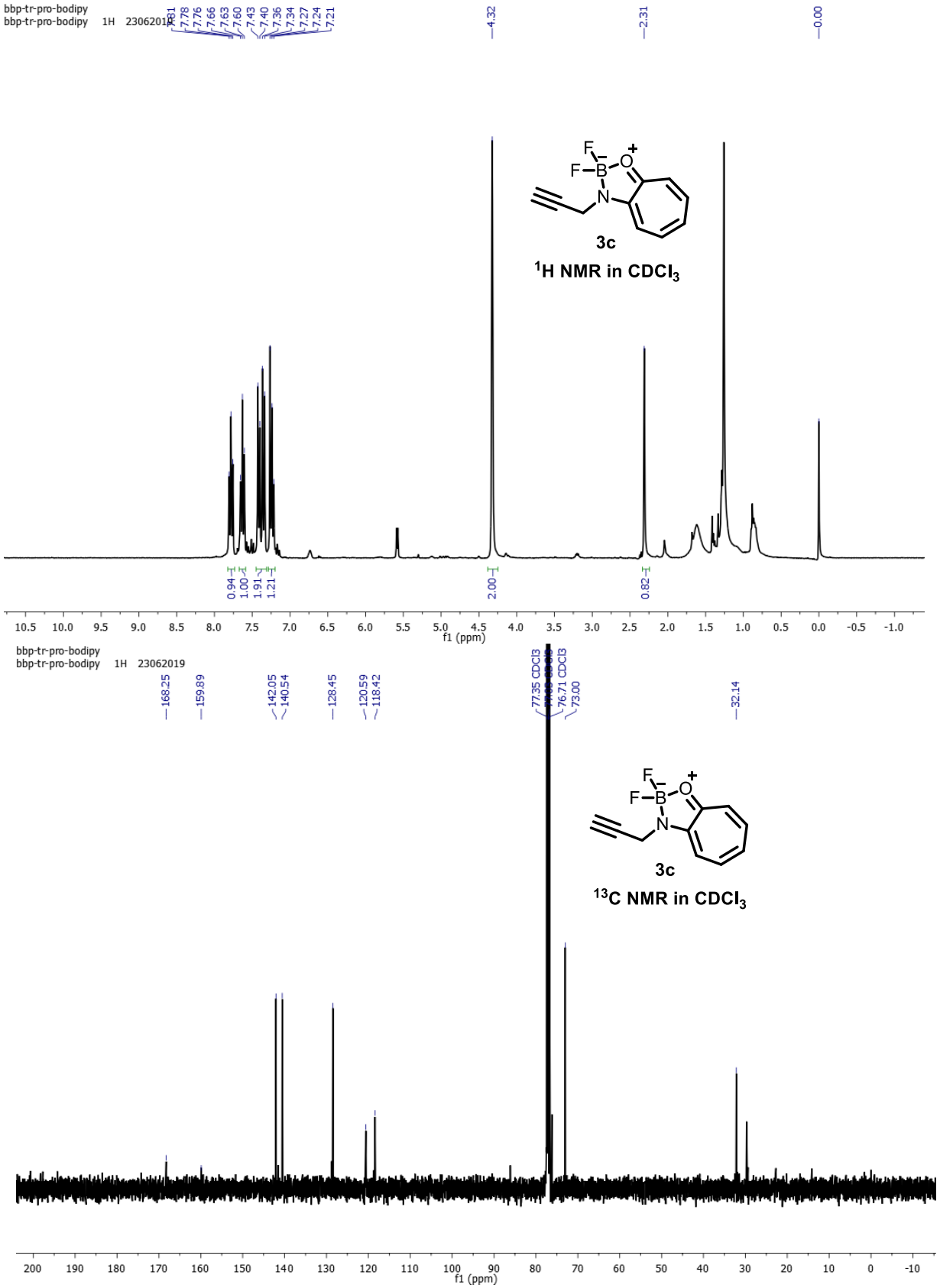

Figure A3. (^{1}H and ^{13}C) NMR spectra of Boron complex **3** in $CDCl_3$.

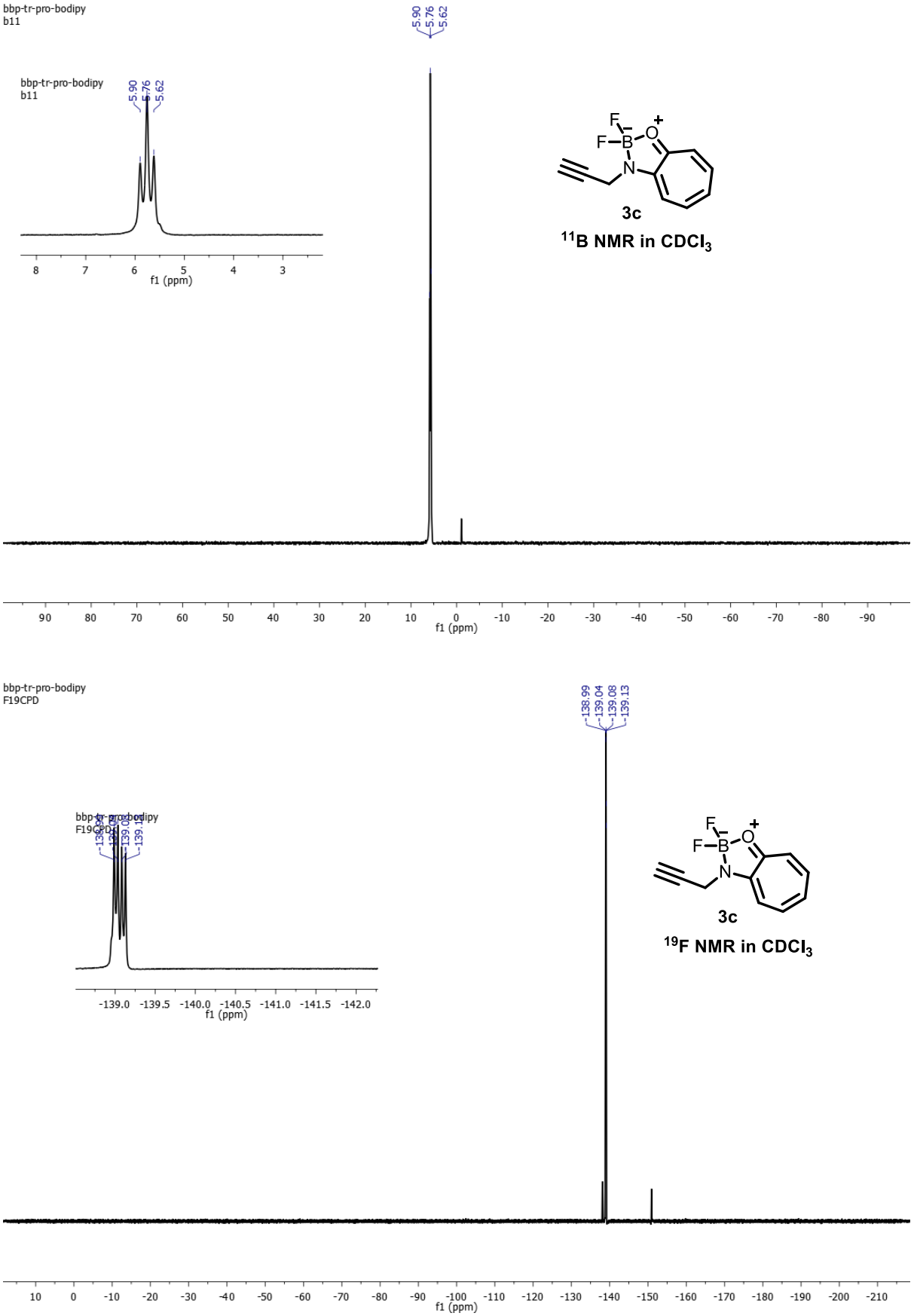

Figure A4. (^{11}B and ^{19}F) NMR spectra of Boron complex **3** in $CDCl_3$.

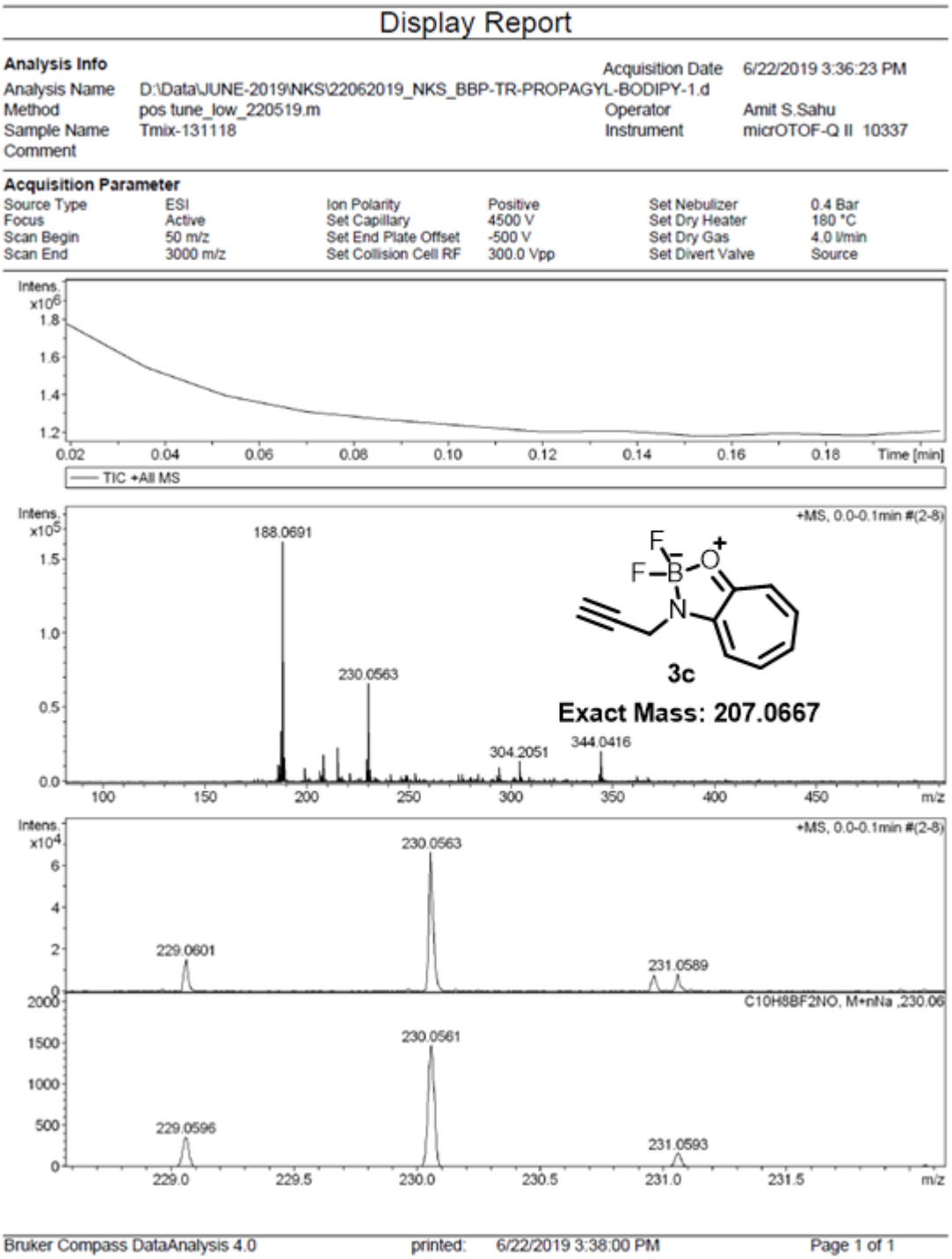

Figure A5. ESI/HRMS spectra of Boron complex **3**.

3. NMR (^{1}H, ^{13}C) and HRMS spectra of compound **5**:

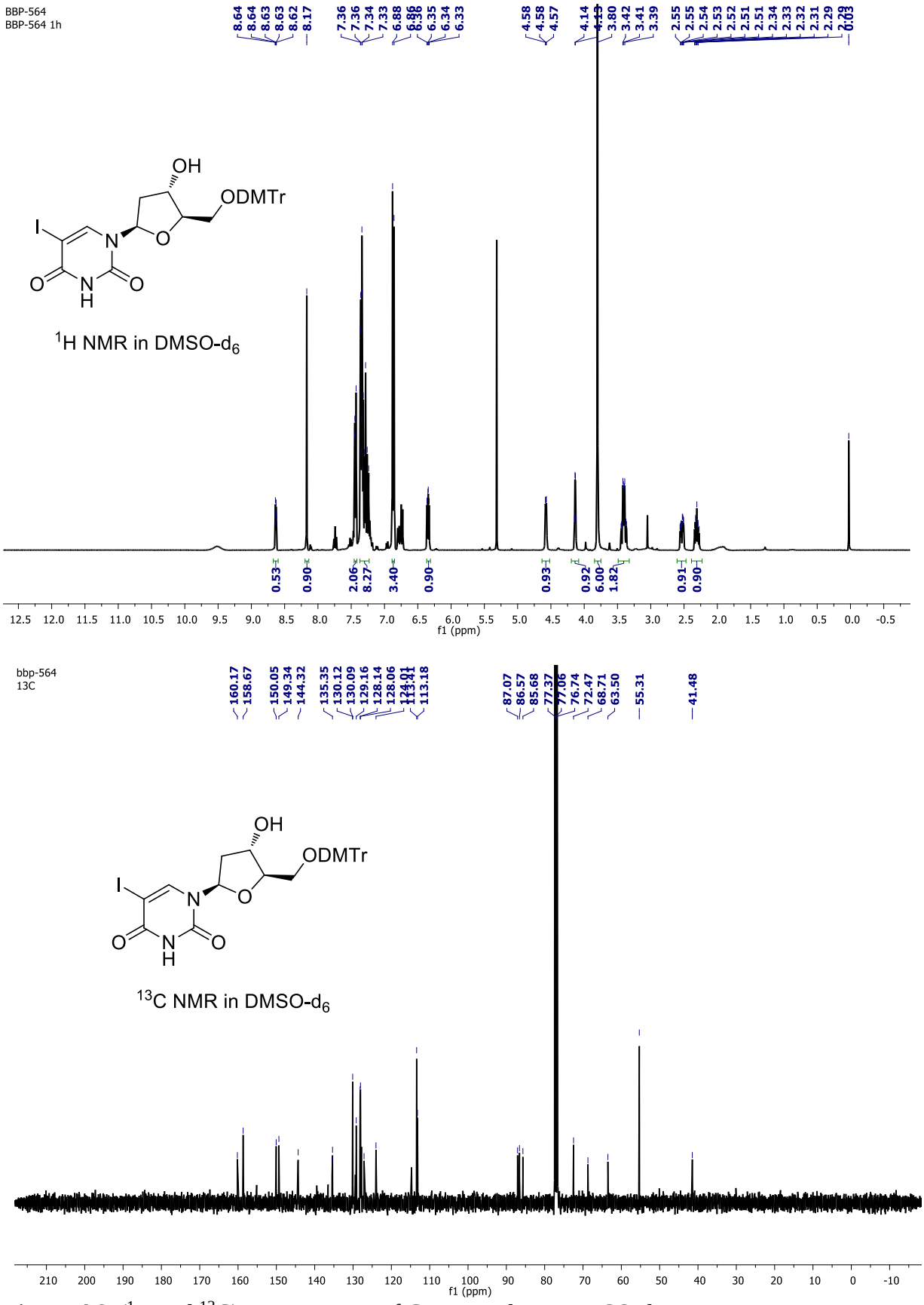

Figure A6. (^{1}H and ^{13}C) NMR spectra of Compound **5** in DMSO-d$_6$.

4. NMR (^{1}H, ^{13}C, ^{11}B, ^{19}F) and HRMS spectra of compound **6**:

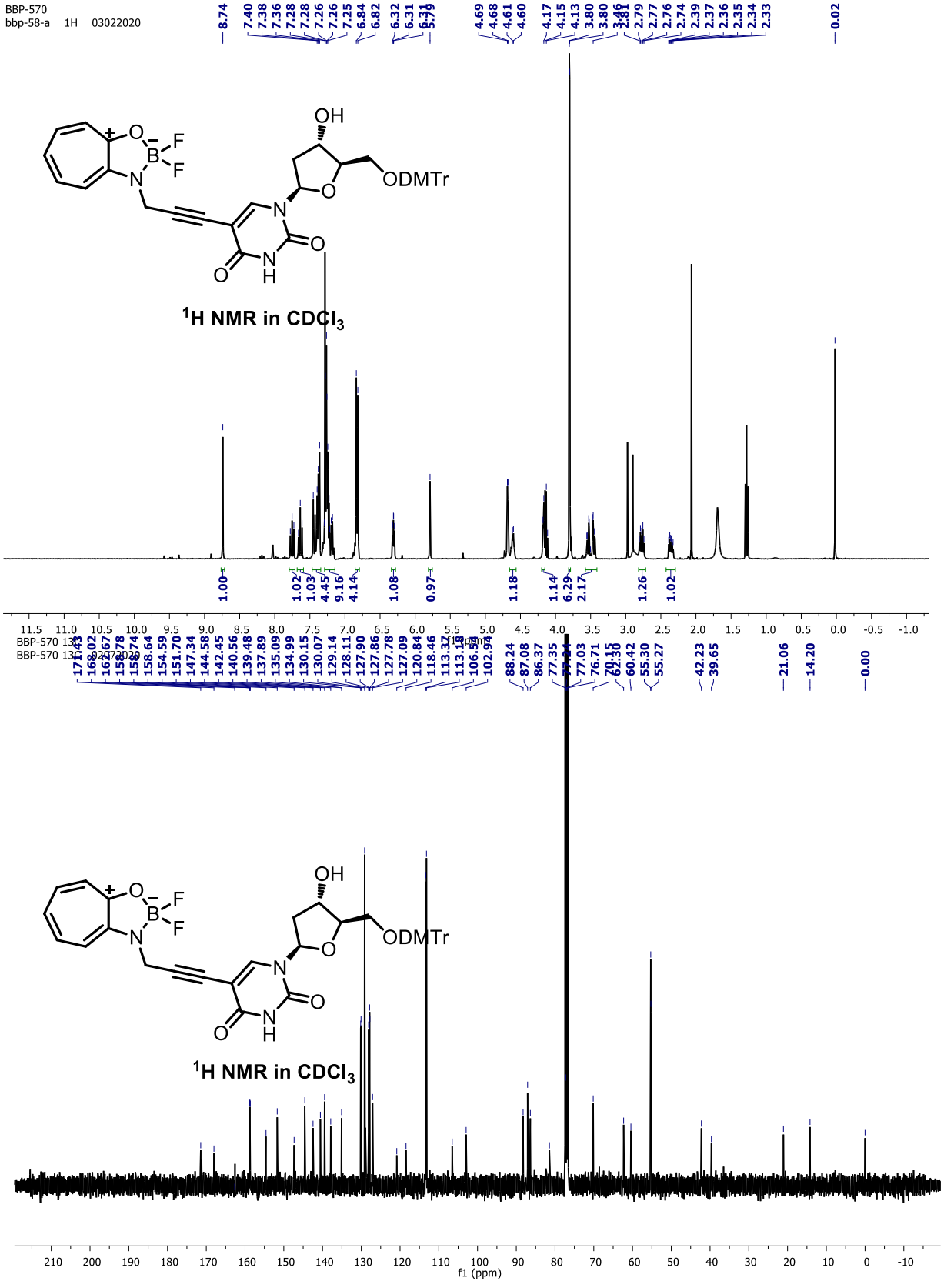

Figure A7. (^{1}H and ^{13}C) NMR spectra of Compound **6** in $CDCl_3$.

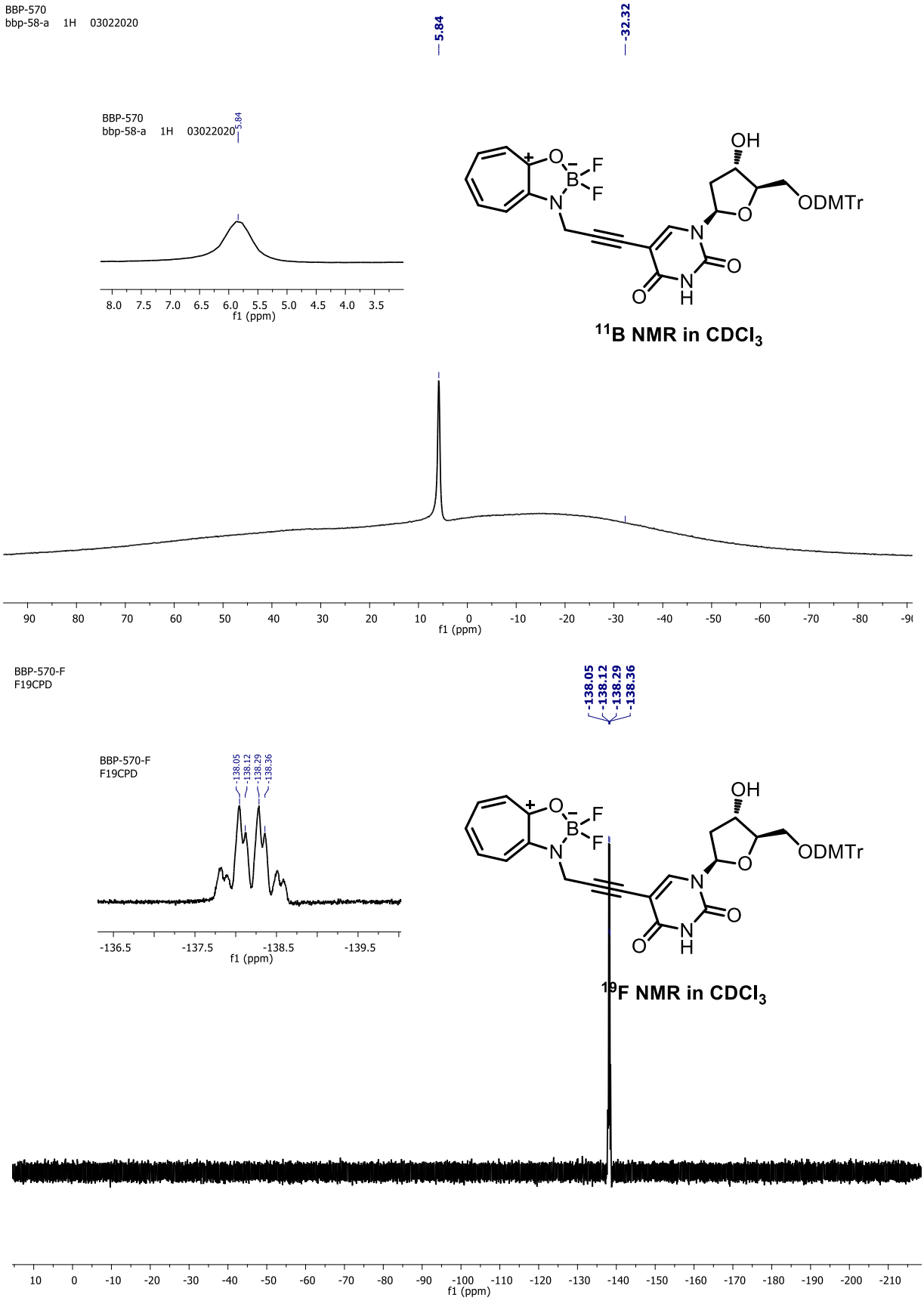

Figure A6. (^{11}B and ^{19}F) NMR spectra of Boron complex **6** in $CDCl_3$.

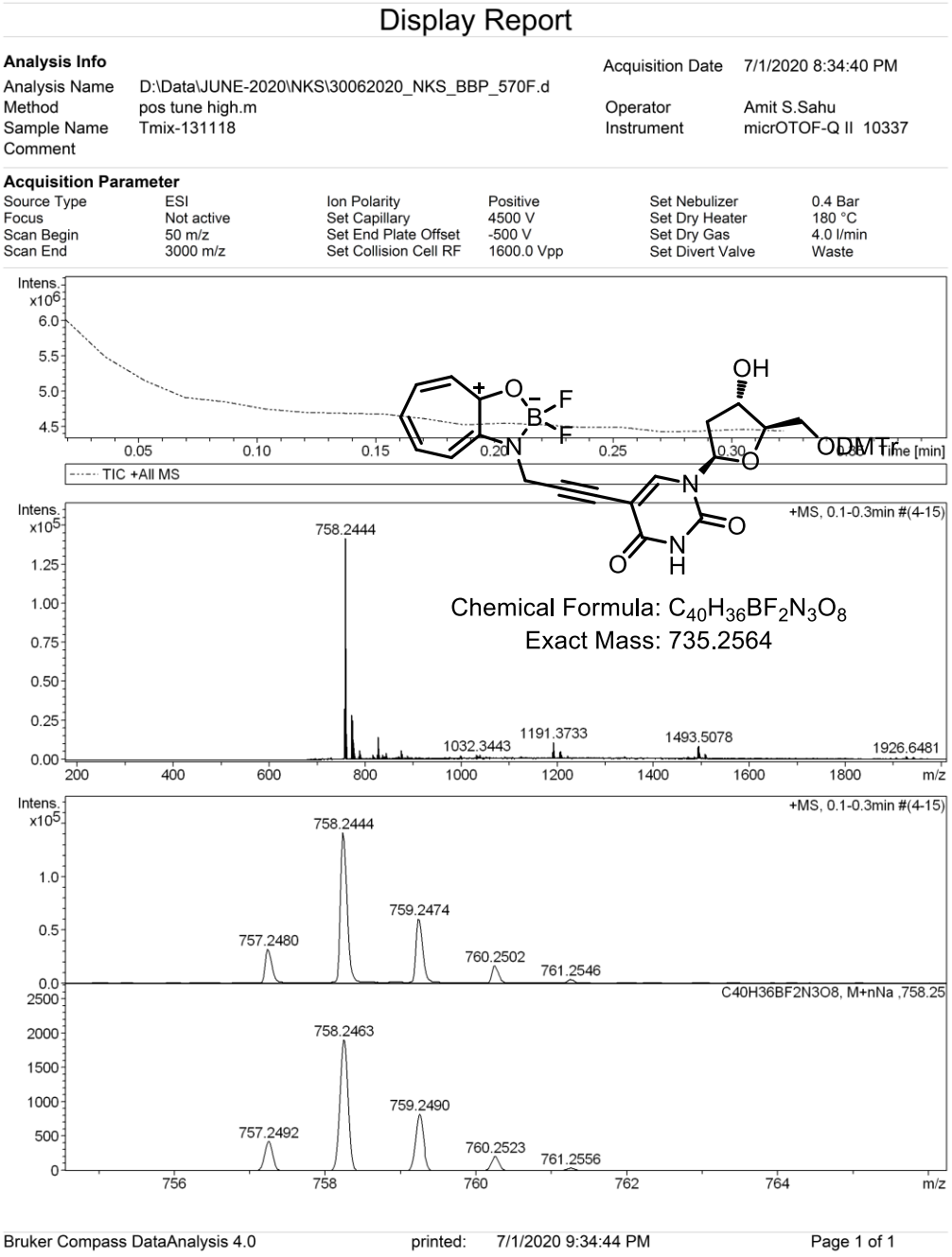

Figure A7. ESI/HRMS spectra of Compound **6.**

5. NMR (^{1}H, ^{13}C, ^{11}B, ^{19}F, ^{31}P) and HRMS spectra of phosphonamidites **7**:

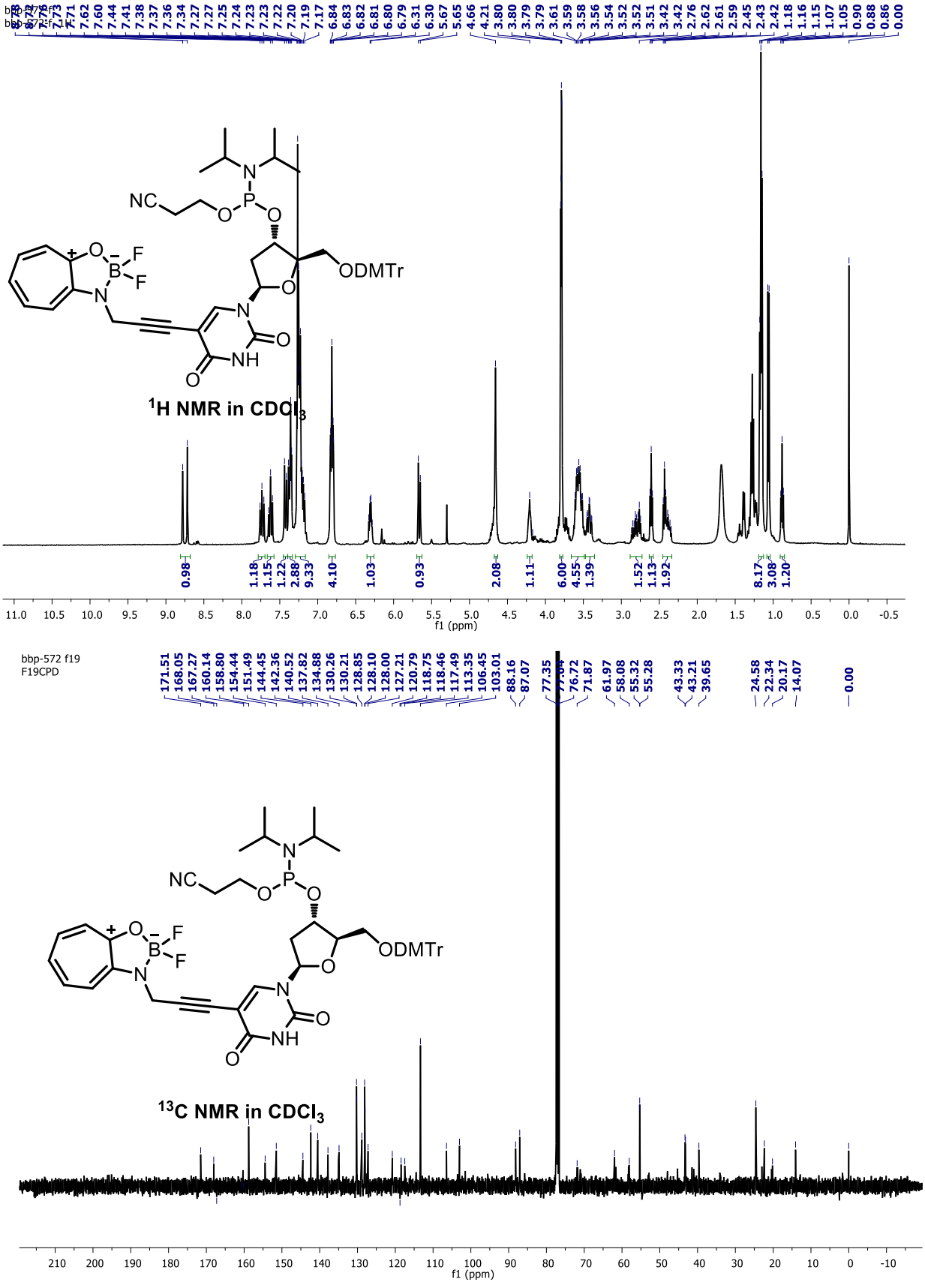

Figure A8. (^{1}H and ^{13}C) NMR spectra of phosphonamidites **7** in $CDCl_3$.

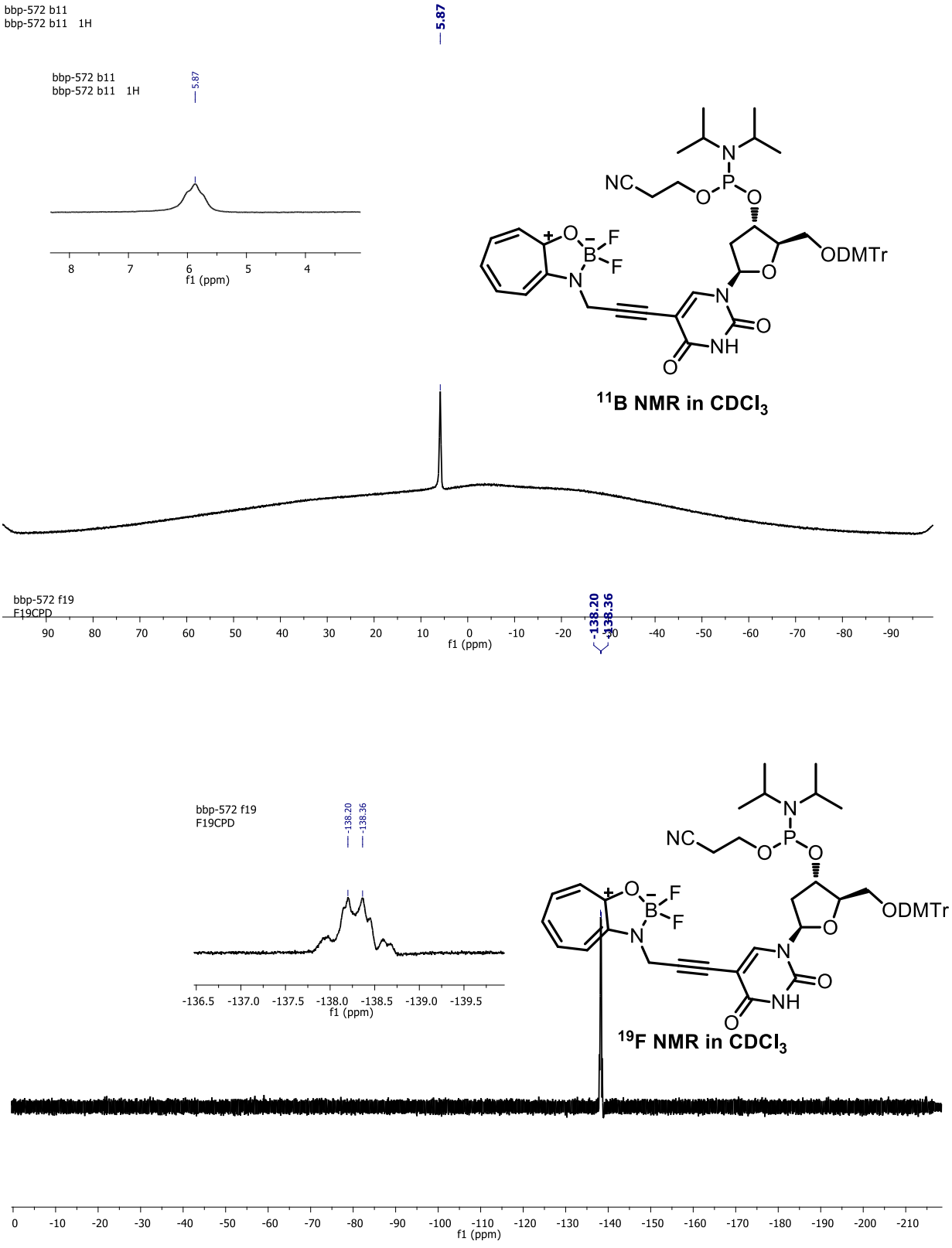

Figure A9. (^{11}B and ^{19}F) NMR spectra of phosphonamidites **7** in $CDCl_3$.

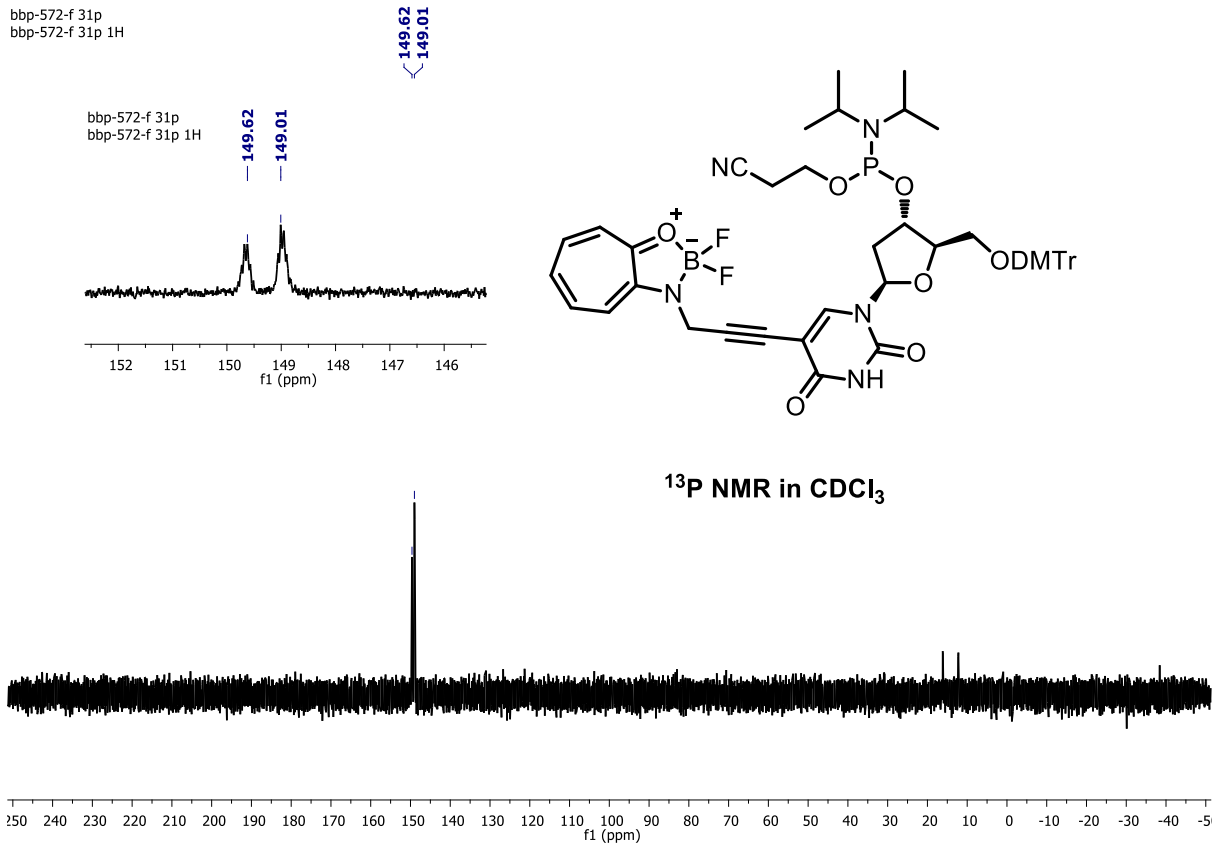

Figure A10. (^{31}P) NMR spectra of phosphonamidites **7** in $CDCl_3$.

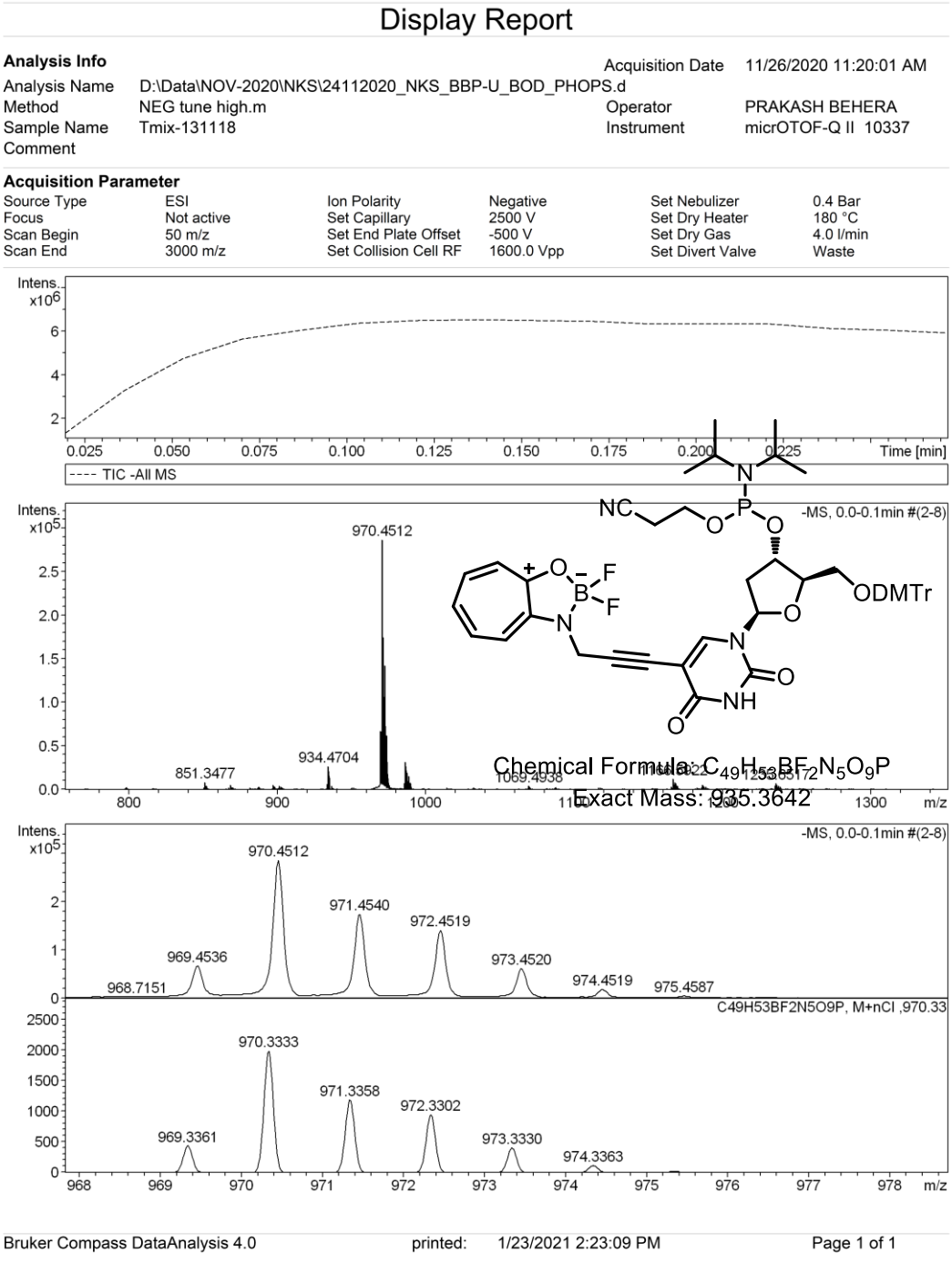

Figure A11. ESI/HRMS spectra of phosphonamidites **7**.

6. NMR (^{1}H, ^{13}C, ^{11}B, ^{19}F, ^{31}P) and HRMS spectra of Trpoponylated BODIPY thymidine **8**:

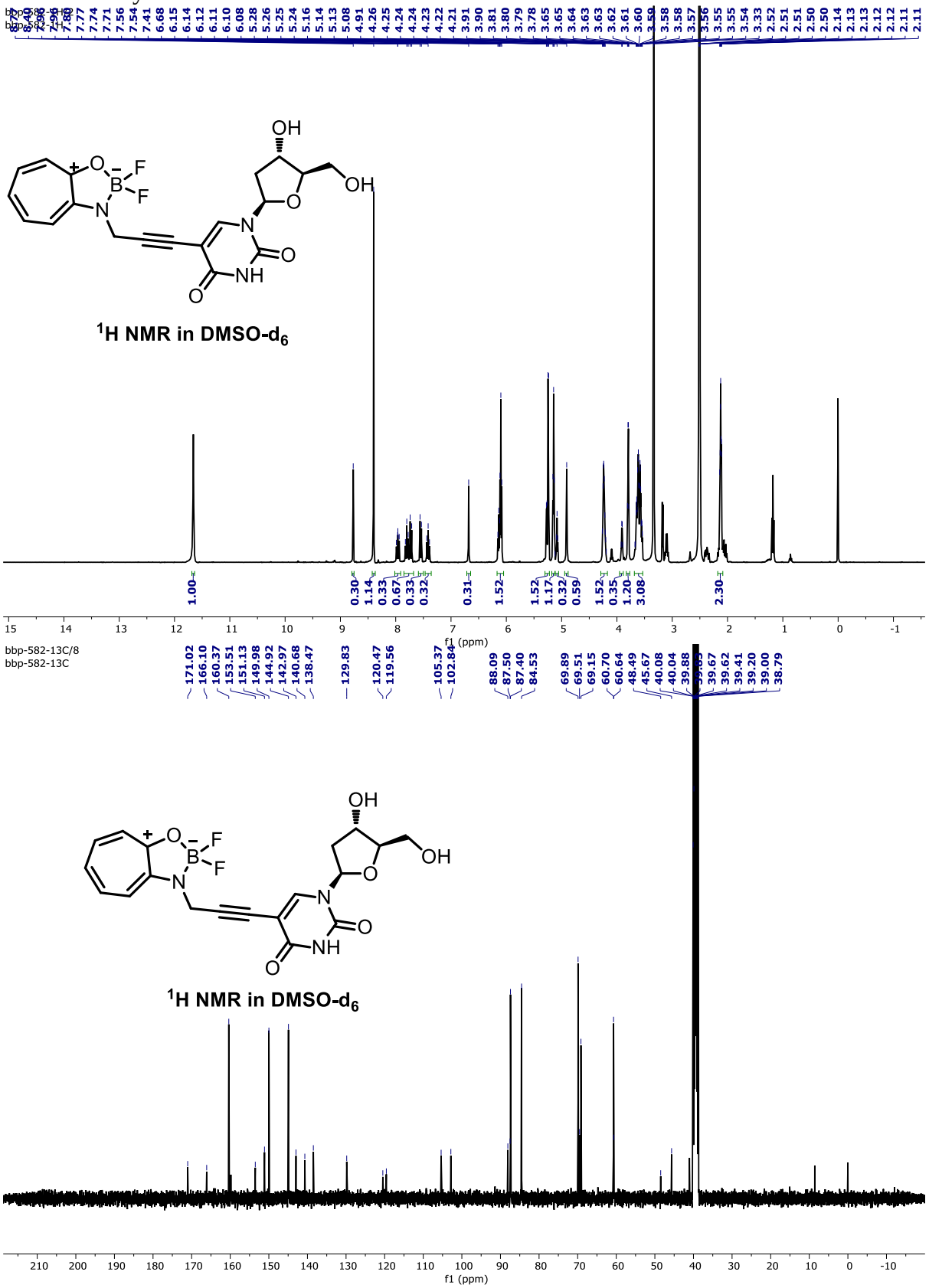

Figure A12. (^{1}H and ^{13}C) NMR spectra of *Troponylated* Nucleoside **8** in DMSO-d$_6$

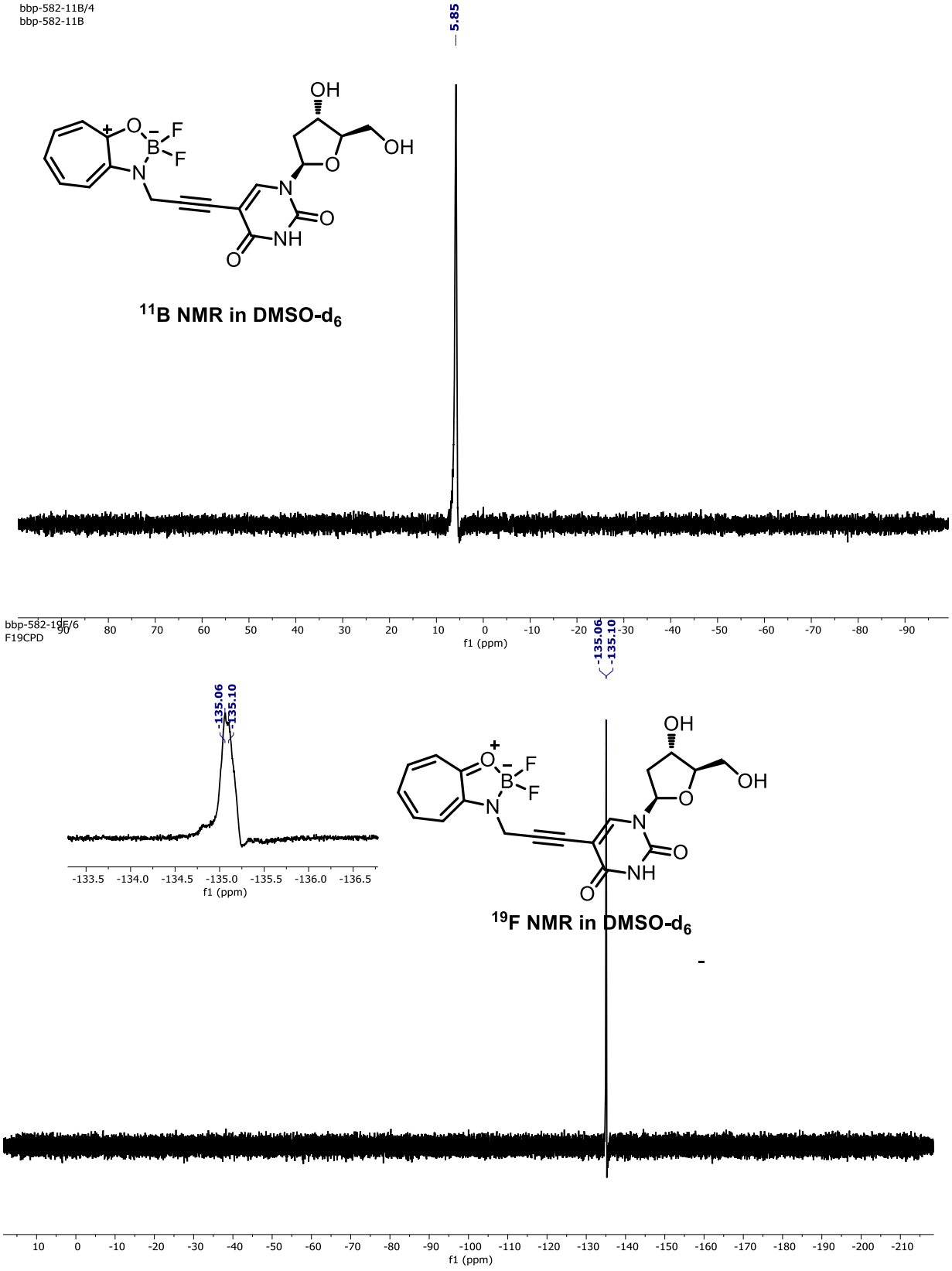

Figure A13. (^{11}B and ^{19}F) NMR spectra of *Troponylated* Nucleoside **8** in DMSO-d_6.

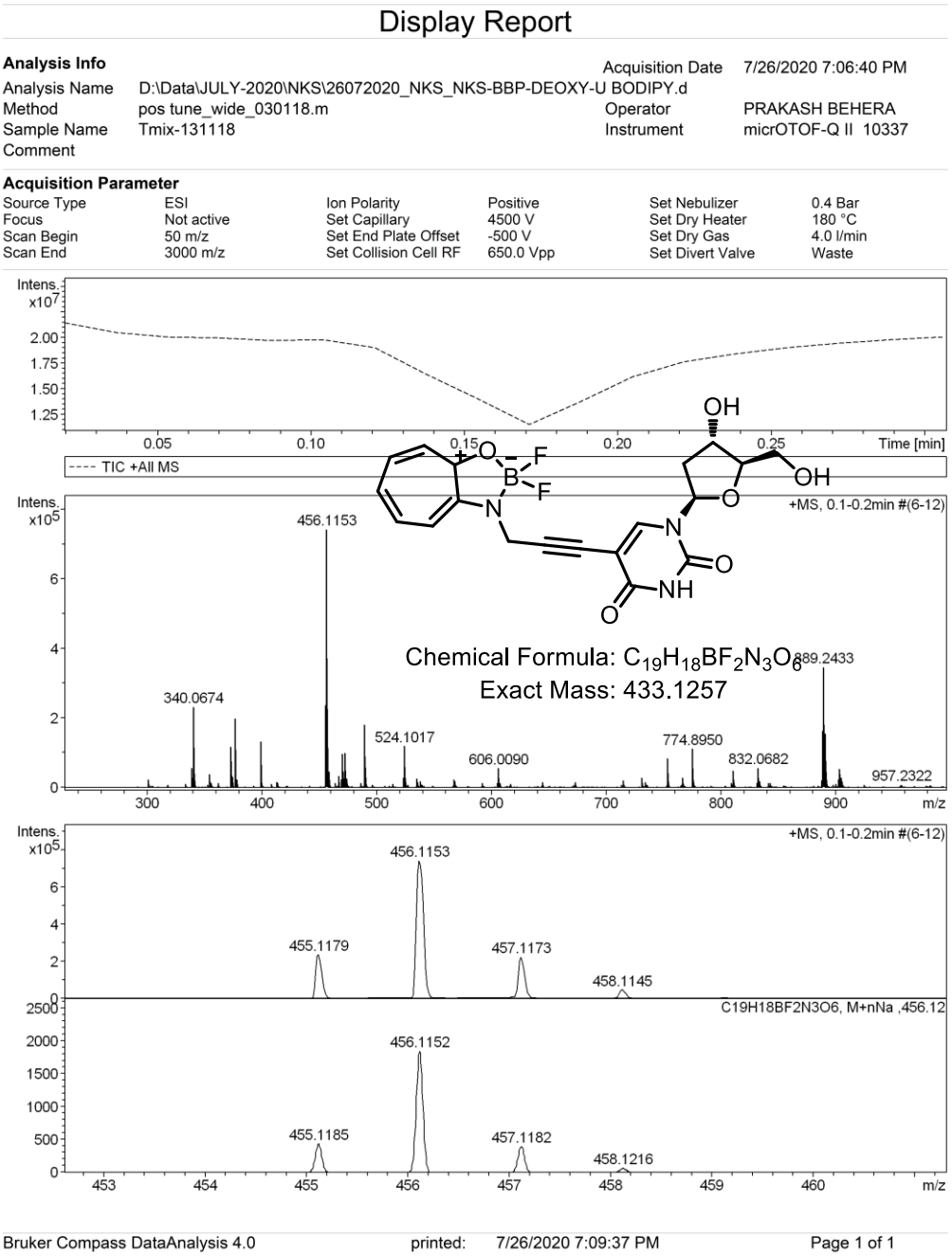

Figure A14. ESI/HRMS spectra of Compound **8**.

7. NMR (^{1}H, ^{11}B, ^{19}F, ^{31}P) and HRMS spectra of Triphosphate **9**:

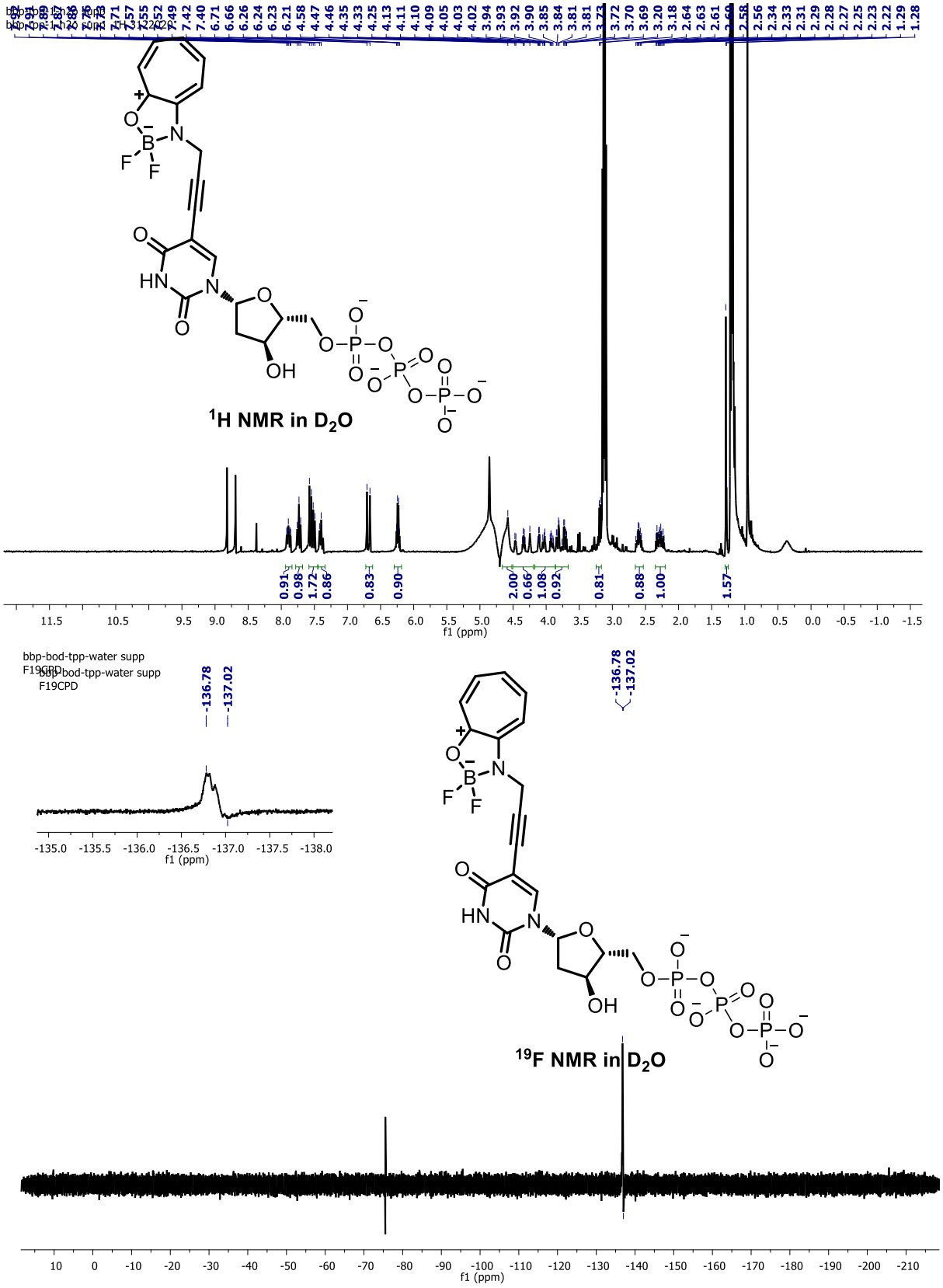

Figure A15. (^{1}H and ^{19}F) NMR spectra of *Troponylated* Triphosphate **9** in D_2O.

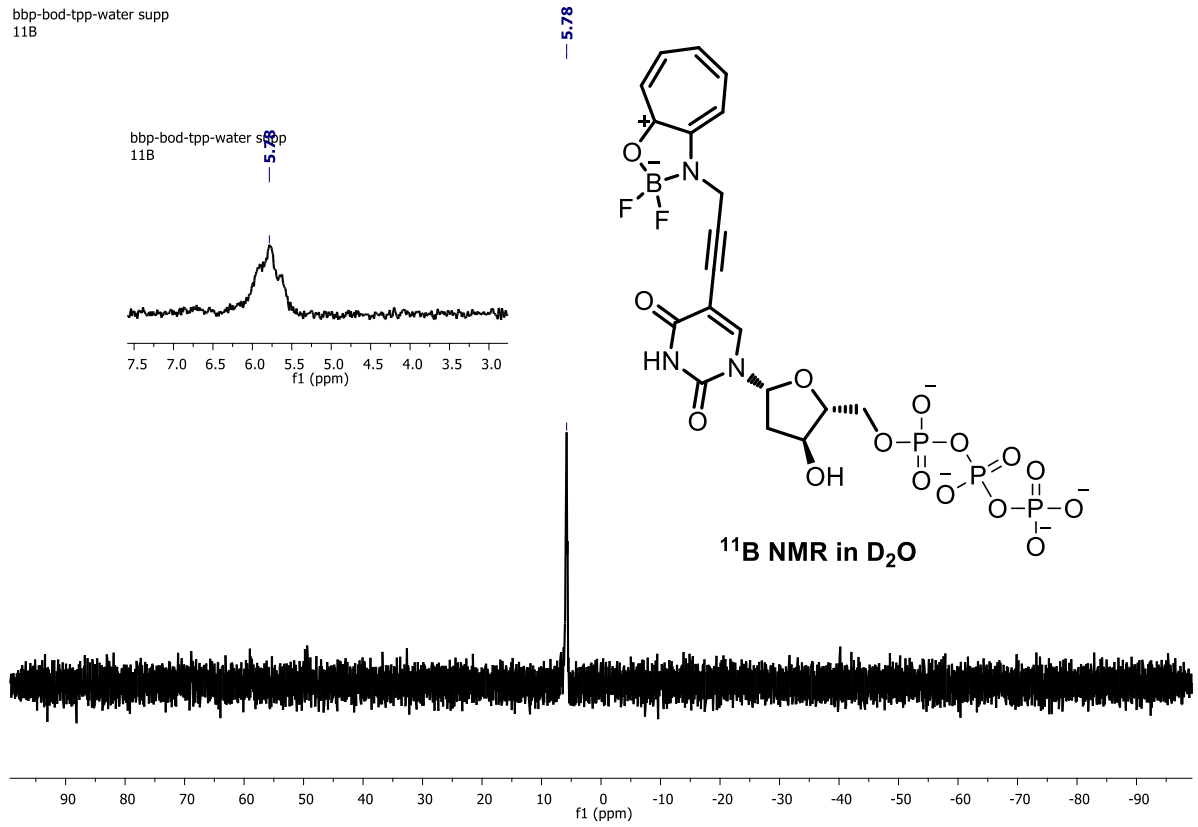

Figure A16. ^{11}B NMR spectra of *Troponylated* Triphosphate **9** in D_2O.

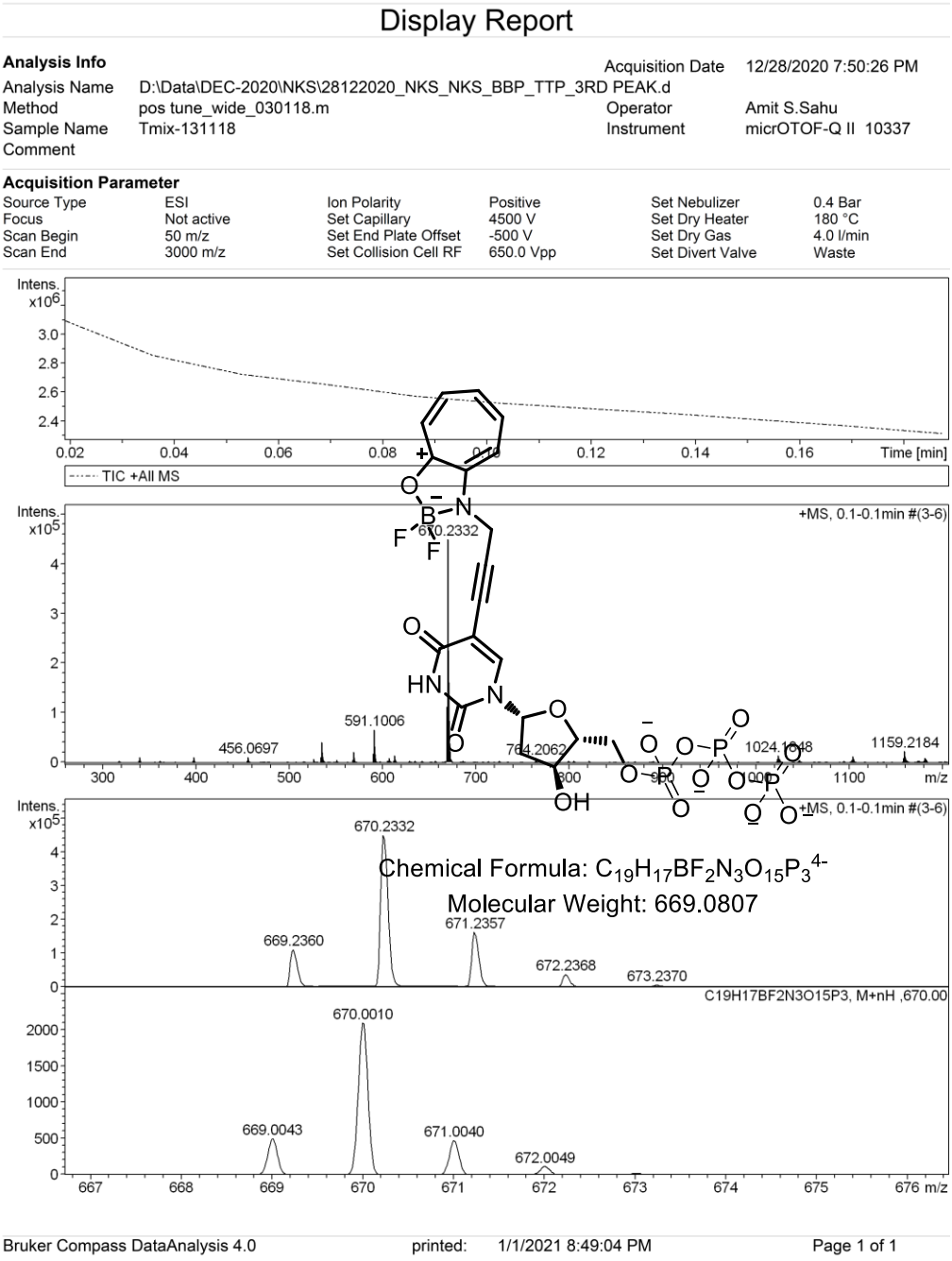

Figure A17. ESI/HRMS spectra of *Troponylated* Triphosphate **9.**

8. NMR (1H, 13C) and HRS spectra of compound 11:

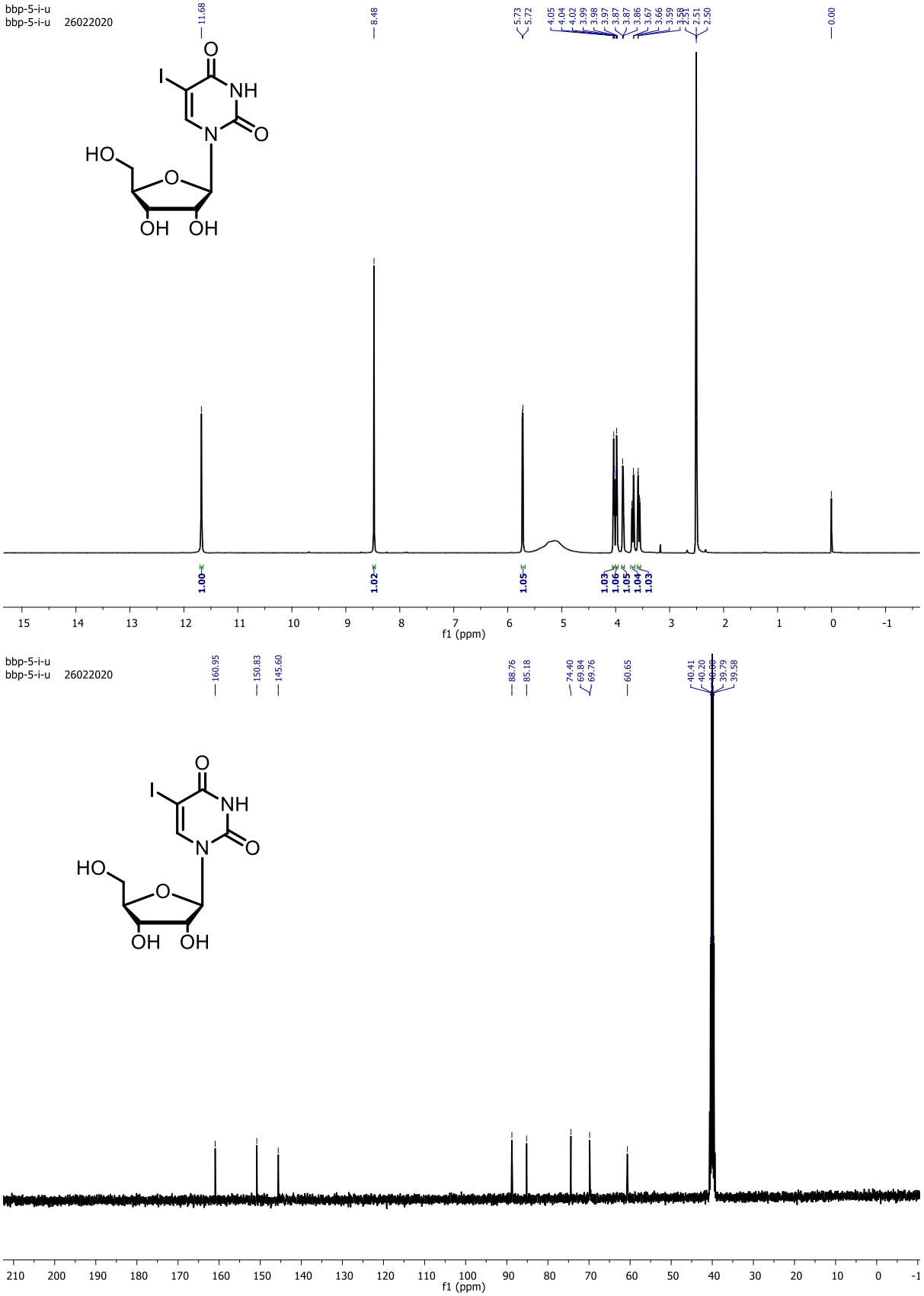

Figure A18. (^{1}H and ^{13}C) NMR spectra of Compound **11** in $CDCl_3$

9. NMR (^{1}H, ^{13}C) and HRS spectra of compound **12**:

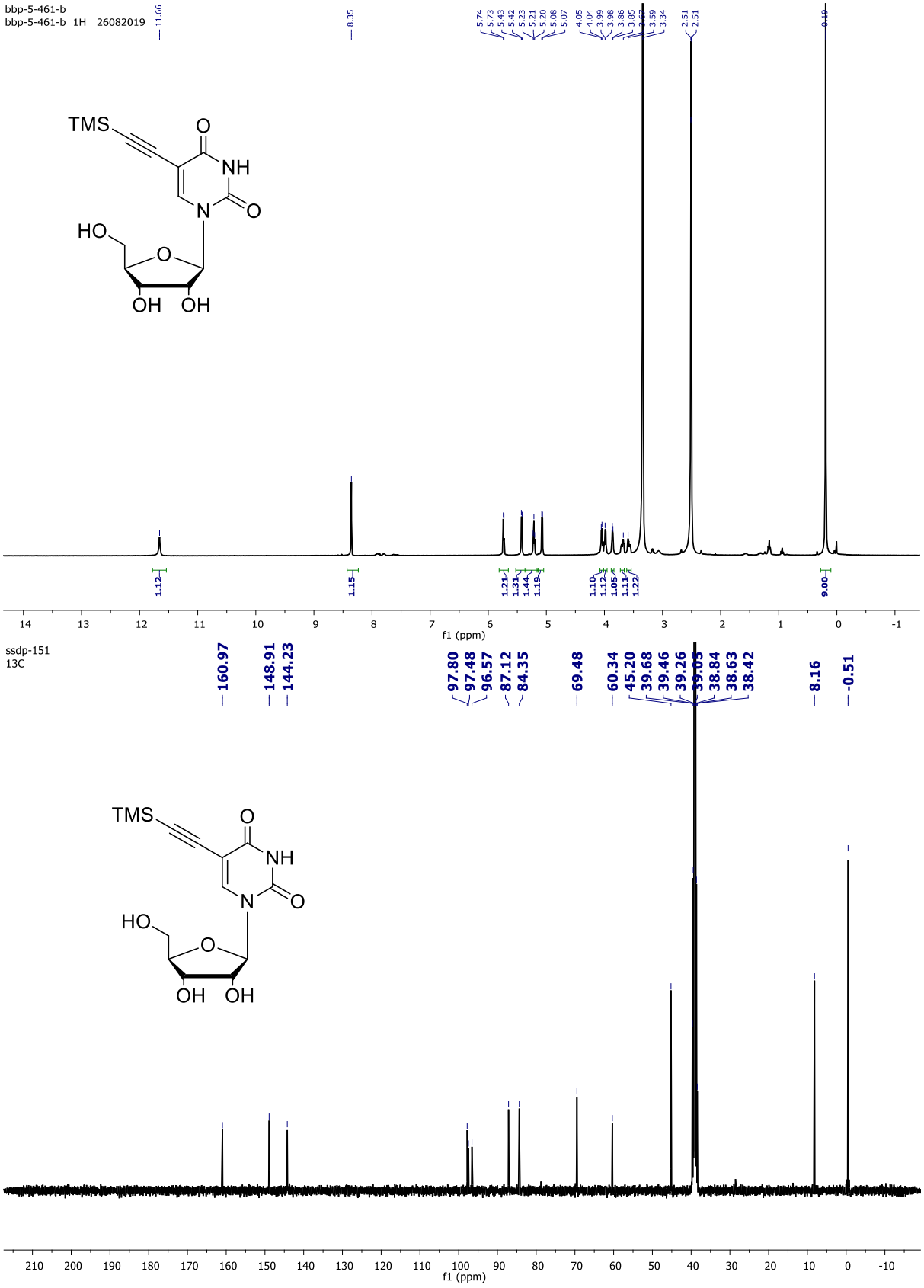

Figure A19. (^{1}H and ^{13}C) NMR spectra of Compound **12** in DMSO-d_6

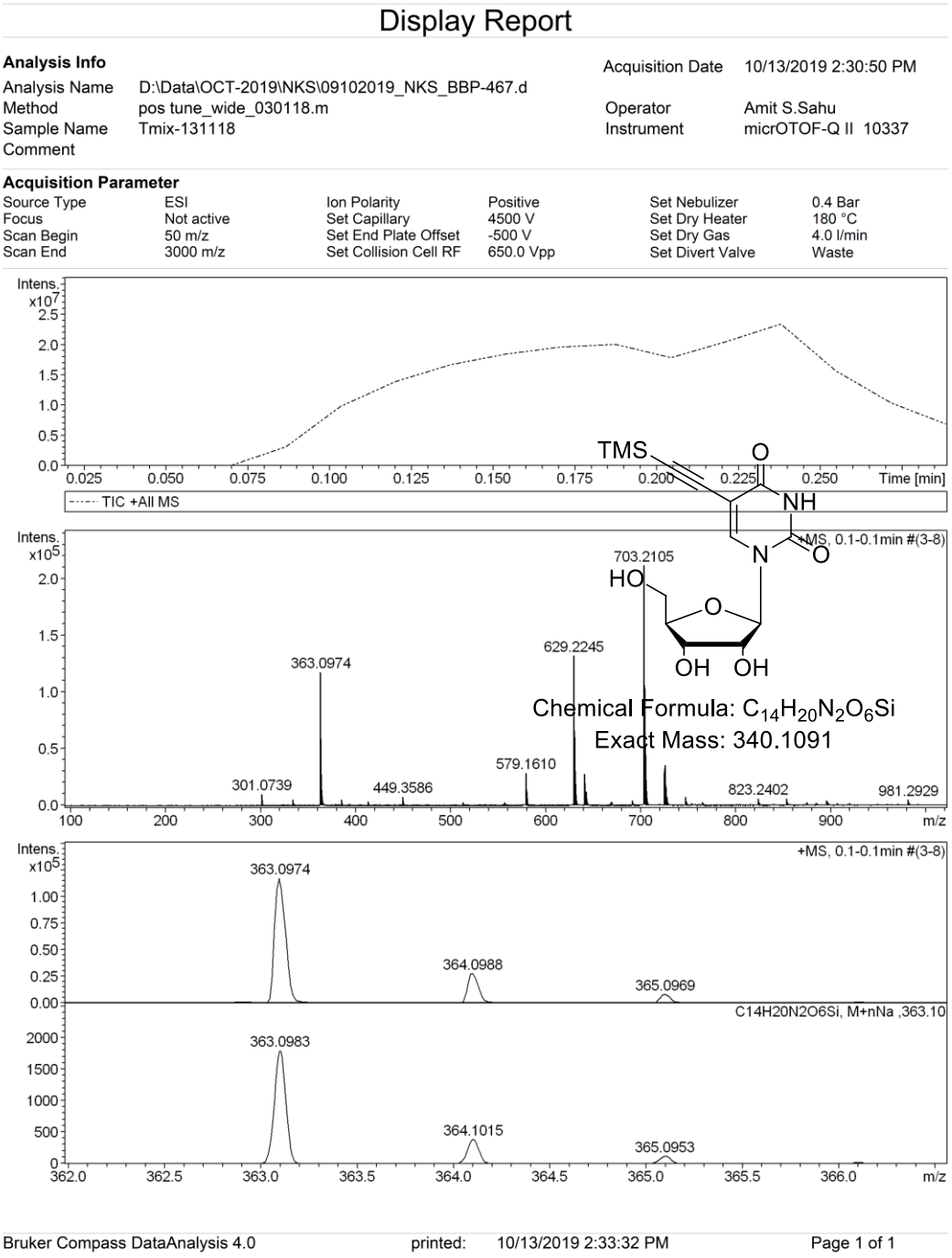

Figure A20. ESI/HRMS spectra of phosphonamidites **3**.

10. NMR (^{1}H, ^{13}C) and HRMS spectra of compound **13**:

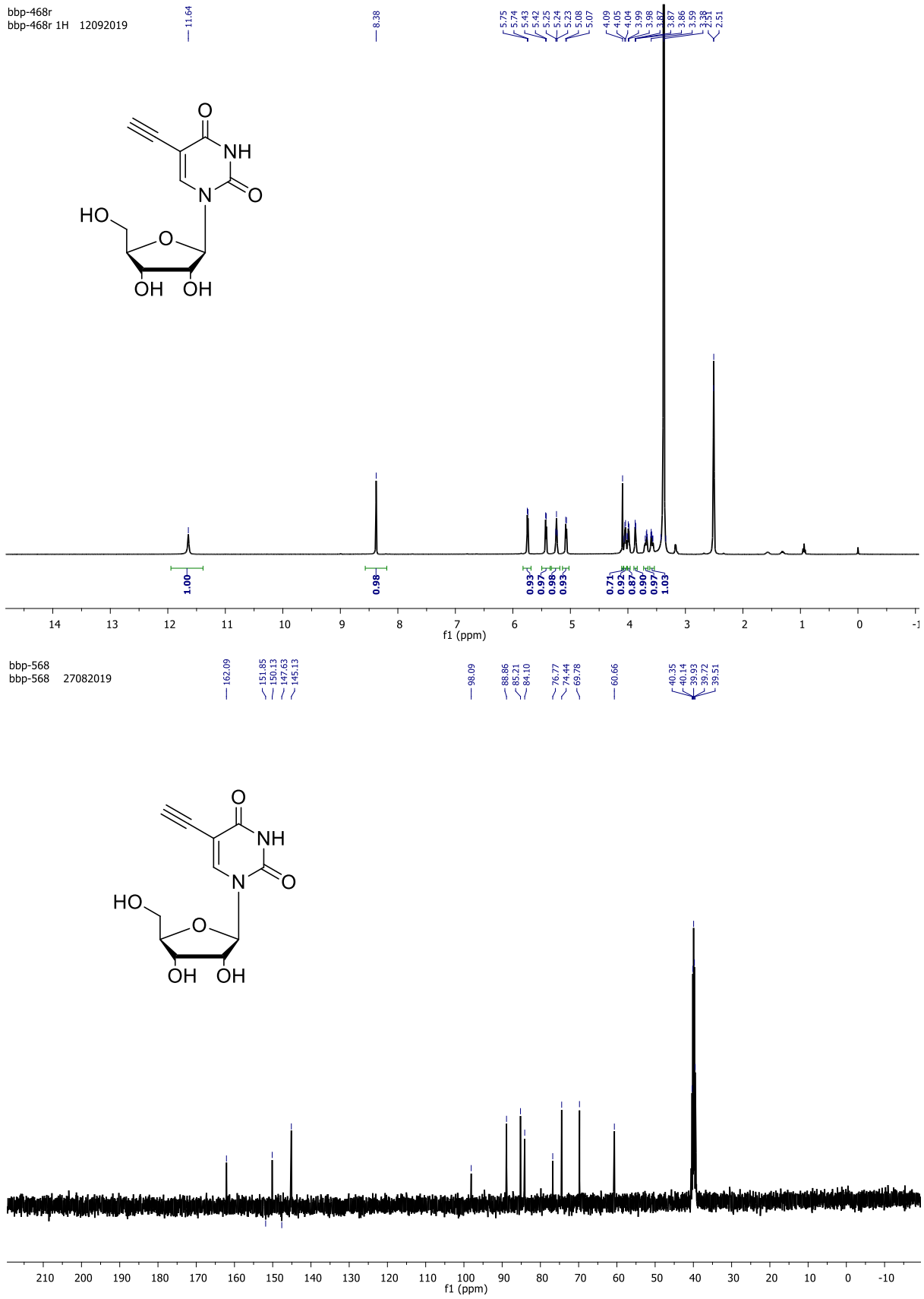

Figure A21. (^{1}H and ^{13}C) NMR spectra of Compound **1** in DMSO-d_6

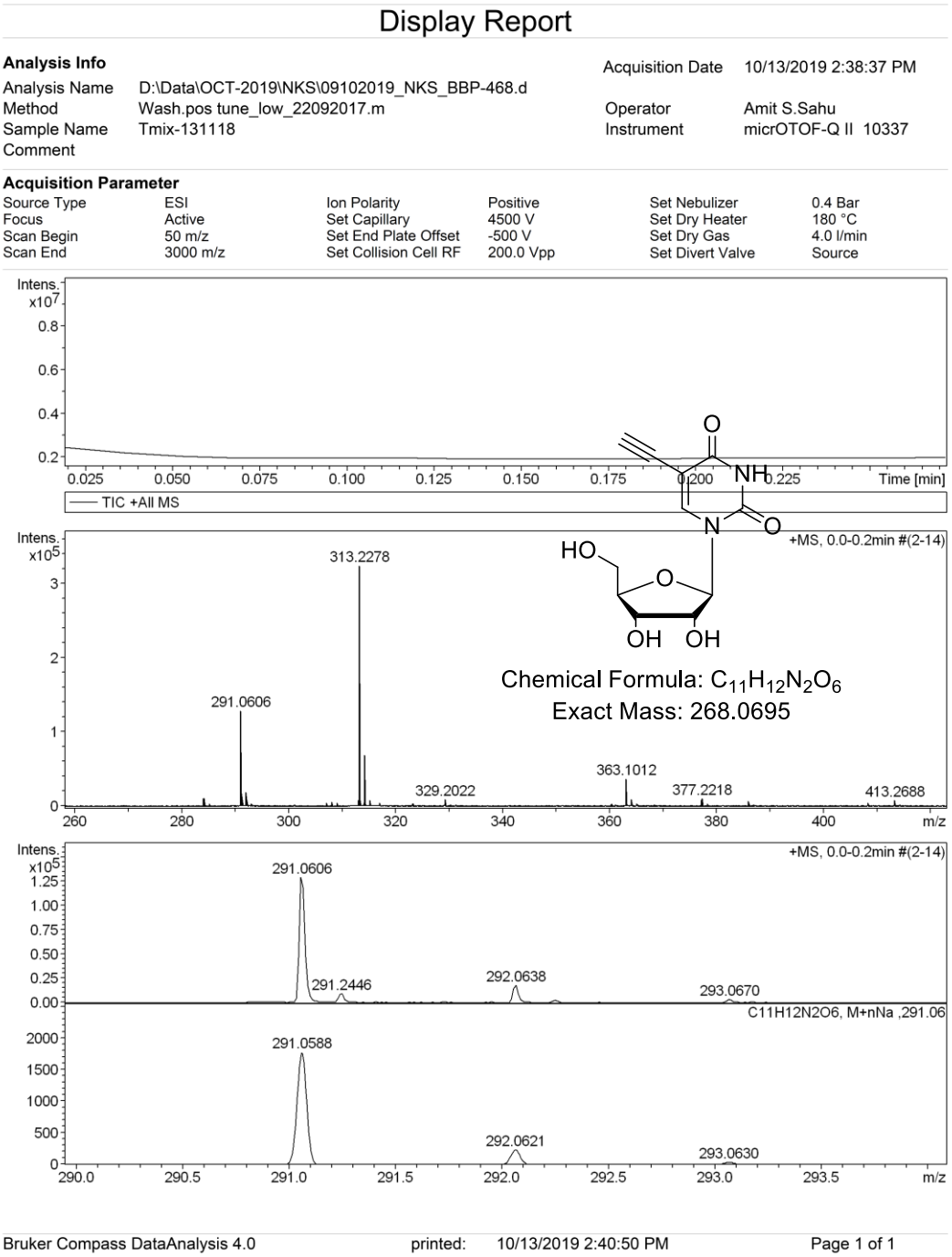

Figure A21. ESI/HRMS spectra of phosphonamidites **3.**

11. NMR (^{1}H, ^{13}C) and HRMS spectra of compound **14**:

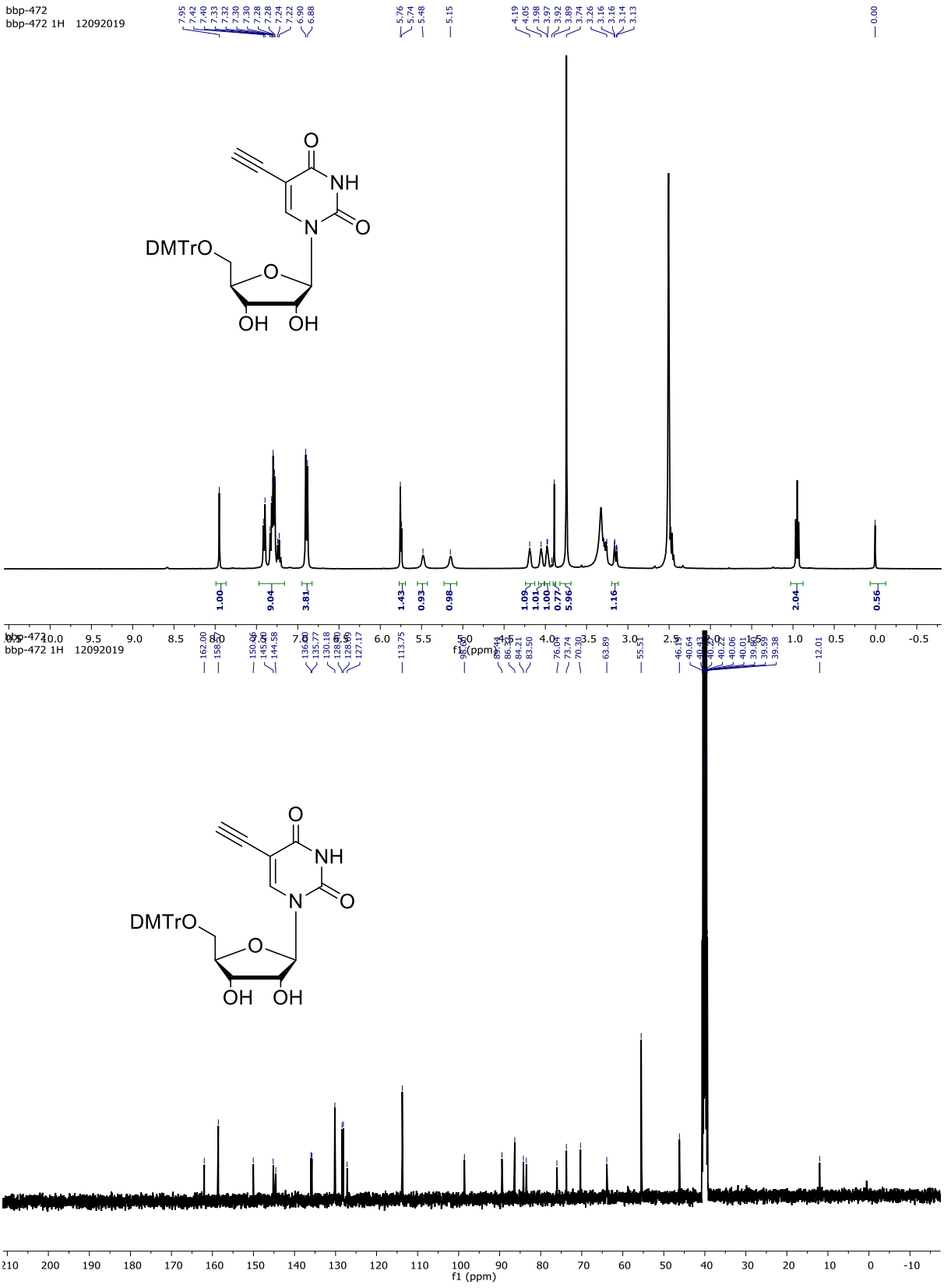

Figure A22. (^{1}H and ^{13}C) NMR spectra of Compound **1** in DMSO-d_6

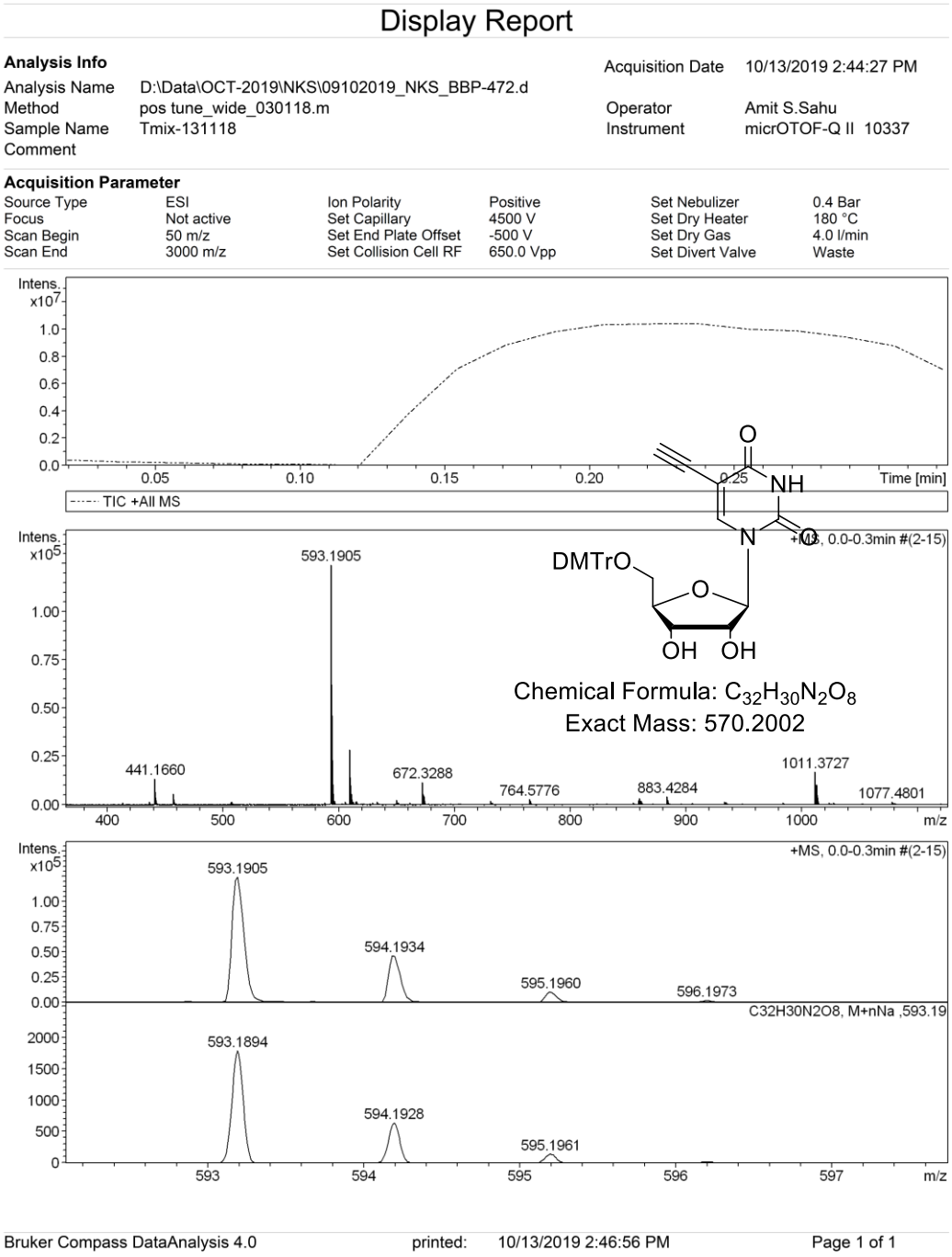

Figure A23. ESI/HRMS spectra of phosphonamidites **3**.

12. NMR (^{1}H, ^{13}C) and HRMS spectra of compound **15**:

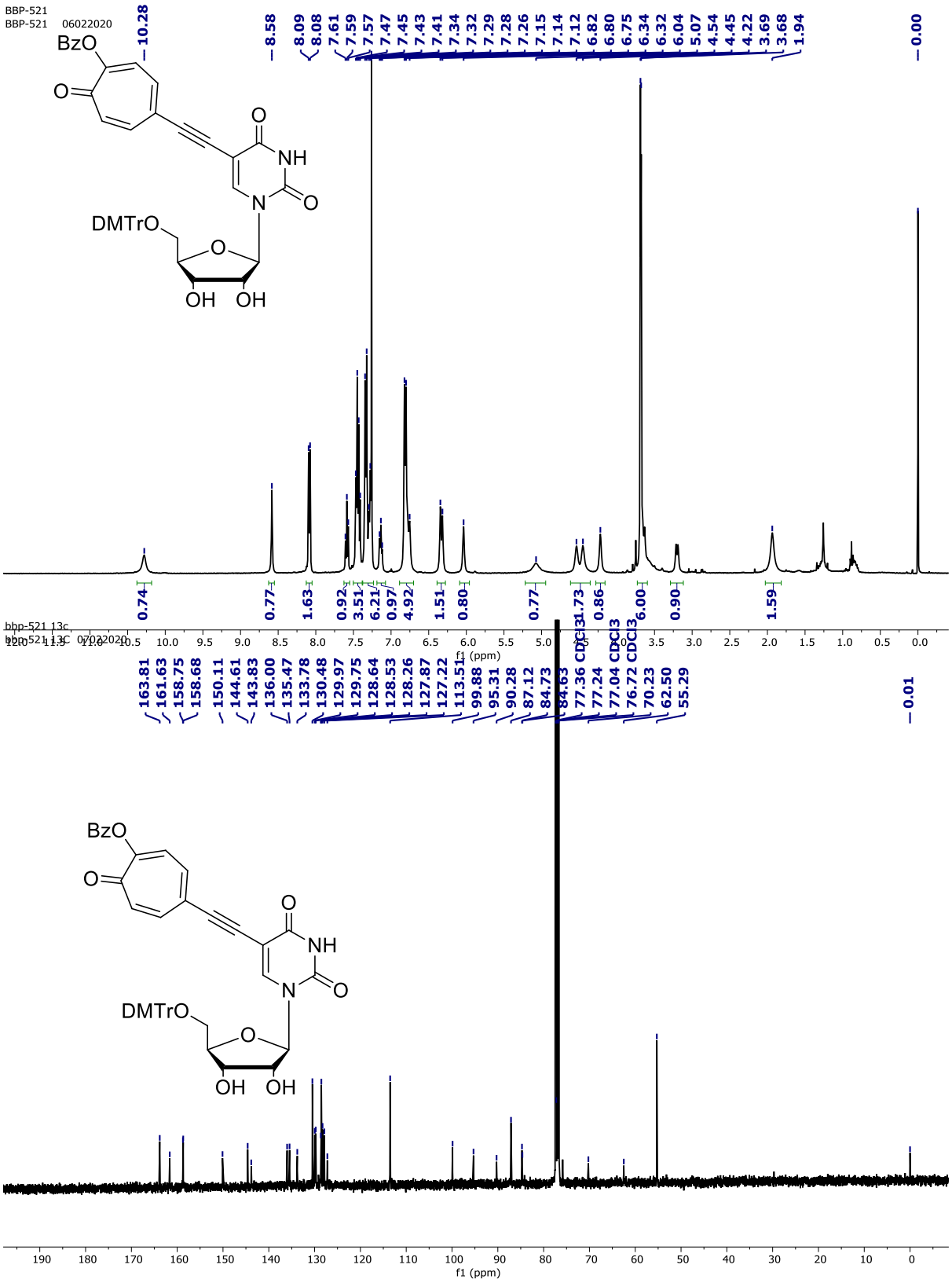

Figure A24. (^{1}H and ^{13}C) NMR spectra of Compound **1** in $CDCl_3$

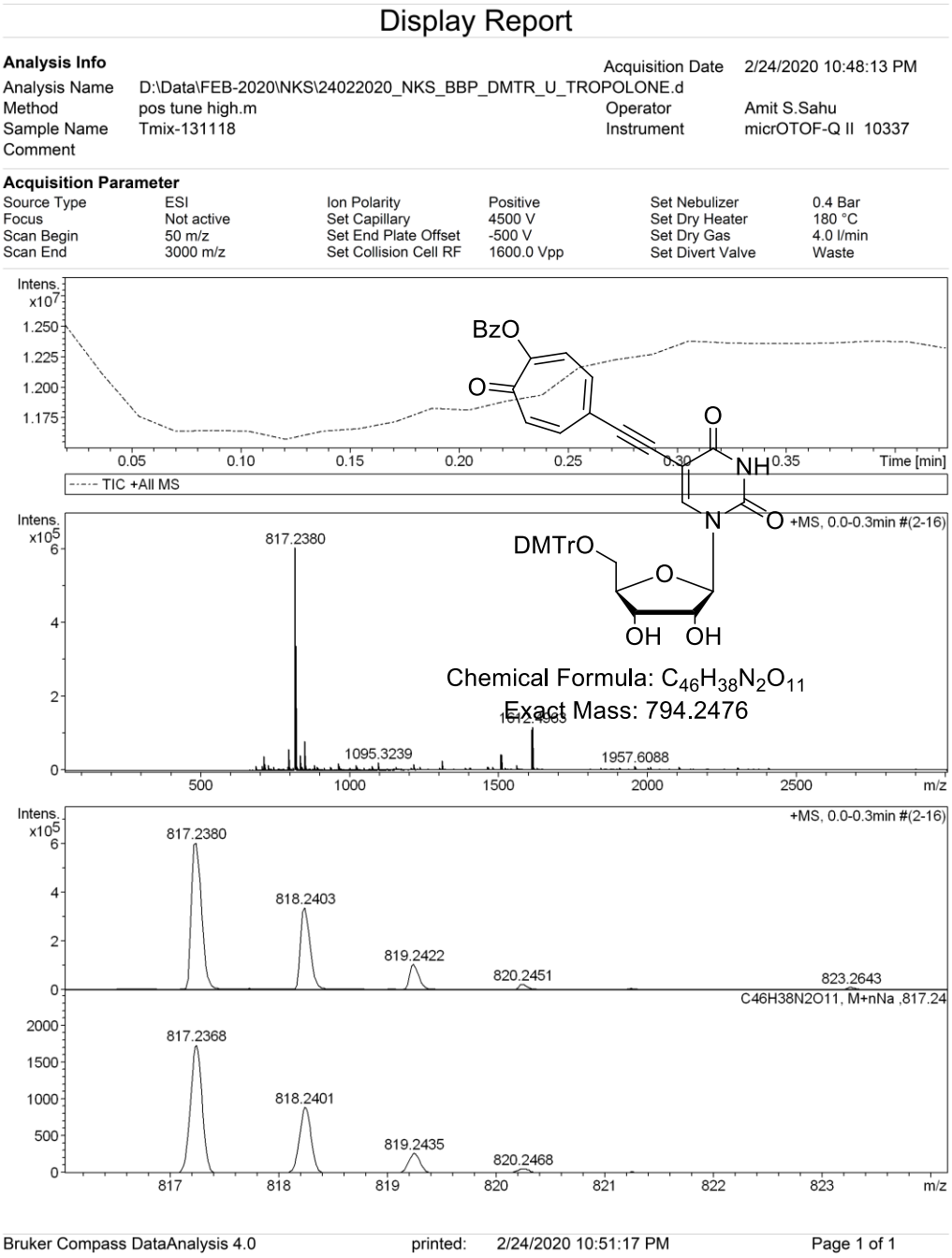

Figure A25. ESI/HRMS spectra of phosphonamidites **3**.

13. NMR (^{1}H, ^{13}C) and HRMS spectra of compound **16**:

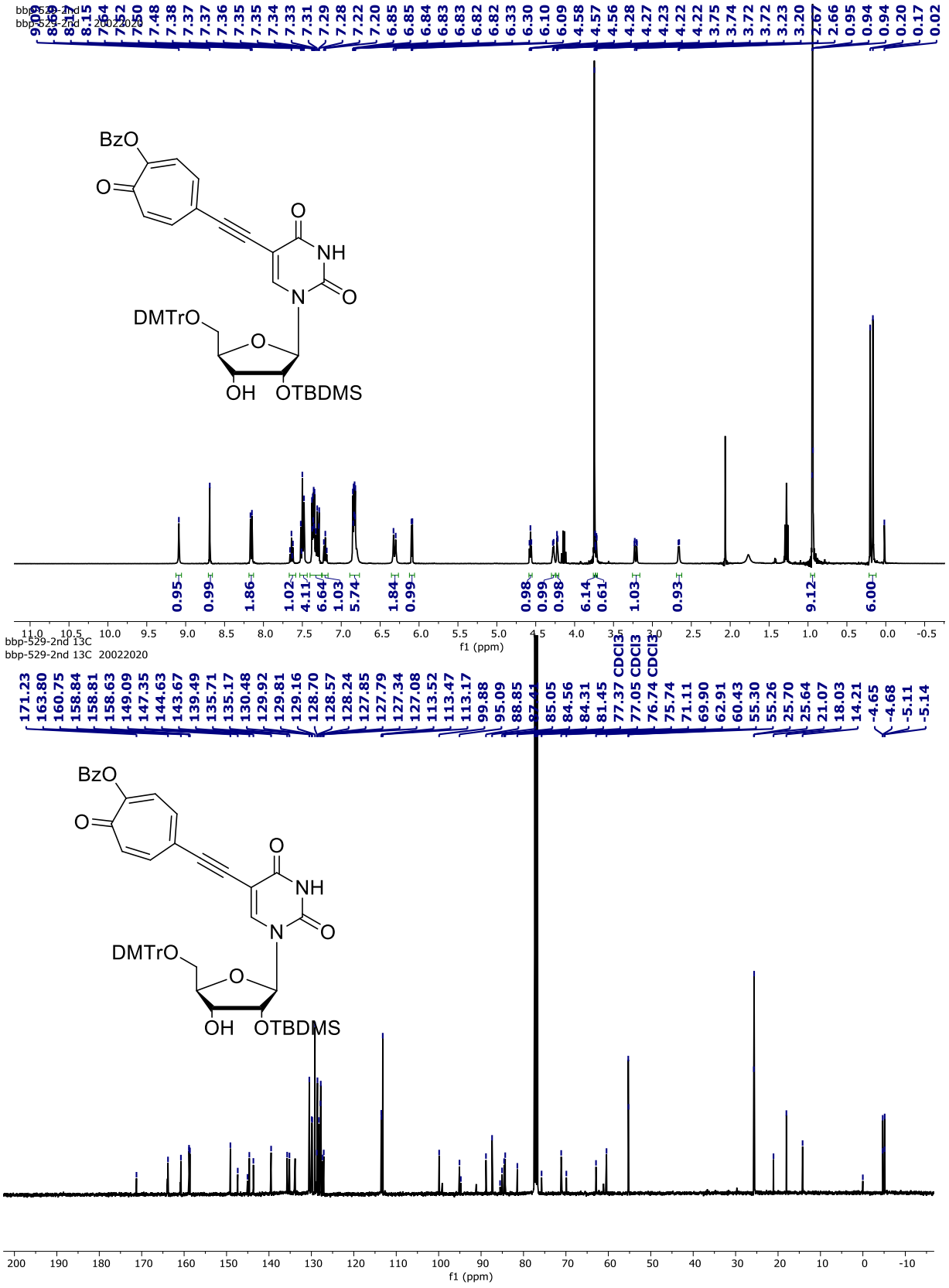

Figure A26. (^{1}H and ^{13}C) NMR spectra of Compound **1** in $CDCl_3$

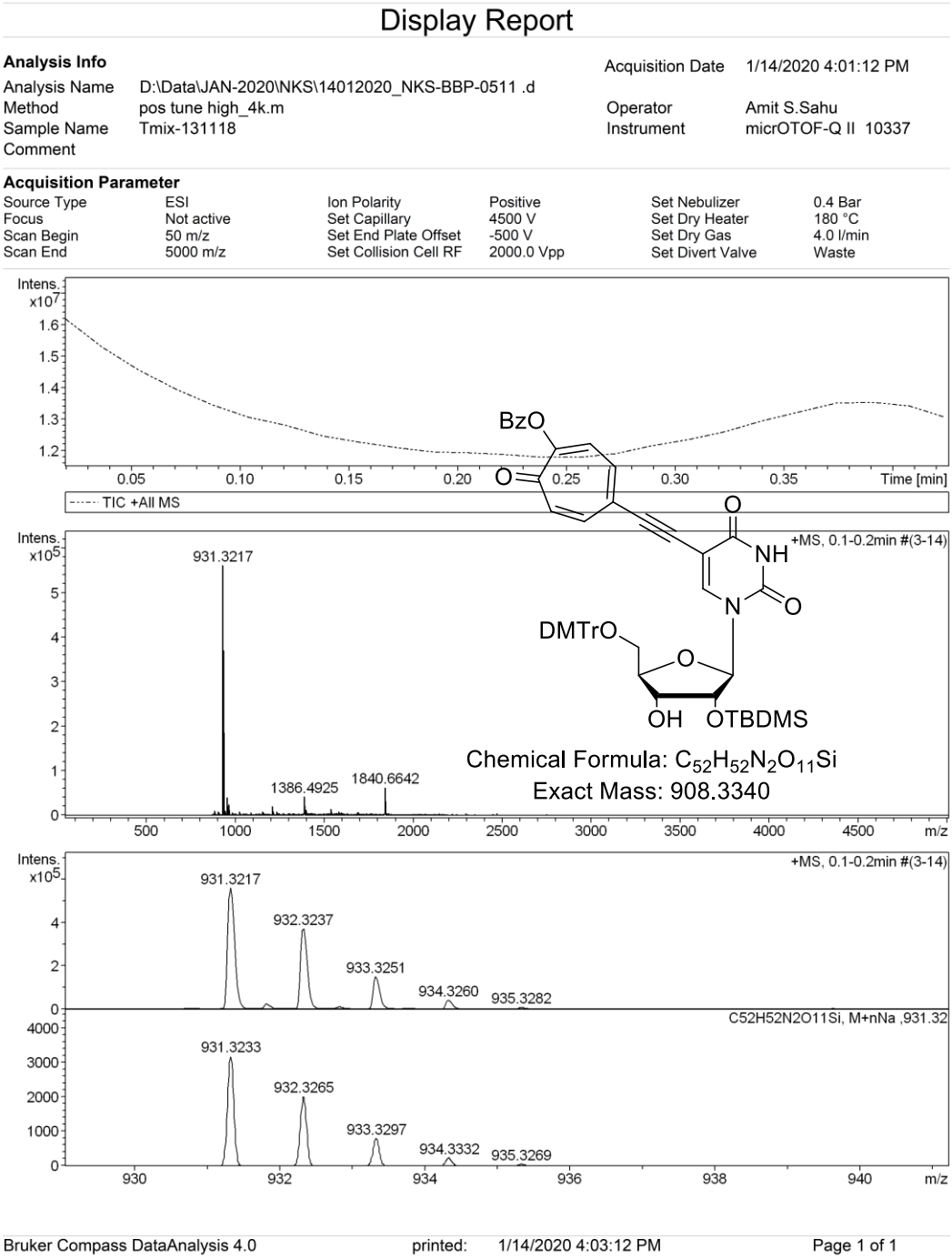

Figure A27. ESI/HRMS spectra of phosphonamidites **3**.

14. NMR (^{1}H, ^{13}C) and HRMS spectra of compound **17**:

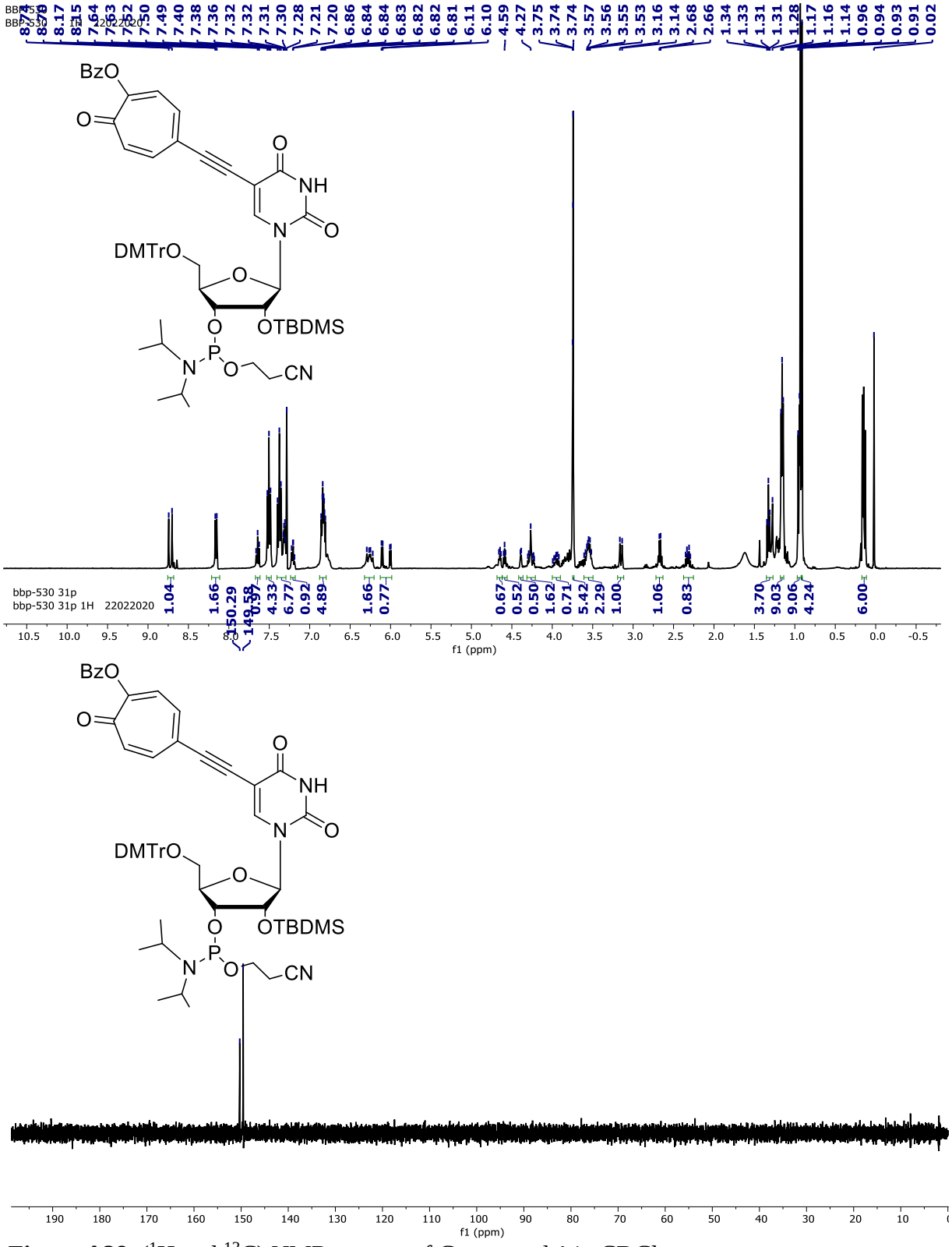

Figure A28. (^{1}H and ^{13}C) NMR spectra of Compound **1** in $CDCl_3$

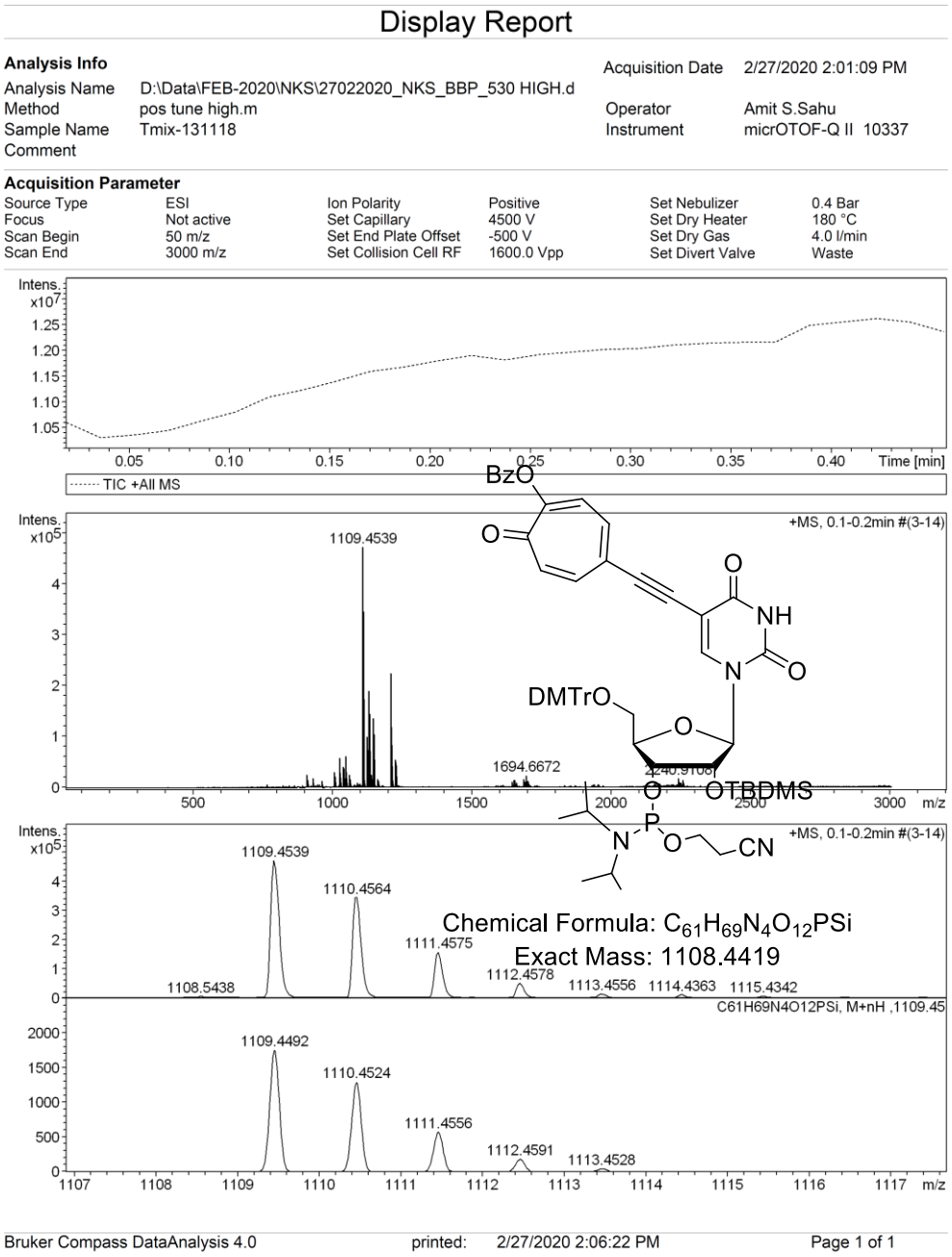

Figure A29. ESI/HRMS spectra of phosphonamidites **3**.

Thesis summary

Title of thesis: "Syntheses and Biochemical Evaluation of *Tropolonylated* Peptide and Nucleic acid Analogues"

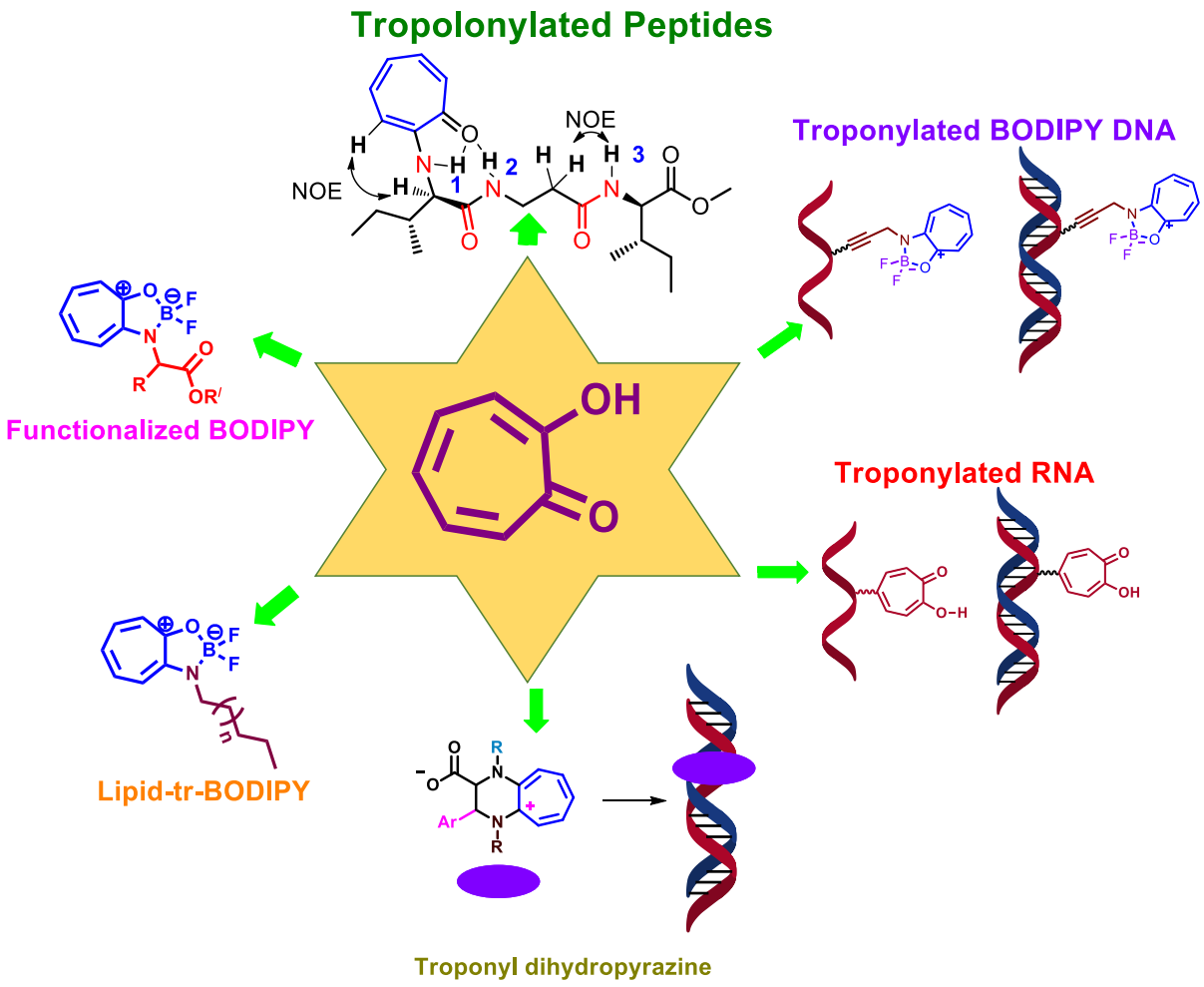

CrystEngComm

ROYAL SOCIETY OF CHEMISTRY

PAPER

View Article Online
View Journal | View Issue

Check for updates

Cite this: *CrystEngComm*, 2021, **23**, 131

N-Arylated peptide: troponyl residue influences the structure and conformation of *N*-troponylated-(di/tri)-peptides†

Bibhuti Bhusana Palai[ab] and Nagendra K. Sharma *[ab]

Received 22nd September 2020,
Accepted 12th November 2020

DOI: 10.1039/d0ce01386b

rsc.li/crystengcomm

Published on 12 November 2020. Downloaded on 5/21/2022 1:58:33 PM.

N-arylated peptides as peptoids influence the structural and conformational changes of small peptides that lead to unique foldamers, even in di-/tri-peptides. This report describes the syntheses, structural and conformational studies of rationally designed non-benzenoid *N*-arylated peptides containing bioactive tropolone molecules such as *N*-troponylated di-/tri-peptides. This report also demonstrates the role of the troponyl group in influencing the structure and conformation of *N*-troponylated short peptides (di-/tri-peptides) by single-crystal X-ray data analyses, circular dichroism (CD) studies, and 2D-NMR and DMSO-d_6 ^{1}H-NMR titration experiments. The tropolonyl residue has a significant role in the formation of unique supramolecular self-assemblies in dipeptide crystalline solids such as helical/β-sheet/β-turn (antiparallel β-sheet) type secondary structures. The sequence-specific tr-di-/tri-peptides exhibit a characteristic β-strand type of characteristic CD-signal in organic solvents (CH_3CN/MeOH). The hydrogen bonding nature of N–H, intra- or intermolecular hydrogen bonding, is also established by DMSO-d_6 ^{1}H-NMR titration experiments in the representative tr-di-/tri-peptides. These results explicitly support the role of the troponyl carbonyl group in the formation of secondary structures of peptides, even in di-/tri-peptides. Hence, the *N*-troponylation of peptides may alter the conformation of peptides to prepare novel peptidomimetics.

Introduction

Protein and peptides form secondary structures such as β-sheets/turns and α-helices, which are vital for their biochemical activities.[1,2] Non-covalent interactions such as hydrogen bonding and π–π interactions guide the formation of secondary structures in peptides as foldamers.[3–5] Generally, the amide carbonyl (–C═O)/amine (N–H) groups of peptides are involved in the hydrogen bonding and form stable secondary structures.[6,7] Sequence-specific structured peptides interact with a specific protein and nucleic acid to maintain the biochemical process. Nowadays, protein–peptide interaction and nucleic acid (DNA/RNA)–peptide interaction studies have emerged as powerful tools for developing peptide-based therapeutic drug candidates. However, naturally occurring peptides and their structures have limitations, such as aqueous solubility, structural stability with peptidase, and cellular uptake affinity, for practical applications in biochemical research. Thus, several structurally modified amino acids are prepared and employed for the synthesis of peptide foldamers. These foldamers are used for the development of novel biomaterials and potential therapeutic drug candidates.[8,9] For example, aromatic amino acids, mainly phenylalanine-rich di-/tri-peptides, have shown a high tendency, because of π–π interactions, for the formation of various types of self-assembled materials.[10] Aromatic tripeptides containing aromatic amino acids (Tyr & Trp) and methionine (or cysteine) are reportedly known to form fibrous aggregates.[11] Bag and co-workers have reported novel scaffolds as β-turn peptidomimetics from the triazole amino acid-containing peptides.[12] Gabapentin based hybrid small peptides reportedly form a double turn conformation by C_{12}/C_{10} hydrogen bonding.[13] N-terminal aromatic acid-containing peptides have the ability to spontaneously self-assemble because of hydrogen bonding and π–π interactions[14–16] The attachment of an alkyl/aryl group at the N-terminal of peptides alters the structure and function of peptides. Recently, the influence of *N*-alkylated/arylated peptides or peptoids has been explored in the structural and conformational changes of peptides.[17–21] *N*-alkylated peptoids

[a] *School of Chemical Sciences, National Institute of Science Education and Research (NISER)-Bhubaneswar, Jatni Campus, Bhubaneswar, 752050 Odisha, India. E-mail: nagendra@niser.ac.in, https://www.niser.ac.in/users/nagendra#profile-main; Fax: +91 0674 249 4141; Tel: +91 (674) 2494004*

[b] *HBNI-Mumbai, Mumbai, India*

† Electronic supplementary information (ESI) available. CCDC 1889029–1889034 (six structures). For ESI and crystallographic data in CIF or other electronic format see DOI: 10.1039/d0ce01386b

Organic & Biomolecular Chemistry

PAPER

View Article Online
View Journal | View Issue

Published on 04 June 2019. Downloaded by National Institute of Science Education & Research on 5/21/2022 1:58:28 PM.

Check for updates

Cite this: *Org. Biomol. Chem.*, 2019, **17**, 6497

BODIPY analogues: synthesis and photophysical studies of difluoro boron complexes from 2-aminotropone scaffolds through *N,O*-chelation†

Bibhuti Bhusana Palai,‡[a,b] Ramachandra Soren‡[a,b] and Nagendra K. Sharma *[a,b]

Received 21st April 2019,
Accepted 4th June 2019

DOI: 10.1039/c9ob00915a

rsc.li/obc

Boron-dipyrromethene (BODIPY) fluorophore derivatives were prepared from a *Pyrromethene* scaffold and di-fluoroboron. To add to the range of biocompatible fluorophores, this report describes the synthesis and photophysical studies of carboxylate-functionalized BODIPY analogues from natural products, *Tropolone* and α-amino acids, through *N,O*-chelation. The structure of a few derivatives was confirmed by single crystal X-ray studies. UV/fluorescence studies revealed their fluorescence behaviors in organic solvents with a quantum yield of ~0–15%, which varied based on the structure of amino acids. Further, electrochemical studies were accomplished by cyclic voltammetry, which confirm only one irreversible reduction reaction with E_{pc} = –1.3 (V). Finally, their HOMO and LUMO molecular orbitals/energy differences were calculated from a theoretically (DFT) optimized structure, which also supported the role of amino group residues in the enhancement of the fluorescence. The glycinate derivative exhibited the greatest quantum yield compared to the other amino groups. Hence, 2-aminotropone containing BODIPY analogues are potential candidates for the development of various types of functionalized fluorophores as BODIPY analogues.

Introduction

Boron-dipyrromethene (BODIPY) derivatives are versatile organic fluorescent dyes and are widely applied in the syntheses of fluorophore materials and s excellent labeling agents of biomolecules for making chemical sensors, cell imaging agents, and energy related cassette entities (Fig. 1A).[1–4] However, a few shortcomings, such as solubility and functionality, persist with BODIPY dyes, which limit their direct use in practical applications. Recently, functionalized BODIPY analogues were prepared from various dipyrromethene-derived scaffolds and other related benzenoid aromatic ligands.[5] For example, alkenyl-BODIPY and C(sp^3) connected dimers exhibited an absorption peak in the near infrared (NIR) region.[6] Dipyridylmethene (DIPYR) dyes, pyridine-based BODIPY analogues, exhibited a wide range of photophysical properties from non-emissive to green fluorescence with a quantum yield of 0.2–0.8.[7] BOIMPYs, benzimidazole-containing analogues, have shown red-emissive fluorophores and are considered as NIR-Dyes.[8,9] Werz and co-workers prepared ethylene-bridged oligo-BODIPYS, which exhibited intramolecular J-aggregation and are considered as super-fluorophores with a quantum yield of almost unity.[10] Further chlorinated dipyrromethene derivatives are desired for tuning their photophysical behaviors. Recently, α-chlorinated-BODIPY analogues were prepared in one step directly from BODIPY using $CuCl_2$.[11] A new family of BODIPY dyes as *N*-BODIPYs (diaminoboron dipyrromethanes) were tested as smart photonic materials.[12] BOAHY, acyhydrozone containing BODIPY analogues, has several unique photophysical properties, such as weak fluorescent in

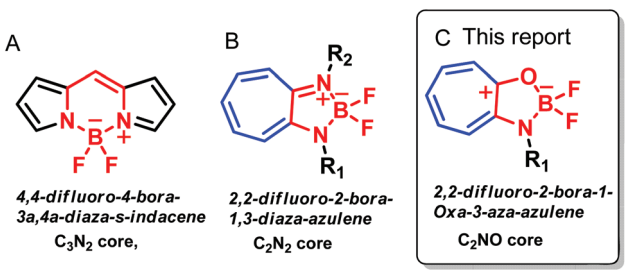

Fig. 1 Chemical structures of (A) BODIPY complex; (B) boron–aminotroponimine complex; and (C) boron–aminotropone complex.

[a]*School of Chemical Sciences, National Institute of Science Education and Research (NISER)-Bhubaneswar, Jatni campus, Bhubaneswar-752050, Odisha, India. E-mail: nagendra@niser.ac.in; https://www.niser.ac.in/users/nagendra#profile-main; Fax: +91 (674) 2494004; Tel: +0674-249-4141*

[b]*HBNI-Mumbai, Mumbai, India*

†Electronic supplementary information (ESI) available: Spectroscopic (MS and NMR) and crystallographic data. CCDC 1888894–1888899. For ESI and crystallographic data in CIF or other electronic format see DOI: 10.1039/c9ob00915a

‡These authors contributed equally.